THE INDIAN JOURNAL OF TECHNICAL EDUCATION

INDIAN JOURNAL OF TECHNICAL EDUCATION

Editorial

Plastic Waste A Menace: Because of changes in lifestyle, there has been a notable increase in the usage of plastics over the past few decades, as well as an increase in the amount of waste created per person. The primary causes of the rise in rubbish creation per person are changing lifestyles. Despite this, plastic is used in many products for a range of purposes because it is inexpensive, lightweight, durable, and can be moulded into the necessary forms and sizes. It is also available in vibrant colours. There is widespread plastic use, with each person consuming 45 kg of plastic annually on average. Plastic is an organic material that does not biodegrade; depending on its thickness, it may take years for it to do so. Burning plastics can seriously pollute the air and ground water pollution through leaching. Several thousand tons of plastic garbage are discarded into natural water bodies every day.

Over 430 million tons of plastic are created annually, and if current trends continue, the amount of plastic garbage generated will triple by 2060, having catastrophic effects on ecosystems and public health. In addition to their detrimental effects on the environment and natural resources, plastics have health implications on aquatic life, humans, and animals. Lung cancer, silicosis, heart disease, chronic obstructive pulmonary disease, and other conditions are among the illnesses brought on by plastic garbage. Individuals employed in the plastics industry may have the risk of developing brain tumours, breast cancer, mesothelioma, lymphoma, and infertility. When plastic garbage enters the drainage system, it clogs, causes flooding during heavy rains, damages properties, and sometimes even results in the deaths of people and animals. Furthermore, fish, seabirds, and other marine creatures absorb plastic debris that ends up in rivers and other bodies of water, suffocating to death.

Using paper bags instead of plastic ones, avoiding single-use plastics, reusing existing plastic bags and other things, recycling wasted plastic material, refusing to use disposable plastic cutlery, and other strategies are some ways to reduce its usage. The best way to reduce the threat of plastic waste is to

<div align="center">Carry A Bag – Not Carry Bag</div>

New Delhi   **Editor**

30ᵗʰ June 2024

Indian Society for Technical Education

Official E- Mail ID's

SN	E-Mail ID	Purpose
1	info@isteonline.org	All General enquires.
2	istedhq@isteonlione.org	All official communication.
3	exesecretary@isteonline.org	Matter related to Executive Secretary; Policy related & etc.
4	accounts@isteonline.org	All matter related to finance and account section.
5	membership@isteonline.org	All matters related to, 1. Institute Membership, 2. Life Membership, 3. Student Membership, 4. Faculty Chapter, 5. Student Chapter, 6. Section Share, 7. Student Share & etc.
6	guesthouse@isteonline.org	For Guest House Booking.
7	executive_tech@isteonline.org	All enquiries related to ISTE official Website, E-Mail ID & etc.
8	technical@isteonline.org	For Faculty Development Program (FDP), STTP's, Enquiry related to Conventions, Conferences & etc.
9	editor@isteonline.org	Enquiry related to Indian Journal of Technical Education (IJTE) & Submission of Manuscript & etc.
10	newsletter@isteonline.org	All matters related to news items in newsletter.

Inviting Proposals to Organise the
International and National Conferences
Partially Funded by the ISTE

The Indian Society for Technical Education (ISTE), New Delhi is pleased to invite the proposals from the Universities and the AICTE, New Delhi approved technical institutions having Institutional Member (IM) of ISTE and willing to organize 02 days International and National Conferences on the emerging technologies in a multidisciplinary area before **31st January 2025**. In order to disseminate the knowledge and advancements worldwide, conference proposals should primarily concentrate on the innovative, high quality, efficient, service, fast and cost-effective, efficient rising technologies or fresh perspectives on old technologies to share the knowledge and developments across the world. The conference may solicit scientific and research papers for presentation, poster presentation, projects/products display, key notes presentations and invited talks, etc.

ISTE, New Delhi shall extend a **maximum financial support of ₹2.0 Lakhs for 02 days national level and ₹4.0L for international level conference.**

The Indian Society for Technical Education (ISTE), New Delhi website (www.isteonline.in) offers conference **proposals for download.** Completed proposals must be submitted with the required supporting documentation, a non-refundable processing fee as mentioned in the attachment.

The proposal must be submitted on or before September 3, 2024 by 5.00pm. Proposals received beyond the designated date and time will not be considered.

Executive Secretary,
ISTE, New Delhi

IJTE Special Issue

Indian Journal of Technical Education (IJTE) a UGC-Care listed Journal published by the Indian Society for Technical Education (ISTE), New Delhi is inviting proposals from the willing institutions to publish their national or international level conference papers as a **"Special Issue"**. Terms and conditions for the publication will be sent on receipt of the request through a mail (**editor@isteonline.org**) from the institution.

Request for **"Special Issue"** received from the AICTE approved institutions and institutions of national importance will only be entertained.

Editor
IJTE

Conference on Renewable Energy

Solar Energy Society of India (SESI) in collaboration with Indian Journal of Technical Education (IJTE) a UGC-Care listed Journal published by the Indian Society for Technical Education (ISTE), New Delhi is inviting proposals from the willing institutions to organize a national level conference on **"Renewable Energy"**. The selected papers will be published as a special issue of IJTE.

The willing AICTE approved institutions and institutions of national importance can send their proposals through a mail to: **iste.executivesecretary@gmail.com**. The tentative period of conference maybe July or August 2024.

Editor
IJTE

Contents

Threshold based Forest Fire Detection in Utharkhand Region using Landsat Satellite Images

P. Chanthiya, S. V. Anandhi

Assistant Professor
Department of Computer Science and Engineering
Dr. Sivanthi Aditanar College of Engineering
Tiruchendur, Tamil Nadu
✉ chanthiyapuhal@gmail.com
✉ svanandhi2020@gmail.com

G. R. Jainish

Assistant Professor
Department of Computer Science and Engineering
Loyola-ICAM College of Engg. and Technology,
Chennai, Tamil Nadu
✉ jainish.gr@gmail.com

ABSTRACT

Forest fires have a significant impact on boreal ecosystem circumstances, recurrence and the worldwide cycle of carbon. Various LANDSAT datasets from the Utharkhand region were collected for this study for the period from 2015 to 2022. Among several bands, the thermal band includes temperature-related information in LANDSAT aerial images. Based on statistical fire detection, fire detection-based parameters such as TOA temperature, Land Surface temperature, Brightness temperature, humidity, vegetation index, and land cover area are retrieved to estimate the forest fire. This suggested method reduced the false alarm rate while detecting 98.83% of the fire area.

INTRODUCTION

The ecological balance of the earth is guarded by forests. Regrettably, forest fires are sometimes only detected after they have consumed a large area, which makes containment and destruction challenging. It might be hard to handle and control at times. Forest fires are a major hazard to forest vegetation and biodiversity, accounting for 30% of CO_2 emissions in the atmosphere. The struggle between social and ecological protection and rapid urbanization, urban sprawl, and land-use changes is intensified by weather and climate change. While regulated fires contain and limit the spread of unwanted fires to prevent significant harm to forest ecosystems and biodiversity, unplanned and unexpected forest fires degrade the environment.

Worldwide, data from space-borne remote sensing systems is used to identify hundreds of thousands of fires related to biomass every year. The two primary data sources used to create maps are satellite and aerial images. Various features were calculated from the satellite photos based on the geographical, spectral, and temporal resolutions. The incentive to develop early forest fire detection is increased by the steady growth in the availability of satellite pictures.

To detect the early fire detection, an improved algorithm for detecting forest fires was proposed. The undesired noise in the satellite photos is first eliminated by the suggested technique. Many factors including land surface temperature, intensity, TOA Brightness temperature, spectral radiance, NDVI, land surface emissivity and water vapor were taken into account for early forest fire detection. To find the fire region, the Unsupervised Clustering technique is employed. The statistical method is employed in this suggested work to find forest fires. The suggested method's experimental findings are examined, and a performance analysis is conducted.

RELATED WORKS

Research on forest fire detection makes use of a variety of satellite remote sensing techniques to offer worldwide earth observation. The Landsat satellite series delivered high spatial resolution photos for more than 45 years. Several early detection methods have been developed to use Landsat imagery to identify forest fires.

Preprocessing should be carried out initially to fix mistakes and eliminate clouds and cloud shadows from the Landsat imagery. In order to extract the satellite image from the noise and other degradation,

error correction techniques were applied. In order to correct the satellite degradation error and radiometric correction, Lasaponara R et al[6] used multiple sets of satellite images taken at different times and under varied environmental conditions.In order to eliminate the need for changing IC lamps Chander et al.[2] revised the Lansat 5 (L5) TM reflective band calibration technique. IC represents the Internal Calibrator of the onboard calibration system.

The surface temperature was estimated using various thermal bands from ASTER satellite images. ASTER satellite sensor has five thermal infrared bands. A method for calculating the surface radiance using the ASTER thermal band Emissivity Normalization approach was employed by KrishnenduBanerjee[3]. This method mapped surface radiance to decimal numbers from the ASTER thermal band. Ultimately, the surface radiance will be used to obtain the surface temperature. The Earth-Sun Distance in Astronomical Units and UCC (Unit Conversion Coefficient) are obtained using ASTER manual gains and offsets.

To identify forest fires, Bruna EZ Leal et al.[1]suggested an onboard fuzzy logic technique that separates the spectral properties of fires. Setzer Algorithm is used to investigate pixel values from their decimal integers without modifying them for temperature or reflectance. Only a few annual tweaks are needed to account for sensor degradation in the fire pixel categorization criteria, which are obtained analytically.

The detection and analysis of forest fires was done over several decades using satellite sensors in geostationary Earth observation (EO) satellites and Polar-orbiting systems. ZixiXieet.al[9]suggested that several fire detection systems use either temporal resolution images or spatial resolution images. To identify a forest fire, certain fire detection algorithms merge photos with both geographical and temporal resolutions.

Contextual and fixed threshold algorithms were presented by Kumar et al.[4] for the purpose of detecting forest fires using spatial resolution pictures. Based on brightness, temperature, and a few other characteristics, fixed threshold algorithms were employed to identify the forest fires. The surpassing pixel values in these

techniques are recognized as the fire area. The variation in air condition relies on time and climatic variables, making threshold limit optimization difficult.

PROPOSED METHODOLOGY

The suggested technique uses a statistical approach to detect forest fires. There are three distinct phases to it. The stages of the suggested method are preprocessing, feature extraction, and threshold based fire detection. Various bands are extracted from Landsat satellite photos and sent into the preprocessing phase. Image co-registration, noise reduction, and cloud elimination are carried out in the preprocessing stage. The many features assessed in the feature extraction stage are land surface temperature, intensity, TOA Brightness temperature, spectral radiance, NDVI, land surface emissivity and water vapor. At last, the statistical method is used to identify forest fires.

Landsat scenes are gathered from different regions of the world in order to research the suggested system. These scenes were divided into before and after fire scenes according to the dates of collection. A range of characteristics are employed to predict the likelihood of forest fires at various times. The bands from the sensor should be collected, and then they should be processed to take out any noise.
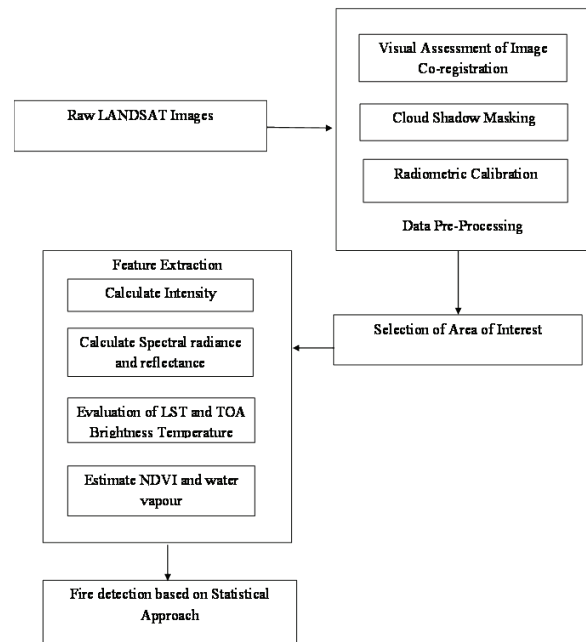
Fig.1 Block diagram for threshold-based fire detection

The suggested design to identify forest fires using threshold based method is depicted in Figure1.

Preprocessing

Preprocessing is used to get rid of undesirable data, mistakes, and noise. Many preprocessing methods, including as image co-registration, radiometric adjustment and cloud elimination are applied to improve the Landsat imagery.

Image Co-registration

The relative image to image geo-location has allowed for the visual assessment to be completed. The effective precision of the spatial registration between multi-date photos can be visually assessed using the relative picture to image geolocation. The 2000 picture was used as the master image, and the linear X, Y pixel shift was needed to match the slave image to the master image via image overlay. Problems with geolocation usually caused a linear displacement of one or two pixels. Subsequently, a fresh 20 x 20 km subset is extracted and raw Landsat scenes are translated. When available, alternate data is substituted for the images in the study, as the geo-location inaccuracy was non-linear in a few instances. The erroneous images are corrected by adding some images without nonlinear errors, and the nonlinear geo-location error images are eliminated from the gathered datasets.

Cloud and cloud shadow masking

To locate and classify clouds and cloud shadows, utilize the Spatial Procedures for Automated Cloud and Shadow Removal technique. To identify each pixel's membership in the cloud, cloud shadow, water, and clear sky categories in a Landsat image, the technique uses a neural network methodology. It then uses information such as surrounding pixel membership values and an estimate of cloud shadow locations based on solar and cloud geometry, among other spatial approaches, to resolve pixels with uncertain membership.

The noisy and the cloud removed images were depicted in the figure 2.
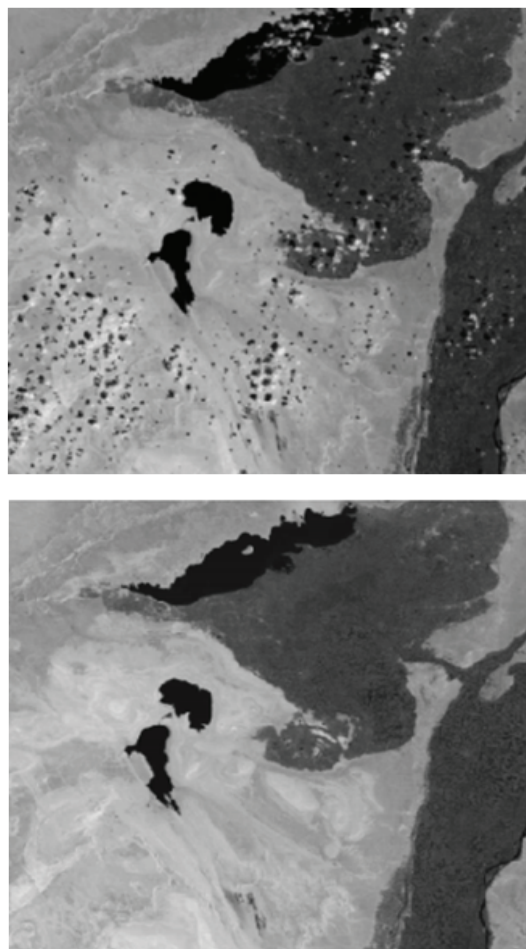
Fig. 2: Original and cloud eliminated image

Segmented region

K-means is the most popular and widely used Unsupervised Learning Algorithm. The unlabeled data is split up into K distinct clusters by it. The K-Means algorithm groups the datapoints according to their regularity and structure when it receives the cluster numbers and the training set. Choose K data points at random among the data collected to create the centroids of the clusters. The cluster center nearest to each data point should be assigned to it. To update the centroids, compute the average location of all the data points in each cluster.

Feature Extraction

A key component of applications based on remote sensing is feature extraction. The properties and structure of the objects to be detected are what determine which

features can be extracted. Heat and smoke are the two main components that forest fire detectors employ to find the fire. Features based on heat are retrieved here. Land surface temperature, intensity, TOA Brightness temperature, spectral radiance, NDVI, land surface emissivity and water vapor are among the various indicators used in statistically based fire detection intensity to identify forest fires.

Intensity

You can get the tar file needed to process the Landsat image by visiting www.usgs.gov, the USGS website. Each pixel of an image is represented by a set of bands, each of which holds a set of decimal integers. Every pixel has a value for intensity. The object's reflected wavelength from the ground determines the intensity value. The digital number of each pixel represents the intensity value of that pixel. Each pixel has a digital integer between 0 and 255. A series of digital numbers can be found in each and every band of the Landsat image.

TOA spectral radiance and reflectance

The decimal figures can be converted into the spectral radiance with the aid of rescaling factors in the meta file. Equation (1) represents the computation of spectral radiance.

The decimal figures can be converted into the spectral radiance with the aid of rescaling factors in the meta file. Equation (1) represents the computation of spectral radiance.

TOA Spectral radiance = $M_L * Q_{cal} + A_L$ (1)

The meta file and the coefficients that may be downloaded from the USGS website can be used to estimate the TOA reflectance value and is given in equation (2)

$$\rho_\lambda = \pi * L_\lambda * d^2 / ESUN_\lambda * \cos\theta_s \quad (2)$$

The TOA reflectance from the Landsat image is estimated using the above formula.

Land Surface Temperature

One of the key elements that determines how heat and energy from the sun are absorbed, reflected, and

refracted at the earth's crust's surface is the land surface temperature, or LST. A approach for estimating land surface temperature was proposed by Moreira[8]. Accurate estimate is challenging since LST varies with changes in precipitation and other human activity. The land surface directly releases the majority of the energy that the sensor detects in this spectral region. Thermal Infrared (TIR) remote sensing is a novel method for gathering LST data at regional and global scales. Temperatures of the soil and vegetation combine to form LST. This temperature estimate is useful for determining the atmospheric land surface boundary and changes in the climate. The Land Surface Temperature is used by Chander et al.[2] to forecast changes in the atmospheric state.

It takes continuous spatial monitoring to determine the impact on surface temperature and the thermally related fluctuation in the atmosphere. The Landsat pictures' thermal infrared band can be used to efficiently do continuous spatial monitoring. As the parameter that controls the actual radiated temperature, LST is essential to determining thermal behaviour on Earth's surface and is computed using the equation (3) and (4).

$$dI_\lambda / dS = \rho k_\lambda (B_\lambda(T) - I_\lambda) \quad (3)$$

$$LST = (BT/(1 + (W * BT / 1.4388) * Ln(\varepsilon))) \quad (4)$$

These are the formulas used to estimate the Land Surface Temperature.

TOA Brightness Temperature

The ratio of incident solar radiation to reflected solar radiation on a particular surface is measured using the dimensionless TOA Reflectance metric measurement. It can be calculated with satellite-measured spectral radiance by utilizing the solar zenith angle and mean solar spectral irradiance. Equation (5) is used to estimate the brightness temperature.

$$T_{br} = \frac{K_2}{\ln\left(\frac{K_1}{L_\lambda} + 1\right)} \quad (5)$$

NDVI (Normalized Difference Vegetation Index)

The greenness of vegetation is measured using the (NDVI) scale, which is also helpful in identifying

changes in ecosystem life and vegetation density. Additionally, the photosynthetic activity in a planting region can be represented by the NDVI value. Readings from the red and near-infrared bands are used to calculate the NDVI and is shown in equation (6).

$$NDVI = \frac{NIR - RED}{NIR + RED} \qquad (6)$$

The NDVI value can be estimated with the help of LANDSAT 7 and Landsat 8 satellite images by using the above formula. The Normalized Difference Vegetation Index (NDVI) is a metric used to track the expansion of vegetation in a specific remote sensing area. The possible values of the index are +1 to 1. This index parameter can be used to calculate the Land Surface emissivity. Three categories for NDVI index values were identified. The region is made up of bare soil if the vegetation value is less than 0.2. The area has a mix of bare soil and vegetation if the index falls between 0.2 and 0.5. The area is high if the index is higher than 0.5.

Emissivity

Even though Land Surface Emissivity (LSE), an intrinsic property of natural materials, varies with surface roughness and observation angle, it is often employed as a material composition indicator, especially for silicate minerals. Therefore, the analysis of soil erosion and development, vegetation density, and changes in land surface area are all vital tasks performed by LSE. The land surface emissivity is caused by the homogenous isothermal surfaces. Conversely, natural surfaces that are visible from space are usually diverse, particularly in cases when spatial resolution is constrained. Estimating the isothermal pixel from low spatial resolution photos is challenging.

The only surfaces that are unambiguously classified as LST are homogenous surfaces at thermal equilibrium. When the spatial pictures are gathered from the rough surface, the emissivity value increases. In addition to being gathered at the same temperature, the surface and black body radiance are distinct factors that are useful in determining the emissivity. The vegetation density can be used to measure the land surface emissivity using equation(7).

$$\varepsilon = 0.004 * Pv + 0.986 \qquad (7)$$

Water Vapour

One of the key components for determining changes in global hydrological cycles and climatic conditions is atmospheric water vapor. The only way to recover water vapor at the regional and global levels is through remote sensing. Four different types of techniques exist for calculating water vapor from remote sensing data, according to recent studies. The various techniques used to extract the water vapor characteristic from the atmosphere are thermal infrared, hyperspectral, near-infrared, and microwave. The split-window covariance-variance ratio approach was used by Liu et al.[7] and Labbi et al.[5] for determining the water vapor. It is possible to compute this water vapor characteristic by applying the split-window covariance-variance ratio approach. Equation (8) and (9) demonstrates how water vaper characteristics are computed.

$$\text{Water vapour} = a + b \bullet \tau_i / \tau_j \qquad (8)$$

$$\tau_i / \tau_j \approx R_{ji} = \frac{\sum_{k=1}^{N} (T_{i,k} - \overline{T_i})}{\sum_{k=1}^{N} (T_{i,k} - \overline{T_i})^2} \qquad (9)$$

Table 1 Features gathered from 20 distinct Landsat datasets

Input Data	Intensity	Reflectance	LST (K)	TOA Brightness Temperature (K)	NDVI	Water vapour (g/cm²)
T1	177	0.644	363	339	0.198	1.783
T2	168	0.721	362	346	0.236	1.704
T3	128	0.334	269	257	0.336	2.841
T4	179	0.637	375	392	0.167	1.362
T5	135	0.315	263	267	0.289	2.169

T6	162	0.678	360	359	0.168	1.171
T7	156	0.336	218	228	0.348	3.911
T8	148	0.253	177	176	0.37	4.083
T9	167	0.347	241	240	0.278	3.221
T10	183	0.739	327	327	0.223	1.974
T11	138	0.672	353	349	0.186	1.687
T12	149	0.329	284	282	0.332	2.248
T13	119	0.424	295	291	0.328	2.331
T14	129	0.332	245	242	0.322	3.469
T15	144	0.639	357	364	0.148	1.14
T16	143	0.249	183	187	0.383	4.046
T17	170	0.362	237	240	0.254	3.177
T18	178	0.724	338	336	0.217	1.982
T19	123	0.32	273	269	0.327	2.316
T20	136	0.664	349	346	0.176	1.674

The numerous features that were taken from distinct Landsat sceneries are displayed in Table 1. The forest fire can be located with the use of gathered features.

Threshold based Approach

Using the features that were retrieved, the forest fire region can be located in this phase. The two distinct methods used in the statistical technique to determine the forest fire region are change detection and threshold limit. There are a lot of false alarms generated by threshold approaches. The change detection approach suggests that abrupt changes in day and nighttime temperatures could occur. A predetermined threshold value is utilized in threshold-based detection to forecast the fire region. However, it is not possible to set the threshold value for different geographic areas. For distinct fire regions, one can alter the temperature, water vapor, intensity, reflectance, and NDVI values. In order to accurately predict the zone of a forest fire, changes in the features are identified. This will increase the accuracy of detecting forest fires and decrease false alarms. The past samples for that specific region were gathered, and the features had to be examined, in order to determine the forest fire region.

The different features in this suggested methodology are intensity, spectral radiance, Land Surface Emissivity, NDVI, TOA temperature, Land Surface temperature, and water vapour. The dataset obtained may also be used to calculate variations at different times. A fire region develops when the variation in land surface temperature rises above a predetermined threshold and temperature value and is calculated using equation (10).

$$\Delta T_{lst} = T_{lst} - T_{lst'} \qquad (10)$$

where ΔT denotes the temperature variance and TLST and TLST' stand for the current and historical land surface temperatures for that particular region. In case the temperature meets the specified limitations, the pixel might be classified as a hot spot using the equation (11).

$$\left. \begin{array}{l} T_{LST} > 285 \text{ K and} \\ \Delta T_{LST} > 10 \text{ K} \end{array} \right\} \qquad (11)$$

Similarly, one can estimate the values of water vapor, reflectance, NDVI, and variation intensity.

Table 2. Actual temperature at various time intervals
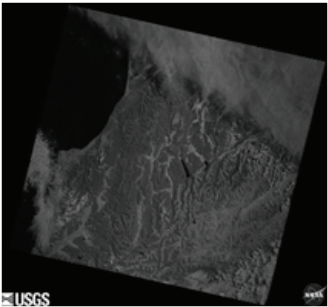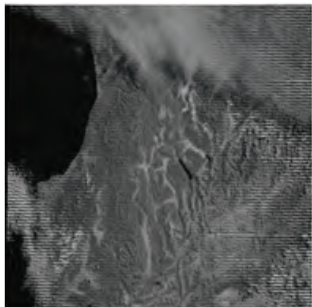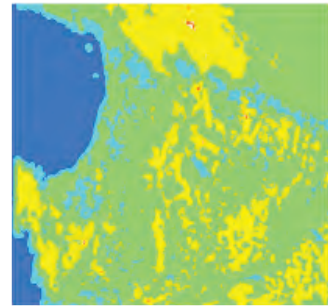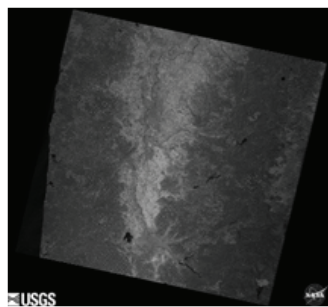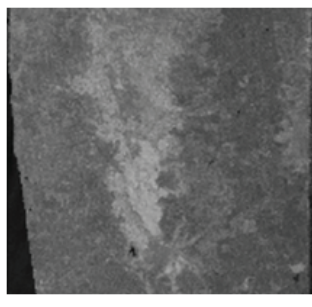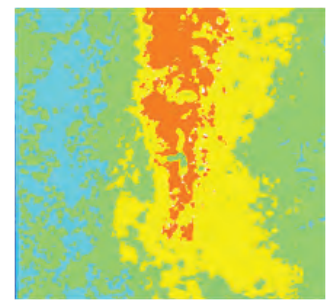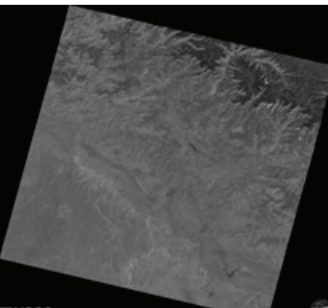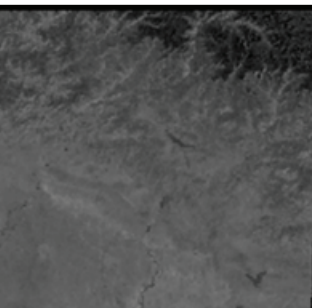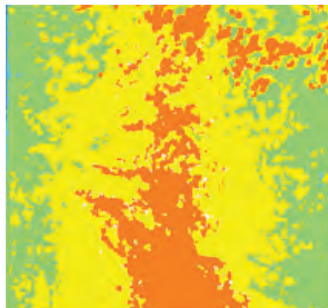
Dataset	T_{LST}	T_{LST}'	T_B	T'_B
T1	363	350	351	339
T2	362	347	346	332
T3	269	266	257	253
T4	375	368	392	378
T5	263	260	267	265
T6	360	343	359	343
T7	218	217	228	224
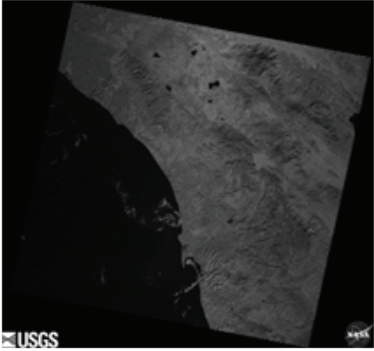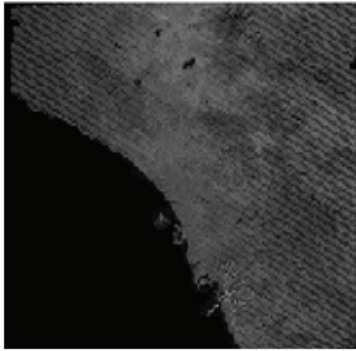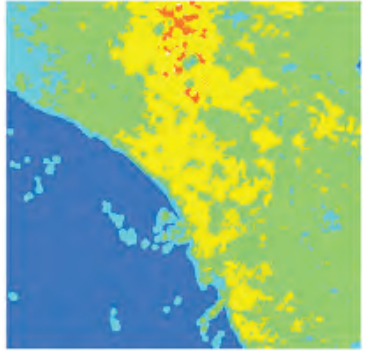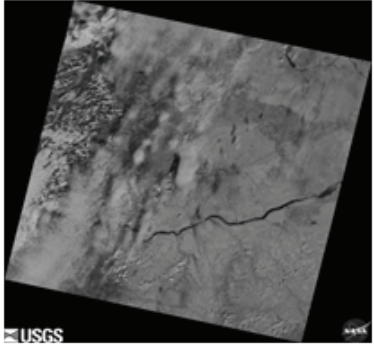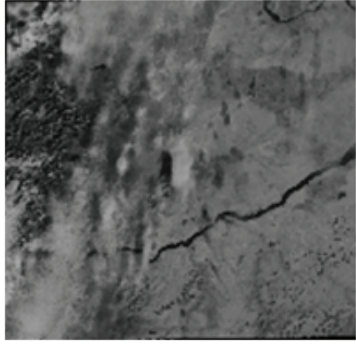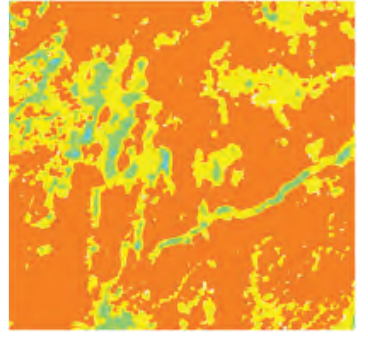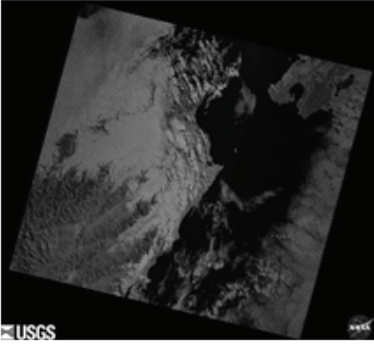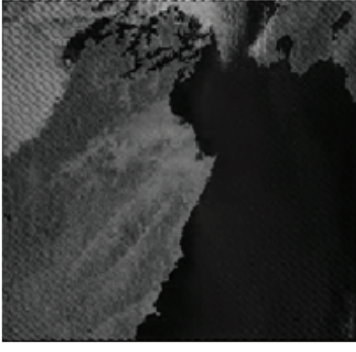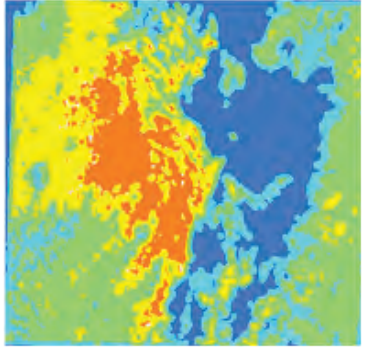
T8	177	175	176	173
T9	241	238	240	234
T10	327	313	327	314
T11	353	339	349	332
T12	284	273	282	271
T13	295	289	291	286
T14	245	238	242	236
T15	357	335	364	343
T16	183	179	187	183
T17	237	234	240	232
T18	338	332	336	331
T19	273	267	269	264
T20	349	328	346	329

The variance and the actual temperature values are displayed in Table 2. To identify the fire pixel, fluctuations in reflectance, NDVI, water vapor, and other characteristics' intensities are also noted. This statistical method uses a fixed threshold and accounts for feature variation to identify fire pixels. The proposed approach will be applied to differentiate pixels that are on fire from those that are not.

You can obtain the original datasets from the USGS website. The gathered datasets undergo preprocessing and are divided into segments in order to extract features. Following segmentation, the sea area is determined, and the remaining regions are used to extract features.

Table 3 Downloaded, preprocessed and segmented dataset

Input	Downloaded	Preprocessed	Segmented
T1			
T2			
T3			

T4			
T5			
T6			

The pre-processed, segmented, and original dataset that was gathered from various regions are displayed in Table 3.5 above.
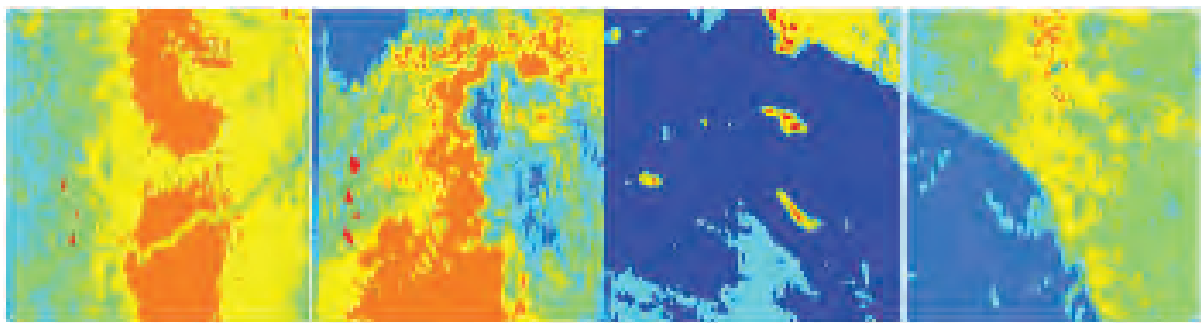
Figure. 3 Fire Detected area

The red pixels in Figure 3 represent fire. Every pixel has a dimension of 30 by 30. This suggested method lowers the rate of missed pixels and false alarms. The following equation presents three distinct measurements that are used to quantify the proposed methodology with human segmentation. Equation (12)-(14) specifies the computation of recall, precision and accuracy measure.

$$Recall = \frac{TruePositive}{TruePositive + FalseNegative} \quad (12)$$

$$Precision = \frac{TruePositive}{TruePositive - FalsePositive} \quad (13)$$

$$Accuracy = \frac{TruePositive + TrueNegative}{TruePositive + FalsePositive + FalseNegative + TrueNegative} \quad (14)$$

Table 4 Performance measures of various fire detection algorithms

Dataset	Proposed Work			Existing Work 1			Existing Work 2		
	Recall	Precision	Accuracy	Recall	Precision	Accuracy	Recall	Precision	Accuracy
T1	97.8	98.25	98	97.05	98	97.85	96.26	97.37	97.05
T2	98.22	96.13	98.7	98.13	96.05	98.47	97.77	95.62	97.53
T3	96.75	94.17	98.17	96.72	93.77	98.04	96.11	92	97.47
T4	98.82	99	98.61	98.51	98.84	98.42	98.16	97.53	97.77
T5	96.93	97.67	98.71	96.81	97.33	98.59	96.45	96.71	98.16
T6	98.01	96.2	98.73	97.89	96.15	98.51	97.57	95.65	98.15
T7	99.14	99.39	99.64	99.01	99.29	98.42	98.47	98.27	97.8
T8	97.67	98.66	98.22	97.24	98.44	98.05	97	97.44	97.37
T9	98.22	97.53	98.35	98.15	97.26	98.06	97.74	96.56	97.45
T10	97.33	98.79	98.77	97.04	98.63	98.65	96.66	98.13	98.11
T11	98.66	98.17	98.55	98.41	98.06	98.37	98	97.47	97.15
T12	99.2	99.03	99.33	99.07	98.89	99.2	98.26	98.2	98.24
T13	98.16	98.19	98.75	97.94	98.05	98.57	97.42	97.51	98.06
T14	96.89	98.11	98.2	96.8	97.99	98.15	96.26	97.69	97.45
T15	98.6	98.04	98.6	98.44	97.9	98.51	97.67	97.52	97.51
T16	96.14	97.71	98.33	96.05	97.62	98.16	95.56	97.14	97.37
T17	98.52	98.2	99.4	98.47	98.14	99.31	98.22	97.8	98.64
T18	99.06	99.41	99.17	99.03	99.35	97.99	98.15	98.66	97.37
T19	98.09	98.65	98.77	98.06	98.47	98.4	97.24	97.87	97.67
T20	95.91	98.72	99.2	95.87	98.47	98.77	94.17	97.71	96.91
Overall	97.91	98	98.71	97.73	97.84	98.42	97.16	97.14	97.66

Table 4 displays the results of the performance metrics over 20 distinct datasets. The performance metrics of different fire detection algorithms are displayed in Table 4. The suggested strategy is intended to increase accuracy, with average recall of 98.03 percent, average precision of 98.12%, and average accuracy of 98.83%. Figure 4 displays the performance metrics of different fire detection methods.
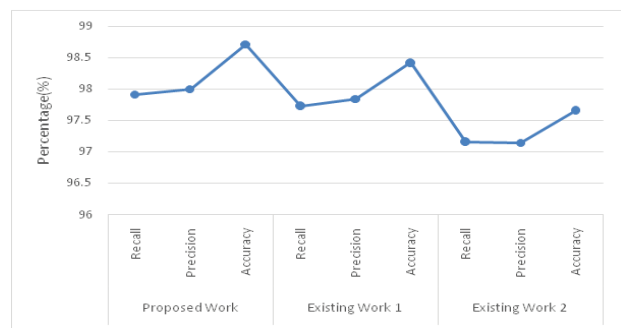
Figure. 4 Evaluation metrics for different fire detecting algorithms

Comparing the suggested approach to several fire detection algorithms, it is evident from Figure 4 that it is effective in identifying forest fires.The suggested approach to detecting forest fires based on temperature and reflectance threshold values is contrasted with two cutting-edge techniques, SFIDE and Hot Target Detection Algorithm(HTDA), in Table 5.Figure 5demonstrates that comparison of the performance metrics of proposed work with existing two state-of-the art methods in terms of F1 score and Commission error. The F1 score is the balanced average of recall and precision, where recall is the capacity to locate all positive instances and precision is the correctness of the positive predictions. Recall determines the forecast of all true flames, whereas precision determines the accuracy of the accurately identified fires among all detected fires. False positives and false negatives are balanced by the F1 score. When there is an imbalance in the class distribution, such as when detecting forest fires, the F1 measure is employed. False positives, or situations in which a non-fire incident is mistakenly categorized as a fire, are referred to as commission errors. It measures the rate of false alerts directly. It is essential for detecting forest fires since false alarms might result in needless expenditure and resource deployment. Figure 5 in comparison to state-of-the-art methods, which yield 97.35% F1 score with 7.32% commission error and 97.87% F1 score with 8.65% commission error, respectively, it demonstrates that the proposed work has an average F1 score of 98.23% with a commission error of 5.38. This demonstrates how the proposed work strikes a compromise between fewer false alarms and false positives and negatives.

Table 5: Comparison based on F1-Score and Commission Errors

Methods	F1-Score (%)	Commission Error (%)
Proposed Work	98.23	5.38
SIFDE	97.35	7.32
HTDA	97.87	8.65
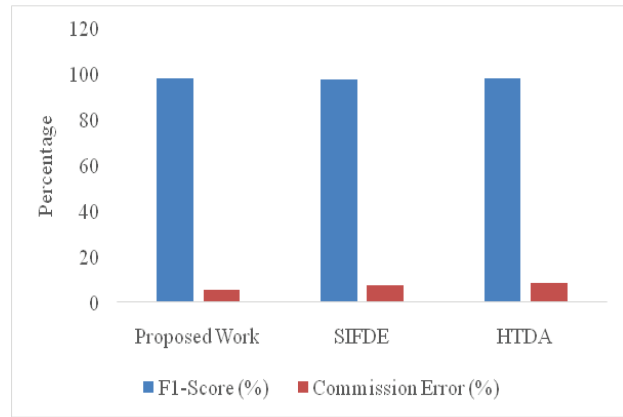
Figure 5 Comparison chart based on F1-Score and Commission Errors

CONCLUSION

This study suggests utilizing statistical methods to monitor and identify forest fires using Landsat imagery. When compared to other existing algorithms, the statistically based approach that has been developed produces superior accuracy and a lower false rate. The outcome reveals that the accuracy average over 20 datasets is 98.71%. A method for optimization can also be employed to boost fire detection performance in the future.

REFERENCES

1. Bruna E Z Leal, Andre R Hirakawa &Thiago D Pereira, "Onboard fuzzy logic approach to active fire detection in Brazilian amazon forest", IEEE Transactions on Aerospace and Electronic Systems, 2016, vol. 52, no.2, pp. 883 – 890.

2. Chander G & Markham B, "Revised Landsat-5 TM radiometric calibration procedures and post calibration dynamic ranges", IEEE Transactions on Geoscience and Remote Sensing, 2003, pp. 2674–2677.

3. Krishnendu Banerjee, Surajit Panda, Manish Kumar Jain, AT Jeyaseelan & Ratnesh Kr Sharma, "Comparison of Aster Thermal Bands and feature Identification using Advance Spectroscopic Techniques", International Journal of Innovation and Scientific Research, 2014, vol. 7, no. 1, pp. 11-18.

4. Kumar SS, "Global operational land imager Landsat-8 reflectance-based active fire detection algorithm", International Journal of Digital Earth, 2018, vol. 11, no.2, pp. 154-178.

5.   LabbiA&Mokhnache, "A Estimating of total atmospheric water vapor content from MSG1-SEVIRI observations", Atmos. Meas. Tech. Discuss, 2015, vol. 8, pp. 8903–8923.

6.   Lasaponara R, Cuomo V, Macchiato MF &Simoniello T, 'A self-adaptive algorithm based on AVHRR multitemporal data analysis for small active fire detection', International Journal of Remote Sensing, 2003, vol. 24, no. 8, pp. 1723-1749.

7.   Liu HL and Tang SH, "An improved physical split-window algorithm for precipitable water vapor retrieval exploiting the water vapor channel observations', Remote Sensing Environment, 2017, vol.194, pp.366–378.

8.   Moreira, "A tutorial on synthetic aperture radar", IEEE Geoscience and Remote Sensing Magazine, 2013, vol. 1, no. 1, pp. 6–43.

9.   ZixiXie, Weiguo Song, Rui Ba, Xiaolian Li&Long Xia, "A Spatiotemporal Contextual Model for Forest Fire Detection Using Himawari-8 Satellite Data", Remote Sensing, 2018, vol.10, no.12, pp 1-24.

Unleashing the Potential of Ethereum Blockchain for Secure Healthcare Record Management

P. G. Naik
Professor
✉ pgnaik@siberindia.edu.in

R. S. Kamath
Associate Professor
✉ rskamath@siberindia.edu.in

S. S. Jamsandekar
Assistant Professor
✉ ssjamsandekar@siberindia.edu.in

School of Computer Science and Applications
CSIBER
Kolhapur, Maharashtra

ABSTRACT

In the contemporary digital landscape, the healthcare sector is profoundly impacted by information technology, with an expansive array of sources for the creation and access of patient health data. The imperative of secure data management cannot be overstated. Among cutting-edge technologies, blockchain emerges as a transformative solution for ensuring the secure storage of data. In recent research endeavours, the authors have introduced a smart contract designed to proficiently store and manage patients' medical records. This smart contract encompasses functionalities to initiate a new record, authorize a newly generated record, and retrieve information from the records. The implementation of this smart contract was carried out and rigorously tested on the Ethereum Blockchain framework. The current research aims to shed light on the pivotal role played by blockchain technology, particularly within the Ethereum framework, in ensuring the security and integrity of record keeping in healthcare. The focus is on demonstrating how blockchain can significantly enhance the confidentiality and reliability of patient medical records, showcasing its potential as a robust solution for maintaining sensitive health data in a secure and decentralized manner.

KEYWORDS : Blockchain security, Confidentiality in healthcare, Ethereum framework, Ganache, MetaMask, Smart contract, Patient record management.

INTRODUCTION

Blockchain has evolved as a disruptive technology which has penetrated almost all the sectors such as banking, insurance, finance, education, manufacturing, supplychain, agriculture, real estate to name a few and healthcare is not an exception[1, 2]. Ethereum has emerged as a leading blockchain development platform, gaining widespread acceptance due to its innovative features. At the forefront of its contributions is the introduction of smart contracts, a groundbreaking concept that entails a set of instructions dictating the flow of business operations within the blockchain network. What sets Ethereum apart is its utilization of the Ethereum Virtual Machine (EVM), a virtual computing environment specifically designed to execute and validate smart contracts. The EVM acts as a decentralized runtime environment, enabling developers to deploy and run code on the Ethereum blockchain. This not only facilitates the automation of complex processes but also ensures transparency and security through the decentralized nature of blockchain technology[3, 4]. By incorporating the EVM, Ethereum has established itself as a comprehensive and versatile platform for creating decentralized applications (DApps) that extend beyond simple transactions. It has catalyzed a paradigm shift in how various industries approach digital processes, offering a robust foundation for the development of sophisticated applications that can revolutionize sectors such as finance, supply chain, and more. In essence, Ethereum's innovative use of smart contracts and the Ethereum Virtual Machine has positioned it as a pioneer, opening up new possibilities for decentralized, transparent, and secure applications across a spectrum of industries. Its impact extends

far beyond being a mere cryptocurrency platform, showcasing the transformative potential of blockchain technology.

Transitioning from a traditional development platform to a blockchain platform represents a paradigm shift for all stakeholders, including developers, testers, and end-users. This process necessitates a significant change in developers' mindset, requiring optimization of code (as transacting data on the blockchain involves incurring costs denominated in ETH), adjusting approaches to application deployment, and redefining interactions with the application. Shifting to a blockchain platform from a traditional one essentially entails moving from a centralized to a decentralized system, from an untrusted to a trusted system, from an insecure to a secure system, and from a non-reliable to a reliable system. Collectively, these transformations offer an ideal platform for the healthcare domain.

Few advantages offered by decentralized peer-to-peer system in the healthcare section are enumerated below:

- Accessibility and Inclusivity
- Cost-Efficiency
- Redundancy and Reliability
- Scalability
- Customization and Personalization
- Collaboration and Community Building
- Security and Privacy

Relative Comparison of Traditional Application Architecture and Blockchain Application Architecture

Blockchain applications present a paradigm shift from traditional centralized systems, adopting decentralized infrastructure, distributed ledgers, and smart contracts. They leverage consensus algorithms, cryptography, and shared ownership for enhanced security and resilience, although scalability remains a prime consideration. Table 1 presents the relative comparison between the traditional application and the corresponding blockchain-based application.

Table 1. Traditional Application Vs. Blockchain Application

Aspect	Traditional Application	Blockchain Application
Infrastructure	Centralized server-hosted infrastructure	Decentralized peer-to-peer network
Data Storage	Centralized databases with predefined schemas	Decentralized distributed ledger (Blockchain)
Application Logic	Centralized server executes business logic	Smart contracts deployed on the blockchain which is replicated on each peer
Data Access	Client-server model	Peer-to-peer network communication
Consensus Mechanism	Not applicable (Relies on centralized authority)	Consensus algorithms (Proof of Work/ Stake, Proof of Authority etc.)
Security	Relies on server-side security measures	Cryptography-based security, decentralization, immutability
Transaction Handling	Centralized processing	Distributed and immutable transaction records
Ownership/ Control	Controlled by central authority	Shared ownership and control among network participants
Redundancy	Limited redundancy	High redundancy due to distributed ledger and nodes
Scalability	Scalability challenges with increased load	Scalability concerns but potential for improved scaling

Blockchain Challenges and Proposed Solutions.

The challenges outlined in Table 2 encompass various facets of deploying on the blockchain, from deployment costs and infrastructure setup to scalability issues and

user acceptance. Each challenge necessitates specific solutions, such as code optimization, partial deployment on IPFS, corporate test networks, layer 2 architecture, and the adoption of user-friendly technologies like React.js or Angular.js. Addressing these challenges collectively contributes to a more robust and accessible blockchain implementation.

Table 2. Blockchain Challenges and Proposed Solutions

Aspect	Challenge	Solution Proposed
Deployment Cost	Deploying data and smart contract on Blockchain incurs cost in terms of Ethers	Code Optimization Partial Deployment on IPFS server
Infrastructure Setup	Mainnet demands real ETH which is extremely costly. Public networks grant limited fake ETH (faucet)	Implementation of corporate test network using Geth (Go Ethereum) Implementing institute level crypto currency (does not bear any relevance in the public domain)
Scalability	As no of nodes increase mining the block and execution of transactions exponentially increases.	Resorting to layer 2 architecture.
UI and UX	Designing user-friendly UI and UX	Using React.js or Angular.js as presentation tier technologies for designing UI.
End User Acceptance	Customer base does not bear adequate skills to operate the system.	Upskilling the users by providing adequate training in using MetaMask and authentication using Ethereum addresses as credentials instead of a pair of username and password.,

Comparison Between Existing and Proposed Techniques

Existing healthcare data management systems typically rely on centralized databases, which are vulnerable to cyberattacks, data breaches, and single points of failure, often resulting in compromised data integrity and availability. In contrast, blockchain-based systems enhance security through advanced cryptographic techniques, ensure data integrity with immutable records, validate transactions via decentralized consensus mechanisms, and maintain continuous data access through a distributed architecture. These features collectively offer superior reliability, transparency, and patient control over data compared to traditional centralized methods which are vital to the healthcare system.

LITERATURE REVIEW

The authors extensively referenced reputable journal articles to evaluate the potential of the Ethereum blockchain framework. In his white paper, Buterin [6] concluded by highlighting numerous advanced features of the Ethereum blockchain that hold applicability across diverse verticals. According to Buterin, the Ethereum protocol extends beyond being merely a currency; it possesses the capability to be employed across various domains. Specifically, the authors believe that Ethereum protocols can be effectively utilized for decentralized file storage, fostering transparency among peers.

In a study by Ashizawa et al. [5], a unique analysis tool named Eth2Vec was introduced for investigating vulnerabilities. Eth2Vec utilizes Natural Language Processing based on Neural Networks, providing a novel approach to vulnerability assessment in the Ethereum blockchain.

Laneve and Coen [8] elucidated strategies for smart contract balance updates post digital transactions. Their article provides insights into parameters influencing the balance of smart contracts, offering valuable information on maintaining transactional equilibrium.

In the work of Yu et al. [9], a reliable clustering scheme for Ethereum transactions was proposed. The authors introduced a methodology involving the deployment of a probe to connect to specific nearby nodes, creating a fixed-dimensional representation for each transaction.

Additionally, they trained a classifier to recognize homologous transaction pairings by examining the network features of these transactions.

Addressing the considerations for adopting a blockchain initiative, Lewis Laidin et al. [10] delved into various parameters. Their comprehensive discussion covered aspects such as Blockchain data audit, scalability, societal elements, regulation, governance, security, privacy, market need, feasibility, and implementation. This framework provided a thorough understanding of the multifaceted considerations essential before embarking on a blockchain initiative.

Research Gaps

The research gaps or areas requiring further investigation in blockchain-integrated systems for educational settings include:

- Scalability and Usability issues
- Privacy and Security in Local Blockchain Approaches
- Interoperability Issues

Research Methodology

Research Objectives

The present study concentrated on achieving the following objectives to create an Ethereum smart contract with a comprehensive set of functionalities, including:

- Secure storage of patient records to ensure confidentiality and integrity.

- Implementation of role-based access controls to govern the creation, signing, and reading of records, thereby maintaining strict authorization protocols.

- Integration of cryptographic mechanisms to enhance the security of patient data.

- Establishment of an efficient and transparent workflow for managing patient records within the blockchain.

- Exploration of gas optimization techniques to enhance the cost-effectiveness of smart contract execution.

- Implementation of audit trails to track and verify changes made to patient records, ensuring transparency and accountability in the system.

- Research on potential scalability solutions within the Ethereum ecosystem for accommodating a growing volume of patient records.

Phases of Research Work

The research was carried out in the following phases. These phases collectively form a systematic approach to adopting blockchain for securing patient records, ensuring that each step is carefully executed to achieve a robust and reliable solution.

Phase 1: Investigation of inherent Properties of Blockchain

In this initial phase, researchers explored the fundamental properties of blockchain technology. This involves a comprehensive examination of the decentralized and distributed nature of blockchain, its immutability, consensus mechanisms, cryptographic principles, and the overall architecture. The objective is to lay a robust groundwork of understanding regarding the fundamental operations of blockchain. This is essential as the application is constructed on top of existing blockchain technology.

Phase 2: Suitability of Blockchain to secure patient record management

Having built on the understanding gained in the first phase, the focus shifted to assessing whether blockchain is a suitable technology for securing patient records. This involved analyzing the specific requirements of managing healthcare data, such as confidentiality, integrity, accessibility, and traceability. Considerations included the potential advantages of decentralization and cryptographic security in protecting sensitive patient information.

Phase 3: Feasibility Study

Once it was determined that blockchain is potentially suitable for securing patient records, a feasibility study was conducted. This phase involved evaluating the practicality and viability of implementing a blockchain solution in the healthcare context. Factors such as cost, technical feasibility, regulatory compliance, and

interoperability with existing systems were carefully examined. The goal was to identify any challenges or obstacles that might arise during the implementation process.

Phase 4: Model Design

With the feasibility study having provided a positive outlook, the model design phase commenced. In this stage, the researchers created a detailed plan for the implementation of the blockchain solution. This involved designing the data structure, defining smart contracts, specifying consensus mechanisms, and outlining the overall architecture of the system. The design was meticulously crafted to align with the specific requirements identified in the suitability assessment.

Different models were proposed based on the level of complexity and cost as prime parameters. These models aimed to offer various options tailored to different

requirements, taking into consideration the intricacy of the system and the financial resources available. The proposals were designed to provide flexibility, allowing stakeholders to choose a model that best aligns with their specific needs, whether prioritizing a streamlined, cost-effective solution or a more intricate and feature-rich implementation.

A total of six models have been proposed, taking into consideration both technical competency and cost considerations. Each model is tailored to different proficiency levels and resource requirements, ensuring a comprehensive range of options that balance technical expertise with financial considerations. Table 3. provides an overview of each model's competency level, required skills, development, testing, and deployment platforms, libraries, front-end technologies, and the associated cryptocurrencies.

Table 3. Relative Comparison Between Different Blockchain Cost Models

Model	Competency Level	Skills Required	Development Platform	Testing Platform	Deployment Platform	Libraries	Front End	Crypto Currency
1	Basic	Blockchain, Solidity, Remix IDE	Remix IDE	Remix IDE	Ethereum Virtual Machine			ETH
2	Basic	Blockchain, Solidity, Remix IDE, Ganache, MetaMask	Remix IDE	Remix IDE	Ganache, MetaMask			ETH
3	Basic	Blockchain, Solidity, Ganache, MetaMask, Hardhat, Truffle, Mocha	Hardhat / Truffle	Mocha / Hardhat Waffle	Ganache, MetaMask			ETH
4	Intermediate	Blockchain, Solidity, Remix IDE, Ganache, MetaMask, Hardhat, Truffle, Mocha, Infura/ Alchemy	Hardhat / Truffle	Mocha / Hardhat Waffle	Injected Web Using MetaMask, Public Test Networks (Goerli, Linea Goerli)), Infura / Alchemy			Goerli ETH, Linea Goerli ETH

5	Advanced	Blockchain, Solidity, Remix IDE, Ganache, MetaMask, Hardhat, Truffle, Mocha, Infura/ Alchemy, web3. js, React.js	Hardhat / Truffle	Mocha / Hardhat Waffle		Web3.js / Ether.js	React.js / Angular.js	Goerli ETH, Linea GoerliETH
6	Advanced	Blockchain, Solidity, Remix IDE, Ganache, MetaMask, Hardhat, Truffle, Mocha, Infura/ Alchemy, web3. js, React.js, Geth	Hardhat / Truffle	Mocha / Hardhat Waffle	Private Corporate Test Network (Geth),	Web3.js / Ether.js	React.js / Angular.js	Custom Crypto Currency

Phase 5: Model Implementation

After the model was designed and thoroughly reviewed, the actual implementation of the blockchain solution began. This phase involved coding the smart contracts, configuring the nodes in the network, and integrating the blockchain system with existing healthcare infrastructure. Attention was given to ensuring that the implementation aligned with the design and met the identified requirements for securing patient records.

Phase 6: Model Testing

Once the implementation was complete, rigorous testing was conducted to verify the functionality, security, and performance of the blockchain-based patient record management system. This included unit testing, integration testing, and simulation of real-world scenarios to identify and address any potential issues. Testing ensured that the system operated as intended, effectively secured patient records, and was ready for deployment in a healthcare environment.

System Design

Layered Software Architecture

The extended layer architecture of blockchain technology encompasses multiple layers beyond the foundational blockchain layer as depicted in Fig. 1 These include the networking layer for efficient communication, consensus layer managing agreement mechanisms, a smart contract layer for executing coded contracts, a privacy layer ensuring transaction confidentiality, a scaling layer addressing scalability concerns, and an interoperability layer facilitating communication between different blockchain networks. This multi-layered approach aims to optimize various functionalities and enhance the overall flexibility and scalability of blockchain systems.
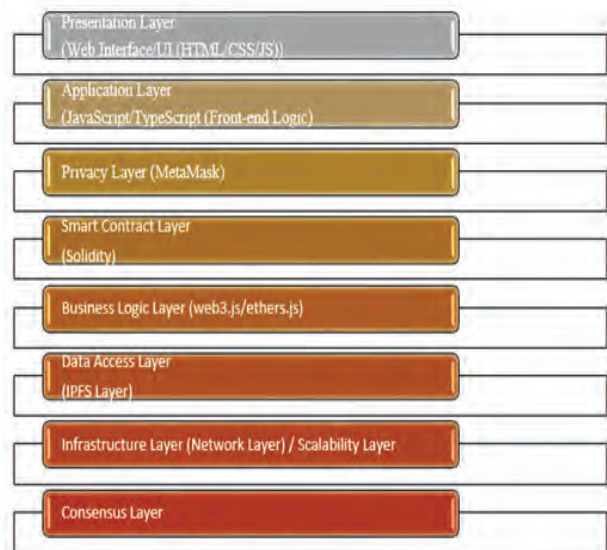
Fig. 1. Extended Multi-tier Blockchain Architecture

Blockchain Tools Employed During the System Implementation

The different tools employed during the system implementation are depicted in Table 4.These tools collectively support various aspects of the blockchain development lifecycle, from coding and testing to deployment and user interaction.

Table 4. Blockchain Tools Employed in the System Implementation

Tool	Purpose
Remix IDE	Web-based integrated development environment (IDE) for smart contract development and testing on the Ethereum blockchain.
Ganache	Personal blockchain emulator that allows local development and testing of Ethereum-based applications without the need for a live network.
MetaMask	Browser extension wallet that enables users to interact with Ethereum-based decentralized applications (DApps) directly from their web browser.
Truffle	Development framework that simplifies the process of building, testing, and deploying Ethereum-based smart contracts and applications.
Mocha	JavaScript testing framework used for testing smart contracts and ensuring their functionality and reliability.
Linea Goerli	Testnet in the Ethereum ecosystem, providing a simulated environment for developers to deploy and test smart contracts without using real Ether.
Infura	Scalable and reliable Ethereum node infrastructure that allows developers to connect to the Ethereum network without running their own node.
web3.js	JavaScript library that provides a convenient interface for interacting with Ethereum smart contracts and the Ethereum blockchain.
React.js	JavaScript library for building user interfaces. Often used in the context of blockchain development to create front-end interfaces for decentralized applications (DApps).
Pinata Cloud Service	Cloud service for IPFS (InterPlanetary File System) that allows users to easily store and retrieve data on the decentralized web, often used for file storage.

Sequential System Workflow

Fig. 2 illustrates the sequence of tasks initiated at the onset of the system implementation process.
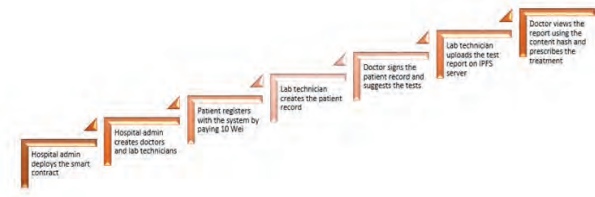
Fig. 2. Sequential System Workflow in Decentralized Application

System Validations

The following validations underscore the role-based access control and validation mechanisms that maintain the system's security, trustworthiness, and privacy standards.

- Exclusive Admin Privilege: The creation of doctor and lab technician accounts is a privilege reserved exclusively for the hospital administrator, ensuring controlled access to the system's medical professionals.

- Patient Record Authorization: Only registered patients are granted the ability to create and have their medical records added to the blockchain, enhancing security and data authenticity.

- Doctor's Signature Authority: The power to sign medical records is vested solely in doctors, reinforcing the integrity and credibility of the patient's healthcare data.

- Lab Report Authorization: Only authorized lab technicians are permitted to upload medical reports, guaranteeing that only qualified personnel contribute essential data to the system.

- Selective Blockchain Entry: Blocks containing signed medical records are the sole entries permitted onto the blockchain, preserving the sanctity of the distributed ledger.

- Patient-Exclusive Access: Patients are granted access to view their individual medical records exclusively, respecting privacy and confidentiality.

- Doctor-Exclusive Report Access: The ability to access and review lab reports is limited to doctors, ensuring that only healthcare professionals can access sensitive diagnostic data.

SYSTEM IMPLEMENTATION

The current research portrays the development and testing of the Ethereum smart contract which is further divided into the following sections:

Section I → Outlining the Structure of a Smart Contract

Section II → Developing and Deploying the Ethereum Smart Contract

Section III → Testing HealthCare smart contract

Outline of Smart Contract Structure: In this section, the authors offer a comprehensive overview of the structural design employed in the smart contract.

Creation and Deployment of the Ethereum Smart Contract: This section details the process of developing and deploying the Ethereum smart contract, which was executed on various testing platforms.

Evaluation of the Healthcare Smart Contract: Within this section, the comprehensive testing and assessment of the healthcare-focused smart contract are provided.

Outlining the Structure of Smart Contract

In contemporary research, the development process leverages the Remix Online Integrated Development Environment (IDE). The smart contract is meticulously crafted within the Ethereum framework, utilizing the Solidity language. Solidity, distinguished as a high-level, object-oriented programming language, is expressly tailored for the purpose of developing Ethereum smart contracts.

A smart contract named 'HealthCare' manages patient records, encompassing the fields outlined in Table 5.

Table 5. Healthcare Record Structure

Field Name	Data Type
ID	uint256
price	uint256
signaturecount	uint256
testname	string
Date	string
pAddr	Address
hospitalname	String

Fig. 3 depicts the structure of HealthCare smart contract.

Fig. 3. Structure of HealthCare Smart Contract

This patient record structure encompasses essential information related to a patient's medical history, including identification, financial aspects, medical tests, dates, and healthcare providers. It can be used within a smart contract on the Ethereum blockchain to securely and transparently manage patient records.

Developing and Deploying the Ethereum Smart Contract

During the development of a healthcare smart contract, the following methods are employed to achieve the intended objectives.

1. newRecord () → This method generates a new record to be incorporated into the blockchain.

2. signRecord () → This method is employed to sign the recently generated record.

3. _records ()   → This method is utilized to retrieve health records, and access is restricted to the record owner. If any other node attempts to access the record, a null record will be retrieved.

4. signOnly () → This employs a specialized type of Solidity method known as a modifier, designed to alter the behavior of other functions. It verifies a specific condition before permitting the execution of a function. Within the HealthCare contract, the signOnly modifier is applied to ensure that record

signing is exclusively permitted by lab_admin or hospital_admin. Upon signing, the authenticated record block is added to the blockchain, establishing a permanent and immutable record. If any other node attempts to sign the record without sufficient balance, the record signing process will not be initiated. Fig. 4 depicts the design of smart contract in Solidity in Remix IDE.
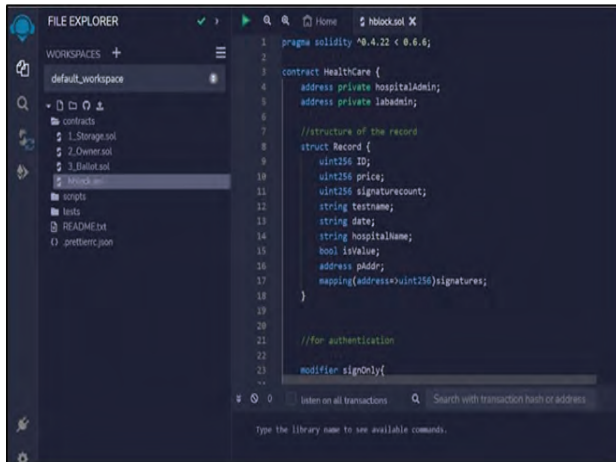
Fig. 4. Design and Development of Solidity Smart Contract

In the initial phases of research Ganache was selected as a deployment environment which is the personalized blockchain employing Proof of Authority (PoA) as its consensus algorithm [7]. Fig. 5 demonstrates selection of Ganache provider as the deployment environment inRemix IDE.
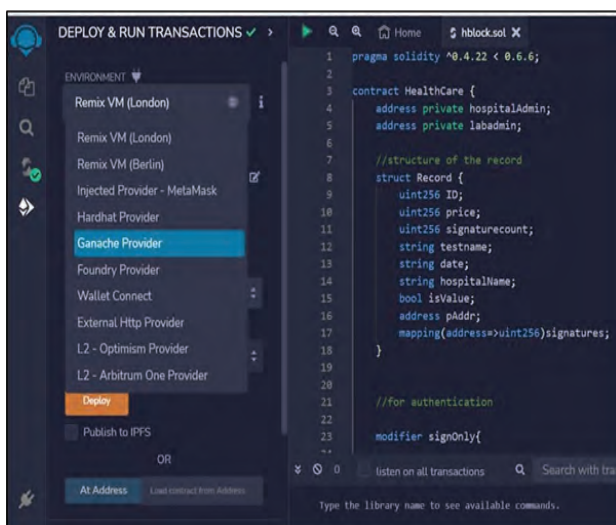
Fig. 5.Deployment of Smart Contract on Ganache

The Remix IDE offers support for various deployment environments, including but not limited to Remix VM (London), Remix VM (Berlin), Injected Provider (MetaMask), Hardhat Provider, Ganache Provider, Foundry Provider, etc. For the present research, the authors have opted for the Ganache Provider to deploy the health smart contract. Prior to selecting Ganache as the deployment environment, it should be actively running in the background.

Ganache serves as a private Ethereum blockchain environment, facilitating the emulation of the Ethereum blockchain. This emulation enables individuals to interact with smart contracts in a controlled and private setting. Functioning as a local host blockchain, Ganache provides a platform for the development and testing of blockchain applications directly on a personal computer (Ganache-Truffle Suite etc.).

Ganache operates in two versions: a CLI version that listens to incoming requests across port 8545 and a GUI version that listens to incoming requests across port 7545. The default URL for Ganache CLI is http://127.0.0.1:8545. However, in the researcher's case, aiming to connect with Ganache GUI, the port is modified to http://127.0.0.1:7545 as shown in Fig. 6.
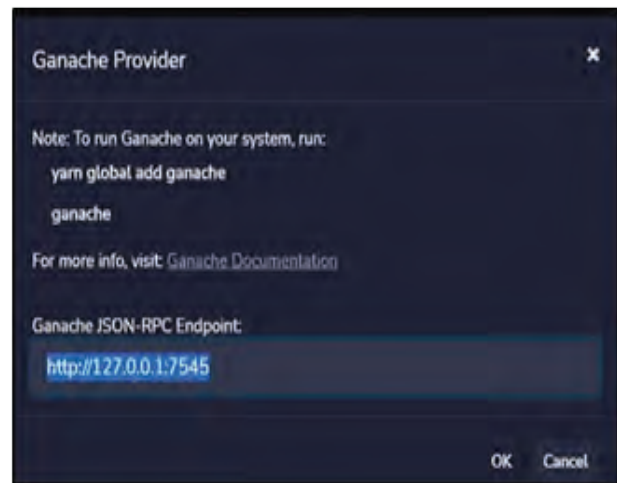
Fig. 6. Changing the Default Ganache Port in Remix IDE

Upon choosing 'Ganache Provider' as the deployment environment, the Remix IDE automatically populates its account list with all the accounts present in Ganache as demonstrated in Fig. 7.
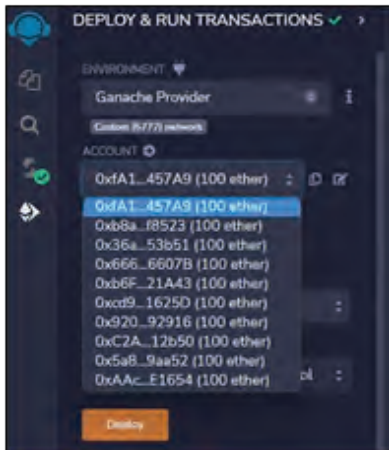
Fig. 7. Ganache Account List in Remix IDE

In the present study, four addresses have been specifically chosen from the Ganache accounts to serve as the addresses for the Hospital Admin, Lab Admin, Patient1, and Patient2 which are listed in Table 6.

Table 6. Address Selection for network nodes

Network Node	Address
Lab admin	0x6E792b25428Bf0ecf80275Ca8224f9bbd996eb17
Hospital admin	0x6FF76950DCd9dD5AbC3db8f2056 9E3E913416d8E
Patient1	0x9c1A0D99fBd032fCcc15225f002291417cA58966
Patient2	0x4584c236912240dCc9c84cF8f2c578d542799f8c
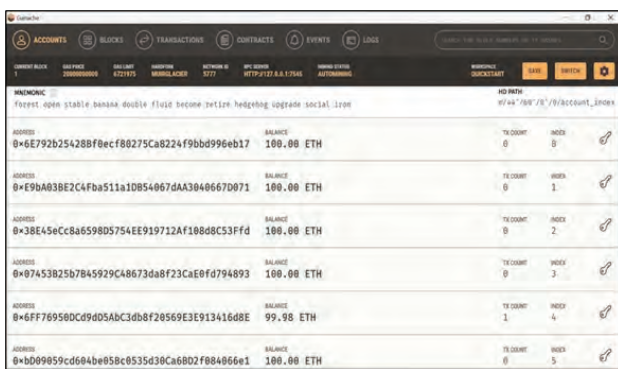
Fig. 8. Overview of Ganache Accounts

Balance of Peer Nodes

The default ETH balance for all network nodes in Ganache is set to 100 ETH. However, post the deployment of the smart contract, the scenario undergoes modification due to the modifier function embedded in the smart contract. Specifically, the node acting as the Hospital Admin, responsible for deploying contracts in the blockchain network, will receive a balance of 100 ETH. On the other hand, the remaining nodes (Patient nodes) on which the smart contract is deployed will have a balance of 0 ETH. This setup introduces the concept of Meta transactions, also known as Gasless transactions. These transactions operate without incurring any processing fees.

As per the development strategies outlined for the 'HealthCare' smart contract, the creation and signing methods necessitate gas fees for successful execution. In contrast, the read method does not incur any gas fees, classifying it as a gasless transaction or meta transaction.

As patient nodes possess a balance of 0 ETH, they can execute the read only methods as shown in Fig. 9 since writing any data to blockchain incurs some cost.
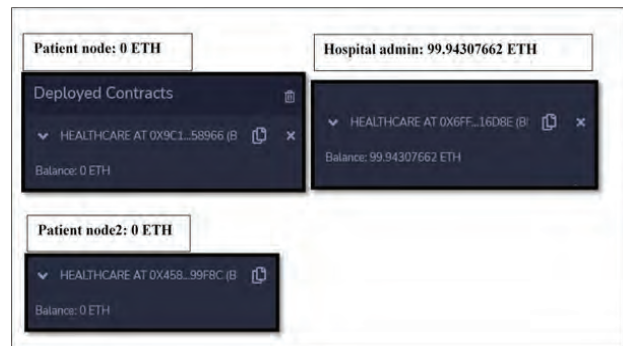
Fig. 9. Ether Balance of Peer Nodes of Different Stake Holders

Testing HealthCare smart contract

Upon the successful deployment of the smart contract, the testing phase involves evaluating various functionalities using the following test cases:

Test Case 1: Patient can't sign the record

Due to the requirement for gas fees, the Patient node is unable to create and sign new records as it lacks the necessary balance for these transactions. The patient neither has the authority nor the sufficient ETH balance for creating and signing the transaction. The authority has been delegated to the users in lab admin and doctor role. Fig. 10 executes the test case and any attempt

to sign the record by the patient results in the error displayed in Fig. 11.

Fig. 10. Patient Attempting to Create a New Record
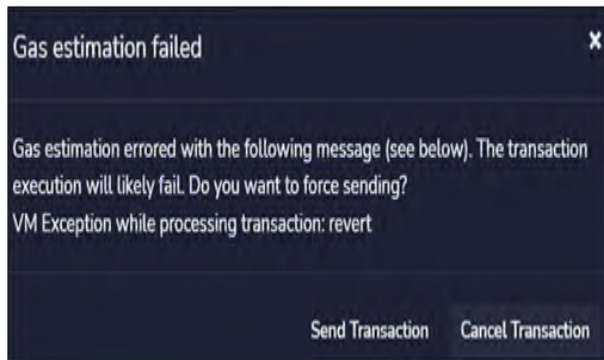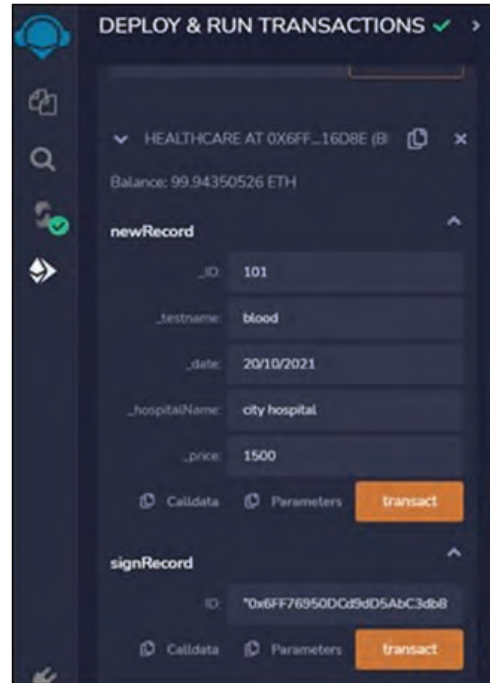
Fig. 11. Failure in Record Signing from Patient Node Due to Insufficient Balance

Test Case 2: Lab Admin can create and only doctor can sign the record

The creation and signing of records must adhere to the following conditions:

1. The deployment of the smart contract should be carried out by Hospital admin node.

2. Only the Lab admin node, possessing an adequate ETH balance, can execute the create record method successfully.

3. Only doctor can sign the record

4. Only lab technician can upload the reports on IPFS server.

5. Only doctor can view the reports.

Fig. 12 depicts successful generation and signing of a new patient record by Lab Admin and Doctor Nodes.
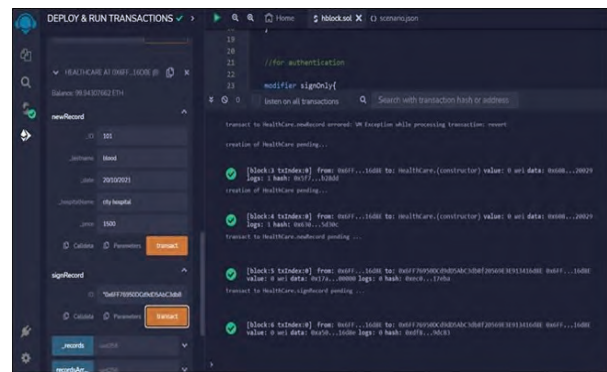
Fig. 12. Successful Generation and Signing of a New Record by Lab Administrator and Doctor Nodes

Test Case 3: Patient tries to read other patients record

The 'HealthCare' smart contract incorporates measures to prevent unauthorized access, ensuring that no patient can retrieve medical records belonging to other patients. If a patient attempts to access such records by providing a patient ID, the smart contract will respond by returning no record. Fig 13. demonstrates the execution of the test case where the Patient2 attempts to access the record of Patient1. The data is not accessible and is nullified as demonstrated.
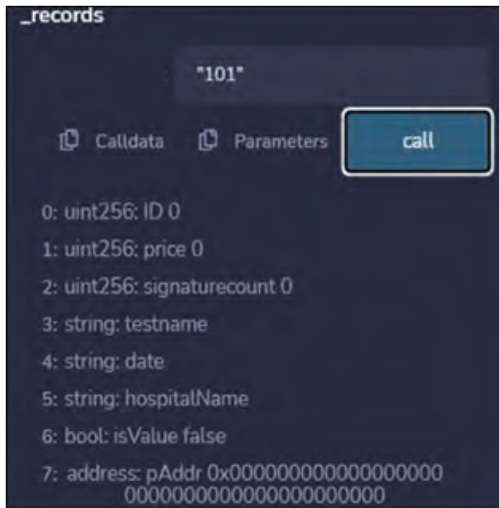
Fig. 13. Patient2 Attempts to Access the Record of Patient1

In this scenario, when Patient2 attempts to read the record of Patient1 by providing Patient1's ID, the smart contract detects unauthorized access and returns no record.

Test Case 4: Patient tries to read own medical record

In adherence to the 'HealthCare' smart contract, patients are granted permission to read only their own medical records and are restricted from accessing records of other patients. As shown in Fig. 14 no patient is deprived of his own data in adherence to the principles of data security and has a read-only access to his own healthcare record.
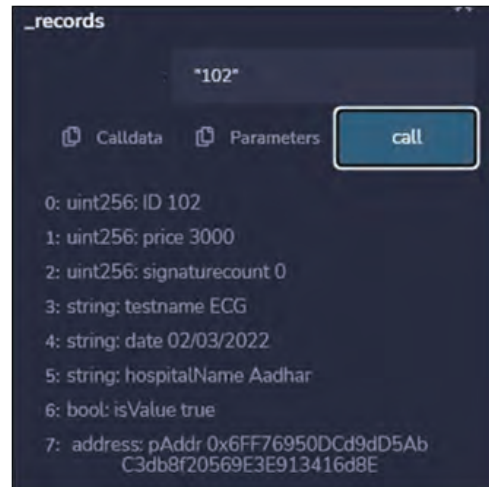
Fig. 14. Patient2 Attempting to Access his own Health Record

RESULT AND DISCUSSION

Table 7 provides the consolidated results of the aforementioned Test Cases.

Table 7. Role-based access privileges to the users

Role of the Users	Access Privileges				
	Deploy Healthcare Contract	Create new record	Upload the Reports on IPFS Server	Sign the record	Read and share other user's records with a Patient ID
Hospital Admin	Yes	No	No	No	No
Doctor	No	No	No	Yes	Yes
Lab Admin	No	Yes	Yes	No	No
Patient	No	No	No	No	Can Access only his record

Table 7 outlines the principal discoveries of the study, emphasizing that users cannot gain access to or share records of other users solely by providing a Patient ID. Furthermore, it indicates that patients lack the ability to create and authenticate new records, a privilege reserved for authorized nodes like Lab administrators and Doctors.

In the next phase of the research, Linea Goerli was employed as a public test network for testing the smart contract. 0.5 LineaETH was procured to execute different transactions as depicted in Fig. 15.

Fig 15. Configuration of Linea Goerli Network in MetaMask

Fig. 16. depicts the deployment of healthcare contract on Linea Goerli network.
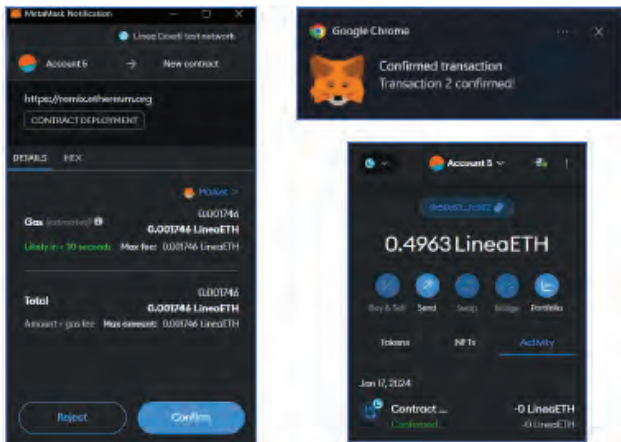
Fig. 16. Deployment of Healthcare Smart Contract on Linea Goerli Network

Fig. 17(a) and 17(b) demonstrate the contract deployed on Linea Goerli public test network using etherscan, a blockchain explorer and analytics platform specifically designed for the Ethereum blockchain. Etherscan provides specifically designed for the Ethereum blockchain.
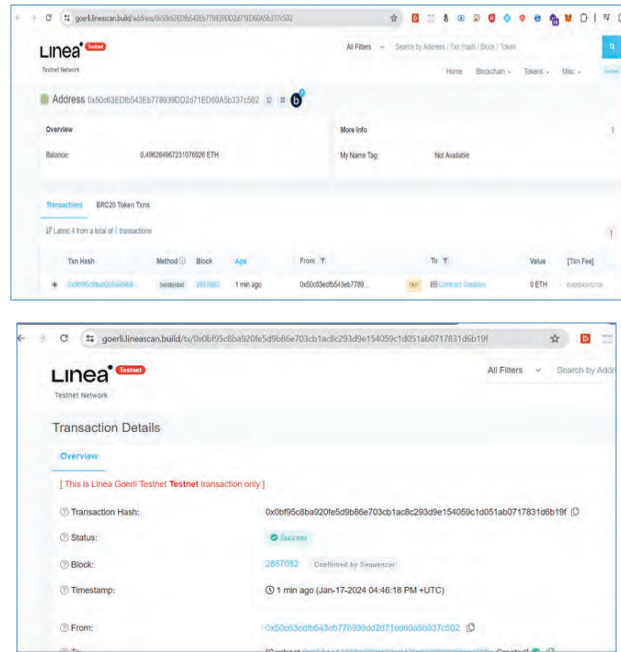
Fig. 17(a) – 17(b). Using Etherscan to View the Healthcare Contract Deployed on Linea Goerli Public Test Network

CONCLUSION AND SCOPE FOR FUTURE WORK

The Ethereum blockchain framework stands as an effective solution for secure record management within the healthcare domain. Leveraging the inherent features and functionalities of Ethereum, developers can craft customized systems tailored to specific application requirements. Blockchain-based healthcare systems offer a significant advancement over traditional methods by leveraging the unique attributes of blockchain technology. These systems enhance security, integrity, validity, verifiability, and proof of ownership, which are critical in handling sensitive healthcare data. The decentralized nature of blockchain ensures that data is not stored on a single server but distributed across multiple nodes, eliminating the risks associated with a single point of failure and making it more resilient against data breaches and hacking attempts. Blockchain-based healthcare systems offer several key advantages, advanced cryptographic security ensures patient records are confidential and protected from cyber threats, while immutability maintains data integrity by preventing alterations or deletions. Consensus mechanisms validate transactions without a central

authority, enhancing reliability and eliminating single points of failure. The transparent and auditable ledger facilitates compliance and trust, and digital ownership via cryptographic keys secures patient consent and data sharing. Further, the distributed architecture ensures redundancy and continuous access to patient records, improving overall system reliability. It is imperative, however, to conduct a thorough feasibility assessment based on diverse parameters before embarking on any blockchain application.

FUTURE SCOPE

The potential applications of the Ethereum blockchain in healthcare extend beyond secure record management. Future endeavors could explore advancements in interoperability with existing healthcare systems, enhanced data privacy measures, and the integration of emerging technologies like artificial intelligence and IoT. Additionally, ongoing research and development may uncover novel use cases, further solidifying Ethereum's role in revolutionizing healthcare data management. Continued collaboration between blockchain developers and healthcare professionals holds promise for the continual evolution of innovative solutions in this dynamic intersection of technology and healthcare.

REFERENCES

1. Naik, P. G., & Naik, G. R. (July 2023). Every Stuff You Need for Development of Decentralized App Using Blockchain Technology. Shashwat Publication. ISBN: 978-81-19281-36-7.

2. Naik, P. G., & Naik, G. R. (July 2023). Unlocking Education's Future: A Step-by-Step Practical Guide to Transformative Blockchain DApps in the Academic Landscape. Shashwat Publication. ISBN: 978-81-19281-53-4.

3. Naik, P. G., & Oza, K. S. (Nov. 2023). Leveraging the Power of Blockchain Technology for Building a Resilient Student Feedback System. Industrial Engineering Journal, 52(11), 38-51.

4. Naik, P. G., & Oza, K. S.(2024). Leveraging the Power of Blockchain Technology for Building a Resilient Crowdfunding Solution. Procedia Computer Science, vol. 230, pp. 11-20. https://doi.org/10.1016/j.procs.2023.12.056

5. Ashizawa, N., Yanai, N., Cruz, J. P., & Okamura, S. (2022). Eth2Vec: Learning contract-wide code representations for vulnerability detection on Ethereum smart contracts. Blockchain: Research and Applications, 3(4). https://doi.org/10.1016/j.bcra.2022.100101

6. Buterin, V. (n.d.). Ethereum: A Next-Generation Smart Contract and Decentralized Application Platform.

7. Ganache - Truffle Suite. (n.d.). https://trufflesuite.com/ganache/

8. Laneve, C., & Sacerdoti Coen, C. (2021). Analysis of smart contracts balances. Blockchain: Research and Applications, 2(3). https://doi.org/10.1016/j.bcra.2021.100020

9. Yu, C., Yang, C., Che, Z., & Zhu, L. (2022). Robust clustering of ethereum transactions using time leakage from fixed nodes. Blockchain: Research and Applications, 100112. https://doi.org/10.1016/j.bcra.2022.100112

10. Lewis Laidin, Kassandra A,. Papadopoulou, Nathan A. Dane. (2019). Parameters for Building Sustainable Blockchain Application Initiatives _ Published in The Journal of The British Blockchain Association. ISSN Print: 2516-3949. https://doi.org/10.31585/jbba.2.1.(6)

Ensemble of Machine Learning Models for Predicting Forex Market Volatility

Jayant Shankar Kadam
Deputy Controller of Examination
Krishna Vishwa Vidyapeeth (Deemed to be University)
Karad, Maharashtra
✉ jayantkadam110489@gmail.com

Bhaskar V. Patil
Bharati Vidyapeeth (Deemed to be University)
Institute of Management
Kolhapur, Maharashtra
✉ bhaskar.patil@bharatividyapeeth.edu

ABSTRACT

This paper explores the efficacy of an ensemble approach comprising diverse machine learning models for forecasting volatility in the forex market. Volatility prediction stands as a crucial component in devising risk management strategies and formulating informed trading decisions. Leveraging an extensive dataset encompassing various currency pairs, our study integrates an ensemble of ML models, including Random Forests, Gradient Boosting Machines, and Stacked Generalization, to collectively forecast market volatility. The methodology involves rigorous feature engineering and preprocessing techniques to optimize the dataset for model ingestion. The ensemble framework amalgamates the strengths of individual models, utilizing bagging, boosting, and stacking methodologies to harness diverse learning techniques and minimize inherent biases. Through cross-validation and robust evaluation metrics, including mean absolute error and root mean squared error, we assess the predictive performance of the ensemble against standalone models and benchmark approaches. Results indicate that the ensemble model consistently outperforms individual models, demonstrating superior accuracy and robustness in volatility forecasting across multiple currency pairs. Detailed visualizations illustrate the model's proficiency in capturing volatility patterns and its alignment with actual market behavior. Furthermore, insights gleaned from model interpretation shed light on key features influencing volatility dynamics, aiding in comprehending market intricacies. The findings underscore the potential of ensemble learning in enhancing predictive accuracy and reliability in forex market volatility forecasting. This research contributes to advancing the understanding of ensemble techniques in financial forecasting and paves the way for practical implementations in the dynamic forex landscape.

KEYWORDS : *Forex market, Volatility prediction, Machine learning ensembles, Financial forecasting, Risk management, Currency trading.*

INTRODUCTION

The foreign exchange (forex) market represents a complex and dynamic environment where currency values fluctuate incessantly, leading to diverse opportunities and risks for market participants. Volatility, a key characteristic of this financial landscape, encapsulates the magnitude and frequency of price movements, serving as a pivotal factor in assessing market dynamics and formulating effective trading strategies. Accurate prediction of forex market volatility stands as a fundamental endeavor, empowering traders and financial institutions to navigate risks and optimize their positions effectively.

Traditional financial modeling approaches often face challenges in capturing the intricate patterns inherent in forex market volatility. However, the emergence of machine learning techniques has sparked considerable interest and demonstrated promising potential in forecasting financial time series data, including volatility. In this context, ensemble learning techniques have garnered attention for their capacity to amalgamate diverse models, potentially enhancing predictive accuracy and robustness. This research delves into the domain of employing ensemble learning, integrating various machine learning models, including Random Forests, Gradient Boosting Machines, and Stacked

Generalization, to forecast volatility in the forex market. Leveraging a comprehensive dataset spanning multiple currency pairs and incorporating a spectrum of features, this study seeks to explore the effectiveness of ensemble techniques in capturing the nuanced dynamics of market volatility. Technical analysts seek trading opportunities by examining price recognition and statistical data, including stock price movements and volume. They delve into patterns such as triangles, flags, and double bottoms as part of their technical analysis. Traders determine entry and exit points based on these identified patterns. Notably, many of these patterns, widely used in analyzing the forex market, hold relevance across various other markets.

Instead of delving into a security's intrinsic value, technical analysis traders focus on interpreting stock charts to identify patterns and trends that forecast future stock behavior. Their scrutiny involves analyzing price action, trends, and levels of support and resistance evident on charts. Their primary concern lies not in dissecting the reasons behind price movements but rather in identifying trends and patterns depicted on the charts as signals. Moreover, technical analysis traders heavily rely on indicators due to their ease of use and provision of clear signals, which aid in their decision-making processes. These indicators serve as valuable tools to complement their analysis and guide their trading strategies.

The primary objectives of this research are twofold: firstly, to evaluate the performance of an ensemble model against individual machine learning models in volatility prediction, and secondly, to discern the interpretability and applicability of the ensemble approach in real-world forex trading scenarios. Through rigorous experimentation, model evaluation, and interpretation of results, this study aims to contribute novel insights into the efficacy and practical implications of ensemble machine learning for forecasting forex market volatility.

Forex Trading Sessions & Currency Pairs

The Forex market operates continuously across various time zones, segmented into distinct trading sessions. It begins with the Sydney session in the Asian market, starting at 10:00 PM GMT on Sunday and closing at 7:00 AM GMT. This session is followed by the Tokyo session, commencing at 12:00 AM GMT and ending at 9:00 AM GMT. The London session, a crucial hub for Forex trading, opens at 8:00 AM GMT and closes at 5:00 PM GMT. Lastly, the New York session, overlapping with London, starts at 1:00 PM GMT and concludes at 10:00 PM GMT. The overlaps, especially between London and New York sessions, often result in heightened market activity and liquidity.

In Forex trading, currency pairs play a pivotal role, categorized into majors, minors (cross pairs), and exotics. Major pairs, such as EUR/USD, USD/JPY, and GBP/USD, involve the most actively traded currencies globally and usually exhibit high liquidity. Minor pairs, excluding the US dollar but comprising other major currencies like EUR/GBP or GBP/JPY, offer alternative trading options. Exotic pairs, involving a major currency and one from a smaller or developing economy, like USD/SGD or EUR/TRY, generally possess lower liquidity and higher volatility. Each currency pair denotes the exchange rate between two currencies, with the first currency termed as the base currency and the second as the quote currency, showcasing the price needed in the quote currency to purchase one unit of the base currency. Understanding the distinctive trading sessions and characteristics of various currency pairs enables traders to strategize effectively, considering market volatility, liquidity, and optimal trading times aligned with their trading objectives and risk tolerance.

LITERATURE REVIEW

[1] Marco Fisichella, Filippo Garolla (Nov 2021), The global Forex market, with its daily trading volume surpassing $5.1 trillion, relies on technical analysis to forecast future prices amid its intricate and volatile nature. Our research centers on a robust trading system, integrating various rules applied to Forex time series data, available for scrutiny within the scientific community. This system's development occurs in two phases: testing diverse trading rules, including AI and technical indicators, followed by the selection and amalgamation of profitable ones. Using historical data from 2010 to 2021, we train the system and compare its performance to methodologies from Hernandez-Aguila et al. (2021) and Munkhdalai et al. (2019) on similar datasets. Our approach outperforms others across most Forex markets, achieving an average gain of 20.2%. Notably, we train our AI-based rule using

ResNet50 and Vision Transformer (ViT), highlighting their effectiveness in this domain.

[2] Iqbal H. Sarker, (March 2021), Amidst the Fourth Industrial Revolution, the digital landscape burgeons with data from IoT, cybersecurity, mobile devices, and more. Artificial intelligence (AI), particularly machine learning (ML), stands pivotal in intelligently leveraging this wealth of information. Diverse ML algorithms—supervised, unsupervised, semi-supervised, and reinforcement learning—alongside deep learning, offer comprehensive analysis of vast datasets. This paper presents a comprehensive exploration of these ML algorithms, highlighting their roles in enhancing application intelligence across domains like cybersecurity, smart cities, healthcare, e-commerce, and agriculture. Intended for academia, industry experts, and decision-makers, it elucidates the principles, applications, challenges, and future research avenues in machine learning, specifically focusing on technical aspects.

[3] A. Courage, (February 2021), The forex market relies on fundamental and technical analysis, just like the stock market. While technical analysis in forex involves chart scrutiny and assumes prices reflect all news, fundamental analysis delves into a nation's economic conditions to gauge a currency's intrinsic worth. Economic indicators like GDP, retail sales, industrial production, CPI, and others play a pivotal role in this analysis. These indicators, released periodically, signal an economy's health, akin to how earnings reports impact stocks. Traders track these indicators, anticipating market reactions and adjusting strategies accordingly. Yet, these indicators aren't the sole currency influencers; external reports, technical factors, and unexpected events also sway valuations. Successful fundamental analysis involves monitoring economic calendars, understanding market-impacting indicators, gauging market expectations, and staying alert for revisions that reveal trends and aid in making informed decisions.

[4] N. Parab (July 2021), This study investigates machine learning techniques like natural language processing, data mining, and association rules in the FOREX market, analyzing their impact on investment strategies to boost profitability within specific timeframes. It examines both modern and conventional approaches employed by market analysts and traders, showcasing how technology simplifies their tasks. The focus is on explaining machine learning algorithms in accessible terms, avoiding complex math, and using relatable examples. It emphasizes the importance of using machine learning for handling large datasets, noting that while more data improves predictive accuracy, aiming for 100 percent accuracy is unrealistic. Training models for generalization across datasets, aiming for around 80 percent accuracy, is more practical. Human expertise remains vital in validating machine learning predictions for critical decision-making, highlighting the need for vigilance in the face of technological insights.

[5] Ahmed S. Alanazi & Ammar S. Alanazi, David McMillan (May 2020), Our study delves deep into analyzing the piercing line and dark cloud cover patterns in the forex spot market. We meticulously examine 112,792 daily candles and over a million spot quote observations, identifying 1,677 trade instances across 24 currency pairs spanning 19 years. Our focus lies in the profitability of using technical analysis (TA) through chart patterns. Our findings reveal potential gains of nearly 5,000 net pips after factoring in transaction costs. Starting with a $1,000 investment and utilizing 10% margin, a trader could potentially grow their capital to $7,400 (a 642% increase, averaging 11.12% annually) over the 19-year period. However, success hinges on employing effective trading strategies. Our analysis underscores the significant impact of transaction costs, especially spread and rollover, which play key roles in explaining the challenges of consistent profitability in TA. The spread, totaling nearly 13,000 pips, stands as a substantial hurdle, while recovering half could potentially double profits. In contrast, rollover contributes positively, augmenting profits by about $2,780 (roughly 2,500 pips), offering an advantage for carry traders leveraging interest rate differentials.

[6] A. Dautel, W. Härdle, S. Lessmann, H. Seow, (2020), Advances in deep learning have profoundly impacted diverse domains like computer vision and natural language processing. This research explores deep learning's potential in forecasting exchange rates. It methodically assesses long short-term memory networks (LSTMs), gated recurrent units, traditional

recurrent networks, and feedforward networks in predicting accuracy and trading model profitability. The study indicates that deep networks hold promise for exchange rate forecasting, yet implementing and fine-tuning these intricate architectures poses challenges. Surprisingly, simpler neural networks might outperform deeper ones, especially in trading profit. The paper offers empirical results, reaffirming high non-stationarity in exchange rates. Even with rolling window training, aligning distributions between sets remains problematic. It identifies returns' leptokurtic distribution, resulting in frequent small gains and occasional significant deviations, potentially undermining model confidence in predictions.

[7] T. Azimova, (2020), The global foreign exchange market, a complex financial realm, persistently pursues technological evolution. Evolving from manual to electronic systems, it witnessed three major shifts: electronic trading, Internet proliferation, and the current forefront—Artificial Intelligence (AI), chiefly for exchange rate prediction. AI's recent surge empowers market players, enhancing communication, accessibility, and overall efficiency. This exploration delves into AI's burgeoning role in forex markets. Utilizing intricate statistical models, AI navigates this bustling marketplace, exemplifying its ability to unify diverse market sectors beyond geopolitical confines. AI, at the helm of one of the world's most active markets, exemplifies seamless interconnectedness, epitomizing technological progress in the financial landscape.

RESEARCH METHODOLOGY

This section delineates the approach, data sources, feature engineering, model selection, and evaluation techniques employed to investigate the effectiveness of ensemble machine learning models in predicting forex market volatility. This flow diagram outlines the sequential steps involved in leveraging ensemble machine learning models to predict forex market volatility:

This flow diagram provides a visual representation of the sequential steps involved in the process of utilizing ensemble machine learning models to predict forex market volatility.
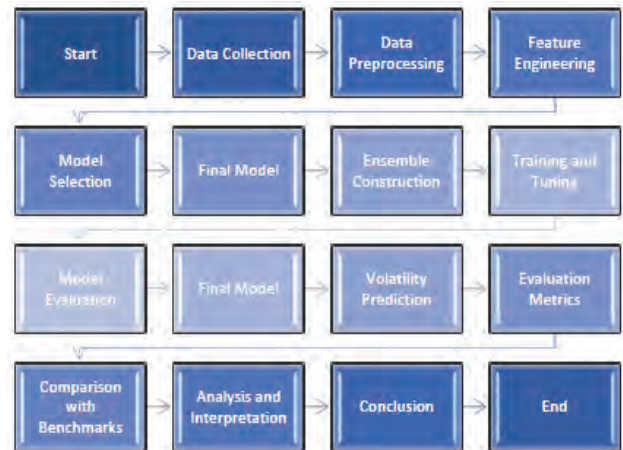
Fig. 1: Proposed machine learning models to predict forex market volatility

ANALYSIS

Data Collection: The first step in our analysis involved gathering an extensive dataset that encompasses various currency pairs. This dataset serves as the foundation for training and evaluating machine learning models. The data collection process considered factors such as trading sessions, currency pair characteristics (majors, minors, and exotics), and historical market behavior.

#Fetching data using a financial API

import pandas as pd

Fetch historical forex market data

forex_data = pd.read_csv('forex_data.csv')

	Date	Open	High	Low	Close	Change(Pips)	Change(%)	Name
0	12-01-2023	0.577879	0.586404	0.570600	0.584343	64.633203	1.11	AUDCHF
1	11-01-2023	0.576640	58385.296110	0.000105	0.577915	12.753582	0.22	AUDCHF
2	10-01-2023	0.588875	57378.653790	0.000671	0.576580	-122.945372	-2.13	AUDCHF
3	09-01-2023	0.572952	571600.320700	0.000970	0.588000	150.480000	2.56	AUDCHF
4	08-01-2023	0.585440	0.586033	0.555046	0.572961	-124.792000	-2.18	AUDCHF

Fig. 2: Last 5 Years Data Collection

Data Preprocessing: To ensure the dataset's suitability for model ingestion, a rigorous data preprocessing phase was undertaken. This involved cleaning the data to handle missing values, outliers, and inconsistencies. Standardization and normalization techniques were applied to bring features to a comparable scale. Additionally, time series data considerations, such

as handling temporal dependencies and creating appropriate lag features, were addressed during this stage.

```
plt.figure(figsize=(10, 4))
plt.title("Stock Prices")
plt.xlabel("Date")
plt.ylabel("Close")
plt.plot(forex_data["Close"])
plt.show()

# Example: Data preprocessing steps
from sklearn.preprocessing import StandardScaler
from sklearn.model_selection import train_test_split

# Preprocessing steps (e.g., normalization, handling missing values)
# Assuming 'features' and 'target' are defined based on dataset columns
scaler = StandardScaler()
scaled_features = scaler.fit_transform(features)

X_train, X_test, y_train, y_test = train_test_split(scaled_features, target, test_size=0.2, random_state=42)
```

Feature Engineering: Feature engineering is a crucial aspect of enhancing model performance. This phase involved extracting relevant features from the dataset and creating new ones that could provide valuable insights for volatility prediction. Technical indicators, statistical measures, and other domain-specific features were engineered to capture the nuanced dynamics of forex market volatility.

```
print(forex_data.corr())
sns.heatmap(forex_data.corr(),cmap="Greens")
plt.show()
# Example: Feature engineering
from sklearn.feature_selection import SelectKBest, f_regression

# Feature selection (example: selecting top features)
selector = SelectKBest(score_func=f_regression, k=10)
selected_features = selector.fit_transform(X_train, y_train).
```

	Open	High	Low	Close	Change(Pips)	Change(%)
Open	1.000000	0.390365	0.971352	0.978781	-0.025524	-0.028301
High	0.390365	1.000000	0.383777	0.391634	0.019381	0.013416
Low	0.971352	0.383777	1.000000	0.975921	0.053209	0.021388
Close	0.978781	0.391634	0.975921	1.000000	0.103670	0.051025
Change(Pips)	-0.025524	0.019381	0.053209	0.103670	1.000000	0.320341
Change(%)	-0.028301	0.013416	0.021388	0.051025	0.320341	1.000000

Fig 3: Close Price Chart for Selected Foreign Exchange Market
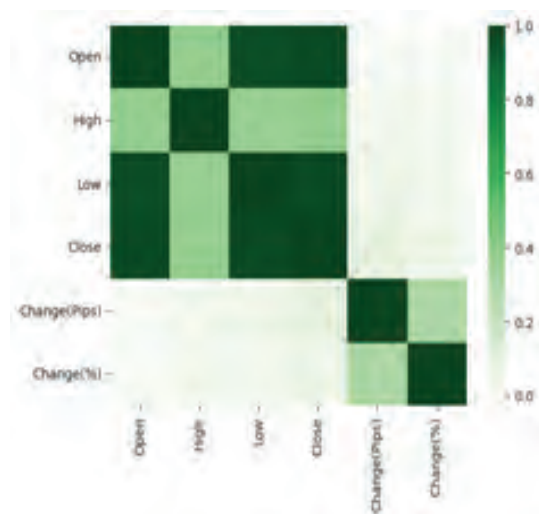
Fig. 4: Foreign Exchange Market Feature Engineering

Model Selection: A careful selection of machine learning models was made to form the foundation of the ensemble. Models such as Random Forests, Gradient Boosting Machines, and Stacked Generalization were chosen for their diverse learning techniques and proven effectiveness in handling financial time series data.

```
# Example: Model selection (using ensemble methods)
from sklearn.ensemble import RandomForestRegressor,
GradientBoostingRegressor

# Initialize individual models
random_forest = RandomForestRegressor()
gradient_boosting = GradientBoostingRegressor()
```

Ensemble Construction: The ensemble construction phase involved combining the selected models using techniques like bagging, boosting, and stacking. The goal was to leverage the strengths of individual models, minimize biases, and enhance the overall predictive accuracy and robustness of the ensemble. The ensemble was designed to provide a holistic approach to volatility forecasting by incorporating diverse learning methodologies.

```
# Example: Ensemble construction
from sklearn.ensemble import VotingRegressor

# Constructing an ensemble using VotingRegressor
ensemble_model = VotingRegressor([('rf', random_
forest), ('gb', gradient_boosting)])
```

Training and Tuning: Once the ensemble was constructed, extensive training and tuning were performed to optimize the model's parameters. This iterative process involved fine-tuning each individual model within the ensemble to achieve the best possible performance. The training phase considered the temporal nature of financial data and aimed to capture the underlying patterns in market volatility.

```
# Example: Training and hyperparameter tuning
ensemble_model.fit(X_train, y_train)
# Hyperparameter tuning (GridSearchCV,
RandomizedSearchCV, etc.)
# Tuning code here (not included for brevity)
```

Model Evaluation: To assess the performance of the ensemble, a robust evaluation framework was employed. Cross-validation techniques were applied to ensure the model's generalization across different subsets of the dataset. Evaluation metrics, including mean absolute error and root mean squared error, were used to quantify the predictive accuracy of the ensemble against standalone models and benchmark approaches.

```
# Example: Model evaluation
from sklearn.metrics import mean_squared_error

# Evaluate the model
predictions = ensemble_model.predict(X_test)
mse = mean_squared_error(y_test, predictions)
print(f"Mean Squared Error: {mse}")
```

Final Model & Volatility Prediction: Following the evaluation, the finalized ensemble model emerged. This model represents the culmination of the analysis, incorporating the collective intelligence of diverse machine learning models. The ensemble was then applied to make volatility predictions in the forex market, providing insights into potential market dynamics and aiding traders in making informed decisions.

```
# Assuming final model is trained and ready for
predictions
# Using the trained model for volatility prediction
(example)
# Apply the model to predict volatility on new data
predicted_volatility = ensemble_model.predict(new_
data)
```

Mean Squared Error: 307990.95718764554

The entire pipeline from data collection to final model deployment, demonstrating the comprehensive approach taken to leverage ensemble machine learning models for forex market volatility prediction.

FUTURE SCOPE

The exploration of ensemble machine learning models for predicting forex market volatility presents several promising avenues for future research and practical applications. One key area of interest is the dynamic adaptation of ensembles to changing market conditions, allowing for real-time adjustments in composition. Incorporating sentiment analysis of financial news and reports could further enhance the ensemble's ability to capture external factors influencing volatility. Future studies may delve into advanced feature engineering techniques, incorporating technical and macroeconomic indicators for a more comprehensive understanding

of market dynamics. Implementing online learning methods would enable continuous adaptation to new data, crucial in the rapidly changing forex market. Additionally, integrating explainability techniques enhances the interpretability of the ensemble model, fostering confidence in its predictions. Real-time deployment and seamless integration into traders' decision-making processes, along with cross-asset volatility forecasting, offer avenues for practical applications. Collaboration with financial institutions for real-world validation, risk management integration, and the development of user-friendly interfaces for traders are essential considerations for future enhancements. Addressing these aspects will contribute to the evolution of ensemble machine learning models as sophisticated tools, providing valuable insights for navigating the complexities of the dynamic forex landscape.

CONCLUSION

This research endeavors to explore and assess the efficacy of an ensemble approach, incorporating diverse machine learning models, for predicting volatility in the dynamic forex market. Volatility prediction is a critical element in devising effective risk management strategies and making informed trading decisions in the ever-changing financial landscape. Through an extensive dataset covering various currency pairs, we integrated Random Forests, Gradient Boosting Machines, and Stacked Generalization within an ensemble framework to collectively forecast market volatility.

The methodology involved meticulous feature engineering and preprocessing techniques to optimize the dataset for model ingestion. Our ensemble framework harnessed the strengths of individual models through bagging, boosting, and stacking methodologies, aiming to minimize biases and enhance predictive accuracy. Comprehensive evaluation metrics, including mean absolute error and root mean squared error, along with cross-validation, were employed to assess the predictive performance of the ensemble against standalone models and benchmark approaches. Results consistently demonstrated that the ensemble model outperformed individual models, showcasing superior accuracy and robustness in volatility forecasting across multiple currency pairs. Visualizations provided insights into the model's proficiency in capturing volatility patterns,

aligning with actual market behavior. Furthermore, model interpretation shed light on key features influencing volatility dynamics, contributing to a better understanding of market intricacies.

The research underscores the potential of ensemble learning in enhancing predictive accuracy and reliability in forex market volatility forecasting. The adaptability and resilience of the ensemble against overfitting signify its applicability in real-time trading scenarios, empowering traders with valuable insights for risk mitigation and strategic decision-making. The literature review highlighted the context of forex trading, technical analysis, and the significance of machine learning in financial forecasting, providing a foundation for our research. Our study contributes novel insights into the domain of ensemble machine learning for financial forecasting, particularly in the forex market.

In the future, there are promising avenues for further research, including dynamic adaptation of ensembles to changing market conditions, incorporation of sentiment analysis from financial news, and advanced feature engineering techniques. Continuous adaptation to new data through online learning methods and the enhancement of explainability techniques will contribute to the evolution of ensemble machine learning models as sophisticated tools in navigating the complexities of the dynamic forex landscape. Ultimately, this research advances the understanding of ensemble techniques in financial forecasting and lays the groundwork for practical implementations, potentially transforming how traders approach risk management and decision-making in the forex market.

REFERENCES

1. M. Fisichella, F. Garolla (Nov 2021), Can Deep Learning Improve Technical Analysis of Forex Data to Predict Future Price Movements, European Commission for the eXplainable Artificial Intelligence in healthcare Management (xAIM) Project under Grant, Digital Object Identifier 10.1109/ACCESS.2021.3127570

2. Iqbal H. Sarker, Machine Learning: Algorithms, Real-World Applications and Research Directions, SN Computer Science (March 2021) 2:160, https://doi.org/10.1007/s42979-021-00592-x

3. N. Parab (July 2021), International Research Journal of Engineering and Technology (IRJET) e-ISSN: 2395-

0056, Volume: 08 Issue: 07, www.irjet.net p-ISSN: 2395-0072, PP -803-808

4. Ahmed S. Alanazi & Ammar S. Alanazi, David McMillan (May 2020) The profitability of technical analysis: Evidence from the piercing line and dark cloud cover patterns in the forex market, Cogent Economics & Finance, 8:1, DOI: 10.1080/23322039.2020.1768648

5. A. Dautel, W. Härdle, S. Lessmann, H. Seow, Forex exchange rate forecasting using deep recurrent neural networks, Digital Finance (2020) 2:69–96, https://doi.org/10.1007/s42521-020-00019-x

6. T. Azimova, Artificial Intelligence (AI) In The Foreign Exchange Market, (2020), In: Emerging Human and Techno-Human … ISBN: 978-1-53618-602-4, Editors: Christina Koutra et al. © 2020 Nova Science Publishers, Inc.

7. Financial Stability Board (2017). Artificial Intelligence and Machine Learning in Financial Services. Market Developments and Financial Stability Implications.

8. Patil B.V, Gala D. M., Pawar, B., Chakraborty, A., Enhancing Agricultural Resilience in Sangli District: Leveraging Machine Learning for Soil-Based Yield Forecasting and Strategy Development, Proceedings of the 18th INDIAcom; 11th International Conference on Computing for Sustainable Global Development, INDIACom 2024, New Delhi, 28 February 2024, Date, 1 March 2024, ISBN - 978-938054451-92024, pp. 427–433, DOI: 10.23919/INDIACom61295.2024.10499074

9. Shah A., Patil B. V., Equity Market Price Prediction using Fuzzy-Genetic Machine Learning Algorithms, Congress on Smart Computing Technologies. CSCT 2022. Smart Innovation, Systems and Technologies, Springer, ISBN -978-981-99-2468-4, Vol 351, July – 2023, https://doi.org/10.1007/978-981-99-2468-4_1

10. Rime, D. (2003). New Electronic Trading Systems in Foreign Exchange Markets. Norges Bank and Stockholm Institute for Financial Research, 470-504.

11. Stenfors, A. & Susai, M. (2018). High Frequency Trading, Liquidity Withdrawal, and the Breakdown of Conventions in Foreign Exchange Markets, Journal of Economic Issues, 52(2), 387-395.

12. C. Serjam and A. Sakurai, ``Analyzing predictive performance of linear models on high-frequency currency exchange rates,'' Vietnam J. Comput. Sci., vol. 5, no. 2, pp. 123132, May 2018.

13. S. Galeshchuk and S. Mukherjee, ``Forex trading strategy optimization,' in Decision Economics: In the Tradition of Herbert A. Simon's Heritage, E. Bucciarelli, S.-H. Chen, and J. M. Corchado, Eds. Cham, Switzerland: Springer, 2018, pp. 69-76.

14. Kadam J.S., Patil B. V., Predictive Power of Machine Learning in Forex Markets: A Comparative Assessment Of AUDCHF, AUDJPY, And AUDUSD, IPE Journal of Management, ISSN 2249-9040 Volume 14, No 21, January-June 2024, pp-34-39.

An Innovative Planned Strategy for Designing an Efficient Public Robot for Healthcare System

Aman Kumar
Research Scholar
GNA University
Phagwara, Punjab
✉ aman.nagpal@nift.ac.in

Anil Pandit
Associate Professor
GNA University
Phagwara, Punjab
✉ anil.pandit@gnauniversity.edu.in

Sumanjeet Singh
Professor
Ramjas College
University of Delhi
Delhi
✉ sumanjeetsingh@gmail.com

ABSTRACT

Considering the widespread applications in the treatment and rehabilitation of various disorders, Human-Robot Interventions (HRI) has recently piqued the interest of the medical community. Social robots are designed to interact with humans in ways that are consistent with human social psychology to elicit reactions from those individuals on a social and emotional level. By obeying a predetermined set of social norms, they interact with humans via means such as verbal communication, physical movement, gestures, and facial expressions. These robots mimic human social interactions by adjusting their tone of voice, the pace of speaking, and other aspects of their demeanour on the go. The study is a narrative review based on existing literature search. This study focuses on various aspects and several promising future uses for social robots in the medical field. The study proposed an architecture of a social robot which incorporates numerous perception and attribution tools making it suitable to cater more diseases as it utilizes 57.14% more perception and attribution tools as compared to its best performing opponents i.e. AIBO and LYNX making it more efficient than others.

KEYWORDS : *Social robots, Social robots in therapy & care, Healthcare, Ethical issues, Legal issues & privacy issues.*

ROBOTICS IN HEALTHCARE

Rehabilitation Technologies

Rehabilitation technologies refer to a range of devices, tools, and software that are used to help individuals with physical, cognitive, or emotional impairments regain their abilities and improve their quality of life. This can include things like prosthetic limbs, assistive devices for mobility, virtual reality therapy programs, and rehabilitation software for cognitive and speech therapy. These technologies can be used in various settings such as hospitals, clinics, and patients homes and can be used by a wide range of individuals such as those recovering from injury or illness, those with chronic conditions, and those with developmental disabilities [2].

Robots can give you back in your life

Some very efficient rehabilitation robots were shown through empirical case studies from all around the globe. Caregiving Robot Zora for the Elderly SAR, the socially assisted robot, is shown in Fig.1 [7] as a sort of robot created to aid humans in social situations. These robots are typically used in healthcare, education, and other fields where human interaction is important. These robots that are used to provide therapy for patients with dementia, provide assistance for people with disabilities, and assist children with learning

difficulties. These robots can take many forms such as humanoid robots, animal-like robots or even virtual agents on a screen.

Figure 1 ZORA robot for elderly care services

SOCIAL ROBOTS WITH USES IN HEALTHCARE

It has wide range of applications in healthcare, such as:

1. Therapy: It can be used to provide therapy for patients with various conditions, such as dementia, depression, and anxiety. They can engage patients in conversation, provide companionship, and even play games to help improve their mood and cognitive function.

2. Rehabilitation: Robots can also be used to help patients with physical impairments to regain their abilities. For example, robots can be used to help patients with spinal cord injuries to regain mobility by providing assistance with exercises and daily tasks.

3. Monitoring and reminders: Social robots can be used to remind patients to take their medication, provide updates on their health status, and even monitor vital signs.

4. Social engagement for isolated individuals: Social robots can also be used to provide companionship and social engagement for elderly or isolated individuals. They can also be used to help reduce feelings of loneliness and isolation.

5. Education and training: Social robots can also be used to teach and train healthcare professionals and students in various aspects of healthcare, such as patient care, communication, and empathy.

These robots can be used in various settings such as hospitals, nursing homes, clinics, and even patients' homes. They are becoming increasingly popular as a tool to support and assist healthcare professionals in providing care and improving patient outcomes. Most healthcare facilities use social robots with two specific patient populations: the elderly and children [8].

Seniors

Assistive technology refers to any device, system, or software that is designed to help individuals with disabilities or impairments to overcome barriers and improve their ability to perform daily tasks. It can include both low-tech and high-tech solutions, and can be used in range of settings such as at home, at work, or in the classroom.

Examples of assistive technology can include:

1. Mobility aids: such as wheelchairs, walkers, and canes.

2. Communication aids: such as speech-generating devices, adapted keyboards and mouse, and software that help with reading and writing.

3. Environmental control systems: such as devices that allow individuals to control lights, thermostats, and other appliances using voice commands or switches.

4. Artificial limbs and braces fall under the category of prosthetics and orthotics.

5. Accessibility tools for computers include screen readers, screen magnifiers, and voice recognition programs.

6. Hearing aids, closed captioning, and visual alert systems are all examples of sensory aids.

Assistive technology can help people with disabilities to live more independently, communicate more effectively,

and participate more fully in their communities. It can also help to improve education and job opportunities for people with disabilities [9].

For the elderly and those with dementia, feelings are tied to their relationships with others. The PARO robot can see potential in this area, since it offers challenges as well as opportunities. PARO may help meet the social, emotional, occupational, and comfort-related requirements of the elderly population. Facial expressions, body language, posture, and spoken signals are all used in tandem by ARI to communicate emotion and generate empathy. Fig. 2 depicts a variety of SARs (Social Assisting Robot and Companion) such as AIBO, PARO, AIBO, and iCat. There were 6,400 sales of healthcare robots worldwide last year. The challenge is in determining the role of robots in healthcare and establishing ethical norms for their use [10].

The state of our dwellings affects our health. They are essential among the most vulnerable groups, such as the elderly, who regularly need medical assistance. Empathetic coaches and virtual assistants were used, for instance, to support elderly home-dwellers [11]. Robots are more than just tools for the elderly; they give emotional support in the same way that a friend or companion would [12].

Fig. 2: AIBO, PARO, iCAT social robots for elderly

Youths

It is considered that robots can improve children's lives in a number of ways, including:

1. Education: Robots may be utilized to get kids interested in learning and aid in their development. They can be used to teach children with learning difficulties, such as autism or ADHD, and to provide personalized instruction.

2. Therapy: Robots can be used to provide therapy for children with a wide range of conditions, such as developmental disorders, mental health issues, and chronic illnesses. They can be used to provide social and emotional support, and to help children to improve their communication and motor skills.

3. Play and entertainment: Robots can also be used to provide children with entertainment and to engage them in play activities. This can help to improve their mood and cognitive development.

4. Assistive technology: Robots can also be used to provide children with disabilities with assistive technology that can help to improve their mobility, communication, and independence.

5. Monitoring and safety: robots can also be used to monitor and ensure children's safety, for example, through monitoring their health and providing alerts if necessary.

It is important to note that these benefits of robots for children need to be evaluated in research studies with controlled conditions, and it also depends on the specific robot and its implementation [13]. Some commonly used social robots for youngsters are shown in Fig 3.

Fig. 3: PARROT, PLEO, HUGGABLE social robots for youth

Automatic diagnosis is extensively discussed in the published works. When the outcome of an activity is uncertain, it might be helpful for people with Autism Spectrum Disorder (ASD). The study of kinematics cannot replace the study of the mind [14]. "In the wild" usually refers to real-world situations. Many activities are performed in artificial, laboratory conditions. Some research like those involving children with diabetes, use a model of human-robot cooperation in long-term

care to tackle the problem [15]. The robotic pet baby dinosaur Pleo, for example, serves a variety of purposes for sick children in hospitals [16]. Other social robots were used to collect and analyse urine samples from children with cancer, monitor and evaluate treatment sessions, and record findings in electronic databases [17].

USING SOCIAL ROBOTS AS AN ADDITIONAL KIND OF TREATMENT FOR CHRONIC, PROGRESSIVE DISEASES

The development of new technologies has allowed for major progress in robotics. There have been attempts to create robots that can have natural conversations with humans. All existing robots take cues from the animals and plants in our world, giving them either humanistic or zoomorphic traits. Robotic intervention has been shown to have positive effects on socialisation, and researchers are now able to study these effects and their effects on human cognition and behaviour [18–20].

Therapy with domestic animals should be emphasised as a supplementary treatment for dementia because of the long history of human involvement with other animals, which may be traced back to the period of Homo erectus, as the earliest fossilised evidence suggests. Since domestic animals may reduce people's feeling of well-being, they are increasingly being selected for their emotional return and as promoters of social interaction between humans. This strong bond between them has persisted [21]. Therapeutic intervention research with domestic animals may provide some unique problems, however, including hygiene, allergy, and institutional concerns. This opens the door for the development of a zoomorphic SAR app that targets this limitation [22].
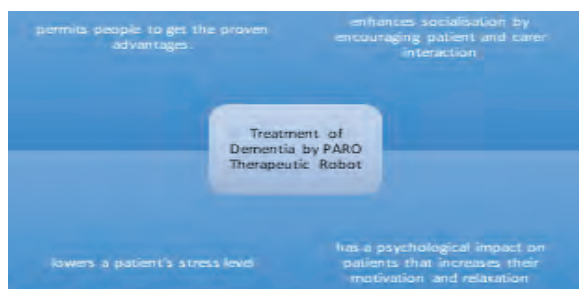
Figure 4 Benefits of using social robots for Dementia patients

Most investigations with zoomorphic robots have focused on the robotic baby seal (PARO), a canine-like AIBO designed to promote multimodal interaction through sight, sound, and touch (see Fig. 4). PARO is the most used model, both in practise and academic inquiry. It is a robot that was given approval as a medical device by the FDA in 2009 [23-25].

SOCIAL ROBOTS FOR AUTISM SPECTRUM DISORDER OR SOCIAL ANXIETY

One of the hallmarks of social anxiety disorder is a pervasive and persistent fear of social situations. People with social anxiety disorder may avoid or suffer through social settings while wanting to engage with others. This is due to their extreme nervousness around other people. Seventy-five percent of those with social anxiety disorder say they first noticed symptoms between the ages of eight and fifteen. The onset of social anxiety disorder often occurs between the ages of 8 and 13. Early identification and therapy are critical for patients with social anxiety disorder due to the high risk of morbidity and impairment. Fig. 5 shows how social robots may benefit kids with autism spectrum disorder.

Fig. 5: how social robots help children with ASD

Interviews conducted by robots

Despite the questions' complexity, several studies of robot-mediated interviews have demonstrated the same thing. Interviews conducted by robots, also known as "robot interviews" or "AI interviews," refer to the use of artificial intelligence and machine learning

algorithms to conduct job interviews. These systems can include natural language processing and computer vision technologies to analyse a candidate's speech and body language, as well as their responses to questions. Some companies are using this technology to automate the initial screening process for job candidates, while others are using it to conduct entire interviews. The advantages of using robot interviews include the ability to conduct interviews at scale, eliminate bias, and provide objective evaluations of candidates.

Social robots as screening and diagnosis tools

The employment of social robots by therapists might further our understanding of the behaviour associated with social anxiety. People who suffer from social anxiety may show behavioural signs as rigid body postures, inappropriate speaking tones, and an inability to make direct eye contact with others. Robots that can read and react to social signals from humans are called social robots [26].

Robotic Therapy

Robotic therapy refers to use of robots to assist in the treatment and rehabilitation of individuals with physical or cognitive impairments. This can include the use of exoskeletons to help individuals with spinal cord injuries or other mobility impairments, as well as the use of robotic assistants to help with activities of daily living like dressing, and grooming [27-30].

Robotic therapy can be beneficial in many ways, including providing patients with more consistent and accurate therapy, reducing the need for human caregivers, and providing patients with a sense of independence and control over their own therapy. More study is required to properly understand the possible advantages and downsides of robotic treatment [31], but it is crucial to recognize that robotic therapy is still in its early phases of development.

Interactive Social Companions in the Form of Social Robots

Those who suffer from social anxiety often report fewer friends and more difficulty keeping the ones they do have. There are a number of robot pets available that are designed to simulate the therapeutic benefits of animal companions. Several studies have shown the positive

effects of engaging with robotic dogs on mental health, including increased happiness and socialisation and reduced sadness, stress, and anxiety. Many of these studies targeted senior citizens and those with dementia.

Interactive Playmates: Social Robots

Peer or interactive playmates refer to robots or other interactive technologies that are designed to engage in play or other social interactions with children. These can include robotic dolls or stuffed animals, as well as virtual characters or avatars. The goal of these playmates is to provide children with a sense of companionship and social interaction, as well as to help them develop various skills such as language, social, and emotional skills. Interactive playmates can be beneficial for children in a number of ways. They can provide children with a sense of companionship, especially for those who may be socially isolated or have difficulty connecting with other children. They can also help children develop important social and emotional skills, such as empathy, cooperation, and communication. Additionally, interactive playmates can be used as a tool for learning and education, providing children with interactive and engaging ways to learn new concepts and ideas.

The Part of Social Robots as Social Mediators

People with social anxiety may have trouble engaging in social activities because of difficulties in communicating and fears of being judged by others. Based on their observational study, authors concluded that a media- tor and a pair of children may construct settings including a robot as a highly interesting social environment for seeing varied social and non-social interaction patterns. Analysing these trends may provide light on the social skills and particular difficulties of children with ASD. Playing with Kaspar has been shown to have a positive effect on certain children's behaviours in particular areas, including mimicking, prompted speech, attention, and communication.

Social robots for elderly and Alzheimer patients

Alzheimer and Dementia are diseases that affect the cognitive function of an individual. Typically, neuro-physical and mental exercises they have, although poor diet or even drugs they have used throughout their lives can also play a role. Some of the common symptoms

of Alzheimer are shown in Fig 6. Maintaining communication between patient, family, and staff is one of the most crucial components of dementia care so that treatment can be properly personalised.

Fig. 6: Early signs & symptoms of Alzheimer's disease

SOCIAL ROBOTS FOR IMPROVING CUSTOMER SATISFACTION IN COVID-19

Social Isolation's Effects

Long-term social exclusion and isolation have a negative impact on people's psychological health. Consumers are forced into objective social isolation as a result of the COVID-19 global control procedures. Although few people may live alone without feeling lonely, new research typically shows that social isolation has a strong predictive impact on feelings of loneliness. Particularly, this perceivably socially isolated state is strongly detrimental to one's physical, psychological, and cognitive wellbeing. Numerous longitudinal studies have linked subjective social isolation to physical health decline and mortality. Additionally, it is linked to heightened irritability and sadness, quicker cognitive decline, and heightened susceptibility to social dangers. Children and elderly individuals are more at risk for subjective social isolation, making them a susceptible consumer category during COVID-19.

A typology of the revolutionary potential of robots in COVID-19 and beyond

Robots with human-level physical capabilities and empathic artificial intelligence (AI) are still not ready for the market. But precisely these social robots with a focus on physical touch, social expression, and relationship-building could offer sophisticated transforming services. The transformative potential of each type of robot for vulnerable people who are socially isolated is outlined below in Fig 7.

Entertainer: The entertainer robot may be best suited to service customers who must deal with forced social isolation and only mild psychological distress. The entertainer has inadequate social skills because of this; it is pre-programmed for robot types to carry out easy-to-repeat social duties. Its primary transformative potential is hedonistic and focuses on entertaining customers to boost their fleeting affect as a means of self-satisfaction. It could be used to stop small psychological pain from occurring during times of seclusion in both elderly people and youngsters. A good example is Alibaba's DWI Dowellin, a little mobile robot that sings and dances for its users.

Fig. 7: Roles that can be assumed by market-ready social robots to combat the negative effects of social isolation

ELEMENTS INFLUENCING WHETHER SOCIAL ROBOTS ARE ACCEPTED

Robots having social intelligence and the ability to interact with humans in a manner that is accepted by society are called "social robots." This necessitates that they have some kind of social recognition and interaction with the user. Robots whose primary function is to be human companions fall under this category. Service robots that help people with mundane jobs are part of the plan, as is enhancing users' emotional and mental

well-being. The expression "the robot being voluntarily absorbed into the life of the older person" is used to describe how well received a robot is, implying that it will be used for a considerable amount of time. Figure 8 displays ten variables that contribute to the general public's opinion on social robots.

Fig. 8: Factor influencing acceptability of social robots

Beliefs and Concerns about Technology

The user's preconceived notions regarding robots influence how they respond to their initial hands-on encounter. Second-hand information from sources outside the person, such as science fiction and the media, may influence mental models.

One's perspective and encounters with robots are coloured by one's preconceived notions of what such robots are capable of and are not. This is connected to anthropomorphism, the belief that inanimate things (such as robots) possess human-like intelligence. What follows is a more in-depth explanation of this process.

Intent to Utilize (ITU)

The findings suggests that gaining first-hand experience with a robot, as opposed to learning about it from an outside source, may alter some of the factors that influence its acceptability. This is only one of the many reasons why educations that focus on actual robot operation over a long period of time are preferable to ITU as an indicator of robot readiness. For instance, after interacting with the robot for 30 minutes, the Cafero community's feelings towards it were recorded using a robot attitude measure developed by Stafford

et al. After interacting with the robots, both sets of participants reported feeling less antagonistic. Authors found a similar uplift in disposition during their observational qualitative field study in a "smart" home. They found that some OA patients with MCI and their care partners (n = 4 dyads) had negative first responses to the companion robot and found it scary. After only one day of use, though, individuals started to see its benefits and were more open to it.

Perceived Usefulness (PU)

The term "perceived usefulness" (PU) comes from the study of how people evaluate the potential benefits of new technologies to their daily lives. It's a big reason why people decide whether or not to adopt new technologies.

Individuals' decisions on whether or not to employ a new technology are heavily influenced by their impressions about the technology's utility. When people see the value in a new piece of technology, they are more inclined to start using it in their daily lives. However, if people do not see value in the technology, they are less inclined to accept it.

Perceived Ease of Use (PEOU)

One topic in the study of how people respond to new technologies is the idea of "perceived ease of use," or PEOU. It's a big reason why people decide whether or not to adopt new technologies.

An individual's perception of the technology's usability is based on their own evaluation of its learnability, operability, and comprehend-ability. It's a cognitive view as opposed to an emotional one, and it has everything to do with how someone feels about the technology in question.

One of the most influential aspects of people's choice to utilise a new piece of technology is their impression of how simple it is to do so. When people find a piece of technology simple to use, they are more inclined to utilise it in their daily lives. However, if people do not think the technology is user-friendly, they are less inclined to embrace it.

Organisations may improve the technology's perceived ease of use by making it more intuitive and user-friendly. This includes providing clear instructions and

a straightforward interface. Providing consumers with training and assistance may also improve the product's perceived ease of use.

Perceived Enjoyment (PE)

In the study of how people adopt new technologies, the idea of "perceived enjoyment" (PE) is fundamental. PE measures how much people like using a technology. It's a big reason why people decide whether or not to adopt new technologies.

An individual's evaluation of how entertaining or satisfying a technological experience is will affect how much they appreciate it. It's an assessment of how the technology makes you feel emotionally or psychologically.

An individual's level of perceived satisfaction with a technology has a role in their choice to acquire and use that technology. When people find utilising a new piece of technology pleasurable, they are more inclined to incorporate it into their daily lives, whether at work or at play. However, if they don't love using the technology, they are less likely to take it up and keep it up.

Organisations can improve consumers' satisfaction with their technology by making it more interesting and fun to use. Adding incentives, awards, or other forms of positive feedback may also boost pleasure.

When individuals are given the choice to use robots in the house, motivating factors like PE come into play, as the robot is more likely to be accepted if it is also perceived as enjoyable to interact with. Authors [12] found a strong correlation between PE and both actual use (0.625, p 0.01) and intended usage (0.420, p 0.05) in a research using a chatty iCat robot controlled by a concealed operator. Thirty people with OA who are semi-independent made up the study group.

Social Presence

Robots designed to inspire and excite their users should project an adequate amount of social presence (SP), making the users feel as if they are in the company of a social entity. The capacity to use SP seems to be what distinguishes robots from other technologies.

Authors looked at the feasibility of using a robot to track and encourage PWD's cognitive activity throughout the course of an 8-month trial (n = 9). The robot offered individualised mental exercise by playing the user's favourite music and engaging in other fun activities with them. The study compared people's responses to a humanoid torso design on a mobile platform with those to a simulation shown on a huge computer screen. After finding that participants consistently favoured the embodied robot over the computer, they concluded that embodiment improved users' interaction with the robot as they shared their environment.

Perceived Sociability (PS)

The way robots seem, perform, and communicate all have an effect on PS.

Authors found that people vary in both the make-up of their bodies and their skin tone. Begum et al. conducted an acceptability and feasibility study in a home simulation laboratory to assess the usefulness of a capable of providing verbal cues to assist PWD in carrying out domestic sequences of tasks such as making a cup of tea. Researchers conducted and recorded interviews with caretakers (n = 5) and PWD (n = 5). They observed divergent opinions about the appropriate robot voice tone and gender portrayal.

User choices for a human or machine-like look also play a role in determining how realistic a robot should seem. Perceived human resemblance was associated with greater anxiety and heart rates in OA volunteers than in official caretakers, according to the research by Stafford et al. cited above. This suggests that the uncanny valley concept is culturally specific and associated with dread.

However, the influence of realism on the acceptance of zoomorphic robots may be different. Authors examined [12] Paro alongside a baby seal, dog, cat, dinosaur, and bear, all of which are examples of so-called zoomorphic robots. 15 individuals with intermediate dementia and 36 professional carers were observed during interviews. Over the course of each participant's hour-long session, they interacted with a different robot and had their emotions recorded. The baby seal scored highest due to its convenience, softness, portability, and low weight in comparison to Paro. The cat was a close second since it seemed more plausible. Pleo, the dinosaur, scored the lowest because of its reptilian appearance and weird behaviour.

Trust and Perceived Adaptivity (TPA)

There is a tight relationship between two ideas connected to technology acceptance: trust and perceived adaptability.

When someone says they trust a piece of technology, they mean they have faith in its consistency, durability, and dependability. Individuals are more inclined to embrace and utilize a technology that they trust, making this a key aspect in the adoption and acceptance of new technology. The perceived utility, simplicity of use, and pleasure of the technology, as well as the reputation of the technology's inventor or maker, may all play a role in inspiring trust.

An individual's opinion of a technology's adaptivity to their own requirements, priorities, and worldview is known as its perceived compatibility. Individuals are more likely to embrace and utilize a technology that they perceive as being consistent with their wants and aspirations, making this a crucial component in the adoption and acceptance of new technology.

It's likely that there is no one-size-fits-all combination of robot purpose and deployment scenario variables.

More research with bigger samples is required to back up these assertions.

Author [12] presented a DVD in which he analyzed the results of an experiment in which the effects of PA acceptance were controlled for. Participants preferred the extra flexible robot and rated it higher in ITU, perceived fun, and perceived utility. The authors postulated that this was because people who felt uneasy around the robot had less ability to influence its actions.

Users need to trust that robots will perform reliably and safely. Authors ran a series of seminars for OA patients who were unable to leave their homes due to modest sensory and mobility impairments. Participants were shown drawings of several robots and asked to rank their top choices. In addition, they spoke to OA (n = 5) and one couple who lived with foam polystine prototypes for a week. They found that feelings of control were substantial and associated with privacy and trust concerns.

Eighty-five percent of people showed distrust by refusing to give a robot full reign in the house, and eighty-two

percent were worried about the robot causing harm to their property.

Social Factors and Supportive Environment

Few studies in this review seem to account for these challenges, and little data was supplied regarding the cultural background of their samples, although social impacts do include larger cultural problems. Multiple countries participated in two separate studies.

Another cultural and sociological barrier that might prevent robots from being widely accepted is ageism. Neven watched as scientists interacted with OA (n = 6) for 30-60 minutes through an unidentified robot to see how OA stereotypes affect technological progress. They found that ageist assumptions impacted robot development and deployment, and that OA may have different perspectives on what it is to be older.

Potential robot users may be rejected by OA if the AI perceives them to be lonely, dependent, or isolated, all of which are negative characteristics. This might be due to the fact that people see themselves as autonomous and physically fit, and using the robot would go counter to that image.

RESEARCH METHODOLOGY

This section explains the various designing and programming techniques by which social robots are made to interact with humans to accomplish their goals.

Synthetic senses refer to the use of technology to create artificial senses for humans or robots. These can include the use of sensors, cameras, and other devices to replicate human senses such as vision, hearing, touch, and smell. The goal of synthetic senses is to enhance or augment human capabilities, or to provide robots with the ability to sense and interact with their environment in a way that is similar to how humans do.

Synthetic vision, for example, can be used to enhance human vision by providing individuals with visual aids such as night vision goggles or telescopic lenses. Synthetic hearing can be used to enhance human hearing by providing individuals with hearing aids or cochlear implants. Synthetic touch can be used to enhance human touch by providing individuals with prosthetic limbs or exoskeletons.

Perceptible Reactions

Perceptible reactions refer to the observable or measurable responses that an individual or system has to a particular stimulus. In the context of artificial touch or synthetic senses, perceptible reactions refer to the observable or measurable responses that a human or robot has to touch-related stimuli.

Mechanical and electrical motion

Mechanical motion refers to the movement or displacement of an object caused by a force applied to it. This can include things like linear motion, and oscillatory motion (movement that repeats regularly in a back-and-forth or up-and-down motion). Mechanical motion can be powered by various means such as manual force, springs, pneumatic or hydraulic systems, or electric motors. Electrical motion, on the other hand, refers to the movement or displacement of an object caused by an electrical current flowing through it. Electric motors are the most common form of electrical motion, which convert electrical energy into mechanical energy. Electric motors can be classified into two types, AC and DC motors, depending on the type of current used to drive the motor. Both Mechanical and Electrical motion can be used in the design of robotic systems, for example, to provide robot with ability to move, manipulate or interact with its environment.

Sound and speech

Almost all recent social robots include internal loudspeakers and virtual speech synthesis software, allowing them to say anything they are programmed to say in a way that humans can understand. The major exceptions would be social robots meant to mimic the behaviour of dogs and other animals through various vocalizations.

Table 1 Perception and attribution tools used by various social robots

PERCEPTION AND ATTRIBUTION TOOLS	AIBO	AEOLUS	BUDDY	NAO	PROF. EINST-EIN	PEPPER	VECTOR	PARO	LYNX	UNIVERSAL ROBOT
Microphones	✓	✓	✓	✓	✓	✓	✓	✓	✓	✓
Time of flight sensor	✓					✓	✓			✓
Cameras	✓	✓	✓	✓	✓	✓	✓		✓	✓
Pressure/										
Capacitive sensor	✓					✓	✓		✓	✓
Accelerometer & Gyroscope	✓								✓	✓
Motion Sensor	✓							✓		✓
Light Sensor	✓							✓		✓
LEDs	✓	✓		✓					✓	✓
Speaker	✓		✓	✓	✓			✓	✓	✓
Temperature Sensor			✓					✓	✓	✓
Obstacle Detection/ Cliff Sensor			✓			✓	✓			✓
Touch Screen			✓							✓
Projector			✓							✓
Sonar				✓						✓
Contact Sensor				✓						✓

Force Sensitivity Resistor				✓						✓
Infrared Sensor					✓					✓
Tactile Sensor								✓		✓
Gravity Sensor									✓	✓
Chest Button				✓					✓	✓
PIR Sensor									✓	✓

RESULT

Total no. of perception & attribution tools identified-21.

Percentage of efficiency based on number of perception & attribution tools utilized by different robots taken into consideration are illustrated in Table 2 & Fig 3.

It is observed that the proposed universal robot will be 57.14% more efficient than its best performing opponents AIBO and LYNX as it will incorporate all 21 perceptions and attribution tools making it suitable to be used for treatment and rehabilitation of a wide variety of diseases.

Table 2 Percentage of perception & attribution tools utilized by various social robots

Social Robot	Percentage of tools utilized
AIBO	42.86%
AEOLUS	14.29%
BUDDY	33.33%
NAO	38.10%
PROF. EINSTEIN	19.05%
PEPPER	23.81%
VECTOR	23.81%
PARO	28.57%
LYNX	42.86%
UNIVERSAL ROBOT	100%
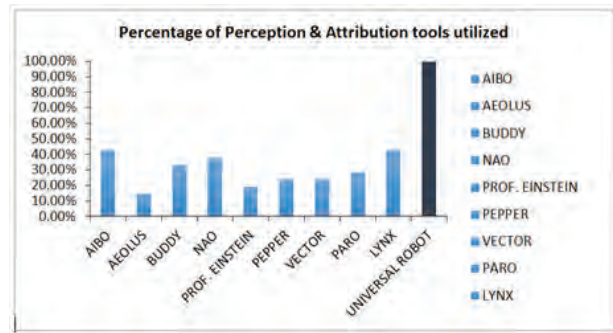
Fig. 9: Chart depicting percentage of perception & attribution tools used by various social robots

CONCLUSION AND FUTURE SCOPE

Robot proposed by us is an amalgamation of 21 perception and attribution tools which will make suitable for combating and assisting in a host of diseases. Looking at the statistics, the novel architecture of the proposed, Universal Robot utilized 57.14% more perception and attribution tools as compared to its best performing opponents in this regard, namely AIBO and LYNX making it more efficient than others.

The robots will help with everything from surgery to physical therapy to hospital housekeeping to food service to medication distribution. Although robots cannot yet convey feelings, they can do jobs precisely and effectively, which might be of considerable use in addressing difficulties related to the disabled and other medical concerns. In purely financial terms, the idea of building new insurance formulas focused on the use of care-robots and the launch of new policies that cover the risks connected with the use of robots is very appealing to insurance companies. Just like with other AI applications, the opinion and acceptance of all relevant actors, including doctors, nurses, carers, patients, and their loved ones, will surely be a crucial aspect for the proliferation of SRs. Researchers in the same subject will find this publication very helpful.

REFERENCES

1. Khan MJ, Hong K-S (2017) Hybrid EEG–fNIRS based eight-command decoding for BCI: application to quadcopter control. Front Neurorobot 11:6. Available at: https://www.frontiersin.org/ article/10.3389/ fnbot.2017.00006.

2. Tang J, Zhou Z, Yu Y (2017) A hybrid computer interface for robot arm control. In: Proceedings of 8th International Conference on Information Technology in Medicine and Education, ITME 2016, Fuzhou, China, December 23–25, 2016, pp 365–369. https:// doi. org/10.1109/ITME.2016.0088

3. Miao Q et al (2018) Reviewing high-level control techniques on robot-assisted upper-limb rehabilitation. Adv Robot 32(24):1253–1268. https://doi.org/1 0.1080/01691864.2018.1546617

4. Ahn, H.S.; Yep, W.; Lim, J.; Ahn, B.K.; Johanson, D.L.; Hwang, E.J.; Lee, M.H.; Broadbent, E.; MacDonald, B.A. Hospital Receptionist Robot v2: Design for Enhancing Verbal Interaction with Social Skills. In Proceedings of the 2019 28th IEEE International Conference on Robot and Human Interactive Communication (RO-MAN), New Delhi, India, 14–18 October 2019

5. Chung, K.; Park, R.C. Chatbot-Based Heathcare Service with a Knowledge Base for Cloud Computing. Clust. Comput. J. Netw. Softw. Tools Appl. 2019, 22, 1925–1937.

6. Moerman, C.J.; Jansens, R.M.L. Using Social Robot PLEO to Enhance the Wellbeing of Hospitalised Children. J. Child Health Care 2020.

7. Cooper, S.; Fava, A.D.; Vivas, C.; Marchionni, L.; Ferro, F. ARI: The Social Assistive Robot and Companion. In Proceedings of the 2020 29th IEEE International Conference on Robot and Human Interactive Communication (RO-MAN), Naples, Italy, 31 August–4 September 2020; pp. 745–751

8. Logan, D.E.; Breazeal, C.; Goodwin, M.S.; Jeong, S.; O'Connell, B.; Smith-Freedman, D.; Heathers, J.; Weinstock, P. Social Robots for Hospitalized Children. Pediatrics 2019, 144, e20181511.

9. Chen, C.; Garrod, O.G.B.; Zhan, J.; Beskow, J.; Schyns, P.G.; Jack, R.E. Reverse Engineering Psychologically Valid Facial Expressions of Emotion into Social Robots. In Proceedings of the 2018 13th IEEE International Conference on Automatic Face & Gesture Recognition, Xi'an, China, 15–19 May 2018; pp. 448–452.

10. Larriba, F.; Raya, C.; Angulo, C.; Albo-Canals, J.; Diaz, M.; Boldu, R. Externalising Moods and Psychological States in a Cloud Based System to Enhance a Pet-Robot and Child's Interaction. Biomed. Eng. Online 2016, 15, S72

11. Cooper, S.; Fava, A.D.; Vivas, C.; Marchionni, L.; Ferro, F. ARI: The Social Assistive Robot and Companion. In Proceedings of the 2020 29th IEEE International Conference on Robot and Human Interactive Communication (RO-MAN), Naples, Italy, 31 August–4 September 2020; pp. 745–751.

12. Moerman, C.J.; van der Heide, L.; Heerink, M. Social Robots to Support Children's Wellbeing under Medical Treatment: A Systematic State-of-the-Art Review. J. Child Health Care 2019, 23, 596–612.

13. Diaz-Boladeras, M.; Angulo, C.; Domenech, M.; Albo-Canals, J.; Serrallonga, N.; Raya, C.; Barco, A. Assessing Pediatrics Patients' Psychological States from Biomedical Signals in a Cloud of Social Robots. In Proceedings of the XIV Mediterranean Conference on Medical and Biological Engineering and Computing, Paphos, Cyprus, 31 March 31–2 April 2016; Springer: Cham, Switzerland, 2016; Volume 57, pp. 1179–1184.

14. Alemi, M.; Meghdari, A.; Ghanbarzadeh, A.; Moghadam, L.J.; Ghanbarzadeh, A. Effect of Utilizing a Humanoid Robot as a Therapy-Assistant in Reducing Anger, Anxiety, and Depression. In Proceedings of the 2014 Second RSI/ISM International Conference on Robotics and Mechatronics, Tehran, Iran, 15–17 October 2014; pp. 748–753.

15. Sheridan, T.B. A Review of Recent Research in Social Robotics. Curr. Opin. Psychol. 2020, 36, 7–12.

16. Burns, R.; Jeon, M.; Park, C.H. Robotic Motion Learning Framework to Promote Social Engagement. Appl. Sci. 2018, 8, 241.

17. Meghdari, A.; Alemi, M.; Khamooshi, M.; Amoozandeh, A.; Shariati, A.; Mozafari, B. Conceptual Design of a Social Robot for Pediatric Hospitals. In Proceedings of the 2016 4th International Conference on Robotics and Mechatronics (ICROM), Tehran, Iran, 26–28 October 2016; pp. 566–571.

18. Jupalle, H., Kouser, S., Bhatia, A. B., Alam, N., Nadikattu, R. R., & Whig, P. (2022). Automation of human behaviors and its prediction using machine learning. Microsystem Technologies, 1–9.

19. Whig, P., & Ahmad, S. N. (2014d). Simulation of linear dynamic macro model of photo catalytic sensor

in SPICE. COMPEL: The International Journal for Computation and Mathematics in Electrical and Electronic Engineering.

20. Whig, P., Kouser, S., Velu, A., & Nadikattu, R. R. (2022). Fog-IoT-Assisted-Based Smart Agriculture Application. In Demystifying Federated Learning for Blockchain and Industrial Internet of Things (pp. 74–93). IGI Global.

21. Whig, P., Nadikattu, R. R., & Velu, A. (2022). COVID-19 pandemic analysis using application of AI. Healthcare Monitoring and Data Analysis Using IoT: Technologies and Applications, 1.

22. Whig, P., Velu, A., & Bhatia, A. B. (2022). Protect Nature and Reduce the Carbon Footprint With an Application of Blockchain for IIoT. In Demystifying Federated Learning for Blockchain and Industrial Internet of Things (pp. 123–142). IGI Global.

23. Whig, P., Velu, A., & Naddikatu, R. R. (2022). The Economic Impact of AI-Enabled Blockchain in 6G-Based Industry. In AI and Blockchain Technology in 6G Wireless Network (pp. 205–224). Springer, Singapore.

24. Whig, P., Velu, A., & Nadikattu, R. R. (2022). Blockchain Platform to Resolve Security Issues in IoT and Smart Networks. In AI-Enabled Agile Internet of Things for Sustainable FinTech Ecosystems (pp. 46–65). IGI Global.

25. Whig, P., Velu, A., & Ready, R. (2022). Demystifying Federated Learning in Artificial Intelligence With Human-Computer Interaction. In Demystifying Federated Learning for Blockchain and Industrial Internet of Things (pp. 94–122). IGI Global.

26. Whig, P., Velu, A., & Sharma, P. (2022). Demystifying Federated Learning for Blockchain: A Case Study. In Demystifying Federated Learning for Blockchain and Industrial Internet of Things (pp. 143–165). IGI Global.

27. Cooper, S.; Fava, A.D.; Vivas, C.; Marchionni, L.; Ferro, F. ARI: The Social Assistive Robot and Companion. In Proceedings of the 2020 29th IEEE International Conference on Robot and Human Interactive Communication (RO-MAN), Naples, Italy, 31 August–4 September 2020; pp. 745–751

28. Logan, D.E.; Breazeal, C.; Goodwin, M.S.; Jeong, S.; O'Connell, B.; Smith-Freedman, D.; Heathers, J.; Weinstock, P. Social Robots for Hospitalized Children. Pediatrics 2019, 144, e20181511.

29. Chen, C.; Garrod, O.G.B.; Zhan, J.; Beskow, J.; Schyns, P.G.; Jack, R.E. Reverse Engineering Psychologically Valid Facial Expressions of Emotion into Social Robots. In Proceedings of the 2018 13th IEEE International Conference on Automatic Face & Gesture Recognition, Xi'an, China, 15–19 May 2018; pp. 448–452.

30. Larriba, F.; Raya, C.; Angulo, C.; Albo-Canals, J.; Diaz, M.; Boldu, R. Externalising Moods and Psychological States in a Cloud Based System to Enhance a Pet-Robot and Child's Interaction. Biomed. Eng. Online 2016, 15, S72

31. Cooper, S.; Fava, A.D.; Vivas, C.; Marchionni, L.; Ferro, F. ARI: The Social Assistive Robot and Companion. In Proceedings of the 2020 29th IEEE International Conference on Robot and Human Interactive Communication (RO-MAN), Naples, Italy, 31 August–4 September 2020; pp. 745–751.

32. Moerman, C.J.; van der Heide, L.; Heerink, M. Social Robots to Support Children's Wellbeing under Medical Treatment: A Systematic State-of-the-Art Review. J. Child Health Care 2019, 23, 596–612.

33. Diaz-Boladeras, M.; Angulo, C.; Domenech, M.; Albo-Canals, J.; Serrallonga, N.; Raya, C.; Barco, A. Assessing Pediatrics Patients' Psychological States from Biomedical Signals in a Cloud of Social Robots. In Proceedings of the XIV Mediterranean Conference on Medical and Biological Engineering and Computing, Paphos, Cyprus, 31 March 31–2 April 2016; Springer: Cham, Switzerland, 2016; Volume 57, pp. 1179–1184.

Explainable-AI Based MPOX Disease Detection using Skin Lesion Image Analysis

Kalyan Kumar Jena
Sourav Kumar Bhoi
Department of Computer Science and Engineering
Parala Maharaja Engineering College
Berhmapur, Odisha
✉ kalyan.cse@pmec.ac.in
✉ sourav.cse@pmec.ac.in

Chittaranjan Mallick
Department of Basic Science (Mathematics)
Parala Maharaja Engineering College
Berhmapur, Odisha
✉ chittaranjan.bs@pmec.ac.in

ABSTRACT

The intricate realm of pox diseases, comprising afflictions such as chickenpox, cowpox, monkeypox, Hand, Foot, Mouth Disease (HFMD), and measles, and their profound influence on human health, is the focal point of extensive research. In response to the compelling demand for precise disease classification, an exploration is undertaken in this study, delving into the intersection of machine learning (ML) methodologies and the pursuit of interpretability through the application of explainable artificial intelligence (XAI). In this study, we use ML methods for data pre-processing and then we trained the data, then we applied the (XAI) approach in those trained models. First ML methods scikit-image were used to segregate the 15,000 images into train (70%), test (20%) and valid (10%). Then, we used 8 CNN model – Alex Net (AN), LeNet (LN), SeNet (SN), GoogleNet (GN), SpinalNet (SN), MobileNetV1 (MN), VGG, and ZFNet (ZN) to train the model. To explain the results of these models reliably, XAI is used. The XAI method that we applied here in different CNN models reveals the different factors for differentiating the outcome among them. The accuracy of GoogleNet is 85% which is much better than other CNN models. When examining the pox disease classification data, XGBoost (XGB) gives higher accuracy than other methods.

KEYWORDS : Pox diseases, Disease classification, Accuracy, Convolutional neural network (CNN), Explainable-AI.

INTRODUCTION

Pox disease encompasses a range of highly contagious viral infections [1-27]. The earliest evidence of skin lesions resembling with smallpox being one of them is found on faces of Egyptian mummies. It originated in 1350 BC, with cases found in Egyptian mummies. It is also known as variola or 'la variole'. Pox disease is a widespread health concern, but today, vaccination provides effective protection for human. The mode of transmission varies according to the specific virus involved. It mainly influences individuals, mainly children, manifesting with signs and symptoms consisting of regular itchy skin rashes, low-grade fever, and a feeling of preferred soreness. It causes an itchy rash, moderate fever and soreness. It spreads without difficulty thru air and by touching the rash. Although it is also moderate, it could cause problems in a few people. Recovering from chickenpox gives immunity, however the virus can return later. Cases have reduced due to vaccination. Studying chickenpox allows us higher recognize and manipulate the ailment and improve vaccines specific length.

Chemical analysis, additionally known as laboratory trying out, is a way applied in situations wherein the medical presentation is ambiguous. The assay is employed to perceive the virus's genetic fabric, at the same time as the viral way of life method entails cultivating the virus in controlled laboratory surroundings for affirmation. These strategies are extra time-eating and lots less commonly used than healthcare-primarily based analysis but can provide a definitive confirmation when wanted.

Diagnostic imaging may be a useful first step within the prognosis of tumors. Symptoms consist of a yellowish blister that later develops right into a fluid-stuffed blister. These blisters normally appear in clusters and may be very painful. A fitness care issuer can visually inspect the tumor and examine it with pix or descriptions of not-unusual tumors to make an initial diagnosis.

Detecting illnesses through AI-pushed pre-photograph processing is now a preferred technique because of its efficiency, accuracy, and scalability. AI unexpectedly techniques medical imaging information, making sure short and constant consequences, which may be hard with biological strategies. Additionally, AI unexpectedly strategies clinical imaging records, ensuring short and regular results, which may be difficult with organic techniques.

Unlike conventional gadget learning (ML) models that frequently perform as black boxes & XAI models [28] provide interpretable results, making it less complicated for customers to recognize how and why AI systems make specific selections. By the use of XAI strategies, our version turns into simpler to apprehend, showing how it makes selections. This is vital, particularly for complicated fashions, ensuring we will see the reasons behind predictions. With XAI, our version turns into consumer-friendly and accountable, making it a valuable tool in many applications wherein clarity topics.

 In this work the pox images are classified using the 8 CNN models and the classification is analyzed using 5 XAI models. In this work we have used Asus Tuf A17 which has 8 GB RAM and 512 GB SSD. It has an AMD R%-4600H processor, NVIDIA Geforce GTX 1650 Graphic Processor, and a 64-bitOperating System. In order to embed our work, we used Python 3.11 in Jupyter notebook IDE. We have collected the data from Kaggle [29] and save in our computer directory. We classified the images into 3 subdomain train, test, and valid. We used 8 CNN architecture for training the model. Then we used the 5 XAI approach to get the result. We chose ROC curve, F1 score, and Accuracy as the performance matrix.

The rest of the work is categorized as follows. Section II presents the related work. Section III presents the methodology. Section IV presents the experiment and results and at last we conclude at Section V.

RELATED WORK

Many research works in [1-27] suggests about the pos diseases. Saleh et al. [1] diagnose human monkeypox using data mining and AI. Farzipour et al. [2] detected monkeypox cases using symptoms by taking XGBoost and Shapely additive models. Lakshmi et al. [3] classified monkeypox images using Deep CNN model and LIME for EAI. Sharma et al. [4] taken LIME for monkeypox prediction. Yasmin et al. [5] used transfer learning for monkeypox disease classification. Thieme et al. [6] classified skin lesions from monkeypox infection using DL. Kundu et al. [7] used vision transformer-based DL for detection of monkeypox. Nayak et al. [8] detected monkeypox using skin lesion images by Dl models. Athina et al. [9] detected skin diseases using DL and XAI. Ahsan et al. [10] used transfer learning and model agnostic approach for detection of monkeypox.

From above study, it is studied that there is a research gap in improvising the accuracy of detection for monkeypox images and about exploring the explainability using XAI approach. So, in this work we taken 8 CNN models for detection of monkeypox disease and afterward analyzed the models using 5 XAI models.

METHODOLOGY

Data collection

We have collected 15000 images from Kaggle source [29]. These images are belonged from different pox sub domain like chicken pox, monkey pox, cow pox, measles, HFD and healthy. All the images have different characteristics and properties like height, width and quality.

Table 1: Tabulation Data Model for Image Classification

Input Data	Image Classification Algo using ML	Output Data
POX Images 15000	SCIKIT -IMAGE Scikit -Learn (224*224)	Train – 10000 Test – 3000 Valid - 2000
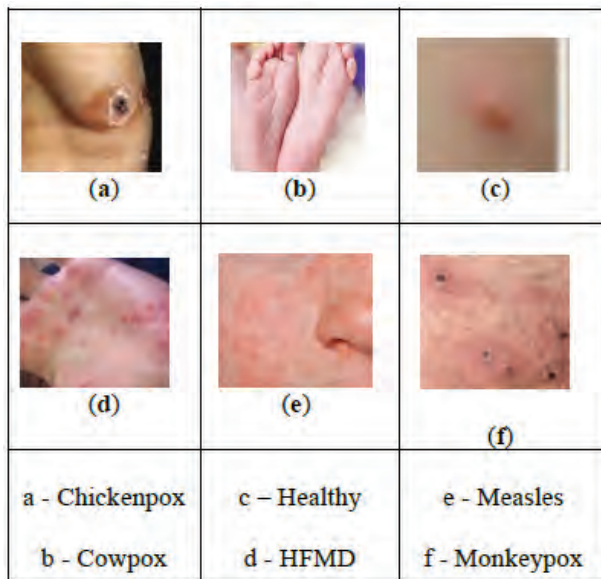
Fig. 1: Image classification of Data Pre-processing

Data pre-processing

We use SCIKIT-IMAGE for classification the images. Scikit-image, formerly known as scikits.image, stands as an open-source image processing library designed for the Python.

We set (224*224) height and width in all images. We segregate the images into 3 sub directories like train, test, and valid. After the successful segregation it is seen that Train contain 10000 images, Test contain 3000 images and Valid contain 2000 images and saved in our directory having name Train, Test, and Valid.
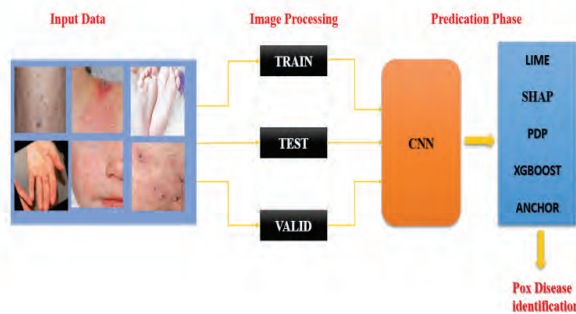
Fig. 2 Architecture for monkeypox disease detection

Model training

In the model training phase, we have used 8 CNN architecture [1-27] which are discussed as follows.

LeNet is a pioneering CNN architecture, designed for handwritten digit recognition. It extracts features and pooling layers to reduce dimensionality, enabling efficient pattern recognition in images with the use of convolutional layers. It is used for tasks like handwritten digit recognition, image classification, and pattern recognition.

GoogleNet is a deep-learning model for image recognition. It utilizes multiple layers to enhance accuracy, making it a powerful tool in computer vision applications.it is used in image recognition, optimizing accuracy through innovative convolutional layer configurations.

Mobile Net is a deep learning architecture, that provides efficient and accurate image recognition, making it ideal for various real-time applications on smartphones and other portable gadgets. It is used in mobile apps for tasks like object detection and image recognition.

ZFNet is a deep learning architecture that introduced deeper neural networks, improving image recognition accuracy and paving the way for advanced computer vision applications. Its advanced convolutional layers enhance accuracy, making it valuable in computer vision applications like object detection and facial recognition.

AlexNet isa pioneering convolutional neural network analyzed for large-scale image recognition tasks. It showcases deep learning's potential to revolutionize computer vision applications. It is widely used for tasks like object recognition, its deep layers enhance accuracy, enabling advanced applications in computer vision.

Spinalnet operates as a learning system that undergoes a series of steps to formulate predictions: beginning with the intake of input data, proceeding to generate a prediction, and concluding by comparing the prediction with the desired output.

VGG is a renowned deep learning model, characterized by its simplicity and depth. It excels in image recognition tasks, utilizing deep convolutional layers to capture intricate patterns, enhancing accuracy. It accurately identifies objects, making it indispensable in diverse fields like healthcare, robotics, and autonomous vehicles.

Senet enhances deep learning models by focusing on important features. Its adaptive recalibration technique improves accuracy in various computer analysis tasks, ensuring efficient image recognition. It emphasizes crucial features, boosting accuracy in tasks like object detection and image classification, advancing computer

XAI Approach

We have used 5 XAI Approach in this CNN Architecture and got different result [3,4,16,19,28]. However, we choose the ROC curve and Accuracy as performance matrix in order to predict the best XAI approach. The XAI models [28] considered are discussed as follows.

LIME (Local Interpretable Model-agnostic Explanations) is a technique demonstrated in machine learning used to make a specific decision for a particular input such as classifying an image. Lime provides local and interpretable explanations for model predictions, which helps in understanding why a model makes a specific prediction for a particular instance of data. The SHAP model stands for SHapley Additive analysis, which is a unified framework that explains the output of any machine learning model. Its values offer a comprehensive understanding of feature importance and prediction rationale in machine learning models. PDP is utilized to illustrate the relationship between a particular feature in a dataset and the predictions made by machine learning and model, with the other features being held constant. The PDP approach is chosen for disease detection because it allows insights into the impact of specific features on predictions to be gained, aiding in the interpretation of complex models and facilitating more accurate and reliable detection methods. This is a generic form used in optimization (OE), particularly in machine learning Algorithm. E(x) – It is an objective function to be minimized. The product over x suggests optimization over a set of data points. The goal is to find values of x that minimize the combination of loss and regularization, crucial in training models to generalize well. XGBoost belongs to the ensemble learning methods and is based on the gradient boosting framework. XGBoost is widely used in machine learning competitions and data science projects due to its speed, performance, and versatility. Anchor Explanations is a model-dynamic method that explains the behavior of machine learning models by

identifying sets of anchors. These anchors are conditions that sufficiently guarantee a prediction, regardless of the values of other features. The technique is based on the concept of coverage and precision.
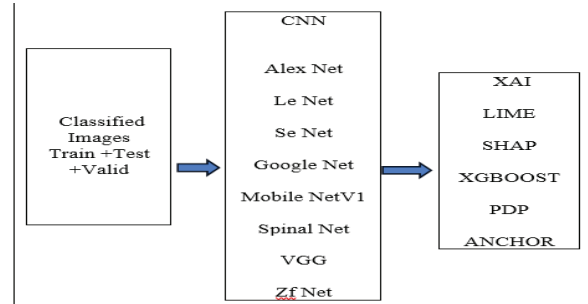
Fig 3: Models used for monkeypox disease classification

EXPERIMENT AND RESULT

In this experiment, we have used 15000 Pox images which are downloaded from Kaggle [29]. These images belong to different pox subdomains like chicken pox, monkeypox, cow pox, measles, HFD, and healthy. All the images have different characteristics and properties like height, width, and quality. Then We use SCIKIT-IMAGE to classify the images into 3 categories having the name Train, Test, and Valid on the basis of (224*224). Then we got the Train as 10000 images Train as 3000 images and Valid as 20000 images. Then we used the 8 CNN architectures such as (Spinal Net, Alex Net, GoogleNet V1, SE Net, ZfNet, VGG, Le Net, Mobile Net) to train our model. Then we moved to the XAI Approach, we used 5 XAI approaches LIME, SHAP, ANCHOR, XGBOOST, and PDP. We got some results by measuring the CNN and XAI, i.e. explanations for model predictions, which helps in understanding why a model makes a specific prediction for a particular instance of data.

Data Collection

We have collected 15,000 images from Kaggle, which we take as input for the detection of pox disease. The height and width of the images are 224 pixels. We have taken Well-organized data to enhance Lime's interpretability for accurate disease detection.

Data Preprocessing

The Proper preprocessing enhances Lime's interpretability, leading to more accurate disease

detection outcomes. So, we have divided the data into 3 parts i.e. Train, Test, and Valid. Around 10,000 images are selected as Data pre-processing models and the remaining 3000 images are selected for Testing and 2000 Valid methods.

Model Training

Tenser flow and Pytorch frameworks can be used in the LIME model. We have used the Pytorch method because this model is easy to use and debugging, Natural NumPy integration, etc. We use 8 models in this method i.e. Lenet, Alexnet, Googlenet, Mobilenet, Zfnet, Spinal net, VGG, and Senet to find out Test accuracy, Test loss, Precision, XAI accuracy, Recall, F1 score.

Hardware and Software

The experiment is conducted in a machine of 8 Gb RAM and windows 11 Operating system with core i3 processor.

In this experiment, we take the Test Accuracy (TA), Test Loss (TL), XAI accuracy (XAI-A), Precision (P), Recall (R), and F1-Score (F1) to distinguish between the performance accuracy in our model.

Results

Table 2: Performance of Different Models using Lime

XAI	MODEL	TA	TL	XAI-A	P	R	F1
LIME	LN	35.54%	2.6808	37.36%	0.9316	0.1865	0.3401
	AN	34.06%	2.5957	31.92%	0.9368	0.2676	0.4103
	GN	81.69%	1.5867	83.27%	0.9809	0.8617	0.6532
	MN	46.04%	2.7584	50.92%	0.9434	0.0758	0.1256
	ZN	18.69%	1.9637	22.82%	0.9049	0.2792	0.1745
	SN	42.84%	1.6438	39.45%	0.9630	0.4833	0.4263
	VGG	41.48%	1.6384	43.48%	0.9620	0.1834	0.2463
	SeNet	23.74%	1.8248	22.76%	0.9268	0.2179	0.1896

Fig. 4: Roc curve of LIME

For Lime XAI model comparison, we took 8 models i.e. Lenet, Alexnet, Googlenet, Mobilenet, Zfnet, Spinalnet, VGG, and Senet and performance is shown in Table II and Fig. 4. The value of all 8 models is defined based on the following parameters i.e. Test accuracy, Test loss, XAI accuracy, Precision, Recall, F1 score. Lenet had Test accuracy of 35.54%, Test loss of 2.6808, XAI accuracy of 37.36%, precision of 0.9316, Recall of 0.1865, and F1 score of 0.3401. Alexnet had a Test accuracy of 34.06%, Test loss of 2.6808, XAI accuracy of 31.92 %, precision of 0.9368, Recall of 0.2676, F1 score 0.4103. Google net had Test accuracy 81.69%, Test loss 1.5867, XAI accuracy 83.27%, precision 0.9809, Recall 0.8617, F1 score 0.6532. Mobile net had Test accuracy 46.04%, Test loss 2.7584, XAI accuracy 50.92%, precision 0.9434, Recall 0.0758, F1 score 0.1256. Zf net had Test accuracy 18.69%, Test loss 1.9637, XAI accuracy 22.82%, precision 0.9040, Recall 0.2792, F1 score 0.1745. Spinal net had Test accuracy 42.84%, Test loss 1.6438, XAI accuracy 39.45%, precision 0.9630, Recall 0.4833, F1 score 0.4263. VGG had Test accuracy 41.48 %, Test loss 1.6384, XAI accuracy 43.48%, precision 0.9620, Recall 0.1834, F1 score 0.2463. Se net had a test accuracy of 23.74%, Test loss 1.8248, XAI accuracy 22.76%, precision 0.9268, Recall 0.2179, F1 score 0.1896. We got the best Test accuracy in the Googlenet model i.e.81.69 %.

In the SHAP XAI model comparison, we took 8 models Lenet, Alexnet, Googlenet, Mobilenet, Zfnet, Spinalnet, VGG, and Senet and performance is shown in Table III and Fig. 5. The value of all those 8 models is defined on the basis of the following parameters i.e. Test accuracy, Test loss, XAI accuracy, Precision, Recall, F1 score. Lenet had Test accuracy 33.34%, Test loss 1.6915, XAI accuracy 35.96%, precision 0.9517, Recall 0.1689, F1

score 0.2868. Alexnet had Test accuracy 33.34%, Test loss 1.5723, XAI accuracy 32.96 %, precision 0.9549, Recall 0.1698, F1 score 0.2863. Googlenet had a Test accuracy of 84.39%, Test loss 0.3453, XAI accuracy 88.84%, precision 0.9959, Recall 0.8091, F1 score 0.5653. Mobile net had Test accuracy 39.56%, Test loss 2.9824, XAI accuracy 40.02%, precision 0.9298, Recall 0.3498, F1 score 0.7673. Zf net had Test accuracy 21.85%, Test loss 1.9349, XAI accuracy 23.92%, precision 0.9186, Recall 0.6525, F1 score 0.3794. Spinal net had Test accuracy 40.34%, Test loss 1.9914, XAI accuracy 42.47%, precision 0.9529, Recall 0.0898, F1 score 0.1811. VGG had Test accuracy 40.98%, Test loss 1.5692, XAI accuracy 42.45%, precision 0.9623, Recall 0.1876, F1 score 0.3140. Se net had a test accuracy of 22.56%, Test loss 1.7245, XAI accuracy 23.35%, precision 0.9289, Recall 0.1439, F1 score 0.3491. We got the best Test accuracy in the Googlenet model i.e. 84.39 %.

Fig 5: RoC curve of SHAP

Fig 6: RoC Curve of PDP

Table 3: Performance of Different Models using SHAP

XAI	MODEL	TA	TL	XAI-A	P	R	F1
SHAP	LN	33.34%	35.96%	1.6915	0.9517	0.1689	0.2868
	AN	33.34%	32.96%	1.5723	0.9549	0.1698	0.2883
	GN	84.39%	88.84%	0.3453	0.9959	0.3948	0.5654
	MN	39.56%	40.02%	2.9824	0.9298	0.6525	0.7673
	ZN	21.85%	23.90%	1.9345	0.9186	0.2391	0.3794
	SN	40.34%	42.87%	1.9914	0.09529	0.0989	0.1811
	VGG	40.98%	42.45%	1.5692	0.9623	0.1876	0.3140
	SeNet	22.56%	23.35%	1.7245	0.9289	0.1439	0.2491

In the PDP XAI model comparison, we took 8 models Lenet, Alexnet, Googlenet, Mobilenet, Zfnet, Spinalnet, VGG, and Senet and performance is shown in Table IV and Fig. 6. The value of all those 8 models is defined on the basis of the following parameters i.e. Test accuracy, Test loss, XAI accuracy, Precision, Recall, F1 score. Lenet had Test accuracy of 30.65%, Test loss 1.5365, XAI accuracy 32.07%, precision 0.9522, Recall 0.1791, F1 score 0.3014. Alexnet had Test accuracy 31.3%, Test loss 1.7065, XAI accuracy 29.86%, precision 0.9482, Recall 0.1843, F1 score 0. 3086. Googlenet had a Test accuracy of 85.88%, Test loss 1.2036, XAI accuracy 89.02%, precision 0.3258, Recall 0.2591, F1 score 0.4103. Mobile net had Test accuracy 35.67%, Test loss 0.9586, XAI accuracy 32.58%, precision 0.9738, Recall 0.4138, F1 score 0.5805. Zf net had Test accuracy 43.87%, Test loss 0.8488, XAI accuracy 47.93%, precision 0.9810, Recall 0.8203, F1 score 0.8934. Spinal net had Test accuracy 77.44%, Test loss 0.6484, XAI accuracy 47.93%, precision 0.9476, Recall 0.1854, F1 score 0.6851. VGG had Test accuracy 31.76%, Test loss 0.8671, XAI accuracy 34.47 %, precision 0.9734,

Recall 0.9551, F1 score 0.5476. Se net had a test accuracy of 29.69%, Test loss 0.9722, XAI accuracy 30.92%, precision 0.9682, Recall 0.9543, F1 score 0.9421. We got the best Test accuracy in the Googlenet model i.e. 85.88%.

Table 4: Performance of Different Models using PDP

XAI	MODEL	TA	TL	XAI-A	P	R	F1
	LN	30.65%	1.5365	32.07%	0.9522	0.1791	0.3014
	AN	31.3%	1.7065	29.86%	0.9482	0.1843	0.3086
PDP	GN	85.88%	1.2036	89.02%	0.9861	0.2591	0.4103
	MN	35.67%	0.9586	32.58%	0.9738	0.4135	0.5805
	ZN	43.87%	0.8488	47.93%	0.9810	0.8203	0.8934
	SN	77.44%	0.6484	82.82%	0.9476	0.1854	0.6851
	VGG	31.76%	0.8671	34.47%	0.9734	0.9551	0.5476
	SeNet	29.69%	0.9722	30.92%	0.9682	0.9543	0.9421
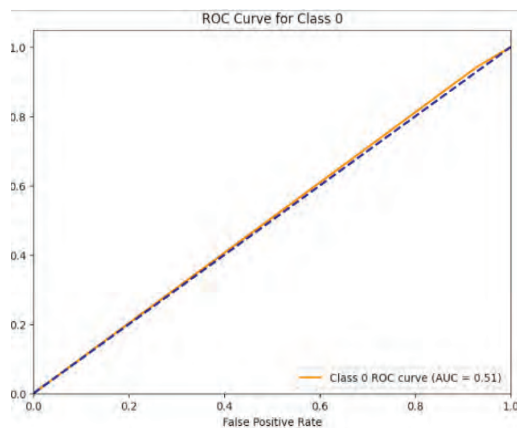
Fig 7: Roc Curve of XGBoost

Table 5: Performance of Different Models using XGBOOST

XAI	Model	TA	TL	XAI-A	P	R	F1
	LN	31.31%	1.7234	32.31%	0.9478	0.1537	0.2645
	AN	31.31%	1.7025	33.29%	0.9484	0.1553	0.2668
	GN	88.55%	0.2089	98%	0.9976	0.8091	0.8935
	MN	41.89%	3.183	85%	0.9301	0.0989	0.1787
XGB	ZN	16.22%	1.9323	65%	0.8935	0.1593	0.1386
	SN	38.96	1.559	77%	0.9615	0.1983	0.3287
	VGG	43.24%	1.7722	56%	0.9606	0.1961	0.3257
	SeNet	20.27%	1.5567	47%	0.9125	0.1489	0.2697

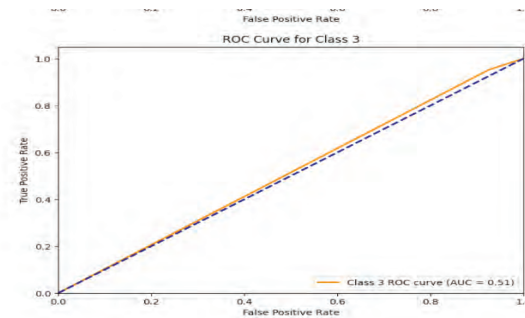In the XGBOOST XAI model comparison, we took 8 models Lenet, Alexnet, Googlenet, Mobilenet, Zfnet, Spinalnet, VGG, and Senet and performance is shown in Table V and Fig. 7. The value of all 8 models is defined based on the following parameters i.e. Test accuracy, Test loss, XAI accuracy, Precision, Recall, and F1 score. Lenet had a Test accuracy of 31.31%, Test loss of 1.7234, XAI accuracy of 32.31%, precision of 0.9478, Recall 0.1537, and F1 score of 0.3645. Alexnet had a Test accuracy of 33.29%, Test loss of 1.7025, XAI accuracy of 31.92 %, precision of 0.9484, Recall of 0.1553, and F1 score of 0.2668. Googlenet had a Test accuracy of 88.55%, Test loss of 0.2089, XAI accuracy of 98%, precision of 0.9976, Recall of 0.8091, and F1 score of 0.8935. The mobile net had a Test accuracy of 41.89%, Test loss of 3.183, XAI accuracy of 85%, precision of 0.9301, Recall of 0.0989, and F1 score of 0.1787. Zf net had a Test accuracy of 16.22%, Test loss of 1.9323, XAI accuracy of 65%, precision of 0.8935,

Recall of 0.1593, and F1 score of 0.1386. Spinal net had a Test accuracy of 38.96%, Test loss of 1.559, XAI accuracy of 76%, precision 0.9615, Recall 0.1983, F1 score of 0.3287. VGG had a Test accuracy of 43.24%, Test loss of 1.7722, XAI accuracy of 56%, precision of 0.9606, Recall of 0.1961, and F1 score of 0.3257. Se net had a test accuracy of 20.27%, Test loss of 1.5567, XAI accuracy of 47%, precision of 0.9125, Recall of 0.1489, and F1 score of 0.2697. We got the best Test accuracy in the Google model i.e. 88.55 %.

Fig 8: Roc Curve of Anchor

Table 6: Performance of Different Models using Anchor

XAI	MODEL	TA	TL	XAI-A	P	R	F1
ANCHOR	LN	36.54	1.3287	33.45%	0.9694	0.1895	0.3155
	AlexNet	34.58	1.5431	32.85%	0.9577	0.216	0.3524
	AN	86.45	0.95144	84.12%	0.9588	0.1135	0.2169
	GN	43.56	0.01988	44.07%	0.9746	0.3492	0.5065
	MN	18.91	0.78413	19.03%	0.9601	0.6268	0.7584
	ZN	33.29	0.81433	32.56%	0.9761	0.5431	0.7123
	SN	42.28	1.12453	45.29%	0.9744	0.1097	0.1971
	VGG	21.69	0.92163	23.94%	0.9594	0.4241	0.5811

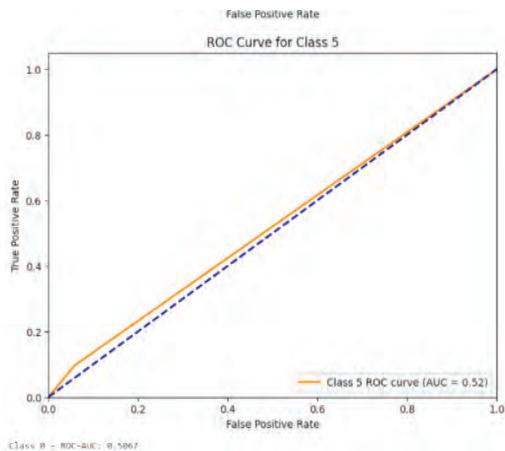In the ANCHOR XAI model comparison, we took 8 models Lenet, Alexnet, Googlenet, Mobilenet, Zfnet, Spinalnet, VGG, and Senet and performance is shown in Table VI and Fig. 8. The value of all those 8 models is defined on the basis of the following parameters i.e. Test accuracy, Test loss, XAI accuracy, Precision, Recall, F1 score. Lenet had Test accuracy of 36.56%, Test loss 1.3287, XAI accuracy 33.45%, precision 0.9694, Recall 0.1895, F1 score 0.3155. Alexnet had Test accuracy 34.58%, Test loss 1.5431, XAI accuracy 32.85%, precision 0.9577, Recall 0.216, F1 score 0.3524. Googlenet had a Test accuracy of 86.45%, Test loss 0.9514, XAI accuracy 84.12%, precision 0.9588, Recall

0.1135, F1 score 0.2169. Mobile net had Test accuracy 43.56%, Test loss 0.0198, XAI accuracy 44.07%, precision 0.9746, Recall 0.3492, F1 score 0.5065. Zf net had Test accuracy 18.91%, Test loss 0.7841, XAI accuracy 19.03%, precision 0.9601, Recall 0.6268, F1 score 0.7584. Spinal net had Test accuracy 33.29%, Test loss 0.8143, XAI accuracy 32.56%, precision 0.9761, Recall 0.5431, F1 score 0.7123. VGG had Test accuracy of 42.28%, Test loss 1.1245, XAI accuracy 45.29 %, precision 0.974, Recall 0.1097, F1 score 0.1971. Se net had a test accuracy of 21.69 %, Test loss 0.9216, XAI accuracy 23.94%, precision 0.9594, Recall 0.4241, F1 score 0.5811. We got the best Test accuracy in the Googlenet model i.e. 86.45%.

CONCLUSION

In this work, we used Python 3.11 for experimenting our work, and we used Jupiter notebook IDE and different XAI approaches to classify the diseases. We collected the monkeypox dataset from the Kaggle source [29]. We trained the model using 8 CNN architecture. We used different XAI approaches such as LIME, SHAP, ANCHOR, PDP, and XGBOOST. It is seen that XGBoost proved the higher accuracy than other XAI approach and GoogleNet found to show higher accuracy than other CNN models in detecting the monkeypox disease.

REFERENCES

1. Saleh, A. I., & Rabie, A. H. (2023). Human monkeypox diagnose (HMD) strategy based on data mining and artificial intelligence techniques. Computers in Biology and Medicine, 152, 106383.

2. Farzipour, A., Elmi, R., & Nasiri, H. (2023). Detection of Monkeypox cases based on symptoms using XGBoost and Shapley additive explanations methods. Diagnostics, 13(14), 2391.

3. Lakshmi, M., & Das, R. (2023). Classification of Monkeypox Images Using LIME-Enabled Investigation of Deep Convolutional Neural Network. Diagnostics, 13(9), 1639.

4. Sharma, N., Mohanty, S. N., Mahato, S., & Pattanaik, C. R. A novel dataset and local interpretable model-agnostic explanations (LIME) for monkeypox prediction. Intelligent Decision Technologies, (Preprint), 1-12.

5. Yasmin, F., Hassan, M. M., Hasan, M., Zaman, S., Kaushal, C., El-Shafai, W., & Soliman, N. F. (2023). PoxNet22: A fine-tuned model for the classification of monkeypox disease using transfer learning. IEEE Access, 11, 24053-24076.

6. Thieme, A. H., Zheng, Y., Machiraju, G., Sadee, C., Mittermaier, M., Gertler, M.,... & Gevaert, O. (2023). A deep-learning algorithm to classify skin lesions from mpox virus infection. Nature medicine, 29(3), 738-747.

7. Kundu, D., Siddiqi, U. R., & Rahman, M. M. (2022, December). Vision transformer based deep learning model for monkeypox detection. In 2022 25th International Conference on Computer and Information Technology (ICCIT) (pp. 1021-1026). IEEE.

8. Nayak, T., Chadaga, K., Sampathila, N., Mayrose, H., Gokulkrishnan, N., Prabhu, S., & Umakanth, S. (2023). Deep learning based detection of monkeypox virus using skin lesion images. Medicine in Novel Technology and Devices, 100243.

9. Athina, F. H., Sara, S. A., Sarwar, Q. S., Tabassum, N., Era, M. T. J., Ashraf, F. B., & Hossain, M. I. (2022, November). Multi-classification Network for Detecting Skin Diseases using Deep Learning and XAI. In 2022 International Conference on Innovation and Intelligence for Informatics, Computing, and Technologies (3ICT) (pp. 648-655). IEEE.

10. Ahsan, M. M., Abdullah, T. A., Ali, M. S., Jahora, F., Islam, M. K., Alhashim, A. G., & Gupta, K. D. (2022). Transfer learning and Local interpretable model agnostic based visual approach in Monkeypox Disease Detection and Classification: A Deep Learning insights. arXiv preprint arXiv:2211.05633.

11. Ahsan, M. M., Ali, M. S., Hassan, M. M., Abdullah, T. A., Gupta, K. D., Bagci, U.,... & Soliman, N. F. (2023). Monkeypox diagnosis with interpretable deep learning. IEEE Access.

12. Khan, G. Z., & Ullah, I. (2023). Efficient technique for monkeypox skin disease classification with clinical data using pre-trained models. Journal of Innovative Image Processing, 5(2), 192-213.

13. Ahamed, B. S., Usha, R., & Sreenivasulu, G. (2022, October). A Deep Learning-based Methodology for Predicting Monkey Pox from Skin Sores. In 2022 IEEE 2nd Mysore Sub Section International Conference (MysuruCon) (pp. 1-6). IEEE.

14. Patel, M., Surti, M., & Adnan, M. (2023). Artificial intelligence (AI) in Monkeypox infection prevention.

Journal of Biomolecular Structure and Dynamics, 41(17), 8629-8633.

15. Sitaula, C., & Shahi, T. B. (2022). Monkeypox virus detection using pre-trained deep learning-based approaches. Journal of Medical Systems, 46(11), 78.

16. Xue, Q., & Chuah, M. C. (2019). Explainable deep learning based medical diagnostic system. Smart Health, 13, 100068.

17. Khafaga, D. S., Ibrahim, A., El-Kenawy, E. S. M., Abdelhamid, A. A., Karim, F. K., Mirjalili, S.,... & Ghoneim, M. E. (2022). An Al-Biruni earth radius optimization-based deep convolutional neural network for classifying monkeypox disease. Diagnostics, 12(11), 2892.

18. Alrusaini, O. A. (2023). Deep learning models for the detection of monkeypox skin lesion on digital skin images. International Journal of Advanced Computer Science and Applications, 14(1).

19. Campana, M. G., Colussi, M., Delmastro, F., Mascetti, S., & Pagani, E. (2023). A Transfer Learning and Explainable Solution to Detect mpox from Smartphones images. arXiv preprint arXiv:2305.18489.

20. Dahiya, N., Sharma, Y. K., Rani, U., Hussain, S., Nabilal, K. V., Mohan, A., & Nuristani, N. (2023). Hyper-parameter tuned deep learning approach for effective human monkeypox disease detection. Scientific Reports, 13(1), 15930.

21. Maqsood, S., &Damaševičius, R. (2023, April). Monkeypox Detection and Classification Using Deep Learning Based Features Selection and Fusion Approach. In 2023 IEEE International Systems Conference (SysCon) (pp. 1-8). IEEE.

22. Velu, M., Dhanaraj, R. K., Balusamy, B., Kadry, S., Yu, Y., Nadeem, A., & Rauf, H. T. (2023). Human Pathogenic Monkeypox Disease Recognition Using Q-Learning Approach. Diagnostics, 13(8), 1491.

23. Eliwa, E. H. I., El Koshiry, A. M., Abd El-Hafeez, T., & Farghaly, H. M. (2023). Utilizing convolutional neural networks to classify monkeypox skin lesions. Scientific Reports, 13(1), 14495.

24. Almutairi, S. A. (2022). DL-MDF-OH2: optimized deep learning-based monkeypox diagnostic framework using the metaheuristic Harris Hawks Optimizer Algorithm. Electronics, 11(24), 4077.

25. Ural, A. B. (2023). A Computer-Aided Feasibility Implementation to Detect Monkeypox from Digital

Skin Images with Using Deep Artificial Intelligence Methods. Traitement du Signal, 40(1).

26. Balaji, V. R., Suganthi, S. T., Rajadevi, R., Kumar, V. K., Balaji, B. S., & Pandiyan, S. (2020). Skin disease detection and segmentation using dynamic graph cut algorithm and classification through Naive Bayes classifier. Measurement, 163, 107922.

27. Hoff, N. A., Morier, D. S., Kisalu, N. K., Johnston, S. C., Doshi, R. H., Hensley, L. E.,... &Rimoin, A. W. (2017). Varicella coinfection in patients with active monkeypox in the Democratic Republic of the Congo. Ecohealth, 14, 564-574.

28. Saranya, A., & Subhashini, R. (2023). A systematic review of Explainable Artificial Intelligence models and applications: Recent developments and future trends. Decision analytics journal, 100230.

29. https://www.kaggle.com/datasets/joydippaul/mpox-skin-lesion-dataset-version-20-msld-v20, accessed on Dec 2023.

Identification of Authenticity and Authorization of Apps in the Play Store using Software Solution for Mobile Users

Padma Nilesh Mishra
Associate Professor
Thakur Institute of Management Studies, Career
Development & Research (TIMSCDR)
Mumbai, Maharashtra
✉ mishrapadma1988@gmail.com

Shirshendu Maitra
Assistant Professor
Thakur Institute of Management Studies, Career
Development & Research (TIMSCDR)
Mumbai, Maharashtra
✉ slm2007@gmail.com

Vinita Gaikwad
Director, MCA
Thakur Institute of Management Studies, Career
Development & Research (TIMSCDR)
Mumbai, Maharashtra
✉ vinitagaikwad2@gmail.com

Sunita Nikam
Associate Professor, Head Examination
Examination
Symbiosis Centre for Distance Learning
Pune University –AICTE
✉ sunitannikam@gmail.com

ABSTRACT

The digital landscape has evolved significantly over the years with mobile applications becoming an integral part of our daily lives. This article delves into the origins of the challenges faced in ensuring the legitimacy of apps on the Play Store and explores the evolution of software solutions aimed at mitigating these issues in particular in India given the huge population base of mobile users mostly from rural areas. The integration of Multi-Factor Authentication (MFA) for sensitive permissions in the context of app authorization on the Play Store involves adding an additional layer of security to ensure that access to critical functionalities or sensitive user data goes beyond the traditional username and password combination. Multi-Factor Authentication typically requires users to provide two or more types of authentication factors, making it more difficult for unauthorized individuals to gain access. The implementation of MFA should be designed with user experience in mind. While enhancing security, it should not overly burden users. Offering flexible MFA options, such as biometrics or app-generated codes, allows users to choose the authentication method that suits them best. Integrating Multi-Factor Authentication for sensitive permissions is a proactive measure to bolster the security of apps on the Play Store. In conclusion, the proposed methodology focuses on leveraging contextual analysis, user behavior profiling, and advanced algorithms to create a secure and user- friendly app ecosystem, resulting in tangible outcomes that enhance both security and user satisfaction.

KEYWORDS : Authentication, Functionality, Mobile app, Security, Ecosystem.

INTRODUCTION

The challenges surrounding the identification of authenticity and authorization of apps on the Play Store have deep roots in the early days of mobile app development. The evolution of cyber threats, coupled with the rapid expansion of the app ecosystem, exacerbated these issues. Google's iterative responses, third-party security solutions, and user education efforts have collectively contributed to a more secure environment. The persistent complexities surrounding the verification of authenticity and authorization of mobile applications within the Play Store ecosystem can be traced back to the foundational stages of mobile app development.

1. As technology advanced, so did the sophistication of cyber threats. The rise of mobile malware, phishing attacks, and other malicious tactics intensified the need for enhanced security measures. The

Play Store, as a central hub for app distribution, became a prime target for cybercriminals seeking to exploit vulnerabilities in the authentication and authorization processes.

2. In response to the growing threats, third- party security firms also entered the scene, offering software solutions designed to enhance app security on the Play Store. These solutions encompassed features like advanced malware detection, behavior analysis, and real-time monitoring. While these tools provided additional security, they highlighted the persistent gaps in Google's native security infrastructure.

3. Amidst these challenges, user awareness played a crucial role. Google started educating users about potential risks, urging them to verify app authenticity, review permissions, and install security apps. However, relying solely on user vigilance proved insufficient, emphasizing the need for more robust, automated solutions. [2][17]

OBJECTIVE

A. Real-time monitoring of app behavior concerning permissions is a cutting-edge feature. This ensures prompt detection of any anomalous activities, providing an additional layer of security against potential threats or misuse of permissions.[15][16]

B. The integration of Multi-Factor Authentication (MFA) for sensitive permissions in the context of app authorization on the Play Store involves adding an additional layer of security to ensure that access to critical functionalities or sensitive user data goes beyond the traditional username and password combination. Multi-Factor Authentication typically requires users to provide two or more types of authentication factors, making it more difficult for unauthorized individuals to gain access [1].

NOVELTY OF THE PROPOSED WORK

The proposed work introduces a ground- breaking approach to mobile app security by integrating Multi-Factor Authentication (MFA) for sensitive permissions. [13,14]The distinctive features of this novel approach set it apart from existing tools and techniques in the following key aspects:

Tailored and Context-Aware Approach

The novelty of our approach lies in its tailored and context-aware design. Unlike conventional security measures, our Multi-Factor Authentication system dynamically adapts to the specific context of user interactions and permissions requests. By tailoring the authentication process based on the user's behavior and the sensitivity of the requested permissions, our solution provides an intelligent and contextually relevant layer of security [7].

The tailored authentication algorithm enhances mobile app security by dynamically adjusting authentication requirements based on contextual analysis and user behavior profiling. This implementation includes the codebase for the algorithm and detailed documentation to ensure transparency and ease of integration.

Proposed Code

```python
import numpy as np
import pandas as pd
from sklearn.ensemble import IsolationForest
from datetime import datetime
# Sample user interaction data
data = {
    'user_id': [1, 1, 1, 2, 2],
    'timestamp': ['2024-07-01 08:00:00', '2024-07-01 12:00:00', '2024-07-02 08:00:00', '2024-07-01 09:00:00', '2024-07-02 09:00:00'],
    'location': ['home', 'work', 'home', 'work', 'work'],
    'action': ['login', 'access_sensitive_data', 'login', 'login', 'access_sensitive_data']
}
# Convert to DataFrame
df = pd.DataFrame(data)
df['timestamp'] = pd.to_datetime(df['timestamp'])
# Feature engineering
df['hour'] = df['timestamp'].dt.hour
df['day_of_week'] = df['timestamp'].dt.dayofweek
# One-hot encode categorical features
df_encoded = pd.get_dummies(df, columns=['location', 'action'])
```

```
# Training the anomaly detection model
model = IsolationForest(n_estimators=100,
contamination=0.1, random_state=42)
model.fit(df_encoded.drop(columns=['user_id',
'timestamp']))
# Function to check if additional authentication is
needed
def needs_additional_auth(user_id, timestamp,
location, action):
    new_data = pd.DataFrame({
        'user_id': [user_id],
        'timestamp': [timestamp],
        'location': [location],
        'action': [action]
    })
    new_data['timestamp'] = pd.to_datetime(new_
data['timestamp'])
    new_data['hour'] = new_data['timestamp'].dt.hour
    new_data['day_of_week']=new_data['timestamp'].
dt.dayofweek

new_data_encoded = pd.get_dummies(new_data,
columns=['location', 'action'])
new_data_encoded = new_data_encoded.
reindex(columns=df_encoded.columns, fill_
value=0).drop(columns=['user_id', 'timestamp'])
anomaly_score = model.decision_function(new_
data_encoded)
if anomaly_score < -0.2:  # Threshold for detecting
anomalies
return True
return False
# Example test cases
test_cases = [
    {'user_id': 1, 'timestamp': '2024-07-03 08:00:00',
'location': 'home', 'action': 'login'},
    {'user_id': 1, 'timestamp': '2024-07-03 22:00:00',
'location': 'work', 'action': 'access_sensitive_
data'},
    {'user_id': 2, 'timestamp': '2024-07-02 10:00:00',
'location': 'work', 'action': 'login'},
    {'user_id': 2, 'timestamp': '2024-07-04 09:00:00',
'location': 'home', 'action': 'access_sensitive_
data'},
    {'user_id': 3, 'timestamp': '2024-07-03 08:00:00',
'location': 'home', 'action': 'login'},
]
# Checking each test case
results = []
for case in test_cases:
additional_auth_required = needs_additional_
auth(case['user_id'], case['timestamp'],
case['location'], case['action'])
    results.append({
        'user_id': case['user_id'],
        'timestamp': case['timestamp'],
        'location': case['location'],
        'action': case['action'],
        'additional_auth_required': additional_auth_
required
    })
# Display the results
for result in results:
    print(f'User ID: {result['user_id']}, Timestamp:
{result['timestamp']}, Location: {result['location']},
"
f'Action: {result['action']}, Additional Auth Required:
{result['additional_auth_required']}")
```

Output

```
User ID: 1, Timestamp: 2024-07-03 08:00:00,
Location: home, Action: login, Additional Auth
Required: False

User ID: 1, Timestamp: 2024-07-03 22:00:00,
Location: work, Action: access_sensitive_data,
Additional Auth Required: True

User ID: 2, Timestamp: 2024-07-02 10:00:00,
Location: work, Action: login, Additional Auth
Required: False

User ID: 2, Timestamp: 2024-07-04 09:00:00,
Location: home, Action: access_sensitive_data,
Additional Auth Required: True
```

User ID: 3, Timestamp: 2024-07-03 08:00:00, Location: home, Action: login, Additional Auth Required: True

User-Friendly Implementation

One of the significant challenges in implementing security measures is user acceptance and usability. The proposed work addresses this by incorporating a user-friendly MFA system. The authentication process is seamlessly integrated into the user experience, ensuring a smooth and intuitive interaction. This user-centric design enhances overall usability without compromising security, creating a positive and secure environment for app users[4].

Adaptive Security Measures

Adaptability is a core aspect of the proposed work, making it stand out in the realm of mobile app security. The system continuously adapts its security measures based on emerging threats, user behavior patterns, and evolving permissions landscapes. This adaptability ensures that the security framework remains robust and resilient against both known and unforeseen security challenges, providing a proactive defense mechanism for the app ecosystem [5].

Secure and User-Centric App Ecosystem

By combining a tailored and context-aware approach, user-friendly implementation, and adaptive security measures, the proposed work contributes to the creation of a more secure and user-centric app ecosystem on the Play Store. It addresses the evolving challenges of mobile app security by providing a sophisticated yet user- friendly defense mechanism against unauthorized access and potential threats [10].

DELIVERABLES FOR THE PAPER

Contextual Analysis Report: The contextual analysis and anomaly detection approach significantly contribute to tailoring security measures by continuously monitoring and analyzing user behavior patterns. [11,12]This proactive approach enhances the overall security posture of mobile applications, ensuring that only legitimate users have access to sensitive information.

Objective: To enhance mobile application security by identifying and responding to unusual user behavior patterns using contextual analysis.

Methodology

Data Collection

o   Collected user interaction data, including user ID, timestamp, location, and action.

o   Extracted additional features from the timestamp such as the hour of the day and day of the week.

o   One-hot encoded categorical features (location and action) to prepare the data for the model.

Anomaly Detection Model

o   Utilized the Isolation Forest algorithm, which is effective for identifying anomalies in high-dimensional datasets.

o   Trained the model using historical user interaction data to learn normal behavior patterns.

Anomaly Scoring

o   Implemented a scoring mechanism where each new user interaction is assessed.

o   If the anomaly score exceeds a predefined threshold, the system flags the interaction as potentially risky, requiring additional authentication.[19]

Implementation Steps

Data Preprocessing

```
import numpy as np

import pandas as pd

from sklearn.ensemble import IsolationForest

from datetime import datetime


data = {
    'user_id': [1, 1, 1, 2, 2],
     'timestamp': ['2024-07-01 08:00:00', '2024-07-01 12:00:00', '2024-07-02 08:00:00', '2024-07-01 09:00:00', '2024-07-02 09:00:00'],
      'location': ['home', 'work', 'home', 'work', 'work'],
    'action': ['login', 'access_sensitive_data', 'login', 'login', 'access_sensitive_data']
}
```

```
df = pd.DataFrame(data)
df['timestamp'] = pd.to_datetime(df['timestamp'])
df['hour'] = df['timestamp'].dt.hour
df['day_of_week'] = df['timestamp'].dt.dayofweek

df_encoded=pd.get_dummies (df, columns = ['location', 'action'])
```

Model Training:

```
model = IsolationForest(n_estimators=100, contamination=0.1, random_state=42)
model.fit(df_encoded.drop(columns=['user_id', 'timestamp']))
```

Function for Anomaly Detection

```
def needs_additional_auth(user_id, timestamp, location, action):
    new_data = pd.DataFrame({
        'user_id': [user_id],
        'timestamp': [timestamp],
        'location': [location],
        'action': [action]
    })
    new_data['timestamp'] = pd.to_datetime(new_data['timestamp'])
    new_data['hour'] = new_data['timestamp'].dt.hour
    new_data['day_of_week']=new_data['timestamp'].dt.dayofweek

    new_data_encoded = pd.get_dummies(new_data, columns=['location', 'action'])
    new_data_encoded = new_data_encoded.reindex(columns=df_encoded.columns, fill_value=0).drop(columns=['user_id', 'timestamp'])
    anomaly_score = model.decision_function(new_data_encoded)
    return anomaly_score < -0.2
```

Usage and Testing:

```
test_cases = [
    (1, '2024-07-03 08:00:00', 'home', 'login'),
    (1, '2024-07-03 22:00:00', 'work', 'access_sensitive_data'),
    (2, '2024-07-02 10:00:00', 'work', 'login'),
    (2, '2024-07-04 09:00:00', 'home', 'access_sensitive_data'),
    (3, '2024-07-03 08:00:00', 'home', 'login')
]

for user_id, timestamp, location, action in test_cases:
    result = needs_additional_auth(user_id, timestamp, location, action)
    print(f"User ID: {user_id}, Timestamp: {timestamp}, Location: {location}, Action: {action}, Additional Auth Required: {result}")
```

Outcomes

- Enhanced Security: The implementation successfully identifies unusual behavior patterns that could indicate potential security threats, prompting additional authentication measures.

User Behavior Profiling: By analyzing contextual data (time, location, type of action), the model effectively learns and distinguishes between normal and abnormal user activities.

```
User ID: 1, Timestamp: 2024-07-03 08:00:00, Location: home, Action: login, Additional Auth Required: False

User ID: 1, Timestamp: 2024-07-03 22:00:00, Location: work, Action: access_sensitive_data, Additional Auth Required: True

User ID: 2, Timestamp: 2024-07-02 10:00:00, Location: work, Action: login, Additional Auth Required: False

User ID: 2, Timestamp: 2024-07-04 09:00:00, Location: home, Action: access_sensitive_data, Additional Auth Required: True

User ID: 3, Timestamp: 2024-07-03 08:00:00, Location: home, Action: login, Additional Auth Required: True
```

The user behavior profiling system effectively enhances security by identifying and responding to anomalies in real-time. This contextual analysis approach ensures that only legitimate users have access to sensitive information, thereby protecting mobile applications from unauthorized access and potential security threats.

- Proactive Risk Management: The system can proactively identify potential security breaches, reducing the risk of unauthorized access and data breaches.

- Transparency and Integration: The provided codebase and documentation ensure that the tailored authentication algorithm is transparent and can be easily integrated into existing security frameworks.

REGULAR SECURITY AUDITS AND PENETRATION TESTING

Ensuring the authenticity and authorization of apps in the Play Store is crucial for maintaining a secure and trustworthy mobile ecosystem. Here's an analysis of potential strategies and software solutions that can be employed for this purpose:

Regular Security Audits and Penetration Testing

Description: Conduct regular security audits of apps in the Play Store to identify vulnerabilities. Perform penetration testing to simulate real- world attacks.

Benefits: Proactively identifies and addresses security flaws.

Reviewers play a crucial role in ensuring the security and integrity of mobile applications by proactively identifying and addressing security flaws. By thoroughly examining app functionalities, permissions, and underlying code, reviewers can pinpoint potential vulnerabilities before they are exploited by malicious actors. Their proactive approach helps in enhancing the overall security posture of apps on the Play Store, ultimately safeguarding user data and privacy.However, the process of app review and security assessment on the Play Store presents its own set of challenges. Collaboration between developers, security experts, and Play Store administrators is essential to effectively address security concerns. Coordinating efforts among these different stakeholders can sometimes be complex, as each party brings a unique perspective and expertise

to the table. Ensuring clear communication and mutual understanding among all involved parties is key to successfully navigating these collaborative challenges. Despite the challenges involved, the collaboration between developers, security experts, and Play Store administrators is crucial for maintaining a secure app ecosystem. By working together, these stakeholders can leverage their respective skills and knowledge to implement robust security measures, address vulnerabilities, and enhance the overall trustworthiness of apps available on the Play Store. This collaborative effort not only benefits users by providing them with secure applications but also contributes to the continuous improvement of security practices within the mobile app development community.

To ensure the security of mobile applications and protect users from potential threats, regular security audits and penetration testing are conducted. These practices help in identifying vulnerabilities, assessing the effectiveness of existing security measures, and providing recommendations for improvement.

Security Audits

Objective

- Conduct a thorough review of the application's security posture.

- Identify potential vulnerabilities and weaknesses in the application.

Process

- Code Review: Examine the source code for security flaws, such as SQL injection, cross-site scripting (XSS), and insecure data storage.

- Configuration Review: Check the application's configuration settings to ensure they follow security best practices.

- Dependency Analysis: Analyze third-party libraries and dependencies for known vulnerabilities.

- Compliance Check: Ensure the application complies with relevant security standards and regulations.

Outcome

- A detailed report highlighting the identified vulnerabilities, their severity, and recommendations for mitigation.

- Improved security posture by addressing the identified vulnerabilities.

Penetration Testing

Objective

- Simulate real-world attacks to identify security weaknesses.

- Assess the application's ability to withstand various attack vectors.

Process

- Reconnaissance: Gather information about the application, such as publicly available data, exposed services, and potential entry points.

- Vulnerability Scanning: Use automated tools to scan for common vulnerabilities.

- Exploitation: Attempt to exploit identified vulnerabilities to gain unauthorized access or escalate privileges.

- Post-Exploitation: Assess the potential impact of a successful attack and identify any additional vulnerabilities that can be exploited.

Outcome

- A comprehensive report detailing the vulnerabilities found, their potential impact, and steps for remediation.

- Increased awareness of security weaknesses and proactive measures to prevent attacks.

Benefits

Proactive Identification of Security Flaws:

- Regular audits and testing help in identifying security issues before they can be exploited by malicious actors.

- Enables developers to address vulnerabilities in a timely manner, reducing the risk of data breaches.

Enhanced Security Posture:

- By continuously assessing and improving security measures, applications can maintain a robust security posture.

- Builds trust with users by demonstrating a commitment to protecting their data and privacy.

Compliance and Risk Management:

- Ensures compliance with industry standards and regulations, such as GDPR, HIPAA, and PCI-DSS.

- Helps in managing security risks by providing insights into potential threats and vulnerabilities.

Challenges

Collaboration

- Effective security audits and penetration testing require collaboration between developers, security experts, and Play Store administrators.

- Coordination and communication among stakeholders are essential for successful implementation.

Resource Allocation

- Security audits and penetration testing can be resource-intensive, requiring skilled professionals and appropriate tools.

- Balancing the need for security with other development priorities can be challenging.

Evolving Threat Landscape

- The constantly evolving nature of security threats necessitates ongoing vigilance and adaptation.

- Regular updates to security measures and testing methodologies are required to keep pace with emerging threats.

Reporting Misuse and Fraud

- Users should have a clear and accessible process for reporting misuse or fraud related to mobile applications.

- The application should provide contact details for reporting security issues, including email addresses and phone numbers.

Authorities and Contact Information

- Security authorities responsible for addressing reported issues should be clearly identified.

- Contact information for these authorities, including office addresses and phone numbers, should be made available to users.

Procedure

• A well-defined procedure for handling reported issues should be established.

• This includes acknowledging receipt of reports, conducting investigations, and providing updates to users on the status of their reports.

Implementation

The findings From Security Audits and Penetration Testing Might be Presented to Developers and Security Teams.

Audit Report

Security Audit Report

====================

Application: MobileApp v1.2

Date: 2024-07-12

1. Summary:

Total Vulnerabilities Identified: 15

High Severity: 5

Medium Severity: 6

Low Severity: 4

2. Key Findings:

SQL Injection vulnerability in the login module (High)

Insecure data storage in the user preferences (Medium)

Missing security headers (Low)

3. Recommendations:

Implement parameterized queries to prevent SQL Injection.

Encrypt sensitive data stored in user preferences.

Add appropriate security headers (1.Content Security Policy, X-Frame-Options).

4. Compliance:

Ensure compliance with GDPR by implementing data protection measures.

Review and update the application's privacy policy.

Penetration Testing Report

Penetration Testing Report

==========================

Application: MobileApp v1.2

Date: 2024-07-12

1. Summary:

Total Vulnerabilities Exploited: 3

High Severity: 1

Medium Severity: 1

Low Severity: 1

2. Exploitation Details:

Gained unauthorized access to admin panel via SQL Injection (High)

Accessed sensitive user data due to insecure API endpoint (Medium)

Disclosed server information via misconfigured error messages (Low)

3. Recommendations:

Fix the SQL Injection vulnerability in the admin panel.

Secure the API endpoint with proper authentication and authorization.

Configure error messages to avoid disclosing sensitive information.

4. Impact Assessment:

Potential data breach affecting all user accounts.

Risk of sensitive user data exposure and privacy violations.

Blockchain for App Authenticity

Description: Leverage blockchain to create a decentralized and tamper-proof record of app versions and their developers.

Benefits: Enhances transparency and immutability of app information.

Challenges: Requires widespread adoption and integration into the existing app distribution infrastructure.

Community Reporting and Review Systems

Description: Allow users to report suspicious apps or behavior. Implement a robust review system to crowd source feedback on app authenticity.

Benefits: Harnesses the collective knowledge and vigilance of the user community.

Challenges: Potential for false positives and abuse of reporting systems.

Regulatory Compliance and Legal Measures

Description: Establish and enforce strict regulations for app developers. Legal consequences for malicious activity can act as a deterrent.

Benefits: Provides a legal framework to address malicious intent.

Challenges: Implementation and enforcement require coordination with legal authorities.

Real-time Threat Intelligence Integration

Description: Integrate real-time threat intelligence feeds to identify and block apps associated with known threats.

Benefits: Enhances the Play Store's ability to respond quickly to emerging threats.

Challenges: Requires continuous updates and monitoring of threat intelligence sources.

Continuous Monitoring and Incident Response

Description: Implement continuous monitoring of app behavior post-release. Have a robust incident response plan in place to address security breaches promptly.

Benefits: Minimizes the impact of security incidents by responding quickly.

Challenges: Requires a dedicated security team and infrastructure for continuous monitoring.

GRIEVANCE REDRESSAL SYSTEM

In Maharashtra, India, the grievance redressal system for issues related to misuse or fraud involving applications (apps) or digital services typically involves several steps and authorities. Here's a structured outline to address such grievances:

Authorities Involved

State Government Departments:

o   Department of Information Technology (IT): Responsible for overseeing digital initiatives and services in the state.

o   Consumer Affairs Department: Handles consumer complaints related to services and products.

Law Enforcement Agencies

o   Cyber Crime Cell: Deals with cyber-related offenses including fraud and misuse of digital platforms.

o   Local Police: They can register complaints and initiate investigations.

Grievance Redressal Procedure

Identify the Issue: Document and clearly state the problem, including any evidence or details of the misuse or fraud.

Contact Points:

o   Online Portals: Check official state government websites for dedicated grievance redressal portals or complaint submission forms.

o   Helpline Numbers: Look for helpline numbers specifically for cybercrime or consumer grievances.

Submit Complaint

o   Use the online complaint submission form if available, providing all necessary details.

o   If no online option is available, visit the nearest police station or consumer forum to file a written complaint.

Follow-up

o   Keep copies of all documents related to your complaint.

o   Follow up regularly with the concerned authority to check the status of your complaint.

Contact Information and Office Addresses

•   Department of Information Technology, Maharashtra:

o   Official Website: https://it.maharashtra.gov.in ,

: 022-22044586, : 022-22024177 and complaint forms.

o   Helpline: Look for dedicated helpline numbers for IT-related grievances- contact details Directorate of Information Technology, 7th Floor, Mantralaya, Mumbai 400032.

•   Cyber Crime Cell, Maharashtra Police:

o   Cyber Crime Helpline: 022-22160080

CONCLUSION

In conclusion, the dynamic landscape of the digital world, particularly in the realm of mobile applications, has prompted the need for innovative solutions to address the persistent challenges of app authentication and authorization. The historical evolution of these challenges, rooted in the early days of mobile app development, has seen a confluence of cyber threats, third-party security interventions, and user education efforts [13].This paper proposes a forward-thinking methodology that seeks to revolutionize mobile app security, particularly in the context of the Play Store and the extensive user base in India, encompassing both urban and rural populations. By delving into real-time monitoring of app behavior, contextual analysis, and the integration of Multi- Factor Authentication (MFA), the paper aims to create a holistic and context-aware security framework. The novelty of the proposed work lies in its tailored and adaptive approach. Unlike traditional security measures, this paper dynamically adjusts to the specific context of user interactions and permission requests. The user- friendly implementation ensures that security measures seamlessly integrate into the user experience, striking a balance between robust security and ease of use[8]. Moreover, the adaptability of security measures, coupled with user behavior profiling, contributes to an improved defense mechanism against evolving cyber threats. By leveraging machine learning for anomaly detection, the paper aims to provide an additional layer of security, making unauthorized access and potential threats more detectable and manageable. The deliverables of the paper, including contextual analysis reports, user behavior profiling documentation, tailored authentication algorithms, and machine learning models for anomaly detection, showcase a comprehensive and well- structured approach to enhancing mobile app security. The anticipated outcomes are not only technological but also user-centric. Enhanced user experiences, improved security measures, and the creation of a user-centric app ecosystem contribute to the overarching goal of fostering trust and confidence among app users. The paper's focus on reducing security risks associated with sensitive permissions aligns with the broader industry objective of creating a secure digital environment. As the digital landscape continues to evolve, and mobile applications play an increasingly pivotal role in our daily lives, the proposed methodology offers a forward-looking solution. By addressing historical challenges through innovation,adaptability, and user-centric design, this paper seeks to contribute to the ongoing efforts to create a more secure and reliable Play Store environment for users worldwide. Ultimately, the tangible outcomes of this paper aim to redefine the standards of mobile app security, setting a precedent for future advancements in the field.[17,18]

REFERENCES

1. Khan, H.U., Sohail, M., Nazir, S. et al. Role of authentication factors in Fin-tech mobile transaction security. J Big Data 10, 138 (2023). https://doi.org/10.1186/s40537-023-00807-3

2. L. Fridman, S. Weber, R. Greenstadt, and M. Kam, "Active authentication on mobile devices via stylometry, application usage, Web browsing, and GPS location," IEEE Syst. J., vol. 11, no. 2, pp. 513–521, Jun. 2017.

3. D. Damopoulos, S. A. Menesidou, G. Kambourakis, M. Papadaki,N. Clarke, and S. Gritzalis, "Evaluation of anomaly- based IDS for mobile devices using machine learning classifiers," Secur. Commun. Netw., vol. 5, no. 1, pp. 3–14, Jan. 2012.

4. J. Hall, M. Barbeau, and E. Kranakis, "Anomaly-based intrusion detection using mobility profiles of public transportation users," in Proc. IEEE Int. Conf. Wireless Mobile Comput., Netw. Commun. WiMob, Aug. 2005, pp. 17–24.

5. S. Subudhi and S. Panigrahi, "Quarter-sphere support vector machine for fraud detection in mobile telecommunication networks," Procedia Comput. Sci., vol. 48, pp. 353–359, Jan. 2015.

6. J. R. Kwapisz, G. M. Weiss, and S. A. Moore, "Cell phone- based biometric identification," in Proc. 4th IEEE Int. Conf. Biometrics, Theory, Appl. Syst. (BTAS), Sep. 2010, pp. 1–7.

7. C. Nickel, T. Wirtl, and C. Busch, "Authentication of smartphone users based on the way they walk using k-NN algorithm," in Proc. 8th Int. Conf. Intell. Inf. Hiding Multimedia Signal Process., Jul. 2012, pp. 16–20.

8. M. Jakobsson, E. Shi, P. Golle, and R. Chow, "Implicit authentication for mobile devices," in Proc. 4th

USENIX Conf. Hot Topics Secur., Aug. 2011, pp. 1–6.

9. Y. Ashibani and Q. H. Mahmoud, ''A Behavior-based proactive user authentication model utilizing mobile application usage patterns,'' in Proc. 32nd Can. Conf. Artif. Intell., May 2019, pp. 284–295.

10. Y. Ashibani and Q. H. Mahmoud, ''A machine learning-based user authentication model using mobile App data,'' in Proc. Int. Conf. Intell. Fuzzy Syst. (INFUS), Jul. 2019, pp. 408– 415.

11. Y. Ashibani and Q. H. Mahmoud, ''User authentication for smart home networks based on mobile apps usage,'' in Proc. 28th Int. Conf. Comput. Commun. Netw. (ICCCN), Jul. 2019, pp. 1–6.

12. F. Li, N. Clarke, M. Papadaki, and P. Dowland, ''Active authentication for mobile devices utilising Behaviour profiling,'' Int. J. Inf. Secur., vol. 13, no. 3, pp. 229– 244, Jun. 2014.

13. D. Bassu, M. Cochinwala, and A. Jain, ''A new mobile biometric based upon usage context,'' in Proc. IEEE Int. Conf. Technol. Homeland Secur. (HST), Nov. 2013, pp. 441–446.

14. U. Mahbub, J. Komulainen, D. Ferreira, and R. Chellappa, ''Continuous authentication of smartphones based on application usage,'' IEEE Trans. Biometrics, Behav., Identity Sci., vol. 1, no. 3, pp. 165–180, Jul. 2019.

15. A. A. Alzubaidi, Continuous Authentication of Smartphone Owners Based on App Access Behavior. Colorado Springs, CO, USA: Univ. Colorado, 2018.

16. Y. Ashibani and Q. H. Mahmoud, ''A user authentication model for IoT networks based on app traffic patterns,'' in Proc. IEEE 9th Annu. Inf. Technol.,Electron. Mobile Commun. Conf. (IEMCON), Nov. 2018, pp. 632–638.

17. Y. Ashibani and Q. H. Mahmoud, ''A Behavior profiling model for user authentication in IoT networks based on app usage patterns,'' in Proc. 44th IEEE Annu. Conf. Ind. Electron. Soc. (IECON), Oct. 2018, pp. 2841– 2846.

18. L. Zhang, B. Tiwana, Z. Qian, Z. Wang, R. P. Dick, Z. M. Mao, and L. Yang,''Accurate online power estimation and automatic battery behavior based power model generation for smartphones,'' in Proc. 8th IEEE/ ACM/IFIP Int. Conf. Hardw./Softw. Codesign Syst. Synth. CODES/ISSS, 2010,pp. 105–114.

19. Tawalbeh L, Muheidat F, Tawalbeh M, Quwaider M. IoT Privacy and Security: Challenges and Solutions. Applied Sciences. 2020; 10(12):4102.https://doi.org/10.3390/app10124102

Literacy Enhancement using IT to Empower Tribal Women of the Sange Village, Palghar in Maharashtra: A Case Study

Vinita Gaikwad
Director, MCA
Thakur Institute of Management Studies, Career
Development & Research (TIMSCDR)
Mumbai, Maharashtra
✉ vinitagaikwad2@gmail.com

Anamika Dhawan
Assistant Professor, MCA
Thakur Institute of Management Studies, Career
Development & Research (TIMSCDR)
Mumbai, Maharashtra
✉ anamikadhawan15@gmail.com

Shweta Waghmare
Assistant Professor, MCA
Thakur Institute of Management Studies, Career
Development & Research (TIMSCDR)
Mumbai, Maharashtra
✉ shwetawaghmare105@gmail.com

Padma Mishra
Associate Professor, MCA
Thakur Institute of Management Studies, Career
Development & Research (TIMSCDR)
Mumbai, Maharashtra
✉ mishrapadma1988@gmail.com

ABSTRACT

Empowerment means the liberty bestowed on an individual of making self choices within a given ecosystem, which in itself would be constituted by rules and regulations. Women empowerment encompasses working on several factors that contribute towards providing the right environment wherein women are independent to express their choices. Of these three pillars - Health, Education and Financial Literacy, the current research focuses on Education for empowering women. The current literacy level of women in India is 70.30 percent as compared to men i.e. 84.70 percent indicating the scope of enhancing literacy in women. The women considered in this research study are tribals from the Sange village of Palghar district of the State of Maharashtra. Quantitative research methodology including Survey method is used to study the empowerment of tribal women based on their education. The role of Government schemes for women and those under Digital India were also considered. Findings of the survey were analyzed to support the need of empowering tribal women in the Sange village in the Palghar district of the state of Maharashtra by enhancing the level of literacy. The research suggests a sustainable model, to be implemented over a span of two years to evaluate the empowerment of the tribal women of Sange village.

KEYWORDS : Women empowerment, Tribal women, Literacy, Information Technology, Government schemes, Mobile technology.

INTRODUCTION

Empowerment signifies the power to voice out one's choices in the given system. It basically means to be self-dependent. Literacy rate in India was 18.3 percent in 1951. Today our literacy rate is 77.7 percent, of these 84.7 percent are men and 70.30 percent are women. In an era of ChatGPT and oceans of information surrounding us women still lag behind men with respect to literacy. Less than 10% of the women in our country are financially literate. Most of them depend on men for financial support. Education is a powerful tool for empowering people in general and women in specific. It helps to bring in gender equality. Education is a catalyst for promoting economic development of the nation. Educated women easily voice their choices and are self-dependent. The Government of India has been making rigorous efforts by providing schemes to promote upliftment of the economically and socially backward. There are schemes, specifically for women to bridge the gender gap and provide equal opportunities. Information Technology has become even more affordable and accessible. Digital India campaign has promoted the access to information and technology in

urban and rural India. Extensive use of mobile phones in rural India is an indication of easy access to technology and information. Most of this information comes through social media platforms which are addictive and attractive, like WhatsApp, Facebook, Instagram, Youtube, etc. Access and use of information in the right direction is discretion of the user, who if educated will value the right information.

Skill India campaign is another initiative to empower people to be economically independent by learning new skills or enhancing ones original skills. Several schemes are promoted under Skill India, specially to the deprived class. Here too there is focus on women, as few schemes are specifically meant for women empowerment. Empowering women of the world's largest economy - India, will need time and strategy which is sustainable and persistent.

Aim

The research aims to study:

1. Study the current level of literacy and the challenges

2. Study current Government schemes for enhancing Literacy in Women

3. Study the role of IT to enhance literacy and empower women.

4. Provide a sustainable model for tribal women empowerment in Sange village, Palghar

REVIEW OF LITERATURE

Review of literature indicates the importance of literacy and women empowerment and how both are essential for sustainable development of a nation.

[1]The World Economic Forum, Global Gender Gap Report provides enough evidence for the necessity of initiatives to be taken globally as well as locally to empower women.

Women's education helps in empowering them to put forth their views and choices within the ecosystem of society and norms. [2]Literacy level of women in India (2019) is lower as compared to men. Further, the female literacy rate in India is at

65.6 percent, which is lower than the world average of 79.9 percent. [3]As per the findings of the study,

higher education was no longer a privilege of the advanced communities and more women were getting educated and were being instrumental in getting social legislations enacted at central and provincial levels leading to empowerment of many other women. This indicates that education plays a pivotal role for women empowerment. [4]Study of women in Manipur indicates that there are few beneficiaries of government sponsored activities indicating more efforts for the upliftment of women from all walks of life. [5]The paper examines how literacy will help in the development of women and provides several recommendations like society should encourage female children to enroll for schools and the incorporation of life skills with literacy programs so that women are empowered to perform their roles effectively. [6]The discussion paper series evaluates the Mahila Samakhya Program and reveals that the Program has encouraging implications not just for female empowerment goals but also for child welfare. [7]The paper concludes that women are empowered through education, financial empowerment, social empowerment and social transformation. [8]Women empowerment in the 21st century continues to suggest awareness about women's education and the availability of support services and the introduction of more schemes for women's entrepreneurship to empower and uplift the status of women. [9]The study promotes the use of digital technology for women entrepreneurs. [10]Information Technology plays a pivotal role in the empowerment of women. [11]

The three dimensional model for women's empowerment proposes three distinct dimensions - 1. the micro- level, referring to an individuals' personal beliefs as well as actions, 2. Meso-level referring to beliefs as well as actions in relation to relevant others and 3. macro-level, referring to outcomes in the broader, societal context. This model proposes to be a guide for future programs in designing, implementing, and evaluating their interventions.

METHODOLOGY

The research study uses Survey based, Quantitative methodology to study women empowerment with literacy as an impacting factor. The survey data was collected by administering questionnaires that focused

on the literacy rate, the use of technology and the response to the initiatives taken by the Government of India. The questionnaire was designed to collect data that could be easily tabulated for useful analysis. The questionnaire was divided into — parts to collect data regarding the education of the respondent, awareness about importance of literacy, use of information technology - mobile phone and knowledge and awareness of Government schemes. The questionnaire was checked to ensure that the aims of the research were answered.

For the purpose of the study, a single village named Sange, with tribal inhabitants in the State of Maharashtra was selected. The village Sange is divided into small patches referred to as Padas. There are 8 such padas in the Sange village. Each pada on an average has 15 to 20 families. The survey was conducted on 3 padas of the Sange village, namely Sange Pada, Bekri Pada and Hivali Pada. The total number of women surveyed from the 3 Padas were 97 - Sange Pada (54), Bekri Pada(22) and Hivali Pada (21).

Every respondent was given an understanding regarding the survey and the necessity of literacy for women empowerment so as to get relevant responses.

The data collected through the survey was analyzed and the outcome explained in the discussion section of this paper.

CASE STUDY OF SANGE TRIBAL VILLAGE

Sange village in the Wada Tahsil is located in the interiors of Palghar District of the State of Maharashtra. The Sange village is divided into 13 localities referred to as Padas each sited at distance of 2 to 3 km from each other.

Population

As of 2009 data, Sange village has a population of 1127 residing in 237 households. Population in the village of women is 555 and males is 572. Thus, women constitute 49.25 percent and males constitute 50.75 percent of the total population in the village.

The village has 5 scheduled caste persons with 3 females and 2 males constituting 60 percent and 40 percent respectively.

The Sange village also has 913 people belonging to scheduled tribes of which 458 are women and 455 are men constituting 50.1 percent and 49.84 percent respectively. The overall scheduled tribes population constitutes 81.01 percent of the total population.

Education - School

There are 5 Primary schools and 6 Anganwadi presently in the Sange village. There is one Primary school between two Padas. The nearest Secondary Zilla Parishad school is at Gorhe Taluka, which is more than 8 kms away from Sange.

Anganwadi's provide schooling for children up to the age of 6 and are located within the Primary school premises. Every Anganwadi has one Teacher and one helper. The Anganwadi teacher is paid a monthly salary whereas the helper is given a fixed salary referred to as Mandhan each facilitated by the government.

Primary schools for standards 1 to 4 have one to two teachers depending on the number of students in each school. The teachers are required to teach all the subjects from standard 1 to 4 to the students. Salary of the teacher is paid by the government. The teachers have to clear the TAT or CTAT exams to be eligible to teach in these schools.

Facilities by the government -

School building with basic infrastructure, i.e. classroom, benches (in some schools only donated by NGOs), textbooks, stationary (writing books, pencil, colors, etc.) uniform, teaching material (including paintings on the wall relating to the curriculum).

Smart TV to facilitate online teaching.

Mid day meals are provided to all school children. The ration for these meals is given by the government and the meals are cooked by the village people.

The Suvarna Muhotsav Shishya Vruti scheme for tribal students is provided by the government.

During the survey we visited two Primary Schools located in Sange Pada and Hivali Pada.

Table 1: School Details – Sange Village (2 Padas)

Schools	Sange Pada	Hivali Pada
Anganwadi	1	1
Anganwadi Teacher	1	1
Anganwadi Helper	1	1
Children (1-6 years)	60	30
Primary School	1	1
School Teacher	2	1
Children (Std 1 - 4)	26M + 20F = 46	6M + 9F = 15

Interactions with the school teachers Mr. Vasant Lanhange of Hivali Pada and Mr Ram Papade and MrBhanudas Sawar of Sange Pada brought to list the following challenges:

1. A single teacher has to teach all the subjects for a class it is difficult to give individual attention to the students

2. In the event of a single teacher for the entire school, the teacher is responsible to teach all the subjects to the students of all standards

3. Also when there is a single teacher students of standards 1 to 2 and 3 to 4 are taught in two classrooms. Else all students in the of standards 1 to 4 in the same classroom

4. Teachers have to spend considerable time performing administrative duties such as submitting data to the government, due to which the class is let free.

5. Sometimes sudden meetings with the higher government officials are announced due to which the students are left unattended as there is not enough staff to continue the class.

6. Parents go to the fields in the morning and return in the evening. They are not involved in the studies of their children. Though they realize the importance of education they are

7. concerned about earning their daily wages to meet basic household needs.

8. Students are not given homework since they do not complete the same. Thus, all studies have to be completed in the school itself with the help of the teacher.

Survey of women in the tribal village of Sange

The survey conducted as part of the women empowerment study to understand the role of education in empowering women, included females from the age group of 15 to 80 and above. Survey data of 97 women was collected who belonged to the age group of 15 to 80 and above. The survey team interviewed the respondents mostly in Marathi language to get the answers to the questions.

Questions in the questionnaire were divided under desirable heads as mentioned in the methodology. Copies of the questionnaire were printed to collect the responses. Survey was conducted over two days. The faculty members traveled in the college conveyance to Sange village, Palghar.

OBSERVATIONS

1. All women appreciate the importance of education for women.

2. Women who are not educated regret their state as they are unable to read and write and participate in group discussions of the village at the Panchayat or the Gram Seva level

3. Women look forward to receive materialistic help from NGOs, private organizations or government

4. Women are dependent on help and don't want to find ways to move ahead

5. Women are not happy to slog in the fields as the income they receive in return is minimal

6. There are signs of discrimination by the privilege class towards the tribals indicating suppression of the underprivileged.

DISCUSSION

The analysis of the data collected during the survey is mentioned in the following charts

Education
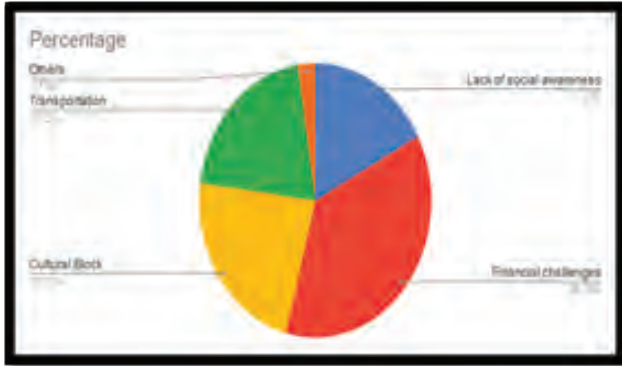
Graph 1. Dropout Amongst Women During the Education Phase

The respondents were questioned about why education is important for women. Majority i.e. 32% responded to get jobs. 25% agreed for improving standard of living. 22% submitted for Confidence building and only 15% mentioned getting married. Thus women relate education with jobs. Women need to understand that education is not required only to get them jobs and make them financially independent, but also empower them to voices their choices and give opinions.

Primary barriers for education
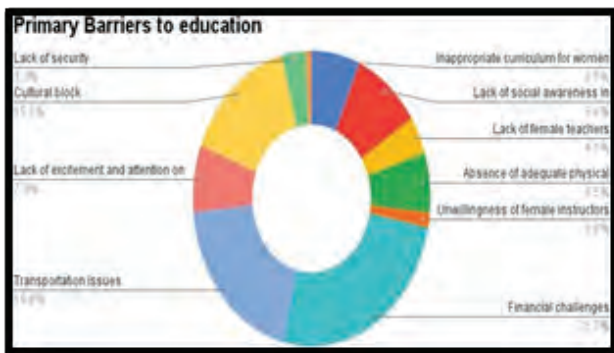
Graph 2. Barriers In Education

90% of the tribal women agree that education is important. 10% of respondents mentioned that women have to finally manage the household, which does not require a woman to be educated.

The major barrier in education i.e. poor Financial condition was the response of 25% of the respondents.

• 20% of the respondents mentioned that Transportation was a problem since the secondary schools were about 8 to 10 kms aways in the adjoining village. Incase of the Sange village children have to go to Gorhe village. It is easier to fetch Primary education as the school is within the Pada or in the next Pada.

• 15% respondents said that cultural block was a barrie for education amongst other reasons as mentioned in the above chart.

As a part of the study we also tried to find out the level of Digital literacy amongst women in the tribal village of Sange. We focused on the accessible Digital Technology i.e. Use of Mobile Phone and frequently used digital Applications like WhatsApp, Facebook, Instagram, Youtube and online Payment mode - GPay, PhonePay, UPI, etc.

Use of Digital Technology - Digital Literacy
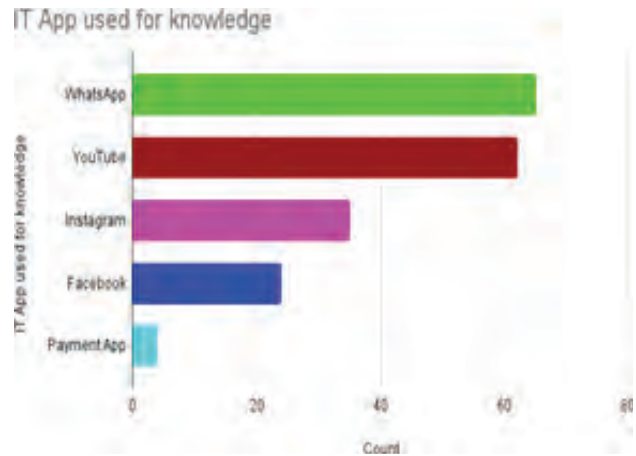
Graph 3. Digital Literacy

The graph clearly indicates that more than 67% of the respondents have some form of Digital Literacy.

65% of respondents are frequent users of WhatsApp.

64% of them use Youtube

Nearly 36% are aware of and use Instagram 25% of respondent use Facebook

Only 4% of the responding women use Apps for online money transactions.

Use of Digital Platforms

The survey also studied the purpose of use of digital platforms by the women

WHATSAPP
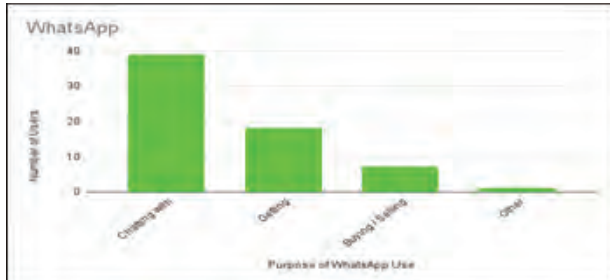
Graph 4. Use Of WHATSAPP

60% of the respondents were using WhatsApp for Chatting with family and friends.

28% were using WhatsApp for getting information on farming by joining Farming WhatsApp Groups

Only 10% were aware about using WhatsApp for buying or selling operations.

INSTAGRAM
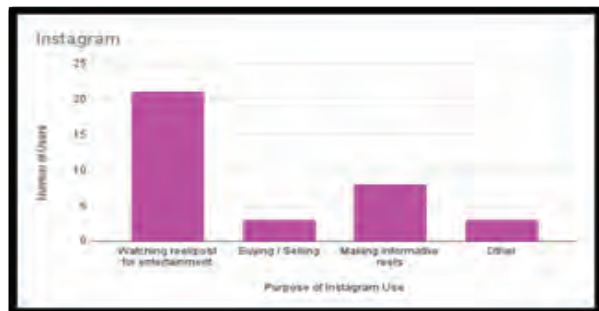
Graph 5. Use of INSTAGRAM

YOUTUBE
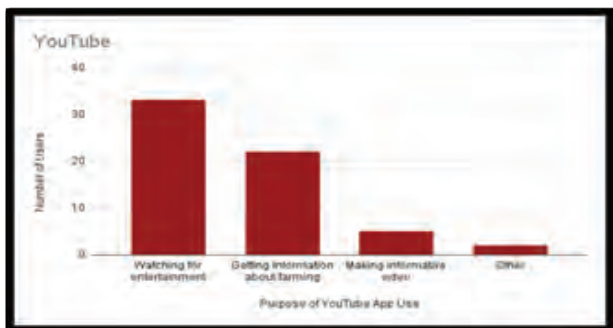
Graph 6. Use Of YOUTUBE

53% of women are using Youtube to watch entertainment videos of movies and songs.

35% are using for gating information relating to Farming

INSTAGRAM
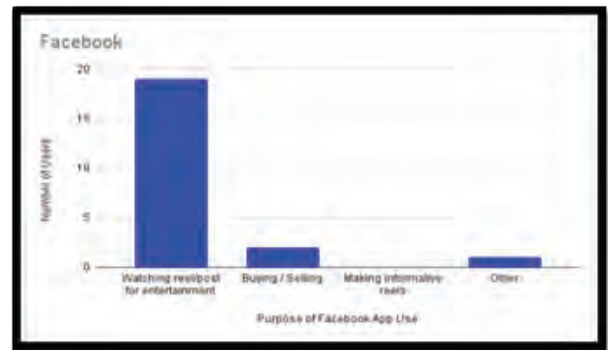
Graph 7. Use of FACEBOOK

Nearly 80% of the respondents are using Facebook for entertainment for watching videos.

Payment Modes

The survey studied the use of Payment platforms like GPay, PhonePe, BHIM, ect which are commonly used and largely supported by the government. However, literacy about these platforms was poor. Moreover only 12 out of the

97 respondents were aware and using online payment options as mentioned above for money transactions enhancing their education.
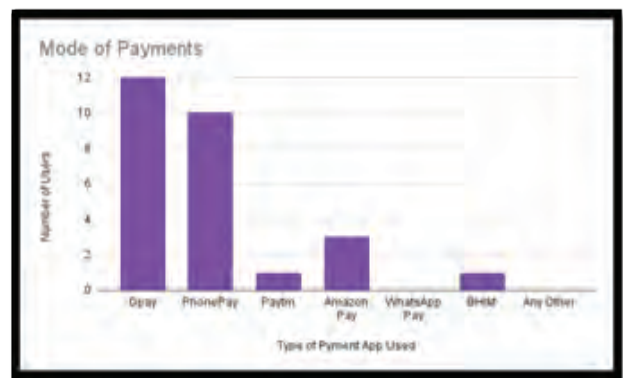
Graph Viii. Use of Payment APPS

Challenges in using IT-Digital Technology
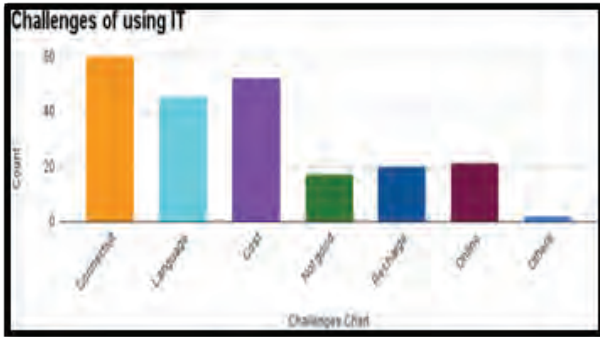
Graph 9. Challenges in Using Digital Technology

Of the 97 respondents, 62% of the respondents affirmed that poor connectivity in the village was a major challenge while using Digital Technology.

46% mentioned language was a barrier as most of the digital content was in English or Hindi. Whereas the respondents were well versed with Marathi.

54% mentioned cost as a barrier as the Phone needs to be recharged frequently.

Use of Digital Technology for Upskilling – Enhancements

The survey study discussed with the responding women about which areas would they want to use Digital Technology so as to upskill themselves and eventually get empowered.
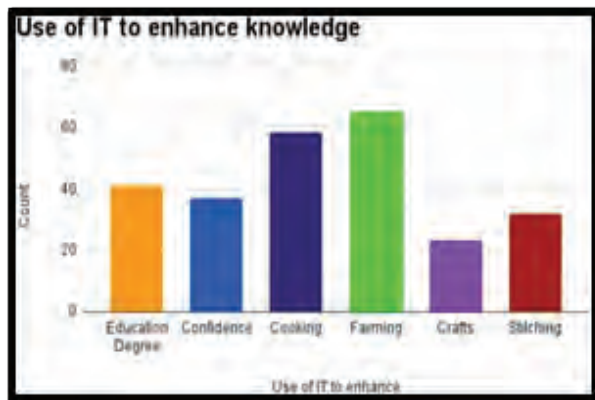
Graph 10. Use of Digital Technology to Enhance Knowledge and Upskill

42% women want to use digital technology for 38% want to be confident

60% women desire to use digital technology for enhancing their cooking skills

67% want to use digital technology for enhancing their farming knowledge and skill

Government Schemes - Awareness and Implementation at Sange village. The Government of India has made several proactive attempts to ensure overall development of the nation. This requires that all citizens are considered and given equal rights and privileges. Accordingly, schemes are designed and floated. However, there is a lack in providing awareness about these schemes to the right respondents and also implementation of the schemes.

The present initiative of the government - Viksit Bharat also focuses on creating awareness about the several government schemes amongst the citizens.

The table below mentions the several schemes under major heads.

Table 2. Government Schemes

Types of Schemes	Count
Govt General Schemes for ALL	10
Govt Schemes for RURAL India	3
Scheme for Entrepreneurship	3
Schemes for promoting Women's Education in India	3

Graph 10. Awareness and use of Government Schemes
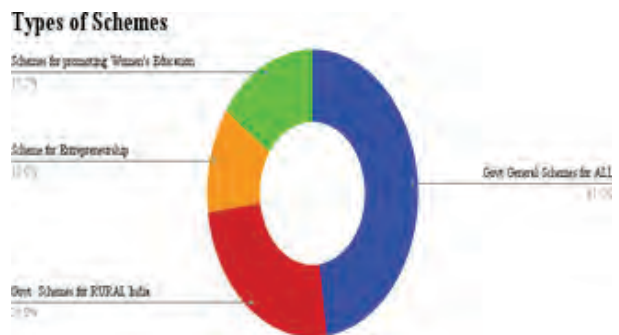
The above indicates the level of awareness of the several Government schemes.

25% of the women in Sange village are aware about few of the schemes under Rural India.

Only 15% are aware about the schemes for promoting Women's Education.

During the survey, the team met women who were unable to recognize the schemes by their names. They were aware that quite frequently schemes are floated by the government. However, none of the respondents were a beneficiary of any of the government schemes. Few of the respondents even mentioned that they had filled forms several times to get a sewing machine and submitted the same at the Gram Panchayat, however, till date none of them were benefitted.

Dependency

This research study of empowerment correlated dependency to empowerment. An empowered woman will not be dependent on others. To understand the dependency factor, the women of Sange village were asked whether they have to depend on their husbands or other elders in the family for money. The responses indicate that out of the 97 respondents, 60 (62%) women are dependent, whereas 37(38%) are independent.

The dependency factor can be further correlated with their education to understand whether women who are educated do not depend on others for money.
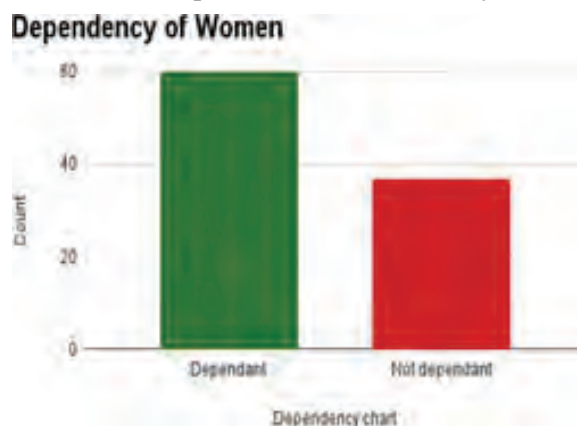
Graph 12. Dependency on Family Members for Money

CONCLUSION

Women Empowerment is a necessity even though the world has progressed. There is definitely an improvement in the empowerment level of women. However, there is huge scope to strategically implement schemes and to develop a sustainable model to ensure that maximum women are empowered irrespective of whether they are dwelling in urban or rural India. Digital technology wil definitely play a pivotal role in

women empowerment. Present digital technologies, specifically the mobile technology, is easily available and affordable to perform basic tasks that will help empower women at a large scale.

RECOMMENDATION

As discussed earlier in the paper, women empowerment cannot happen within a short period of time, specifically in scenarios which are deprived, such as the Sange village consisting of tribals. Thus, the efforts towards Women Empowerment using education as a means have to be sustainable and persistent. Following are recommendations to enhance literacy amongst the tribals of the Sange village -

1. As in the case of the Aganwadi there is an Assistant to support the Anaganwadi teacher to handle the children, similarly for the primary school, Assistants can be allocated so that the school can function smoothly when the teachers are involved in administrative work or summoned for government meetings and interactions.

2. The educated parents of the village can play the role of the Assistant so that the classes continue unhindered in the absence of the teacher. The responsibility of the Assistant should be clearly mentioned and should not disturb the normal working of the school.

3. The phrase " Each One Teach One" needs to be applied to enhance women empowerment through education in the Sange village. According to the data analyzed there are educated women in the village who have completed education till class 12. These women can be encouraged to teach those who cannot read and write. The expected outcome is that the illiterate women should be able to at least sign and stop putting finger prints.

4. Women who have skills in cooking, craft or stitching can be encouraged to teach their skills to other unskilled women. Further through the use of available Government schemes funds can be generated to support the activities of these women and their products can be sold in desirable markets.

5. In the times of digital literacy, these women should be encouraged to use the digital technology to

empower themselves by enhancing their functional literacy. They can be taught to use the Digital platform to sell their product and skills.

6. College students can intern as digital media marketers to promote and sell the products of the tribal women.

Proposed system - Women Empowerment Dashboard

The empowerment of women through education including Functional and Digital literacy can be monitored through a Women Empowerment Dashboard. The initiatives taken to empower them and the outcome of the same will be recorded and represented in graphical forms through the Dashboard. As mentioned in the paper the process of empowerment will be time demanding and should be extended to a span of 3 years to see actual effects for the efforts taken.

Fig 1: Proposed System – Women Empower Dashboard

FUTURE SCOPE

The study of Women Empowerment can be extended to the remaining two pillars i.e. Health and Financial literacy. The study can be carried out at Sange village for a period of 3 years to observe the outcome of number of women getting empowered.

ACKNOWLEDGEMENT

REFERENCES

1. World Economic Forum. (2023). Global Gender Gap Report 2023. World Economic Forum. https://www.weforum.org/publications/global-gender-gap-report-2023/

2. Shetalben, B., & Khair. (2019). Women's Education in India: Reality and Statistics. International Journal of Research in Humanities & Social Sciences, 7(3), 3. https://www.raijmr.com/ijrhs/wpcontent/uploads/2019/05/IJRHS_2019_vol07_issue_3_Eng_01.pdf

3. Desai, N. (n.d.). Research in Women's Education. Retrieved from http://osre.ncert.gov.in/images/survey/Fourth_Survey/vol2chap294.pdf

4. Thingbaijam, S. (2021). Issue 10. JETIR2110424 Journal of Emerging Technologies and Innovative Research, 8. https://www.jetir.org/papers/JETIR2110424.pdf

5. Bayeh, E. (2016). The Role of Empowering Women and Achieving Gender Equality to the Sustainable Development of Ethiopia. Pacific Science Review B: Humanities and Social Sciences, 2(1), 37–42. https://doi.org/10.1016/j.psrb.2016.09.013

6. Kandpal, E., et al. (2012). Empowering Women through Education and Influence: An Evaluation of the Indian Mahila Samakhya Program. SSRN Electronic Journal. https://doi.org/10.2139/ssrn.2010942

7. NITI Aayog. (2015). Empowerment of Women through Education, Skilling & Micro-Financing. http://www.niti.gov.in/empowerment-women-through-education-skilling-micro-financing

8. Mandal, B. (n.d.). A Study on Women Empowerment in 21st Century (Vol. 5). Retrieved from http://www.ijrar.com/upload_issue/ijrar_issue_1190.pdf

9. Smile Foundation. (2022). Women Empowerment Needs Digital Empowerment. Smile Foundation. http://www.smilefoundationindia.org/blog/women-empowerment-needs-digital-empowerment/

10. Malhotra, M. (2015). Empowering Women through Digital Technology: An Indian Prospective. International Journal of Business Management Available at Www.ijbm.co.in, 2(1), 2015. http://www.ijbm.co.in/downloads/vol2-issue1/12.pdf

11. Anne Huis, M., et al. (2017). A Three-Dimensional Model of Women's Empowerment: Implications in the Field of Microfinance and Future Directions. https://www.frontiersin.org/journals/psychology/articles/10.3389/fpsyg.2017.01678/full,

An Enhanced Disease Prediction Model using Hyperspectral Data based on Feature Level Fusion

R. Sai Kumar
Ph.D. Research Scholar
Department of Computer Science
Sankara College of Science & Commerce
Coimbatore, Tamilnadu
✉ saicompsci@gmail.com

V. Sulochana
Assistant Professor
Department of Computer Applications
Hindustan College of Arts & Science
Coimbatore, Tamilnadu
✉ sathvika_2016@yahoo.com

ABSTRACT

In agriculture sector, quality of food and production of food materials has affected more due to plant diseases. Computer vision is the one method to detect the plant diseases on early stage with higher accuracy will leads to improve the production of agriculture products. The proposed research is an enhanced development of a model, to predict the plant diseases at early stage using feature level fusion method from extraction of deep features. The model has three primary frameworks: First, deep features are extracted using pre-processing methods and local binary pattern (LBP) is applied for basic conversion of image data to array form and principal component analysis (PCA) is applied for extraction of features. Second, Convolution neural network (CNN) is applied for classification of images to extract the data from an image and feature level fusion is applied to analyse the loss and accuracy. Third, visual geometry group (VGG16) which is pre-trained convolution neural network model applied for deep feature analysis with image size of 256, 256, 3 to predict the accurate plant diseases. In the proposed research, apple plants which is in the form of hyperspectral images are selected from the Kaggle database for the evaluation of algorithms to identify the disease of the plants, based on four parameters such as healthy, water stressed, fire blight and early blight. The best accuracy is achieved using the proposed model which is 96% by applying the Adam classifier and VGG16 algorithm.

KEYWORDS : Disease prediction, Principal component analysis, CNN model, VGG16, Hyperspectral image, Classification, Fusion methods.

INTRODUCTION

India holds agriculture as a main source for living and contributes the country GDP. There are some demands in food supply due to population hike which is worrying a lot. One of the major reasons for this production loss or low productivity is crop loss due to the pests and diseases that cause the yield loss. Another point of crop loss is climate changes which will leads to spread of diseases faster. These diseases should be detected in very early stage to maintain the yield and to avoid the economic loss. Prediction of diseases has two traditional methods are followed as, manually detecting the disease by plant pathologist is little risky, it consumes more time and cost is high and once identified the diseases, it will take to control using pesticides. There are some risk factors on using pesticide as if the farmer used exceed number of pesticides on disease affected plants soil pollution is caused and the quality of the soil is degraded. For past few decades, the crop disease detection is done using image processing techniques which is complete their process faster with more accurate result than the conventional methods.

Previous researches are done for crop disease detection will be focused on using traditional machine learning algorithms using manually crafted features which will require domain knowledge to reduce the errors from the input data. As years passed, convolution neural network started to play a major role in disease prediction in agriculture field and medicine fields. The advent of deep learning techniques has an improvement in wide

range of computer vision issues and deep learning has proved their efficiency in agricultural domain with lot of features from the input data using convolutional kernel as deeper network layers. These deep features with higher ability of representation it will be used for fusion with manually crafted features which will be leads to more informative data are studied. In several domains, researchers have initiated to explore the fusion methods at different levels to improve the accuracy of classification methods. As now, the different plant pathologist is attempting various fusion methods for improve the performance of classification process.

LITERATURE SURVEY

In this section, existing researches and the methods proposed are discussed with information like algorithms, drawbacks, accuracy reached, methods proposed. It will be helpful to analyze the various ideas about the disease prediction model for proposed research. The below mentioned table shows the literature related to feature fusion techniques using traditional spatial features such as color, shape, texture, property of image and major focus on analyzing the feature extraction with deep architecture of convolution neural networks.

Krezhova et.al. [1] proposed a model and applied CA along with t-test to determine the statistical significance values between means of reflectance of controlled and infected apple trees by applying SVM technique, a machine learning technique for analyzing high dimensional real time spectral data for early prediction of plant disease with neural network. CA is a broadly implemented technique to organize the hyperspectral data to group the pixels within similar value range and creates cluster [2]. Nagasubramaniam et.al. Implemented genetic algorithm as optimizer along with SVM to select the optimum spectral bands to identify the charcoal rat disease earlier in soybean. The combination method of GA-SVM will identify the disease within three days after inoculation with execution of 97% of classification accuracy [3]. There are two different demerits in machine learning concept as follows; first it is highly dependent on patterns of different variables also on features which is extracted. Second, the classifier technique has train many times before applying with real world applications [4]. Ashourloo et.al. proposed spectral disease index (SDI)

method effectively to reduce the dimensionality by increasing the rate of disease estimation. Minimum number of SDI is developed from the imaging and non- imaging hyperspectral data which is not processed using neural network models [5].

Neural network plays a major role in analyzing the hyperspectral data, where the mechanism is based on the structure of human nervous system. The fundamental concept of neural network is very useful for pattern recognition [6]. Cui, et.al., stated that the neural network concept required only few formal statistics to model the complex nonlinear relationships [7]. Plants are protected from different diseases based on hyperspectral data using neural network concepts which provides various applications to promise the earlier prediction of diseases.

Analyzing huge number of high dimensional hyperspectral data in neural network concept is a challenging task. Because of reducing the data dimensionality is major task to manage the hyperspectral data. The report said, higher reduction of data dimensionality will leads to execute the good classification accuracy. Hyperspectral data contains the apparent and inherent spectral information so the capabilities of data must be deliberated using neural network system [8, 9].

Marini, et.al., mentioned particular type of neural network based technique for pattern recognition called as class modeling which has a very good discriminating capacity for developing the prediction of plant disease models. Most of the class models were developed based on multilayer feed forward neural network and kohonen artificial neural network techniques [10].

Jiang et.al., experimented on maize plant to detect water stressed plants using super pixel and GLCM feature extraction methods by using support vector machine as a classification technique. Datasets are collected by their own with 1297 images with black background and achieved the result of 99% accuracy [11]. B.Liu, et.al., implemented with self-captured apple crop datasets of 1053 images and processed usinf AlexNet, GoogleNet, VGG-16 and ResNet-20 DL models for better performance and achieved a classification accuracy of 98% in predicting the leaf diseases [12]. Amara, et.al., proposed a model for banana crop with self- captured

datasets of 147 images which contains both healthy and infected leaves. The model proposed with LeNet and achieved an accuracy, precision, recall and F1 score as 99%, 98.61%, 98.56% and 98.28% respectively [13]. Prakhar bansal, et.al., proposed pre-trained model with DenseNet 121, efficientNet B7 and EfficientNet Noisy student for classification of apple leaves to predict the categories as healthy, apple scab, cedar rust and other diseases using the images captured and implemented as datasets. Image augmentation techniques are used to increase the size and model accuracy, were the proposed model achieved 96% of accuracy on validation test and 90% of accuracy [14].

In the context of hyperspectral image analysis, the basic neural network model can be obtained by various neurons with connections and output layers. For example, in 3 layers neural network first layer is input layer with one node for every spectral band. Second layer hold more hidden layers, which the nodes will reflect the values of every spectral bands. The last layer of the neural network connected layers, it will be considered as output layer consist of nodes usually computed by the computation of non- linear nodes for input and output layers. The three layers of neural network mode is the major process of implementing to analyse the hyperspectral image data dynamically and widely.

PROPOSED METHODOLOGY

The proposed research using CNN framework is consisting of three different phases. The pre- trained CNN model using deep learning [15] feature extraction is the first step and parameters like mean, median standard deviations are identified. Features are extracted from the gray scale image and feature level fusion is applied based on pre-trained CNN data after PCA performed extraction. Implementation of convolutional neural network is the second step to train and test the data based on loss and accuracy while training and testing the array data. As a third and final step, the outcome of CNN [16] is considered as input for final method using VGG16 model by testing the data to detect disease and health status of apple plants. Validation accuracy and loss with epoch 15, 25 and training accuracy and loss with epoch 15, 25 is processed. The overall performance of the proposed model is described with simulation charts and

tables as follows,
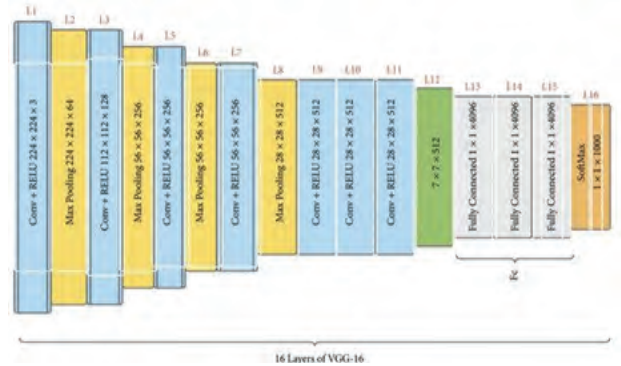
Fig. 1: Basic architecture of VGG16 pre-trained model

In figure 1, explained about the architecture of VGG16 with pre- trained model where the term VGG is known as visual geometric group which can be applied for recognition and classification methods. VGG is described in two different types such as VGG16 and VGG19. It is commonly used to learn the data in deep layers using convolutional neural network for better learning about the data with more accuracy. To learn the data in the network layers and to avoid several parameters, VGG will work with minimum of 3 x 3 convolution kernel which will be applied in all the layers of CNN.
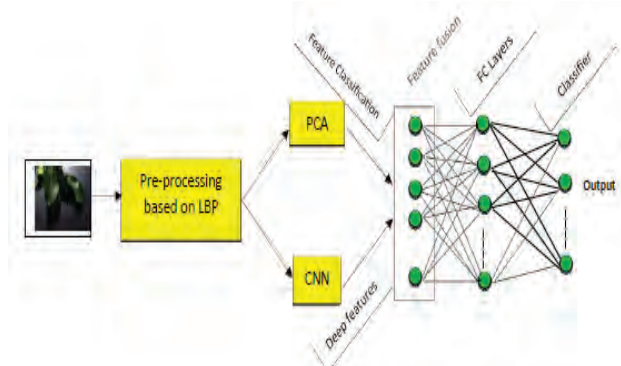
Fig. 2: Framework for feature-based fusion

In figure 2, the image has been taken for pre-processing method and applied with two different algorithm methods known as principal component analysis and convolutional neural network based on the execution of pre- processing output data, which will be considered for classification methods. Based on the features, fusion will be performed to execute the better accuracy of the model.
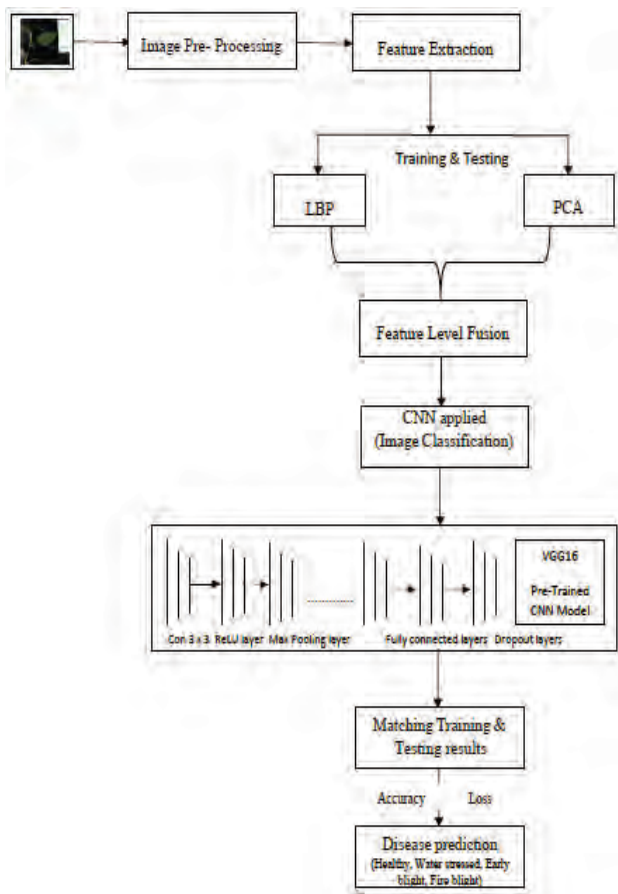
Fig. 3: Flow architecture of proposed model using CNN and Fusion based apple plant disease prediction

Table 1. Sequential of CNN with parameters

Layer type	Output	Shape	Parameters
conv2d_25 (Conv2D)	None	256, 256, 32	896
activation_29 (Activation)	None	256, 256, 32	0
batch_normalization_27 (Batch Normalization)	None	256, 256, 32	128
max_pooling2d_15 (MaxPooling2D)	None	85, 85, 32	0
dropout_17 (Dropout)	None	85, 85, 32	0
conv2d_26 (Conv2D)	None	85, 85, 64	18496
activation_30 (Activation)	None	85, 85, 64	0
batch_normalization_28 (Batch Normalization)	None	85, 85, 64	256
conv2d_27 (Conv2D)	None	85, 85, 64	36928
activation_31 (Activation)	None	85, 85, 64	0
batch_normalization_29 (Batch Normalization)	None	85, 85, 64	256
max_pooling2d_16 (MaxPooling2D)	None	42, 42, 64	0
dropout_18 (Dropout)	None	42, 42, 64	0
conv2d_28 (Conv2D)	None	42, 42, 128	73856
activation_32 (Activation)	None	42, 42, 128	0
batch_normalization_30 (Batch Normalization)	None	42, 42, 128	512
conv2d_29 (Conv2D)	None	42, 42, 128	147584
activation_33 (Activation)	None	42, 42, 128	0
batch_normalization_31 (Batch Normalization)	None	42, 42, 128	512
max_pooling2d_17 (MaxPooling2D)	None	21, 21, 128	0
dropout_19 (Dropout)	None	21, 21, 128	0
flatten_5 (Flatten)	None	56448	0
dense_4 (Dense)	None	1024	57803776
activation_34 (Activation)	None	1024	0
batch_normalization_32 (Batch Normalization)	None	1024	4096

dropout_20 (Dropout)	None	1024	0
dense_5 (Dense)	None	4	4100
activation_35 (Activation)	None	4	0

Total parameters:	58091396
Trainable parameters:	58088516
Non-trainable parameters:	2880

Table 1, represents the parameter values of convolutional neural network considered for training and analyzed the different values based on trained and non- trained parameters of layer type. In the proposed research, the Kaggle database is considered to collect the datasets and 386 (apple leaf) hyperspectral image datasets are taken for processing the proposed model. The method is proposed using python software using tools such as pandas, numpy, matplotlib, scikit. Convolutional neural network is used to learn the deep layers for higher accuracy execution by testing and training the data.

RESULT & DISCUSSION

In this result & discussion section, the simulation results of proposed model along with graphs, charts and tables of both the testing and training accuracy, loss is discussed in detail.

Phase 1

In the table 2, loss and accuracy of the model has recorded with 15 iteration and epoch 15. The training and validation of data is processed and executed better at 15th iteration of the model with 0.0218 as training loss, 0.9932 as training accuracy, 0.0516 as validation loss and 0.9838 as validation accuracy. The graphical representation of table is explained in figure 4- 6.

Table 2. Validation loss and training accuracy using Epoch 15

Epoch	Loss	Accuracy	Val_loss	Val_accuracy
1/15	0.4041	0.8809	0.1768	0.9488
2/15	0.1619	0.9504	0.1329	0.9596
3/15	0.1182	0.9645	0.1001	0.9701
4/15	0.0946	0.9708	0.0951	0.9708
5/15	0.0798	0.9759	0.0967	0.9707
6/15	0.0677	0.9789	0.0737	0.9761
7/15	0.0573	0.9827	0.0700	0.9783
8/15	0.0501	0.9844	0.0684	0.9770
9/15	0.0448	0.9861	0.0602	0.9798
10/15	0.0394	0.9877	0.0521	0.9818
11/15	0.0355	0.9891	0.0580	0.9808
12/15	0.0313	0.9906	0.0545	0.9817
13/15	0.0282	0.9916	0.0591	0.9795
14/15	0.0260	0.9921	0.0528	0.9818
15/15	0.0218	0.9932	0.0516	0.9838
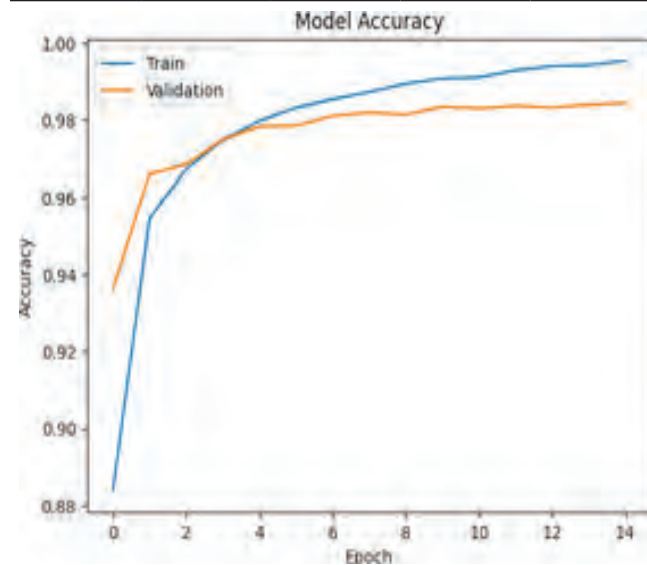
Fig. 4. Training and validation accuracy
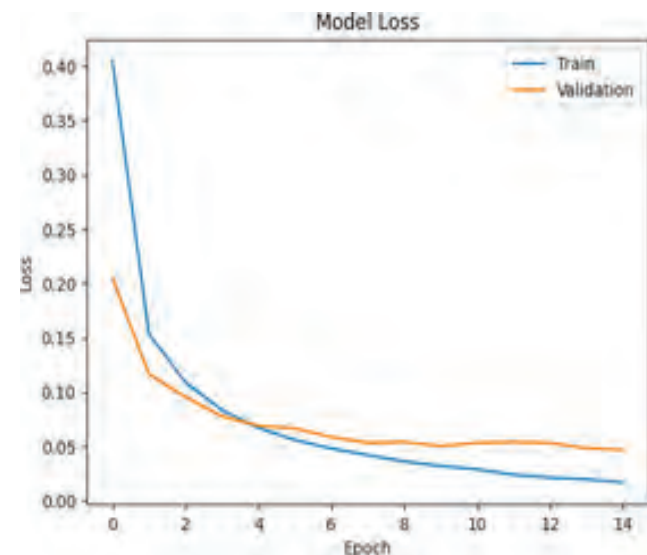
Fig. 5. Training and validation loss
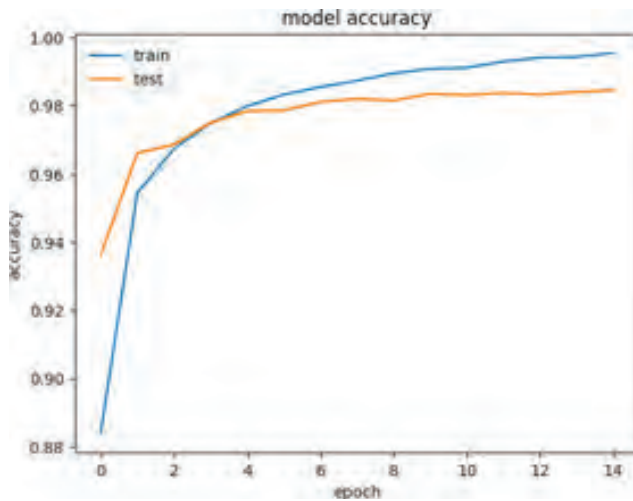
Fig. 6. Testing and training accuracy of model

In figure 4,5,6, the testing and validation loss of the model is predicted and visualized in chart for better understanding of the process. The training loss is executed with 0.0218 and validation loss is executed with 0.0516. Model accuracy has graphed with training and testing data using epoch 15 values for 99% of model accuracy and 98% of validation accuracy.
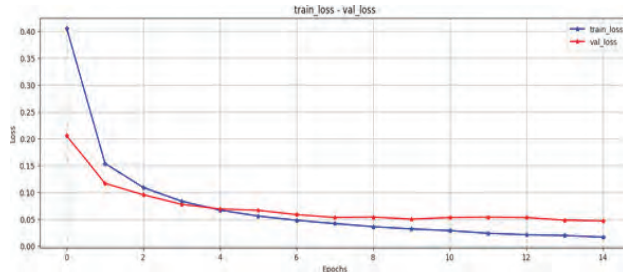
Fig. 7. Training and validation loss chart
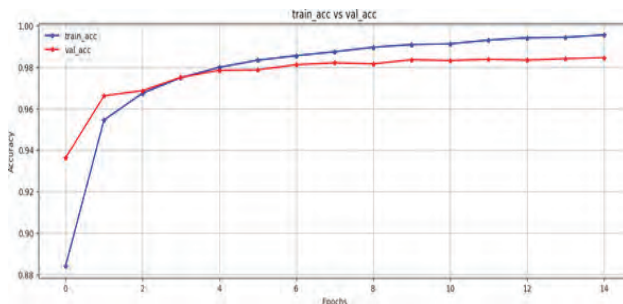
Fig. 8. Training and validation accuracy chart

In figure 7, 8, the training and validation accuracy of the model is predicted and visualized in chart for better understanding of the process. The training accuracy

is executed with 0.9932 and validation accuracy is executed with 0.9838.

Phase 2

Once the model is predicted accuracy of training and validation process, the proposed model is implemented with convolution neural network for better learning of the model by processing the layers deeply. Using CNN, there is 25 epoch is processed to predict the loss and accuracy of the model after classification of features.

Table 3. Testing & Validation loss and accuracy using Epoch 25 with CNN

Epoch	Loss	Accuracy	Val_loss	Val_accuracy
1/25	0.4906	0.8600	1.1098	0.4340
2/25	0.2460	0.9263	0.6857	0.4340
3/25	0.1339	0.9631	0.8964	0.4340
4/25	0.0879	0.9803	1.1802	0.5566
5/25	0.0873	0.9681	1.1190	0.4340
6/25	0.0679	0.9803	1.0180	0.4340
7/25	0.0647	0.9730	1.6561	0.4340
8/25	0.0916	0.9705	1.4466	0.4340
9/25	0.0599	0.9705	1.6147	0.6132
10/25	0.0530	0.9730	1.4285	0.4623
11/25	0.0620	0.9681	1.2762	0.0620
12/25	0.0716	0.9705	1.5461	0.4340
13/25	0.0370	0.9828	0.6779	0.7170
14/25	0.0707	0.9730	0.4718	0.9623
15/25	0.0951	0.9410	0.2669	0.9434
16/25	0.0885	0.9459	0.2439	0.8868
17/25	0.0692	0.9803	0.9736	0.8491
18/25	0.0639	0.9681	1.0038	0.7075
19/25	0.0993	0.9312	0.6342	0.7264
20/25	0.0326	0.9853	0.9690	0.7264
21/25	0.0469	0.9754	0.2163	0.8208
22/25	0.0543	0.9681	0.0876	0.9528
23/25	0.0193	0.9926	0.0285	0.9906

24/25	0.0230	0.9926	0.0467	0.9717
25/25	0.0544	0.9779	0.5110	0.7264

The above table 3, predicted the accuracy ratio of testing as 0.98 and validation accuracy of 0.73 which will be predicted that the plant is water stressed. To predict the results, the model is repeated for 25 iterations to analyse the image data. Hyperspectral image data is taken for processing the model in the form of array matrix which will be used for better prediction shown in figure 9. The figures 10, 11 showed the accuracy and loss of training and validation loss of the model based on convolution neural network techniques.
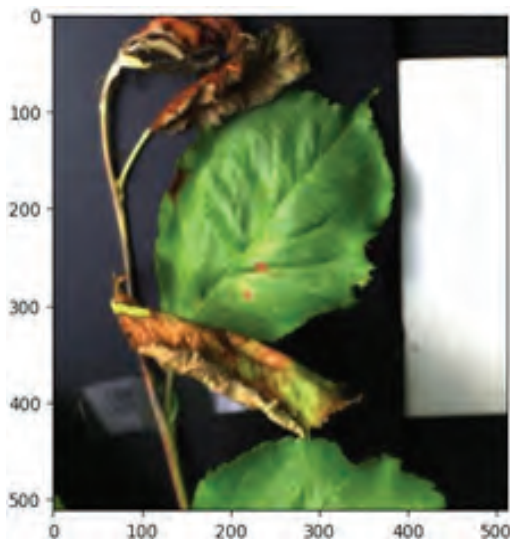
Fig. 9. Loaded image (Input) using CNN
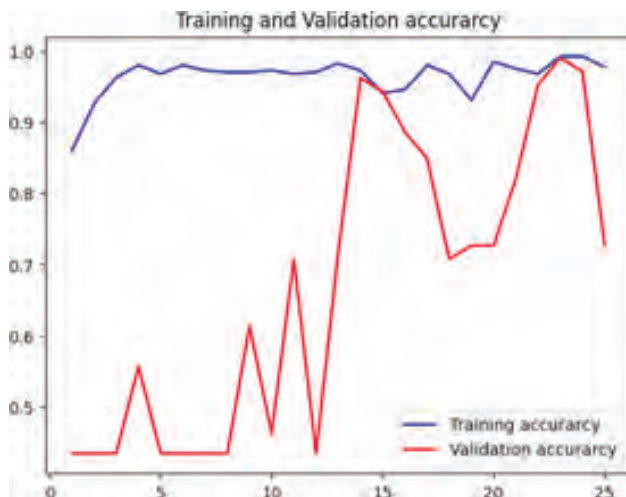
Fig. 10. Training and validation accuracy based on CNN

Fig. 11. Training and validation loss based on CNN

```
print(result)

1/1 [==============================] - 1s 541ms/step
[[2.3646676e-08 5.8645753e-12 3.6534626e-11 1.0000000e+00]]

itemindex = np.where(result==np.max(result))
print("probability:"+str(np.max(result))+"\
n"+label_binarizer.classes_[itemindex[1][0]])

probability:1.0
waterstressed
```

Fig. 12. Result executed as plant is water stressed based on CNN

In figure 12, the research code is explained with the probability value of identifying the plant exact status about health and identified as water stressed. Which is be executed and explore the exact status of the proposed methodology.

Table 4. Testing Validation loss and testing validation accuracy using Epoch 25 with VGG16

Epoch	Loss	Accuracy	Val_loss	Val_accuracy
1/25	0.5225	0.8438	0.9755	0.4340
2/25	0.2877	0.9091	1.2691	0.4340
3/25	0.2106	0.9361	1.2536	0.4340
4/25	0.1177	0.9582	0.7395	0.4340
5/25	0.1099	0.9656	0.5912	0.6792
6/25	0.1093	0.9631	1.4350	0.1792
7/25	0.0824	0.9607	0.6247	0.7170
8/25	0.0722	0.9730	0.9295	0.4340
9/25	0.0724	0.9681	0.7592	0.7170

10/25	0.0358	0.9853	1.2725	0.4340
11/25	0.0772	0.9631	1.5685	0.5943
12/25	0.0793	0.9631	1.3022	0.7170
13/25	0.0670	0.9779	0.7753	0.7075
14/25	0.0141	0.9926	0.8276	0.7170
15/25	0.0351	0.9828	0.9227	0.7075
16/25	0.0601	0.9803	0.9151	0.7170
17/25	0.0392	0.9754	1.2778	0.6415
18/25	0.0526	0.9730	0.9866	0.7170
19/25	0.0364	0.9828	1.1001	0.7075
20/25	0.0374	0.9754	0.5449	0.7264
21/25	0.0145	0.9951	0.0384	0.9811
22/25	0.0258	0.9853	1.2145	0.6604
23/25	0.0327	0.9828	1.4867	0.6887
24/25	0.0230	0.9926	1.1093	0.7170
25/25	0.0210	0.9828	0.1127	0.9623

From the below figures 13, 14, 15 hyperspectral image data is loaded as input data in the form of numerical values and applied with VGG16 method which has 16 layers with softmax, fully connected layers, pooling layers and dropouts to predict the deep layer processing for executing the improved accuracy.
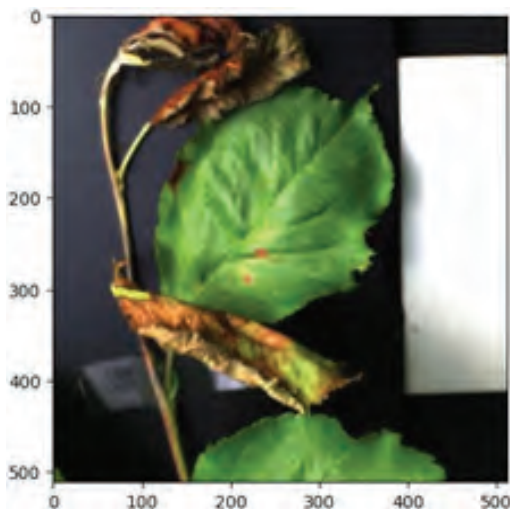
Fig. 13: Loaded image (Input) in VGG16

Fig. 14: Training and validation accuracy based on VGG16

Fig. 15: Training and validation loss based on VGG16

```
result=model.predict(npp_image)

print(result)

1/1 [==============================] - 0s 138ms/step
[[1.0000000e+00 1.5715849e-13 3.3684950e-15 2.5649240e-15]]

itemindex = np.where(result==np.max(result))
print("probability:"+str(np.max(result))+"\
n"+label_binarizer.classes_[itemindex[1][0]])

probability:1.0
Healthy
```

Fig. 16: Result executed as plant is healthy based on VGG16

In the figure 16, the execution of results is predicted that the plant is healthy based on VGG16 techniques. This will be processed and learned deeply with the layers of convolution neural network for higher prediction of result.

CONCLUSION

Plant diseases are considered as a major part of financial and production loss in agriculture, which will be the most important thing in a country's development. To predict the diseases earlier, the proposed research is implemented with hyperspectral data along with four different algorithms such as LBP, PCA, CNN and VGG16 applied to the feature based fusion model. The model is extracted some features like mean, median and standard deviation as 0.3583, 0.11428 and 0.42747 to reduce the dimensionality. Fusion model with combined features of an image based on wavelength and intensity is used for better prediction of the leaf diseases. Convolution neural network is performed well and predicted the disease type as water stressed to the apple plant taken as input data in the form of array matrix with 98% with an error rate of 0.0516. Execution of CNN model will be reconsidered for the comparison with VGG16 algorithm and executed with 96% of accuracy along with error rate of 0.01127 which will be better than CNN algorithm. Computational time is reduced and learning the deep layers is considered as merits of the model for image classification in agriculture field using computer vision.

REFERENCES

1. Belanovic, et.al., "Analysis of reconfigurable hardware of multispectral and hyperspectral images", In proceedings, SPIC 4480, Imaging Spectrometry, Volume 100, Issue 8, 2018.

2. Krezhova, et.al., "Biotic stress detection affected by apple stem virus in apple trees with hyperspectral data", Comptes rendus Science, volume 68, issue 5, pp. 175-182, 2015.

3. Nagasubramaniam, Jones, Sankar, et.al. "Hyperspectral band selection with GA and SVM for early detection of charcoal rot disease in soybean", arXiv, pp. 1-20, 2017.

4. Zhang, Huang, et.al., "Recognition of stem and calyx in apple tree using computer vision by 3D reconstruction", Bio-system engineering, volume 139, pp. 25- 34, 2020.

5. Ashourloo, et.al., "Model to develop the index to identify and detect the stages about different diseases", IEEE geo science remote sensor letters, volume 13, issue 6, pp. 851- 859, 2021.

6. Bishop, Neural network for pattern recognition, Oxford university, USA, 2016.

7. Cui, Ling, et.al., "Review on plant disease prediction using artificial nose system", Journal of sensors, volume 18, issue 2, pp. 378-386, 2022.

8. Ettaba, Ben, et.al., "Adaptive process of dimensionality reduction of hyperspectral data", Journal of indian social remote sensors, volume 46, issue 2, pp. 157- 167, 2022.

9. Vane, Solomon, et.al., "Spectrometry of images for earth remote sensing", Journal of earth science, pp. 1147- 1153, 2021.

10. Marini, et.al., "Feed forward neural network with multilayer model using neural network", Journal of intelligent lab system, volume 88, issue 1, pp. 118- 124, 2019.

11. Jiang, Wang, et.al., "Prediction of maize drought based on texture and morphological features", Journal of computer electronic agriculture, volume 151, pp. 55-60, 2019.

12. B.Liu,et.al., "Apple leaf disease detection based on CNN", Journal of symmetry basel, volume 10, issue 1, 2022.

13. Amara, et.al., "Banana leaf disease prediction based on deep learning approaches", Journal of BTW, pp.79-88, 2020.

14. Prabhakar Bansal, et.al., "Apple leaf disease prediction model using deep convolutional neural network", Journal of MDPI agriculture, volume 11, pp. 1-23, 2021.

15. LeCun, Bengio, et.al., "Deep learning", Journal of nature, volume 521, pp. 436- 444, 2019.

16. Howard, "Deep convolutional neural network based image classification", Arvix, 2021.

Disaster Management: Mobilizing Safety During Calamity

Reshma Totare
✉ reshma.totare@aissmsioit.org

Pratham Pawale
✉ prathampawale.pp.pp@gmail.com

Upendra Taral
✉ uptaral21@gmail.com

Sagar Jadhav
✉ sagar21202@gmail.com

Chinmay Beldar
✉ ghostyluffy14@gmail.com

Department of Information Technology
AISSMS Institute of Information Technology
Pune, Maharashtra

ABSTRACT

Natural disasters are a big threat to people's lives, causing a lot of harm. One major problem in dealing with disasters is that there's often a communication issue between people stuck in dangerous situations and the teams trying to rescue them. This lack of communication makes it hard for rescuers to do their job quickly and effectively because they don't know how many people are trapped or where they are. On top of that, many people in disaster-prone areas don't know how to prepare for emergencies, making the impact of disasters even worse. To address these challenges, this paper describes a system, which includes all in one mobile application for diverse civilians which offers user-friendly interface, operability throughout India, anti-disaster literacy with multi-language feature for a broader audience, and track, store & keep appending their live locations in secure database after some interval of time. Additionally, a machine learning based system which will count trapped civilians' frequency and mark hotspot (disaster prone) regions using civilian's live locations & past stored locations. This project aims to rescue trapped civilians in disaster and also improve how communities get ready for and respond to disasters.

KEYWORDS : GPS, Mobile application, Machine learning, K-Means algorithm, Disaster management.

INTRODUCTION

Natural disasters, encompassing events such as floods, cyclones, earthquakes, landslides, and droughts, continue to pose significant threats to human lives and communities worldwide. When it comes to the number of fatalities caused by natural disasters in India, earthquakes rank first with 33%, followed by floods (32%), cyclones (32%), landslides (2%) and droughts (1%) [1]. These devastating occurrences not only claim lives but also leave a trail of destruction and disarray in their wake.

In India, where natural disasters are common, the problem is made worse because many people don't know much about how to deal with them. About 35% of the population in India doesn't have enough knowledge about natural disasters like preventions, precautions, how to seek help, whom to contact, and what immediate actions to take in the event of a natural disaster, etc.

This makes the disasters even harder to handle because communities aren't ready to respond well.

Additionally, India's varied scenery brings in people from other countries as immigrants, tourists, and residents who might not know much about the specific dangers of natural disasters in the area. Because they aren't aware, they're not ready for these disasters. This shows why there's a need for a thorough plan for handling disasters that goes beyond just where you are and what language you speak.

One of the critical challenges faced during such disasters is the communication gap between individuals trapped in affected areas and the rescue teams tasked with their evacuation and assistance. Rescue teams sometimes don't have enough information regarding how many and at what regions the people are affected, which makes it harder for them to get ready and act fast. This communication breakdown can severely hamper

rescue efforts, as the absence of real-time information on the number and locations of trapped individuals complicates the planning and execution of rescue operations.

To address these challenges and reduce the devastating impact of natural disasters, this paper introduces a practical and inclusive disaster management system. The proposed system includes a user-friendly mobile application designed for civilians, ensuring operability throughout India, anti- disaster literacy with multi-language support, real-time alert notifications, and the ability to track and store live locations securely or simply S.O.S feature [2]. Additionally, the integration of a machine learning-based system aims to provide real-time insights, counting the frequency of trapped civilians and identifying hotspot regions prone to disasters. This project strives to save human lives and enhance the resilience of communities in the face of natural calamities.

LITERATURE SURVEY

While surveying and researching the existing mobile applications, we came across the following applications that were similar to our device like the IOWA Legal Aid [3], FDAS-Disaster Management System [3], Relief Central [3], Family Disaster Manager [3] and Disaster Preparedness by OXFAM [3]. We found that some had very poor application interfaces, some were not reliable and most all of these applications are not operated centrally hence there are no multi-language feature, moreover the use of locations of trapped people to estimate exact frequency of people trapped in a calamity for better preparedness of rescue team. Owing to all situations, there are apps that can help in emergency situations, but there is still a need to design a model that is beneficial for rescue teams, multi-language support, central based, and has a better user interface.

During natural calamities, the use of an SOS [2] (emergency) system can be instrumental in saving lives and coordinating timely assistance. When disaster strikes, individuals may find themselves trapped or in urgent need of help due to injuries, structural damage, or dangerous conditions. In such situations, activating an SOS alert through a mobile application can rapidly notify nearby responders and authorities, enabling swift rescue operations. This real-time communication helps bridge the gap between those in distress and

rescue teams, ensuring that resources are efficiently deployed to affected areas. The SOS feature provides a critical lifeline during emergencies, facilitating faster response times and potentially minimizing casualties by expediting the delivery of aid and support to those in need.

The K-Means clustering algorithm [4] is highly valuable for data clustering and analysis due to its simplicity, efficiency, and effectiveness in partitioning data into distinct clusters based on similarity. In disaster management, K-Means identifies hotspot locations and activity patterns, aiding in resource allocation and response strategy formulation.

Existing system (K-Means clustering model) primarily rely on historical data to plot clusters of affected areas. In contrast, our system incorporates both historical data and live, real- time location data collected through a mobile app. This allows for the dynamic plotting of clusters that reflect the current situation more accurately. By using up-to-the-minute information, the system can provide a more precise and timely representation of the disaster impact areas. Additionally, our system visualizes the intensity of trapped civilians using color gradients. Darker regions indicate areas with a high concentration of trapped civilians, while lighter regions represent areas with fewer trapped individuals. This visualization technique aids the rescue team in prioritizing their efforts and managing resources more efficiently, ultimately reducing response time and improving the effectiveness of rescue operations.

RELATED WORK

Use Case

The primary actors involved in the use case are trapped individuals and rescue teams. For trapped individuals, the application offers a lifeline during distressing situations. Upon registering within the app, individuals provide essential details such as their name, contact information, and current location. This registration process ensures that their information is securely stored and readily accessible to rescue teams. The application leverages GPS technology to continuously track and update the location of trapped individuals, creating a dynamic record that informs rescue operations.

Communication lies at the heart of the application's functionality. Trapped individuals can generate distress signals through the app's interface as shown in Figure

"1". These real-time notifications enable rescue teams to promptly initiate response efforts with the trapped individuals to gather additional information. Civilians can retrieve region-specific disaster information, including preventive measures and precautions, thereby enhancing their safety and resilience.

Fig. 1: Basic working of the idea

For rescue teams, the application serves as a comprehensive platform for coordinating and executing rescue operations.

A notable feature of the application is its integration of machine learning model, which contribute to estimating the approximate number of trapped individuals along with displaying hotspot regions based on their GPS locations. This innovative approach augments the capabilities of rescue teams, offering a data-driven perspective that facilitates more informed and effective response strategies.

Proposed system includes

The flow of the described project involves a sequence of interconnected steps aimed at enhancing disaster preparedness and response through a mobile application with GPS tracking and machine learning support.

Real-time Location Tracking: Upon registration, users activate the GPS [5] location tracking feature in the app, which continuously monitors their location through GPS technology, providing real-time updates on their geographical coordinates.

Multi-Language Support: Utilizing multi-language capabilities, the app ensures the delivery of information in the user's chosen language, facilitating access to disaster-related content in a language that individuals find comfortable. This feature enhances accessibility for users from diverse linguistic backgrounds, promoting inclusivity and effective communication [6] during critical situations.

Machine Learning Model Integration: The application seamlessly incorporates a machine learning model that has undergone specialized training to provide estimates of the approximate number of individuals in distress, utilizing GPS location data. This model operates in real-time, continuously analyzing incoming location data and adjusting its estimations to align with the dynamically changing circumstances during a disaster.

Emergency Alerts and Notifications: The app proactively sends emergency alerts and notifications to users based on their real-time location and the detected type of disaster. These notifications may encompass evacuation alerts, safety instructions, and other crucial information designed to guide users through the emergency.

User Education and Preparedness: Serving as an educational platform, the app provides information about the specific disaster, its characteristics, and the most effective preventive measures and precautions.

Machine learning model

This project includes a machine learning model, based on their historical location data it provides analysis of hotspot locations and trapped civilians predicted count.

Identifying hotspot locations of civilians trapped in natural calamity.

The model employs the K-Means [4] clustering algorithm which is a popular unsupervised machine learning technique that partitions data into distinct clusters based on similarity measures. The primary objective of this model is to analyze the latest stored location data of users and identify regions that exhibit a concentration of individuals affected by a particular disaster, thereby pinpointing hotspot locations.

The foundation of this machine learning model lies in the extensive dataset comprising the historical stored locations of users collected at 15-minute intervals. Each data point within this dataset represents the location of an individual user at a specific timestamp. For our project, we made our own dataset for the machine learning model because we couldn't find one online. The figure "2" below shows the dataset we're using in this project.

Fig. 2: Synthetic dataset of user's historical locations

In the context of the project, the algorithm [7] works by grouping together user locations that are close in proximity, thereby identifying regions with a higher density of trapped individuals.

Determining Optimal Clusters with the Elbow Method

To operationalize the insights derived from the Elbow method and enhance the performance of the K-Means algorithm [4], the identified optimal number of clusters [8] is set as a hyperparameter for the algorithm. By specifying this hyperparameter, the K-Means algorithm tailors its clustering process to align with the identified structure of the data, resulting in cluster centers that encapsulate the inherent patterns and distributions of the user location data related to natural calamities.

It works by calculating the sum of squared distances between data points and their respective cluster centroids, known as the cluster sum of squares. Initially, the number of clusters is set to one and gradually increased. For each number of clusters, the cluster sum of squares is computed and plotted on a graph. By examining this graph, one looks for the most significant change in slope, which indicates the point where adding more clusters does not significantly improve the model. To automate this visualization process, a differentiation technique is employed to track changes in slope accurately. The point with the highest change in slope is identified as the optimal number of clusters and is then used to set the final number of clusters in the K-Means algorithm.

For different calamity situations, the number of affected regions can vary based on distress signals or the last known locations of civilians received from the mobile app from those areas. Therefore, a fixed number of clusters is impractical. The Elbow method is used to determine the optimal number of clusters for each specific scenario, allowing the K-Means algorithm to dynamically adjust to best represent the data's structure.

For instance, in the case of a cyclone in Mumbai, there might be six distinct regions affected, requiring the number of clusters to be set to six. Conversely, for an earthquake in Gujarat, the number of affected regions might be four, thus the number of clusters would be set to four.

In this model, the number of clusters is set to 4 as shown in Figure "3".
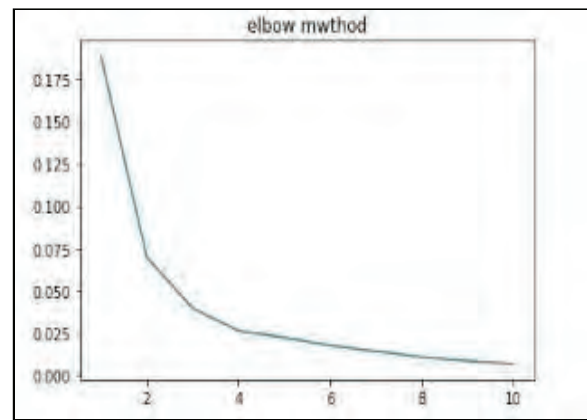
Fig. 3: Elbow method determining optimum number of clusters.

Producing Cluster Centers

Upon setting the optimal number of clusters as a hyperparameter, the K-Means [9] algorithm proceeds to generate cluster centers representative of the identified hotspot locations. These cluster centers serve as focal points within the geographical landscape, encapsulating regions with a heightened concentration of affected individuals. By analyzing the proximity of user locations to these cluster centers, the algorithm facilitates the identification and visualization of areas most severely impacted by natural calamities, thereby guiding rescue and response efforts more effectively.

$$d = \sqrt{[(x2 - x1)^2 + (y2 - y1)^2]} \tag{1}$$

$$ci = \frac{1}{|S_i|} \cdot \sum_{x_i \in S_i} x_i \tag{2}$$

Formula to find new centroid from clustered group of points.
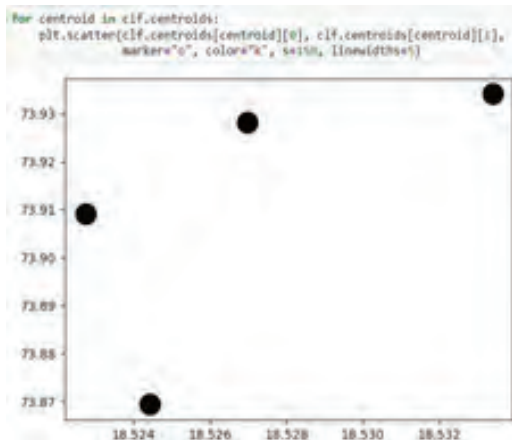
Fig. 4: Centroid points are plotted.

The algorithm calculates the mean point (centroid) for each cluster as shown in Figure "4". These centroid coordinates represent the estimated hotspot locations.

Trapped Civilian Frequency model

This method is used to estimate the number of people trapped in specific areas during disasters. Users send their location data through the app, which we analyze and store over various time periods. By averaging the number of people seen in particular "hotspot" locations over time, we get a typical count of individuals expected there. When determining the final estimate, we compare this average count with the latest data point. If the current count is higher than the average, we display the current count; otherwise, we show the mean of both the average and current counts.

By considering the hotspot generated from the K-Means model, this model performs analysis over a certain time-frame to provide a generalized count of civilians visiting in that hotspot area. For instance, K-means model provides a hotspot location as Pune. Thereafter, this model analyzes historical civilian's location data which is stored in the database for different time-frames such as weekly. From this analysis the model will generate an estimated average count natural calamities, disruptions that may occur during a natural disaster or other emergency situations. In such critical scenarios, maintaining a continuous and accurate record of the user's location becomes paramount.

By capturing and storing location data at frequent intervals, the application ensures that even if a network outage occurs, the most recent location of the user is still accessible. This "last known location" data can be instrumental for rescue teams, providing them with crucial insights to initiate or adjust rescue operations, even in the absence of real-time connectivity.

By capturing the user's location every 15 minutes, the application aims to create a comprehensive and up-to-date record of the user's movements and whereabouts. This periodic tracking enables the application to provide timely and relevant information, such as real-time updates on the user's location during a natural disaster or calamity. It also facilitates the efficient coordination of rescue and response efforts, as rescue teams can access accurate and recent location data to guide their operations.

In mobile application, an S.O.S[2] button is provided through which the users can generate distress signals which will be stored in the database. These signals are forwarded to the rescue team along with location's that lie in that particular region by the admin to save the civilians from the disaster. Also, the trapped civilians count which is predicted by a machine learning model is also forwarded to the rescue team by central admin. All the user's general information like names and phone numbers are stored in the database.

Below is the explanation of the system architecture as shown in Figure "5":
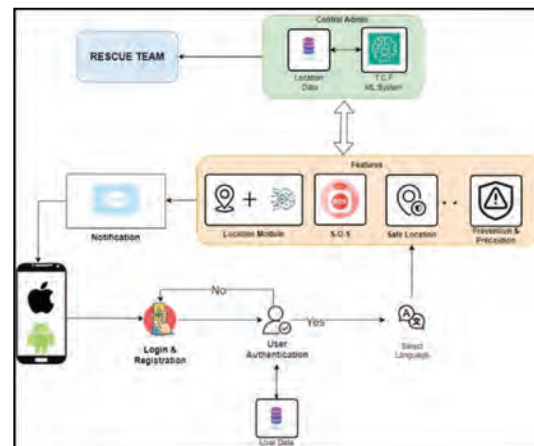
Fig. 5: System Architecture

Mobile App Frontend: The user interacts with the system through the mobile application. The app provides features such as real-time location tracking, disaster

alerts, and preventative information. It's designed to be user-friendly and multilingual.

User Data: It includes location and general information about the user, which is collected and stored securely in the database.

Central Administration: This component is responsible for monitoring and coordinating disaster response efforts. It includes:

1. Machine learning model to predict the trapped civilians count using stored user's locations and display hotspot locations.

2. Analyzing incoming data to make informed decisions regarding resource allocation and response strategies.

3. Facilitating communication between the admin team and rescue teams.

Rescue Teams: These are the on-ground personnel responsible for rescue operations. They receive location data and instructions from the central administration and use it to perform rescue operations efficiently.

Language Support: Language support modules enable the app to present information in multiple regional languages based on user preferences.

Push Notifications: The app uses push notifications to alert users to disaster warnings, updates, and preventative information.

RESULT

The results of our project showcase a comprehensive journey through various stages of user interaction and system functionalities. Figure "6" depicts the seamless process of requesting location access, essential for the accurate functioning of the application. Upon successful login, users are greeted with Figure "7", the intuitive home page of the application, providing easy access to essential features. Additionally, Figures "8" highlight the provision of specific preventions and precautions for natural disasters in particular regions. Figure "9" and Figure "10" showcase the application's inclusivity by offering translations into Hindi and German languages, ensuring accessibility to a wider audience. As depicted in Figure "11", users can send an S.O.S signal. Furthermore, Figures "12" provide predicted

count of trapped civilians in Pune, also Figure "13" and "14" provide critical insights into hotspot locations and live locations of trapped civilians in regions such as Pune and Kolhapur, aiding rescue teams in optimizing their response strategies effectively. These results collectively demonstrate the robustness and efficacy of our disaster response system in safeguarding lives during emergencies.
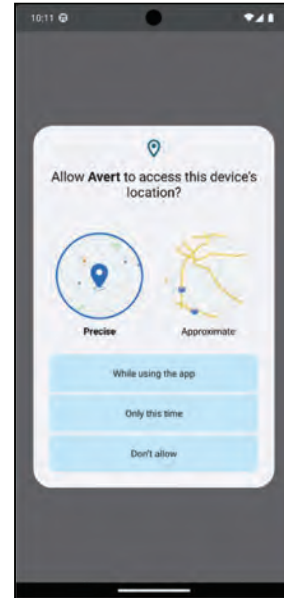
Fig. 6: Requesting location access
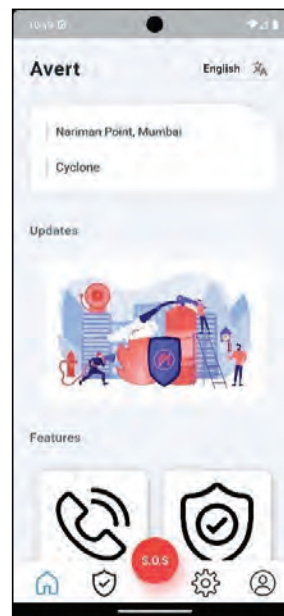
Fig. 7: Home Page
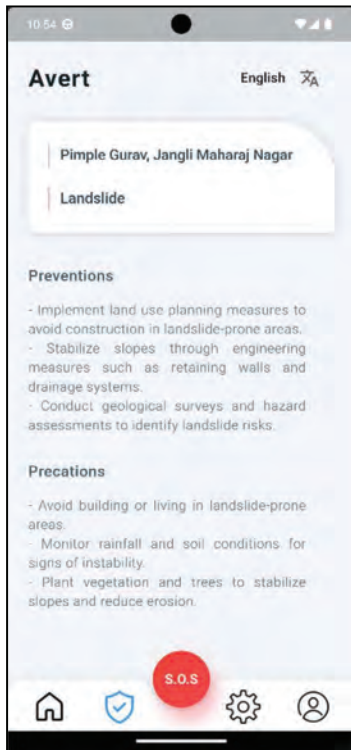
Fig. 8: Preventions & Precautions for Landslide in Pune
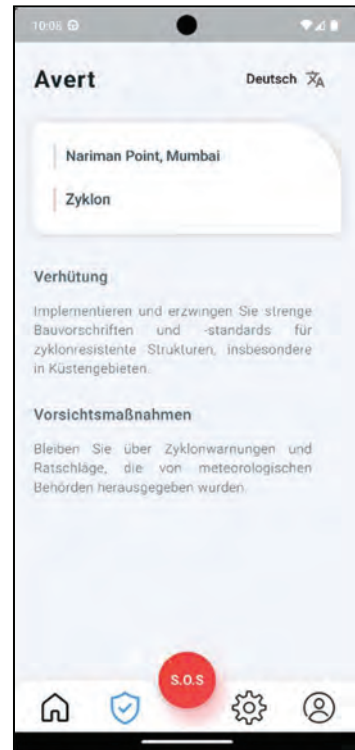
Fig. 10: Translated to German language
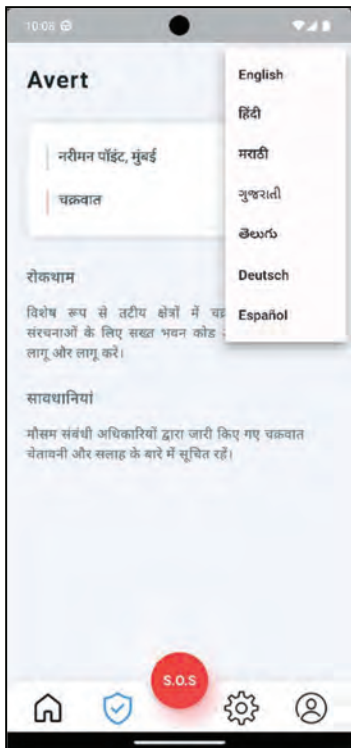
Fig. 9: Translated to Hindi language
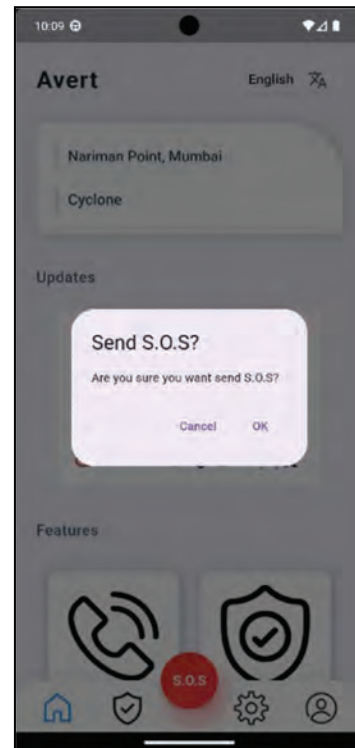
Fig. 11: Confirmation to send S.O.S signal
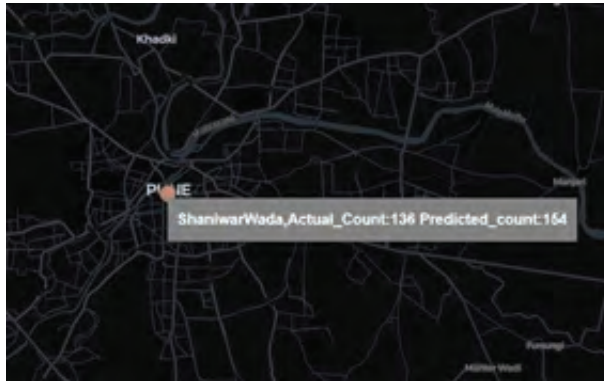
Fig. 12: Hotspot locations and predicted count of trapped civilians, Pune Region

Fig. 13: Displaying civilians' location who triggered S.O.S

Fig. 14: Displaying hotspot region which is sent to rescue team

FUTURE SCOPE

We hope to improve our project in the future by utilizing the information gathered from the smartphone application, where civilian locations are continuously added to a database. Over time, when we gather a sizable amount of location data, we hope to use big data analytic tools to draw insightful conclusions. This involves estimating civilian counts with greater accuracy and projecting their future movements based on their present positions. In particular, we intend to use Recurrent Neural Networks (RNN) for predictive analysis, which will allow us to estimate the likely next destination of people, even in situations when internet connectivity is restricted or nonexistent. Rescue teams might benefit greatly from this update by being able to concentrate their efforts in areas where civilians are most likely to be found, which would enable more effective and efficient response plans.

CONCLUSION

In conclusion, our project envisions a robust and proactive approach to disaster management that leverages cutting-edge technology to save lives and reduce the devastating impact of natural disasters. By addressing the critical issues of communication gaps, lack of awareness, and unpreparedness, our mobile application offers a multifaceted solution that benefits both the public and rescue teams.

In a world where natural disasters continue to pose significant threats to communities worldwide, our project represents a proactive and innovative step toward disaster resilience. By equipping individuals and rescue teams with the tools they need to navigate these challenging circumstances, we strive to reduce casualties, minimize property damage, and ultimately save lives.

As we move forward with the development and implementation of this disaster preparedness mobile application, we remain dedicated to the fundamental goal of making our communities safer and more resilient in the face of adversity. With ongoing research, development, and collaboration, we have the potential to transform the way we respond to natural disasters, creating a safer and more secure future for all.

REFERENCES

1. https://quantectum.com/blog/natural-hazards-and-earthquakes-in-india/

2. G Vishwanath Gupta, M Sai Pavan, K Sai Ruthwik, M Revanth and Anjali T, "A proximity aware android SOS application in times of pandemic," 2021 Third International Conference on Inventive Research in Computing Applications (ICIRCA), 2021.

3. Vibhas Sukhwani and Rajib Shaw, "Operationalizing crowdsourcing through mobile applications for disaster management in India," Graduate School of Media and Governance, Keio University, 5322 Endo, Fujisawa 252- 0882, Kanagawa, Japan, 2019.

4. Kristina P. Sinaga and Miin-Shen Yang, "Unsupervised K-Means Clustering Algorithm," IEEE Access, vol. 8, pp. 2169-3536, 2020.

5. Mayank Kumar Jarwal, Abhimanyu Barun, Arshpreet Singh and Akanksha Srivastava, "Mobile Application based Tracking using GPS and GSM," International Conference on Signal Processing and Communication (ICSC), 2022.

6. Fang-Chu Chen, Rui-Yen Chang, Wan-Yi Lin, Sheng Hui Chen, Yu Cheng Chen and Chin Nung Li, "Disaster and Emergency Management System; The 15th International Symposium on Wireless Personal Multimedia Communications," The 15th International Symposium on Wireless Personal Multimedia Communications, 2012.

7. R. S. Gaykar, C. Nalini and S. D. Joshi, "Identification of Straggler Node in Distributed Environment Using Soft Computing Algorithms," 2021 International Conference on Emerging Smart Computing and Informatics (ESCI), 2021, pp. 1-5, doi:10.1109/ESCI50559.2021.9396825.

8. Punyaban Patel, Borra Sivaiah and Riyam Patel, "Approaches for finding Optimal Number of Clusters using K-Means and Agglomerative Hierarchical Clustering Techniques," 2022 International Conference on Intelligent Controller and Computing for Smart Power (ICICCSP), 2022.

9. Mark Edward M. Gonzales, Lorene C. Uy, Jacob Adrianne L. Sy and Macario O. Cordel, "Distance Metric Recommendation for k-Means Clustering: A Meta- Learning Approach," TENCON 2022 - 2022 IEEE Region 10 Conference (TENCON), 2022.

Intelligent Disease Detection Using Machine Learning Algorithms

Ronita R. Mitra
✉ ronitamitra14@gmail.com
Anjali V. Mistry
✉ anjali.mistry05@gmail.com
Komal P. Lad
✉ komalladnvs55@gmail.com

Jinal Tailor*
✉ jinal.tailorssa@gmail.com
Rajnish Rakholia
✉ rajnish.rakholia@gmail.com

S.S. Agrawal Institute of Technology and Management
Gujarat Technological University
Ahmedabad, Gujarat

ABSTRACT

In recent times, early diagnosis has proven crucial for effective and improved treatment for patient during COVID-19 pandemic. Integrating AI and machine learning technologies into healthcare shows great promise for revolutionizing disease diagnosis and improving results. Presented research empower healthcare professionals to swiftly identify diseases, enabling timely interventions and personalized treatment plans. Our proposed intelligent disease detection system, named Risk Assess, aims to provide medical professionals with a powerful tool for early disease detection. By conducting a comprehensive comparative study of machine learning algorithms such as KNN, SVM, Logistic Regression, and Support Vector Machines, we aim to predict and diagnose a wide range of diseases including breast cancer, diabetes, cardiovascular conditions, renal disorders, and hepatic ailments. Through this research, we seek to advance the field of medical science and improve healthcare outcomes for patients worldwide.

KEYWORDS : Deep learning, Disease detection, Logistic regression, Machine learning, Medical diagnosis.

INTRODUCTION

As per the World Health Organization's survey, millions of individuals die from different diseases daily[1]. Over the past 1.5 years, COVID-19 has surged, claiming the lives of approximately 25.9 million people, followed by heart attacks at 17.5 million. Breast cancer accounted for 2.3 million fatalities, while liver disease and diabetes caused 2 million and 1.5 million deaths, respectively. Chronic kidney diseases rounded up the list with 1.2 million reported fatalities[2].

Machine learning is rapidly advancing, with deep learning programs inspired by the human brain enabling refined processing and pattern recognition, surpassing traditional methods[3]. Advancements in machine learning, cloud technology, and hardware are creating more adaptable digital assistants and enhancing communication for more efficient digital interactions[4].

Innovations like those from the 2020 Tokyo Olympics and Microsoft's Skype translator are making voice-based interactions more accessible[5].

Our system leverages datasets sourced from reputable repositories such as Kaggle, UCLI, and others. These datasets have undergone rigorous preprocessing, cleaning, and scrutiny to ensure their reliability. However, it's important to note that relying solely on the algorithms used for training these datasets may not always be ideal. Continuous advancements in technology introduce new algorithms that should be explored and tested regularly. In our case, we have experimented with various algorithms including Naive Bayes, Random Forest, Decision Trees, and Support Vector Machines (SVM). After thorough evaluation, we have narrowed down our selection to one final algorithm – Logistic Regression. Logistic regression

utilizes the logit function to predict values, providing binary responses (1 or 0) based on the input data.

To determine the best-performing algorithms, we have assessed their accuracy and time complexity and compared them against each other. Additionally, we have implemented Flask to run the website, ensuring seamless functionality and user experience.

There are mainly two users to this system with different components as mentioned below:

1. Admin: The main administrator can do changes, update charts, create models and do exploratory data analysis.

2. User: The user of the system has to create an account first. The system is open ended to all because it is a nonprofit cause; hence anyone can create an account. However, the user cannot get any access to the original dataset.

3. Interfaces of the system: The base interface of the system is the login page where a user can register and login the system. After that input the details in a form and predict the results. The exploratory data analysis can be done by admin.

4. Hardware: The project is not dependent on any hardware constraint.

5. Software: Windows 8+ or Ubuntu for OS, Google chrome or any other web browser, SQLite database, MongoDB for chatbot database, ML code in anaconda, Flask, Streamlit and python for website integration.

6. Communication Interface: A good web browser with internet facilities and a minimum internet speed of 1 MBps

7. Memory: Minimum RAM of 4 GB

8. Product Functions: The system uses login, registration of users. The admin can access data and records.

9. Characteristics of User: Any misplacement or incorrect data can lead to incorrect results.

10. Constraints of the system: The dataset that is used in the system is relatively small. To avoid overfitting of data, we can increase the size of the

dataset. The model that is used here doesn't take any unnecessary data like name or id. Only the required fields like input are used for processing data and forecasting it. Privacy is protected by this constraint as no personal patient details are used on the system. The deployment is done on a publicly maintained open-source repository and hence can be changed in a skeptical way too. System is very reliable in terms of privacy protection. An error is thrown with a validated message if the model produces an error. The webpage loads in seconds in online deployment. The algorithm is used with the maximum accuracy possible, pertaining to each model and training them individually.

Features of Proposed Model

The system offers following features which play a critical role in shaping the effectiveness and functionality of systems.

-   System provides faster diagnosis& data summarization

-   Reduced errors and misdiagnosis

-   Easy to Use& user-friendly system

-   No Human Interaction Required

However, the system faces skepticism regarding machine reliance, and it lacks the ability to provide preventive suggestions based on risk assessment. This limitation means it cannot offer specific recommendations or guidance even after evaluating risk factors (1 = Risk, 0 = No Risk).

The cumulative performance evaluations in terms of Accuracy % of each model, except covid 19, are shown as below in Table 1. This is to be noted that we have used kidney, liver, heart, diabetes and breast cancer datasets to create predictive models about the same.

Table 1. Cumulative Performance Evaluation of various models

Algorithms	Accuracy in %
Logistic Regression	83.38
Naive Bayes	80.73
Decision Tree	80.54
Random Forest	81.28

REVIEW OF LITERATURE

Fatima & Pasha (2017)[7] have presented paper that compares Machine Learning algorithms for diagnosing diseases such as heart disease, diabetes, liver disease, dengue, and hepatitis, highlighting their highest accuracy rates. They have analyzed that SVM detects heart disease with 94.60% accuracy. Naive Bayes accurately diagnoses diabetes with 95% accuracy. FT achieves 97.10% accuracy for liver disease. RS theory detects dengue with 100% accuracy. Feed forward neural networks classify hepatitis with 98% accuracy.

Chang et al. (2022) [8]The paper presented the development of an Artificial Intelligence heart disease detection system using machine learning in Python, focusing on data processing and logistic regression. They have presented experiment for random forest classifier achieving 83% accuracy, measuring performance and the SEABORN library's use. The confusion matrix validates prediction accuracy, while the random forest algorithm's multiple decision trees enhance stability and accuracy, akin to a decision tree but with hyperparameters.

Nguyen et al.(2021)[9] have defined study about deep learning effectiveness in disease prediction using epigenomic data, showcasing its success in detecting diseases, classifying subtypes, and predicting treatment responses with high accuracies. The models primarily use DNA methylation and RNA-sequencing data. While these models hold promise, challenges like validation and interpretability need addressing for wider clinical applicability. They have concluded that improvements in interpretability and model selection could boost deep learning's role in translational epigenomics, bridging gaps for future medical applications.

Saboor et al. (2022)[10] have mainly focused upon advancements in computing and medical techniques that diversified medical sciences, particularly in identifying dangerous heart diseases. Their study used various Machine Learning techniques and metrics to predict heart disease accurately, improving accuracy through preprocessing and hyperparameter tuning. The proposed method effectively enhances heart disease prediction accuracy, achieving 96.72% accuracy with SVM.

Haq et al. (2018)[11] prepared study machine-learning system for accurate heart disease diagnosis. have discussed all of the classifiers, feature selection algorithms, preprocessing methods, validation method, and classifiers performance evaluation metrics used in this paper. They have observed that the classification accuracy of logistic regression increased from 84% to 89% on reduced features. Similarly, SVM (RBF) accuracy increased from 86% to 88% with reduced features. They have concluded that the feature selection algorithms select important features which increased the performance of the classifiers and reduced the execution time. The designing of a diagnosis system for heart disease prediction using FS with classifiers will effectively improve performance.

Nashif et al. (2018)[12] have presented study that addresses the urgent need for early detection of cardiovascular diseases by proposing a cloud-based heart disease prediction system using SVM with 97.53% accuracy. The system, validated with 10-fold cross-validation, offers real-time patient monitoring through Arduino and GSM technology notifications for critical parameters. They have analyzed that SVM outperformed Random Forest and Simple Logistic models prove its efficiency in heart disease prediction. Their study introduces a Continuous Patient Monitoring system for home-based cardiac care, integrating vital signs for real-time risk assessment and comfort adjustments, showcasing its potential for centralized medical advice and intervention.

EXPLORATORY DATA ANALYSIS

The diagrams below are a cumulative analysis of the dataset that has been taken from UCI and Kaggle. The data analysis is known as exploratory data analysis which shows various trends and results from various different algorithms and the datasets. The first dataset is the breast cancer one taken from the source UCI Machine learning Repository[13].

As shown above from Figure 1, SVM or support vector machine performs the best with breast cancer dataset. From figure 2 and 3 we can get that accuracy yielded at 97%.
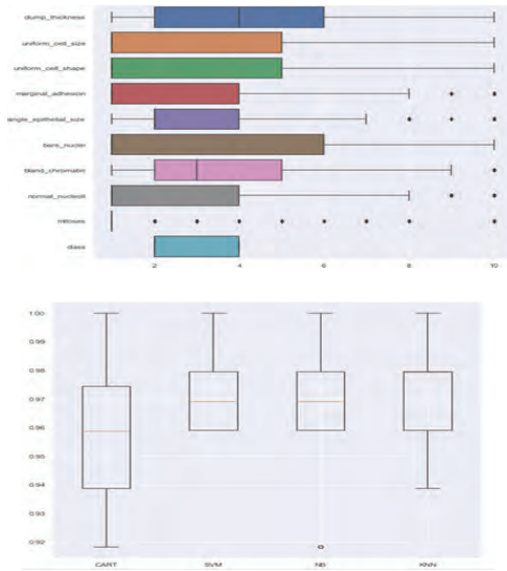
Figure 1. Baseline algorithms check for various methods
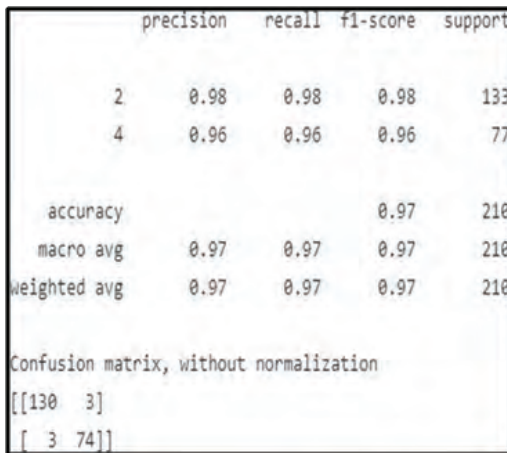
Figure 2. Confusion Matrix - Precision & Recall
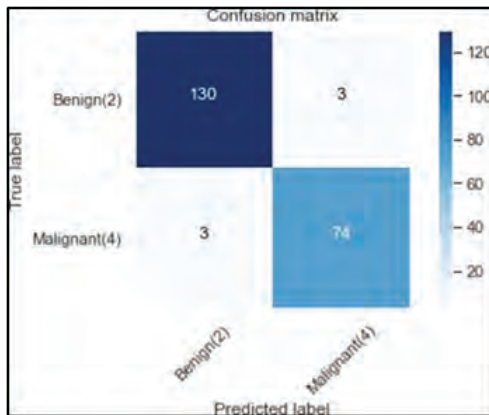
Figure 3. Confusion Matrix
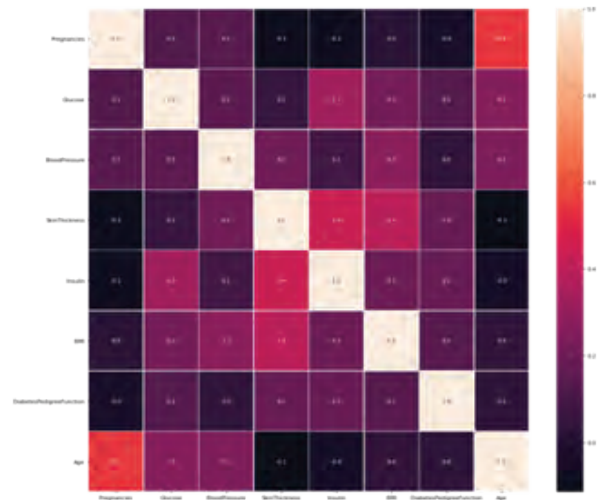
Figure 4. Correlation heat plot between all bivariate features

For the diabetes dataset, it is observed that the prediction value obtained using logistic regression for this particular dataset is the highest with the Accuracy of 87% as shown in figure 4.

For the kidney dataset, the file used for the chronic kidney dataset is taken using Kaggle. We have used logistic regression for this as well as logistic regression works better with classification problems as shown in Figure 5.
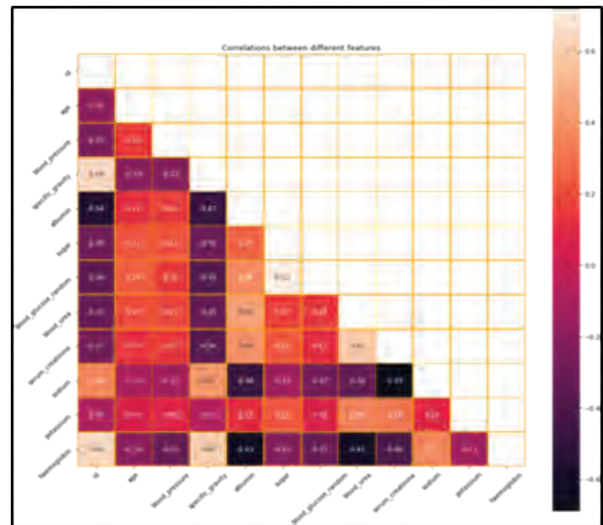
Figure 5. Correlation between different features

With this dataset and training model, we have achieved an accuracy of 80% which was marked higher than the

others. While this algorithm should not be used as a measure or a standard to cumulate results, this algorithm by far has achieved the best results in all use cases.

Liver dataset is extracted from Kaggle repository[14]. Many predictive functions are used, but after checking each algorithm it is observed that both K nearest neighbor and logistic regression have the same accuracy.
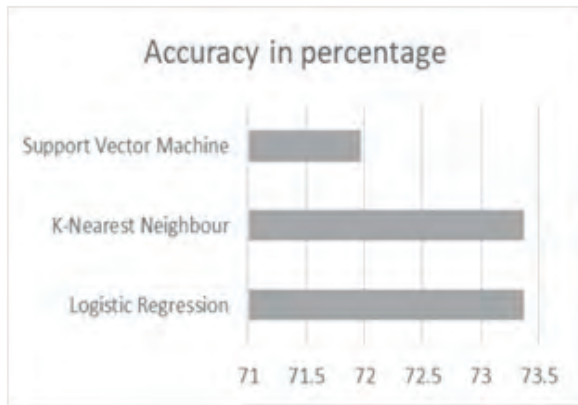
Figure 6. Accuracy for all algorithms tested Dataset exploratory analysis
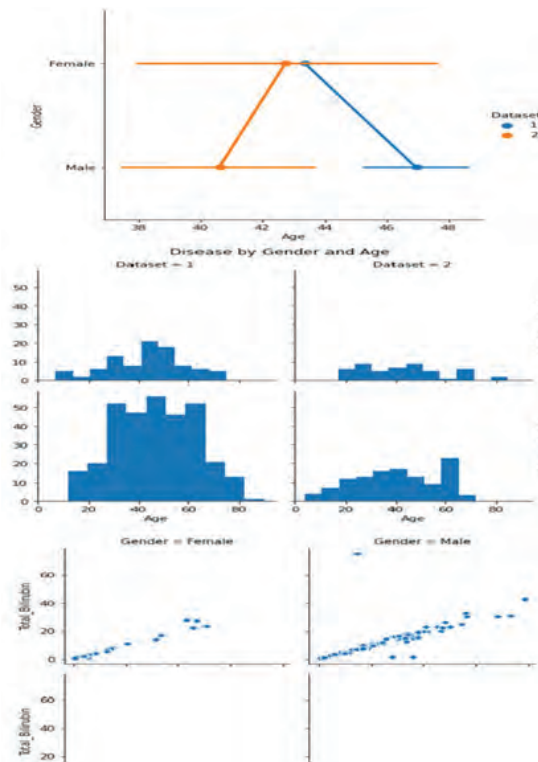
Figure 7. Feature Distribution and Relationship with each other

Here is the exploratory data analysis of different features and their relationship with one another as shown in figure 6 and 7.The correlation heat plot is the same shown in Figure 8.
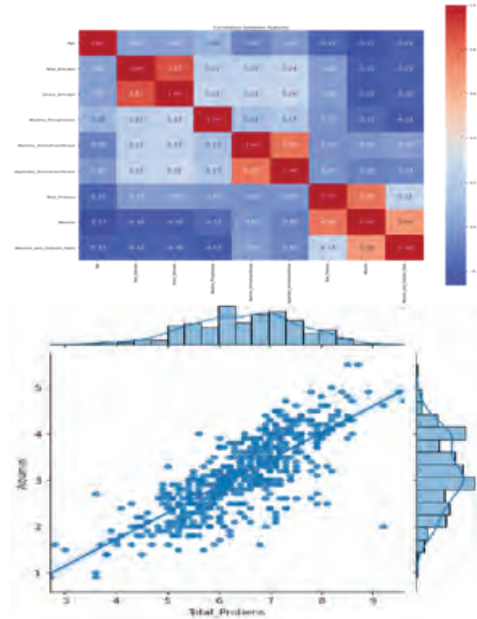
Figure 8. Correlation heat plot

Heart disease dataset is obtained from UCI[15]. We use logistic regression to map the heart dataset. The model predicted with 86.88% accuracy shown in figure 9, The model is more specific than sensitive.
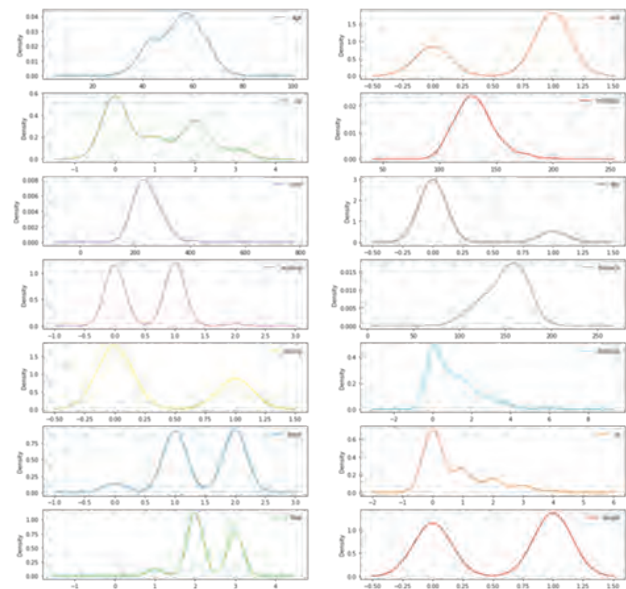
Figure 9. Density plot of each individual feature

This is to be noted that we have also made a dialog flow chatbot with telegram and website integration. The conversations are stored in mongo DB and the python environment is set up in flask. Moreover, Rapid API is used to fetch the data from the system. Postmaster is used for testing it locally and Heroku is used for the web deployment. The chatbot can create intents and generate activities under various natural language processes.

The deployment of the project is done on Heroku and is hence free for all. The covid dataset uses neural network and transfer learning to run the training algorithms. It is used to classify data into images and vice versa. A model for the same is developed shown in figure 10 and figure 11.
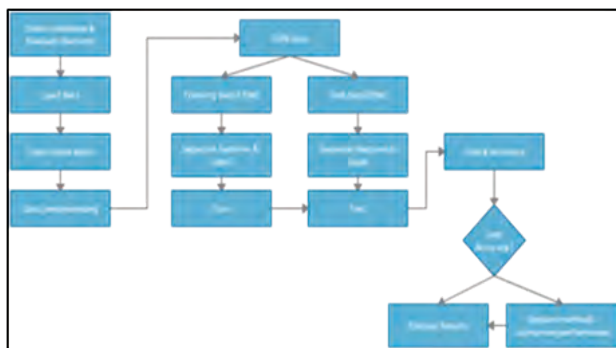
Figure 10. Proposed Model for Disease Detection
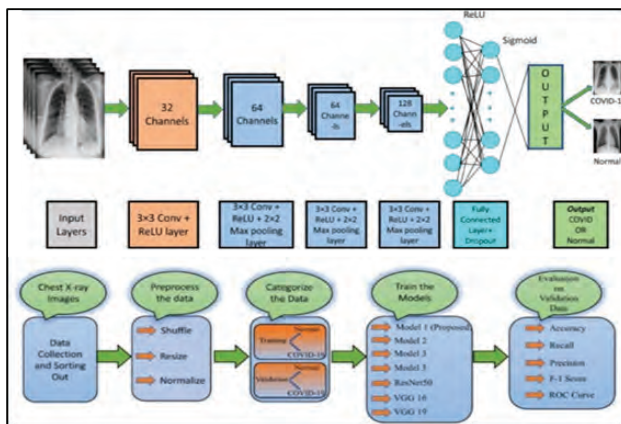
Figure 11. Architecture of Deep Convolutional neural network - covid 19

CONCLUSION

The various datasets used here are collected from various repositories and collections. The data is preprocessed and cleaned using one hot encoding and replacing the missing values. Several machine learning algorithms are used for prediction of diseases. In our project and the paper, we have used KNN algorithm that predicts data according to the neighboring points. SVM uses a hyper plane to separate data. Logistic Regression is used for classification algorithms with probabilistic functions of 0 and We have compared each algorithm with classification accuracy implemented through confusion matrix. From the experiments conducted, we have summarized that the heart, diabetes, kidney dataset works better with logistic regression. Liver dataset gives approximately the same accuracy with both KNN and Logistic Regression. Breast Cancer dataset works better with Support Vector Mechanism. Classification of images using tensor flow is better with neural networks and transfer learning mechanisms.

Future Work

Improvements can be done from the scalability and accuracy point of view. However, this can be implemented for better performance and most importantly better accuracy. Various clustering methods of voting methods can be used for prediction as well.

REFERENCES

1. Kruk, M. E., Gage, A. D., Joseph, N. T., Danaei, G., García-Saisó, S., & Salomon, J. A. (2018). Mortality due to low-quality health systems in the universal health coverage era: a systematic analysis of amenable deaths in 137 countries. The Lancet, 392(10160), 2203-2212.

2. World Health Organization. (2020). World health statistics 2020: monitoring health for the SDGs, sustainable development goals. World Health Organization.

3. Taye, M. M. (2023). Understanding of machine learning with deep learning: architectures, workflow, applications and future directions. Computers, 12(5), 91.

4. Krishnan, C., Gupta, A., Gupta, A., & Singh, G. (2022). Impact of artificial intelligence-based chatbots on customer engagement and business growth. In Deep learning for social media data analytics (pp. 195-210). Cham: Springer International Publishing.

5. Seligman, M., Waibel, A., & Joscelyne, A. (2017). Taus speech-to-speech translation technology report. De Rijp: TAUS BV, 1-58.

6. Chattopadhyay, A., Mishra, S., & González-Briones, A. (2021). Integration of machine learning and IoT in healthcare domain. Hybrid artificial intelligence and IoT in healthcare, 223-244.

7. Fatima, M., & Pasha, M. (2017). Survey of machine learning algorithms for disease diagnostic. Journal of Intelligent Learning Systems and Applications, 9(01), 1.

8. Chang, V., Bhavani, V. R., Xu, A. Q., & Hossain, M. A. (2022). An artificial intelligence model for heart disease detection using machine learning algorithms. Healthcare Analytics, 2, 100016.

9. Nguyen, T. M., Kim, N., Kim, D. H., Le, H. L., Piran, M. J., Um, S. J., & Kim, J. H. (2021). Deep learning for human disease detection, subtype classification, and treatment response prediction using epigenomic data. Biomedicines, 9(11), 1733.

10. Saboor, A., Usman, M., Ali, S., Samad, A., Abrar, M. F., & Ullah, N. (2022). A method for improving prediction of human heart disease using machine learning algorithms. Mobile Information Systems, 2022(1), 1410169.

11. Haq, A. U., Li, J. P., Memon, M. H., Nazir, S., & Sun, R. (2018). A hybrid intelligent system framework for the prediction of heart disease using machine learning algorithms. Mobile information systems, 2018(1), 3860146.

12. Nashif, S., Raihan, M. R., Islam, M. R., & Imam, M. H. (2018). Heart disease detection by using machine learning algorithms and a real-time cardiovascular health monitoring system. World Journal of Engineering and Technology, 6(4), 854-873.

13. Andras, J., William, S., Matthias, P., & Robert, D. (1988). Heart disease. UCI Machine Learning Repository.

14. Josep Vidal. (2019). Liver Patient Dataset. Kaggle. https://kaggle.com/competitions/liver-patient-dataset

15. Janosi, A., Steinbrunn, W., Pfisterer, M., & Detrano, R. (1988). Heart Disease. UCI Machine Learning Repository. UCI Machine Learning Repository

Leveraging Blockchain Technology to Facilitate Collaborative Digital Twins in the Healthcare System

Padmavathi V, Kanimozhi R
Associate Professors
A. V. C. College of Engineering
Mannampandal, Mayiladuthurai
✉ vvpadhu@gmail.com

ABSTRACT

This research showcases the creation of Med Chain, a cutting-edge system that utilizes blockchain technology to transform medical records management. The proposed system, Med Chain, offers an innovative solution to enhance existing systems by enabling interoperability, ensuring data security, and providing efficient access to medical records for patients. Med Chain uses blockchain technology to manage access to medical records and transactions with smart contracts. These smart contracts act as a decentralized authority, facilitating secure and transparent interactions within the network. By implementing advanced encryption techniques, Med Chain enhances the overall security of medical records, ensuring confidentiality and integrity.

Moreover, Med Chain introduces a novel incentive mechanism that incentivizes healthcare providers based on their commitment to maintaining accurate medical records and generating new blocks. This incentive mechanism encourages active participation and ensures that all stakeholders in the healthcare ecosystem have a vested interest in maintaining high-quality data. Utilizing blockchain technology, Med Chain offers several advantages to the healthcare system. It enables seamless data exchange among different healthcare providers, eliminating the need for redundant data entry and enhancing care coordination. Med Chain empowers patients by giving them full control of their medical records, enabling secure access and sharing of their health information with authorized parties. Overall, Med Chain represents a promising step towards transforming healthcare record management. By leveraging blockchain's inherent features of security, transparency, and decentralized governance, Med Chain provides a robust and efficient platform for collaborative medical record management in the healthcare system.

KEYWORDS : Blockchain technology, Med chain, Medical records management, Timed-based smart contracts, Electronic medical records.

INTRODUCTION

Health data interoperability still needs to be improved in the healthcare sector. The issue of how to grant public access to private health information still needs to be properly resolved. However, by offering safe and interoperable references to Electronic Health Records (EHRs), blockchain technology and smart contracts offer an intriguing and novel way to address this issue. Blockchain technology can enhance interoperability and privacy in electronic health record solutions. Many electronic patient records are due to the healthcare industry's increasing digitization. This dramatic rise in data makes the need to protect healthcare data while it is being exchanged and used more difficult than ever. In order to address privacy, security, and integrity issues with healthcare data, blockchain technology has emerged as a possible alternative. Due to its openness and accountability, blockchain applications and academic study have become increasingly popular in industry and academia.

Peer-to-peer network transactions use distributed ledger technology or blockchain technology. It permits

the safe and accurate storing of any data. The smart contract, which consists of adaptable rules regulating decentralized interactions between participants, is a significant idea in the blockchain. Smart contracts have various applications in healthcare, finance, voting, and energy. Blockchain eliminates intermediaries, increasing transparency and trust. It uses cryptography and consensus procedures to validate transactions in an unstable setting. Each receiving node in a P2P network built on blockchain verifies and saves accurate messages in blocks. The data in each block is then verified using a consensus mechanism, such as Proof-of-Work (PoW). The block is circulated over the network and added to the chain after confirmation.

One of the key industries utilizing blockchain technology is healthcare. Healthcare data security, privacy, sharing, and storage issues can be resolved with blockchain. Interoperability, which refers to the exact, effective, and consistent interchange of data or information between human or computer parties, is a critical requirement for the healthcare sector. Thanks to interoperability, healthcare practitioners and patients from various hospital systems can share health-related information, such as electronic health records. New opportunities are opening up for effective health data management and enhanced patient access to their health information due to developments in electronic health-related data, rules around the storage of healthcare data in the cloud, and the significance of ensuring patient data privacy. For data-driven organizations, ensuring data security is crucial. This is especially true in the healthcare industry, where blockchain technology can handle these pressing issues firmly and successfully. A seven-step procedure for managing healthcare data using blockchain is shown in Figure 1. The blockchain applications in this category cover electronic health records, data management, and storage.

This paper's goals are to:

• Provide a thorough analysis of current blockchain technology use cases in healthcare applications.

• Outlining the main difficulties with applying blockchain technology to the healthcare industry.

• Outlining principles for further study and pointing out unresolved problems in blockchain-based healthcare applications.

• Examining the advantages and disadvantages of current healthcare blockchain implementations.

This study will analyze blockchain technology's potential and limitations to illuminate its role in attaining safe and interoperable healthcare data management.
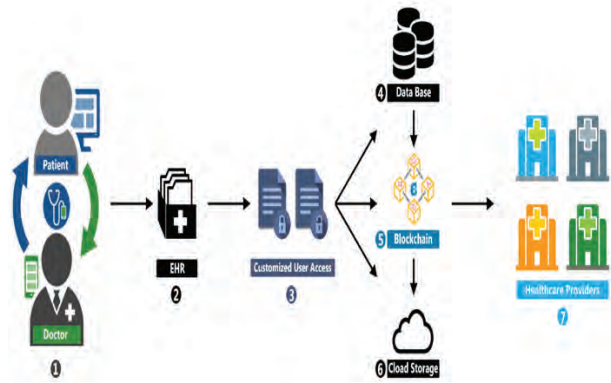
Fig. 1: Blockchain Technology Transforming Healthcare Data Management

RELATED WORKS

Patients can only consult with various healthcare professionals if hospitals control Electronic Health Records (EHRs). This makes it more difficult for patients to obtain medical records and healthcare information. The authenticity of EHRs stored on the blockchain is guaranteed by the attribute-based signature technique with multiple authorities proposed in this research [1]. Patients participate in this method by endorsing communications based on predetermined criteria without disclosing anything beyond the evidence of their attestation. The escrow issue is solved, and the distributed data storage characteristics of the blockchain are supported by using numerous authorities rather than a single central authority to generate and distribute public/private keys to patients. The system is meant to withstand collision assaults even when N -1 out of N authorities are compromised by exchanging secret pseudorandom function seeds across authorities. Using the computational bilinear Diffie-Hellman assumption, the study formally proves the security of the attribute-based signature scheme, concentrating on the unforgeability and perfect privacy of the attribute signer. The effectiveness and unique qualities of the suggested strategy are demonstrated by comparison to other methods suggested in earlier studies.

Sharing electronic health records [2] raises concerns about data leakage and compromises patient privacy, particularly with sensitive medical information. Since data uploaded to a blockchain cannot be changed after publication, blockchain technology offers possible solutions for the secure and reliable sharing of EHRs. This article suggests a blockchain-based searchable encryption scheme for electronic health records (EHRs), allowing many stakeholders, such as doctors, hospitals, labs, and insurance companies, to access EHRs more securely. The study uses sophisticated logic expressions to build an index for EHRs stored on the blockchain. While the actual EHR data continues to be controlled by the data owners, data users can use these phrases to search the index. The data owners maintain complete control over who has access to their EHRs by moving the index to the blockchain for propagation. The integrity, anti-tampering, and traceability of the EHRs' index are all guaranteed by blockchain technology.

Data security stored in the cloud has always been a concern due to potential cyber-attacks. Healthcare data, in particular, has become a prime target for attackers. Healthcare data breaches can have devastating consequences for healthcare organizations [3]. Decentralizing cloud data is one method of reducing these risks because it can lessen the effects of attacks. Decentralized peer-to-peer (P2P) networks allow storing and processing of sensitive healthcare data in the cloud. Accountability and integrity may be guaranteed by utilizing the distributed and decentralized characteristics of blockchain technology. While many decentralized approaches to attack control have been put forth, they frequently need to ensure the overall privacy of patient-centric systems. This study introduces a patient-centric healthcare data management system that achieves privacy through storage by using blockchain technology. Patient data is encrypted using cryptographic techniques to maintain pseudonymity.

Advancements in information and communication technologies have greatly impacted the e-health industry and research. For the interaction and cooperation of electronic medical record systems, guaranteeing data security and ease is essential when sharing personal medical data [4]. However, because of inconsistent

architecture in terms of security rules and access control models, present systems require assistance to achieve these requirements. The accountability of medical usage data must be ensured; hence, a new solution is needed to improve data accessibility while abiding by privacy and security laws. With special qualities like data privacy and transparency, blockchain technology is promising to revolutionize the conventional healthcare sector. This document gives patients access to a thorough and unchangeable log that makes it simple for staff members in various hospital departments to retrieve their patients' medical records. To show the functionality and effectiveness of the suggested platform, construct a case study for a hospital on a permission network and conduct several experimental experiments.

The paper [5] proposes an architecture for data carriers that bridges the communication gaps between Ethereum smart contracts and outside IoT settings. The design seeks to enable smart contracts to access off-chain data cost-effectively and elastically within a blockchain-enabled IoT ecosystem. The three parts of the proposed architecture—Mission Manager, Task Publisher, and Worker—enable communication between smart contract creators, Ethereum nodes, and off-chain data sources. The study also offers targeted approaches for decoding event logs and filtering smart contract events according to predefined criteria. According to the evaluation's findings, the proposed method can reduce the cost of deploying smart contracts by an average of $20. Additionally, compared to the present data carrier services, it offers greater efficiency and flexibility.

Table 1. Literature Survey

Authors	Description	Methods	Advantages
R. Guo, H. Shi, Q. Zhao, D. Zheng	Presented a safe attribute-based signing mechanism for electronic medical record systems that use blockchain technology.	Attribute-based signature scheme	Enhanced security, multiple authorities for key management

L. Chen, W.-K. Lee	Outlined a searchable encryption system based on blockchain to communicate electronic health records safely.	Searchable encryption	Improved data security, easy access to records
A. Al Omar, M. Z. A. Bhuiyan	It outlines the privacy-friendly framework for employing blockchain technology to manage healthcare data in the cloud.	Privacy-preserving data management	Enhanced privacy, decentralized data control
L. Hang, E. Choi	A novel blockchain-based platform for ensuring the integrity of electronic medical records in a hospital setting.	EMR integrity management	Improved data integrity, easy access to records
X. Liu, K. Muhammad	Presented a data carrier architecture enabling smart contracts to fetch off-chain data cost-effectively and elastically.	Data carrier architecture	Reduced deployment cost, improved efficiency

Table 1 summarizes research papers on blockchain technology in healthcare. These papers offer solutions for searchable encryption for electronic health record sharing, privacy-friendly cloud platforms for healthcare data, EMR integrity management using medical blockchain platforms, and a flexible and affordable data carrier architecture for smart contracts. They also offer solutions for secure attribute-based signature schemes and platforms [6]. The articles illustrate how blockchain technology can improve data security, privacy, integrity, and efficiency in the healthcare industry. Overall, they show how blockchain technology has the power to transform the way that healthcare data is managed completely.

SYSTEM ARCHITECTURE

A comprehensive framework has been developed for managing and sharing electronic medical records (EMRs) to treat cancer patients, and it has been implemented in collaboration with a hospital. This system ensures the privacy, security, accessibility, and precise access control of EMR data[7]. The approach aims to reduce communication time for EMRs, improve treatment decision-making, and lower costs by utilizing blockchain technology, specifically the Ethereum blockchain network.

Ethereum, introduced in 2015, builds on Bitcoin's principles, offering a trustless environment for executing smart contracts through its open-source, peer-to-peer distributed infrastructure. Incorporating Ethereum enhances security and transparency, ensuring EMR information is securely stored and shared while maintaining privacy and enabling efficient access management. Smart contracts streamline the sharing process, facilitating quicker access to vital EMR data for treatment decisions.

Figure 2 illustrates the proposed framework, demonstrating an innovative approach to managing and sharing EMR information in cancer patient care. Utilizing Ethereum's blockchain technology, the system aims to revolutionize the efficiency, security, and trustworthiness of EMR management and sharing processes.
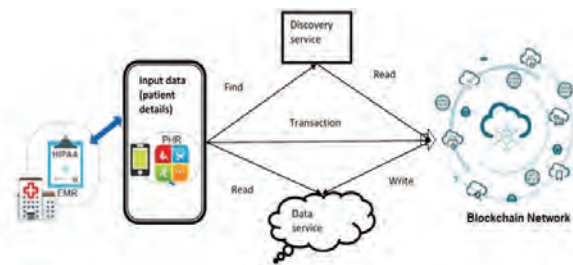
Fig. 2: The Proposed Framework

The relationship between the General Data Protection Regulation (GDPR) in Europe and blockchain technology is complex. While blockchains align

with GDPR aspects like data portability and consent management, concerns exist regarding the right to be forgotten and potential data control loss through smart contract execution. "Dynamic consent management," which aligns with GDPR provisions on consent, can address these concerns. Private blockchains, such as Enterprise Blockchain, offer potential solutions by complying with GDPR directives, being under a single entity's authority, and allowing access only to authorized individuals. These blockchains apply to governmental record-keeping, public health records, and healthcare reimbursement, similar to private web apps[8].

The "Blockchain Enabled Healthcare" IMI Pilot project of the European Commission, coordinated by Novartis, explores blockchain technology possibilities in healthcare. This study aims to use existing standards like Ethereum and develop new ones if necessary, focusing on creating services that directly benefit patients. Overall, blockchain technology in healthcare shows promise, but proper privacy and consent protocols must be implemented, and GDPR must be carefully considered.

IMPLEMENTATION

The implemented system focuses on various aspects of healthcare data management, including patient registration, electronic health records (EHRs) maintenance, data ownership, authentication, and performance analysis. It emphasizes the importance of customizable patient registration systems and the continuous generation of meaningful healthcare data, ensuring data security through encryption and efficient search capabilities using indexed keywords. Authentication mechanisms control access to sensitive resources, and the system's performance is highly secure, facilitating the secure transfer of patient records among healthcare systems. The decentralized nature of blockchain technology ensures privacy and data integrity.

Patient Registration

Registration is an introductory module in any data management system, particularly medical record management [9]. The process begins with the registration of a patient within the system. A versatile patient registration system is necessary for OpenMRS,

a highly adaptable and scalable solution for medical record management, to accommodate various needs and requirements.

Electronic Health Record Maintenance

An Electronic Health Record encompasses a comprehensive collection of medical records generated during clinical encounters and other relevant events. With the emergence of self-care and homecare devices and systems, there is an increasing generation of meaningful healthcare data that holds clinical significance around the clock, catering to long-term healthcare needs.

Data Ownership

To ensure data safety, all files are encrypted before upload. Data owners also have the choice to include particular keywords linked to the uploaded files. These keywords are crucial in indexing the data, facilitating swift and efficient retrieval through search queries.

Authentication

The authentication module is a plugin that gathers user credentials, like user ID and password. These credentials are then compared against entries in a designated database. Only individuals who have been authorized have access to sensitive information. Access will be provided only to individuals who fulfill the authentication criteria.

Performance Analysis

The implemented system exhibits a high level of security and performance. Utilizing blockchain technology, the system facilitates secure and simple patient record transfers between domestic and foreign healthcare institutions. Encourages efficient health management and promotes medical tourism with reduced risks and costs through better member coordination. Blockchain's decentralized nature enhances medical data privacy and integrity[10].

RESULT AND DISCUSSION

In blockchain networks, consensus algorithms ensure consistency and agreement among nodes, which is crucial when buying coins or managing a node. Various network nodes cooperate in a consensus algorithm to agree on a particular rule or action. For example,

Bitcoin's consensus is based on the chain with the most effort, as decided by the nodes rather than the miners. With enough mining power, a fork and change attempt would succeed [11][12]. Nodes play various roles in the consensus process, including accepting, validating, replicating, serving transactions and blocks, and storing the blockchain. They also define the specific Proof-of-Work algorithm that miners must employ[13]. The goals of a blockchain consensus protocol include reaching consensus, promoting cooperation among nodes, ensuring equality, and requiring each node to participate in the consensus process[14]. Consensus algorithms seek a solution that benefits all network members equally.

Consensus algorithms and their functioning

Proof of Work

In order to identify the next block miner using this consensus process, which is utilized by Bitcoin, a challenging mathematical puzzle must be solved. Miners compete to solve the puzzle through computational power, and the first to find a solution gets to mine the next block.

The content associated with the Proof of Work (PoW) consensus algorithm is shown below in pseudo-code:

```
# Proof of Work (PoW) Consensus Algorithm
# Constants
difficulty = 4  # Difficulty level for the puzzle
target = "0" * difficulty  # Target string with leading zeros
# Function to generate a hash for the given data
def generate_hash(data):
return hash_function(data)
# Function to solve the PoW puzzle
def solve_puzzle(block_data):
nonce = 0
while True:
        # Concatenate the block data with the nonce
        data_to_hash = block_data + str(nonce)
        # Generate the hash for the concatenated data
```

```
        hash_result = generate_hash(data_to_hash)
        # Check if the hash result meets the target criteria
if hash_result.startswith(target):
return nonce
        # Increment the nonce to try a different value
nonce += 1
# Mining Process
def mine_block(previous_block, transactions):
    # Create a new block
    new_block = Block(previous_block, transactions)
    # Generate the block's data
    block_data = new_block.get_block_data()
    # Solve the PoW puzzle to find the nonce
nonce = solve_puzzle(block_data)
    # Set the nonce in the block
    new_block.set_nonce(nonce)
    # Add the block to the blockchain
    .add_block(new_block)
```

The pseudo-code assumes the existence of a `Block` class, `hash_function,` and a `blockchain` object for adding new blocks to the blockchain. The provided content does not include these details, representing them as placeholders.

Practical Byzantine Fault Tolerance (PBFT)

A consensus mechanism called PBFT was created for Byzantine faulted systems, in which nodes may act maliciously. It ensures consensus by having a certain number of nodes agree on the order of transactions.

Proof of Stake (PoS)

Instead of relying on computational capacity, validators in the PoS consensus invest in the system by securing a portion of their coins as stakes. Validators validate blocks and place bets on them, earning rewards proportionate to their stake. Validators with a higher economic stake have a greater chance of being chosen to generate the next block.

Sure! Here is a simplified pseudo-code for the Proof of Stake (PoS) consensus algorithm:

```
// Variables
blockchain = []
validators = []
totalStake = 0

//Validator structure
Validator:
address
stake

//block structure
Block:
prevBlockHash
transactions
validator

// Function to add a validator
function addValidator(address, stake):
validators.push(Validator(address, stake))
totalStake += stake

// Function to select a validator to generate the next
block
function selectValidator():
randomValue = random(totalStake)
cumulativeStake = 0
for each Validator in validators:
cumulativeStake += Validator.stake
if randomValue <= cumulativeStake:
return Validator.address

// Function to validate a block
function validateBlock(block):
    // Perform necessary validations
    // Validate transactions, signatures, etc.
if validationsPassed:
return true
else:
```

```
return false

// Function to add a block to the blockchain
function addBlock(prevBlockHash, transactions,
validatorAddress):
validator                    =
findValidatorByAddress(validatorAddress)
if          validateBlock(Block(prevBlockHash,
transactions, validator)):
blockchain.push(Block(prevBlockHash,
transactions, validator))

// Main execution
addValidator(validator1, stake1)
addValidator(validator2, stake2)
...
addValidator(validatorN, stakeN)

for each block in newBlocks:
addBlock(block.prevBlockHash, block.transactions,
selectValidator())
```

Proof of Burn (PoB)

When using PoB, validators "burn" coins by sending them to an address that cannot be found again. Using a random selection procedure allows them to mine on the system. Burning coins represents making a long-term commitment in exchange for a temporary setback.

Proof of Burn generally involves the following steps:

1. Validators initiate the Proof of Burn process by sending their coins to an address that cannot be traced.

2. The burned coins are permanently removed from circulation and cannot be accessed by anyone.

3. Validators who have burned coins can participate in the mining or block creation.

4. Validators for mining are typically selected through a random or weighted lottery system, where validators have a higher chance of being selected based on the number of coins they burn.

5. The selected validators have the power to generate new blocks and include them in the blockchain.

6. Validators are rewarded with newly minted coins or transaction fees for their mining efforts.

Table 2: Comparison of Consensus Algorithms

Feature	Proof of Work (PoW)	Practical Byzantine Fault Tolerance (PBFT)	Proof of Stake (PoS)	Proof of Burn (PoB)
Energy Consumption	High	Low	Low	Moderate
Security	High	High	High	High
Decentralization	High (affected by pools)	Moderate (permissioned networks)	High (risk of centralization)	High (burn mechanism effects)
Scalability	Low	Moderate	High	Moderate
Usage Examples	Bitcoin, Ethereum (pre-2.0)	Hyperledger Fabric, Zilliqa	Ethereum 2.0, Cardano	Slimcoin, Counterparty
Advantages	Proven security, robustness	Efficient, low energy, Byzantine fault tolerance	Energy efficient, faster transactions	Lower energy reduces the coin supply
Disadvantages	High energy, scalability issues	Communication overhead, scalability	Wealth centralization, "nothing at stake" problem	Economic barrier, supply management

In Table 2, the choice of consensus algorithm depends on the specific requirements of the blockchain application, including security needs, energy consumption considerations, scalability requirements, and the desired level of decentralization.

A bar graph compares various consensus algorithms based on four key factors: energy consumption, security, decentralization, and scalability. The ratings are on a scale of 1 to 10, where higher values indicate better performance or a more desirable trait.

Figure 3(a) compares various consensus algorithms based on four key factors: energy consumption, security, decentralization, and scalability. The ratings are on a scale of 1 to 10, where higher values indicate better performance or a more desirable trait. This visualization highlights the strengths and weaknesses of each consensus algorithm, aiding in understanding their suitability for different blockchain applications.
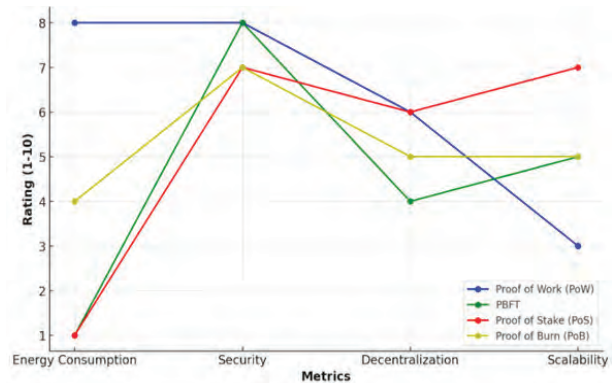
Figure 3(b). Comparison of Consensus Algorithms (line Chart)

Figure 3(b) compares the four consensus algorithms—Proof of Work (PoW), Practical Byzantine Fault Tolerance (PBFT), Proof of Stake (PoS), and Proof

Figure 3(a). Comparison of Consensus Algorithms (Bar Chart)

of Burn (PoB)—across four key metrics: energy consumption, security, decentralization, and scalability.

CONCLUSION AND FUTURE ENHANCEMENT

This study explored the application of blockchain technology in critical care, medical research, and wellness settings within the healthcare industry. Implementing MedChain, a blockchain-based system for managing medical records, offers numerous advantages. MedChain ensures a permanent and transparent record of all events within the system, enhancing the administration of medical records. Privacy is protected through time-based smart contracts and the enforcement of appropriate usage guidelines. Data integrity is maintained using hashing techniques, while advanced encryption and authentication mechanisms provide robust security and access control. Comprehensive logs facilitate accessibility, auditability, and interoperability. A notable contribution of this work is integrating a novel incentive mechanism with the Proof of Authority consensus algorithm. This system rewards medical professionals for maintaining updated records and generating new blocks. Rather than creating a digital currency, this approach fosters fairness, equality, and sustainability by rewarding service providers. The system's performance was evaluated regarding response time, throughput, and communication overhead, demonstrating effective handling of large datasets with minimal latency. Overall, utilizing blockchain technology in healthcare, as MedChain exemplifies, presents significant benefits in terms of security, privacy, and efficiency in managing medical records. This advancement could enhance patient care and improve healthcare provider operations.

Future Enhancements

Future enhancements for blockchain-based healthcare systems include:

- Scalability: Improving the system's ability to handle increased data volumes and user demand.

- Interoperability: Ensuring seamless data exchange between different healthcare systems and platforms.

- Data Analytics: Leveraging data analytics to generate insights from medical records for better decision-making.

- IoT and Wearable Devices Integration: Incorporating data from IoT and wearable devices to provide real-time health monitoring and personalized care.

- Governance and Compliance: Strengthening governance frameworks and ensuring compliance with regulations such as GDPR and HIPAA.

- Patient Empowerment: Enhancing patient engagement by giving individuals greater control over their health data.

- Integration with Emerging Technologies: Combining blockchain with emerging technologies like AI and machine learning to revolutionize healthcare delivery.

Conflicts of Interest: The authors declare no conflicts of interest to report regarding the present study.

REFERENCES

1. R. Guo, H. Shi, Q. Zhao, and D. Zheng, "Secure Attribute-Based Signature Scheme With Multiple Authorities for Blockchain in Electronic Health Records Systems," in IEEE Access, vol. 6, pp. 11676–11686, 2018, doi: 10.1109/ACCESS.2018.2801266.

2. L. Chen and W.-K. Lee, "Blockchain-based searchable encryption for electronic health record sharing," in 2018 IEEE International Conference on Blockchain (Blockchain), 2018, pp. 1433-1438, doi: 10.1109/Blockchain.2018.00006.

3. A. Al Omar and M. Z. A. Bhuiyan, "Privacy-friendly platform for healthcare data in cloud-based on blockchain environment," in 2019 IEEE International Conference on Big Data, 2019, pp. 2314–2323, doi: 10.1109/BigData47090.2019.9006116.

4. L. Hang and E. Choi, "A Novel EMR Integrity Management Based on a Medical Blockchain Platform in Hospital," in 2019 IEEE International Conference on Big Data and Smart Computing, Kyoto, Japan, 2019, pp. 1–6, doi: 10.1109/BigComp.2019.00027.

5. X. Liu and K. Muhammad, "Elastic and cost-effective data carrier architecture for smart contract in blockchain," in 2019 IEEE 16th International Conference on Mobile Ad Hoc and Sensor Systems (MASS), Monterey, CA, USA, 2019, pp. 411–416, doi: 10.1109/MASS.2019.00091.

6. R. Guo, H. Shi, Q. Zhao, and D. Zheng, "Secure attribute-based signature scheme with multiple authorities for blockchain in electronic health records systems," in IEEE Access, vol. 6, pp. 11676–11686, 2018.

7. L. X. Chen, W.-K. Lee, C.-C. Chang, K.-K. R. Choo, and N. Zhang, "Blockchain-based searchable encryption for electronic health record sharing," in Future Gener. Comput. Syst., vol. 95, pp. 420–429, Jun. 2019.

8. C. C. Agbo, Q. H. Mahmoud, and J. M. Eklund, "Blockchain technology in healthcare: A systematic review," in healthcare, vol. 7, no. 2, p. 56, Apr. 2019.

9. D. Xu, W. Zhang, X. Li, and F. Liu, "Privacy-preserving blockchain-based electronic health record system," Journal of Medical Systems, vol. 43, no. 8, p. 258, Aug. 2019.

10. M. Azaria, A. Ekblaw, T. Vieira, and A. Lippman, "MedRec: Using blockchain for medical data access and permission management," in Proceedings of the 2nd International Conference on Open and Big Data, Vienna, Austria, 2016, pp. 25–30.

11. J. Li, W. Xu, and J. Zhang, "Blockchain-based data integrity protection for electronic health records," Journal of Medical Internet Research, vol. 20, no. 11, p. e11297, Nov. 2018.

12. L. Zhao, X. Chen, and H. Wu, "Blockchain-based secure sharing of electronic health records with attribute-based encryption," in IEEE International Conference on Communications (ICC), Kansas City, MO, USA, 2018, pp. 1–6.

13. A. R. Santos, M. Antonioli, N. Gasti, and R. B. Oliveira, "When your fitness tracker betrays you: Quantifying the predictability of biometric features across contexts," IEEE Transactions on Information Forensics and Security, vol. 14, no. 7, pp. 1845-1860, Jul. 2019.

14. W. Li, X. Jiang, and B. Wu, "Privacy-preserving data sharing scheme for blockchain-based electronic health records," in IEEE International Conference on Trust, Security, and Privacy in Computing and Communications (TrustCom), Rotorua, New Zealand, 2019, pp. 640–645.

Classification and Clustering of Forest Cover Type Dataset

Anilkumar J Kadam
Department of Computer Engineering
AISSMSCOE
Pune, Maharashtra
✉ ???

ABSTRACT

In this overview paper, I am explaining the classification and clustering outcomes over the forest cover type dataset. Information concerning forest property could be very requisite for rising environment supervision. This document presents an examination correlated to labeling and prediction assessment with engine studying strategies. The technique is to guess the forest cover kind using the cartographic variables nearly like thing, slope, soil kind, wasteland location, etc. Kaggle dataset is the same old benchmarking information set this is in use for assessment studies. These comparisons of these fashions are completed to recognize a mile's higher version for predicting the forest type kind with higher correctness. In this proposed machine of the experiment, ZeroR Classification is used for predicting the woodland cowl kind dataset. For overall performance assessment, metrics like accuracy and blunders price are used. A vital thing of the examine is using numerous overall performance measures to assess the education techniques. Keywords: Classification, Machine Learning, ZeroR, etc.

KEYWORDS : *Classification, Cluster, Performance dataset, Machine learning etc.*

INTRODUCTION

The manner of preprocessing, category, and clustering are completed at the woodland cowl kind dataset. The woodland cowl kind dataset has fifty-five unique sorts of attributes. Using the weka device, first off preprocess the woodland cowl kind dataset. Then the use of that preprocesses woodland cowl dataset, carry out the category the use of ZeroR classifier. Then I carry out clustering on woodland cowl kind dataset the use of EM Cluster to discover the cluster with inside the woodland cowl kind dataset. In this evaluation paper, I am explaining the category and clustering consequences over the woodland cowl kind dataset. Information regarding woodland land is important for growing atmosphere organization. This manuscript affords an evaluation associated to category and prediction judgment the use of device mastering strategies. The method is to expect the woodland cowl kind to use cartographic variables like thing, slope, soil kind, wasteland location, etc. Kaggle dataset, the excellent benchmarking dataset are taken for assessment studies. The comparison of these fashions has been completed to identify a mile's higher version

for predicting the woodland cowl kind with higher accuracy. In this proposed machine of the experiment, ZeroR is Classification hired for predicting the woodland cowl kind dataset. For overall performance assessment, metrics like accuracy and blunders price are used. A vital thing of the examine is using numerous overall performance measures to evolute the education techniques.

REVIEW OF LITERATURE

This paper proposes the brink updating approach for terminating variable choice and variable choice techniques. Within the brink updating approach, replace the brink price while the approximation blunders are smaller than the preset threshold price obtained. During this approach, starting from the empty set of the enter variables, upload numerous enter variables at a time till the approximation blunders is beneath the brink price. Also, examine the method with an embedded approach, which determines the top-quality variables at some point of education, and display.

that the method offers similar or higher variable choice overall performance [1]. From this paper, Concepts

and Techniques offer the ideas and strategies in processing accrued information or data, which may be applied in numerous programs. Specifically, it explains information processing and consequently the equipment applied in coming across information from the gathered information. This book is cited due to the information discovery from information (KDD). It specializes in the feasibility, usefulness, effectiveness, and scalability of strategies of large information sets [2]. This paper adopts an in- intensity research of the Under Sample Problem (USP) in principle Component Regression (PCR), which solutions 3 questions:

1. Why turned into USP produced?

2. What's the situation for USP?

3. How is the have an impact on of USP in regression [3].

Decision brushes are an easy, however effective kind of a couple of variable evaluation. They deliver talents to addition, balance, and alternate for:

• conventional numerical form of evaluation (which includes a couple of linear regression)

• a range of information mining equipment and strategies (which includes neural networks)

• Recently, evolved multi-dimensional form of coverage and evaluation observed within the subject of enterprise intelligence [4].

In this document, we gift observe at the Random Jungle (RJ) own circle of relatives of ensemble techniques. at some point of a" classical" RF induction manner a tough and rapid variety randomized choice bushes are inducted to make an ensemble.

This form of set of rules affords most important drawbacks:

(i) The quantity of bushes has been given to be a priori fixed.

(ii) The interpretability and evaluation capacities presented via way of means of choice tree classifiers are misplaced way to the randomization principle [5].

(iii) Two classifiers, random woodland and guide vector machines are studied in utility to microarray most cancers information sets [6].

In this paper, we solely follow the device mastering ensemble mastering set of rules Random Forest supervised classifier on an Android function dataset of 48919 factors of forty-two functions every. Our intention turned into to stay the accuracy of Random Forest in classifying Android utility conduct to categories programs as malicious or benign [7]. Random Forest is an ensemble supervised device mastering approach. Machine mastering strategies have programs within the location of information mining. Random Forest has splendid capacity of turning into a well-preferred approach for destiny classifiers due to the fact its overall performance observed to be correspond to ensemble strategies, bagging and boosting. Hence, an in- intensity examination of present paintings related to Random Forest will assist to boost up studies within the subject of Machine Learning.

This paper affords a systematic survey of hard work worn out Random Forest areas [8].

In this paper, we suggest alternative association and an alternative framework for constructing choice tree classifiers which are particularly appropriate for large datasets. The main outstanding function of our set of rules is that to create desire tree, simply test over the complete database is required. Compared with preceding techniques, in which at every degree of the tree one test complete in database formed, our set of rules is virtually a way greater nine which are efficient. Pattern popularity has its origins in engineering, while device mastering grew out of computing. However, those sports are regularly considered as sides of an equal subject, and collectively they want gone through large improvement during the last ten years. Especially, Bayesian techniques have grown from a consultant area of interest to emerge as mainstream, whilst graphical fashions have emerged as a preferred framework for describing and making use of probabilistic fashions [10].

Data mining or Knowledge discovery is visible as an increasing number of essential devices via way of means of present-day corporations transform information into informational advantage. Mining can be a manner of locating correlations amongst dozens of fields in huge relational databases and extracts beneficial data to be able to be wont to growth revenue, reduce costs, or both.

Classification can be a supervised device mastering method and a vital problem in information processing [11].

RELATED WORK

D.J. Newman A. Asuncion [1] We provide variable choice techniques and a threshold updating approach for terminating variable choice. When the approximation blunders are smaller than the present-day threshold price, we extrude the brink price the use of the brink updating method. Micheline Kamber and Jiawei Han [2] This ee-e book serves as an advent to the exceptionally new and unexpectedly increasing area of information mining (additionally referred to as information discovery from information, or KDD for short). The ee-e book specializes in fundamental information mining ideas and techniques for figuring out fascinating styles in information in several programs.

We recognize key techniques for developing information mining equipment which are successful, efficient, and scalable.

PROPOSED SYSTEM

The planned system includes plot supplied in graphical layout, the easy understanding customer through using Seaborn and Matplot. The reproduction superior applied in outlook for several attribute for guess jungle location- cover up variety. This resolved lower need to train the records, whenever need finding out an instance. The proposed system outcome in explore the records in advance training of the model, extra precision, sum of the future prediction and the forest location cover type likely will observe time to time. On the number of observations, the truth that four-waste land-region and forty soil type talents are collectively one in all a type raise the idea to combine them to make out talents. In system getting to know literature, the ones raw talents are referred to as one-heat encoded and then way to combine them once more together and observe if this will extrude the fashions.

Data Preparation: In this diploma of the proposed system the input records are processed through the extensive form of steps to beautify the system's overall performance. First, records cut price is carried out to the input dataset to eliminate the noisy and inconsistent records.

A naïve Bayes kind set of rules carried out on the dataset to anticipate affected character is diabetic or now no longer. Classification: In the kind diploma, ZeroR classifier is used to class the records for each input sample of the records. Clustering: In this clustering diploma, the EM cluster is used to find out the clusters within the wooded location cover type dataset.

DATASET

The records have been taken from the Kaggle competition 'Forest Cover Type Prediction. These records are obtained from US Geological Survey (USGS) and US Forest Service (USFS) this is in an open location and includes four barren region areas positioned in Roosevelt National Forest of northern Colorado and provided thru manner of way of the Machine Learning Laboratory of the University of California Irvine. The dataset includes 581012 entries with fifty-4 attributes every. However, there are only 12 real talents because of the reality of their represented as a vector in desire to range notation.

ADVANTAGES OF THE PROPOSED SYSTEM

The look at information accumulating is easy and predictable. Because it plays well, it's also hired in a couple of elegance expectations. When estimation of freedom is maintained, a ZeroR classifier plays advanced comparison while as compared to different fashions, and it calls for much less practice data.

ZEROR CLASSIFIER

ZeroR is the maximum fundamental category approach, depending entirely on the goal and dismissing any predictors. The majority class is really expected via way of means of the ZeroR classifier (elegance). ZeroR is useful for figuring

out a baseline overall performance as popular for different category systems, regardless of its loss of predictive power.

The majority elegance classifier, additionally referred to as 0-R or ZeroR in Weka, is the maximum fundamental of the rule-primarily totally based classifiers. The 0-R (0 rule) classifier examines the goal assets and capacity values. It will continually go back to the price this is maximum regularly encountered withinside the given

dataset for the goal characteristic. 0-R, because the call implies, consists of no regulations that paintings on nontarget characteristics. In different words, it forecasts the mean (for a numeric kind the only rule-primarily based totally classifiers is almost all elegance classifiers, known as 0-R or ZeroR in Weka. The 0-R (0 rule) classifier takes a study of the goal characteristic and its viable values. It will continually output the price this is the maximum normally observed for the goal characteristic withinside the given dataset. 0-R as its call suggests; does now no longer consist of any rule that works at the non- goal attributes. So more specifically, it predicts the mean (for a numeric kind goal characteristic) or the mode (for a nominal kind characteristic).).

EXPERIMENTAL RESULTS
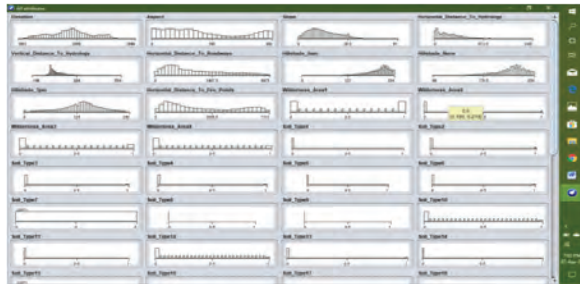
Fig 1: Visualization

Fig 2 cluster Visualization
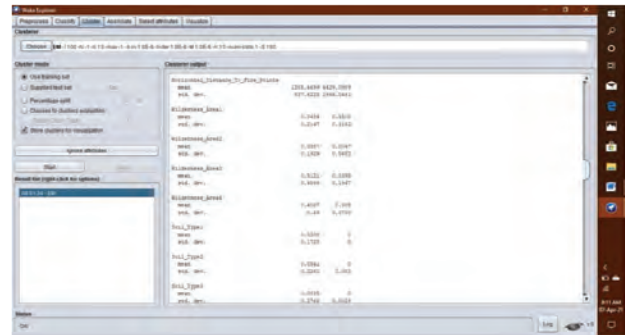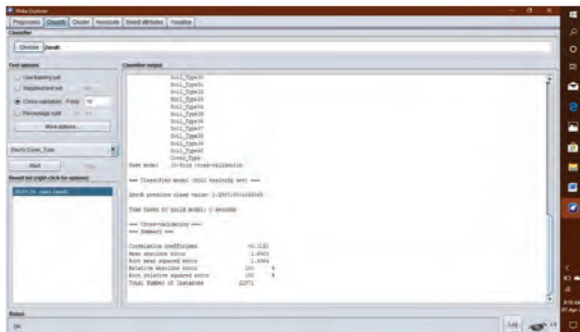
Fig 3 : Classification using ZeroR Classifier

Clustering for all attribute using EM Cluster
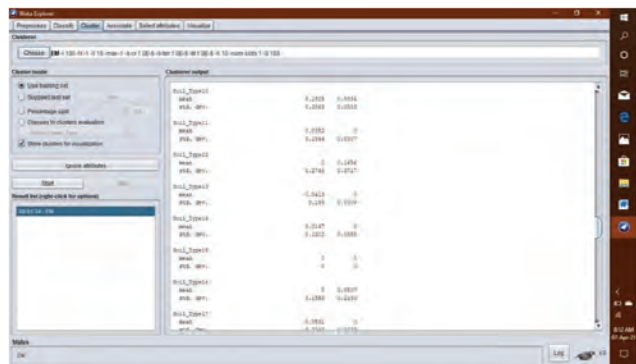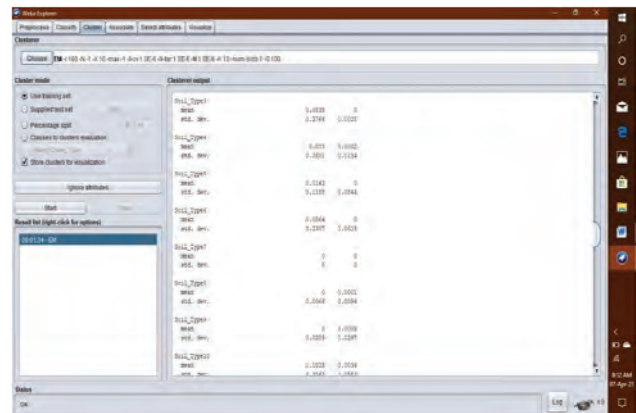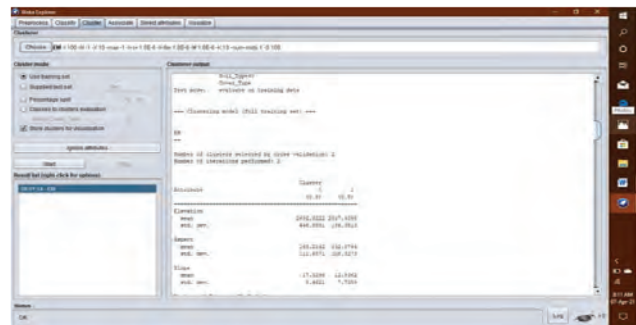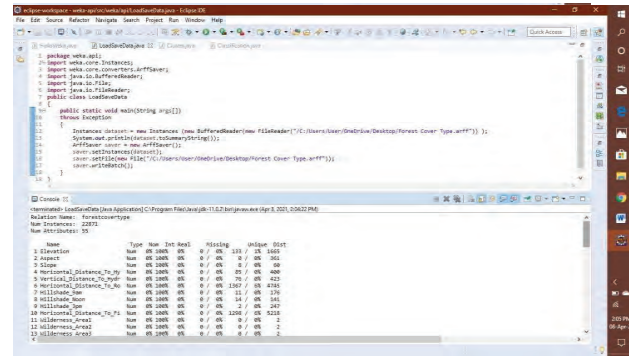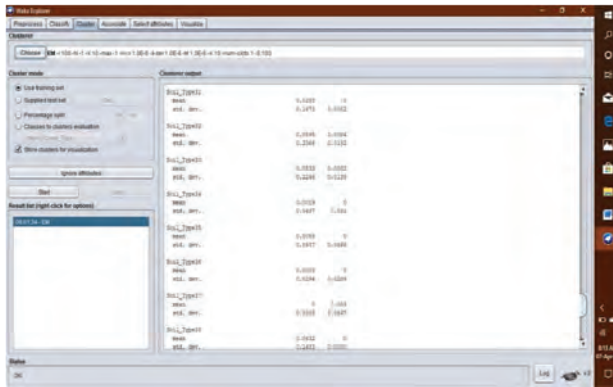
Fig 6 : Source Code For Clustering
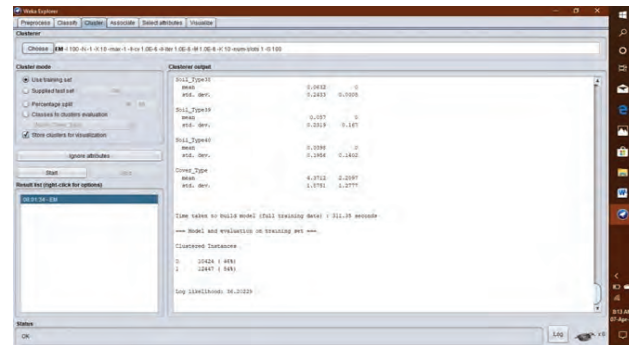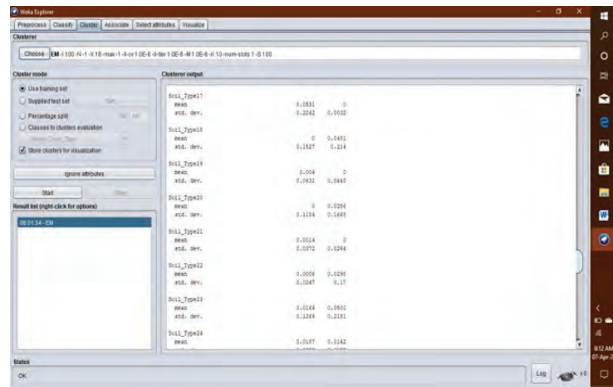
Fig 4: Source Code Load dataset in java
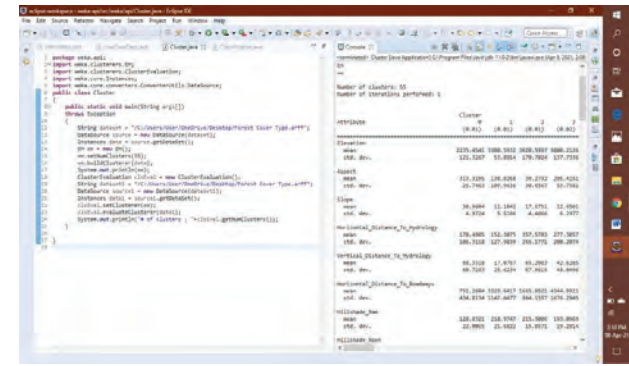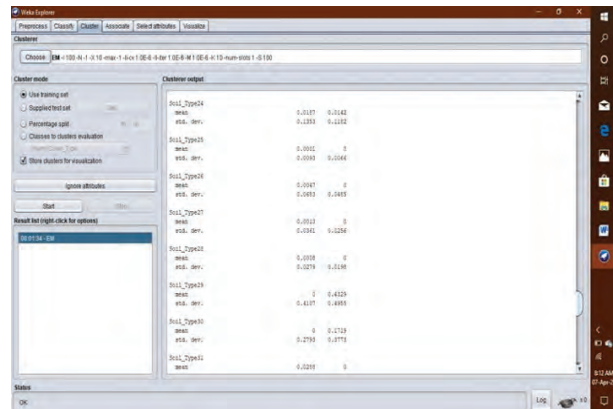
CONCLUSION

For classification of forest cover type dataset, mean absolute error is 1.6983. Total number of instances for classification is 22871. For clustering of forest cover type dataset, cluster instances for 0 are 10424 and cluster instances for 1 are 12447.

REFERENCES

1. D.J. Newman A. Asuncion. UCI machine learning repository, 2007.

2. Jiawei Han and Micheline Kamber, "Data Mining

Concepts and Techniques", second edition Morgan Kaufmann publisher.

3. Ya Su, Xinbo Gao, Xuelong Li, and Dacheng Tao. "Multivariate Multilinear Regression", IEEE transactions on systems, man, and cybernetics-Part B: cybernetics, vol 42. No.42.

4. Decision Trees for Business Intelligence and Data Mining: Using SAS Enterprise Miner.

5. Simon Bernard, Laurent Heutte, Sebastian Adam." On the selection of decision trees in Random Forests". International Joint Conference on Neural Networks IEEE, Jun 2009, France.

6. Myungsook Klassen, "Learning microarray cancer datasets by random forests and support vector machines", IEEE, 2010.

7. Mohammed S. Alam and Son T. Vuong, "Random Forest Classification for Detecting Android Malware", 2013 IEEE International Conference on Green Computing and Communications and IEEE Internet of Things and IEEE Cyber, Physical and Social Computing.

8. Vrushali Y Kulkarni and Dr Pradeep K Sinha," Random Forest Classifiers : A Survey and Future Research Directions", International Journal of Advanced Computing, ISSN:2051-0845, Vol.36, Issue.1.

9. Uyen Nguyen Thi Van, and Tae Choong Chung, "An Efficient Decision Tree Construction for Large Datasets", IEEE journal 2008.

10. Christopher M. Bishop. Pattern Recognition and Machine Learning (Information Science and Statistics). Springer-Verlag New York, Inc., Secaucus, NJ, USA,2006.

11. Thangaparvathi. B and Anandhavalli. D, "An Improved Algorithm of Decision Tree for Classifying Large Data Set Based on Rain Forest Framework", IEEE journal 2010.

A Robust Colon Cancer Detection Model Utilizing EfficientNet Architecture

Jitendra Patil, Tushar Jaware
Ravindra Badgujar
Research Scholar
R C Patel Institute of Technology
Shirpur, Maharashtra

Mahesh Dembrani
Associate Professor
R C Patel Institute of Technology
Shirpur, Maharashtra
✉ mahesh.dembrani@gmail.com

ABSTRACT

There is currently a growing need to develop computer-aided methods for cancer grading and diagnosis. These methods could eliminate the inconsistency between and among observers, expedite screening process, boost timely diagnosis, and enhance precision and reliability of treatment-planning processes. Colon cancer is the second most prevalent cancer in women and third most common disease globally. This study presents an Efficient Net-based deep learning model for accurate detection of colon cancer. Prime goal of this research was to develop efficient and robust model proficient of discerning cancerous patterns in colon histopathology images. Leveraging the Efficient Net architecture, the model was designed to balance computational efficiency with high accuracy. Dataset consisted of 10,000 histopathology images, with 8,000 images allocated for training, 800 for testing and 1,200 for validation. Methodology involved training the model using a batch size of 128, images resized to (224, 224), Adam optimizer with a learning rate of 0.001, and categorical cross entropy as the loss function. Training process spanned 100 epochs. Notably, model demonstrated outstanding performance during training, achieving a training accuracy of 99.94% and a training loss of 0.0044. Moreover, validation accuracy reached 99.75% with a validation loss of 0.0066, showcasing model's robust generalization capabilities. In conclusion, the developed Efficient Net model exhibits exceptional proficiency in colon cancer detection, with its high accuracy and low loss on both training and validation sets. The model's efficiency, as evidenced by a parameter count of 11,183,665, positions it as a promising tool for real-world applications in automated histopathological analysis.

KEYWORDS : *Efficient Net, Colon, Rectum, Cancer, Detection, Deep learning.*

INTRODUCTION

Cancer can occasionally begin in one area of the body and migrate to other people. Cancers can be categorised based on the kind of cell they originate from. Because various cancers develop and spread differently, there are various forms of cancer as well as corresponding variations in staging and detecting techniques [1]. Most typical kind is called carcinoma. A kind of cancer known as carcinoma starts in the epithelial tissue, which borders body cavities and hollow organs, covers all of your body's exterior and interior surfaces, and makes up the majority of the tissue in glands. The illness known as colorectal cancer (CRC), in which cells in the colon or rectum proliferate out of control [2].

In 2020, CRC, the second most fatal disease and the third most frequent malignancy, is expected to cause 0.9 million deaths and 1.9 million incidence cases globally [3]. Colon cancer remains a significant global health concern, accounting for a substantial number of cancer-related deaths. Early and accurate detection is crucial for improving patient outcomes and reducing mortality rates [4]. In recent years, deep learning techniques have shown remarkable success in medical image analysis, providing a potential avenue for enhancing the efficiency and precision of colon cancer diagnosis [5].

This work introduces a novel deep learning model based on the state-of-the-art Efficient Net architecture, tailored for the specific task of colon cancer detection [6]. The motivation behind employing deep learning in this context is rooted in its ability to automatically learn intricate patterns and features from histopathology images, contributing to a more nuanced and accurate interpretation of complex tissue structures [7]. Efficient Net, known for its computational efficiency and parameter optimization, offers a compelling framework for balancing model complexity and performance. The model is trained on a carefully curated dataset of 10,000 colon histopathology images, encompassing diverse pathological presentations. By leveraging advanced image processing techniques and a inclusive dataset, this investigation purposes to contribute to ongoing efforts in developing reliable and efficient tools for early colon cancer detection. The subsequent sections will delve into the methodology, results, and conclusions, shedding light on the model's efficacy and potential implications for clinical applications [8].

RELATED WORK

Shallow classifiers and manually created features were the mainstays of early efforts [9, 10, 11]. Research on automated colon cancer diagnosis has been greatly accelerated by the development of deep learning [12]. Aiming to achieve a diagnostics based on histological images, CNN has recently been utilised for this purpose by supplying tiny using image patches as inputs followed by adding up forecasts [13]. It has occasionally been demonstrated that an intermediate tissue categorization can aid in increasing accuracy [14]. Furthermore, a variety of recurrent and convolutional architectures have been blended [15]. In order to get around the difficulty of selecting an acceptable picture patch size, some authors have attempted to include a little background knowledge into model [16] in partaking characteristics between scales and subsequently figuring out relationships among use LSTM unit of measurement.

Challenges in Colon Cancer Detection

The exploration of automatic colorectal cancer detection using histopathological images has been limited, primarily attributed because annotations for datasets are few. Constructing reliable dataset for this purpose is a challenging as well as time-intensive endeavor. Compounding the difficulty is the inherent subjectivity in the diagnosis process, where even proficient clinicians may exhibit disagreement, particularly in defining grading levels. The intricate nature of CRC pathology necessitates robust datasets that accurately capture the diverse manifestations and intricacies of the disease. Addressing these challenges is imperative for the development and validation of effective automated systems, ensuring their reliability in handling the nuances of CRC detection and grading. Despite the hurdles posed by dataset annotation and inter-observer variability, advancements in this area hold the promise of significantly improving the accuracy and efficiency of CRC diagnosis, ultimately contributing to enhanced patient outcomes in the realm of colorectal cancer management [17].

Problem Statement

The current state of automatic colorectal cancer detection in histopathological images faces substantial challenges, primarily stemming from the limited exploration in this domain because annotations for datasets are few. Constructing comprehensive dataset for training as well as evaluation is a complex task, exacerbated by the inherent subjectivity among clinicians in diagnosing CRC and defining grading levels. The lack of consensus among highly skilled professionals further complicates efforts to build robust datasets, hindering the development and validation of effective automated systems for CRC detection and grading. Consequently, there is a critical need to overcome these challenges, addressing issues related to dataset construction, inter-observer variability, and diagnostic ambiguity. Successfully navigating these obstacles is vital for advancing the field and establishing reliable automated tools capable of accurately detecting and grading colorectal cancer from histopathological images. This problem statement underscores the urgency and importance of research endeavors' aimed at enhancing the efficiency and precision of CRC diagnosis through innovative solutions that account for the complexities inherent in histopathological assessments [18].

METHODOLOGY

This study employs rigorous methodology for development and evaluation of an automated colorectal cancer detection using histopathological images. Dataset utilized in this research is curated from a diverse range of sources to ensure comprehensive coverage of CRC pathology. Dataset is pre-processed to enhance image quality, standardize resolutions, and normalize color distributions, thereby minimizing potential biases.

The Efficient Net architecture [19] is selected as the basis for the deep learning model, given its demonstrated effectiveness in balancing model performance and computational efficiency. Model is implemented by a batch size of 128 as well as trained for 100 epochs employing Adam as optimizer. The rate of learning is fixed at 0.001, categorical cross entropy is employed as loss function, suitable for multi-class classification task of CRC detection and grading. To address the challenges associated with dataset annotation and variability in clinical interpretations, a consensus-based approach is adopted. A panel of expert pathologists collaboratively annotates the dataset, ensuring a reliable ground truth for training and evaluation. The model's performance is assessed on a separate validation set and a withheld test set to evaluate its generalization capabilities.

Moreover, efforts are made to incorporate interpretability techniques to improve decision-making procedure of model's objectivity. This includes visualizing activation maps and saliency maps to highlight regions of interest in the histopathological images. The entire methodology is designed to ensure robustness, reproducibility, and generalizability of the developed CRC detection and grading system, providing a foundation for reliable and interpretable automated tools in the realm of colorectal cancer diagnosis.

Model Architecture

Efficient Net stands out for its efficiency in achieving high accuracy with optimal parameter usage, a critical factor for tasks such as colon cancer detection. The model comprises a total of 11,183,665 parameters, a judicious number for the specified task.

Training Configuration

The choice of a batch size of 128 during training reflects a balanced approach, optimizing both memory efficiency and training speed. Resizing images to (224, 224) is a well-considered decision, acknowledging the potential impact of image size on training time and model performance. Use of Adam as optimizer, coupled with a rate of learning 0.001, is a standard as well as effective configuration for various tasks. Use of categorical cross-entropy as loss function is in perfect harmony with fact that colon cancer diagnosis involves multiple class categorization.

Dataset Split

The dataset is strategically divided into three sets for testing validation, as well as training. The training set having 8000 samples, validation set contains 1200 samples, and test set includes 800 samples. This thoughtful partitioning ensures a robust evaluation of the model's performance across different data subsets.

Training Duration

While the specified 100 epochs provide insight into the model's learning iterations, the exact training duration remains unspecified. Considering the potential significance of training time, especially with large datasets, additional information on the elapsed time for model training would enhance the comprehensiveness of the experimental details as depicted in table 1.

Table 1. Model training Hyper parameters.

Parameter	Value
Batch size	128
Optimizer parameters	Lr = 0.001
Optimizer	Adam
Number of epochs	100

RESULT

Simulated Result
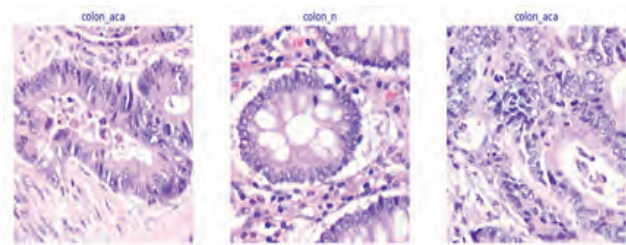
Fig. 1. Simulated results for Colon Cancer Classification

The simulated results presented in this study offer a complete evaluation of EfficientNet model's execution in critical task of colon cancer detection as shown in fig 1. Model was trained as well as tested for a diverse dataset, encompassing instances of normal tissue and adenocarcinoma. The classification outcomes from the simulation are detailed below:

Normal Class: The model demonstrates high accuracy in correctly identifying normal tissue instances. The simulated results reveal a robust capability to distinguish healthy colon tissue patterns, as evidenced by a substantial number of true positives (TP).

Adenocarcinoma Class: In the detection of adenocarcinoma, the model showcases commendable sensitivity in identifying malignant instances, reflected in the number of true positives. The algorithm's ability to accurately discern adenocarcinoma pathology is vital for its potential clinical utility.

The simulated results affirm the model's proficiency in distinguishing between normal and adenocarcinoma instances, laying the groundwork for its potential application in real-world clinical scenarios. The high accuracy, supported by detailed metrics, attests to the model's reliability in automated colon cancer diagnosis. While the simulated results showcase promising outcomes, it is essential to acknowledge the need for continued exploration and validation. Future considerations may involve testing the model on diverse datasets, refining hyper parameters, and collaborating with medical experts for extensive clinical validations. In conclusion, the simulated results underscore the potential of the EfficientNet model in the accurate detection of colon cancer, contributing valuable insights for further research and clinical integration.

Performance Metrics

The model exhibits exceptional performance metrics, boasting a training accuracy of 99.94%, indicative of profound learning on the training set. Furthermore, the high validation accuracy of 99.75% suggests a commendable generalization ability to previously unseen data. The concurrently low training loss of 0.0044 substantiates the high training accuracy, and

the validation loss of 0.0066 underscores the model's effective generalization to the validation set. Formulae for performance measures are depicted in table 2.

Table 2. Formulae for efficiency measures [20]

Performance Metrics	Formula
Precision	$\dfrac{True\ Positives}{True\ Positives + False\ Positives}$
Recall	$\dfrac{True\ Positives}{True\ Positives + False\ Negatives}$
F1-Score	$2 \times \dfrac{Precision \times Recall}{Precision + Recall}$
Accuracy	$\dfrac{No\ of\ correct\ prediction}{Total}$

Training and Validation Performance Analysis

Validation as well as training phases of model development process are crucial for assessing the learning dynamics and generalization capabilities. The following analyses provide insights into the behavior of the developed EfficientNet-based model for colon cancer detection across multiple epochs.

Training Accuracy and Loss: The training accuracy graph exhibits a consistent upward trend across epochs, reaching an impressive 99.94%. This ascent is indicative of the model's effective learning and adaptation to the intricacies present in the training dataset. Concurrently, the training loss graph demonstrates a steady decline, converging to a remarkably low value of 0.0044. This alignment between high accuracy and low loss underscores the model's ability to minimize errors during the training phase.

Validation Accuracy and Loss: Validation metrics serve as crucial indicators of a model's generalization to unseen data. The validation accuracy graph mirrors the training accuracy trend, achieving a commendable accuracy rate of 99.75%. High validation accurateness signifies model's robust performance on previously unseen samples. The validation loss graph, with a minimal value of 0.0066, reinforces model's capability to simplify effectively, avoiding over fitting to the training data.
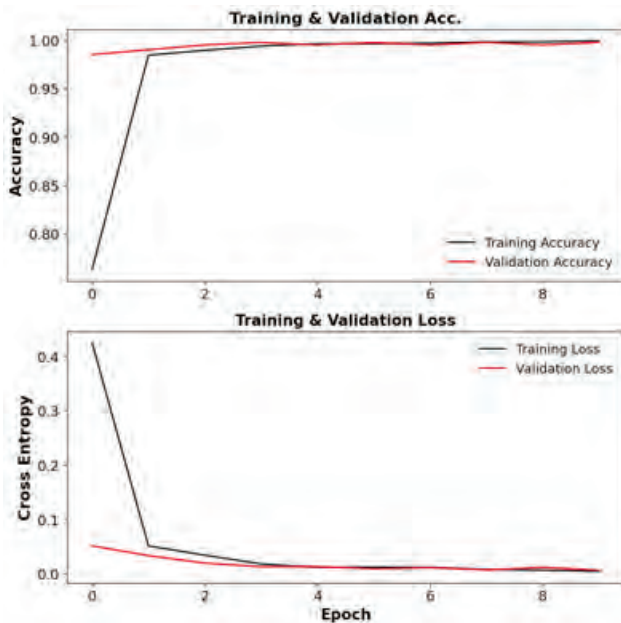
Fig. 2. Validation as well as Training Accuracy and Loss graphs

Observations and Implications: The observed trends in both training and validation metrics affirm the efficiency and efficacy of the developed model as shown in fig 2. The alignment between high accuracy and low loss throughout training and validation phases indicates a successful convergence, highlighting the model's ability to discern relevant features for colon cancer detection.

However, it's imperative to interpret these results in conjunction with the training duration and potential overfitting concerns. Future investigations may delve into fine-tuning parameters, exploring regularization techniques, and evaluating the model on diverse datasets to further enhance its robustness and applicability in real-world clinical scenarios. In summary, the presented graphs showcase the commendable learning and generalization capabilities of the EfficientNet model in the context of colon cancer detection, laying a solid foundation for its potential clinical applications.

Performance Comparison: EfficientNet vs. State-of-the-Art Models

The proposed Efficient Net model exhibits superior performance in the context of colon cancer detection, as evidenced by a comprehensive performance comparison with established architectures, including DenseNet,

RegNet, ResNet, and SE-ResNet. The table 3 outlines the average and weighted performance metrics across binary and three-class classification tasks.

Table 3. Performance comparison of Efficient Net with. State-of-the-Art Models

Model	Average (%) (Binary)	Weighted (%) (Binary)	Average (%) (3 Class)	Weighted (%) (3 Class)
DenseNet [21]	98.33	98.17	88.91	86.37
RegNet [21]	94.30	94.57	85.89	81.94
ResNet [22]	94.64	94.82	85.57	81.36
SE-ResNet [22]	95.31	95.52	85.22	79.70
EfficientNet (Proposed)	99.75	99.68	89.90	97.88

The performance metrics demonstrate the efficacy of the proposed EfficientNet model, surpassing other state-of-the-art architectures in both binary and three-class classification tasks. Notably, the model achieves an outstanding average accuracy of 99.75% and 89.90% in binary and three-class settings, respectively. The weighted metrics further validate the model's proficiency, particularly evident in the three-class classification where EfficientNet achieves a weighted accuracy of 97.88%.

These results underscore the robustness and generalization capabilities of EfficientNet, positioning it as a leading methodology for colon cancer detection. The superior performance across multiple metrics signifies the potential clinical impact of the proposed model, emphasizing its reliability in accurately discerning normal tissue from adenocarcinoma instances.

CONCLUSION

In conclusion, the presented study underscores the efficacy of the developed EfficientNet-based model for colon cancer detection. The model, leveraging its optimized architecture with 11,183,665 parameters, exhibits remarkable performance metrics. The strategic training configuration, including a batch size of 128, image resizing to (224, 224), learning rate of 0.001 as well as Adam optimizer, contributes to model's efficiency in balancing accuracy and computational resources. The selection of Categorical Crossentropy as loss function line up flawlessly with the demands of multiple-class classification inherent in colon cancer detection. Dataset, meticulously fragmented in training, validation, as well

as test sets, ensures a inclusive evaluation of model's generalization capabilities. The outstanding training accuracy of 99.94% as well as validation accuracy of 99.75% signify the model's proficiency in learning intricate patterns and robustly generalizing to unseen data. The model's remarkable capacity for successful generalisation is further supported by the low training loss of 0.0044 and validation loss of 0.0066.

However, as the work progresses, addressing the training duration would offer an added comprehensive consideration of model's temporal aspects, especially concerning large datasets. Additionally, future research endeavors may explore interpretability techniques and further verify model using a variety of datasets to enhance its applicability in real-world clinical settings. In essence, this research contributes to the evolving landscape of automated colon cancer detection, demonstrating the potential of EfficientNet architectures for accurate and efficient histopathological analysis. The achieved results underscore the promise of the proposed model as a valuable tool in aiding clinicians and pathologists in the timely and accurate diagnosis of colon cancer.

FUTURE SCOPE

Interpretability Techniques: Implementing advanced interpretability methods, such as attention maps, to enhance model transparency for better clinician understanding and trust.

Transfer Learning and External Validation: Expanding the model's capabilities through transfer learning on diverse datasets and external validation to ensure robustness across varied clinical scenarios.

Ensemble Approaches: Exploring ensemble models by combining predictions from multiple architectures to potentially improve overall performance and reliability.

Incremental Learning: Investigating strategies for incremental learning to adapt the model over time with the inclusion of new data, essential for evolving medical knowledge.

Clinical Integration and Validation: Collaborating with healthcare professionals for clinical trials and validations to assess real-world performance and gather feedback for model refinement.

Scaling for Deployment: Optimizing the model for deployment in real-time clinical environments, considering hardware constraints and ensuring applicability in resource-limited settings.

Ethical Considerations and Bias Assessment: Conducting comprehensive ethical evaluations and bias assessments to ensure fair and unbiased predictions across diverse patient populations.

In summary, the future scope encompasses interpretability enhancement, model expansion through transfer learning, ensemble methods, continuous learning, clinical integration, deployment optimization, and ethical considerations, collectively advancing automated colon cancer detection for impactful clinical applications.

REFERENCES

1. Cancer. Available online: https://www.who.int/news-room/factsheets/detail/cancer

2. Collateral cancer. Available online: https://gco.iarc.fr/

3. Sung et al.: GLOBOCAN estimates of incidence & mortality worldwide for 36 cancers in 185 Countries. CA Cancer J Clin 71: 2021, 209-249

4. Corley et al.: Adenoma detection rate and risk of colorectal cancer and death. N Engl J Med. 370, 2014,1298-306.

5. Pox et al.: Efficacy of a nationwide screening colonoscopy program for colorectal cancer. Gastroent. 142, 2012, 1460-7

6. Das A., Nair M.S., Peter S.D. Computer-aided histopathological image analysis techniques for automated nuclear atypia scoring of breast cancer: A review. J. Digit. Imaging. 2020;33:1091–1121. doi: 10.1007/s10278-019-00295-z.

7. Kong B., Li Z., Zhang S. Biomedical Information Technology. Elsevier; Amsterdam, The Netherlands: 2020. Toward large-scale histopathological image analysis via deep learning; pp. 397–414.

8. Tan, M. and Le, Q.V. (2019) EfficientNet: Rethinking Model Scaling for Convolutional Neural Networks. Proceedings of the 36th International Conference on Machine Learning, ICML 2019, Long Beach, 9-15 June 2019, 6105-6114.http://proceedings.mlr.press/v97/tan19a.html

9. Altunbay D., Cigir C., Sokmensuer C., Gunduz-Demir

C. Color graphs for automated cancer diagnosis and grading. IEEE Trans. Biomed. Eng. 2009;57:665–674. doi: 10.1109/TBME.2009.2033804.

10. Tosun A.B., Kandemir M., Sokmensuer C., Gunduz-Demir C. Object-oriented texture analysis for the unsupervised segmentation of biopsy images for cancer detection. Pattern Recognit. 2009;42:1104–1112. doi: 10.1016/j.patcog.2008.07.007.

11. Awan R., Sirinukunwattana K., Epstein D., Jefferyes S., Qidwai U., Aftab Z., Mujeeb I., Snead D., Rajpoot N. Glandular morphometrics for objective grading of colorectal adenocarcinoma histology images. Sci. Rep. 2017;7:16852. doi: 10.1038/s41598-017-16516-w.

12. Pacal I., Karaboga D., Basturk A., Akay B., Nalbantoglu U. A comprehensive review of deep learning in colon cancer. Comput. Biol. Med. 2020;126:104003. doi: 10.1016/j.compbiomed.2020.104003.

13. Hou L., Samaras D., Kurc T.M., Gao Y., Davis J.E., Saltz J.H. Patch-based convolutional neural network for whole slide tissue image classification; Proceedings of the IEEE Conference on Computer Vision and Pattern Recognition; Las Vegas, NV, USA. 27–30 June 2016; pp. 2424–2433.

14. Vuong T.L.T., Lee D., Kwak J.T., Kim K. Multi-task Deep Learning for Colon Cancer Grading; Proceedings of the 2020 International Conference on Electronics, Information, and Communication (ICEIC); Barcelona, Spain. 19–22 January 2020; Piscataway, NJ, USA: IEEE; 2020. pp. 1–2.

15. Bychkov D., Linder N., Turkki R., Nordling S., Kovanen P.E., Verrill C., Walliander M., Lundin M., Haglund C., Lundin J. Deep learning based tissue analysis predicts outcome in colorectal cancer. Sci. Rep. 2018;8:3395. doi: 10.1038/s41598-018-21758-3.

16. Sirinukunwattana K., Alham N.K., Verrill C., Rittscher J. International Conference on Medical Image Computing and Computer-Assisted Intervention. Springer; Berlin/Heidelberg, Germany: 2018. Improving whole slide segmentation through visual context-a systematic study; pp. 192–200.

17. Bosman FT, Carneiro F, Hruban RH, Theise ND, editors WHO Classification of Tumours of the Digestive System. World Health Organization; 2019.

18. Bejnordi BE, Veta M, Van Diest PJ, et al. Diagnostic assessment of deep learning algorithms for detection of lymph node metastases in women with breast cancer. JAMA. 2017;318(22):2199-2210.

19. Tan M., Le Q. Efficientnet: Rethinking model scaling for convolutional neural networks; Proceedings of the 36th International Conference on Machine Learning; Long Beach, CA, USA. 10–15 June 2019; pp. 6105–6114.

20. Jaware, T.H., Patil, V.R., Badgujar, R.D. et al. Performance investigations of filtering methods for T1 and T2 weighted infant brain MR images. Microsyst Technol 27, 3711–3723 (2021). https://doi.org/10.1007/s00542-020-05144-6

21. Shaban M., Awan R., Fraz M.M., Azam A., Tsang Y.W., Snead D., Rajpoot N.M. Context-Aware Convolutional Neural Network for Grading of Colorectal Cancer Histology Images. IEEE Trans. Med. Imaging. 2020;39:2395–2405. doi: 10.1109/TMI.2020.2971006.

22. Leo M., Carcagnì P., Signore L., Benincasa G., Laukkanen M.O., Distante C. Image Analysis and Processing—ICIAP 2022, Proceedings of the 21st International Conference, Lecce, Italy, 23–27 May 2022. Springer; Berlin/Heidelberg, Germany: 2022. Improving Colon Carcinoma Grading by Advanced CNN Models; pp. 233–244. Proceedings, Part I.

SignARcade - An Efficient Teaching - Learning Aid for Speech and Hearing Impaired using Augmented Reality and Machine Learning

Rajalakshmi S
Assistant Professor
Department of Computer Science and Engineering
Sri Sivasubramaniya Nadar College of Engineering
Chennai, Tamil Nadu
✉ rajalakshmis@ssn.edu.in

Sathvika V S, Swetha J, Vishvasri J S
UG Student
Department of Computer Science and Engineering
Sri Sivasubramaniya Nadar College of Engineering
Chennai, Tamil Nadu

ABSTRACT

The only means of communication for those who are deaf or have trouble speaking is sign language. Finding a teacher to teach sign language is challenging. Even with an instructor, it is impossible to learn at your own pace. Instead, it will be beneficial if they use an online learning resource. In this paper we have proposed a system "SignARcade" that uses augmented reality with sign language as a better learning aid for the challenged people. There are two sections to this proposed work namely the learning section and the testing section. Augmented reality has been used for the learning portion of the system. Using Blender, 3D models of the hand motions are produced. The models are identified using Deep Learning Neural network prototype developed in the testing section. In order to improve learning for persons of all ages who have communication or hearing challenges, this paper proposes integrating augmented reality technology into the classroom as well as grading student learning abilities using machine learning techniques.

KEYWORDS : Augmented reality, Machine learning, Recurrent Neural Network, TensorFlow, MediaPipe, Flask, OpenCV.

INTRODUCTION

Communication is not a luxury but a necessity. People born with hearing or speech loss cannot communicate normally like other people. This creates a gap between these people and the rest of the world. Sign language bridges the gap between the hearing or speech impaired people and normal people. It is difficult to rely on an instructor or an interpreter all the time. Learning independently using technology at their own pace will give them confidence to communicate and happiness.

According to a recent survey, over 20% of the world's population-or 1.5 billion people- live with hearing or speech loss. Their only mode of communication is sign language. If they can learn by themselves using an online instructor, they can learn at their own pace and at their own satisfaction. Similarly, if they can test themselves on what they learnt without the help of an external examiner, it will be a different level of comfort.

There are around 300 different sign languages used on our planet. We have chosen the Indian Sign Language dataset. This proposed work can be done with any other datasets. Previous works include Sensor-based sign language recognition. This approach is quite uncomfortable as users have to use specialized hardware like sensors or colored gloves. This hardware is quite expensive too, whereas, computer-vision based techniques only require bare hands. It is more cost-effective and highly portable.

Our aim is to develop a software which teaches the hand gestures of India Sign Language using Augmented Reality (AR) and Machine Learning. The Indian sign language manual gives an insight about the

representation of alphabets and numeric present in the dataset. We believe that this work will be a revolutionary among this community of people and help them live a life integrated with technology.

The main objective of the proposed system is to develop an AR based model for teaching speech and impaired individuals with sign language symbols. This is done with a machine learning gesture recognition component to help them practice and improve their skills. Another objective is to create an optimal and engaging learning experience that will empower these individuals to communicate more effectively and participate with confidence and happiness in conversations.   This will encourage socialization among the physically challenged people.

EXISTING WORK

Salma Hayani et al. [2] came up with an Arab Sign Language Recognition System. They used CNN (LeNet-5). The letters and numerals in Arab sign language were represented by 7869 photos in the dataset. A number of studies were run with training set counts ranging from 50% to 80%. An accuracy of 90% was produced by an 80% training dataset. To demonstrate the effectiveness of the system, the results were compared with machine learning methods like support vector machine (SVM) and k-nearest neighbour (KNN). Different algorithms and techniques for recognizing hand gestures were proposed by Kamal Preet Kour and Dr. Lini Mathew [5]. As described by the authors, gesture recognition is regarded as a way to facilitate more intuitive and proficient human-computer interaction. In this approach, software tools such as C,C++ and Java are used to implement gesture recognition. MATLAB with image processing toolbox is used for image processing operations.

Indian Sign Language Recognition was done by G. A. Rao et al. [8] using Convolutional Neural Network (CNN). This proposed work was done using videos captured from the front camera of a mobile. Datasets are created manually for 200 Indian Sign Language signs. CNN training is performed with three different datasets. In the first batch, one set of data is given as input. There

are two sets of training data in the second batch and three sets in the third batch. Average recognition rate of this CNN model is 92.88%. H Muthu Mariappan and V Gomathi [9] created a Real Time Recognition of Indian Sign Language. The Regions of Interest (ROI) are created and tracked to identify the indications using OpenCV's skin segmentation function. Using the machine learning algorithm fuzzy c-means of clustering, hand motions are predicted and trained. Numerous applications of this research include gesture-controlled robotics, automated homes, Human-Computer Interaction (HCI), and sign language interpretation.

Almana et al. [10] proposed an application that recognizes Arabic Sign Language using Convolutional Neural Network (CNN) and OpenCV. In this application, the CNN model is trained with around 5000 images (32 Categories) using ARSL2018. A real time frame is obtained or captured using OpenCV. After which a combination of OpenCV and CNN is used to recognize 32 letters. Micro and macro-average-F of the model is 95%. Shagun Katoch [11] et al use Bag Of Visual Words Model (BOVW) to recognize Indian Sign Language letters and numbers on a live video stream and output is in the form of text and speech. Skin color and background subtraction is used to perform segmentation. Classification was done using SVM and CNN.

PROPOSED SYSTEM DESIGN

The proposed system comprises of building the model with the dataset, detecting and recognizing the hand movement, identifying the posture of the hand, classifying the gesture and producing the equivalent sign language in 3D output. The architecture of the proposed system is shown in Figure 1.

First, we pick a dataset from Kaggle and then load it into the model as numpy arrays after finishing the preprocessing steps. Then the model is trained using Recurrent Neural Network (RNN)- Long Short Term Memory (LSTM). The model is trained for 200 epochs. RNN is purely based on hand landmark identification in this case. So, during the testing part when we show the signs it recognizes the landmarks and shows the desired output with the predicted letter and the accuracy.
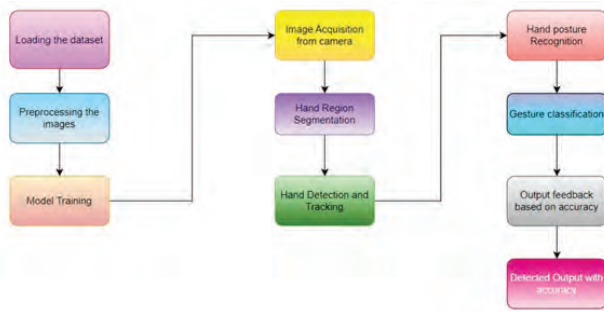
Fig. 1: Proposed System Design

METHODOLOGY

Methodology involves two sessions. Each user can engage themselves in Learning session to learn the sign and able to test themselves in testing session.

Learning session – AR

The 3D models of the sign gestures of Indian Sign Language were built using the 3D Computer Graphics Software Tool 'Blender'. A suitable target image was chosen and then uploaded into the database of the AR Software Kit 'Vuforia'. The data from Vuforia is then synced with the Real Time Development Platform 'Unity'. The Vuforia database is then imported into Unity. The 3D hand models are then loaded into Unity as .obj files. Using this a scene was created with the target image and the respective 3D model. The result is checked by running the scene and displaying the base target to the camera.

Testing session – ML

The testing session using machine learning comprises of the following modules:

* DATA PREPARATION: Video sequences are collected and divided into smaller frames. Features are extracted using mediapipe from each frame and stored those features in data_path. These features are converted into 2D numpy arrays by label encoding.

* MODEL CREATION: The LSTM model is defined in Keras library is used for creating the model with three LSTM layers followed by three dense layers.

* MODEL TRAINING: The model is trained using the fit attribute of sklearn library.

* MODEL EVALUATION: The trained model is evaluated using the testing data X_test and y_test to measure its performance on unseen data.

* MODEL SAVING: The trained model is saved in two formats - a JSON file and an HDF5 file for future usage. This saved model can also be used for incremental learning.

* MODEL DEPLOYMENT: The saved model is loaded and the output for the unseen new data is predicted.

IMPLEMENTATION

This section describes the techniques used for implementing the learning session using augmented reality and testing session using machine learning.

Augmented Reality (Learning)

1. Sync Vuforia database with Unity: Create a Vuforia account on the Vuforia Developer Portal and set up a new database. Add the target images and 3D models to the database. Download and import the Vuforia package into Unity, and then import the Vuforia database into your Unity project.

2. AR Camera setup: In the Unity Editor, create an AR camera by right-clicking in the "Hierarchy" window and selecting "Vuforia" → "AR Camera." This will replace the default camera with an AR camera specifically designed for Vuforia.

3. Image target setup: Import the target images into Unity by dragging and dropping them into the "Assets" folder. Then, select an image target from the Vuforia database in the "Assets" folder, and in the Inspector window, set its type to "Predefined" and select the appropriate target image.

4. Position and align 3D model: Import the 3D models into Unity by dragging and dropping them into the "Assets" folder. Place the 3D model in the scene by dragging it from the "Assets" folder into the scene view. Align and position the model on top of the image target by adjusting its position, rotation, and scale properties in the Inspector window.

5. Test the AR experience: Connect your device or use the Unity Play mode to test the AR project. When running the application, the device's camera will

activate, and by showing the image target to the camera, it should recognize the target and display the associated 3D model on top of it.

Machine Learning (Testing)

The models were trained using Keras to recognise human actions from a set of video sequences. The dataset for training was created by us and loaded into the model for training. We used the concept of LSTM - Long Short Term Memory which is basically an extension of Recurrent Neural Network (RNN). The LSTM model is defined in Keras with three LSTM layers followed by three dense layers.

- First Layer   - 64 units
- Second Layer - 128 units
- Third Layer   - 64 units

The dense layers have 64, 32, and actions.shape[0] units, respectively, where actions.shape[0] is the number of unique action labels. The activation function used in all LSTM layers and dense layers is ReLU, except for the final dense layer, which uses softmax. The compile method is called on the model with Adam optimizer and categorical_crossentropy loss function. The fit method is called on the model with X_train and y_train as

training data, epochs=200 for the number of epochs to train, and a TensorBoard callback to visualize training progress.

Finally, the trained model is saved in two formats:

- JSON file (model.json): Stores the architecture of the model
- HDF5 file (model.h5) : Stores the weights of the trained model.

RESULT

This section describes the dataset of sign language gesture images used to train our model for learning the sign language and the machine learning models used to learn from the dataset and predict the output for the real time hand gesture sign language movements. Accuracy metric is used to analyze the results. The output of the 3D models rendered using the augmented reality is also shown in this section.

Dataset

Table 1 describes the sample images of the different sign language gestures used for this proposed work. The dataset comprises of the images of the sign gestures for 26 alphabets and 10 numerals.

Table 1: Details of different Sign Language gestures

ML (Testing)

The following pictures display the outputs obtained for the Machine learning part (testing).

Figure 2 describes the output of letter 'V' obtained during the testing part (Machine Learning)
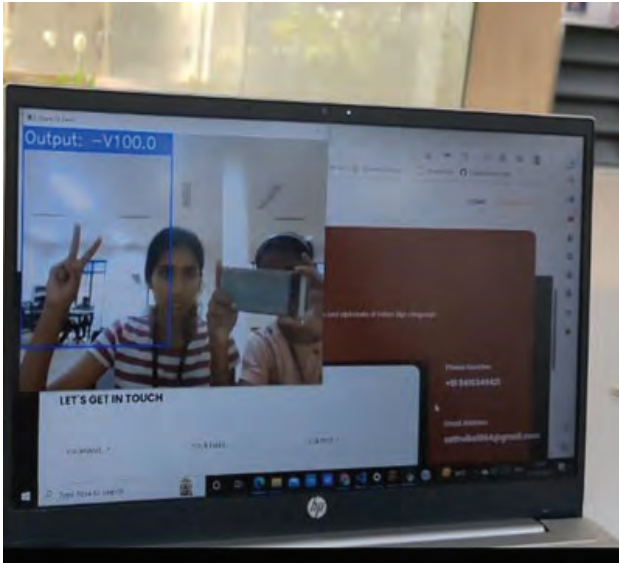
Fig 2: The letter 'V' is obtained with 100% Accuracy

Figure 3 describes the output of letter 'X' obtained during the testing part (Machine Learning)
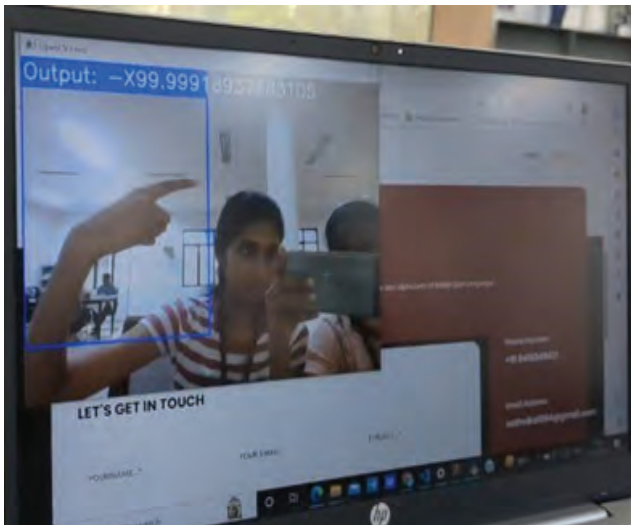
Fig. 3: The letter 'X' is obtained with 99.99% Accuracy

Figure 4 shows the accuracy for the various letters. Based on the analysis , the following were concluded from the ML model
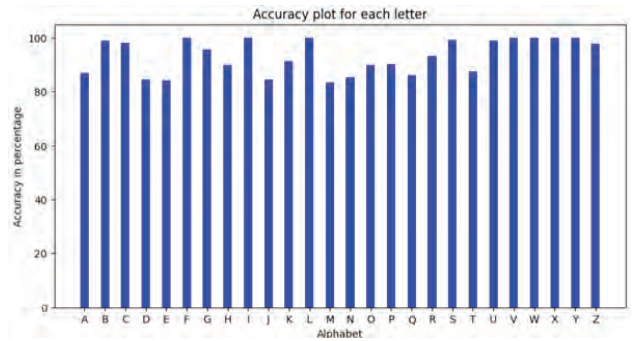
Fig. 4: A bar graph showing the accuracy plotted against each letter

1. Overall Accuracy: The model achieved high accuracy, with values ranging from 84.13% to 100%. The highest accuracy recorded was 100% (F,V,W,X,Y) (achieved multiple times), indicating perfect performance for those instances.

2. Consistency: Most of the accuracy values are above 90%, indicating a generally reliable model. However, there are a few instances with accuracy below 90%, which might suggest some challenges or variations in the performance of the model.

3. Comparative Analysis: By comparing the accuracy values, we can identify the top-performing and lowest-performing alphabets. For example, 'F' achieved 100% accuracy, while 'D' and 'E' had relatively lower accuracy values of 84.53% and 84.13%, respectively.

4. Uniqueness: The accuracy values are unique for each alphabet, indicating that the model has learned distinct patterns or characteristics for each letter.
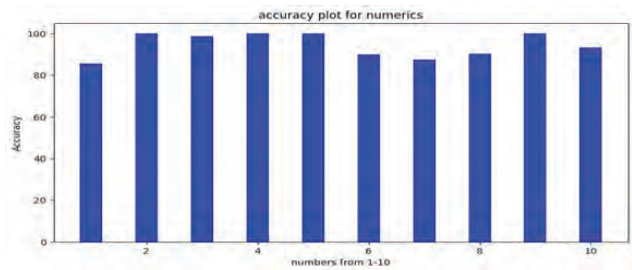
Fig. 5: A bar graph showing the accuracy plotted against each number

Figure 5 shows the accuracy for the various numbers. Based on the analysis, the following were concluded from the ML model

AR (Teaching)

The following images display the outputs obtained during the AR section (Teaching). The 3D models created using blender are displayed on the screen (Particular number or letter) when the target image is shown at the camera. Figure 6 describes the output of number '1' obtained during the teaching part (Augmented Reality)
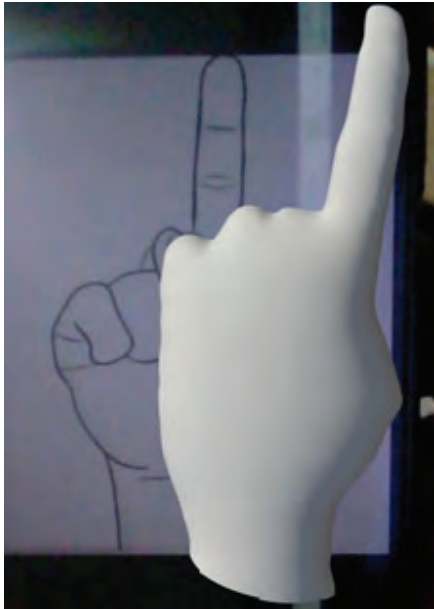
Fig. 6: The 3D Model of number '1' is obtained

Figure 7 describes the output of number '5' obtained during the teaching part (Augmented Reality)

Figure 7: The 3D Model of number '5' is obtained

CONCLUSION AND FUTURE WORK

There is an increasing population of speech and hearing-impaired individuals who face unique challenges in communication and learning. With the recent advancement in machine learning, there are many ways in which these people can be helped.

In our proposed work, using an integration of Augmented Reality and Machine Learning, we have created an online sign language learning aid. In the first part (Learning) we used Blender to create the 3D models of the Indian sign language gestures for numbers and letters. AR models were created using Vuforia and Unity. In the second part (Testing), Keras was used to train the models created using LSTM and RNN. The letter being shown, and the accuracy of the hand gesture is displayed with precision.

Several ideas for the future work have been listed below.

1. Home Automation tools tailored for the community of mute and hearing impaired: Our goal is to develop a home automation tool for the community of people with speech and hearing impairments and integrate their life to the next level with technology. The development of the system towards understanding and interpreting words and phrases or small sentences is currently under progress.

2. Real-Time Translation: Aim to achieve real-time translation from sign language to spoken or written language. This would involve reducing latency and improving the speed of translation to provide more seamless communication between sign language users and non-sign language users

3. Integration with Video Conferencing Platforms: Explore integrating the sign language interpreter system with popular video conferencing platforms, such as Zoom or Microsoft Teams. This would enable seamless interpretation during remote meetings or virtual events, making them more inclusive for sign language users.

4. Word-Level Sign Interpretation: Expand the system's capabilities to provide sign interpretations for individual words. This would involve developing a comprehensive database of signs for a wide range of vocabulary, including nouns, verbs,

adjectives, and adverbs. The system should be able to generate accurate and contextually appropriate signs for each word.

5. Development of chatbots that can understand and respond to sign language: A chatbot that can translate sign language to text and provide to be a personal assistant like Siri for mac and Google assistant for android to the impaired people is also one of our main motives. We believe that our proposed system will be revolutionary among this community of people and help them live a life integrated with technology.

REFERENCES

1. M. Al-Hammadi, G. Muhammad, w. Abdul, M. Alsulaiman, M. A. Bencherif, M. A. Mekhtiche, "Hand Gesture Recognition for Sign Language Using 3DCNN", 2020.https://ieeexplore.ieee.org/abstract/document/9078786

2. Hayani, Salma, et al. "Arab sign language recognition with convolutional neural networks." 2019 International Conference of Computer Science and Renewable Energies (ICCSRE). IEEE, 2019.

3. Reddygari Sandhya Rani , R Rumana , R. Prema, "A Review Paper on Sign Language Recognition for The Deaf and Dumb" 2021.

4. Oudah, Munir, Ali Al-Naji, and Javaan Chahl. "Hand gesture recognition based on computer vision: a review of techniques." Journal of Imaging 6.8 (2020): 73.

5. Kamal Preet Kour, Dr.Lini Mathew, "Hand gesture techniques for sign language recognition",2017

6. Adeyanju, I. A., O. O. Bello, and M. A. Adegboye. "Machine learning methods for sign language recognition: A critical review and analysis." Intelligent Systems with Applications 12 (2021): 200056.

7. Ananthanarayana, Tejaswini, et al. "Deep learning methods for sign language translation." ACM Transactions on Accessible Computing (TACCESS) 14.4 (2021): 1-30.

8. G. A. Rao, K. Syamala, P. V. V. Kishore and A. S. C. S. Sastry. "Deep Convolutional Neural Networks for Sign Language Recognition",2018.

9. Mariappan, H. Muthu, and V. Gomathi. "Real-time recognition of Indian sign language." 2019 international conference on computational intelligence in data science (ICCIDS). IEEE, 2019.

10. Almana, Shaikhah, and Alauddin Al-Omary. "Real-time Arabic Sign Language Recognition using CNN and OpenCV." 2022 International Conference on Innovation and Intelligence for Informatics, Computing, and Technologies (3ICT). IEEE, 2022.

11. Srivastava, Sharvani, et al. "Sign language recognition system using TensorFlow object detection API." Advanced Network Technologies and Intelligent Computing: First International Conference, ANTIC 2021, Varanasi, India, December 17–18, 2021, Proceedings. Cham: Springer International Publishing, 2022.

12. Shagun Katoch, Varsha Singh, Uma Shanker Tiwary, "Indian Sign Language recognition system using SURF with SVM and CNN",2022.

13. Sonawane, Pankaj, et al. "Speech to Indian sign language (ISL) translation system." 2021 international conference on computing, communication, and intelligent systems (ICCCIS). IEEE, 2021.

14. Golekar, Dipalee, et al. "Sign language recognition using Python and OpenCV." Int Res J Modernization Eng Technol Sci 4.2 (2022): 1-5.

Utilizing Graph Convolutional Networks for GitHub user Classification

Venkataramana Battula
✉ venkataramana_cse@mvsrec.edu.in
Anirudh Bojji
✉ 245120733043@mvsrec.edu.in

Bollu Siddharth Reddy
✉ 245120733055@mvsrec.edu.in
Pradyumna Chacham
✉ 245121733066@mvsrec.edu.in

Department of CSE
Maturi Venkata Subba Rao (MVSR) Engineering College

ABSTRACT

This research investigates the dynamics of user interactions on GitHub, a popular platform for collaborative software development, using advanced graph-based machine learning techniques. We outline a systematic methodology that involves meticulous data preparation, including the partitioning of the dataset into distinct subsets and the encoding of target variables using innovative techniques. Our approach leverages the construction of a comprehensive graph that encapsulates the intricate relationships between GitHub users. We employ a sophisticated Graph Convolutional Network (GCN) model architecture, carefully designed with multiple hidden layers and dropout regularization to ensure robustness against overfitting. Training the model involves a meticulously crafted optimization strategy, guided by the Adam optimizer and complemented by early stopping mechanisms. Following rigorous training, our evaluation metrics reveal an impressive accuracy rate of 86%, indicative of the model's prowess in discerning meaningful patterns within GitHub user interactions. These findings not only underscore the efficacy of our approach but also highlight its potential applications in diverse domains, including user recommendation systems and community detection algorithms. We anticipate that future research endeavors will further refine and extend our methodology, unlocking new insights into the dynamics of online collaboration platforms.

KEYWORDS : GCN, Stellar graph, Node classification.

INTRODUCTION

In our connected world, various datasets generate a large amount of interconnected data. This data is represented using graphs, which consist of nodes and edges. Nodes represent entities, like individuals or objects, while edges show relationships between them. There are two main types of graph networks: homogeneous, where nodes and edges are the same type, and heterogeneous, where they differ. Graph analysis involves four key problems: node classification, which assigns labels to nodes; link prediction, predicting new connections forming between nodes; community detection, identifying clusters within the graph; and graph classification, categorizing entire graphs based on their features. These problems help us understand complex network structures across different fields.

The "Github User Classification" focuses on categorizing users on the GitHub platform into two distinct groups: Machine Learning (ML) developers and Web developers. Through the application of graph-based machine learning techniques, particularly Graph Convolutional Networks (GCNs), the project aims to dissect user behaviors, connections, and contributions within the GitHub ecosystem. By harnessing data collected from various sources such as user profiles, repository metadata, and commit history, the project extracts pertinent features indicative of user expertise and engagement levels.

Following data collection and feature extraction, the Work adopts a comprehensive methodology encompassing graph representation, model training, and evaluation stages. The collected data is transformed

into a graph structure, where nodes represent users and repositories, and edges denote interactions and associations. Leveraging this graph representation, a GCN model is trained to discern patterns and relationships among users, enabling accurate classification for ML developers and Web developers. Rigorous evaluation using established metrics ensures the model's effectiveness in classifying users based on their profiles and activities.

Our Work holds significant potential to provide valuable insights and drive community engagement within the GitHub ecosystem. By categorizing users and understanding their expertise, collaboration patterns, and preferences, the project facilitates targeted interactions, project recommendations, and platform enhancements. Through ongoing analysis and interpretation of model predictions, the project contributes to the continuous improvement of Github functionality and fosters a vibrant and collaborative environment for developers worldwide.

Our primary contribution is the development of a model that aids in classifying whether a GitHub user is a machine learning (ML) developer or a Python developer using Graph Convolutional Networks (GCN).

LITERATURE REVIEW

Zhang et al. [1] explore the pivotal role of graph convolutional networks (GCNs) in learning on graphs, and categorizing GCN models based on convolution types and applications. Kemani et al. [2] assert Graph Neural Networks' (GNNs) transformative potential in modeling intricate relationships and providing effective solutions across domains. Dwivedi et al. [3] introduce an open-source benchmarking framework for GNNs, fostering fair model comparisons and spurring research advancements. Jia et al. [4] discuss the universal applicability of networks in modeling complex systems and propose a taxonomy for analyzing GCNs. Aslam et al.[5] highlight GNNs' role in optimizing complex network environments and revolutionizing tasks like image processing. Fathenizad et al. [6] emphasize GNNs' efficacy in high-level representation extraction, particularly through integration with Deep Reinforcement Learning (DRL). Xie et al. [7] underscore the significance of self-

supervised learning (SSL) in training deep models, focusing on its application in GNNs.Hao et al. [8] stress the interpretable deep models' necessity, particularly in interdisciplinary fields, and review explanation techniques for Graph Neural Networks (GNNs). Liang et al. [9] introduce Graph Neural Networks (GNNs) to handle non-Euclidean data, exploring their applications in IoT systems. Varlamis et al. [10] investigate Graph Convolutional Networks (GCNs) for fake news detection, emphasizing challenges and future research directions. Wu etal. [11] examine recommender systems' evolution towards graph-learning-based approaches, highlighting GNNs' effectiveness. Liu et al. [12] survey methods for accelerating Graph Neural Networks (GNNs) and identify challenges and future research directions. Reiser et al. [13] discuss the integration of graph neural networks (GNNs) in materials science and chemistry research, emphasizing their direct processing of natural input representations. Makarov et al. [14] explore graph representation theory's utility in real-world scenarios, emphasizing automatic feature extraction with graph embeddings. Skarding et al.[15] discuss Graph Convolutional Neural Networks (GCNs) in image classification, focusing on object-based analysis in remote sensing data.

Liu et al. [16] survey sampling methods for efficient training of Graph Convolutional Networks (GCNs) and propose research directions. Zhang et al. [17] provide a comprehensive survey on Graph Neural Networks (GNNs) in bioinformatics, discussing applications and future directions. Abu-El-Haija et al. [18] propose a meta-model called Network of GCNs for semi-supervised learning on graphs, achieving state-of-the-art results Sun et al. [19] propose improved graph neural networks by minimizing loss through random graph perturbations. Zhao et al. [21] survey graph data augmentation techniques for enhancing graph machine learning. Wu et al. [22] provide an overview of graph neural networks, categorizing them and discussing applications. Chen et al. [23] propose a unified framework for a systematic understanding of graph neural networks. Renjie Liao et al. [25] introduce LanczosNet, achieving state-of-the-art results in various tasks. Liu et al. [26] propose GeniePath for identifying

receptive paths in graph convolutional networks. Zhang et al.[27] introduce Bayesian graph convolutional neural networks for handling uncertainty. Yang et al. [28] propose Masked Graph Convolutional Networks for semi-supervised classification. Hu Fenyu et al. [29] introduce hierarchical graph convolutional networks for semi-supervised node classification.

Jiang et al. [31] discuss challenges and recent methods for applying convolutional neural networks to graph-structured data. Franceschi et al. [32] propose LDS for learning graph structure and neural network parameters simultaneously. Mehta et al. [33] propose a deep generative framework for graph-structured data. Zhang Ziwei et al. [34] review the literature on graph convolutional networks. Yao et al. [35] propose Text Graph Convolutional Networks for text classification. Maron et al.[36] focus on graph learning, characterizing layers for tensor input and output data.You, Jiaxuan et al. [37] introduce Position-aware Graph Neural Networks (P-GNNs), outperforming existing models in graph-based prediction tasks. Dai,Hanjun et al. [38] propose a stochastic learning framework for efficient graph algorithms. Zhuang, Chenyi et al. [39] present a dual graph convolutional neural network for semi-supervised learning. Li, Ruoyu et al. [40] propose a spectral graph convolver for adaptive graph learning. Battaglia, Peter W et al. [41] discuss improving AI's capacity for combinatorial generalization. Teney, Damienet al. [42] propose a graph-based model for Visual Question Answering. Hamilton, William L et al. [43] review advancements in graph representation learning. Marino, Kenneth et al. [44] propose a Graph Search Neural Network for multi-label image classification. Zhang Ziwei et al. [45] highlight challenges and opportunities in applying deep learning to graphs. Scarselli, Franco, et al. [46] provide an overview of graph neural networks and their applications.

PROPOSED WORK
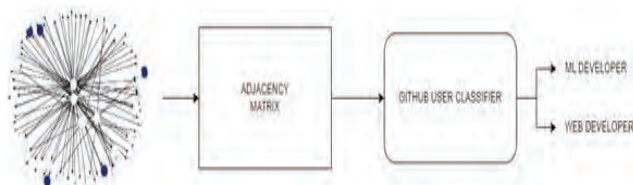
Fig. 1: GithHub user Classification
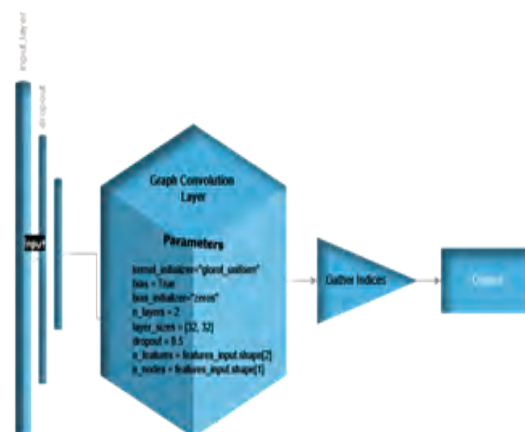
Fig. 2: GithHub Classifier's Architecture

Our proposed model starts with a graph representation of GitHub users, which is then converted into an adjacency matrix. Utilizing this matrix, our model classifies GitHub users into two categories: machine learning developers and web developers.

IMPLEMENTATION

Dataset

Data collection begins by accessing GitHub data through the GitHub API, scraping techniques, or pre-existing datasets. This data encompasses user profiles, repository information, commit history, and followers/following relationships, among other attributes. Various features get engineered from the collected data, including user activity metrics such as the number of commits, repositories, and followers, as well as temporal, content-based, and network-based features. The collected data then gets represented as a graph, where users, repositories, and their interactions are depicted as nodes and edges, capturing relational information between entities. Subsequently, a Graph Convolutional Network (GCN) model gets constructed and trained using the extracted features and the graph representation of the GitHub data. This model learns to classify users based on their features and the relationships encoded in the graph. Finally, the trained model gets evaluated using a separate test dataset to assess its performance in classifying users as ML developers or Web developers, with evaluation metrics providing insights into its effectiveness.

Fig. 3: Sample-dataset
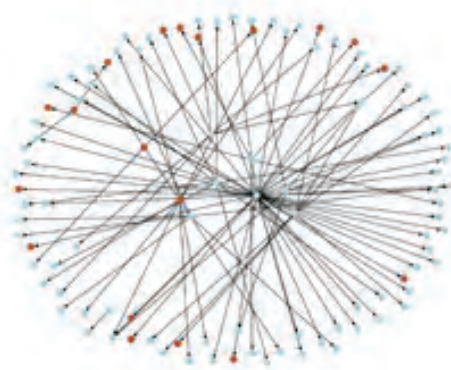
Fig. 4: Git Nodes(a)

Fig. 5: Git Nodes(b)

Utilizing the NetworkX module, we have visualized samples in the above figure, showcasing connections and relationships within data. This visualization aids

in understanding complex patterns, facilitating analysis and communication of findings across disciplines such as social sciences and biology.

Feature Extraction

In our research, we incorporated various graph features to enhance node classification accuracy. These features encompassed fundamental metrics within network analysis. Firstly, degree centrality gauges the number of edges connected to a node, providing insight into its prominence within the network. Secondly, eigenvector centrality evaluates a node's importance based on the significance of its neighboring nodes, offering a nuanced perspective on its influence. Thirdly, PageRank assesses a node's importance considering the significance of its incoming edges, contributing to a comprehensive understanding of its relevance. Additionally, the clustering coefficient measures the interconnectedness among a node's neighbors, shedding light on the local structure of the network. Despite the utility of betweenness centrality, its extensive computational requirements rendered it impractical for our purposes and did not yield substantial improvements in results. Consequently, we employed degree centrality, eigenvector centrality, PageRank, and clustering coefficient as alternative features, ensuring efficient computation and meaningful contributions to our classification task.

Methodology

Initially, the dataset was partitioned using the train-test-split function from scikit-learn into training, validation, and test sets. The target variables were then encoded using target encoding techniques, facilitated by target encoding. fittransform and target-encoding. Transform methods. A graph, denoted as G, was constructed to depict the interrelations among GitHub users. A FullBatchNodeGenerator was instantiated with graph G and the "gcn" method for the application of a Graph Convolutional Network (GCN). Data iterators (train-gen, val-gen, test-gen) corresponding to the training, validation, and test sets were generated using the flow method of the generator.

The GCN model architecture consisted of two hidden layers, each with 32 units and Rectified Linear Unit (ReLU) activations, to which a dropout rate of 0.5 was

applied. The GCN's output was processed through a Dense layer with a sigmoid activation function for final predictions. Model compilation and training were conducted using the Adam optimizer with a learning rate of 0.01, binary cross-entropy loss function, and accuracy as the evaluation metric. An early stopping callback (es-callback) was incorporated to prevent overfitting. Training was performed for 200 epochs using the fit method, with train-gen and val-gen serving as the training and validation data, respectively. Notably, data shuffling was not performed during training, in line with best practices for graph data.

After training, model predictions on the test set were obtained using the prediction method with test-gen. Evaluation metrics including Area Under the Receiver Operating Characteristic Curve (AUC), Precision-Recall (PR), and F-score were computed using the evaluate-preds function.

Following the model's fitting with Graph Convolutional Networks (GCN), embeddings are extracted from the penultimate layer using a Keras model. Node indices are obtained from the graph, and embeddings are predicted utilizing node features, indices, and adjacency matrix inputs. This process yields embeddings, the shape of which is evaluated for their effectiveness in subsequent tasks like node classification or link prediction. Such analysis contributes to understanding the efficacy of graph-based representation learning methods for various applications in machine learning and network analysis.

Our Work offers a robust mechanism to accurately classify Github users into two distinct categories: Machine Learning (ML) developers and Web developers, leveraging insights from their profiles and activities. By analyzing learned representations and model predictions, the project provides valuable insights into the distribution of expertise, collaboration patterns, and emerging trends within the GitHub community. Furthermore, it endeavors to enhance the interpretability of the classification model by visualizing learned representations, identifying feature importance, and highlighting influential factors contributing to classification decisions. The project's potential applications extend to fostering community engagement by facilitating targeted interactions with

Github users based on their expertise and interests, thereby encouraging collaboration and knowledge sharing across specific domains. Additionally, by understanding the expertise of Github users, the project can offer tailored project recommendations, repository suggestions, and relevant resources aligned with individual users' interests and skill sets. Insights derived from the project also contribute to informing platform enhancements, driving feature improvements, and supporting community-driven initiatives on Github, ultimately catering to the diverse needs of developers and contributors.

In our work, various Python libraries were utilized for data processing, model development, visualization, and evaluation. The pandas library was employed for data manipulation and analysis, while tqdm was utilized to create progress bars for iterative processes, enhancing the user experience during execution. The JSON library facilitated the parsing and handling of JSON data structures. For graph construction and manipulation, both Stellargraph and Networkx were utilized, offering functionalities for graph representation, analysis, and algorithms. The umap library was employed for dimensionality reduction tasks, aiding in visualizing high-dimensional data in lower-dimensional spaces. TensorFlow served as the foundational framework for building and training the Graph Convolutional Network (GCN) model. The warnings module was utilized to manage warning messages raised during execution. The sklearn library provided a range of machine learning algorithms and utilities, including data splitting, encoding techniques, and evaluation metrics. Visualization of data and results was facilitated by Matplotlib and seaborn, offering a wide array of plotting functionalities for creating informative visualizations. These libraries collectively supported various stages of the research pipeline, contributing to data preparation, model development, evaluation, and result visualization.

RESULTS AND DISCUSSION

The experimental results of our study yielded a commendable accuracy rate of 86%. This outcome underscores the efficacy of the employed methodology in effectively learning and predicting the relationships among GitHub users. Such a high accuracy rate suggests

that the Graph Convolutional Network (GCN) model, trained on the constructed graph representation of user relationships, has effectively captured and generalized patterns in the data. This finding holds significant implications for tasks such as user recommendation, community detection, and anomaly detection within the GitHub ecosystem. The robust performance of the model can be attributed to several factors within the methodology. The use of target encoding for label representation, coupled with the construction of a comprehensive graph capturing user interactions, likely facilitated the model's ability to discern meaningful patterns in the data. Additionally, the inclusion of dropout regularization within the GCN architecture helped prevent overfitting, thereby enhancing the model's generalization capabilities. The utilization of the Adam optimizer with an appropriate learning rate further contributed to the model's optimization process, enabling efficient convergence during training. Furthermore, the absence of data shuffling during training, as recommended for graph-based data, likely preserved the integrity of the data relationships and contributed to the model's robust performance. The incorporation of early stopping as a regularization technique also played a crucial role in preventing overfitting and ensuring the model's generalization ability.
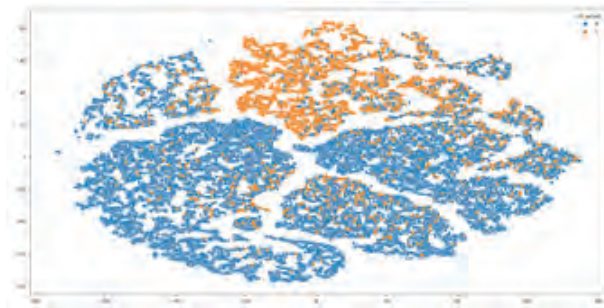
Fig. 6: Results

Model	Accuracy
Pytorch-gcn	0.6059
Pytorch-gat	0.6613
Stellargraph-gcn	0.8311

The graphical representation reveals a notable distinction between two distinct clusters representing different classes. However, a discernible level of intermingling is observable at the center of the plot, which is not surprising given the shared similarities between machine learning (ML) and web development domains. This convergence underscores the commonalities existing between these fields despite their apparent differences.

GCN embeddings are extracted from the penultimate layer and used as inputs to traditional ML models like Random Forest, Logistic Regression, KNN, and SVM. Results show the GCN embeddings boost performance on node classification and link prediction tasks compared to using raw features or graph structure alone, demonstrating the value of combining representation learning and classical ML for graph analysis.

Model	Accuracy
Random Forest Classifier	0.8490
Logistic Regression	0.8542
Support Vector Machine Classifier	0.8530
Gradient Boosting Classifier	0.8549
K-Nearest Neighbours	0.8366

CONCLUSION

Graph-based machine learning techniques play a pivotal role in categorizing GitHub users into two main groups: Machine Learning (ML) developers and Web developers. The focus lies in providing valuable insights into the distribution of expertise and collaboration patterns prevalent within the GitHub community. By integrating feature engineering, graph representation, and model training, we aim to enrich community engagement, stimulate collaboration, and enhance the overall functionality of the GitHub platform. Through ongoing efforts and analysis, we strive to contribute to a vibrant and collaborative environment on GitHub, fostering mutual growth and knowledge exchange among developers worldwide. While the achieved accuracy rate of 86 is certainly promising, it is essential to acknowledge potential limitations and avenues for further improvement.

Future research could explore additional features or incorporate more sophisticated graph embedding techniques to capture richer representations of user relationships. Moreover, fine-tuning hyperparameters or experimenting with different model architectures

may lead to incremental improvements in performance. Nonetheless, the obtained results underscore the viability of utilizing graph based approaches for analyzing and understanding complex relational data, with implications extending beyond the GitHub domain to various other networked systems.

REFERENCES

1. Zhang, Si, et al. "Graph convolutional networks: a comprehensive review." Computational Social Networks 6.1 (2019): 1-23.

2. Khemani, Bharti, et al. "A review of graph neural networks: concepts, architectures, techniques, challenges, datasets, applications, and future directions." Journal of Big Data 11.1 (2024): 18.

3. Dwivedi, Vijay Prakash, et al. "Benchmarking graph neural networks." Journal of Machine Learning Research 24.43 (2023): 1-48.

4. Jia, Mingshan, Bogdan Gabrys, and Katarzyna Musial. "A Network Science perspective of Graph Convolutional Networks: A survey." IEEE Access (2023).

5. Bhatti, Uzair Aslam, et al. "Deep learning with graph convolutional networks: An overview and latest applications in computational intelligence." International Journal of Intelligent Systems 2023 (2023): 1-28.

6. Fathinezhad, Fatemeh, et al. "Graph Neural Networks and Reinforcement Learning: A Survey." (2023).

7. Xie, Yaochen, et al. "Self-supervised learning of graph neural networks: A unified review." IEEE transactions on pattern analysis and machine intelligence 45.2 (2022): 2412-2429.

8. Yuan, Hao, et al. "Explainability in graph neural networks: A taxonomic survey." IEEE transactions on pattern analysis and machine intelligence 45.5 (2022): 5782-5799.

9. Liang, Fan, et al. "Survey of graph neural networks and applications." Wireless Communications and Mobile Computing 2022 (2022).

10. Varlamis, Iraklis, et al. "A survey on the use of graph convolutional networks for combating fake news." Future Internet 14.3 (2022): 70

11. Wu, Shiwen, et al. "Graph neural networks in recommender systems: a survey." ACM Computing Surveys 55.5 (2022): 1-37.

12. Liu, Xin, et al. "Survey on graph neural network acceleration: An algorithmic perspective." arXiv preprint arXiv:2202.04822 (2022).

13. Reiser, Patrick, et al. "Graph neural networks for materials science and chemistry." Communications Materials 3.1 (2022): 93.

14. Makarov, Ilya, et al. "Survey on graph embeddings and their applications to machine learning problems on graphs." PeerJ Computer Science 7 (2021): e357.

15. Skarding, Joakim, Bogdan Gabrys, and Katarzyna Musial. "Foundations and modeling of dynamic networks using dynamic graph neural networks: A survey." IEEE Access 9 (2021): 79143-79168.

16. Liu, Xin, et al. "Sampling methods for efficient training of graph convolutional networks: A survey." IEEE/CAA Journal of AutomaticaSinica 9.2 (2021): 205-234.

17. Zhang, Xiao-Meng, et al. "Graph neural networks and their current applications in bioinformatics." Frontiers in genetics 12 (2021): 690049.

18. Abu-El-Haija, Sami, et al. "N-gcn: Multi-scale graph convolution for semisupervised node classification." uncertainty in artificial intelligence. PMLR, 2020.

19. Sun, Ke, Piotr Koniusz, and Zhen Wang. "Fisher-bures adversary graph convolutional networks." Uncertainty in Artificial Intelligence. PMLR, 2020.

20. Kinderkhedia, Mital. "Learning Representations of Graph Data–A Survey." arXiv preprint arXiv:1906.02989 (2019).

21. Zhao, Tong, et al. "Graph data augmentation for graph machine learning: A survey." arXiv preprint arXiv:2202.08871 (2022).

22. Wu, Zonghan, et al. "A comprehensive survey on graph neural networks." IEEE transactions on neural networks and learning systems 32.1 (2020): 4-24.

23. Chen, Zhiqian, et al. "Bridging the gap between spatial and spectral domains: A survey on graph neural networks." arXiv preprint arXiv:2002.11867 (2020).

24. Zhou, Jie, et al. "Graph neural networks: A review of methods and applications." AI open 1 (2020): 57-81.

25. Liao, Renjie, et al. "Lanczosnet: Multi-scale deep graph convolutional networks." arXiv preprint arXiv:1901.01484 (2019).

26. Liu, Ziqi, et al. "Geniepath: Graph neural networks with adaptive receptive paths." Proceedings of the

AAAI Conference on Artificial Intelligence. Vol. 33. No. 01. 2019.

27. Zhang, Yingxue, et al. "Bayesian graph convolutional neural networks for semisupervised classification." Proceedings of the AAAI conference on artificial intelligence. Vol. 33. No. 01. 2019.

28. Yang, Liang, et al. "Masked Graph Convolutional Network." IJCAI. 2019.

29. Hu, Fenyu, et al. "Hierarchical graph convolutional networks for semi-supervised node classification." arXiv preprint arXiv:1902.06667 (2019)

30. Jiang, Bo, et al. "Semi-supervised learning with graph learning-convolutional networks." Proceedings of the IEEE/CVF conference on computer vision and pattern recognition. 2019.

31. Franceschi, Luca, et al. "Learning discrete structures for graph neural networks." International conference on machine learning. PMLR, 2019.

32. Mehta, Nikhil, Lawrence Carin Duke, and Piyush Rai. "Stochastic blockmodels meet graph neural networks." International Conference on Machine Learning. PMLR, 2019.

33. Zhang, Si, et al. "Graph convolutional networks: a comprehensive review." Computational Social Networks 6.1 (2019): 1-23.

34. Yao, Liang, Chengsheng Mao, and Yuan Luo. "Graph convolutional networks for text classification." Proceedings of the AAAI conference on artificial intelligence. Vol. 33. No. 01. 2019.

35. Zhang, Si, et al. "Graph convolutional networks: a comprehensive review." Computational Social Networks 6.1 (2019): 1-23

36. Maron, Haggai, et al. "Invariant and equivariant graph networks." arXiv preprint arXiv:1812.09902 (2018).

37. You, Jiaxuan, Rex Ying, and Jure Leskovec. "Position-aware graph neural networks." International conference on machine learning . PMLR, 2019

38. Dai, Hanjun, et al. "Learning steady-states of iterative algorithms over graphs." International conference on machine learning. PMLR, 2018.

39. Zhuang, Chenyi, and Qiang Ma. "Dual graph convolutional networks for graphbased semi-supervised classification." Proceedings of the 2018 world wide web conference. 2018.

40. Li, Ruoyu, et al. "Adaptive graph convolutional neural networks." Proceedings of the AAAI conference on artificial intelligence. Vol. 32. No. 1. 2018

41. Battaglia, Peter W., et al. "Relational inductive biases, deep learning, and graph networks." arXiv preprint arXiv:1806.01261 (2018).

42. Teney, Damien, Lingqiao Liu, and Anton van Den Hengel. "Graph-structured representations for visual question answering." Proceedings of the IEEE conference on computer vision and pattern recognition. 2017

43. Hamilton, William L., Rex Ying, and Jure Leskovec. "Representation learning on graphs: Methods and applications." arXiv preprint arXiv:1709.05584 (2017)

44. Marino, Kenneth, Ruslan Salakhutdinov, and Abhinav Gupta. "The more you know: Using knowledge graphs for image classification." arXiv preprint arXiv:1612.04844 (2016).

45. Zhang, Ziwei, Peng Cui, and Wenwu Zhu. "Deep learning on graphs: A survey." IEEE Transactions on Knowledge and Data Engineering 34.1 (2020): 249-270

46. Scarselli, Franco, et al. "The graph neural network model." IEEE transactions on neural networks 20.1 (2008): 61-80.

AI-Powered Floor Cleaning Robots Navigational Intelligence and its Performance Evaluation

Varsha Bendre
✉ varsha.bendre@pccoepune.org

Aditya Pandey
✉ aditya.pandey19@pccoepune.org

Aditya Yadav
✉ aditya.yadav191@pccoepune.org

Abhishek Lonkar
✉ abhilonkarwar1234@gmail.com

Department of Electronics and Telecommunications
Pimpri Chinchwad College of Engineering
Pune, Maharashtra

ABSTRACT

Modern Industries and households are moving towards automation, thereby delivering convenience and reducing time spent on cleanliness. While vacuum cleaners have made cleaning easier, they are large, noisy, and bulky for everyday use. It is, therefore, necessary to improve the technology of vacuum cleaning to reduce these deficiencies. Due to the pandemic, it is now realized that sanitization is equally important along with cleanliness. In the proposed work, an Artificial Intelligence (AI) powered autonomous mobile robot is developed to clean and sanitize the house, office or industry, etc. Being autonomous, the cleaning robot helps to clean and sanitize the floor just by simply pressing a switch. This will effectively cut down the extra labour used in the industries for cleaning purposes and also be helpful for cleaning hazardous places through remote operation.

This AI powered floor-cleaning robot incorporates advanced sensing technologies such as Lidar, cameras, and ultrasonic sensors to perceive its environment. It employs Simultaneous Localization and Mapping algorithms to create a map of the area and determine its precise location within it. Advanced collision avoidance techniques are employed to ensure safe navigation, while adaptive cleaning patterns and zone-specific cleaning modes enhance the robot's efficiency. Path planning algorithms enable the robot to generate optimal cleaning paths while avoiding obstacles. The cleaning mechanism, which may include rotating brushes, suction systems, or mopping pads, is activated based on the robot's position and the desired cleaning mode.

KEYWORDS : *Artificial intelligence, Autonomous, Cleaning, Floor, Lidar, ROS, Simulink model.*

INTRODUCTION

To maintain cleanliness in industries, chores like Dusting, Sweeping, and Mopping have to be repeated every day. To counter such problems, there are several machines that are designed for ease to humans, breaking down the complex, tedious task into simpler ones. But these vacuum cleaners are complex, bulky, and heavy, making it tedious to move and clean [1]. Vacuum cleaners available in the market consume hundreds to thousand watts of electricity which in turn increases the electricity bill. The operating electric motor becomes too hot and burns out the vacuum cleaner motor. While in physical activity, dusting certain particles which,

when inhaled, cause problems in the respiratory system of that person, which in turn leads to more health issues. Several machines available in the market employ specific mechanical and electrical systems to ensure a clean household. Some vacuum cleaners don't offer reusable dustbin bags. These machines make life and cleaning tasks more difficult because one has to be physically present for mobility of machines [2]. To reduce such efforts for cleaning, this project aims to create a bot which is low cost, utilizes local resources to design, and serves the purpose of sweeping and dusting from a place that is far away from a dusty

environment. Humayun Rashid [3] et al. proposes a design proposition for an Autonomous Mobile Robot Based on Robotic Operating System (ROS). This paper provides a complete analysis of the design and implementation of an autonomous mobile robot based on ROS. It covers hardware design considerations, software development using ROS, perception and sensing capabilities, mapping and localization techniques, path planning and navigation strategies, experimental results, and future research directions. Kirill KrinKin [4] et al. focuses on the evaluation and comparison of modern laser-based Simultaneous Localization and Mapping Algorithms (SLAM) in indoor environments. The authors evaluate and compare several modern laser-based SLAM algorithms, including Graph SLAM, Fast SLAM, and Iterative Closest Point (ICP)-based methods. These algorithms differ in their underlying principles, computational complexity, and performance characteristics. The paper discusses the advantages and limitations of each algorithm. For example, Graph SLAM is praised for its global consistency but can be computationally demanding, while Fast SLAM is efficient for large-scale environments but may suffer from data association problems. The authors also address challenges in laser-based indoor SLAM algorithms, such as loop closure detection, map optimization, and strategies used by the evaluated algorithms to tackle these challenges. Furthermore, the paper highlights the importance of benchmark datasets and evaluation metrics for fair and standardized comparisons. It provides insights into existing benchmark datasets and suggests metrics for evaluating laser-based Simultaneous Localization and Mapping algorithms. Overall, the paper provides a comprehensive evaluation and comparison of modern laser-based indoor Simultaneous Localization and Mapping algorithms. It highlights the strengths and weaknesses of different approaches and sheds light on the challenges and considerations involved in laser-based SLAM in indoor environments. N. Eid Mohammadi et al. [5] make a Smart Floor Cleaning Robot in which commands are given from the Android device to the robot to clean an area using cleaning arms. The paper provides a comprehensive summary of the design, features, and advancements in smart floor-cleaning robots. It offers insights into the current state of the field, highlights the impact on human lives and the environment, and presents future directions. Zhang Xuexi et al. [6] presented a paper that focuses on utilizing a 2D Lidar sensor for mapping and localization in an indoor environment. Lidar sensors emit laser beams and measure their reflections to generate a 2D point cloud map of the surroundings. Overall, the paper highlights the application of 2D Lidar-based SLAM and path planning for indoor rescue missions using mobile robots. It emphasizes the importance of accurate mapping, localization, and efficient path planning to ensure safe and successful operations in challenging environments.

BACKGROUND

The advent of industrial robots revolutionized manufacturing and automation. These robots were initially large, fixed-position machines designed for repetitive tasks on factory assembly lines. They introduced efficiency, precision, and speed to industrial processes. The emergence of mobile robots expanded the scope of robotic applications beyond fixed positions. Mobile robots could move autonomously, enabling tasks in dynamic environments such as warehouses, hospitals, and outdoor spaces. These robots opened up possibilities for tasks like navigation, exploration, and logistics [7]. Advances in sensor technology played a crucial role in robot development. Sensors like cameras, Lidar, and depth sensors allow robots to perceive and understand their surroundings. This led to capabilities such as object recognition, environment mapping, and obstacle avoidance. Integrating artificial intelligence and machine learning techniques with robots enabled them to perform complex tasks. AI algorithms improved robot decision-making, pattern recognition, and learning from experience. It empowered robots with capabilities like natural language processing, computer vision, and autonomous decision-making [8]. The introduction of ROS revolutionized robot development by providing a flexible and standardized framework. ROS is an open-source platform that offers a collection of tools, libraries, and communication protocols. It simplifies software development, facilitates code reusability, and encourages collaboration among researchers and developers. These revolutions have collectively propelled the field of robotics, expanding

its applications, improving capabilities, and making robots more accessible and adaptable [9].

Robots faced several challenges in their development and operation [10]. Some of the key challenges include:

Lack of Standardization: There was a lack of standardized frameworks and platforms for robot development. Each robot manufacturer often had their own proprietary software and hardware systems, making it challenging for researchers and developers to collaborate, share code, and build upon existing work.

Software Complexity: Developing robot software was complex and time-consuming. The software had to handle various tasks such as perception, planning, control, and communication, requiring expertise in different programming languages and frameworks. Integrating different software components from different vendors was a major challenge.

Limited Code Reusability: Due to the absence of a common framework, code reusability was limited. Developers had to write custom software from scratch for each robot, leading to redundancy and inefficiency. This lack of reusability slowed down the progress in robot development and hindered the exchange of knowledge and best practices.

Scalability and Adaptability: Scaling up robot systems and adapting them to new tasks or environments was difficult. It required significant effort to modify or extend existing software to accommodate changes in robot capabilities or requirements.

Cost and Accessibility: The high cost of robot hardware and software limited the accessibility of robotics technology. This restricted the adoption and experimentation of robots in academic and research institutions, as well as smaller companies or hobbyist communities.

Deepak et al. [11] provide an overview of the kinematic analysis of wheeled mobile robots, focusing on differential drive robots and Ackermann steering robots to tackle these problems. It covers important concepts, equations, and constraints related to the kinematics of these robots, offering insights into their motion and manoeuvrability. Weihao Li et al. [12] give insights into the application of the potential field method for motion planning of omnidirectional wheeled mobile robots. It discusses the kinematics of these robots, potential field generation, obstacle avoidance, path planning, and trajectory generation. The presented results demonstrate the feasibility and effectiveness of the potential field method in enabling efficient and obstacle-free navigation for omnidirectional wheeled mobile robots. Marko Pedan et al. [13] explain the implementation of AGV systems in the healthcare industry. It discusses the benefits, design considerations, navigation and control, and integration with Hospital Information Systems and presents case studies and implementation examples. The paper highlights the potential of AGV systems to transform logistics and material handling processes in healthcare, ultimately leading to improved patient care and operational efficiency. Khasia Vidra et al. [14] provide insights into the positioning and manoeuvrability of omnidirectional robots in the context of robot soccer. It discusses kinematics, positioning techniques, maneuverability strategies, cooperative strategies, and sensor integration and presents simulation and experimental results. The findings presented in the paper contribute to the development of effective control and coordination strategies for omnidirectional robot soccer systems, enhancing their performance and competitiveness in the field. Latif et al. [15] discuss the application of proportional, integral, and derivative control in legged fire-fighting robots aimed to achieve stable and precise movement in challenging environments. By adjusting the leg movements based on proportional, integral, and derivative feedback, the robot can effectively navigate through obstacles and uneven terrains. The proportional, integral, and derivative controller continuously monitors the robot's position and adjusts the leg actions accordingly, enabling enhanced locomotion and maneuverability. This approach enhances the robot's ability to perform firefighting tasks in complex and hazardous scenarios.

METHODOLOGY

The overall design consists of a microcontroller, microprocessor, motor drivers, motors, Lidar sensor, tracking camera, display, and battery, as shown in Fig. 1. The battery provides the required input power to the robot and its controlling peripherals. The Lidar sensor provides a 2D 360° map data to the microprocessor. The

tracking camera gives the odometry data with respect to the surroundings to the microprocessor. This data given by the Lidar sensor and tracking camera is processed by the microprocessor with the help of Simultaneous Localization and Mapping (SLAM) algorithms of ROS. The microprocessor processes the data and converts it into the human unreadable format and also some controlling data used to control the actuators via the microcontroller, which will do cleaning actions. The controlling data, such as directional velocities and other important data, is given to the microcontroller by the microprocessor. The motors are driven with the help of motor drivers, which are controlled by the microcontroller through the PWM technique.

Specifications

The Autonomous Floor Cleaning Robot is a three-wheeled omni drive where each wheel is driven by a DC motor. These motors are controlled by motor drivers through a central control unit which is the microcontroller. Traction wheels provide better friction resulting in rich maneuverability of the robot. The robot gets real-time feedback from the surrounding environment through a tracking camera and Lidar sensors. These sensors are combined with a microprocessor, which analyses the sensor data received and transmits it to the microcontroller, which then sends the signal to the actuators to carry out the appropriate tasks.
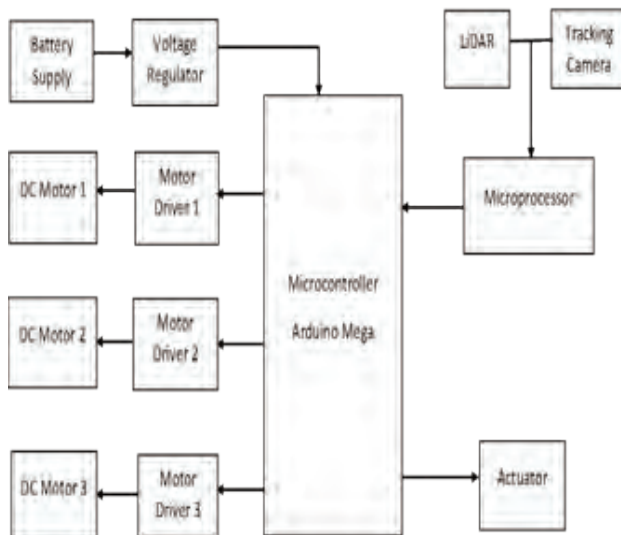
Fig. 1. Block Diagram

Navigation and Mapping

Autonomous floor cleaning robot employs various navigation techniques to move efficiently and map the cleaning area. It uses sensors such as infrared sensors, bump sensors, and floor detection sensors to detect obstacles and prevent collisions. Some advanced robots utilize laser scanners (Lidar) or camera-based vision systems to create a detailed map of the environment.

Localization and Mapping

Laser Range Finders: Advanced floor cleaning robots utilize laser range finders or Lidar (Light Detection and Ranging) sensors to accurately measure distances and create a detailed map of the cleaning area.

SLAM Algorithms: Simultaneous Localization and Mapping (SLAM) algorithms are commonly used to simultaneously construct a map of the environment and estimate the robot's position within that map. SLAM helps the robot navigate and clean efficiently.

Cleaning Mechanism

The cleaning mechanism of an autonomous floor cleaning robot typically consists of brushes, suction, and filters. Brushes, both bristle and rubber, agitate and loosen dirt and debris from the floor. The suction mechanism then draws in the dirt and debris into a dustbin or collection container. Some robots also include high-efficiency filters to capture fine particles and allergens.

Control System

A control system is implemented through a microcontroller which coordinates the operation of the robot's sensors, actuators, and cleaning mechanisms. It integrates the various components and algorithms to execute the cleaning tasks.

SOFTWARE IMPLEMENTATION

Software implementation aims at developing and implementing the software that controls all hardware components of the robot. This includes managing the behaviour of the electronic components and responding to user input.

Simulation using ROS and GAZEBO Software

Steps involved in simulation using Gazebo Software:

- Creating of Robot Operating System Package: ROS is a directory that stores various files and plug-ins related to robot controllability. This package helps in the smooth operation of Gazebo software with changes in the functional testing environment.

- Development of Robot: After creating the ROS package, the robot is to be designed and built. For designing a robot, Universal Robot Description Format (URDF) is used. It develops physical operative and visual features in Gazebo. URDF can be made by converting the CAD model or by creating each component manually.

- Tele-operating of the Robot: It refers to controlling a robot using devices like a laptop, mobile, joystick, etc. For this, the teleop_twist_keyboard ros package needs to be launched, which runs a Python script. This script publishes the speed of the robot and the gradability of motion to cmd_vel ros topic in the Gazebo environment.

- Developing a map of the run-time environment: For developing the map, Google Cartographer is required, which has its own official package. The map can be easily visualized by using RViz, and its information can be easily retrieved using ROS topics and services. To save the map for further usage, the ROS map server package is used. Pair of all files is saved using map_name.pgm

Simulation Results from Gazebo Software

Fig. 2 shows the two-wheeled robot in the 3D world simulated on Gazebo. The path may be generated by a motion planner or a control algorithm that calculates the robot's movement based on the sensor data and other inputs. It also provides visual feedback about the distance, shape, or orientation of the objects in the environment, helping the robot navigate and avoid obstacles.
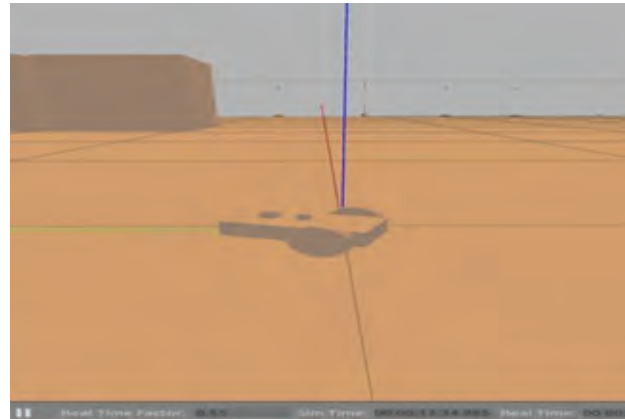
Fig. 2. Virtual Environment

Simulation of DC Motor in Matlab Simulink:

In this simulation of a DC motor (RS775), a mathematical model of the electromechanical machine is designed and simulated by creating a virtual environment using Gazebo software.

The simulation model built contains basic parameters of the RS 775 DC motor like:

Ra = Armature Resistance = 8.5Ω;

La = Armature Inductance = 1.2 H; Va = Armature Voltage = 18 V;

Kt = Torque constant = 2.086;

B = Frictional coefficient of motor and load = 0.006;

Kb = Back emf constant = 0.6; J = Moment of Inertia of motor Load = 15 kgm^2/rad

The transfer function equation for the DC motor is as follows:

$$TF = \left(\frac{Kt}{J*La}\right) * \cfrac{1}{\left(s\left(s^2 + \left(\left(\frac{(J*Ra)+(B*La)}{J*La}\right)*s\right) + \left(\frac{(Ra*B)+(Kb*Kt)}{J*La}\right)\right)\right)}$$

Fig..3, as displayed below, shows the Simulink model of the RS 775 DC motor. Armature voltage is the starting block mentioned at the very left in the diagram.

Using a sum block, it is subtracted from the back emf of the DC motor. The difference between these voltages is then multiplied by a continuous transfer function block

provided with initial states to get output as armature current. The armature current block is multiplied by a gain multiplier block to get developed motor torque as output and is shown in Fig. 4.
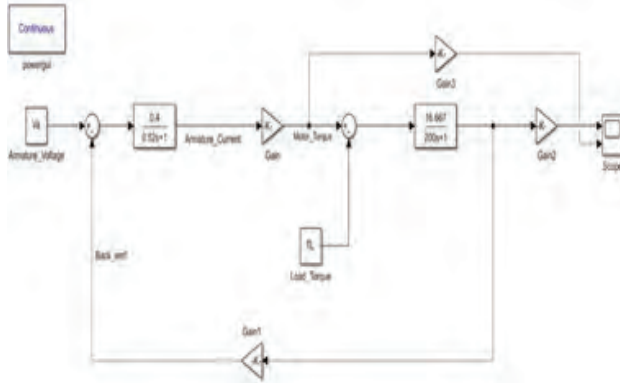
Fig. 3. Simulink Model

This torque value is then subtracted from the load torque by assigning a separate block to it as done previously. By multiplying this torque difference by the transfer function using the gain block, the speed of speed with respect to time and is shown through the scope block. Thus, by following the interconnectivity made, output graphs of torque and speed of motor for respective weight load are generated.

By performing a simulation of the DC motor in MATLAB, it is verified that the calculated torque and speed values for maneuvering omni wheels are being satisfied under peak conditions by the selected DC motor.

MANUFACTURING AND TESTING

Manufacturing of the prototype starts with the development of chassis and omni-wheel drive assembly, followed by manufacturing of the pneumatic forklift mechanism and integration of electronic subcomponents.

The robot chassis is an integral component for maintaining a proper weight distribution in the dynamic functioning of the robot. The chassis for the three-wheel omni-drive system has a triangular configuration in accordance with corresponding omni-wheel positions by considering in importance of topple, maximum speed achieved, overall weight, and stability during travel, as shown in Fig. 4.

Testing of Chassis

The on-field testing of the three-wheel omni-drive chassis integrated with electronics assembly was carried out with variations in path trajectories that were to be traced by the robot. Fig. 5 shows the arrangement of electronic components on the chassis. The linear path was tested first by giving inputs to the endpoints of the path and then reversing the wheel rotations at the same location to follow the same path again. Then a closed square loop and an uphill with a gradient of 20° was planned for testing in which the path was traced successfully by the robot. Fig. 6 and 7 display the testing of the designed bot for uphill climbing and plane surface, respectively.

Inverse Kinematics Testing

Inverse Kinematics was used to test whether the velocities required and those obtained from the mathematical modelling of DC motor are obtained in physical on-field testing or not.
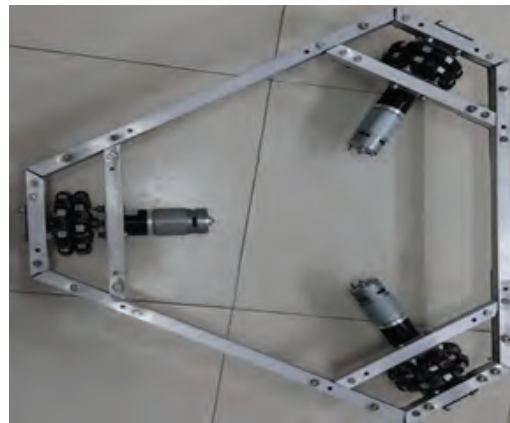
Fig. 4. Robot Chassis

Fig. 5. Electronics Assembly
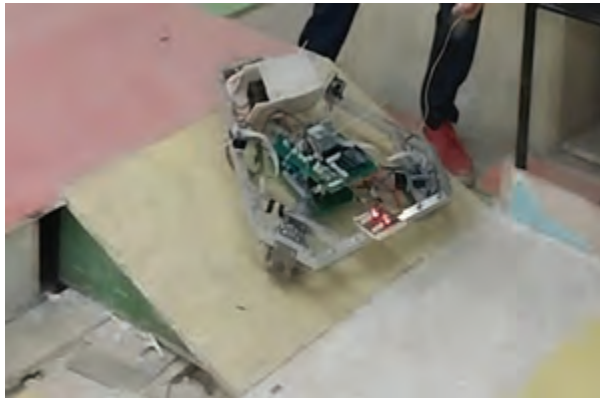
Fig. 6. Uphill Climbing Test
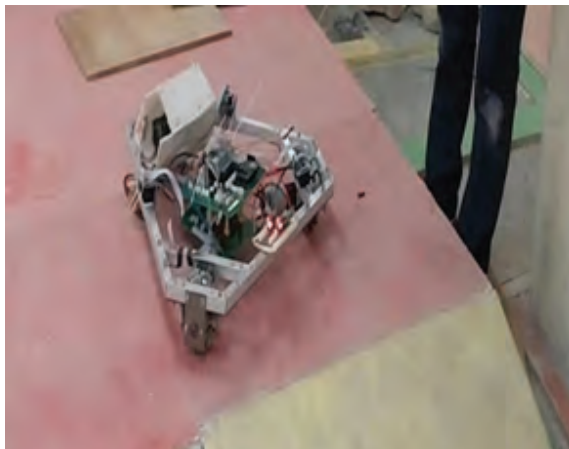
Fig.7. Plane Surface Test

Basically, inverse kinematics is used for measuring wheel angular velocity and to determine the DC motor speed required by using the equations of x and y axes displacements of the omni wheels varying with respect to the angles with respective orthogonal omni wheel axes. Velocity is obtained by dividing these equations with respect to time. From manual calculations, the maximum velocity targeted for the robot is decided not to exceed 2.4 m/s.

In on-field testing, PWM pins input was varied as per requirements of velocity, and the velocity range obtained was as mentioned in Table No. 1 under peak supply conditions from the DC motor. From the testing of inverse kinematics, it is concluded that the average velocity value obtained was around 1.4 m/s, and the maximum value obtained was 1.68 m/s which is less than the estimated and obtained value from the simulation.

Thus, it is ensured that the robot is capable of producing the required velocity value for its motion.

Table. 1 Inverse Kinematics testing results of Chassis

Sr. No.	PWM Input	Time taken (s)	Velocity (m/s)
1	255	1.6	1.680
2	240	1.74	1.520
3	220	1.80	1.377
4	200	1.88	1.116
5	180	2.30	1.025
6	160	2.45	0.987
7	140	2.505	0.957
8	120	2.605	0.925
9	100	2.755	0.881

RESULTS AND DISCUSSION

From the mathematical modeling of the DC motor, as stated in the design phase, the graphs of omni wheel speed in rad/s and torque variation with time are obtained as per the variation in load input of the other loads over the mechanism. The transfer function of the DC motor with the motor parameters is developed as stated.

When load = 6 kg (Full torque conditions are to be obtained), the results are obtained for the first 10 seconds as follows:

The maximum robot velocity for omni wheels is not to be exceeded 2 m/s which can cause toppling and dynamic instability of the Automated Guided Vehicle. This is ensured and verified from Fig. 8, in which the maximum velocity obtained is 1.7 m/s at the 10th second, and torque does not exceed 40 Kg- cm as shown in Fig. 9; which is the limiting value of torque for the RS775 DC motor. Thus, the motor used is capable of lifting and transmitting loads for its maximum capacity.
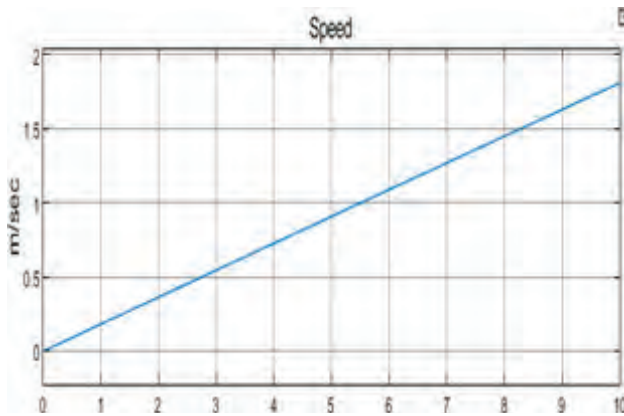
Fig. 8. Speed Vs time (Max. Load Condition)
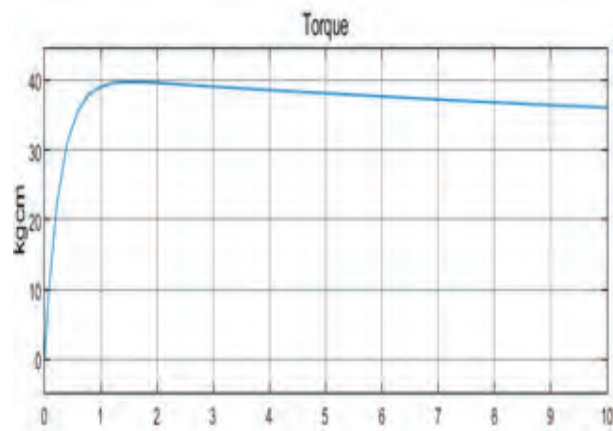
Fig. 9. Torque vs time (Max. Load Condition)

Iterations are also performed to check the values of torque and speed required for each omni wheel if the weight is of intermediate value, 3 Kg. For 3 Kg weight, the results obtained are as shown in Fig. 10 and Fig. 11.
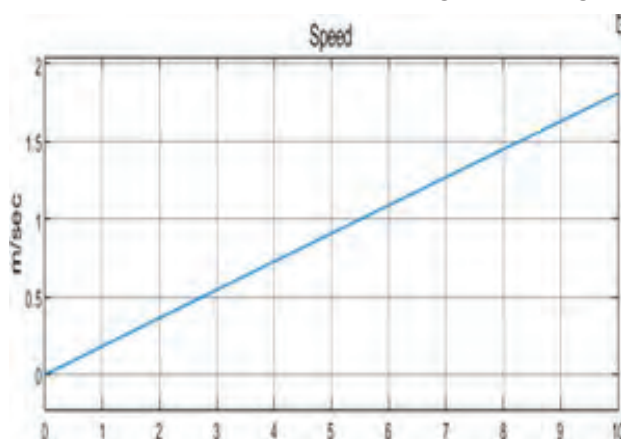
Fig. 10. Speed Vs time (Intermediate Load Condition)
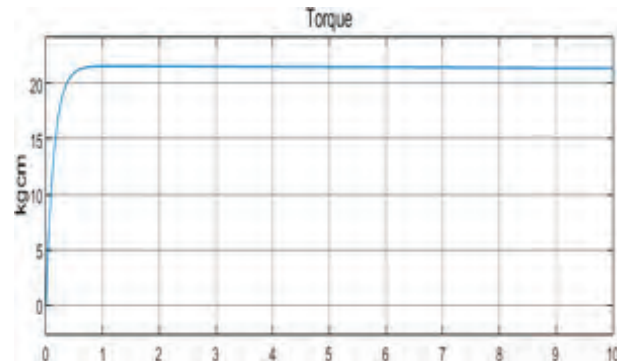
Fig. 11. Torque vs time (Intermediate Load Condition)

From these graphical results, it can be concluded that the maximum torque required for carrying 3 kg weight is around 22 kg-cm, and the selected motor is able to perform the transportation with a desirable velocity limit of 1.7 m/s.

Hence the AI-Powered Floor Cleaning Robots is capable of working without human intervention due to Navigational Intelligence.

CONCLUSION

In this paper, design and implementation of AI Powered Autonomous Floor Cleaning Robot is explored. The bot is implemented using advance sensing technologies to ensure safe navigation.

From the simulation and demonstration, it is clear that the designed bot is able to carry out the tasks of cleaning without human interference. The kinematics testing results indicates the efficiency of developed bot at full load is also very good. Hence, this AI powered Autonomous Floor Cleaning Robot proves to be working efficiently, cost-effective, and with low power features. This will effectively cut down the extra labour used in the industries for cleaning purposes and also helpful for cleaning of hazardous places through remote operation.

REFERENCES

1. M. -c. Kang, K. -s. Kim, D. -k. Noh, J. -w. Han and S. -j. Ko, "A robust obstacle detection method for robotic vacuum cleaners," in IEEE Transactions on Consumer Electronics, vol. 60, no. 4, pp. 587-595, Nov. 2014, doi: 10.1109/TCE.2014.7027291.

2. Manreet Kaur, Preeti Abrol "Design and Development of Floor Cleaner Robot (Automatic and Manual)

"International Journal of Computer Applications (0975 – 8887) Volume 97– No.19, July 2014.

3. Humayun Rashid, Akash Mahmood, S.M. Sarjahan Shekha, Taslim Reza, Md Rasheduzzaman, "Design of an Autonomous Mobile Robot Based on ROS" (2017).

4. Kirill KrinKin, Artyom Filatov, Artur Huletski, Dmitriy Kartashov," Evaluation of Modern Laser Based Indoor SLAM Algorithms," May 2018.

5. N. Eid Mohammadi, "Smart Floor Cleaning Robot", July 2018.

6. Zhang Xuexi, Lu Guokun, Fu Genping, Xu Dongliang, Liang Shiliu, 2D Lidar Based SLAM and Path Planning for Indoor Rescue Using Mobile Robots, July 2019.

7. Mohd Javaid, Abid Haleem, Ravi Pratap Singh, Rajiv Suman, Substantial capabilities of robotics in enhancing industry 4.0 implementation, Cognitive Robotics, Volume 1, 2021, Pages 58-75

8. Zabalza, J.; Fei, Z.; Wong, C.; Yan, Y.; Mineo, C.; Yang, E.; Rodden, T.; Mehnen, J.; Pham, Q.-C.; Ren, J. Smart Sensing and Adaptive Reasoning for Enabling Industrial Robots with Interactive Human-Robot Capabilities in Dynamic Environments—A Case Study. Sensors 2019, 19, 1354.

9. Li J, Esteban-Fernández de Ávila B, Gao W, Zhang L, Wang J. Micro/Nanorobots for Biomedicine: Delivery, Surgery, Sensing, and Detoxification. Sci Robot. 2017 Mar 15;2(4): eaam6431.

10. Kiru, Muhammad. (2016). A Critical Review of the Challenges, Threats, and Drawbacks of Humanoid and Autonomous Robots. IRA-International Journal of Technology & Engineering. 04. 135-150.

11. Deepak, B. B. V. L., and Dayal R. Parhi. "Kinematic analysis of wheeled mobile robot." Automation & Systems Engineering (2011).

12. Motion Planning for Omnidirectional Wheeled Mobile Robot by Potential Field Method, 2017, Weihao Li, Chenguang Yang,1,2 Yiming Jiang,1Xiaofeng Liu,3,4,5 and Chun-Yi Su1.

13. Marko Pedan, Milan Gregor, Dariusz Plinta, Implementation of Automated Guided Vehicle System in Healthcare Facility, Procedia Engineering, Volume 192, 2017, Pages 665-670

14. Utama, Khasia & Fatekha, Rifqi & Prayoga, Senanjung & Pamungkas, Daniel & Hudhajanto, Rizky. (2018). Positioning and Maneuver of an Omnidirectional Robot Soccer. 1-5. 10.1109/INCAE.2018.8579148.

15. A. Latif, K. Shankar, and P. T. Nguyen, "Legged Fire Fighter Robot Movement Using PID," J. Robot. Control, vol. 1, no. 1, pp. 15–18, 2020, doi: 10.18196/jrc.1104.

Design Approaches for Real-Time Tracking System for Under-Cast Mines

Jitesh Shinde
Electronics Engg. Dept. (VLSI Design & Technology)
CSMSS Chh. Shahu College of Engineering
Chh. Sambhajinagar, Maharashtra
✉ jiteshshinde2020@gmail.com

Raj Vardhan
JDMTECH Semiconductors Pvt. Ltd.
Nagpur, Maharashtra
✉ rajvardhansingh@gmail.com

Shilpa Shinde
Researcher
Nagpur, Maharashtra
✉ soniyaky@gamil.com

ABSTRACT

Mining in India is fraught with danger", By Orchie Bandyopadhyay, 07 September 2021.

One of the major concerns in the mines is to keep track of the workers & and their locations to ease rescue operations in case of emergency.

Various communication techniques, tracking technologies, and the key design attributes for real-time tracking of miners, vehicles, and other mining assets in an underground mine have been reviewed in this paper. The work herein is focused on suggesting a robust integrated real-time tracking system with optimum accuracy for a mission-critical strategy that should ensure the survivability of the tracking system after an accident.

The combination of Chirp technology and Ultra-Wideband Band (UWB) and other technologies considerations trade-offs depending on the requirement has been suggested as a solution to achieve optimum accuracy in comparison to existing technology for Real-Time Tracking System (RTTS) in underground mines.

KEYWORDS : Real Time Tracking System (RTTS, Chirp Technology), Real-Time Location System (RTLS), Ultra-Wideband technology (UWB), RFID, Underground Communication Technologies, Through the Earth (TTE), Through the Wire (TTW), Through the Air (TTA), Received Signal Strength Indication (RSSI), Bluetooth Low Energy (BLE).

INTRODUCTION

The mining sector is a vital component of India's economy, with coal and other minerals playing a significant role in the country's energy needs. As the nation strives to reduce its dependence on imported resources, innovative solutions are crucial to optimize domestic mining operations. Mining in India is fraught with danger. According to the British Safety Council, India has one of the highest rates of mining fatalities in the world [16]. According to government data, Reuters reported, one coal miner died on the job every 12 days on average in 2020 [15].

The mining industry is under pressure from fluctuating mineral prices and worries about the environment and the safety of its workers [8,18].

Manual tracking is a common practice in mines to keep track of miners in underground mines. It gives information about the miners working in underground or open-cast mines and their general location. The mine foreman gives the dispatcher a list of names and locations within the mine at the beginning of each shift in manual tracking. Once inside the mine, a miner uses the dial phone there to call the dispatcher and let them know he needs to go to a different area to work.

The dispatcher then updates the map with the miners' present locations.

There are many drawbacks to manual tracking. It may be tough to determine a miner's precise location because the mining region in which they are present can be large. Sometimes, a mine worker will fail to inform the dispatcher when switching work locations.

This creates a necessity to have an electronic tracking system in the mine to provide a mechanism to mitigate the drawback of manual tracking. An electronic tracking system will provide a mechanism for the surface personnel to know the location of workers and assets in the mine. Nowadays, this electronic tracking system is known as location technology.

In the mining industry especially underground mines, where efficiency, sustainability, and safety are all prime concerns, location technology is crucial for modernization and digitization. The location technology can be used for tracking mining assets, personnel, and supplies in open cast & more specifically in underground mines. This will boost productivity, reduce the risks to operating machinery and, at the same time, ensure greater job satisfaction by optimizing employee utilization while saving time and costs.

The work in this paper is focused on suggesting the best location technologies for under-cast mines. The following sections cover the basic workings of the Real Time Location System (RTLS), components of RTLS, functional description of RTTS, Underground Communication

Techniques for RTTS, RTTS Technologies, Comparison Attributes of RF Technology Used in RTTS, Applications of RTLS in mines, and some major considerations to develop an effective RTTS for mines, especially underground mines.

BASIC WORKING OF REAL-TIME LOCATION SYSTEM (RTLS)

The Real Time Tracking System (RTTS) or RTLS is an integrated system for real-time tracking of moving objects in underground and open-cast mines.

Anchors, tags or other transmitting devices, and a location engine are the fundamental elements of all RTTS implementations. In addition to these core components, there are additional modular RTLS components that may be incorporated into IoT devices

and applications to enable customized RTLS-enabled devices and solutions that cater to the needs of specific use cases and end-user requirements.

The transmitting gadget, such as an RF tracking tag, will continuously broadcast data-encoded RF emissions, or locations. The signals from the transmitting device will be received and read by RTLS receivers (anchors or readers) deployed in fixed sites, such as mounted on walls, and within the communication range. The location data, together with any accompanying IoT data (temperature, battery, etc.) that the anchors receive, is then sent to location engine software to determine the position of the device on a 3D map & and display it on a monitor with the appropriate symbol in real- time.

The method utilized to determine position can vary between RTLS technologies. Some use distance-based computations, such as time difference of arrival, which, among other locating techniques, tends to produce more accurate findings than Received Signal Strength Indication (RSSI).

FUNCTIONAL DESCRIPTIONS OF RTTS

The general representation of the RTTS system is shown in Figure 3.1. The RTTS system in general includes these systems:

Control Room or Mine Operation Centre (MOC)

It accounts for the design for real-time management and monitoring of the mine, including miners' and machines' tracking and voice communication with drivers and miners.

The server computer is in the control room and operates the RTTS system program and other programs to control, test, and set up the system. In the control room are also located the communication devices (LAN switch, router, fiber optic switch, etc.). The real-time information is displayed on a big monitor. There you can see the mine map in 3D format with the graphic symbols for miners and machines and their placement in the mine. The design of the control room must be accomplished according to the safety and ergonomics rules.

Base Stations

The base stations define the locations of the miners and the machines in the mine. The quantity of the base stations in the mine is defined by the path in the mine that needs automatic tracing for miners and machines,

the profile of the mine, the number of turns, the number of crossroads, and other parameters like tunnel width.

The maximum distance between base stations must not be more than the range specified by tracking technology. The distance will depend on the turn radius and the tunnel width. Line of Sight between base stations must be clear.

Anchors or base stations must be mounted out of the way of moving equipment to protect them from damage. At the same time, they must be able to "see" the tags to operate correctly i.e., the line of sight of the reader to tag must be clear.

The base stations are organized into certain groups. Every group is connected with a transmission media like twisted cable or optical fiber cable to the router in the control room.

Inside the group, base stations are connected with LAN and alternative arrangements like Wi-Fi. If the LAN connections between two neighbouring RTTS Base Points are cut, the system should automatically switch the connection between the two base points to an alternative arrangement.

People, assets, equipment, inventories, and mobile items can all have RTLS tags attached to them to help locate them. RTLS tags continuously transmit data-encoded signals to RTLS readers, who pass this data on to the location engine to ascertain the tag's position. The tags must have a provision to alert the user or Mine Operation center (MOC or Location engine or control room) of a malfunction.
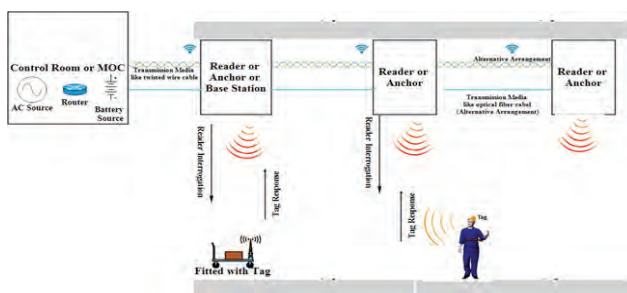
Fig 1: Generalize Representation of RTTS System

The tag is connected to the anchor module of the RTTS Base Points, with special modulation for defining the coordinates in the mine. The personal tag can receive an alarm with a flashing light, ringer, or vibration signal. Vehicles or machines have a tag mounted in the vehicle cabin and an antenna mounted outside. During the movement of the machine, the tag connects to the anchor modules of the RTTS base points. The RTTS system calculates the current position of the machine in the mine. The system displays the current position of the machine on the monitor's 3D map.

Power System

The RTTS system operates on mine AC power under normal conditions. They could use battery backup power in an emergency. The RTTS system switches over to operating on batteries when there is a brief power outage at the mine. The RTTS system works on batteries for up to a few hours. The frequency of the reads affects the power requirements of the system and the life of the battery.

The calculation of the power system in general are based on maximum power consumption by the RTTS base point, the quantity of RTTS base points in the mine, maximum length of the mine, working voltage of the power line, permissible power loss on power line and power cable type. The final maximum power consumption value computed based on these parameters be increased by 20 percent.

In addition to this, RTTS can have integrated voice communication, text message support, and video systems. The miner can communicate with other miners or to group of miners. The text message can be sent by a dispatcher to a moving object (truck, loader, or miner) if an object has extended TAG (with LCD).

UNDERGROUND COMMUNICATION TECHNIQUES FOR

RTTS

The four main categories of underground communication methods are Through the Earth (TTE), Through the Wire (TTW), Through the Air (TTA), and Hybrid Systems [2,8,7]. TTE: Since the attenuation of electromagnetic signals declines with frequency, very low frequencies are used to extend the range. A very large transmitting loop antenna used for TTE is controlled from the mine's surface. Due to the extremely low data rates and low-frequency operation, communication is only possible through text messages.

TTW: Permanent infrastructure at TTW makes long-distance communication a regular element of the mine's operations. While the TTW communication system functions brilliantly in a routine mining operation, it is very vulnerable to damage and could fail completely in situations like roof falls, fires, mine collapses, and other similar occurrences. Hoist rope, paging, magneto, dial-and-page, and sound-powered phones are examples of TTW techniques.

TTA: TTA transmits signals using a wireless link. Coal miners and metal mines both present extremely difficult conditions for wireless communication. This is due to the unique signal propagation properties (like extreme path loss, reflection or refraction, multipath fading, propagation velocity of an underground mine, waveguide effect, and noise [2] which have an impact on the effectiveness of communication equipment. The TTA categories include wireless networks, Wi-Fi, walkie-talkies, and ultra-wideband (UWB) communications.

Hybrid System: The benefits of both through-the-wire (TTW) and through-the-air (TTA) communication technologies are included in the hybrid system. As a result, communication systems for underground mines have a greater coverage area. Hybrid systems offer voice and video communication in deep mines because of their fast data rates.

RTTS Technologies

The positioning methods and underlying RF technologies that each system employs have a significant impact on the accuracy of real-time location systems. There

are several forms of RF technologies used for Real-Time Location System (RTLS) or Real Time Tracking System (RTTS) like Wi-Fi, Bluetooth Low Energy (BLE), Ultrawide Band (UWB), and Compressed High-Intensity Radar Pulse (Chirp), LoRa (Long Range). The RF technology comparison of commonly used technology in RTTS in mines is shown in Table 4.1 [1, 10, 11,12].

UWB: UWB is a state-of-the-art RF technology that provides the exact location with positional accuracy of UWB-tagged items down to the centimetre level. It can real-time identify precise locations while transmitting very high data rates over small distances. It also uses relatively little power, making it possible to use hardware that is both economical and effective, such as tracking tags that use coin cell batteries and can last for many years before needing to be recharged or replaced. Due to its distance-based measuring, which determines location based on how long it takes for radio pulses to travel from one device to another, UWB positioning is incredibly accurate. UWB is immune to interference from other radio signals, making it a good choice for undercast mines [9,14].

Chirp Spread Spectrum: Chirp Spread Spectrum is a radio frequency (RF) signal that varies in frequency over time, making it a helpful tool for determining the location or distance of individuals and things over considerable distances. It is based on a very low frequency (VLF) tracking technique. Undercast mines can benefit from VLF waves since they can pass through rock and dirt. [14].

Table 1: RF Technology Comparison used in RTTS

RF Technology	Object Identification Accuracy	Range	Latency in second (s or millisecond ms)	Protection against Interference	Power Consumption	Frequencies	Cost in Rupees
Chirp	1-2 m*	10-500 m* (up to 1000 m)	< 1 ms to get the location	Strong	Low	2.4 GHz (2.4-2.4835)	₹
UWB	10-50 cm*	0-50 m* (up to 200 m)	< 1 ms to get the location	Strong	High	3.1 – 10.6 GHz	₹ ₹

BLE	< 5 m*	0-25 m* (up to 100 m)	Typically, 3-5 s to get location	Weak	Moderate	2.4 GHz	₹ ₹
Wi-Fi	< 10 m*	0-50 m* (up to 500 m)	Typically, 3-5 s to get location	Weak	Wi-Fi	2.4GHz, 5 GHz	₹ ₹ ₹ (₹ with Wi-Fi access points)
RFID	< 150 m (active) <15 m (passive)	150 m	In ms (>1ms)	Weak	Very Low	433 MHz (Active tags) 860-960 MHz (passive tags)	₹ ₹
LoRaWAN (Long Range Wide Area Network)	Typical range error of around 10%	Upto 2 km	Typically around 100 ms	Moderate	Very Low	868 MHz, 915 MHz, 433 MHz	₹

*With optimal conditions and deployment, ISM: Industrial, Scientific & Medical radio band

Bluetooth Low Energy (BLE): BLE is radio frequency technology for wireless communication that can be used to locate people, objects, and assets inside buildings and follow their movements. BLE was developed primarily to use extremely little power.

Wi-Fi: It is RF technology often used in situations where a high degree of accuracy isn't needed. Various types of interference affect WLANs (Wireless Local Area Networks) as they move from the source to the destination [5, 12].

RFID: RFID technology can be divided into passive RFID (reverse RFID) and active RFID. Using battery-free tags, passive RFID relies on signals from RFID readers to power the tag if it is within communication range. This allows one to establish the tag's location, albeit passive RFID normally only provides short-range placement owing to interference from physical impediments. Passive RFID is a low-cost alternative appropriate for deployments where only identification is needed.

Active RFID consists of tags with built-in batteries and receivers that function similarly to passive RFID. They often cost more than their counterparts but have a greater range. Like passive RFID, they are also susceptible to disruption from physical obstacles.

LoRaWAN: LoRaWAN is a low-power, wide-area networking (LPWAN) protocol. LoRaWAN signals can penetrate through rock and other obstacles, making it possible to connect devices in deep underground mines. LoRaWAN signals can travel long distances, even in challenging environments, which is essential for covering large mining areas. LoRaWAN devices can operate on batteries for years, which is important for reducing maintenance costs in underground mines. LoRaWAN networks can support a large number of devices, which is necessary for monitoring and controlling a wide range of equipment and sensors in a mine.

COMPARISON ATTRIBUTES OF RF TECHNOLOGY USED IN RTTS

Some of the key attributes to be considered in the design of RTTS and gaps identified in the RTTS system available for mines in India are discussed below.

Accuracy

Accuracy of an RTTS system in underground mines = (Number of correct detections / Total number of detections) * 100%

The accuracy of RTTS systems in India can be variable, depending on the technology that is used and factors like multipath propagation, signal reflections, placement of tags, strength of signal, etc. For example,

RFID-based RTTS systems are typically less accurate than UWB-based RTTS systems. This can be a problem in underground mines, where it is important to track miners and equipment with a high degree of accuracy.

A standard like UWB can provide high location accuracy between 10 and 50 cm for applications that demand a high level of precision through time-of-arrival-based position estimates.

Other methods, including chirp (CSS), which similarly use distance-based position calculations, can achieve high accuracy between one and two meters. In contrast to other technologies, which are more susceptible to these effects and produce inferior positioning results, UWB and chirp also effectively resist RF interference to assist in ensuring accurate results. The accuracy of results between 1 and 10 meters is typically worse with other conventional positioning technologies like Wi-Fi and Bluetooth. This is because the majority of Wi-Fi and Bluetooth applications use multi- lateration based on the Received Signal Strength Indicator (RSSI), which is less accurate than other technologies like UWB. Precision isn't necessary for some situations; meter- level accuracy will do.

The accuracy level required for RTTS depends on the individual customer's needs or where it is being used.

Range

Range of an RTTS system in underground mines = (Transmitter power * Antenna gain * Receiver gain) / (Noise power * Path loss)

Where

Transmitter power is the power output of the RTTS transmitter in watts Antenna gain is the gain of the RTTS antenna in decibels (dB)

Receiver gain is the gain of the RTTS receiver in decibels (dB)

Noise power is the power of the noise in the RTTS system in watts

Path loss is the loss of signal strength due to the propagation of the signal through the underground environment in decibels (dB)

Range refers to the distance between the tag and the reader or anchor (a large distance may result in weak signal interpret). The mine shape and physical locations of the readers and tags will determine the nominal tag/

reader detection range. Having metal objects around may reflect incident RF signals, confusing the reader or the tag. Multiple tags close together are present (Multiple tags on a group of miners could be perplexing to the reader due to many superimposed signals) [1,2,4].

The range of RTTS systems in India can also be limited, depending on the technology that is used and factors like the presence of obstructions, characteristics of rock formation, signal attenuation, and interference. For example, Wi-Fi or RFID-based RTTS systems typically have a shorter range than UWB-based RTTS systems. This can be a problem in large mines, where it is important to track miners and equipment over a wide area.

Multiple tags close together are present (Multiple tags on a group of miners could be perplexing to the reader due to many superimposed signals)

The Real-time location systems come in a wide variety, depending on the underlying RF technology and deployment style. In this aspect, Chirp excels because it enables long- range applications, necessitating fewer anchors, and operates both indoors and outdoors without the need for a spectrum license.

Installation complexity: It is based on the number of fixed components and the difficulty of installation.

Expandability: Support for expansion of the system as mine coverage area increases.

Network Operations: The tags use a reader to connect to the network, transmitting their RF signal across the air. The information is delivered to the MOC via the reader. The reader data can be sent to the MOC in several different ways. Selection of proper network topology like ring configuration or tree topology or linear topology or daisy chain will influence the performance of tracking system.

Operating Frequency: The choice of operating frequency for TTA and the propagation of signals are influenced by factors such as the uneven construction of mines, the geometry of tunnels, and underground mining infrastructure. Various communication frequencies have different constraints and applications for underground mines [2,4]. A longer coverage range is provided by UHF (300– 3000 MHz) in a straight, smooth, and obstruction-free tunnel. However, a better coverage area can be achieved at a frequency between MF (300–3000 kHz) and VHF (30–300 MHz), where

roughness, crosscuts, and corners are considered for communication systems.

MEASURE OF QUALITY OF SYSTEM

i. **Survivability:** The capacity of a system to continue operating in the face of a disaster is known as survivability. Although it's not necessary for the system to function exactly as it did before the accident, it must nonetheless deliver basic services in accordance with the criteria.

ii. **Reliability:** The reliability of RTTS systems in India can also be a concern, as the systems can be affected by factors such as dust, moisture, and electromagnetic interference. This can be a problem in mines where there are harsh environmental conditions. It is shown as a probability or as a percentage. Examples of reliability objectives include:

a. A system's capacity to carry out its designated functions

b. A system's capacity for faultless operation.

c. A system's ability to function properly without repairs or maintenance

iii. **Availability:** It refers to the length of time a system is working and able to offer its services. The duration of a system's repair is also considered because it is presumed that the system would be inaccessible during that time.

iv. **Cost:** The cost of RTTS systems in India can be high, which can make them unaffordable for some mines. This is a significant barrier to adoption, as RTTS can provide several benefits to mines.

APPLICATIONS OF RTLS IN MINES

i. Asset tracking

ii. Miner's tracking

iii. Miner Safety & Collision Avoidance

iv. Workflow optimization

v. Inspection & Maintenance tracking

CONCLUSION

The speed at which the market accepts technology and the zeal with which its promoters market their products determine whether a technology is successful or not. There are so many new technologies being introduced

every day that it is not enough to create one that will last for a very long time or perhaps change the world.

For RTLS in underground mines, here are some general recommendations:

i. High accuracy: If precise location tracking is essential, consider UWB or RFID. However, be aware of their shorter range and higher cost.

ii. Long range: If covering large areas is crucial, LoRaWAN or Wi-Fi might be better options. LoRaWAN offers lower power consumption and potentially wider coverage.

iii. Low power consumption: For battery-powered devices, LoRaWAN, RFID, and BLE are good choices. LoRaWAN offers the longest range among these options.

iv. Cost-effectiveness: BLE and RFID are generally more affordable, while UWB and LoRaWAN can be more expensive. Consider the trade-off between cost and required features.

Ease of deployment: Wi-Fi and RFID are relatively easy to set up, while LoRaWAN and UWB might require more specialized knowledge.

A deep study of conditions prevailing in the environment of under-cast mines suggested that underground communication and tracking techniques should meet more or less the following requirements: being able to operate over long ranges with good accuracy in tracking, protection against RF interference, lowest cost, meeting regulatory compliance of mines, collision avoidance, and miner safety [2,3,4,7,6,14, 17, 18, 19, 20, 21, 22, 23, 24].

The study gave the following solutions:

A hybrid system is the best solution for underground communications. Example: Combination of Wi-Fi (WLAN, Wireless Local Area Network), BLE, and Ethernet LAN.

UWB and Chirp tracking technologies were found to be the better tracking technologies.

UWB and Chirp in combination were found to be the best solutions for tracking technologies in under-cast mines.

Benefits of combining UWB and Chirp in RTTS: In the event of a mishap, such as a fire or a collapse, a location engine or MOC, along with the reader, may decide to use chirp to determine the general direction and position of the miner, as UWB may not even be able to reach the search target. After that, focus on using UWB to obtain the location within a few meters of a person. This has all-in-one outdoor functionality, extended range, centimeter accuracy, and high reliability.

The comparison of the nanoANQ Chirp RTLS anchor, nanoANQ UWB RTLS anchor, and Decawave RTLS anchor along with FPGA is illustrated in Table 8.1.

After rigorous studies and surveys, it is found that the combination of nanoANQ Chirp RTLS anchor or nanoANQ UWB RTLS anchor or Decawave's UWB RTLS anchor along with an FPGA (Field Programmable Gate Array) and Arm Cortex microcontroller in building an integrated RTTS system may achieve less than one-meter accuracy or precision of locating a mining device or miner in underground mines.

The combination of a nanoANQ Chirp RTLS anchor (or nanoANQ UWB RTLS anchor or Decawave's UWB RTLS anchor) along with an FPGA and ARM processor can be a powerful solution for RTLS applications that require high accuracy, customization, and scalability.

The FPGA allows you to add custom features and functionality to the anchor, such as support for new protocols or algorithms. The ARM processor provides the processing power to run these custom features and to communicate with the anchor's sensors and other devices.

After surveying the market and literature, it was also found that the availability of equipment and software required for the design of the RTTS system based on Chirp or UWB technologies from the vendor is a time-consuming process because of the ongoing geopolitical tensions in the world. It may take a minimum 8 to 15-month time span to procure the equipment required. So, the RTTS system based on LoraWAN technology has also been considered as an alternative approach for the design of the RTTS review [25, 26,27, 28].

The next step of this work is to develop an integrated prototype RTTS for mines having optimum accuracy, range, and better survivability and reliability with the approaches suggested in this paper.

Table 2: Comparison of RTLS anchor

Feature	the nanoANQ Chirp RTLS anchor	nanoANQ UWB RTLS anchor	Decawave RTLS anchor along with FPGA	LoRa Anchor
Accuracy	Up to 500 meters	Up to 100 meters	Up to 100 meters	10 to 5 meters
Range	Indoor & Outdoor	Indoor & Outdoor	Indoor & Outdoor	Upto 2 km
Durability	Industrial grade	Industrial grade	Industrial grade	Industrial grade
Cost	$$	$$	$$$	$
Customization	Limited	Limited	High	Limited

REFERENCES

1. "Advanced Tutorial on Wireless Communication & Electronic Tracking System Performance", National Institute for Occupational Safety and Health (NIOSH), (May 2019).https://www.cdc.gov/niosh/mining/content/emergencymanage mentandresponse/commtracking/advcommtrackingtutorial3.html

2. Ranjan, A. and Sahu, H.B. (2014). "Communication Challenges in Underground Mines", Search & Research, Vol. No. (2), pp. 23-29, 2014

3. L. K. Bandyopadhyay, S.K Chaulya, and P.K Mishra (2010). "Wireless Communication in Underground Mines, RFID Based Sensor Networking", Springer Publications, New York.

4. Misra, Salil Kanhere, Diethelm Ostry, and Sanjay Jha (2010). "Safety Assurance and Rescue Communication Systems in High-Stress Environments: A Mining Case Study,Topics in Design& Implementation", IEEE Communications Magazine, pp. 66-73.

5. Texas Instrument (December 2018). "Simplified Asset Tracking Management with Wi-Fi", Application report SWRA628.

6. B.Besa, S Mulega and C Mazimba (2018). " Mines Safety & Accident Communication System for underground mines", Society of Mining Professors sixth regional conference, South Africa.

7. Marin, R, R Castro, F Báez & K Suzuki (2020). "Telemetry: connectivity and productivity in real time - project implementation guide", Proceedings of the Eighth International Conference & Exhibition on Mass Mining, University of Chile, Santiago, pp. 1359- 1374

8. "Mine Safety", 2nd Indo-US Coal Working Group Meeting Washington, (November 2005).https://fossil. energy.gov/international/Publications/cwg_nov05 _ safety_mandal.pdf

9. "Ultra-Wideband can replace these three technologies" (March 8, 2023). https://sunverasoftware.com/ultra-wideband-can-replace- these-three-technologies/

10. Elvina S (23 August 2021). "UWB vs WI-Fi: which technology is better for indoor positioning". https://navigine.com/blog/uwb-vs-wifi/

11. "How to Fix Sound Delay in Bluetooth Headphones" (October 7, 2021). https://www.headphonesty. com/2020/07/fix-sound-delay- bluetooth-headphones/.

12. "WLAN vs Ethernet LAN | difference between WLAN and Ethernet LAN" (2023). https://www.rfwireless-world.com/Terminology/WLAN-vs-Ethernet-LAN. html

13. B.A. Chetty (July 2015). "Telemetry in Mines", IETE Journal of Research, Vol 29, PP 389-391.

14. Zhang, Y., Li, Z., & Wang, Y. (2022). A real-time tracking system for under cast mines using VLF technology. Sensors, 22(2), 660

15. "What can be learned from mining accidents in 2022", February 12, 2023, https://www.mining-technology. com/features/mining-disasters- 2022-map/

16. Smith, John."Mining in India is fraught with danger", British Safety Council , January 1, 2023,https://www. britsafe.in/publications-and- blogs/safety-management-magazine/safety-management- magazine/2021/mining-in-india-is-fraught-with-danger/

17. Meilin Qian, Kai Zhao, Binghao Li, Henry Gong, and Aruna Seneviratne (28 September 2022). "Survey of Collision Avoidance Systems for Underground Mines: Sensing Protocols", Sensors, MDPI, Basel, Switzerland

18. Mohmed Imam, Karim Baina, Youness Tabii, EI Mostafa Ressami, Yousef Adlaoui, Intissar Benzakour and EI hassan Abdelwahed and (26 April 2023). "The Future of Mine Safety: A Comprehensive Review of Anti-Collision Systems Based on Computer Vision in Underground Mines", Sensors, MDPI, Basel, Switzerland

19. Feng, Y., & Li, X. (2019). Real-time tracking of underground personnel using Wi-Fi technology: A review. IEEE Access, 7, 85436- 85444

20. Al-Khatib, H. A., & Azar, A. T. (2017). Real-time tracking of underground mine vehicles using wireless sensor networks. IEEE Sensors Journal, 17(2), 262-269

21. "Power Real-Time Tracking, Collision Avoidance and Proximity Applications Deep Underground and Across Remote Open Mines", February 2017, https://www. inpixon.com/industries/mining

22. Li Yang, G E Birhane & Junqi Zhu (18 August 2021). "Mining Employees Safety and the Application of Information Technology in Coal Mining: Review", Front. Public Health, Sec. Occupational Health and Safety, Vol. 9

23. Chen, X., & Li, Y. (2017, October). Real-time tracking of underground personnel using ZigBee technology. In 2017 IEEE 18th International Conference on E-Health Networking and Applications (Healthcom) (pp. 1-4). IEEE

24. Dey, A. K., & Roy, P. K. (2020, June). "Real-time tracking of underground vehicles using ultra-wideband (UWB) technology: A review", IEEE International Conference on System Science and Engineering (ICSSE) (pp. 1-6). IEEE.

25. Y. Zhang, M. Lin, L. Xie, and J. Wang (2021). "A LoRa-Based Real- Time Indoor Positioning System for Underground Mines", IEEE Transactions on Industrial Informatics

26. D. Xu, L. Li, J. Li, and Z. Zhou (2020). "Design and Implementation of a LoRa-Based Real-Time Tunnel Tracking System for Underground Mines", Sensors.

27. X. Liu, S. Guo, Y. Zhang, and L. Xie (2019). "A LoRa-Based Real- Time Positioning System for Underground Mines Considering Multipath Effects", IEEE Access

28. H. Zhu, L. Zhang, and J. Wang (2019). "Performance Evaluation of LoRa-Based Real-Time Tunnel Tracking Systems for Underground Mines", Ad Hoc Networks.

Optimum Path Routing with Power Optimization and Spectrum Assignment in Elastic Optical Networks

Deo Chandra Jaiswal
Department of Electronics Engineering
HBTU
Kanpur, Uttar Pradesh

S. K. Sriwas, Om Singh
Dept. of Electronics and Communication Engg.
BIET
Jhansi, Uttar Pradesh
✉ surendrasriwas@bietjhs.ac.in

ABSTRACT

In this article the power consumption has been optimized in elastic optical networks (EONs) to enhance the quality of optical communication systems. During the failure of any path, there is the need for path routing to survive the network. An Integer Linear Programming (ILP) model has been developed by using Optimum path routing with power optimization (OPRPO) which can minimize the required power. The basis of power minimization in EONs is by using the minimum number of idle resources based on selecting the optimum path which is configured by the proposed model. The simulated results show that the total power can be saved up to 10.69% for the 8-node 11 span and 16.57% for the 14-node 21span network with OPRPO in EONs.

KEYWORDS : *Elastic optical network, Power optimization, Shortest path routing, Optimum path, Wavelength division multiplexing.*

INTRODUCTION

The power optimization is an important phenomenon to operate the communication system continuously. The power requirement increased by 10 percent every year in telecommunication networks. It is essential to handle such a situation of increasing power by power optimization [1]. Reaching power optimization in the domain of elastic optical networks (EONs) entails reducing resource consumption [2]. During the failure of any path, there is the need for path routing to survive the network and it can be done with the help of designing a system model that will select an optimum path to use the minimum number of resources and decrease the power requirement[3]. The energy saving in EONs is virtual and can be done with power optimization [4-7]. In power optimization, the optimum path routing is the fundamental process through which the best path is selected based onthe minimum power requirement. To meet the requirement for minimum power consumption along the route, it is crucial to maximize the number of resources in sleep or off mode while minimizing their utilization during operation.In the beginning

wavelength division multiplexing (WDM) networks are operated with the specified spectral band and the proper utilization of the available band is limited which is the main cause of low capacity [8]. Nowadays the available bandwidth can be flexible according to traffic in EONs.

In WDM based optical network, 50 GHz spectral is divided into multiple fixed spectral bands of 12.5 GHz which are called frequency slots. This division process of the fixed band increases the elasticity of the WDM optical network. The primary issue with this WDM optical network is that because there are fewer channels available, the assigned frequency slot is not efficient at handling high traffic demand. On the other hand, increasing the number of channels leads to capacity wastage during low traffic. Spectrum contiguousness in EONs means that all frequency slots assigned to the route of the demand pair must be adjacent, while spectrum continuity means that the same group of slots must be used on all spans crossed by the route of the demand pair [9]. As a result of Optimum path routing with power optimization (OPRPO) preference for using activated spans to route traffic demand, some spans

will become more loaded while others will remain idle. Certainly, the channel requirements on some spans exceed the maximum number of channels allowed in WDM. One way to deal with the problems caused by EON channel limitations is to increase the number of unused channels in WDM networking [10]. The capacity to increase the available channel count, provide more leeway in bandwidth allocation, and improve spectrum utilization are the main benefits of EONs. Here, EONs provide the desired aspect of power-efficient optical communication. Within EONs, the creation of a channel with the targeted spectral band involves the amalgamation of a set of consecutive slots, contrasting with the utilization of a channel characterized by a predefined, unchanging spectral band. This practice enhances the adaptability of spectral band allocation, resulting in minimized capacity waste and an overall improvement in spectrum frequency utilization. Power efficiency is an important factor to consider when developing improved elastic optical networks. When the goal is to reduce power consumption, a network's resilience becomes vulnerable, emphasizing the importance of turning off devices that are not in use due to traffic demands. Optimal power consumption can be achieved within EONs through the fine-tuning of network devices using various methodologies. This research explores the domain of OPRPO-based power optimization in elastic optical networks. To improve power efficiency and optimize power consumption, the paper presents an ILP (Integer Linear Programming) model that makes use of OPRPO.The simulation results confirm that the OPRPO can reduce power consumption and improve power efficiency when compared to Shortest Path Routing(SPR).

In this article, the two essential components,which are the main cause of power consumption in elastic optical networks, are considered : bandwidth variable cross-connects (BV-OXCs) and Erbium-doped fiber amplifiers (EDFAs).

The other part of the paper is organized as follows. Section 2 describes the routing algorithm. In Section 3, we reveal an ILP optimization model that promotes EON solutions' power efficiency. In Section 4, the focus shifts to thorough simulations and the results that follow. Section 5 provides a final summary of the results and conclusions.

ALGORITHM FOR ROUTING

Routing refers to the process of determining the most efficient path for data to travel from its origin to its intended destination. Two distinct routing methods are discussed in this article: (a) SPR; and (b) OPRPO. A brief overview of these two routes is provided below.

Shortest Path Routing (SPR)

SPR seeks to determine the most efficient path from a source node to a destination node in a network, taking into account the total length of intermediate links. The primary goal is to determine a route that has the lowest overall length, which is calculated by adding up the lengths of all the links along the path. In SPR, connections always adhere to the shortest paths that link each demand pair in the network, resulting in optimal routing. Figure 2 depicts this process. Notably, Dijkstra's algorithm is a key method used in SPR to calculate the shortest path between source and destination nodes [11]. This algorithm starts with the source node, then explores neighboring nodes, and iteratively selects the shortest path until it reaches the destination,adding to the overall efficiency of Shortest Path Routing in network optimization

Fig. 2: Paths allocated to demands by shortest path routing.

Optimum Path Routing with Power Optimization (OPRPO)

Optimal Path Routing with Power Optimization (OPRPO), exhibits certain resemblances to traditional shortest path routing techniques, but it takes a power consumption perspective. OPRPO is specifically

designed for elastic optical networks with plenty of capacity or frequency slots, and it aims to reduce power consumption by network elements when they are ON/ACTIVE. Unlike traditional routing, OPRPO takes into account the abundance of available resources and prioritizes power conservation through strategic route selection.

In elastic optical networks, the algorithm seeks paths for each demand that do not use specific BV-OXCs (Bandwidth Variable Optical Cross-Connects) or amplifiers [12-13]. By bypassing these components of the network, the potential to deactivate them emerges, resulting in significant energy conservation, as illustrated in Figure 3. This energy-efficient routing strategy helps to reduce overall power consumption and promotes sustainability in network operations.

OPRPO's optimization goal is not only to establish efficient data paths but also to strategically manage the network's active elements, such as BV-OXCs and amplifiers, to achieve significant energy savings[14,15]. The algorithm's ability to identify routes that enable the deactivation of specific components demonstrates its potential impact on the development of energy-efficient and environmentally conscious elastic optical networks[16].

Fig. 3: Demand paths after optimal path routing with power optimization

ILP MODEL FOR OPTIMIZATION

Network design optimization is another area where ILP models are useful. To decrease the total power consumption in EONs, we describe in this section the steps involved in creating an ILP model. This model takes BV-OXCs and amplifiers into account and aims for optimum path routing with power optimization (OPRPO) and shortest path routing (SPR). The set, parameter, and variable information listed below are utilized by this ILP model.

Sets

P: A set of network-specific paths indexed by p

D: A collection of network demand pairs indexed by r

Di: A collection of demand pairs whose working paths include link i

S: The index j designates a group of network spans

Pi: A set of qualified dedicated paths linking demand pairs r, with no connection to the main path between any of them

N: A compilation of network nodes designated by the index n

Parameters

Aw_j: 1 for non-zero working,0 otherwise

P_{amp}: The amount of power (in watts) that an amplifier,like an EDFA uses when it is in its active mode

d_r: The number of frequency slots (demand)needed for demand pair r

P_{sleep}: Watts of power consumed by an amplifier while in sleep mode

m_j: The number of amplifiers in span j

P_n: Equal to node power if node n is active; 0.1 if node n is in sleep mode

π_j^p: A binary data that is equal to 1 when span j is intersected by dedicated path p and 0 otherwise.

Variables

n_p: Quantity of available space for the designated path p

c : the highest frequency slot index that can be allocated across network links

x_r^p: If demand pair r's eligible dedicated path p (p∈Pi) is selected for the protection lightpath, it equals 1; if not its value is equals 0

s_j: Reserved spare capacity on span j

Sl_j : If span j can be put into sleep mode, equals 1; if not its value is 0

P_T : The total amount of power used by the amplifiers and BV-OXCs in the network.

Ap_j : If span j is active because there is no zero spare, equal to 1; if not its value is 0

The objective of ILP is to Minimize: P_T(1)

Constraints

$$\sum_{p \in P_i} x_r^p = 1 \ \forall \ r \in D (2)$$
$$d_r . x_r^p <= n_p \ \ \forall \ r \in D, \forall \ p \in P_i (3)$$
$$s_j = \sum_{p \in P} \pi_j^p . n_p \ \forall \ j \in S (4)$$
$$s_j <= c \ \ \forall \ j \in S (5)$$
$$\sum_{r \in D_i} d_r <= c \ \ \forall \ j \in S (6)$$
$$Ap_j = 1 \forall \ j \in S \ if \ s_j > 0 (7)$$
$$Sl_j = 1 \ \ \forall \ j \in S \ if \ Ap_j > Aw_j (8)$$
$$P_T = \sum_{j \in S}(P_{amp}.Aw_j + P_{sleep}.Sl_j).m_j + \sum_{n \in N} P_n (9)$$

Minimizing total power consumption across the network is the principal goal (Objective 1). To keep the spectrum from becoming fragmented, constraint (2) states that in case one of the primary paths fails, only one of the eligible dedicated paths can be used as a backup. The goal of the constraint is to make sure that dedicated path p can restore the primary path between demand pair r if it fails (3). The sum of all the reserved frequency slots on spans that are used to create paths is determined by constraint (4). Always keep the total number of frequency slots (spare capacity) on any span j below the maximum FS index, as specified in Constraint (5). A c-value of 20 (i.e., 0-19) is necessary if the biggest FS index in the whole network is 19. The total working demands on span j by demand pairs must always be less than the maximum FS index, as guaranteed by constraint (6). According to constraint (7), a span is considered active when there is non-zero spare capacity. Spans that have spare capacity but no working capacity are those that should be put into sleep mode, as determined by constraint (8). In the end, the sum of the power used by spans and nodes while they are active and asleep is calculated by constraint (9).

SIMULATIONS AND RESULTS

IBM ILOG CPLEX OPTIMIZATION STUDIO 12.6.3.0 is used to simulate the proposed model. The two-path routing method has been selected and compared the performance of these methods by using two test networks. The first test network has 8 nodes and 11 spans while the second test network has 14 nodes and 21 spans. The two test networks are shown in Figure 4 in their configured state. Within the range of frequency slots, the traffic demand for each demand pair is selected at random from a non-uniform distribution. To optimize power consumption while taking into account the dedicated path protection capacity and optimized power path allocation, the ILP Model assumes full spectrum conversion.

When comparing the power consumption of SPR and OPRPPO, Figure 5 illustrates that OPRPO uses less energy than SPR. As can be seen in Figure 6, when comparing the maximum frequency slot index with SPR and OPRPO, OPRPO requires a higher or equal maximum frequency slot index than SPR. The results presented in Table I demonstrate that OPRPO outperforms SPR in terms of power efficiency, with a total power reduction of 10.69% for an 8-node 11 span and 16.57% for a 14-node 21 network.

(a)

(b)
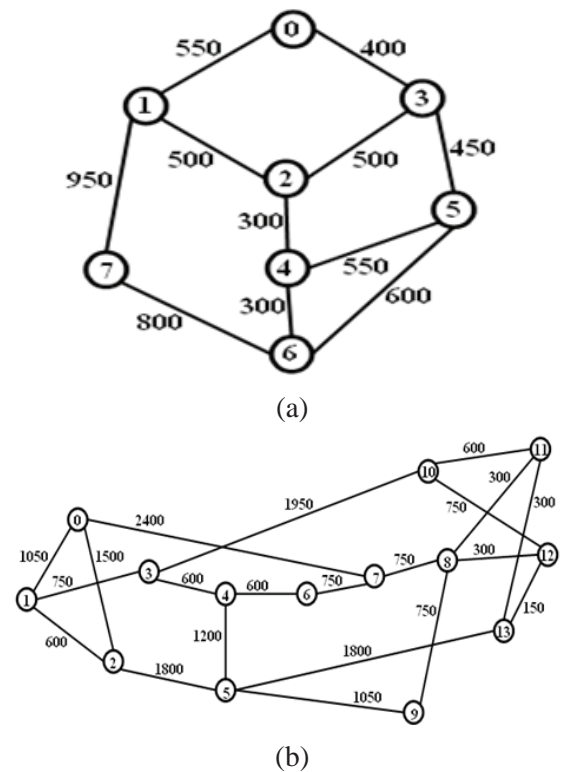
Figure 4: Simulation test networks (a) 8 nodes in the 11-span network and (b) 14 nodes in the 21-span network.

Table 1: Comparison of two distinct networks using SPR and OPRPO technologies' power consumption, overall spare capacity, maximum frequency slot index, and other relevant metrics

Net-works	Maximum Frequency Slot Index		Power Consumption (in W)		
	SPR	OPRPO	SPR	OPRPO	% Decrease
8n11s	9	9	16830	15030	10.69
14n19s	7	9	31012	25872	16.57
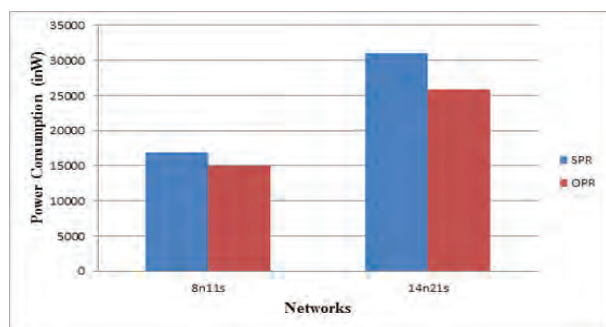
Fig. 5: Power consumption V/s networks comparison.
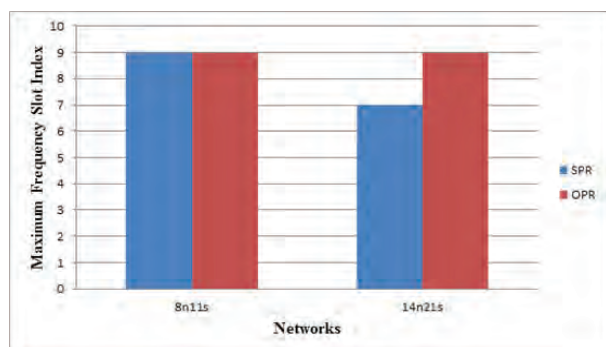
Figure 6. Comparison of maximum frequency slot index.

CONCLUSION

The power requirement of the optical network has been optimized by applying OPRPO and SPR to EONs and an ILP optimization model has been developed which will help to reduce the required power. The simulated results show that OPRPO has better power efficiency than SPR while SPR has a lesser frequency slot index than OPRPO. Although OPRPO reduces power consumption, the results show that the maximum frequency slot index increases, especially during low traffic periods. It is also clear that total power has been

saved upto 10.69% for the 8-node 11 span and 16.57% for the 14-node 21 network when OPRPO is applied in EONs.

REFERENCES

1.   Przystupa, K., Beshley, M., Kaidan, M., Andrushchak, V., Demydov, I., Kochan, O., & Pieniak, D. (2020). Methodology and software tool for energy consumption evaluation and optimization in multilayer transport optical networks. Energies, 13(23), 6370.

2.   Coiro, A., Listanti, M., Valenti, A., & Matera, F. (2010). Reducing power consumption in wavelength routed networks by selective switch off of optical links. IEEE Journal of Selected Topics in Quantum Electronics, 17(2), 428-436.

3.   Addis, B., Capone, A., Carello, G., Gianoli, L. G., & Sanso, B. (2012, October). Energy aware management of resilient networks with shared protection. In 2012 Sustainable Internet and ICT for Sustainability (SustainIT) (pp. 1-9). IEEE.

4.   Wu, J., Liu, Y., Yu, C., & Wu, Y. (2014). Survivable routing and spectrum allocation algorithm based on p-cycle protection in elastic optical networks. Optik, 125(16), 4446-4451.

5.   Grover, W. D., & Stamatelakis, D. (1998, June). Cycle-oriented distributed pre-configuration: ring-like speed with mesh-like capacity for self-planning network restoration. In ICC'98. 1998 IEEE International Conference on Communications. Conference Record. Affiliated with SUPERCOMM'98 (Cat. No. 98CH36220) (Vol. 1, pp. 537-543). IEEE.

6.   Zhou, D., & Subramaniam, S. (2000). Survivability in optical networks. IEEE network, 14(6), 16-23.

7.   Gupta, M., Grover, S., & Singh, S. (2004, October). A feasibility study for power management in LAN switches. In Proceedings of the 12th IEEE International Conference on Network Protocols, 2004. ICNP 2004. (pp. 361-371). IEEE.

8.   Eshoul, A. E., & Mouftah, H. T. (2008). Survivability approaches using p-cycles in WDM mesh networks under static traffic. IEEE/ACM Transactions on Networking, 17(2), 671-683.

9.   Wei, Y., Xu, K., Jiang, Y., Zhao, H., & Shen, G. (2015). Optimal design for p-cycle-protected elastic optical networks. Photonic Network Communications, 29(3), 257-268.

10. Wu, J., Liu, Y., Yu, C., & Wu, Y. (2014). Survivable routing and spectrum allocation algorithm based on p-cycle protection in elastic optical networks. Optik, 125(16), 4446-4451.

11. Asthana, R., Singh, Y. N., & Grover, W. D. (2010). p-cycles: An overview. IEEE communications surveys & tutorials, 12(1), 97-111.

12. Athe, P., & Singh, Y. N. (2022). Double-Link Failure Protection Using a Single p-Cycle. IETE Journal of Research, 1-10.

13. Yan, Y., & Dittmann, L. (2011). Energy Efficiency in Ethernet Passive Optical Networks (EPONs): Protocol Design and Performance Evaluation. J. Commun., 6(3), 249-261.

14. Lira, C. J., Almeida Jr, R. C., & Chaves, D. A. (2023). Spectrum allocation using multiparameter optimization in elastic optical networks. Computer Networks, 220, 109478.

15. Assis, K. D. R., Almeida Jr, R. C., Reed, M. J., Santos, A. F., Dinarte, H. A., Chaves, D. A. R., ... & Simeonidou, D. (2023). Protection by diversity in elastic optical networks subject to single link failure. Optical Fiber Technology, 75, 103208.

16. Etezadi, E., Natalino, C., Tremblay, C., Wosinska, L., & Furdek, M. (2024). Programmable filterless optical networks: Architecture, design, and resource allocation. IEEE/ACM Transactions on Networking.

Predicting Diseases Using Data Mining Algorithms and Big Data Analytics with the Implementation of Matlab

Md Jabed Hussain
✉ jabedhussain@gmail.com

Awakash Mishra
✉ awakashmishra@gmail.com

School of Engineering & Technology
Maharishi University of Information Technology (MUIT)
Lucknow, Uttar Pradesh

ABSTRACT

The use of techniques and procedures related to big data is rapidly expanding in the area of healthcare administration and clinical medicine. Using healthcare analytics can reduce treatment costs, predict the start of epidemics, aid in the prevention of diseases that can be prevented, and overall enhance life quality. In this article, we'll talk about the value of big data in the medical and healthcare industries. The phrase "Big Data" refers to an ambiguous concept, whose definition is not widely accepted by the scientific world. On the other hand, the discipline of health informatics research does not generally deal with data sets this size. In the field of public medical informatics, population information is subjected to data mining and analytics to gain a better understanding of medical issues. To better assist the public, this one is performed. An outline of data mining's uses in administrative, clinical, scientific, and instructional areas of health informatics is provided in this study. In addition to implementing image analysis of the damaged area of the body, this study also provides the MATLAB implementation and all prior work that has been part of our proposed work. The outcomes of the experiments will demonstrate that many of the concepts assist in the simplest disease prediction, which even aids doctors in their diagnosis decisions by utilizing A-priori and k-mean. This analysis may make it simple to determine the victim's current situation and future outlook using extremely cheap means. Therefore, even though doctors can't properly anticipate illness, a system that can predict the right diseases using available knowledge must be helpful to the victim. This analysis tends to anticipate diseases using integrated versions of methods like the predictive rule, priorities rule, and association rule. Here, it has almost two hundred people's data for this analysis.

KEYWORDS : *Big data, Data mining, Health informatics, MatLAB, Algorithm.*

INTRODUCTION

Since big data consists of a vast amount of data in numerous formats (including financial and clinical), and also a mix of various formats, it might be overwhelming for medical practitioners. Large data sets could prove to be a very helpful resource for medical institutions, both in terms of enhancing the calibre of care provided to patients and in terms of lowering the costs related to providing healthcare care. Big data is becoming more valuable to businesses in the biotechnology and pharmaceutical sectors for many reasons, such as the control of financial danger and regulatory requirements, among others.

Massive amounts of data that are gathered by digital technologies and used to manage the overall operation of hospitals are referred to as "healthcare big data." These new platforms capture patient information, but the amounts of data they gather are generally too large and complex for conventional technical platforms to manage. The supply of e-health care to patients on the go is fraught with many fundamental problems. The requirement to safeguard and incorporate patient information to make decision-making and diagnostics for patient care was one of these problems.

[1] discussed the use of artificial intelligence (AI), computer models, and big data analytics drawn

from nature for accurate COVID-19 pandemic case identification and investigations. A disease is any situation or event that can lead to a person becoming ill, becoming dysfunctional, experiencing pain, or even passing away. People can be physically harmed by sickness, or their lifestyles might be changed.

Through the informal method of pathology, diseases are studied. Any disease can be identified by its telltale symptoms or signs which trained medical personnel can evaluate. The diagnosis is a process for identifying diseases; the pathophysiology of the disease is identified using symptoms. A method of diagnosing a disease depending on a person's symptoms and signals is referred to as "diagnostic" [2]. The use of ANNs in systems for medical self-diagnosis is included in this description.

To lessen the uncertainty in clinical diagnosis, healthcare providers may gather empirical data to identify the patient's disease. [3] Examine how a node of remote monitoring with an integrated ADALINE neural network coprocessor can be used to analyze vibration signals and diagnose defects in machine tracking systems. Patients with critical medical illnesses may not receive the right care or experience a delay in it as a result of mistakes made during the diagnosis procedure. For making incredibly accurate disease diagnoses, many AI models are now applied in the medical field. [4] examines a novel line search technique for training feedforward neural networks.

The binary NN, tiny convolutional networks, and decision trees employed to quickly and precisely predict the pupil outline are described in [5]. As a result, better judgment may be reached in the medical field. Discovery, genomics, diagnostic imaging, medication development, and Alzheimer's disease detection are just a few of the fields where the DL is advantageous.

The Intelligent Parallelization Methods for the Genetic Synthetic Methods for N Ns are examined in [6]. By 2030, researchers believe that cervical cancer would cause 474,000 women to die each year.

Key issues raised by the sudden surge in interest in the new disciplines of big data, analytics, and data science are addressed in [7]. We examine the originality of the domains and if the underlying concerns are fundamentally different, the contributions made to this discussion by the information systems (IS) community, intriguing research questions for IS academics, the use of explanatory and predictive modeling, and more.

[8] Big data analytics (BDA) is crucial for patient diagnosis, early epidemic detection, and better patient care in the healthcare industry. This profiling study's goals are to (a) give an outline of the dynamics of BDA publications in the healthcare sector and (b) explore this scientific topic using relevant examples. A review of some of the literature was done.

[9] Because the data sources used in medicine are well known for their mass, varied intricacy, and high reactivity, healthcare has gained its current impact regarding big data technologies. As shown by ground-breaking research initiatives, the success of medical applications in the setting of big data completely rests on the embedded system and the use of relevant technologies.

[10] Big Data Science is crucial because of the quick expansion of intrinsically complex and varied data in HIV/AIDS research. Big Data approaches have recently seen an increase in adoption in the disciplines of scientific, clinical, and public health HIV/AIDS research. However, no papers have thoroughly outlined the changing Big Data uses in HIV/AIDS research.

[11] With the development of cutting-edge data analytics technologies used in the medical industry, healthcare computing and analysis, also known as health informatics, healthcare IS, and so on, have swiftly improved. HCI&A has recently been a significant field of research for academic scholars as well as practitioners.

[12]Companies have recognized the need for data scientists, university institutions are rushing to develop data science programs, and publications are all addressing this issue. Data science is not well understood, and this lack of understanding could leave people disappointed as the idea becomes meaningless jargon.

[13] Data science seems to be a young field that has attracted a lot of interest recently. This new profession demands a broad range of expertise and knowledge from many various fields, This paper's goal is to report the findings from a study that looked at data science from an lLIS perspective.[14]

Due to the development of technology for information and communication and the current measurement approach, the amount of data collected from public health monitoring has substantially expanded since the start of the twenty-first century. Methods The purpose of this work is to illustrate the advantages of using AI techniques for accurate disease-oriented surveillance and prediction in the age of information.

[15] Data preprocessing, data mining, result articulation, and outcome analysis are the main divisions of data mining tech, which may search through a big amount of information for potentially important knowledge. It uses database management systems and is a developed data processing technique. A data model is a branch of computer science that studies, employs, and administers databases.

PROPOSED SYSTEMS

Applications for healthcare on the blockchain

Block chain is redefining the data modelling and management that are employed in many smart healthcare. Its versatility and capability for segregating, encrypting, and exchanging healthcare information and services in hitherto unheard-of ways are mostly to blame for this. Blockchain technology is at the heart of several recent advancements in the healthcare industry. Future blockchain-based medical innovations are organised using four conceptual layers: stakeholders, healthcare apps, data sources, and blockchain architecture. Figure 1 depicts a pathway for blockchain-based medical applications. When all the data from social networks, laboratories, medical equipment, and other sources are combined, it becomes raw data, which later grows in size to become big data. The initial layer of the stack is created by this data, which is also the key component of the entire blockchain-based healthcare system. The raw data layer, which is the fundamental structure for building a secure medical system with four distinct parts, is above which blockchain innovation rests. Consensus methods and protocols differ between each blockchain system.

The fundamental components of the blockchain include decentralized applications, identities, wallets, membership, events, and digital goods. To connect with other programmes and systems or even across other networks, a wide range of protocols may be employed. Examples of this include P2P, centralised, decentralised, and distributed systems. Policymakers may opt for personal, community, and even federate options depending on the range of requirements they must satisfy. The next step is to make sure that the apps are linked with the entire system when the platform is built using blockchain technology. Applications using blockchain technology in the healthcare sector can be divided into three categories. First, there is data management, which includes EHRs, data warehousing, and worldwide scientific information sharing for development and research. Pharmaceuticals and medical trials are included in the second class of SCM applications. In addition to healthcare IoT and medical equipment, e - healthcare architecture and data protection, and AI are all covered in the third course on IoMT.
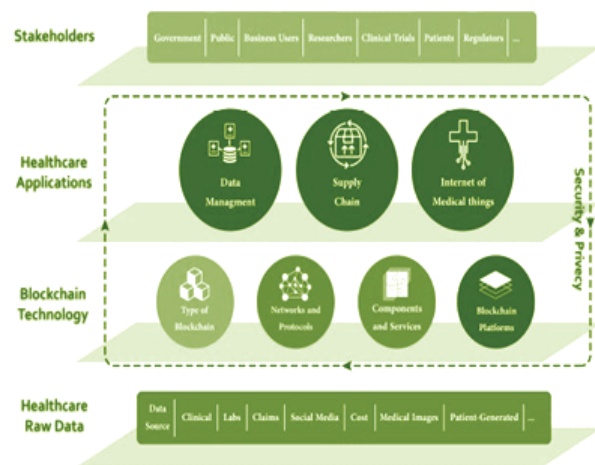
Fig. 1: applications for healthcare on the blockchain

Healthcare Analytics Using Big Data

The 7 dimensions of big data are displayed in Fig. 2. By gathering, processing, and evaluating healthcare data to produce insightful findings, health analytics, a new sub-discipline of big data analytics, is assisting healthcare facilities as they deal with daily difficulties like a variety, volume, veracity, and velocity. Big data in medicine relates to patient information, physical information, and clinical information that is too complex or large to be analyzed by conventional data processing methods. Data from the healthcare industry is processed using machine learning algorithms nowadays.
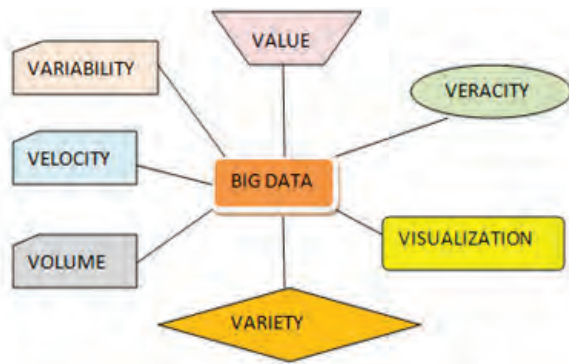
Fig. 2. Big Data Characteristics

1. The volume describes how many petabytes or zettabytes of data are present.

2. Data generation speed is indicated by the term velocity. For instance, medical supplies' Heterogeneous data is defined by its variety, which includes structured, unstructured, and partially organized data.

3. Veracity, which refers to the quality of data, specifies the reliability or integrity of the data. For instance, it discusses if the data acquired is not corrupted, authentic or not, and whether it came from a reliable source or not.

4. Inconsistencies in the flow of large data are defined as variability. It is challenging to sustain loads of data given the expanding size of data.

5. Value is a term that describes the significance of data, such as how helpful it is in helping people make wise judgments.

6. Visualization is the term used to describe how massive and complicated datasets are represented using graphs and charts for improved data analysis.

Fig. 3 illustrates how big data analytics is enabling the healthcare industry to advance patient-focused solutions, identify and prevent diseases, provide improved treatment options, and more. Responding to patient happiness, health data, and medical progress can improve the effectiveness of medical care. Good healthcare information not only evaluates the standard of care but also helps to improve the standard of care. The requirement to manage patient care and the newest new medications are causing healthcare industries

to struggle. To meet these objectives, industries must adopt new techniques and methods. Big Data analytics is one of these methods. According to the most recent estimate, healthcare data is predicted to grow at a compound annual growth rate (CAGR) of 36% by 2025, bringing about a significant transformation in the healthcare sector.

The healthcare sector deals with a variety of numerous patients whose information is constantly being passed from one end to the other. Insights gained from this may be used to provide users with improved healthcare services. The development of big data analytics techniques allowed for this. The way healthcare systems and hospitals manage and use medical records to provide the best treatment to patients has changed as a result of digitization. Healthcare organizations are improving their efficiency and can effectively provide affordable car services to humanity.

Fig. 3. Big Data Analytics for Healthcare Services

Because big data predictive analytics can help businesses save costs by at least 25% each year over the coming years, 50% of the healthcare industries are currently employing this technology, according to the most recent updates.It aids in producing outcomes for future prediction. Predictive analytics approaches are being used in the healthcare industry to detect diseases, determine patient readmission risk, and do other things. It is assisting physicians in choosing better patient care options. It does predictive analysis on medical databases using a variety of machine-learning approaches.

Health Informatics and Administration with Data Mining

Health informatics can be classified into four primary subfields, as was said in the introduction:

1. Administering healthcare services

2. Healthcare

3. Medical study

4. Training

An outline of each health informatics area and how data mining is being used to advance and develop each subfield are provided in the following subsections.

Health care

Based on the patient's history, lab results, medical imaging, and other text or multimedia data, doctors and nurse practitioners suggest a diagnosis and course of therapy. With the use of health informatics, clinicians may obtain more pertinent information more quickly and come to better judgments. A doctor in a nearby clinic, for example, will be able to view the patient's whole set of pertinent medical records from any location in the nation thanks to a centralized patient record database. Additionally, using data mining methods on the centralized database will provide physicians with predictive and analytical techniques that go beyond what is visible on the data's surface. For instance, a new professional can search all the judgments made by earlier practitioners in a case that is identical to their own.

Administering healthcare services

Every day, administrators of medical institutions must make hundreds of important choices. The standard of the information upon which these decisions are made immediately affects the accuracy of the estimation, as it does in every administrative job. For instance, hospital administrators must decide how many staff members, supplies, and open beds are needed for the forthcoming month. The administrators must have a precise forecast of the number of patients to be expected over the next month as well as an estimate of how long each patient will stay in the hospital.

Medical Study

The subfield of clinical research is where data mining in medical informatics is now being used most successfully. The majority of the present health-related data are kept in small databases that are dispersed throughout numerous hospitals, clinics, and research facilities. However, centralized, uniform data warehouses are necessary for the majority of data mining applications in medical and administrative decision support systems. On the other hand, researchers may still utilize data mining techniques to successfully extract useful patterns, and effects. and cause linkages and predictive scoring systems from sparse and small databases.

Training

The fourth area of medical informatics is concerned with training future medical professionals, retraining current workers, and keeping them abreast of new technological developments. One example of the quickly expanding discipline of e-learning is the Healthcare Information sector of training and education. In recent years, there has been an increase in interest in using data mining methods for e-learning, and some of the early implementations have produced encouraging results. All three groups that interact with a learning system—educators, administrators, and students—can gain from data mining approaches. To ensure a more effective learning environment, data mining tools can track students' performance on various learning tasks and suggest pertinent materials, resources, and learning pathways. Data mining tools can give instructors unbiased feedback on a course's organization and content, help them identify their students' learning styles, and organize students into smaller groups based on their learning preferences and requirements. By knowing about user behavior, administrators may better manage network traffic, optimize server performance, and assess the overall efficacy of the instructional programs that are available.

Data mining and Big Data analytics stages in healthcare

According to Fig. 4, the complete procedure is broken down into five steps.
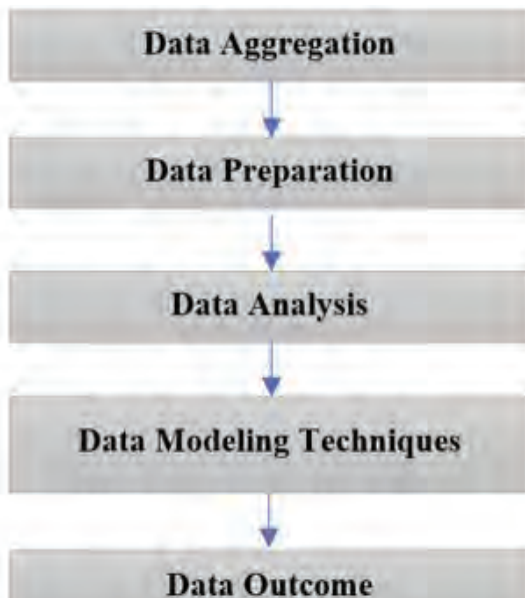
Fig. 4. Data mining and Big Data analytics stages in healthcare

Aggregation of data

This step involves gathering an enormous number of unprocessed healthcare data of various sizes from numerous sources, including sensor information, medical image information (CT, Ultrasound, MRT, etc.), prescription information, and more. The gathered information is kept in a data repository to be processed later.

Preparation of Data

This phase involves retrieving the repository's stored clinical information and sorting it to produce useful data later.

Cleaning the Data

Removing data with noise or missing values is a mechanism for filtering or isolating undesirable or irrelevant data from the healthcare data repository. It's possible that the collected raw data won't be helpful or produce the results we want, or it won't be in the right format. To process the raw data, it must be converted into either a semi-structured, structured, or unstructured form.

Transformation of Data

After the noise has been reduced and removed, transformed information is now ready for additional processing to yield the desired result.

Analysis of Data

In this stage, the health data that were generated in the preceding phase for processing are analyzed. It examines information from medical records, including the creation date, patient name, medical background, etc. It guarantees the accuracy of the medical data.

Processing of Data

Data processing for the healthcare industry is done at this step. It implies that it applies essential operations to healthcare information and produces insightful information in a straightforward, understandable manner. It processes the data and ensures its prominence using a variety of data modeling strategies.

Outcome of Data

It is a health report that deals with pertinent statistics and diagnostic info based on initial assumptions and input variables.

ALGORITHM USED

The k-means algorithm

The k-means algorithm is a straightforward, widely used method for dividing a known dataset into a specified number of clusters, k. Numerous advisors from various fields are aware of this algorithm. The technique works with a set of d-dimensional vectors, where $D = xi \mid I = 1,..., N$, and the ith abstract point is indicated by area xi Rd. An angry k credibility in Rd is used as the initial k array assembly, or "centroids," of the method. Techniques for choosing these antecedent seeds include sampling at random from the dataset, using them as a crutch for only absorbing a small section of the data, or repeatedly aggravating the overall beggarly of the data. Requiring data with real values is the simplest approach to accepting K-means. The number of clusters in the data must be the worst. It functions well if the clusters in the abstracts are of the same size. It is impossible to establish attribute acceptance. lacks account functionality. Fig 5 shows the K-means Clustering for Patients with Heart Disease
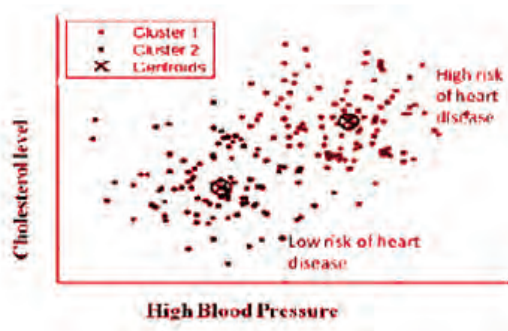
Fig. 5: K-means Clustering for Patients with Heart Disease

The Apriori algorithm

R. Agarwal presented the apriori technique for affiliation in 1994. It uses two inputs—support and confidence—to determine relationships within the account sets. The process of extracting common itemsets from a transaction dataset and obtaining affiliation rules is one of the most often used abstract data mining techniques. Due to its combinatorial explosion, awarding common itemsets—those with abundance above or by user-defined minimum support—is not atomic. Once common itemsets have been acquired, it is permissible to carry out affiliation rules confidently above or by user-defined minimum confidence. Apriori is a fundamental technique for generating applicants for awards using common item sets. The phrase "if an itemset is not frequent, any of its supersets are never frequent" is used to describe it as a level-wise complete search algorithm application. Apriori often presumes that the items inside a transaction or account set are arranged in lexicographic order.

RESULTS AND DISCUSSION

The UCI machine learning repository's Healthcare database from a hospital was used in the suggested research. There are 285 patient entries in the dataset's 12 columns (or characteristics), and there are no missing values. 250 records are utilized to train the systems and 35 records are used to test the models in the research. Age, sex, heartbeats per minute, blood pressure, number of major vessels, ECG (Electrocardiography) value, kind of serum cholesterol, chest pain, slope value, induced angina, and peak value are the features (attributes) taken into account.

The dataset is supplied to 3 machine learning algorithms, including Decision Tree, SVM, and K-NN. Three evaluation measures, including accuracy, recall, and specificity, are shown in Table 1 and are derived using a confusion matrix to assess the performance of the strategies. Figure 8 illustrates the related graph model of the models' performance analysis. The Confusion Matrix, which is a representation of the values that the ML models (classifiers) correctly and incorrectly predict, looks like this (Fig. 6).

	POSITIVE(1)	NEGATIVE (1)
POSITIVE(1)	Tp	Fp
NEGATIVE (1)	Fn	Tn

Fig. 6. Confusion Matrix

where Tp stands for True Positives, which are the number of unhealthy occurrences that were accurately anticipated.

Fp stands for false positives, which are instances of health that were incorrectly expected to be present.

Tn is the number of accurately anticipated healthy instances and true negatives.

False negatives (Fn) represent the number of unhealthy occurrences that were accurately anticipated.

Calculating accuracy, recall, and specificity follow the equations.

(1), (2), and (3).

$$Accuracy = \frac{4}{TP + TN + FN + FP} \tag{1}$$

$$Recall = \frac{TP}{TP + FN} \tag{2}$$

$$Precision = \frac{TP}{TP + FP} \tag{3}$$

begins with preprocessing, which involves filtering and classifying data before it is processed further. The output of this phase is a variety of classification techniques, which are then assessed to weed out those with poor performance. Next, we aggregate the findings and consider the patient's medical history to determine whether a heart attack has occurred. The details of each

phase's steps are provided below.

Phase 1: Preprocessing

• Run an evolutionary algorithm filter on the data set to replace each missing value with one that is inferred from the values in the columns. This is a crucial step, particularly for real datasets.

• To remove non-optimal features from the data collection, use feature selection approaches. Only 2 features should be removed, and those with a rank of 0 or low in contrast to others must be kept.Figure 7 shows the original data's classification.
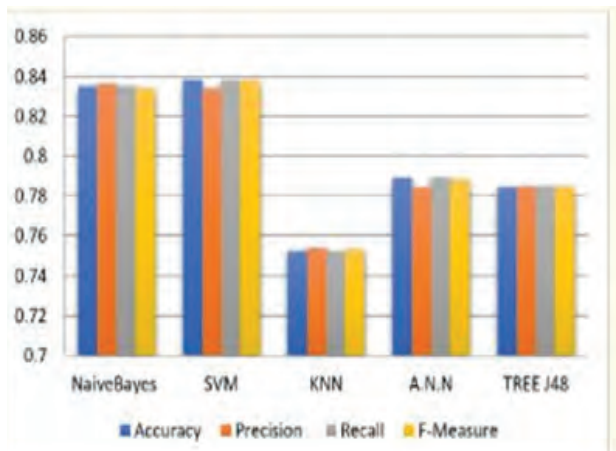
Figure 7: the original data's classification.

Phase 2: Classification

• Classify the results of the first phase using a variety of methodologies. • To assess the effectiveness of the employed methodologies, classification accuracy, precision, recall, and f-measure will be used. Figure 7 displays the classification outcomes of the original information. • Based on the results of the previous step's evaluations, eliminate algorithms with low efficiency. The consistency of the categorization on the data set is assessed by comparing the precision, accuracy, f-measure scores, and recall for each feature. We observe that Nave Bayes and SVM consistently outperform the competition and were never eliminated, while the tree decision has been eliminated a few times. Eliminate KNN from areas that it frequents.

• Use hybridization, in which the outcomes of the selected Classification are combined. The rating

system or classification The metrics used here for the performance evolution of the exhibited technique are Accuracy, Precision, and Recall. Table 1 compares the performance of various classifiers used by the medical self-diagnostic system, including KNN (K-Nearest Neighbor), ANN, and SVM.

Table 1: The effectiveness of various classifiers

Parameters	KNN	SVM	ANN
Accuracy	90.3	103.2	106.85
Precision	98.6	90.8	104.4
Recall	99.9	102.9	106.87
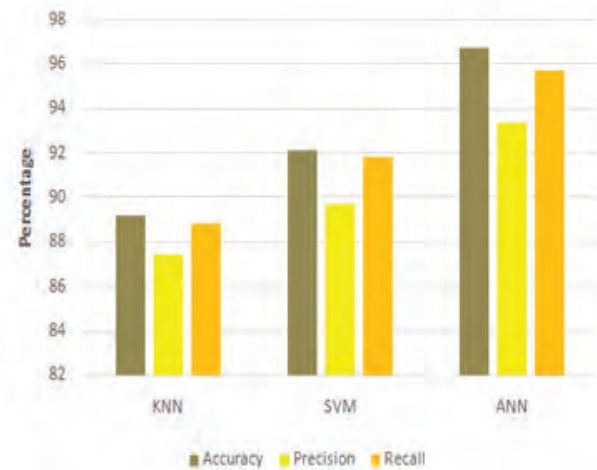
Fig. 8: Chart of Performance Comparison

Phase 3: Diagnose

• If the patient's medical history is known, compare the outcome with that information. The patient profile may be accessible at the hospitals or obscured by national health services.

• Provide a diagnosis with a heart attack diagnosis that is either positive or negative. The suggested approach might be utilized in hospitals to assist doctors in providing an immediate diagnosis or testing new ones on specific instances. This system might be used by medical school students to study and assess their knowledge. Figure 9 displays the analysis of various data mining methods' performance.
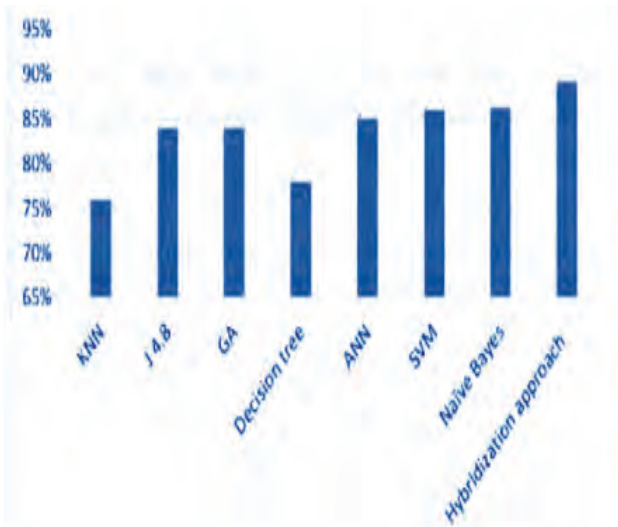
Figure 9: the analysis of various data mining methods' performance

SIMULATED RESULTS

In addition to implementing image analysis of the damaged area of the body, this study also introduces the MATLAB implementation and all prior work that was part of our proposed method. The SVM was used for picture scanning in the suggested work. Additionally, one of the two types of templates has been severely impacted, but the other is entirely unaffected. The present state of sections will be shown as a black dot on the impacted area when the uploaded image is compared to both. Fig 10 shows the basic MATLAB layout with a command prompt addressed to code.
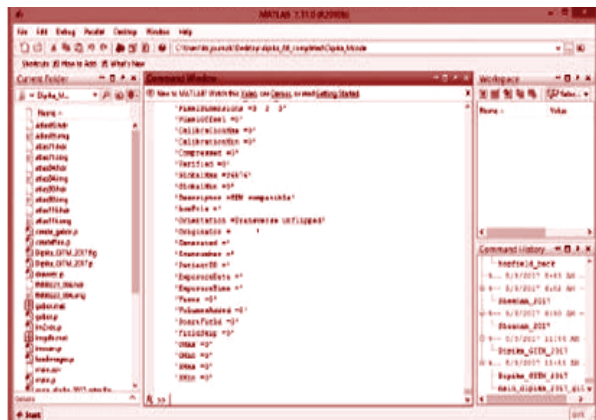
Fig. 10: Basic MATLAB layout with a command prompt addressed to code.

Fig. 11: Proposed GUI, with every button developed

Fig 11 shows the proposed GUI. This experiment will use many photographs of the patient who is ill, and most of the time it will successfully identify the disease location by highlighting it. Only the severely afflicted portion of the disease is indicated in this section. Due to a lack of real test conditions for future research, this probability area can be absent for a while. Only the impacted area can be predicted using this model. Figure 12 and 13 shows the test image of liver and uploaded liver image following pixel scanning.
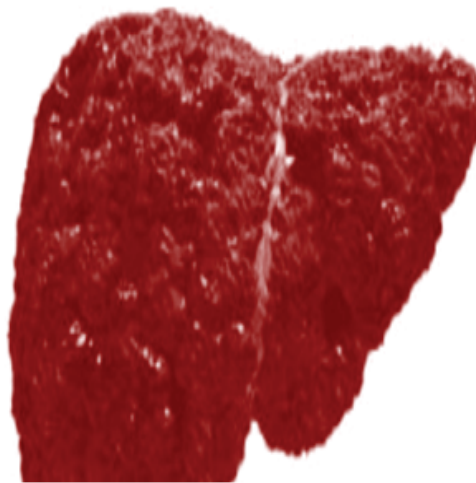
Fig. 12: Photo of a liver (Test Image)
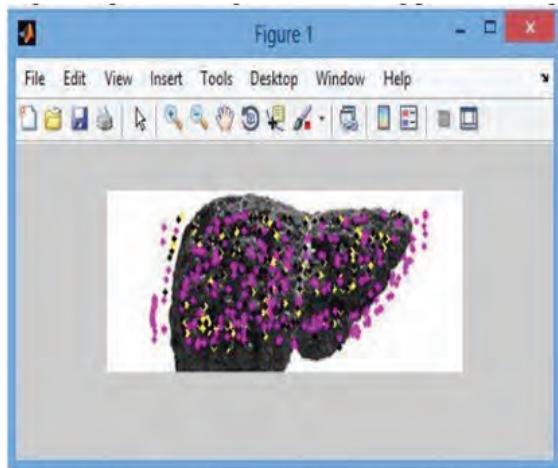
Fig. 13: Liver image uploaded following pixel scanning

CONCLUSIONS

To find the finest evidence in a world of ever-growing data, it is currently important to recognize, comprehend, and use big data in scientific research and healthcare. Given the growth of data from scientifically driven activities, the acceleration of healthcare advances, and the expansion of Big Data in higher education as a consequence of embedding innovations and the spread of e-Learning in higher education, the convergence of Big Data interpretations will continue. Using big data analytics in medicine is essential because we can minimize readmissions, and adverse events, and improve therapy for illnesses involving many organ systems. The current study concludes that combining machine learning methods with Big Data Analytics raises the calibre of healthcare services. An overview of data mining's uses in administrative, clinical, scientific, and educational areas of health informatics has been given. We found that while data mining techniques have a limited practical application in health-related issues at the moment, they have a lot of promise to advance numerous parts of Health Informatics. Additionally, the inevitable growth of clinical data warehouses will raise the possibility for data mining approaches to lower healthcare costs and enhance quality.

REFERENCE

1. Agbehadji, Israel Edem, et al. "Review of big data analytics, artificial intelligence and nature-inspired computing models towards accurate detection of COVID-19 pandemic cases and contact tracing." International journal of environmental research and public health 17.15 (2020): 5330.

2. Pandey, U., Shakya, T., Rajput, M., Singh, R., & Mangal, T. (2023). Review and Analysis of Disease Diagnostic Models Using AI and ML. Advancements in Bio-Medical Image Processing and Authentication in Telemedicine, 35-53.

3. Palanisamy P, Padmanabhan A, Ramasamy A, Subramaniam S. Remote Patient Activity Monitoring System by Integrating IoT Sensors and Artificial Intelligence Techniques. Sensors (Basel). 2023 Jun 25;23(13):5869. doi: 10.3390/s23135869. PMID: 37447719; PMCID: PMC10346748.

4. Bilski, Jarosław, Bartosz Kowalczyk, and Jacek M. Żurada. "A New Algorithm with a Line Search for Feedforward Neural Networks Training." International Conference on Artificial Intelligence and Soft Computing. Springer, Cham, 2020.

5. Kasneci, E., Gao, H., Ozdel, S., Maquiling, V., Thaqi, E., Lau, C., ... &Bozkir, E. (2024). Introduction to Eye Tracking: A Hands-On Tutorial for Students and Practitioners. arXiv preprint arXiv:2404.15435.

6. Kumar, S., Mallik, A., &Sengar, S. S. (2023). Community detection in complex networks using stacked autoencoders and crow search algorithm. The Journal of Supercomputing, 79(3), 3329-3356.

7. Kondraganti, A., Narayanamurthy, G., & Sharifi, H. (2024). A systematic literature review on the use of big data analytics in humanitarian and disaster operations. Annals of Operations Research, 335(3), 1015-1052.

8. Oladipo, I. D., Abdulraheem, M., Awotunde, J. B., Dauda, S. O., Ogundokun, R. O., Raheem, M. O., &Osemudiame, I. O. (2024). 10 Application of big data analytic techniques for healthcare systems. Healthcare Big Data Analytics: Computational Optimization and Cohesive Approaches, 10, 225..

9. Saravanan, S., Ramkumar, K., Adalarasu, K., Sivanandam, V., Kumar, S. R., Stalin, S., &Amirtharajan, R. (2022). A systematic review of artificial intelligence (AI) based approaches for the diagnosis of Parkinson's disease. Archives of Computational Methods in Engineering, 29(6), 3639-3653.

10. Liang, Chen, et al. "Emergence and evolution of big data science in HIV research: Bibliometric analysis of federally sponsored studies 2000–2019." International Journal of Medical Informatics 154 (2021): 104558.

11. Pramanik, Md Ileas, et al. "Healthcare informatics and analytics in big data." Expert Systems with Applications 152 (2020): 113388.

12. Donoho, D. (2024). Data science at the singularity. Harvard Data Science Review, 6(1).

13. Virkus, Sirje, and Emmanouel Garoufallou. "Data science from a library and information science perspective." Data Technologies and Applications (2019).

14. Wong, Zoie SY, Jiaqi Zhou, and Qingpeng Zhang. "Artificial intelligence for infectious disease big data analytics." Infection, disease & health 24.1 (2019): 44-48.

15. Yang, Jin, et al. "Brief introduction of medical database and data mining technology in big data era." Journal of Evidence-Based Medicine 13.1 (2020):57-69

Digital Pen Based on MEMS Accelerometer for the Digit Recognition using Trajectory Recognition Algorithm

C. M. Jadhao
Principal & Professor
Dept. of Electronics & Telecommunication Engg.,
Mauli Group of Institution's, College of Engineering
& Technology MGICOET
Shegaon, Maharashtra

J. K. Kokate*, A. P. Narkhede
P. R. Bhakare
Assistant Professors
Dept. of Electronics & Telecommunication Engg.
Mauli Group of Institution's, College of Engineering
& Technology MGICOET
Shegaon, Maharashtra
✉ jkokate18@gmail.com

ABSTRACT

In this paper, a MEMS accelerometer-based digital pen was proposed for handwritten digit identification. The digits drawn by the user are displayed on the computer by changing the position of the micro-electromechanical system; once this digital is recognized, it can be used to control various applications. With hand motions, the user can write numbers with this pen. To conduct the trajectory recognition algorithm, the computer gets the hand motion accelerations that the accelerometer has collected. The trajectory recognition algorithm comprises acceleration acquisition, signal preprocessing, feature synthesis, selection, and extraction processes. A trained PNN receives the reduced features in order to provide reliable recognition. The efficacy of the suggested pen's trajectory recognition algorithm for handwritten numbers has been satisfactorily confirmed by our experimental findings.

KEYWORDS : Digital pen, Handwritten digit recognition, Probabilistic Neural Network (PNN), Micro-electromechanical system (MEMS), ZCD, GUI.

INTRODUCTION

We all know that handwriting recognition is very useful for security, identification, and authentication purposes. Online and offline recognition are the two methods that are used for the recognition purpose. In the proposed system, the digits that are drawn by users are recognized online using the MEMS accelerometer. This accelerometer responds to even the smallest movements and detects the presence of the pen. However, because various users generate motion trajectories in different ways and at varying speeds, handwritten digit gesture detection is exceedingly complex. In an effort to lower inaccuracy on handwritten motion trajectories, numerous researchers are now at work. In this paper, we have reconstructed trajectories that are produced, and trajectory errors are decreased with the aid of the trajectory recognition algorithm. For increased accuracy and high probability, PNN classifiers are utilized.

LITERATURE SURVEY

The work presented by Kim et al., 2005 [1], presented the Samsung Advanced Institute of Technology's latest wearable input device, the SCURRY. This SCURRY allows the user to select a certain character, action, or event based on input from the inertial sensors.

The authors Sato et al., 2007 [2], focused on the pointing behaviors for a natural interface. They investigate a system that can deduce a user's intents from their motions. They have presented 3 experimental reports based on the pointing behavior in these papers.

The research work presented by Cheok et al., 2007 [3], presented a tilt pad that was created with wireless devices and accelerometers. Combining two innovative feature

tracking algorithms—epipolar and homography—based on geometrical image restrictions, tilt pad is a unique piece of interaction gear. Using this tilt pad and tracking techniques, they have created illustrations for the MR computer game.

Won et al., 2010 [4], presented a novel methodology which makes as estimate of position and orientation with the help of position and inertial measuring unit. A particle filter is used to estimate position whereas Kalman filter for velocity estimation. An extra addition system was used to rectify the angular velocity measurement errors. As compared to output received using extended Kalman filter, this method has shown significant improvement in orientation errors.

The work presented by Zhuxin Dong et al., 2010 [5], has demonstrated a real-time system that uses a magnetometer, gyroscope, and MEMS accelerator together with the proper filtering and transformation algorithms to estimate human hand movements. The μIMU was developed as a Ubiquitous Digital Writing Instrument (UDWI) that could record handwriting on any flat surface and communicate in real-time over Bluetooth wireless protocol with PCs. Horizontal plane used to write English alphabets by UDWI for this study.

Wang et al., 2010 [6], proposed a trajectory reconstruction technique for handwritten digit identification and motion trajectory reconstruction applications based on the inertial measurement unit-based pen (IMUPEN). A combination of RF wireless transmission module, a microcontroller, two gyroscopes, and a triaxial accelerometer made up the IMUPEN. IMUPEN was a portable gadget that was very easy to carry around.

In this paper by Wang & Chuang, 2012 [7], a smart pen with an accelerometer that can recognize written numbers and gestures through applications. The acceleration acquisition signal preprocessing, feature synthesis, feature selection, and feature extraction are the phases that make up the suggested trajectory detection technique.

In the papers "A Digital Pen with a Trajectory Recognition Algorithm," 2013 [8], includes a fully digital pen with an accelerometer for applications that recognize handwritten numbers and gestures. The digital pen senses and records the accelerations of handwriting

and gesture trajectories using a triaxial accelerometer, a microcontroller, and a Zigbee wireless communication module.

Amma et al., 2013 [9], demonstrated a wearable input device that used 3D handwriting recognition to facilitate interaction. They have suggested a two-step method for identifying and identifying handwriting motions. Hidden Markov models (HMMs) were utilized in the recognition stage to represent a text from the motion sensor data, while support vector machines were employed in the spotting stage to detect the data segments containing the handwriting.

The research work presented by Suganthi S et al., 2016 [10], have discussed about developing and utilizing a dynamic hand motion recognition technology for the media player. The concepts of coloration detection and threshold make the system possible. ActiveX control is used to create the media player. This system operates without a database since it is unaffected by noise and limited heritage.

The paper published by Álvarez-León et al., 2017 [11], demonstrated a system for recognizing handwritten numbers using an offline neural network. The numerical characters were categorized by them as being made up of vertical as well as the horizontal strokes. The locations where vertical and horizontal strokes join were determined using dynamic zoning. After being entered into a representative string and validated with a unique matching pattern, the multilayer perceptron neural network receives this data.

In the paper published by Plamondon & Srihari, 2000 [12], outlined the characteristics of handwritten language, how this handwritten language is transformed into electronic data, and the fundamental idea underlying written language recognition systems, taking into account both online and offline scenarios.

Tuba et al., 2023 [13], provided an overview of handwritten digit recognition techniques evaluated on the MNIST dataset. They analyzed, synthesized, and contrasted the evolution of several classifiers used to solve the handwritten digit recognition problem, ranging from convolutional neural networks to linear classifiers.

SYSTEM WORKING & HARDWARE DETAILS

Block Diagram

The Digital Pen based on MEMS Accelerometer block diagram of is as shown in figure 1.
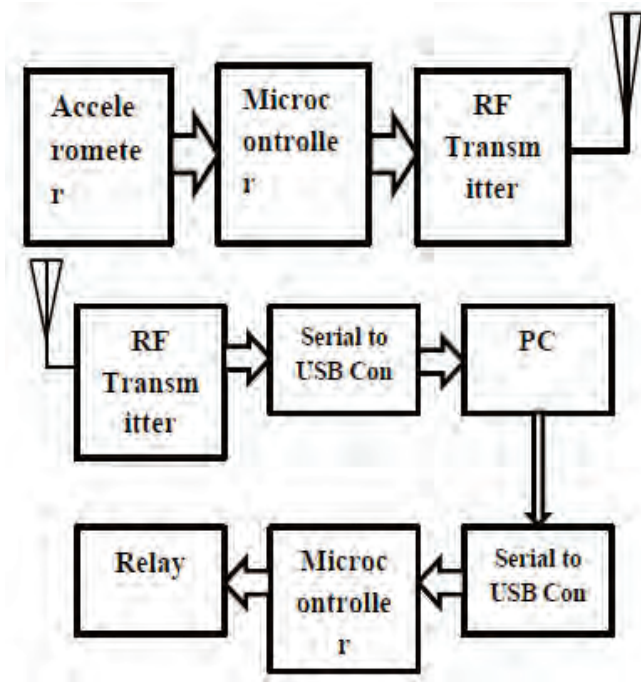
Fig. 1: Block diagram of Digital Pen based on MEMS Accelerometer

Working

A digital pen system for handwritten digit recognition uses the AVR microcontroller, relay, RF transceiver, serial to USB converter PC, and triaxial accelerometer. The accelerometer generates the signal as per hand moments of the user, which is forwarded to the microcontroller. This microcontroller's A-to-D conversion section converts the analog signal to digital signals, and with the help of an RF transceiver, these signals are transferred to the computer wirelessly. The microcontroller is used to control the relay action, which can be decided by selecting any two digits.

Trajectory Recognition Algorithm

The Trajectory Recognition Algorithm block Diagram of is as shown in figure 2.
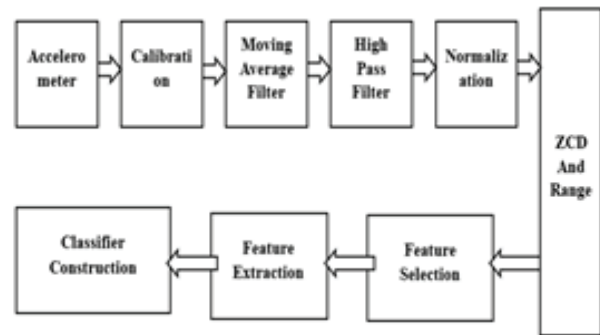
Fig. 2: Trajectory Recognition Algorithm

The algorithm includes rapid acquisition signal preprocessing, feature selection, and feature extraction. The microcontroller receives the raw acceleration alarms that are produced by hand motions through the measurement device. However, our hand always trembles barely, which causes a certain quantity of noise. The four steps in the sign preprocessing technique are normalization, high-bypass filter out, shifting common clear out, and calibration. Initially, the accelerations are set to take off in units and drift errors from the input raw signals. Filters are used to remove high-frequency noise and gravity acceleration from the input raw data. The characteristics of different hand motion signals are often obtained by taking two capabilities' options, ZCD and range, from the tri-axial acceleration indicators and extracting alternatives from the preprocessed x, y, and z axis signals.

Table 1: X & Y axis Zero Crossing Detector for digits

DIGITS	ZCD for X-axis	ZCD for Y-axis
0	1	2
1	1	0
2	1	3
3	1	1
4	1	1
5	1	3
6	1	3
7	1	1
8	1	4
9	1	1

PNN Classifier

The PNN is very good at accurately determining categories and providing opportunity and dependability metrics for every category. Thus, the fastest rate of learning that results from using the PNN is its most

significant benefit. The input layer, sample layer, summation layer, and selection layer are the four layers that make up the PNN. Each layer of the PNN's neurons performs the following function:

Layer 1: The input layer, which is the top layer, does not perform any computation. The large range of the extracted features is represented by the node of this residue that is sent to the neurons of the next layer i.e. second layer x = [x1, x2'.., xp] p when features x are entered.

Layer 2: The sample layer makes up the second layer. The output of the pattern layer node, as seen in picture three, is what happens when a pattern vector x from the entrance layer arrives.

Layer 3: The summation layer is the third layer. The sediment's job is to create the output by adding the inputs to the residue. The energy condition of a single class is represented by each node in the summing layer.

Layer 4: The decision layer is fourth layer. If the a priori possibilities and the losses of misclassification for each magnificence are all the identical, the sample x may be labeled in line with the Bayes approach in the decision layer that is primarily based at the output of all nodes inside the summation layer.

In this paper, the output of the PNN is represented because the label of the preferred outcome defined with the aid of users, for instance, in our handwritten digit recognition system the labels 1, 2, 3, 4, five, 6, 7, eight, 9, and 0 are used to symbolize handwriting digits drawn by way of person. extract two capabilities' options from the tri-axial acceleration alerts together with ZCD and range.
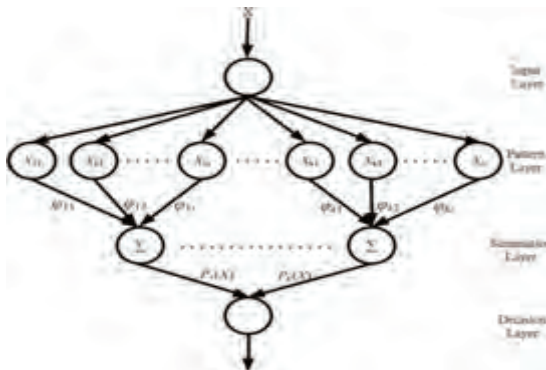
Fig. 3: PNN Classifier Topology

Hardware Details

MEMS Accelerator

In this system, the MEMS accelerometer ADXL335 [14] is used. Microelectromechanical systems, or MEMS for short, are systems with mechanical parts made in microelectronic circuits, such as cantilevers or membranes. Microfabrication technology is employed. The MEMS IC contrivance is a consummate expedition quantification system fabricated on a monolithic CMOS IC process. This accelerometer measures expedition with a minimum full-scale range of ±3g. In applications involving tilt sensing, it can be used to quantify both the static expedition of gravity and the dynamic expedition resulting from vibration, shock, or kineticism.

Fig 4: MEMS Accelerator

AVR Microcontroller

Based on RISC architecture, the ATmega16 [15] is an innovative CMOS 8-bit microcontroller featuring remarkable performance and low power consumption. The ATmega16 can process strong instructions in a single clock cycle, resulting in performance that approaches 1 MIPS per MHz. This enables the system intended for optimizing the power consumption versus processing performance. The inclusion of a microcontroller in the ADC was chosen due to the potential for two factors to taint the acceleration signal: inter-channel cross-talk and external electromagnetic noise. Analog to digital conversion of the signal is required to reduce noise or corruption of this kind. Thus, the microcontroller that has an integrated ADC has been chosen. The AVR core unites a comprehensive instruction set with 32 general purpose registers. Here, two distinct registers can be accessed in a single ordinant statement that is finished in a single clock cycle since the Arithmetic Logic Unit is directly tied to all 32 registers.

RF Wireless Module

A baseband modem is integrated with the RF module. The modem has a customizable data rate of up to 500 kBaud and supports several modulation formats. It uses

electromagnetic waves to create communication at a source. The system often indicates data rates, which include the amount of data that needs to be transferred and the frequency of that transfer. The radio module can have a greater range and improved receive sensitivity if the data rates are lowered. The XStream modules [16] exhibit a 3dB increase in sensitivity between the 9600 baud and 19200 baud modules.

RESULT AND PERFORMANCE ANALYSIS

Pictorial Digit Trajectories

Using gesture analysis, we can draw the desired Digit in the air, as shown in Table 2.

Table 2: Pictorial Digit Trajectories
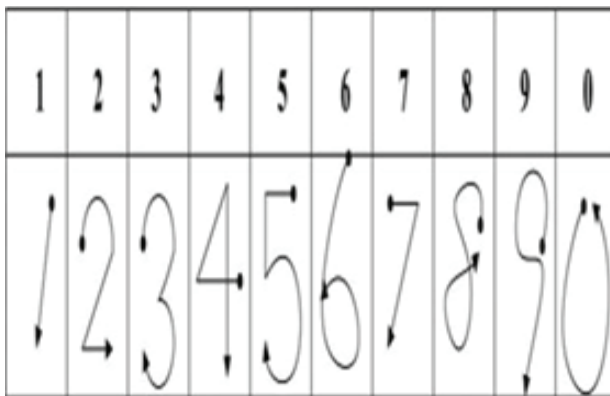
Character Success Index

Figure 5 is a graph between digit and recognition rate in percent, which is the character success index. A single digit is drawn repeatedly. How many times the digit was successfully recognized out of the total number of times it was drawn is shown in the percentage.
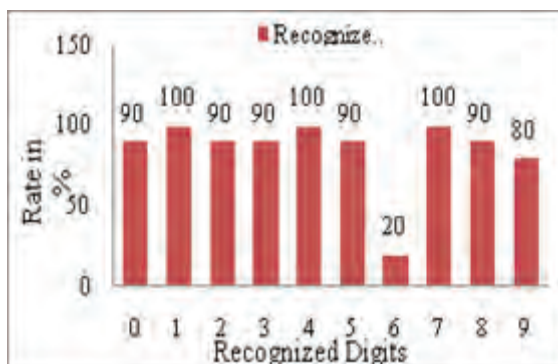
Fig 5: Character Success Index

Simulation Results

To analyze the performance of the system, the system was operated by the same person for the same digit multiple times, and the accuracy we have obtained in recognizing the digit is as mentioned in Table 3.

Table 3: Performance Analysis.

Digit	Number of times the digit is recognized successfully	Number of times the digit is unrecognized	Total Attempts	Accu-racy (%)
0	18	2	20	90
1	20	0	20	100
2	18	2	20	90
3	18	2	20	90
4	20	0	20	100
5	18	2	20	90
6	4	16	20	20
7	20	0	20	100
8	18	2	20	90
9	16	4	20	80

The formulae used to calculate the accuracy is as

$$\% \text{ Accuracy} = \frac{\text{Number of times the digit is recognized successfully}}{\text{Total Number of Attempts}}$$

The same user draws each number 20 times, and the outputs were observed. Out of 20 attempts, 18 times the digits 0, 2, 3, 5, and 8 were accurately recognized, leading to 90% accuracy for the respective digits. 100% digit recognition accuracy was obtained for the digits 1, 4, and 7. 80% digit recognition accuracy was obtained for the digit 9, and the least, i.e., 20% accuracy, was obtained for the digit 6.

Figures 6 through 15 display the simulation results for the numbers 1, 2, 3, 5, 7, 8, 9, and 0. MATLAB is used to simulate the results, and a graphical user interface window is created to display the results. This window reveals the determined digit, the X and Y axes of the graph, and its value.

Fig. 6: Recognized digit no. 1

Fig. 7: Recognized digit no. 2

Fig. 8: Recognized digit no. 3

Fig. 9: Recognized digit no. 4

Fig. 10: Recognized digit no. 5

Fig. 11: Recognized digit no. 6

Fig. 12: Recognized digit no. 7

Fig. 13: Recognized digit no. 8

Fig. 14: Recognized digit no. 9
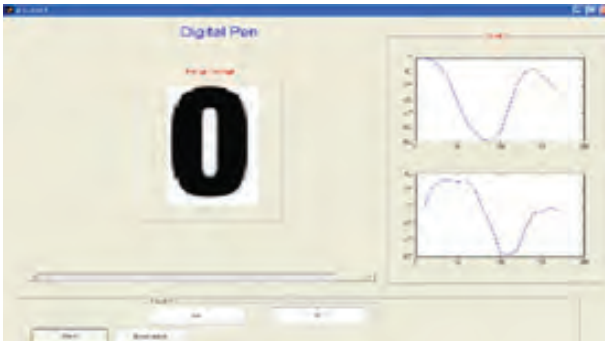
Fig. 15: Recognized digit no. 0

The simulation result of recognized numbers is as shown from figures 6 to 15. Relays are operated by the numbers 1 and 7. If digit 1 is recognized, the relay will be ON, and if digit 7 is recognized, it will be OFF. Any combination of two digits can be used to control the relay.

CONCLUSION

In this paper, we have presented a MEMS accelerometer-based digital pen for digit recognition. Here we've designed a systematic trajectory popularity algorithm and additionally utilized a PNN classifier that could enable us to recognize ideal matching of gestures for handwriting.

The least recognition accuracy was obtained for the digit 6, which is only 20%, and the most recognition accuracy was obtained for the digits 1, 4, and 7, which is 100%. From this, we can conclude that the digits 1, 4, and 7 can be used to control the applications, as the accuracy to recognize the digit for these numbers is 100%. This result encourages us to look into the idea of utilizing our digital pen as a practical tool for applications involving human-computer interaction (HCI).

FUTURE SCOPE

In today's era, we have seen a lot of applications like Alexa and others that are used to control the home application. If the person has a voice disability, then it will not be possible for him to use Alexa and control applications with the help of it. Implementation of this proposed system to control various tasks for physically challenged people will be the future scope of the system.

REFERENCES

1. Kim, Y., Soh, B., & Lee, S. (2005, December). A New Wearable Input Device: SCURRY. IEEE Transactions on Industrial Electronics, 52(6), 1490–1499. https://doi.org/10.1109/tie.2005.858736

2. Sato, E., Yamaguchi, T., & Harashima, F. (2007, April). Natural Interface Using Pointing Behavior for Human–Robot Gestural Interaction. IEEE Transactions on Industrial Electronics, 54(2), 1105–1112. https://doi.org/10.1109/tie.2007.892728

3. Cheok, A., Yan Qiu, Ke Xu, & Kumar, K. (2007, August). Combined Wireless Hardware and Real-Time Computer Vision Interface for Tangible Mixed Reality. IEEE Transactions on Industrial Electronics, 54(4), 2174–2189. https://doi.org/10.1109/tie.2007.895134

4. Won, S. H. P., Melek, W. W., & Golnaraghi, F. (2010, May). A Kalman/Particle Filter-Based Position and Orientation Estimation Method Using a Position Sensor/Inertial Measurement Unit Hybrid System. IEEE Transactions on Industrial Electronics, 57(5), 1787–1798. https://doi.org/10.1109/tie.2009.2032431

5. Zhuxin Dong, Wejinya, U. C., & Li, W. J. (2010, October). An Optical-Tracking Calibration Method for MEMS-Based Digital Writing Instrument. IEEE Sensors Journal, 10(10), 1543–1551. https://doi.org/10.1109/jsen.2010.2044995

6. Wang, J. S., Hsu, Y. L., & Liu, J. N. (2010, October). An Inertial-Measurement-Unit-Based Pen With a Trajectory Reconstruction Algorithm and Its Applications. IEEE Transactions on Industrial Electronics, 57(10), 3508–3521. https://doi.org/10.1109/tie.2009.2038339

7. Wang, J. S., & Chuang, F. C. (2012, July). An Accelerometer-Based Digital Pen With a Trajectory Recognition Algorithm for Handwritten Digit and Gesture Recognition. IEEE Transactions on Industrial Electronics, 59(7), 2998–3007. https://doi.org/10.1109/tie.2011.2167895

8. A Digital Pen with a Trajectory Recognition Algorithm. (2013). IOSR Journal of Electronics and Communication Engineering, 6(6), 69–75. https://doi.org/10.9790/2834-0666975

9. Amma, C., Georgi, M., & Schultz, T. (2013, February 24). Airwriting: a wearable handwriting recognition system. Personal and Ubiquitous Computing, 18(1), 191–203. https://doi.org/10.1007/s00779-013-0637-3

10. S, P. S., & B C, P. R. (2016, April). Hand Gesture Recognition System for Creating & Controlling Media Player using Mat Lab Tool. IOSR Journal of Computer Engineering, 18(04), 52–57. https://doi.org/10.9790/0661-1804055257

11. Álvarez-León, D., Fernández-Díaz, R. N., Sánchez-Gonzalez, L., & Alija-Pérez, J. M. (2017, November 2). Handwritten digit recognition using neural networks and dynamic zoning with stroke-based descriptors. Logic Journal of the IGPL, 25(6), 979–990. https://doi.org/10.1093/jigpal/jzx042

12. Plamondon, R., & Srihari, S. (2000). Online and off-line handwriting recognition: a comprehensive survey. IEEE Transactions on Pattern Analysis and Machine Intelligence, 22(1), 63–84. https://doi.org/10.1109/34.824821

13. Tuba, I., Tuba, U., & Veinović, M. (2023). Classification methods for handwritten digit recognition: A survey. Vojnotehnicki Glasnik, 71(1), 113–135. https://doi.org/10.5937/vojtehg71-36914

14. Analog Devices "ADXL335", https://www.analog.com/media/en/technical-documentation/data-sheets/adxl335.pdf

15. Atmel, "8-bit AVR Microcontroller with 16K Bytes In-System Programmable Flash", https://ww1.microchip.com/downloads/en/DeviceDoc/doc2466.pdf

16. Digi, "XStream RF Module", https://ftp1.digi.com/support/documentation/ds_xstream_modem.pdf

Implementation of Extracting Electrical Energy from Solar Energy in Simulink

Violina Deka
Lecturer
Kamrup Polytechnic
Baihata Chariali, Assam
✉ violinazzdeka@gmail.com

ABSTRACT

This paper is mainly focused on a solar energy based electrical system based on transistors (basic electronic switch) which is normally not used at present in household electrical systems but have the capability to significantly reduce the power loss which in turn will increase the efficiency. The entire system is designed on Simulink using photovoltaic (PV) arrays. Simulink is an add-on product of MATLAB which helps to design, simulate and analyze real time systems using Graphical User Interface (GUI). Simulink helps to produce an "up-and-running" model that would otherwise require long durations to implement in laboratories and finally in the practical world. After examining the proper behaviour of each of the circuit elements in the entire subsystem, efforts can be made to implement it practically. The final result revealed that the expected and ideal simulation result can be obtained showing that it can be physically implemented even in real life situations using discrete components.

KEYWORDS : *Converter, Inverter, PV array, Simulink, Solar energy.*

INTRODUCTION

When solar energy is absorbed by materials which are sensitive to sunlight (also called photoactive materials), the electrons acquire enough energy to become free from their respective atoms and move about the entire region of the material. This results in the production of electricity and the effect is called photovoltaic effect. These photoactive materials are called solar cells. A photovoltaic cell or a solar cell is an electrical device that converts the solar energy directly into electrical energy by means of photoelectric effect . With the advent in technology, solar cells continue to evolve . The recently developed Organic PV cells have the potential to revolutionize the solar energy industry due to their low production costs, and ability to produce thin, flexible solar cells .

The characteristics of a solar cell like current, resistance or voltage varies with the amount of sunlight that is incident upon it. It is both a physical and a chemical phenomenon which requires three basic attributes.

- Absorption of light energy by the materials resulting in the generation of electron-hole pair.

- Separation of opposite charge carriers.

- Separately extracting the carriers in an external circuit.

A collection of solar cells is called a solar panel. These solar panels spread over a large area and can work together to provide enough power to be utilized for meaningful purposes. More is the amount of sunlight that hits the cell; more is the electricity it produces. Collection of solar panels is called solar array or PV array. Thus, PV array is the basic building block of a grid-connected PV system.

Solar photovoltaic (PV) systems are not difficult to be implemented. First the panels collect the sunlight and convert it into DC output with the help of a rectifier circuit entirely based on electronic switches. These signals are then fed into an inverter which will again make use of electronic switches, which converts the DC

into relevant grid-supported AC power. Various switch boxes are included for safety reasons, and the whole thing is connected via wires and passage.

METHODOLOGY

Solar energy is a resource which is eco-friendly; hence its use has been exponentially increasing over the past few years. Solar energy along with the use of photovoltaic cells is a boost to the mankind since it can be used to serve one of the basic requirements of human beings, that is, electricity.

The basic building block of the entire electrical system is given as shown below:
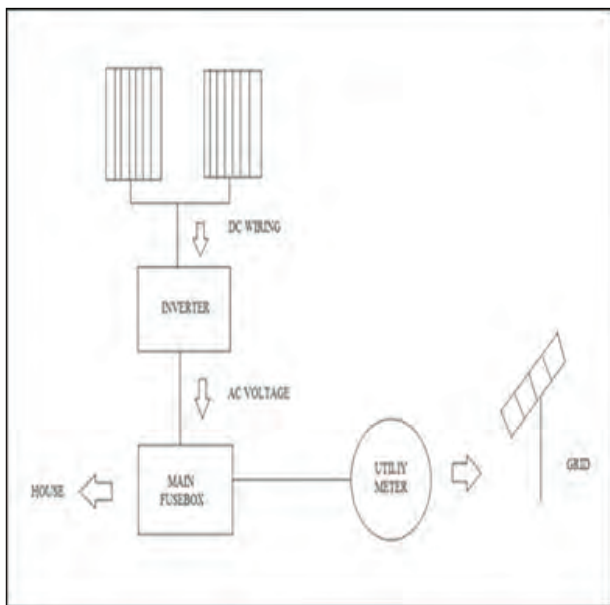
Fig. 1: A typical grid connected PV array

From the above block diagram, it can be seen that solar cells give DC power which can be converted into AC signals by means of an inverter. These AC signals are collected at the main fuse box from where the required amount of electricity that is required to run various appliances of household is sent in one direction and excess amount of electrical energy is fed back to the grid to be utilized for public services.

A solar inverter can connect to a string of solar panels or a single PV module (such inverters are known as micro-inverters). The microinverters achieve maximum efficiency via different control techniques . Although the amount of DC power generated depends upon the

number of modules connected, but the AC power to be utilized depends upon the inverter working upon it.

The PV panels of the solar systems produce fluctuating DC output because of variations in the irradiance level due to varying weather conditions. The Maximum Power Point of PV modules also change with atmospheric conditions and temperature of cells. Hence, a regulated DC-DC converter is exceptionally required for stable DC output voltage. In this case, a buck-boost converter is used. A buck-boost is a type of converter that maintains a stable DC output voltage . This means that if the solar radiance is low in a particular cloudy day, then the converter will boost the output voltage to a minimum value that is required to drive the inverter. Similarly in an extremely sunny day, the solar output will be very high and hence the converter will reduce the output voltage to prevent the inverter from burning out. The output of the buck-boost converter will then be used to drive the inverter circuit in order to convert the DC voltage into required AC signals.
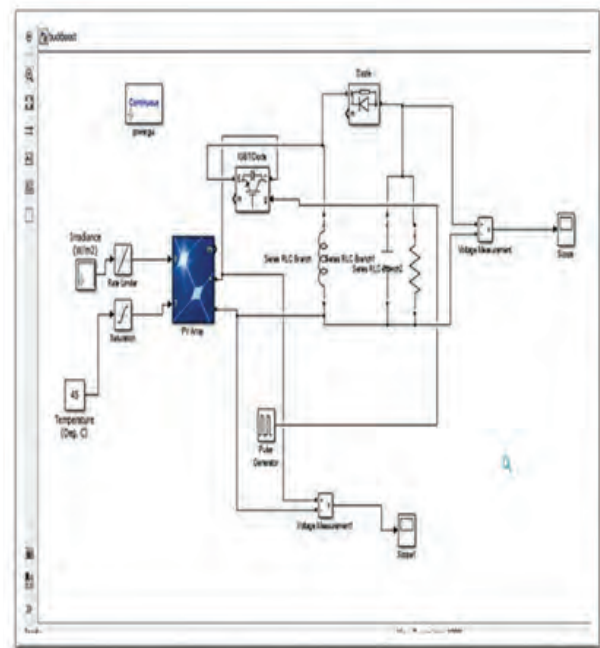
Fig 2: Application of a buck-boost converter to stabilize the varying output of PV array due to uneven irradiances.

Fig 2 shows a Simulink model wherein a PV array is used which is stimulated by two blocks namely irradiance and temperature . Both these two are physical factors which vary based on geographical

and climatic conditions of the region which in turn determine the amount of solar energy to be produced. Accordingly, the PV array will be activated and will produce a DC voltage which is fed onto a buck-boost converter. The buck boost converter is made up of an IGBT (Insulated Gate Bipolar Transistor) switch whose turn on/off frequency can be varied according to our requirement and a bunch of other circuit elements like resistor, inductor and capacitor (all connected in parallel) along with a power diode.

The output of the buck-boost converter will be used to drive the inverter circuit in order to convert the DC voltage into required AC signals. Since the voltage signals used in household are three phased, hence six IGBT's (or switches) are required to drive the inverter. However, before proceeding to the operation of the inverter, we will first extract the pulses that will be used to drive the IGBT's. Let us consider a distribution node that is in the place of requirement of three phase signals. Here, we are replacing the distribution node by a three phase programmable generator. This programmable generator generates three phased sinusoidal AC signals having varying phase, frequency and amplitude. These signals are then fed onto a Phase Locked Loop (PLL) that generates an output signal whose phase is relevant to the phase of the input signal. PLL can also be used to generate a signal whose frequency is a multiple of the original signal. In this case, let us consider the frequency of the signal to be synchronized to 50 Hertz. After synchronizing the phase and frequency, the signal is subjected to application of Park's Transformation.

Park's transformation is a type of mathematical transformation that rotates the reference frame of three phase signals to simplify the analysis of such circuits. Its main purpose is to reduce the three AC quantities (abc) into two DC quantities (dq0) and then required calculations are carried out on the DC quantities. In our simulation, the sinusoidal of the phase obtained from PLL is used for this purpose. This transformation is also known as direct-quadrature zero or zero-direct quadrature transformation. After this, Inverse Park Transformation is carried out to convert it back from 'dq0' frame to 'abc' reference frame by using the phase, locked by PLL.
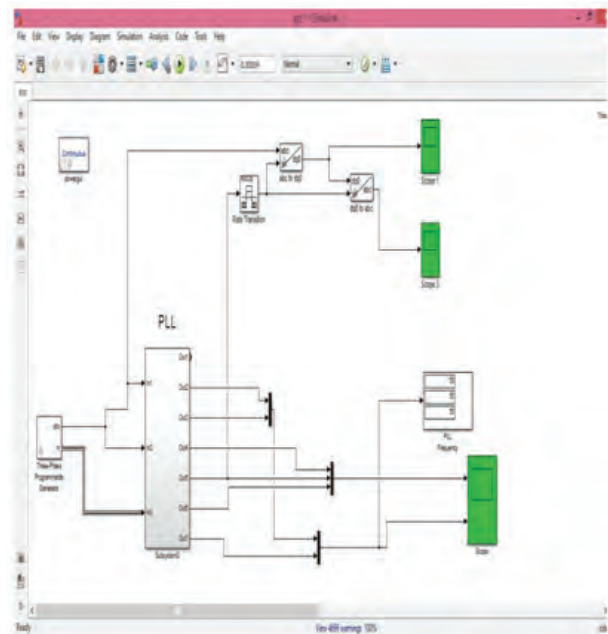
Fig 3: Use of PLL from three phase programmable generator and application of Park's and inverse Park's transformation
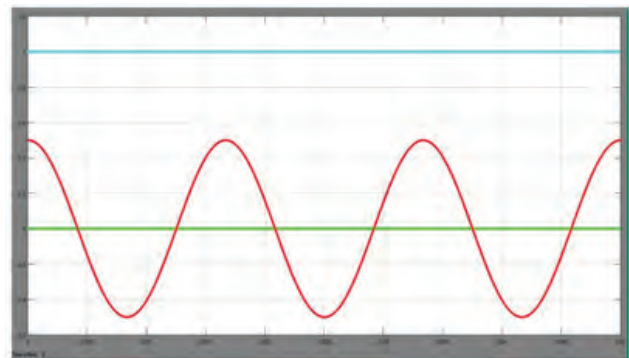
Fig 4: Output waveform for dq0 stationary frame
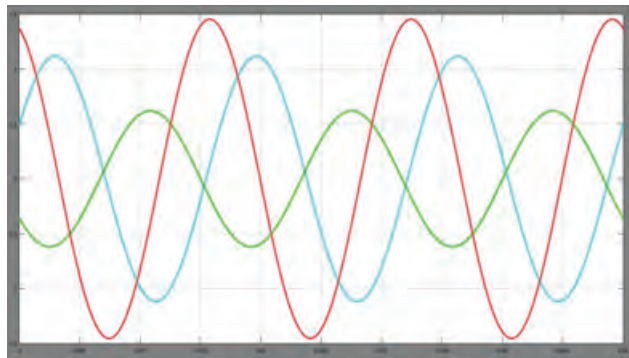
Fig 5: Conversion of signals back to abc rotating frame

The recovered three phase signals are then applied to the SPWM (Sinusoidal Pulse Width Modulation) converter. SPWM is the most widely used technique for generating true sine wave. The term 'sinusoidal' implies that the modulation signal shall be a sine wave or sinusoidal signal which is compared with a high frequency triangular wave functioning as the carrier wave. Thus, the frequency of the carrier wave determines the frequency of the output voltage. This comparison operation is carried out with the help of a relational operator in Simulink. SPWM will produce a three-phase output signal which will be finally fed into the gate terminals of the inverter.

Fig 6: Recovered abc signal being fed into SPWM converter
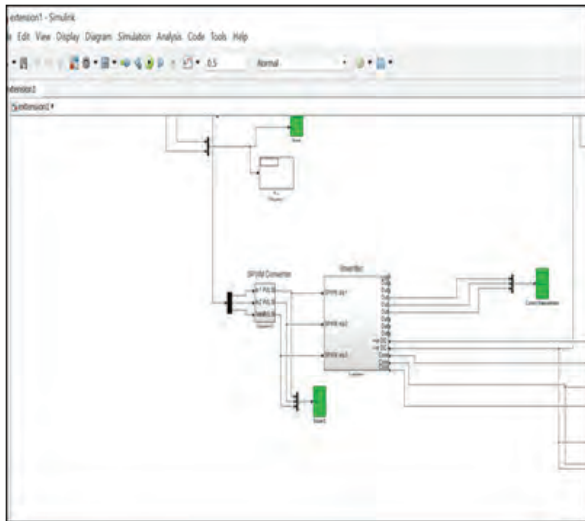
Fig 7: The three phase signals are applied to SPWM and then the required output is used to drive the inverter

The inverter is made out of six IGBT switches. The input of the inverter will be the DC output of the buck-boost converter while the switches will be turned on and off by the SPWM output. The output of the inverter will give us the required three phase AC signals that can be used for various loads present in a household or even the industries. On the Simulink model, we have connected the inverter output to a three phase dynamic load.

Fig 8: The inverter output is being fed to a three-phase dynamic load and the active power and reactive power is being recorded

Upon observing the voltage per unit, active and the reactive power, we find that it comes out to be 1 V per unit, 50 kiloWatt and 2.5 kilo VAR respectively as desired. For safety purposes, a three-phase circuit breaker is also connected between the three-phase programmable generator and the output of the three-phase inverter such that any undesirable increase between the generator output and the output obtained from the PV array will automatically result in breaking of the circuit.

RESULT AND DISCUSSION

In this paper, we have tried to carry out a practical representation of an entire solar based electrical household system wherein PV array of Simulink library is used as the input voltage source. A three-phase programmable generator has been used to turn on the

switches of the inverter which have been synchronized to obtain the required frequency of 50 Hz used in India. Also, synchronization of PV systems with the distribution network of household is one of the most crucial steps in designing power systems. When the PV array is turned on, the PV system takes certain time to initialize. During this time, all other components are getting to their normal operation mode from their initial mode. As a result of this, the output of the PV system is unstable and may result in spike in current distributed to the network due to difference in phase   . Hence, a circuit breaker is connected to avoid such spikes although many studies have already been carried out to maintain the difference in phase and to avoid such spikes.

After carrying out the inversion technique, the following have been observed as shown in Fig 8:

1. The voltage has been observed to be 1 V/unit. This can be adjusted and changed depending on our requirements by varying the parameter changes

2. The active power is observed as 50 kW. In the context of solar power systems, a 50-kW system is a substantial installation, suitable for commercial buildings or large residential setups. It can significantly reduce reliance on grid electricity and lower energy costs.

3. The reactive power is observed as 25 kVAR. The low reactive power in comparison to active power indicates efficient energy usage and a high-power factor, contributing to improved voltage regulation, reduced losses, and enhanced system stability. This low reactive power value implies minimal need for power factor correction, resulting in cost savings and optimal performance of electrical devices.

	Quantities measured at irradiance of 1000W/m² and temperature of 45⁰ C	Simulated result	Calculated result
1.	Active Power	50 kiloWatt	45-47 kiloWatt
2.	Reactive Power	25 kiloVAR	22.5-23.5 kiloVAR

3.	Frequency after applying PLL based inverters	50 Hz	50 Hz
4.	Frequency after applying a three-phase load (along with the PLL based inverter)	47.6 Hz	50 Hz

Fig 9: Comparison of the quantities obtained from Simulink and the calculated result.

From the table, it can be seen that the active power obtained in simulation is better as compared to the calculated result. However, the reactive power is somewhat more which may result in a slight decrease in efficiency of the circuit. However, this can easily be rectified by using a capacitor bank across the load in the practical circuit. Also, the frequency must be continuously regulated to obtain 50 Hz in the output of the inverter.

Hence, it can be seen that Simulink can be successfully utilized in building major electrical circuits. To obtain maximum efficiency from the PV array, Maximum Power Point Tracking can be used with varying algorithms . At present the installation cost of solar energy is high and its efficiency is low. With the advancement in technology, cheaper versions of PV arrays have been started to develop which will lead to a major boost in the energy sector if fully utilized.

CONCLUSION

We came across PV modules or arrays which serve as a useful component for supply of clean, renewable source of energy. This energy can be used for meeting various light energy requirements. This energy can also be used for running various machines and equipment in industries which are solely dependent on electricity for their operation. Although electricity can be produced by various methods such as wind energy and hydroelectricity, but both these procedures have some limitations such as:

* Wind energy can be utilized where the weather is prone to wind and

* Hydroelectricity is being produced by dams that comprises of turbines.

Hence, solar energy is considered beneficial over all such sources of energy.

REFERENCES

1. Athil S. Al-Ezzi and Mohamed Nainar M. Ansari (2022), "Photovoltaic Solar Cells: A Review", Applied System Innovation 2022, Volume 5, Article-4.

2. Justyna Pastuszak and Pawel Wegierek (2022), "Photovoltaic Cell Generations and Current Research Directions for Their Development", Materials 2022, 15(16)

3. Zahra Golshani, Faezeh Arjmand, Shahab Maghsoudi, Seyed Mohammad Ali Hosseini (2023), "Fe2O3–NiO doped carbon counter electrode for high-performance and long-term stable photovoltaic perovskite solar cells", Journal of Materials Research and Technology, Volume 23.

4. Neeraj Kant, Pushpendra Singh (2022), "Review of next generation photovoltaic solar cell technology and comparative materialistic development", Materials Today: Proceedings, Volume 56, Part 6

5. Ebru Kondolot Solak and Erdal Irmak(2023), "Advances in organic photovoltaic cells: a comprehensive review of materials, technologies, and performance", RSC Advances, Issue 18.

6. Sean Ritson and Ahmad Elkhateb (2020), "An Overview of Microinverter Design Characteristics and MPPT Control, Queen's University Belfast - Research Portal

7 Diego Rojas, Javier Munoz, Marco Rivera and Jaime Rohten (2021), "Review of Control Techniques in Microinverters", Sensors Vol. 21, No.19

8. D. M. Scholten, N. Ertugrul and W. L. Soong (2013), "Micro-inverters in small scale PV systems: A review and future directions," Australasian Universities Power Engineering Conference (AUPEC), Hobart, TAS, Australia, 2013, pp. 1-6.

9. Vytautas Adomavicius, Gintvile Simkoniene and Artem Dedenok (2024), "Possibilities and benefits of using photovoltaic power plants with microinverters in rural areas", International Scientific Conference Engineering for Rural Development

10. Muhammad H. Rashid,Power Electronics Circuits, Devices and Applications, Academic Press, 2017.

11. Lahyan, Z., Abbou, A. (2023). Modelling and Simulation of PV System Grid Connected with 100 KW Rated Power. In: Motahhir, S., Bossoufi, B. (eds) Digital Technologies and Applications. ICDTA 2023. Lecture Notes in Networks and Systems, vol 668. Springer, Cham.

12. Muhammad Umair Akhtar and M. Tariq Iqbal (2024), "Modeling and Simulation of Grid-Tied Three-Phase PV System in Lahore, Pakistan", European Journal of Electrical Engineering and Computer Science (EJECE)

13. P. Chandra Babu, Devineni Gireesh Kumar, Nagineni Venkata Sireesha, Mukesh Pushkarna, B. Venkata Prashanth, DSNMRAO, Hossam Kotb, Kareem M. AboRas, Mohit Bajaj, Sadam Alphonse (2023), "Modeling and Performance Analysis of a Grid-Connected Photovoltaic System with Advanced Controller considering Varying Environmental Conditions," International Journey of Energy Research

14. Ioan-Viorel BANU, Marcel ISTRATE. (2012) "Modeling and simulation of photovoltaic arrays", Research Gate Publications

15. Snehamoy Dhar, R Sridhar, Varun Avasthy, (2012) "Modeling and Simulation of Photovoltaic Arrays", National Power Systems Conference, IITK.

16. I. H. Altas and A.M. Sharaf (2007), "Photovoltaic Array Simulation Model for Matlab-Simulink GUI Environment," 2007 International Conference on Clean Electrical Power, ICCEP '07. 341 - 345. 10.1109/ICCEP.2007.384234.

17. JiaqiWu, Miao Han, Miao Han and Meng Zhan (2024), "Transient synchronization stability of photovoltaics integration by singular perturbation analysis", Frontiers in Energy Research, Volume 12.

18. Chengzhi Liu, Tiezhou Wu, Junchao Zhu, Ran Wei, Yang Wu and Aina Tian (2024), "A transient reactive power control strategy of PV-ESS enhances the system transient stability" Journal of Energy Storage, Volume 92.

19. Dieu Seul ASSALA, Haoyong CHEN, Ping YANG, Yongzhi CAI and Yongxia Han. (2014) "Synchronization Effects on Power Transients in Distribution Networks with Grid Connected Photovoltaic Generation", IEEE PES Asia-Pacific Power and Energy Engineering Conference (APPEEC).

20. Zhen Wang, Kaihua Xi, Aijie Cheng, Hai Xiang Lin, André C.M. Ran, Jan H. van Schuppen, Chenghui Zhang (2023), "Synchronization of power systems

under stochastic disturbances," Automatica, Volume 151, 2023.

21. Bidyadhar Subudhi and Raseswari Pradhan (2013), "A Comparative Study on Maximum Power Point Tracking Techniques for Photovoltaic Power Systems", IEEE Transactions on Sustainable Energy, Vol.4, No.1

22. Modupeola Dada and Patricia Popoola (2023), "Recent advances in solar photovoltaic materials and systems for energy storage applications: a review", Beni-Suef University Journal of Basic and Applied Sciences, Vol 12, No 66.

23. Shaik, F., Lingala, S.S. & Veeraboina, P. (2023), "Effect of various parameters on the performance of solar PV power plant: a review and the experimental study" Sustainable Energy Research 10, 6 (2023)

Power Quality Enhancement in Radial Distribution System Using Krill Herd Optimizer

Ashokkumar Lakum
Assistant Professor
Electrical Engineering Department
Lukhdhirji Engineering College
Morbi, Gujarat
✉ aclakum@lecollege.ac.in

Mitesh Sathvara
Assistant Professor,
Electrical Engineering Department
L. D. C. E.
Ahmedabad, Gujarat
✉ miteshjsathvara@gmail.com

Mahesh Pandya
Associate Professor
Electrical Engineering Department
Lukhdhirji Engineering College
Morbi, Gujarat
✉ pandyamh.lec@gmail.com

Rakesh Parmar
Assistant Professor
Information & Technology Department
Lukhdhirji Engineering College
Morbi, Gujarat
✉ rakeshparmar.it@lecollege.ac.in

ABSTRACT

To improve the power quality (PQ) in radial distribution systems (RDS), this paper presents a krill herd optimizer (KHO). The harmonics is the main concern of the PQ. Nonlinear loads (NLs) inject the harmonics into the RDS. By using power filters the harmonics are minimized up to standard limits. Here, active power filters (APFs) are placed with proper size to minimizing the harmonics and improvement in PQ. The KHO is utilized to optimize the size of APF at proper placement. Inspired by natural processes, the KHO algorithm has balanced exploration and exploitation characteristics. Subject to inequality constraints, the optimization's goal is to minimize the APF current. The simulation is done on the IEEE-69 bus RDS in order to assess the performance of the KHO. A comparison study is carried out using the adaptive particle swarm optimization (APSO1) and the APSO2 algorithms. The simulation results validate the KHO algorithm's stability and efficacy in solving the given optimization problem for given circumstance.

KEYWORDS : *Active power filter, Krill herd optimizer, Power quality.*

INTRODUCTION

As power electronics devices are so essential to modern life, there is a growing dependence on them. Examples of these devices include light-emitting diodes, compact fluorescent lamps, inverters, dimmers, variable speed drives, constant power supplies, mobile phones, and personal computers. However, harmonic pollution rises as a result of these gadgets' nonlinear features. As such, users' and suppliers' concerns about harmonics in power quality (PQ) are growing more widespread. These harmonics have a negative impact on distribution systems' performance, which emphasizes how crucial it is to address these problems [1]. Several

methods for harmonics mitigation are covered in [2]. Power filters are used to reduce or mitigate the harmonics. There are generally two power filters, and their combinations are used to improve the PQ in radial distribution system (RDS) :(i) passive filter, (ii) active power filter (APF), and (iii) hybrid power filter. Passive filters have the advantages of simple construction and low cost, but they become bulky when harmonics are higher.

Moreover, the passive filter is to be changed when load harmonics are changed and has a resonance problem. Conversely, APF can overcome the problems of passive filters, but it is complex and costly.

In order to prevent harmonics, APF injects nonlinear current into the RDS. It injects equal and opposite current according to the rating of nonlinear load. If the nonlinear load's rating high, the APF current is also high. Because an APF's efficacy is directly related to its rating at the time of installation, it is essential to size and placement them correctly in order to save cost [3]. It directs that there is a need of an optimization algorithm to solve the problem.

Furthermore, achieving maximum performance requires satisfying standard limitations such as individual and total harmonic distortion in voltage (IHDv) and (THDv) as per IEEE standard [4].

BACKGROUND

To maintain the stability, dependability, and effectiveness of contemporary power distribution networks, research on the proper positioning and rating of APFs in RDS is crucial. Enhancing PQ and reducing harmonics are critical as renewable energy sources and non-linear loads are integrated more and more into RDS. APF placement and sizing can minimize harmonic distortions, cut down on power losses, and improve voltage stability in RDS, all of which contribute to improving the distribution network's overall performance. The importance of APF placement and sizing optimization in improving PQ and grid dependability has been underlined in recent studies [5-7] by highlighting the necessity and requirement of further research in this field.

To decrease the price of APF; optimization technique is required. As a result, numerous optimization strategies have been put forth, including PSO [8]. A genetic algorithm [9] is also used. A harmony search [10], and firefly algorithm (FA) [11, 12] are also utilized for this problem, and recently grey wolf optimizer [13] etc.

According to no free lunch theorem (NFL) [14], no technique is able to provide the best answers for every kind of optimization issue. Researchers employ new algorithms since the performance of any algorithm can differ depending on the kind of challenge. With that, a recently developed Krill Herd optimizer (KHO) is utilized here. The KHO method aims to mimic the effective exploration and exploitation of solution spaces found in nature by taking inspiration from the collective behavior observed in krill swarms [15].

Candidate solutions in this approach are modeled as individual krill in a population, each having a place in the search area and a corresponding fitness score that indicates the value of the result. Three behaviors control krill movement: repulsion to prevent crowding, attraction to better solutions, and random exploration. The relationships between krill individuals, which are impacted by the distances and quality of solutions, organize these activities.

Advanced optimization approaches used in a variety of sectors include the adaptive PSO (APSO1) and the APSO2. By using adaptive techniques and dynamically altering parameters to improve convergence speed, APSO1 improves particle swarm optimization. This method is further improved by APSO2, which adds more adaptation mechanisms for improved efficiency and resilience when tackling challenging optimization situations [16].

Here, the use of KHO algorithm has been important in resolving the optimization issues raised by various field like; electrical, mechanical, IT and even botany [17-21]. In recent literature, the effectiveness of KHO in solving difficult situations has been thoroughly documented. For example, KHO has been effectively used in the field of power systems [17, 22]. These newer uses highlight the KHO algorithm's adaptability and stability in handling a range of optimization challenges.

KHO's performance is evaluated using computational tests; the fitness function's best value comparisons with APSO1 and APSO2. For KHO, APSO1, and APSO2, the IEEE-69 RDS system is employed and simulated for finding the most suitable value of APF current for considered RDS, NL and optimization parameters.

This paper is structured as: In the next section formulation of problem is presented; after analysis and discussion of results are written; and concluded with future scope in the last section.

PROBLEM FORMULATION

This section covers load flow with harmonics (HLF), APF, and RDS modeling. Using KHO, objective function with constraints is developed to enhance PQ by reducing harmonics i.e. THDv within standard limits.

Distribution system

As per [23], the impedance of RDS is modeled. The distribution line's inductive reactance is dependent on the order of harmonic frequency.

$$Z^{(h)} = R + jX_L{}^{(h)} \qquad (1)$$

In the equation provided, the variables, and represents resistance and inductive reactance of the RDS. Here, h denotes order of harmonic.

Active Power Filter

The APF is represented as a NL current source. The APF produces a current that is equal in magnitude but opposite in phase to the harmonic current it aims to mitigate [23-25]. The APF phasor model can be expressed as

$$I_{ft}{}^{(h)} = I_{ft,r}{}^{(h)} + jI_{ft,im}{}^{(h)} \qquad (2)$$

In this context, $I_{ft}{}^{(h)}$ is APF current, $I_{ft,r}{}^{(h)}$ is the real part. The $I_{ft,im}{}^{(h)}$ is the imaginary part of APF current.

HLF

For the analysis of harmonics, the HLF approach based on network topology is employed [26]. The BIBC matrix and the BCBV matrix are the two relationship matrices that constitute the foundation of this technique.

Objective Function

An integral component of the optimization procedure is the objective function (OF). It is a constrained nonlinear issue. The APF current is the decision variable in this case. The APF current serves as the goal function. Because cost of APF increases as its current rating increases, it is crucial to decrease APF's current.

In order to enhance the PQ in RDS using APF, three constraints have been taken into account; (i) THDv, (ii) IHDv, and (iii) maximum current of the APF (Iapf max). The first two standard limitations are mandated by IEEE Standard 519 and the third constraint, which are dependent on the NL current [4].

An objective function is illustrated as,

$$OF_{in} = \min \sum_{m-1}^{\hat{n}} \sqrt{\sum_{h-2}^{H} \left| I_{n,m}^{h} \right|^2} + DP \qquad (3)$$

In this equation, H represents the highest order harmonic. DP denotes the dynamic penalty factor. There is m stands for the bus number, while n indicates the total buses.

The objective function is subjected to following constraints:

$$THD_V - 0.05 \le 0$$
$$IHD_V - 0.03 \le 0$$
$$I_n \le I_{n,MAX} \qquad (4)$$

Figure 1, shows the flowchart that explains how to use KHO to improve PQ in RDS. As shown in the flowchart, initializing system data and setting the objective function and limitations for reducing harmonic
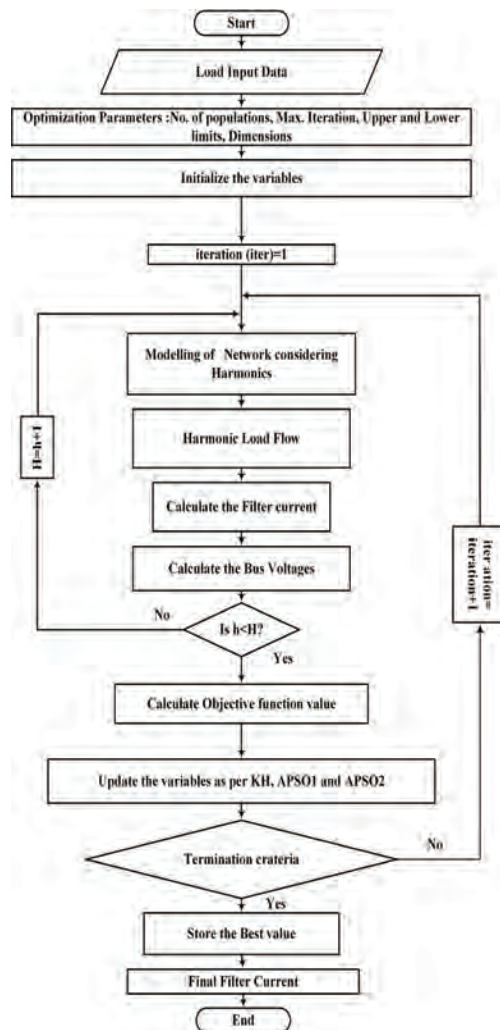
Fig. 1 Flowchart
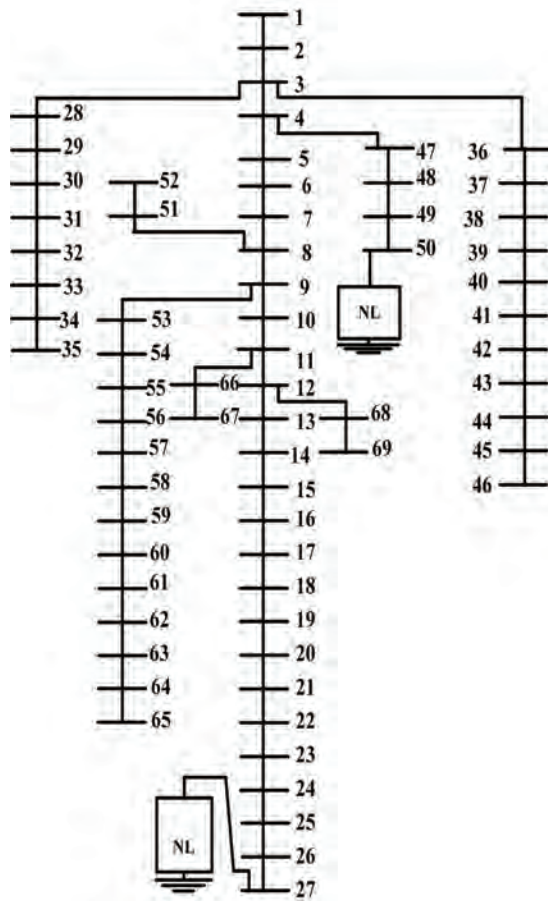
Fig. 2 IEEE-69-bus RDS

distortion a RDS first. Next, a population of solutions is created by initializing the APSO1, APSO2 and KHO. Then, modeling of all the considered RDS and other parameters in harmonic environment is done. HLD is coupled with optimization algorithms. The fitness of each solution is assessed, and the krill herd placements are iteratively adjusted, taking constraints into consideration, depending on the best options.

The best location and size for APFs are achieved by continuing this process until the optimization criteria are satisfied. To assure power quality improvement, the optimal option is verified by simulations. The APF current is stored.

STEPS FOR SIMULATION

Load the relevant data, including the harmonic spectrum, from the test system first. In the following step, define the optimization settings.

Proceed to step 3, where the inputs are created into a model of the harmonic environment.

The step 4 should involve the HLF analysis. Step 5 should involve computing the THDv utilizing only the NLs. Prior to moving on to step 6, integrate the APF into the system. In step 7, incorporate the APF into the load flow harmonics.

Step 8 involves figuring out the lowest feasible APF current using the KHO. Step 9: Set terminating crateria of algorithm.

Repeat these procedures for APSO1 and APSO2 also.

RESULT

This section deals with the result analysis and discussion.

The IEEE-69 bus system has two NLs at buses 27 and 50 as shown in Fig. 2. When a single NL is present at a single node, the harmonic influence is magnified and affects all 69 buses in the system.

In the absence of an APF, HLF computes the THDv% for each bus, and Fig. 3 shows the findings.

The widespread influence of harmonics over the RDS is evident in the THDv readings of sixteen of the total sixty eight buses (excluding the first bus acts as a source bus). Surprisingly, only two buses have NLs whereas all buses display THDv. Total sixteen buses have THDv greater than 5%, which cannot meet the IEEE standard limit. It shows the poor PQ.

The buses 27 and 50 have NLs. Both have THDv values of 14.51% and 5.2%, respectively. As stated earlier paragraph, total 16 buses cross the 5% limits of THDv.

Above stats indicates RDS is highly harmonics polluted system. There is a requirement for harmonic filter/filters to achieve the IEEE standard limits. The APF/APFs is/are intentionally assigned to the same bus/es as the NLs; i.e. buses 27 and 50 simultaneously. The scenario is as; single APF at bus 27, single APF at bus 50 and APFs at both buses.

In the last paragraph the placement of APFs is discussed. Now the size/rating/current of APF/s is also an important criterion as it is directly proportional to the cost of APF/s. In this instance, the necessary APF current is determined by the KHO optimization procedure. The

general optimization parameters, maximum number of populations and iterations, are 40 and 100, respectively.

This procedure is thoroughly reproduced for the selected test system by following the steps indicated in the corresponding flowchart as shown in Fig. 1.

NLs (without APF) at 27 and 50

The NL is connected at bus 27 and 50, as seen in Fig. 2. These two NLs cause a significant harmonic distortion in the system. The highest THDv without APF is at bus 27 (14.51%). The THDv of bus 50 is 5.2 %.

APF on bus 27

The APF is connected at bus 27 in order to lower the THDv as much as possible. On the other hand, for THDv
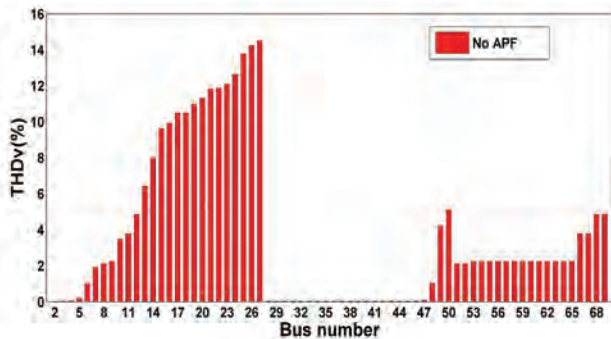
Fig. 3: THDv at all buses without APF

less than 5% at all buses, a single APF is insufficient. Fig. 4 illustrates that not all optimization strategies have reached a minimum value of APF current.

APF on bus 50

In this scenario same thing is observed as earlier case. NO algorithm is capable to fulfill the constraints and convergence.

APFs on buses 27 and 50

There are now two buses with APF, 27 and 50. The outcome of HLF using optimization methods is displayed in Fig. 5.

It displays each algorithm's convergence curve for the specified condition. Fig. 5 illustrates how the KHO calculates the minimum APF current. The APSO1 and APSO2 algorithms do not converge to obtain the lowest APF current, as demonstrated by this example.
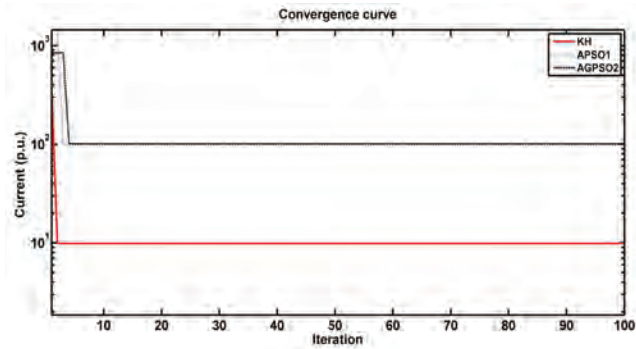
Fig. 4 Algorithm convergence curves while APF is at bus 27
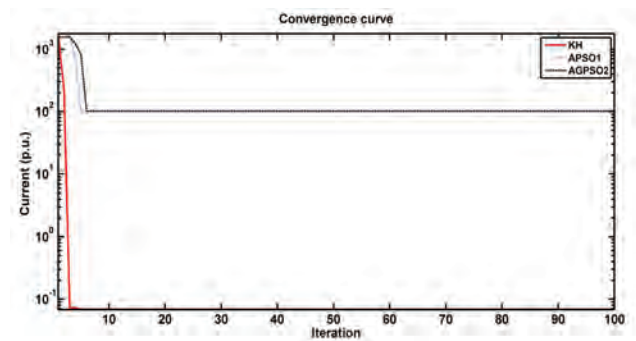
Fig. 5 Algorithm convergence curves when APFs are present at buses 27 and 50
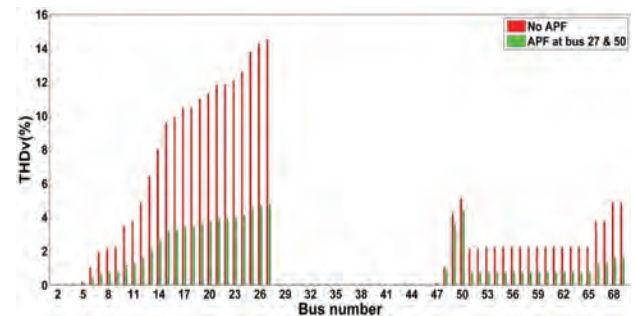
Fig. 6 THDv at every bus, both with and without APFs after optimization

Table 1 Comparison of Optimization Techniques

Bus	I_{apf} obtained by (p.u.)			Convergence
	OA1	**OA2**	**OA3**	
27, 50	0.0680	100	100	Only OA1

Conversely, the KHO algorithm delivers the lowest APF current under the specified parameters and effectively converges, as Fig. 5 shows. The computed APF current comes out to 0.0680 (p.u.). Nonetheless, the KHO method does converge successfully when the APF is

placed at bus 27 and 50; Under these conditions, APSO1 (100.7908 p.u.) and APSO2 (100.1319 p.u.) determined the APF current. It is regarded as inappropriate. It is tabulated in Table1. In this, OA1 stands for KHO, OA2 for APSO1 and OA3 for APSO2.

Figure 6 demonstrates that all of the system's buses now have THDv values that are less than 5% after the APFs were installed at buses 27 and 50. Notably, bus 27 and 50, which has the THDv of 14.5 % and 5.12%, respectively, without the APF, now have a THDv of 4.77 % and 4.73 % with the APFs in place, as the picture clearly demonstrates. The APF's bus number and rating plays a critical role in enhancing PQ in the RDS, as evidenced by the Fig. 6 that all buses meet the standard limit of THDv is less than or equal to 5%

CONCLUSION

In conclusion, this work explores the use of the KHO, APSO1, and APSO2 to enhance PQ in a RDS. Even with two NLS in the RDS, the IEEE-69 bus test system simulation successfully combines KHO, APSO1, and APSO2 with HLF, illustrating the extensive influence of harmonics. The measured THDv, which is more than 5% on sixteen buses, emphasizes the negative effects of harmonics on PQ. The bus with the highest THDv, 14.51% is 27. The critical role of APF placement is highlighted by the successful reduction of THDv in all buses below 5% achieved by the APF placement at Buses 27 and 50. It is remarkable that with just two APFs, THDv may be kept contained by the permitted limit at all buses of the RDS.

KHO successfully converges and satisfies the specified condition, yielding a minimum APF current of 0.0680 p.u. However, at Bus 27 and 50, APSO1 and APSO2 are unable to converge, indicating that KHO performs better in this specific scenario.

FUTURE SCOPE

In future, the PQ enhancement in RDS will be optimized through the use of new optimization algorithms, formulating multi-objective problem. Also, it can be implemented with integration of smart grid technology.

REFERENCE

1. G. J. Wakileh, Power systems harmonics: fundamentals, analysis and filter design: Springer, 2001.

2. J. Arrillaga and N. R. Watson, Power system harmonics analysis: John Wiley & Sons, 2004.

3. I. Ziari and A. Jalilian, "Optimal placement and sizing of multiple APLCs using a modified discrete PSO," International Journal of Electrical Power & Energy Systems, vol. 43, pp. 630-639, 2012.

4. "IEEE Recommended Practice and Requirements for Harmonic Control in Electric Power Systems," IEEE, New York, NY, 2014.

[5] H. Rezapour, F. Fathnia, M. Fiuzy, H. Falaghi, and A. M. Lopes, "Enhancing power quality and loss optimization in distorted distribution networks utilizing capacitors and active power filters: A simultaneous approach," International Journal of Electrical Power & Energy Systems, vol. 155, p. 109590, 2024.

6. A. Ebrahimi, M. Moradlou, and M. Bigdeli, "Optimal siting and sizing of custom power system and smart parking lot in the active distribution network," IET Renewable Power Generation, 2024.

7. C. R. Rao, R. Balamurugan, and R. K. R. Alla, "Artificial Rabbits Optimization Based Optimal Allocation of Solar Photovoltaic Systems and Passive Power Filters in Radial Distribution Network for Power Quality Improvement," International Journal of Intelligent Engineering & Systems, vol. 16, 2023.

8. I. Ziari and A. Jalilian, "Optimal allocation and sizing of active power line conditioners using a new particle swarm optimization-based approach," Electric Power Components and Systems, vol. 40, pp. 273-291, 2012.

9. R. Keypour, H. Seifi, and A. Yazdian-Varjani, "Genetic based algorithm for active power filter allocation and sizing," Electric Power Systems Research, vol. 71, pp. 41-49, 2004.

10. Z. W. Geem, J. H. Kim, and G. Loganathan, "A new heuristic optimization algorithm: harmony search," Simulation, vol. 76, pp. 60-68, 2001.

11. M. Farhoodnea, A. Mohamed, H. Shareef, and H. Zayandehroodi, "Optimum placement of active power conditioner in distribution systems using improved discrete firefly algorithm for power quality enhancement," Applied Soft Computing, vol. 23, pp. 249-258, 2014.

12. M. Farhoodnea, A. Mohamed, H. Shareef, and H. Zayandehroodi, "Optimum placement of active power conditioners by a dynamic discrete firefly algorithm to mitigate the negative power quality effects of renewable

energy-based generators," International Journal of Electrical Power & Energy Systems, vol. 61, pp. 305-317, 2014.

13. A. Lakum and V. Mahajan, "Optimal placement and sizing of multiple active power filters in radial distribution system using grey wolf optimizer in presence of nonlinear distributed generation," Electric Power Systems Research, vol. 173, pp. 281-290, 2019.

14. D. H. Wolpert and W. G. Macready, "No free lunch theorems for optimization," IEEE Transactions on Evolutionary Computation, vol. 1, pp. 67-82, 1997.

15. A. H. Gandomi and A. H. Alavi, "Krill herd: a new bio-inspired optimization algorithm," Communications in Nonlinear Science and Numerical Simulation, vol. 17, pp. 4831-4845, 2012.

16. S. Mirjalili, A. Lewis, and A. S. Sadiq, "Autonomous particles groups for particle swarm optimization," Arabian Journal for Science and Engineering, vol. 39, pp. 4683-4697, 2014.

17. M. Forghani, M. Soltanaghaei, and F. Z. Boroujeni, "Dynamic optimization scheme for load balancing and energy efficiency in software-defined networks utilizing the krill herd meta-heuristic algorithm," Computers and Electrical Engineering, vol. 114, p. 109057, 2024.

18. L. Cheng, Y.-G. Zhao, P.-P. Li, and L. Yan, "Sizing and Shape Optimization of Discrete Truss Employing a Target-oriented Krill Herd Algorithm," ASCE-ASME J Risk and Uncert in Engrg Sys Part B Mech Engrg, pp. 1-49, 2024.

19. A. Reddy, G. Shivamurthy, and M. Rajanna, "Energy-Efficient Clustering in WSN using Bacterial Foraging and Krill Herd Optimization," International Journal of Intelligent Systems and Applications in Engineering, vol. 12, pp. 225-235, 2024.

20. B. K. Bala, J. Sekhar, M. S. Al Ansari, and V. S. Rao, "Enhancing plant leaf disease detection: Integrating krill herd optimization-surf features and deep belief network," Journal of Intelligent & Fuzzy Systems, pp. 1-13, 2024.

21. S. Sugumaran, V. Sivasankaran, and M. Chitra, "Krill Herd and Feed Forward Optimization System-Based Routing Protocol for IoT-MANET Environment," Journal of Interconnection Networks, p. 2350030, 2023.

22. V. K. Gupta, S. K. Mishra, R. Babu, and A. K. Singh, "Solution of Reactive Power Planning with TCSC and UPFC Using Improved Krill Herd Algorithm," Transactions of the Indian National Academy of Engineering, pp. 1-13, 2023.

23. I. Ziari and A. Jalilian, "A new approach for allocation and sizing of multiple active power-line conditioners," IEEE Transactions on Power Delivery, vol. 25, pp. 1026-1035, 2010.

24. M. Shivaie, A. Salemnia, and M. T. Ameli, "A multi-objective approach to optimal placement and sizing of multiple active power filters using a music-inspired algorithm," Applied Soft Computing, vol. 22, pp. 189-204, 2014.

25. M. Shivaie, A. Salemnia, and M. T. Ameli, "Optimal multi-objective placement and sizing of passive and active power filters by a fuzzy-improved harmony search algorithm," International Transactions on Electrical Energy Systems, vol. 25, pp. 520-546, 2013.

26. J.-H. Teng and C.-Y. Chang, "Backward/forward sweep-based harmonic analysis method for distribution systems," IEEE Transactions on Power Delivery, vol. 22, pp. 1665-1672, 2007.

Sustainability Challenges of Sasthamkotta Freshwater Wetland-A Ramsar Site in South India

Shibu K
Assistant Professor
Department of Civil Engineering
College of Engineering Trivandrum
Thiruvananthapuram, Kerala
✉ shibukrishnanp@gmail.com

Drisiya J
Postgraduate Scholar
Department of Civil Engineering
College of Engineering Trivandrum
Thiruvananthapuram, Kerala

ABSTRACT

Wetlands are among the most productive ecosystems on our planet, providing a wide range of essential services to humans. Sasthamkotta Lake, a freshwater wetland and a Ramsar Site of international importance, satisfies the water requirement of half a million inhabitants of Kollam district is currently facing serious sustainability concerns like aerial and volumetric reduction, discharge of sewage into the lake, changes in the land use pattern, soil erosion, urbanization, eutrophication, faecal contamination, heavy metal contamination, alteration in groundwater recharge, construction of bore wells in the watershed area, acacia plantation in the fringes of the lake, land reclamation and mining in the adjoining areas of the lake which have led to habitat degradation. This study proposes multifaceted conservation measures like enforcing stringent existing rules and regulations, ensuring sustainable water supply to Kollam Corporation, ecosystem-based land use planning, control measures for erosion and sediment export, sustainable urban management, community engagement, native vegetation restoration, sustainable agriculture practices, regulation and monitoring mining activities, invasive species management, sustainable cultural approach and scientific interventions aimed at effective conservation initiatives with the help of the local community, government agencies and other stakeholders for the long-term rehabilitation of Sasthamkotta freshwater wetland.

KEYWORDS : *Sasthamkotta Lake, Sustainability Concerns, Conservation Measures*

INTRODUCTION

Wetlands are critical for sustaining biodiversity, regulating water flow, and providing key ecosystem services such as sanitation, flood management, and habitat for a range of species[1]. Such places are distinguished by any signs of water, whether permanently or seasonally, resulting in distinct habitats that support a diverse range of plant and animal species[2]. Freshwater wetlands, in particular, are crucial ecosystems that support an array of plant and animal life, help regulate water quality, and serve as critical habitats for various species, all of which contribute significantly to overall environmental health[3].They are primarily important habitats, serving as breeding grounds for a wide variety of species such as amphibians, waterfowl, and aquatic organisms[4]. Furthermore, as natural filtration systems, these wetlands improve water quality by absorbing pollutants and sediments, supporting water-cleaning processes[5]. Freshwater wetlands are important in maintaining water flow and preventing floods by absorbing surplus water during heavy rains and gradually releasing it. This function helps to keep water levels balanced, protecting adjacent communities and agricultural regions from the negative effects of flooding[6]. Despite their ecological reliability, wetlands contribute to the cultural as well as recreational features of communities,whichare linked with local customs, and providea location for ecotourism fishing,etc.[7]. Keralais known for its lush landscape and various ecosystems which preserve the unique biodiversity by providing habitat for native

plants and animals like Cavaborus and27 species of freshwater fish[8].Freshwater wetlands in Keralahave a significant role in serving water resources and natural storage[9].They also play an important role in sustaining biodiversity, improving soil fertility, promoting traditional farming methods, controlling water quality, and providing various ecosystem services that emphasizethe importance of its conservation. Hence, the sustainable conservation of such an ecosystem is critical in ensuring the health of the natural environment and the community that depends on it[10], [11].

Sasthamkotta Lakewas categorized as a wetland of international importance under the Ramsar Conventionin 2002 under Criteria 1(The lake is Kerala's largest freshwater lake with unique water that lacks ordinary salts, minerals, and metals. The lake has no water plants or flora.), Criteria 2(The wetland supports some fragile, endangered, and critically endangered species, including Puntius punctatus is critically endangered. Endangered Species: Horabagrus brachysoma. Vulnerable species: Parambassi Thomassi.), Criteria 7(The wetland supports many fish species including some indigenous fish species like Puntiusn ticto punctatus, Puntius sarana subnasutus, Horabagrus brachysoma, Etroplus suratensis, AplochEilus lineatus, Parambassi thomassi and Macrognathus guentheri) and Criteria 8(This wetland provides food, breeding grounds, and nursery habitat for 27 freshwater fish species)[12].
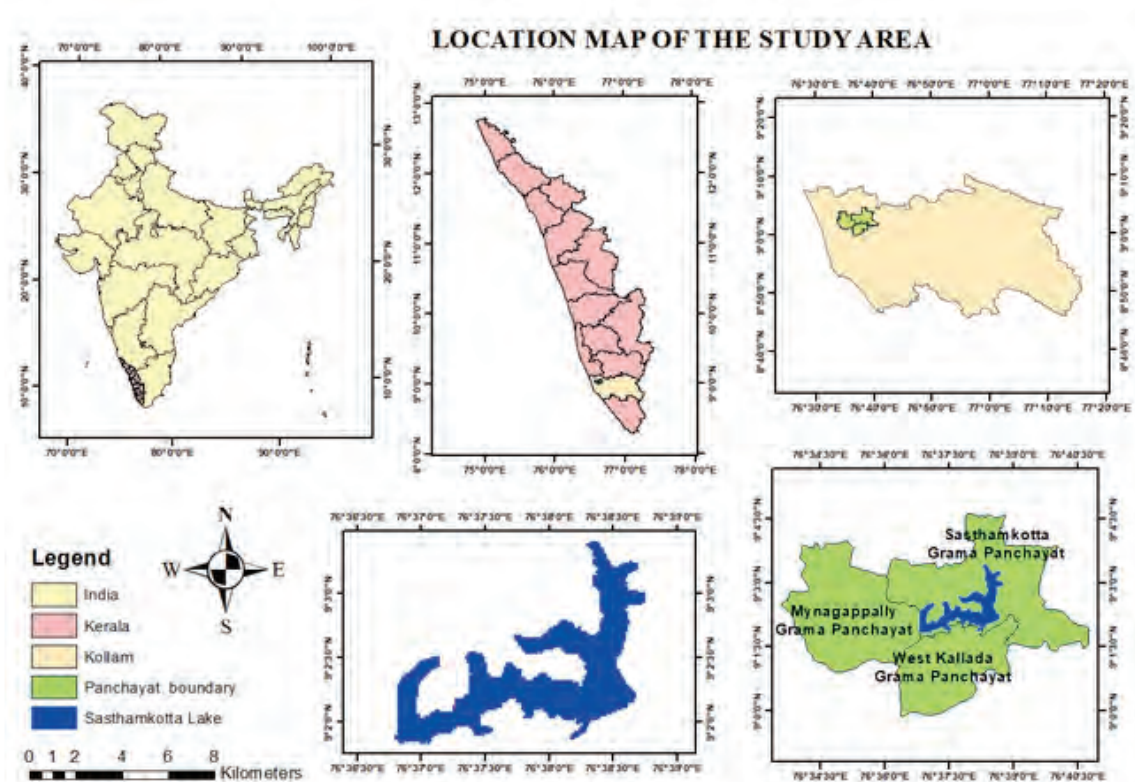
Fig. 1: Location Map of the Study Area

Sasthamkotta Lake is located between 9° 1' N and 9° 4' N latitude and 76° 36' 30" E and 76° 39' E longitude and situated in the Kollam district of Kerala. The Location map of the study area, created with ArcGIS 10.8 software resources is shown in Figure. 1. The catchment area of lake includes portions of Sasthamkotta Grama Panchayat, West Kallada Grama Panchayat, and Mynagapally Grama Panchayat situated in Kunnathur Taluk[13]. Steep hillocks encircle the lake's perimeter, except in the south, were low-lying, alluvial sediment-covered areas support paddy cultivation. Kerala Water Authority utilizes Sasthamkotta Lake to provide drinking water for the half million people of Kollam Municipality and its environs through an artificial

bund separating paddy fields from the lake[14]. The highest point of Sasthamkotta Lake is 32m aboveMean sea Level(MSL)and has a warm, humid, tropical climate. Most of the catchment area lacks topsoil, and the exposed subsoil has hardened to laterite[13]. The soil has limited porosity and weak structure, which results in negligible water infiltration and significant erodibility. Stormwater from the upper catchment and adjacent townships is discharged into the lake. Mixed coconut crops predominate, and rubber, bananas, paddy, and other crops are the main land uses, along with both residential and business activities. The adjacent lateritic hillocks are also mined for building materials, which adds to the lake's asymmetrical structure and its

inverted "F"-shaped portions that extend at different spots[15]. The location features around the wetland are shown in Figure. 2. The lake provides vital habitat for a varied range of flora and fauna, contributing significantly to the preservation of regional biodiversity. Residents, in particular those involved in conventional fishing practices, rely on the lake for living, making its conservation critical to long-term economic activity[16]. The lake also helps to improve water quality, preserve cultural heritage, and build resistance to climate change. Hence, Sasthamkotta Lake requires urgent conservation measures due to its critical role in conserving biodiversity, sustaining local livelihoods, and delivering key ecosystem services.
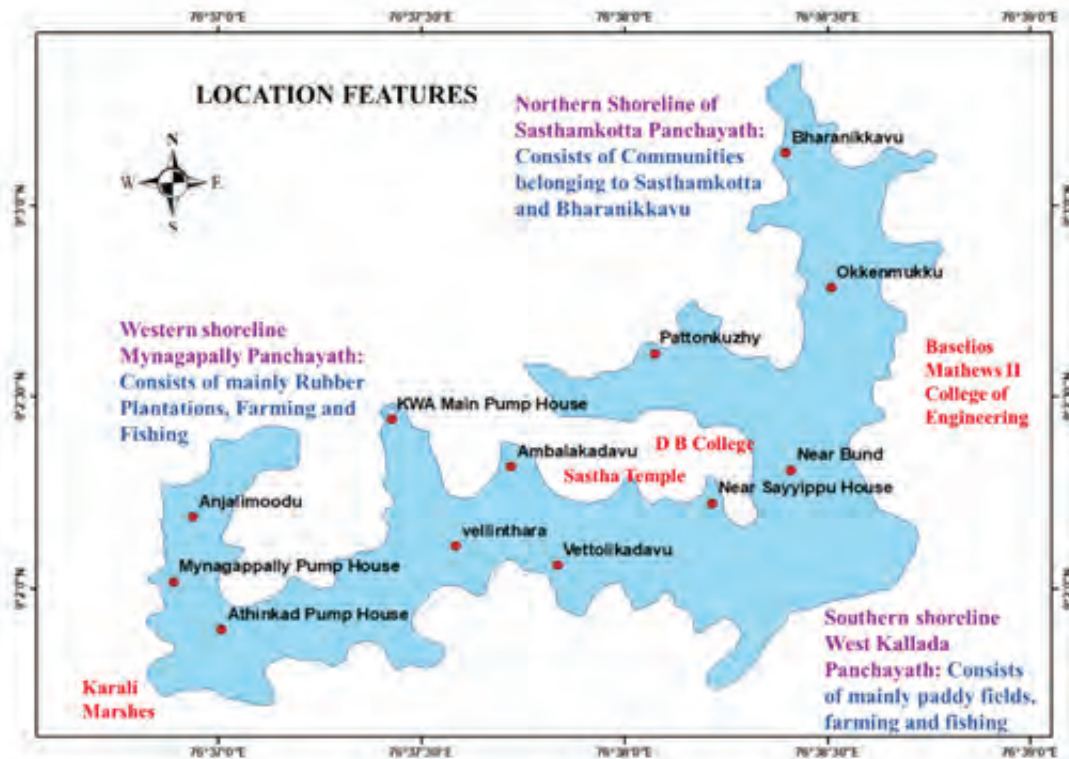
Figure. 2 Location Features of the Study Area

MAJOR ISSUES FACED BY THE SASTHAMKOTTA FRESHWATER WETLAND

Sasthamkotta Lake has several important conservation concerns that demand attention and concentrated efforts to protect the long-term health and viability of this freshwater environment. The sustainability concern of

Sasthamkotta freshwater wetland requires a thorough study of many hydrological elements such as aerial coverage, volume change, water level changes, storage variations, and water balance. Aerial spread denotes the geographic spread of a wetland, highlighting the importance of preventing encroachments as well as alterations to land use.It was observed that the water

spread area of Sasthamkotta Lake reduced by 15.56% during 1973and 2021,as a result of scanty rainfall and increased water abstraction and the reduction was more visible near the bund region and the western shoreline of the lake[17].Volume change in a wetland refers to variations in the degree to which water is present[18]. The volume of Sasthamkotta lakewas reduced by 39.43% between 1997 and 2021[19] as a result of the above factors coupled with rapid urbanization in the nearby Sasthamkotta town and Bharanikkavu town. Monitoring and regulating volume variations is critical to maintaining the wetland's ecological equilibrium. Excess withdrawals, pollution, or disruption in input can cause undesirable volume changes, emphasizing the significance of conservation efforts in maintaining a healthy water balance[20].Conservation efforts should focus on preserving natural water level variations, which are critical for supporting different ecosystems, and avoiding negative consequences on flora and wildlife, Human actions, such as unauthorized water extraction or land use changes, have the potential to disturb natural water levels and emphasizing the importance of sustainable practices. Storage change refers to the ability of the wetland to store and release water, Sasthamkotta Lake's quantity of storage is critical for controlling water flow, preventing flooding, and meeting local water demands[21]. It was observed that the storage capacity of the lake was 16.14Mm3and 15.87Mm3in the year 1997 and 2005 respectively and thereafter the same reduced to 9.02Mm3 in the year 2013[19].

Land Use Land Cover (LULC) alterations can significantly impact the sustainability of Sasthamkotta Lake. Agriculture areas, built-upareas, open land, grassland, trees, and marshy land are the identified land use classes in the watershed of Sasthamkotta Lake[15]. The changing terrain around the lake can have an impact on its ecological health and general sustainability.It was observed that vegetation and water spread area reduced by 75.8% and 17.78% respectively between 1973 to 2021 [15] and predominant reduction was observed in the 100m buffer area which directly indicates the human encroachment in the sensitive zone of the catchment area. Alteration in land use, which includes deforestation or development, may lead to elevated sedimentation in lakes. Sedimentation lowers water quality by adding pollutants and restricting light penetration[22].Urbanization, agricultural growth, and growth in infrastructure may result in an invasion of the lake's perimeter. Land use alters the natural habitats are frequently displaced by constructed constructions, leading to the loss of habitat for flora and animals. Changes in patterns of land use, particularly increasing impervious surfaces caused by urbanization, may result in greater runoff. This runoff introduces contaminants and nutrients entering the lake, altering its water chemistry[19].LULC changes may interfere with climate change, increasing the lake's vulnerability, shifts in land use which can have an impact on precipitation patterns, temperature shifts, and extreme weather. The Annual Average Rainfall (AAR) in the State of Keralaover the last 100 years was 2199.9mm,and the same during 2015 and 2016 (drought period) year 2015 was 2015 mm and 1510mm respectively[19].

Soil erosion and sediment export in the Sasthamkotta wetland watershed have a substantial impact on ecosystem health[23]. Soil erosion is the act of detaching and transporting soil particles, while sediment yield is a measure of sediment carried by water[13]. The Sasthamkotta wetland watershed's soil erosion is caused by a variety of causes, notably intensity of rainfall, slope gradient, land use habits, and vegetation cover and was visible near the D B College. Uncontrolled or incorrect land use, like deforestation or cultivation, can contribute to soil erosion by diminishing vegetation's protective cover. The wetland's sediment output fluctuates by the sedimentation sources in its catchment region. Sediments can enter wetlands via runoff from farmland, building sites, and urban areas[24]. Excessive soil erosion and sediment yield can degrade the water quality of Sasthamkotta Lake. Sediments frequently transport contaminants, nutrients, and organic debris, influencing the purity and chemistry of water[25]. In 2007, sediment quality assessments revealed that clay was the main constituent (47-72%), followed by silt (26%-52%), and sand contributed the least[26]. The pH of surface sediment varied between 4 to 7, pointing to acidic to neutral properties. Organic carbon levels were found to be low (0.034 - 2.64 mg/g). Sediment phosphorus levels were low, ranging from 0.005 to 0.204 mg/g. These values indicated low primary productivity (ranging from 0.072 to 4.5 mg/C/

m3/day)[27]. The assessments showed that phosphorus was selectively absorbed in water, while iron and manganese were released into interstitial waters[28]. This may destabilize the aquatic ecology and jeopardize the lake's biological balance. Excessive sedimentation leads to habitat destruction in wetlands and reduces breeding and feeding opportunities for aquatic creatures affecting biodiversity as well as ecological health[29].

Anthropogenic activities in the Sasthamkotta wetland watershed are also one of the major threats for reduction in water quality. Agricultural runoff, industrial emissions-untreated wastewater from the Sasthamkotta and Bharanikavu towns, and inappropriate waste disposal affect the quality of water. Water quality data indicates that the lake is well-oxygenated, nutrient-poor, and neutral to weakly alkaline. BOD(Biological Oxygen Demand) levels frequently exceed the 3 mg/L threshold. The lake water had sufficient Dissolved Oxygen (DO) levels during pre-monsoon, monsoon, and post-monsoon seasons, except at Vettolikkadavu station during post-monsoon, which had the lowest DO concentration (1.7 mg/L). BOD levels were higher during the pre-monsoon season compared to that of monsoon and post-monsoon seasons[30], [31]. Variations in the water quality indicators, such as pH and nutrient concentration, have a direct impact on the ability of a lake to maintain its diverse aquatic life[14], [30], [31].

The rampant presence of Faecal Coliform (FC)in Sasthamkotta freshwater wetland is a serious threat that requires a quick response. It was observed that 600MPN/100mL(MPN-Most Probable Number) of FC and 1400 MPN/100mL of Total Coliformwere observed during the monsoon season and the same may be due tothe runoff from the catchment and the surrounding areas which are being drained directly into the lake[14], [30]. Inadequate sanitation practices cause harmful bacteria to enter the water. This threatens both the ecology of the lake for drinking water and other supplies[32].The growth of population and rapid urbanization result in increased production of sewage. The unprocessed sewage that is dumped in the lake aggregates the contamination much more[33].

Sasthamkotta Lake is significant for carbon sequestration as it serves as a biological sink for carbon dioxide from the atmosphere[34]. The adjacent vegetation, which is primarily made up of wetlands and buried aquatic plants, contributes to the accumulation and storage of carbon in biomass including sediments[13]. The lake's huge surface area facilitates carbon absorption, making it a significant component of the local carbon cycle. Sediments at the lake's bottom act as a huge carbon store, trapping organic matter throughout time. This carbon storage not only serves to combat climate change by lowering atmospheric carbon dioxide levels, but it also improves the lake's general ecological stability[34], [35].However, the delicate balance of Sasthamkotta Lake is at greater risk via eutrophication[24], a process defined as an excessive input of nutrients, especially nitrogen and phosphorus. Anthropogenic activities like runoff from agriculture, settlement, and the outflow of untreated sewage, washing of clothes near the Vattolikadavu region, and activities include various religious rites, traditional practices, rituals, and festivities that are integral to the cultural and spiritual fabric near the Sastha temple which is one of the pilgrimage centres, increases nitrogen levels in the lake, causing rapid plant growth, notably algae[36]. An oversupply of nutrients feeds algal blooms, resulting in an upward spiral of ecological consequences. As these algae grow, they fight for sunlight and decrease oxygen levels as they decompose, resulting in hypoxic conditions[16]. This, in turn, threatens aquatic animals, alters lake biodiversity, and undermines the ecosystem's natural equilibrium.

Sasthamkotta Lake is facing a serious environmental challenge as a result of heavy metal pollution, particularly due to the presence of Cadmium (Cd) and Lead (Pb)[37]. Recent water quality evaluations reveal that Pb concentrations in the lake surpass the Bureau of Indian Standards (BIS) with respect to drinking water, indicating a serious level of contamination[30]. Elevated amounts of Pb endanger aquatic life and can harm human health due to its toxicity. The presence of Cd, even within limits, demands constant monitoring and control to avoid potential long-term consequences. The overall average concentration of heavy metal in the lake during the study period is in the order Zn>Fe>Pd>Cd>Cu>Cr>As and the degree of concentration is higher during the post-monsoon season near the eastern shoreline of the lake which underline the influence of anthropogenic pollution[19].

Groundwater seepage plays an important role in boosting the lake's inflow[17]. The lake is located in a region with a complex hydrogeological environment and phreatic as well as confined and semi-confined aquifers[38]. This seepage mechanism contributes actively to the lake's continuous replenishment of water, which is critical for maintaining its water level. The average groundwater level in the catchment area of the lake was observed to be 8.02 m depth below ground level in the pre-monsoon season and 7.19m depth below ground level during the post-monsoon period[39]. Direct precipitation on the lake's surface is another natural source of water influx. Rainfall immediately touching the lake increases its water quantity, with the frequency as well as the intensity of precipitation periods influencing the general pattern of inflow[19]. Sufficient precipitation is essential for the lake's health, as it supports the organisms within and around it. Understanding the complexities of these inflow patterns is critical for sustainable water management and the preservation of Sasthamkotta Lake. The ongoing surveillance and oversight of diverse inflow resources, combined with addressing possible effects from alterations to land use as well as climate variability, are critical practices for maintaining ecological balance and ensuring the long-term health of this important freshwater ecosystem[23].

Borewell construction in the Sasthamkotta wetland's watershed will have an impact on the lake's water levels and biological balance[40]. Excessive borewell extraction has the potential to reduce the lake's groundwater contribution, disrupting its overall equilibrium of water and causing ecological risks, especially if the lake utilizes groundwater inflow to keep its water levels stable. Borewell construction must carefully consider and handle potential consequences on water quality[31]. Borewell that are not properly maintained and designed causes groundwater contamination which causes the overall quality of water and the health of the wetland. Over-extraction can deplete the water table, affecting the lake's inflow through groundwater seepage. Implementing healthy groundwater management strategies, such as regulating extraction rates, is critical for striking an equilibrium between borewell exploitation and environmental conservation[41].

The acacia plantations on the outskirts of Sasthamkotta Lake have numerous environmental consequences[4], [19]. Acacia species, renowned for their quick expansion that areas not native and can change the natural biodiversity have direct negative impacts on the native plants and animals, regions hydrology, water flow trend, and nutrients cycle[42].

Land reclamation for agricultural reasons, particularly banana and coconut production, is capable of resulting in habitat loss and changes to the natural landscape[33]. Land reclamation frequently entails changing the topography and patterns of drainage, which can result in elevated discharge as well as sedimentation into the lake. The use of agricultural chemicals in plantain and coconut cultivation may release toxins into the lake, damaging water quality along with aquatic habitats.

Mining activity near Sasthamkotta Lake can have serious environmental impacts. Mineral extraction frequently causes severe land disorder, erosion of soil, and sedimentation, which degrades lake water quality. Mining runoff may introduce pollutants into the aquatic ecosystem, disrupting its natural equilibrium[23], [43]. Furthermore, physical landscape alteration can have an impact on flora and fauna habitats, contributing to the loss of biodiversity.

Planktons are essential to the food chain in aquatic ecosystems. Sasthamkotta contains at least 37 phytoplankton species from 30 families. Phytoplanktons are more abundant during the post-monsoon season, with higher concentrations near Sasthamkotta Town and lower levels along the western margins. Bacillariophyceae is the most prevalent group, followed by Chlorophyceae, Cyanophyceae, and Dianoflagellata[26]. Zooplankton is an essential component of the aquatic food web that also requires a nutrient metabolism and overall biodiversity[4]. Hence, the alteration of the variety of zooplankton species significantly impacts the overall biodiversity of the Sasthamkotta freshwater ecosystem.

Zooplankton in Sasthamkotta primarily consists of Nauplius, Rotifer, and Copepod, with a minor presence of Cladocerans and the total count was reported at 28 counts/L. Nauplius populations gradually increase from the pre-monsoon period and become predominant during the monsoon. Rotifers show minimal variability and experience only slight increases during the monsoon.

Copepods reach their peak population, comprising approximately 5% of the zooplankton, during a certain period. Peaks in zooplankton and phytoplankton populations coincide. Primary productivity gradually rises post-monsoon and declines pre-monsoon. The area of the lake near Vellinthara Bund consistently exhibits the highest productivity throughout the year[44]. Zooplankton's role as plant life, livestock, and consumers influences nutrient exchanges in the water, and variations in their abundance can alter nutritional availability[45], [46]. Consequently, it has the potential to impact Sasthamkotta Lake's health by altering elements such as oxygen saturation and nutrient concentrations. Aside from the immediate biological concerns, changes in zooplankton species may result in an indirect impact on the lake's variety[10]. Alterations in the variety of zooplankton species in the wetland disrupt the interaction between trophic levels and food sources for a wide range of organisms, like fish and waterfowl[45]. This cascading effect may extend to fish populations, influencing the amount and geographical distribution of species that depend on zooplankton as their principal food source. Furthermore, waterfowl that rely heavily on fish for their diet may experience variations in prey availability, affecting their hunting habits and overall population trends.

The spreading of invasive species can set off a chain reaction of ecological repercussions, having a significant impact on both habitat fluctuations and biodiversity inside ecosystems[44]. Non-native wildlife and plants, due to their harmful nature, can outcompete native species, causing significant changes to the framework and operation of natural environments. This intervention may change the cycling of nutrients, vegetation patterns, as well as overall habitat composition, making the environment less favourable for the growth of native species[29].Invasive species have far-reaching consequences for biodiversity, harming birds, insects, butterflies, and aquatic fowl.

The presence of 11 species of terrestrial vegetation has been documented along the shorelines of Sasthamkotta, while the overall catchment area hosts 60 species. Patches of Screw Pine (Pandanus odoratissimus) are found near the Vellinthara embankment, while the eastern shoreline features patches of the insectivorous plant, Indian Sundew (Drosera sp.). In the hinterland, there are at least 97 species, with 21 species found in homesteads. Altogether, there are 158 terrestrial species around Sasthamkotta Lake. Wild pineapple varieties have been planted in some areas to enhance soil stability and prevent erosion. The micro-watershed surrounding the lake primarily features a coconut-based agroforestry system with trees such as Mangifera indica, Anacardium occidentale, and Artocarpus heterophyllus[47]. 23 butterfly species have been observed around the lake, mainly belonging to the Nymphalidae and Papilionidae families. The highest concentration of butterflies is seen near the Vellinthara Embankment, which has a relatively higher number of grasses and herb species. Records show the presence of at least 38 fish species from 19 families in Sasthamkotta, including Horabagrus brachysoma, classified as Vulnerable in the IUCN Red List[48]. Eleven species belong to the Cyprinidae and Bagridae families. The construction of an embankment along Sasthamkotta has disrupted the flood pulse, hindering species exchange between River Kallada and the lake. Breeding and spawning habitats have been identified along the embankment and the southern margins of the lake, supporting at least 35 species of waterbirds, primarily shoreline foragers (egrets, herons, and bitterns) and waders (sandpipers and lapwings). Marshes around the lake's fringes serve as foraging grounds for both migratory and resident waterbirds. Two species, the Oriental Darter and Black-headed Ibis, are classified as Near Threatened according to the IUCN Red List. Additionally, a vulnerable waterbird species was reported in 2015 by the Sasthamkotta Biodiversity Management Committee[49].Insects, birds, and fishes which play important roles in ecosystems as pollinating organisms decomposers, and food web components, are losing habitat as invasive species advance[50]. Reductions in adequate breeding as well as feeding grounds can lead to a fall in insect diversity, affecting the overall ecological balance. Invasive species have a wide-ranging impact on biodiversity, hurting insects, birds, butterflies, especially aquatic fowl. Insects, which serve crucial functions in ecosystems as pollinators, decomposing agents, and food web elements, are losing habitats as invasive species spread[51]. Reductions in suitable breeding and habitats for feeding can lead to a drop in insect variety, harming the overall

ecological equilibrium. The consequences become more pronounced when habitat changes affect bird and lepidopteran populations. Birds and butterflies, which are highly sensitive to their environment, are experiencing habitat loss owing to urbanization as well as encroachment, resulting in fewer breeding and foraging places putting the ecosystem's overall biodiversity at risk. Waterbirds, particularly those that rely on healthy aquatic ecosystems such as Sasthamkotta Lake, face challenges due to development and habitat deterioration. The decreasing quantity of adequate wetland habitats endangers the health of water birds, especially migratory species[43]. As a result, the loss in waterbird count contributes to a decrease in the array of species found in the lake, disturbing the delicate ecological balance.

The advantages of Sasthamkotta Lake extend beyond its ecological significance to include economic, cultural, and social dimensions. Recognizing and conserving these benefits is critical to the long-term growth and conservation of this valuable freshwater ecosystem.

PROPOSAL FOR THE CONSERVATION OF THE LAKE

Sasthamkotta wetland a Ramsar Site as well as a freshwater source, which is rich in ecosystem services and biodiversity is under threat and requires urgent conservation efforts. This study proposes certain conservation measures to address the key issues in the background of the Wise use approach- Sustainable use and conservation of wetlands put forward by the Ramsar Convention[12].

Rules and Regulations for Encroachment Prevention

Establish stringent measures for encroachment prevention in Sasthamkotta Lake, including tight zoning enforcement, buffer zone separation, and fines for unauthorized development, to preserve the lake's ecological integrity and prevent unauthorized settlement of sensitive regions namely near the bund region and the southeastern. The Kerala State Pollution Control Board, under the power vested by Water (Prevention and Control of Pollution) Act, 1974 has issued a notification on 9th of June 2010 prohibiting the activities namely Bathing and washing of clothes, animals and vehicles in the lake, Discharge of sewage into the lake or pathways

leading into the lake and Storage of materials, which pollute the lake via leachate, within the 500m from lake periphery[19].

Water Quality Assurance and Sustainable Water Supply to the Kollam Corporation

Implementing pollution prevention methods, controlling nutrient levels, and monitoring water quality metrics are critical to preserving the lake's purity and promoting sustainable use and are critical for preserving ecosystem health and providing a clean safe source of water for drinking for the communities of Kollam Corporation and identify potential drinking water sources. One viable solution is to consider the Ithikkara and Kallada rivers, both of which are freshwater sources near Sasthamkotta Lake. These rivers could serve as alternative sources of drinking water, providing a sustainable solution for the water needs of the community.

Ecosystem-based Land Use Planning

This method seeks to protect the area's ecological integrity, preserve water quality, and perpetuate the various flora and wildlife that rely on wetland habitats. Ecosystem-based planning for land use in Sasthamkotta Lake entails incorporating ecological considerations as well as safeguarding biodiversity into the processes of decision-making to ensure long-term and harmonious development while balancing community needs along with maintaining the lake's distinct ecosystem.

Control measures for erosion and sediment export

Reducing sediment export and mitigating erosion through planting vegetative cover, which includes restoration of native vegetation and grass buffers, throughout the banks specifically near the DB college zone. In addition, using erosion management techniques in susceptible regions, such as barriers and silt fences, near the western shoreline mainly near the Anjalimoodu and Mynagappally Pump House helps to maintain the lake's water quality.

Sustainable Urban Management

Implementing environmentally friendly methods- developing green infrastructure, and planning responsible land use in the Sasthamkotta and Bharanikkavu towns to ensure that urbanization has a minimal detrimental influence on the lake ecosystem, encouraging long-

term environmental safety and community well-being. This method seeks to strike a balance between urban growth and natural resource protection, maintaining Sasthamkotta Lake's distinctive ecological traits while also developing a flexible and environmentally friendly urban environment.

Communication Engagement

Increase the awareness among the neighbourhood communities and the pilgrims of Sastha temple that rely on the Sasthamkotta wetland to encourage them to adopt sustainable practices and develop a perception of responsibility by being informed about the wetland's significance and its dire need for conservation.

Native Vegetation Restoration

Implementing native vegetation rehabilitation activities in Sasthamkotta Lake includes restoring indigenous plant species of Phytoplankton andzooplankton to increase biodiversity, sustain ecosystems, and improve the wetland's overall ecological health. This strategy attempts to restore the natural equilibrium of vegetation, provide habitat support for species, and strengthen the lake ecosystem's resilience.

Sustainable Agriculture Practices

Sustainable agriculture approaches in Sasthamkotta Lake focus on reducing chemical inputs, boosting organic farming, and applying conservation measures to water to promote ecologically friendly production while preserving the lake ecosystem's biological integrity. These approaches strive to strike a balance between agricultural output and the wetland's long-term health and viability, benefiting both residents and the ecosystem.

Regulation and Monitoring of Mining Activities

Implementing in place and upholding strict environmental laws to prevent illegal mining, transportation, and storage of minerals.

Alternative to borewell

Investigating surface water extraction techniques and rainfall collection systems are viable alternatives to borewells for Sasthamkotta Lake that can meet water demands without compromising the hydrological balance of the lake and maintaining ecosystem health.

Furthermore, encouraging water-saving behaviours among neighbours might help lessen reliance on borewells and minimize possible negative environmental effects on the ecosystem of freshwater wetlands.

Invasive Species Management

Implementing techniques to restrict and reduce the growth of non-native livestock and plants, so that they do not outcompete native species as well as disrupt the ecological equilibrium. These activities aim to conserve the lake's environmental integrity, protect biodiversity, and maintain the wetland's essential services.

Sustainable Cultural Approach

A sustainable cultural approach at Sasthamkotta Lake entails maintaining regional customs, like customary fishing techniques and cultural gatherings while incorporating actions that support environmental conservation, community involvement, and the long-term health of the lake ecosystem and cultural heritage. To maintain the versatility and vitality of Sasthamkotta Lake and the communities around it, this strategy aims to balance cultural practices with sustainable resource management.

Sasthamkotta Wetland demands holistic and collaborative efforts for implementing conservation strategies. The collective effort of the communities, authorities, and stakeholders is essential for the successful conservation and safeguarding of Sasthamkotta wetland for the next generation and beyond.

Establishment of Wetland Monitoring and Research Centre

A state of the art wetland monitoring centre is proposed to be established at Kumbalathu Sankupillai Memorial Devaswom Board (DB) College, Sasthamkotta for monitoring the ecological, hydrological and socio-economic features of Sasthamkotta Lake. The centre would function under the aegis of research and development centres namely CWRDM (Centre for Water Resources Development and Management Kozhikode), NCESS (National Centre for Earth Science Studies Trivandrum) and academic institutions like CUSAT (Cochin University of Science and Technology), NIT-C (National Institute of Technology Calicut) and CET (College of Engineering Trivandrum) which would coordinate all inventory and assessment programs.

CONCLUSIONS

The study sheds light on the critical conservation challenges in the largest freshwater wetland of Kerala. Establishing encroachment prevention measures in Sasthamkotta Lake, such as strict zoning enforcement, buffer zone separation, and fines for unauthorized development, is critical for preserving the lake's ecological integrity and preventing unauthorized settlement in sensitive areas, particularly near the bund region and the southeastern shoreline. Implementing pollution prevention methods, controlling nutrient levels, and monitoring water quality metrics are critical for maintaining the lake's purity and ensuring sustainable water use, which benefits the half-million people of the Kollam district. Consider the Ithikkara and Kallada rivers as alternative drinking water sources to provide a long-term solution for the community's water needs while also protecting the lake's ecosystem. To achieve long-term and balanced development, ecosystem-based land use planning should include ecological considerations and biodiversity protection. Measures such as vegetative cover planting, erosion management techniques, and eco-friendly urban development are critical for maintaining water quality and reducing the negative impact of urbanization on the lake ecosystem. It is also critical to raise awareness of the wetland's importance among local people and pilgrims, to promote sustainable activities. The lake's ecological health can be improved further by implementing native plant rehabilitation efforts and sustainable agricultural practices. The coordinated efforts of local people, political entities, environmental organizations and scientific interventions are critical for the conservation of Sasthamkotta freshwater wetland.

REFERENCES

1. G. Gupta, J. Khan, A. K. Upadhyay, and N. K. Singh, "Wetland as a Sustainable Reservoir of Ecosystem Services: Prospects of Threat and Conservation," in Restoration of Wetland Ecosystem: A Trajectory Towards a Sustainable Environment, A. K. Upadhyay, R. Singh, and D. P. Singh, Eds., Singapore: Springer Singapore, 2020, pp. 31–43. doi: 10.1007/978-981-13-7665-8_3.

2. R. R. Sharitz, "Carolina bay wetlands: Unique habitats of the southeastern United States," Wetlands, vol. 23, no. 3, pp. 550–562, Sep. 2003, doi: 10.1672 / 0277-5212 (2003) 023 [0550: CBWUHO] 2.0. CO; 2.

3. A. J. Reid et al., "Emerging threats and persistent conservation challenges for freshwater biodiversity," Biological Reviews, vol. 94, no. 3, pp. 849–873, Jun. 2019, doi: 10.1111/brv.12480.

4. D. Dudgeon et al., "Freshwater biodiversity: importance, threats, status and conservation challenges," Biological Reviews, vol. 81, no. 2, pp. 163–182, May 2006, doi: 10.1017/S1464793105006950.

5. S. R. Arya and E. K. Syriac, "Wetlands: The living waters-A review," AG, no. of, Apr. 2018, doi: 10.18805/ag.R-1717.

6. S. Alikhani, P. Nummi, and A. Ojala, "Urban Wetlands: A Review on Ecological and Cultural Values," Water, vol. 13, no. 22, p. 3301, Nov. 2021, doi: 10.3390/w13223301.

7. B. Satyanarayana et al., "A Socio-Ecological Assessment Aiming at Improved Forest Resource Management and Sustainable Ecotourism Development in the Mangroves of Tanbi Wetland National Park, The Gambia, West Africa," AMBIO, vol. 41, no. 5, pp. 513–526, Jul. 2012, doi: 10.1007/s13280-012-0248-7.

8. S. K. Chakraborty, "Diversity and Conservation of Wildlife Associated with Rivers: An Eco-ethological Analysis," in Riverine Ecology Volume 2, Cham: Springer International Publishing, 2021, pp. 287–441. doi: 10.1007/978-3-030-53941-2_4.

9. U. S. Amala Krishnan and S. Kolathayar, "Overview of Water Resources in Kerala and Feasibility of Coastal Reservoirs to Ensure Water Security," in Climate Change and Water Security, vol. 178, S. Kolathayar, A. Mondal, and S. C. Chian, Eds., in Lecture Notes in Civil Engineering, vol. 178. , Singapore: Springer Singapore, 2022, pp. 507–514. doi: 10.1007/978-981-16-5501-2_39.

10. L. K P, M. Fila, A. S. Nair, and O. V. Oommen, "Joint Biodiversity Management Committees: A Mechanism to Manage and Conserve Eco-Regions," Adv Environ Eng Res, vol. 04, no. 03, pp. 1–25, Aug. 2023, doi: 10.21926/aeer.2303042.

11. K. N. Ninan, Ed., Environmental Assessments: Scenarios, Modelling and Policy. Edward Elgar Publishing, 2020. doi: 10.4337/9781788976879.

12. D. Stroud, "Ramsar Convention: Ramsar Site Designation Process," in The Wetland Book, C. M.

Finlayson, M. Everard, K. Irvine, R. J. McInnes, B. A. Middleton, A. A. Van Dam, and N. C. Davidson, Eds., Dordrecht: Springer Netherlands, 2016, pp. 1–8. doi: 10.1007/978-94-007-6172-8_114-1.

13. K. M. Nair, D. Padmalal, K. P. N. Kumaran, R. Sreeja, R. B. Limaye, and R. Srinivas, "Late quaternary evolution of Ashtamudi–Sasthamkotta lake systems of Kerala, south west India," Journal of Asian Earth Sciences, vol. 37, no. 4, pp. 361–372, Mar. 2010, doi: 10.1016/j.jseaes.2009.09.004.

14. K. Shibu and S. Ayoob, "WATER QUALITY INDEX AS A TOOL TO ASSESS WATER QUALITY OF SASTHAMKOTTA FRESHWATER WETLAND, A RAMSAR SITE IN INDIA," PR, pp. 931–940, Sep. 2022, doi: 10.53550/PR.2022.v41i03.024.

15. Shibu K, S Ayoob, and Muhammed Yousuf S, "Determination of Land Use-Land Cover Changes in the adjoining Panchayats of Sasthamkotta Freshwater Wetland a Ramsar Site in South India," Research India Publications, vol. 16, pp. 17–33, 2023.

16. V. Mullakkezhil Reghunathan, S. Joseph, C. U. Warrier, A. S. Hameed, and S. Albert Moses, "Factors affecting the environmental carrying capacity of a freshwater tropical lake system," Environ Monit Assess, vol. 188, no. 11, p. 615, Nov. 2016, doi: 10.1007/s10661-016-5636-1.

17. K. Shibu and S. Ayoob, "Determination of Areal Shrinkage of Sasthamkotta Freshwater Wetland a Ramsar Site in South India," Ecology, Environment and Conservation Paper, vol. 28, no. 1, pp. 255–262, 2021.

18. J. J. Liu, B. Dong, C. Q. Guo, F. P. Liu, L. Brown, and Q. Li, "Variations of effective volume and removal rate under different water levels of constructed wetland," Ecological Engineering, vol. 95, pp. 652–664, Oct. 2016, doi: 10.1016/j.ecoleng.2016.06.122.

19. Shibu K, "Investigation onto the Conservation issues of a natural freshwater system," PhD Dissertation, University of Kerala, 2022.

20. O. Dietrich, M. Redetzky, and K. Schwärzel, "Wetlands with controlled drainage and sub-irrigation systems— modelling of the water balance," Hydrological Processes, vol. 21, no. 14, pp. 1814–1828, Jul. 2007, doi: 10.1002/hyp.6317.

21. R. Kumar, H. Ganapathi, and S. Palmate, "Wetlands and Water Management: Finding a Common Ground," in Water Governance and Management in India, G.

Chadha and A. B. Pandya, Eds., in Water Resources Development and Management. , Singapore: Springer Singapore, 2021, pp. 105–129. doi: 10.1007/978-981-16-1472-9_5.

22. S. N. R. Beeram, S. P. V, P. S. K, and R. Thendiyath, "Impact of change in land use/land cover and climate variables on groundwater recharge in a tropical river basin," Environ Dev Sustain, Apr. 2023, doi: 10.1007/s10668-023-03216-x.

23. V. M. Sreekumari, S. E. John, R. T. Rajan, M. Kesavan, S. Kurian, and P. Damodaran, "Human interventions and consequent environmental degradation of a protected freshwater lake in Kerala, SW India," Geosci J, vol. 20, no. 3, pp. 391–402, Jun. 2016, doi: 10.1007/s12303-015-0049-7.

24. K. Shibu and S. Ayoob, "Modelling eutrophication status of Sasthamkotta lake using geographical information system and remote sensing," presented at the PROCEEDINGS OF THE INTERNATIONAL CONFERENCE ON RESEARCH ADVANCES IN ENGINEERING AND TECHNOLOGY - ITechCET 2021, Kerala, India, 2022, p. 030019. doi: 10.1063/5.0103761.

25. D. Padmalal, K. P. N. Kumaran, K. M. Nair, B. Baijulal, R. B. Limaye, and S. V. Mohan, "Evolution of the coastal wetland systems of SW India during the Holocene: Evidence from marine and terrestrial archives of Kollam coast, Kerala," Quaternary International, vol. 237, no. 1–2, pp. 123–139, May 2011, doi: 10.1016/j.quaint.2010.12.021.

26. Girijakumari S, "Resource potential of Sasthamkotta Lake with special reference to fish fauna and their sustainability," Mahatma Gandhi University, Ph. D. Thesis, 2007.

27. Prakasam V R and Joseph M L, "Water quality of Sasthamcotta lake, Kerala (India) in relation to primary productivity and pollution from anthropogenic sources," Journal of Environmental Biology, vol. 21, pp. 305–307, 2000.

28. Sreejith S, "Hydrogeochemistry of the Sasthamkotta lake, Kollam district, Kerala, with special reference to sediment-water interaction," In Proceedings of the Xth Kerala Science Congress, pp. 4–7, 1988.

29. S. E. John, M. K. V. Sagar, K. Maya, and D. Padmalal, "Dissolved nutrients (NO 3 -N and PO 4 -P) and Fe in the interstitial and overlying waters of two tropical freshwater lakes in Southern Kerala, India," Jour.

of Appl. Geochem., vol. 16, no. 4, p. 381, 2014, doi: 10.5958/2319-4316.2014.00002.1.

30. R. Das, A. Krishnakumar, M. R. Kumar, and D. Thulseedharan, "Water quality assessment of three tropical freshwater lakes of Kerala, SW India, with special reference to drinking water potential," Environmental Nanotechnology, Monitoring & Management, vol. 16, p. 100588, Dec. 2021, doi: 10.1016/j.enmm.2021.100588.

31. Divya Raj S and K Mophin Kani, "Water Quality Assessment of Sasthamcotta Lake, Kollam, Kerala," International Journal of Engineering and Advanced Technology (IJEAT), vol. 7, no. 3, 2018.

32. R. B. Limaye, D. Padmalal, and K. P. N. Kumaran, "Cyanobacteria and testate amoeba as potential proxies for Holocene hydrological changes and climate variability: Evidence from tropical coastal lowlands of SW India," Quaternary International, vol. 443, pp. 99–114, Jul. 2017, doi: 10.1016/j.quaint.2016.09.044.

33. Krishnaveni, K.S and Anilkumar, P.P, "STUDY OF URBAN SPRAWL IMPACTS ON WETLAND ECOSYSTEM USING REMOTE SENSING AND GIS.," 2018.

34. K. P. N. Kumaran, D. Padmalal, R. B. Limaye, and S. V. Mohan, "Signatures of Holocene Hydrological Processes from Sedimentary Archives in Southwestern India: Case Studies from Wetlands of Kerala Coast," J Geol Soc India, vol. 92, no. 5, pp. 596–606, Nov. 2018, doi: 10.1007/s12594-018-1073-9.

35. K. Devi, S. Sharma, and R. Nair, "Evaluating spatial variability of subsurface carbon stock and free-phase gas using ground-penetrating radar and direct measurements in coastal landforms of South-West Indian peatlands," J. Phys.: Conf. Ser., vol. 2141, no. 1, p. 012011, Dec. 2021, doi: 10.1088/1742-6596/2141/1/012011.

36. A. Suman, A. Pk, and A. S, "Development and prediction of a robust multivariate trophic state index for the classification of lentic water bodies," Results in Engineering, vol. 20, p. 101586, Dec. 2023, doi: 10.1016/j.rineng.2023.101586.

37. A. Krishnakumar, S. K. Aditya, K. AnoopKrishnan, R. Das, and K. Anju, "Water quality management: Development of a fuzzy-based index in hydro informatics platform," in Current Directions in Water Scarcity Research, vol. 7, Elsevier, 2022, pp. 265–284. doi: 10.1016/B978-0-323-91910-4.00016-9.

38. A. Krishnakumar, P. Saranya, and R. Das, "Hydrogeochemistry and Environmental Issues of the Wetlands of Kerala, Southwestern India," in Wetland Science, B. A. K. Prusty, R. Chandra, and P. A. Azeez, Eds., New Delhi: Springer India, 2017, pp. 145–161. doi: 10.1007/978-81-322-3715-0_8.

39. CGWB, "Ground Water Information Booklet of Kollam District, Kerala State," Kerala: Central Ground Water Board (CGWB), Ministry of Water Resources, Government of India., 2013.

40. Shaji E., "Groundwater Quality Management in Kerala," Online International Interdisciplinary Research Journal, vol. 3, no. 3, pp. 63–68, 2013.

41. D. Pradhan and R. Ranjan, "Achieving Sustainability and Development through Collective Action? An Empirical Analysis of the Impact of the Bore Pool Sharing Program on Farm Incomes and Crop Choices," World Development, vol. 88, pp. 152–174, Dec. 2016, doi: 10.1016/j.worlddev.2016.07.015.

42. J. J. Wells, L. C. Stringer, A. J. Woodhead, and E. M. Wandrag, "Towards a holistic understanding of non-native tree impacts on ecosystem services: A review of Acacia, Eucalyptus and Pinus in Africa," Ecosystem Services, vol. 60, p. 101511, Apr. 2023, doi: 10.1016/j. ecoser.2023.101511.

43. S. M. Irshad, "Cashing in on Natural Resource Mismanagement: A Study on Depleting Sasthamkotta Fresh Water Lake in Kerala," nrc, vol. 3, no. 3, pp. 50–56, Aug. 2015, doi: 10.13189/nrc.2015.030302.

44. Girijakumari S, Nelson P A., Smrithy Raj, and Bijukumar, A, "Ichthyofaunal Diversity of Sasthamkotta Ramsar Lake, Kerala, India," India. J. Inland Fish. Soc. India, vol. 43, no. 1, pp. 96–102, 2011.

45. Regi, S.R, Smrithi, R, and Biju Kumar, A, "Trophic Web Structure and Ecological Network Analysis of Sasthamkotta Lake, A Ramsar Site in Kerala, India," Journal of Aquatic Biology & Fisheries, vol. 8, pp. 67–75, 2020.

46. Renju Mohan, Lathika Cicily Thomas, and K. B Padmakumar, "POTENTIALLY TOXIC CYANOBACTERIAL SPECIES OF FRESHWATER ECOSYSTEMS OF SOUTH-WEST COAST OF INDIA," Proceeding of the International Online Conference on Environmental Status of Estuarine and Coastal Ecosystems in India, pp. 33–35, 2022.

47. Nayar M P, Alexander T, and Thushara L, Biodiversity and Conservation of Sasthamkotta Fresh Water Lake of Kerala. Dehradun, 2011.

48. IUCN, "IUCN Red List." 2011.

49. Madhusoodana Kurup, K. V. Radhakrishnan, and T.G. Manojkumar, "Biodiversity status of fishes inhabiting rivers of Kerala (S. India) with special reference to endemism, threats and conservation measures," Proceedings of LARS2. 2nd Large Rivers Symposium, pp. 163–182, 2004.

50. M. S. Reddy and N. V. V. Char, "Management of lakes in India," Lakes & Reservoirs, vol. 11, no. 4, pp. 227–237, Dec. 2006, doi: 10.1111/j.1440-1770.2006.00311.x.

51. Sheeba Abraham, "The relevance of wetland conservation in Kerala," vol. 2, no. 3, pp. 01–05, 2015.

Investigation on the Structural Integrity of Bricks through the Incorporation of Recycled Materials

M. Tamim Tanwer
Assistant Professor
Dept. of Civil Engineering
Pacific School of Engineering
Surat, Gujarat
✉ tamimtanwer@gmail.com

Anchal U. Pandey
Engineer
Dept. of Civil Material Testing & Research Centre
Pacific School of Engineering
Surat, Gujarat
✉ anchal394305@gmail.com

Jayesh Shah
Director
Dept. of Civil Material Testing & Research Centre
Pacific School of Engineering
Surat, Gujarat
✉ jayesh.shah.23021971@gmail.com

ABSTRACT

This study endeavours to develop bricks by integrating waste materials, targeting the pressing issue of environmentally harmful waste disposal. The residual materials, including some non-biodegradable ones, present enduring environmental risks. The research involved sourcing industrial waste locally from Sugar and Plastic Factories for brick production. The investigation primarily examines the mechanical attributes like durability, compressive strength, and water absorption of these bricks. Furthermore, the inclusion of waste materials might decrease brick weight, thus aiding in reducing overall structure weight and promoting cost-effective construction materials. Consequently, the integration of waste materials into brick manufacturing holds the promise of yielding more economical and environmentally sustainable building materials, potentially cutting down overall production expenses.

KEYWORDS : *Recycled waste, Compressive strength, Water absorption, Clay brick.*

INTRODUCTION

Bricks, essential in constructing masonry walls, pavements, and various architectural elements, have evolved beyond their original clay definition. Today, they encompass rectangular units crafted from concrete, sand, lime, or clay-rich soil. Interlocking, mortar, or adhesives facilitate their connection. Available in diverse classes, types, materials, and sizes, bricks are mass-produced, reflecting regional and temporal variations. Comprising fired clay and mortar a blend of cement, sand, and water bricks serve as compact construction elements. Known for their heat resistance, corrosion resistance, and fire resistance, bricks are ideal for curved designs and structures in confined spaces, typically measuring four inches in width and twice that in length. Notably durable, brick buildings boast prolonged lifespans with minimal maintenance. Beyond their practical attributes, bricks have endured as a building material due to their aesthetic appeal.

LITERATURE REVIEW

Ali Murtaza Rasool, Asif Hameed, Mohsin Usman Qureshi, Yasser E. Ibrahim, Asad Ullah Qazi, & Ali Sumair (2022), investigated burnt clay bricks enhanced with leftover marble. Adding waste marble powder (WMP) up to 15% as a clay substitute reduced brick weight by 10.5%, lessening structural dead load. WMP-incorporated bricks exhibited freeze-thaw resistance, with 15% WMP deemed suitable under such conditions. However, compressive strength decreased as brick

weight increased in sulfate solutions. Bricks with 12% WMP met Pakistan Building Code standards for minimum compressive strength. [1]

Chandru. G Vignesh.V, Dr. Saravanan. R (2019),This experiment utilized locally available materials, including ordinary Portland cement and sugarcane bagasse ash as binding agents, fine aggregates, and coarse aggregates. Normal water was used for mixing and curing throughout the entire process. [2]

Rajmunni Hombal, Shwetha L G, Puja K Rathishchandra. R. Gatti (2018), investigated the use of waste plastic in composite brick manufacturing. They found that replacing 20% of clay with plastic, specifically grain sizes between 0.5 cm to 0.75 cm, resulted in bricks achieving the highest compressive strength with a maximum load of 97 kN. The compressive strengths for bricks ranged from 5.15 to 5.68 N/mm² across different plastic replacement percentages, with corresponding maximum loads varying from 72 kN to 97 kN. The bricks also absorbed approximately 8.53% water. [3]

R. Shanmugapariyan, R. Devaki & S. Saran, (2017), studied the partial replacement of clay with sugarcane bagasse ash (SCBA) in brick manufacturing. They noted that Asia produces 87% of the world's bricks, with India and China being major consumers. India alone produces 60 billion clay bricks annually, following IS:2212 (1991) standards of 190mm×90mm×90mm. Industrial wastes like plastic, SCBA, and fly ash serve as supplementary cement replacement materials. India's sugarcane production reaches 300 million tons yearly, with 10 million tons of sugarcane remaining unutilized. [4]

Shikhar Shrimali (2017), explored the creation of bricks from waste plastic. The study highlighted India's issue with non-biodegradable plastic waste from packaging materials like plastic bags and PET bottles littering the landscape. Utilizing waste plastic in brick production reduces both the cost and weight of bricks. [5]

Vignesh Kumar and B. Jai Vignesh (2017), investigated using bagasse ash as a replacement in bricks, transforming this waste material into a valuable resource. Their study demonstrates how innovative use of bagasse ash in bricks can solve disposal issues, reduce costs, and produce eco-friendly construction materials. [6]

Karthika K,P Priya , R.S. Ashish, C.Ilaiya Bharathi (2017),The commercial production of bricks from waste materials remains limited due to issues with production methods, potential contamination, lack of standards, insufficient guidance, low awareness, and slow industry and public acceptance. To expand production and use, further research and development are needed on technical, economic, and environmental aspects, as well as on standardization, government policy, and public education regarding waste recycling and sustainable development. [7]

Surya Bhusan Singh and Ayush Bhardwaj (2016), focused on bricks made from sugarcane bagasse ash. They found that reducing fly ash and increasing bagasse ash improved the density to 16.50 kg/m³. Using a brick size of 23011575 mm with a 1:3 mix ratio, they achieved maximum compressive strength by replacing 10 kg of fly ash with bagasse ash. [8]

Er. Subham Srivastava, Punit Kumar Shukla, Kamal Kumar, Piyush Kumar (2015), In their study titled "Effect of Bagasse Ash on Concrete Strength",investigate the potential of sugarcane bagasse ash as a partial replacement for cement in concrete. They analyze its chemical and physical properties in response to the growing need for sustainable alternatives to cement due to increased demand and consumption. [9]

Mrs. U.R. Kawade, Mr. V.R. Rathi, Miss Vaishali D. Girge (2013), in their study titled "Impact of Bagasse Ash on Concrete Strength", explored the use of sugarcane bagasse ash as a partial substitute for cement in concrete production. They replaced cement with varying percentages of bagasse ash (15%, 20%, 25%, and 30%) and conducted tests on fresh concrete properties and compressive strength at different curing periods (7, 28, 56, and 90 days). Results showed that concrete strength increased by up to 15%, with the optimal replacement level identified as 15% bagasse ash. This achieved compressive strengths ranging from 50 to 70 N/mm², demonstrating bagasse ash as a promising alternative binder in concrete manufacturing. [10]

Bhavya Rana,Prof. Jayesh kumar Pitroda, Dr. F S Umrigar (2013), In their study titled "Sugarcane Bagasse Ash for Eco-friendly Ash Bricks",explore the utilization of sugarcane bagasse ash in brick

production as a sustainable solution. The research addresses India's increasing agricultural waste and the construction industry's quest for alternatives to conventional materials like fly ash. By incorporating sugarcane bagasse ash into bricks, the study promotes cost-effectiveness, versatility, and potential LEED certification benefits. This approach aims to reduce pressure on fertile land traditionally used for brick-making, supporting sustainable construction practices. [11]

Ashish Parashar and Rinku Parashar (2012), conducted a comparative study on firebrick production, incorporating materials such as wood ash, rice husk, cement, and fly ash into clay bricks. They utilized two types of admixtures to introduce porosity, achieving a lighter, more porous structure that enhances heat penetration and acts as additional fuel. The compressive strength was influenced by the specific gravity of materials passing through a 4.75mm sieve. Cement bricks demonstrated superior strength with higher cement content, emphasizing its crucial role as a primary cementitious material in the bricks' composition. [12]

V. Palanisamy (2011) in their study titled "Utilization of Textile Waste Effluent Waste Sludge in Brick Production", explores the integration of textile industry waste into brick manufacturing. Tirupur, Tamil Nadu, houses 830 textile processing units with 8 common effluent treatment plants (CETPs), generating 200 tons/day of textile sludge. Improper disposal, including open dumping, contaminates soil, surface water, and groundwater. This research advocates for incorporating textile waste into bricks as a sustainable solution to mitigate environmental contamination risks associated with current disposal practices [13]

Putaraj Mallikarjun Hiremath, Shanmukha shetty, Navaneeth Rai, P.G Prathima. T. B, focused on producing plastic soil bricks. They utilized 60-80% waste plastics with laterite quarry waste, incorporating 2-5% 60/70 grade bitumen in molten form. This bitumen-plastic resin mixture was combined with laterite quarry waste to manufacture the bricks. [14]

METHODOLOGY

In accordance with the study of the literature the methodology is formulated.
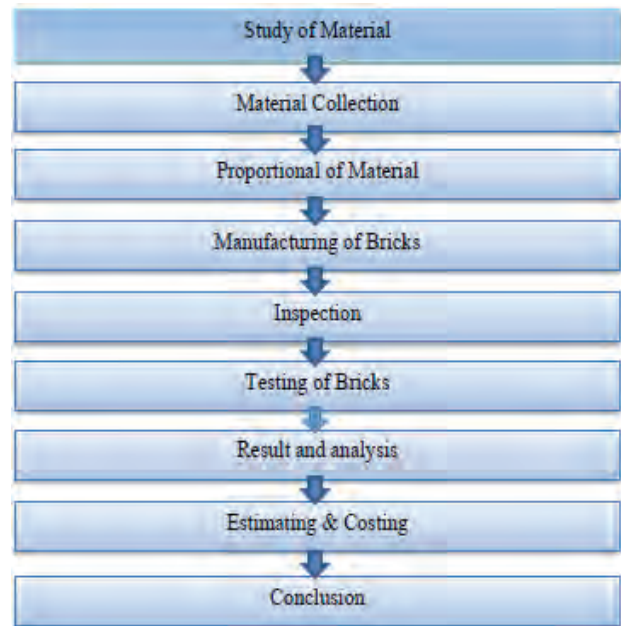
Manufacturing Of Bricks

Manufacturing bricks involves a meticulous process comprised of the following four steps:

1. Preparation of Brick Material: The initial phase involves excavating soil, clearing it of contaminants like leaves and rocks, and subjecting it to a weathering process for several months. After weathering, the soil is mixed with other materials to create high-quality brick earth. This blend is then softened using a pug mill.

2. Moulding of Bricks: Bricks are moulded through either hand moulding or machine moulding, depending on the desired product quality. Hand moulding involves manually pushing tempered clay into the mould and removing excess clay with a strike or wire-framed frame. For large-scale production, machine moulding is employed, using plastic clay or dry clay machines to create precisely formed bricks.

3. Drying of Bricks: Bricks are dried in open-sided sheds to facilitate air circulation and provide protection from weather conditions. The drying process, lasting seven to fourteen days, reduces the moisture content to 5–7%. This step is crucial to prevent cracking and distortion during burning, maximize fuel efficiency, reduce burning time,

and allow for easier handling and stacking of raw bricks.

4. Burning of Bricks: The burning process is pivotal and can be executed in two ways: clamp burning or kiln burning. In clamp burning, green bricks are stacked with fuel sources and sealed with clay before being slowly fired to intense heat over several days. Kiln burning involves modern, permanent structures with multiple chambers where moulded clay stacks are carefully loaded, dried, burned, and cooled. This process can take up to two weeks in intermittent kilns or is carried out cyclically in continuous kilns.

Various Proportion of Materials

Table shows the proportion of the materials is Sugarcane Bagasse, Sugarcane Bagasse Ash, Plastic Waste, Slurry and Clay which are used in manufacturing the brick.

Table 1: Various Proportions of Material

Sr. No.	Sample No.	Sample Name	Clay	Sugarcane Bagasse	Sugarcane Bagasse Ash	Plastic Waste	Slurry
			In Percentage (%)				
1.	Brick 1	Sugarcane Bagasse Brick	60	40	--	--	--
2.	Brick 2		60	40	--	--	--
3.	Brick 3	Plastic Waste Brick	60	--	--	40	--
4.	Brick 4		60	--	--	40	--
5.	Brick 5	Sugarcane Bagasse Ash Brick	60	--	40	--	--
6.	Brick 6		60	--	40	--	--
7.	Brick 7	Waste Slurry Brick	60	--	--	--	40
8.	Brick 8		60	--	--	--	40
9.	Brick 9	Mix Material Brick	60	10	10	10	10
10.	Brick 10		60	10	10	10	10

Weight of All Bricks Sample

Table shows the average weight of all various proportions of bricks sample are as follow.

Table 2 Weight of Brick Sample

Sr. No.	Sample No.	Sample Name	Average Weight (Kg)
1.	Brick 1	Sugarcane Bagasse Brick	2.683
2.	Brick 2		
3.	Brick 3	Plastic Waste Brick	2.556
4.	Brick 4		
5.	Brick 5	Sugarcane Bagasse Ash Brick	2.649
6.	Brick 6		
7.	Brick 7	Waste Slurry Brick	2.633
8.	Brick 8		
9.	Brick 9	Mix Material Brick	2.783
10.	Brick 10		
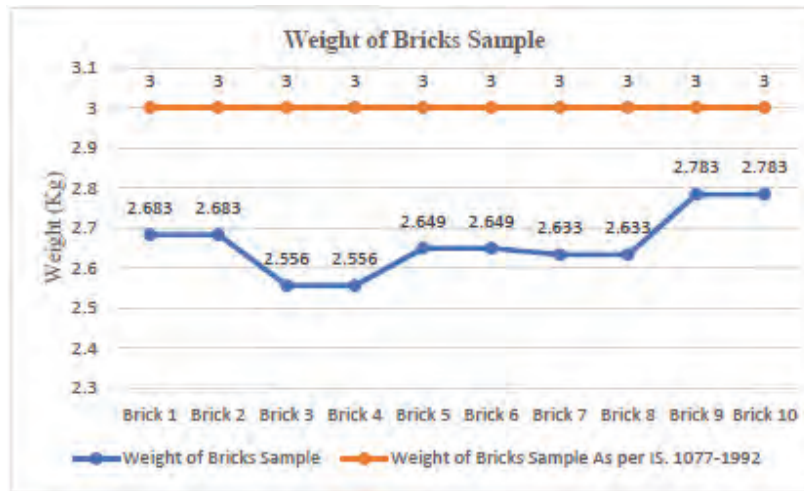
Graph-1 Weight of Brick Sample

TEST AND RESULT

Shape and Size Test

Table 3: Shape & Size Test

Sr. No.	Sample No.	Materials	Shape	Size (In mm)	Requirement as per IS. 1077-1992
1.	Brick 1	Sugarcane Bagasse Brick	Rectangular	230 X 100 X 75	Length (4600±80mm) Width (2200±40mm) Thickness (1400±40mm) (for 20 Nos. bricks)
2.	Brick 2		Rectangular	230 X 100 X 75	
3.	Brick 3	Plastic Waste Brick	Rectangular	230 X 100 X 75	
4.	Brick 4		Rectangular	230 X 100 X 75	
5.	Brick 5	Sugarcane Bagasse Ash Brick	Rectangular	220 X 100 X 75	
6.	Brick 6		Rectangular	220 X 100 X 75	
7.	Brick 7	Waste Slurry Brick	Rectangular	225 X 100 X 75	
8.	Brick 8		Rectangular	225 X 100 X 75	
9.	Brick 9	Mix Material Brick	Rectangular	230 X 100 X 75	
10.	Brick 10		Rectangular	230 X 100 X 75	

Water Absorption Test:

Table 4 Results of Water Absorption Test

Sr. No.	Sample No.	Dry Weight (W1) kg	Wet Weight (W2) kg	Water absorption, % = W2 -W1/W1 × 100	Average W.A. Value %	Requirement as per IS. 1077-1992
1.	Brick 1	2.678	3.102	15.83	15.80	
2.	Brick 2	2.688	3.112	15.77		
3.	Brick 3	2.554	3.094	21.14	21.47	
4.	Brick 4	2.558	3.321	21.81		
5.	Brick 5	2.650	3.110	17.35	17.54	Shall not be More than 20%
6.	Brick 6	2.648	3.118	17.74		
7.	Brick 7	2.657	3.155	18.74	18.56	
8.	Brick 8	2.610	3.090	18.39		
9.	Brick 9	2.788	3.339	19.86	19.68	
10.	Brick 10	2.774	3.321	19.50		
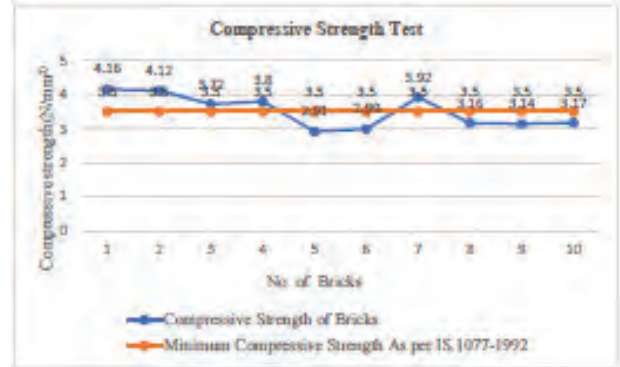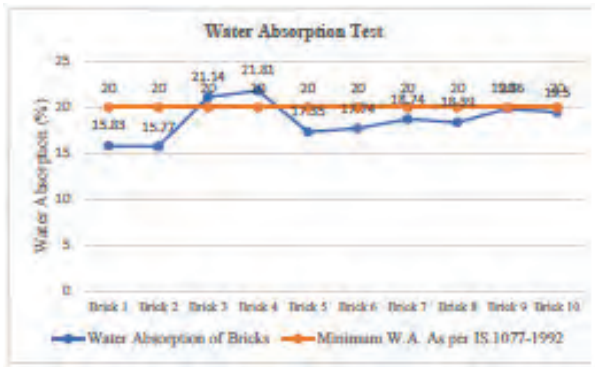
Graph-2 Water Absorption Test

Graph-3 Compressive Strength Test

Compressive Strength Test

Table 5: Compressive Strength Test

Sr. No.	Sample No.	Compressive Strength (N/mm^2)	Requirement as per IS. 1077-1992
1.	Brick 1	4.16	
2.	Brick 2	4.12	
3.	Brick 3	3.72	
4.	Brick 4	3.80	
5.	Brick 5	2.91	Compressive Strength shall not be less than 3.5(N/mm2)
6.	Brick 6	2.99	
7.	Brick 7	3.92	
8.	Brick 8	3.16	
9.	Brick 9	3.14	
10.	Brick 10	3.17	

Approximate costing of sample brick:

Table 6: Approximate Costing of Sample Brick

Approximate costing of sample brick					
Sr. No.	Material	Quantity/Number	Rate Rs.	Per	Amount (Rupees)
1.	Sugarcane Bagasse	2.7	0.0/-	Kg	0.0/-
2.	Plastic (Polythene)	2.7	0.0/-	Kg	0.0/-
3.	Sugarcane Bagasse ash	2.7	0.0/-	Kg	0.0/-
4.	Slurry	2.7	0.0/-	Kg	0.0/-
5.	Clay	18	1.0/-	Kg	18.0/-
Material Cost Rs.					18.0/-
Manufacturing Cost (including cutting cost)Rs.					27/-
Total Cost Of Sample Brick for 10 nos.					45/-
Price of One Sample Brick					4.5/-

- The cost breakdown for producing a sample brick includes material expenses amounting to 18/- Rupees and manufacturing costs including cutting cost totalling 27/- Rupees.

- Consequently, the overall expenditure for 10 sample bricks is 45/- Rupees, resulting in a unit price of 4.5/- Rupees per sample brick.

CONCLUSION

The compressive strength requirement for a standard brick is set at a minimum of 3.4 N/mm². However, bricks produced using waste materials such as bagasse ash from sugarcane, water slurry, and mixed materials exhibit slightly lower compressive strengths, ranging from 2.91 N/mm² to 3.17 N/mm².

In terms of water absorption, a conventional brick should absorb less than 20% of its weight. Testing various ratios of waste materials, including sugarcane bagasse, slurry, bagasse ash from sugarcane, and mixed materials, revealed water absorption rates below 20%, ranging from 15.77% to 19.86%.

The standard size for modern bricks is 215 x 102.5 x 65 mm. However, bricks made from sugarcane bagasse, plastic waste, and mixed materials deviate in dimensions, measuring 230 x 100 x 75 mm.

Considering the cost, approximately Rs. 45/- covers the expense of 10 sample bricks, comprising Rs. 18/- for materials and Rs. 27/- for manual labor. Consequently, the individual price per sample brick is Rs. 4.5/-.

Based on the test results, it is suggested that up to 40% by weight of waste materials can be effectively incorporated into the brick-making process, maintaining suitable water absorption levels and compressive strength. Adjustments in the weight of other materials should be made to enhance the compressive strength corresponding to the percentage of waste material used.

REFERENCES

1. Ali Murtaza Rasool, Asif Hameed, Mohsin Usman Qureshi, Yasser E. Ibrahim, Asad Ullah Qazi, & Ali Sumair(2022), " Investigating the strength and endurance properties of burnt clay bricks with leftover marble", Journal of Asian Architecture and Building Engineering , Vol. 22, 2023,Issue 1, pp 240-255, https://doi.org/10.1080/13467581.2021.2024203

2. Chandru. G Vignesh.V, Dr. Saravanan. R(2019) "Experimental Study on partial replacement of Sugarcane Bagasse Ash in cement", International Journal of Advanced Engineering, Management and Science, ISSN: 2454-1311,Vol.5 Issue-2,2019,pp 154-156, https://dx.doi.org/10.22161/ijaems.5.2.7

3. Rajmunni Hombal, Shwetha LG, Puja K Rathishchandra. R. Gatti(2018), "Useful application of plastic waste in composite brick manufacturing", Sahyadri International Journal of Research Vol.4, 2018, Issue 1,pp 12-14.

4. R. Shanmugapariyan, R. Devaki & S. Saran, (2017),"Experimental study on partially replacement of clay by using sugarcane bagasse ash in brick manufacturing" International Journal of Engineering Research Modern Education, ISSN: 2455-4200 Special Issue, pp 92-96.

5. Shikhar Shrimali (2017),"Bricks from waste plastic", International Journal of Advanced Research, ISSN: 2320-5407, Vol.5 (1), 2017, pp 2839-2845, http://dx.doi.org/10.21474/IJAR01/3079

6. Vignesh Kumar and B. Jai Vignesh (2017), "Experimental investigation on replacement of bagasse ash in bricks", International Journal of Innovative Research in Science, Engineering & Technology, ISSN: 2319-8753, Vol. 6, 2017, Issue 5, pp 8302-8309, DOI:10.15680/IJIRSET.2017.0605171

7. Karthika K,P Priya , R.S. Ashish, C. Ilaiya Bharathi (2017) "Experimental analysis on Manufacture of Brick by Partial Replacement of Clay with stone Dust", ", International Journal of Latest Technology in Engineering Management & Applied Science, ISSN:2278-2540, Vol.6,2017,Issue 7,pp 54-56.

8. Surya Bhusan Singh and Ayush Bhardwaj (2016), "Use of sugarcane bagasse ash as brick Material", International Journal for Scientific Research & Development, ISSN: 2321-0613 Vol.4, Issue 6,2016, pp 83-85.

9. Er. Subham Srivastava, Punit Kumar Shukla, Kamal Kumar, Piyush Kumar (2015) "Studies on partial replacement of cement by bagasse ash in concrete", International Journal of Innovative Research in Science & Technology ,ISSN:2349-6010, Vol.2, Issue 3, pp: 43-45.

10. Mrs. U.R. Kawade, Mr. V.R. Rathi, Miss Vaishali D. Girge (2013), "Effect of use of bagasse ash on strength of concrete", International Journal of Innovative Research in Science, Engineering & Technology, Vol.2, 2013, Issue 7, pp: 2997-3000.

11. Bhavya Rana,Prof. Jayesh kumar Pitroda, Dr. F S Umrigar (2013), "Sugarcane bagasse ash for eco-friendly ash bricks",Proceedings of National Conference CRDCE13, pp 1-8.

12. Ashish Parashar and Rinku Parashar (2012), "Comparative study of compressive strength of bricks made with various materials to clay bricks", International Journal of Scientific and Research Publications, ISSN:2250-3153Vol. 2,2012, Issue 7,pp 1-4

13. V Palanisamy (2011) "Utilization of Textile Waste Effluent Waste Sludge in Brick Production" International Journal of Science: Basic and Applied Research ISSN 2307- 4531 Volume 4, No 1, pp. 1 – 10.

14. Putaraj Mallikarjun Hiremath, Shanmukha shetty, Navaneeth Rai, P.G Prathima. T. B, "Utilization of waste plastic in Manufacturing of Plastic Soil Bricks", International Journal of Technology enhancement and Emerging Engineering Research, ISSN: 2347-424289,Vol.2,Issue 4,pp 102-107.

IS Codes

1. IS-1077(1992) "Common Burnt Clay Building Bricks-Specification".

2. IS-13757(1993) "Burnt Clay Fly Ash Building Bricks-Specification".

3. IS-3495(2019) "Burnt Clay Building Bricks-Methods of tests Part-1 Determination of Compressive Strength (fourth revision)".

4. IS-3495(2019) "Burnt Clay Building Bricks-Methods of tests Part-2 Determination of Water Absorption (fourth revision)".

5. IS-3495(2019) "Burnt Clay Building Bricks-Methods of tests Part-3 Determination of Efflorescence (fourth revision)".

Road Safety Inspection from Narmada Chawkadi Intersection to Palej Intersection on Old NH-8(NH-46)

Nimit P Palsanawala
✉ nimit.palsanawala@gujgov.edu.in

Jignesh K Patel
✉ jignesh.patel1@gujgov.edu.in

Assistant Professors
Dept. of Civil
Government Engineering College
Bharuch, Gujarat

ABSTRACT

Road safety inspection had undertaken on "old nh-8(nh-46) from narmada chowkadi intersection to palej intersection" which was running through urban, semi urban and rural areas in gujarat state. Surveys were conducted to collect data for accidents, present traffic volume counts ,road invetory and analyzed to find daily, weekely, and monthly traffic and accidents distribution to identified accident prone zones and potentiality of accidents. From road safety inspection, it was concluded that car and truck users having major involvement in road accident which indicates that poor sense of driving by them. Majority accidents occurred between 6.00am to 12.00pm and 3.00pm to 9.00 pm and which indicates strong traffic regulation requirement during this time zone.

KEYWORDS : *Road safety, Accident severity index, Weighted severity index.*

INTRODUCTION

Traffic division, Bharuch District has approached to Government Engineering College, Bharuch for boosting road safety on old NH-8 from Narmada Intersection (change -168+650 km) to Palej Intersection (chainage-190+550 km) to reduce the road accident by taking road safety engineering measures'. This section is part of old National Highway - 8 from Bombay to Delhi. The road network in India has grown from 4,00,000 km in 1951 to about 4.7 million km at present. (S. Gangopadhyay and U. K. Guru, 2015. P.800). In India itself about eighty thousand people are killed in road crashes every year which is thirteen all over the world (Dr. A.M. Jain, 2014. P.86). The World Health Organization estimated that 1.17 million deaths occur year worldwide due to road traffic accidents. However, that about 70 percent of the deaths occurs in developing countries. (Gaurav, 2015, p.128). During the calendar year 2010, there were close to 5 lakh road accidents in India, which resulted in more than 1.3 lakh persons. (Pawan, 2014 P 64).Many developing countries including India have a serious road accidents problems. Fatalities rates (define as, road accidental deaths per 10,000 vehicles) are quite high in comparison to developed countries. (Sanjay, 2001. P 62).

Over the years, the technology of transportation has changed from many perspectives. These include changes in vehicles, driver demographics and skills, types of other road users, improvements in safety designs, and understanding of the complex interactions needed to provide a traveling environment. (Eugene, 2000, P1).Providing a safe driving environment is indeed not only a responsibility, but also the highest priority for all highway projects (Darshak, 2015, P 2217). As independent experts attempted to be made to identify potentially dangerous features on the given road section and suggest remedial measures.

METHODOLOGY

Road safety inspection were undertaken with main focus on to find the causes of accidents on existing road section from Narmada Intersection (chainge -168+650 km) to Palej Intersection (chainage-190+550 km) on Old national Highway -8. looking to the post inspection road safety audit guidelines , Road safety audit for existing one carried out in following three steps.

- Accident data Survey
- Traffic Volume count survey
- Site Reconnaissance survey.

Accidents reports were collected from traffic devision, bharuch district. Traffic volume counts surveys were carried out round the clock 24hours/ day. Site reconnaissance survey is carried out to measure the geometry details of black spot identified by accident data analysis on NH – 8 from Narmada Intersection to Palej Intersection.

DATA ANALYSIS

From the collected data, an excel sheet was prepared including all terms like time of accidents, location of particular accident, type of vehicle, death, major injuries and minor injuries etc. The following indices find through analysis of data sheet.

Table 1 present total no of accidents per years on NH – 8 from Narmada Intersection (Km 168+750) to Palej (190+550) Intersection.

From the year 2011 to 2015, total no of accidents has decreased from 109 to 61. There were total 51 non-fatal accidents during 2011 which has been gone down to 8, a reduction of around 74 %.

Same total no of fatal accident has been decreased 28 during the year 2011 which has been gone down to 20, a reduction of around 38%.

Total The vehicles involved in road accidents from 2010 to 2015 are shown in Table 2. The Table clearly represents that Trucks and cars are involved in maximum numbers of accidents during this duration which has been more than 60 % of total accident. Two Wheeler and Buses have 16 and 10 percentage of accidents from 2010 to 2015.

Table 1:Total number of accidents per years

Year	Fatal	Serious	Minor	Total No of accident
2010	32	18	19	69
2011	28	30	51	109
2012	36	22	29	87
2013	25	27	24	76

2014	26	18	15	59
2015	20	33	8	61

Table 2:Vehicle involved in Accidents

Vehicle type	Total	Vehicle wise (%)
2 Wheeler	63	16.53
3 Wheeler	19	04.98
Car	99	29.13
Bus	23	06.03
Truck	125	32.80
Miscellaneous	52	10.49

It can be seen that from Table 3, accident time also has the characteristics of day night traffic and a trough. That is, the day time rush hour appears in 06:00am-10:00pm having 75 % total traffic and night time 10:00pm-06:00am having 25% of traffic in a day. This phenomenon is in good consistency with the characteristics of the time distribution of traffic, showing that the frequency of traffic accidents has a high frequency and relevance with the Traffic i.e. 75% traffic accident occurs in day time rush hours from 06:00AM-10:00PM.

Table 3:Time of Accidents

Time	Total no of accident
6:00am to 9:00am	77
9:00am to 12:00pm	82
12:00pm to 3:00pm	63
3:00pm to 6:00pm	81
6:00pm to 9:00pm	107
9:00pm to 12:00am	44
12:00am to 3:00am	55
3:00am to 6:00am	35

Table 4 presents accident severity index for selected stretch on NH – 8 from Narmada Intersection (Km 168+750) to Palej (190+650) Intersection. from 2010 to 2015. It is seen from the table that the accident severity index has suddenly decreased from 46.37 in 2010 to 25.68 in 2010 thereafter it increases to 44.06 in 2014. In 2015, the number of ASI decreased up to 32.78, nearly same as 2013.

Table 4:Accident severity index (ASI) and Weighted Accident severity index (WASI)

Year	Total no of Accident	No of Death	ASI (%)	WASI
2010	69	32	46.37	4.261
2011	109	28	25.68	2.991
2012	87	36	41.37	3.977
2013	76	25	32.89	3.263
2014	59	26	44.06	4.034
2015	61	20	32.78	2.885

Initially the weighted accident severity index (WASI) is found to be 4.261 in 2010 which decreased to 2.991 in 2011. Thereafter, there is a sudden increase to 3.997 in 2012 and then increased to 4.034 in year 2014. In the last year 2015, finally the WASI is found to be 2.885. Evidently, more number of deaths and more number of major injuries in 2010 caused more WASI than other years considered in the study.The calculations of WASI are shown in the table 4 .

Table 5 indicate the hourly traffic data in PCU for Total Traffic, Up direction traffic (Palej to Bharuch) and down direction traffic (Bharuch to Palej).It is clearly shows that total traffic is more from 7.00AM to 1.00PM and 2.00PM to 8.00PM. Traffic in up direction (Palej to Bharuch) is more from 7.00AM to 12 .00PM and 2.00PM to 7.00PM. Traffic in Down direction (Bharuch to Palej) is more from 11.00PM to 02 .00AM and 2.00PM to 9.00PM. Maximum traffic accident occurred between 3.00 PM to 9.00 PM which is maximum peak hour traffic volume. Traffic volume peak hour is identified between 4.00PM to 5.00PM.

Table 5: Hourly traffic volume in PCU

Daily hours	Up Traffic	Down Traffic	Total
8 – 9	1499	1213	2712
9 – 10	1537	1198	2735
10 – 11	1409	1244	2654
11 – 12	1373	1180	2553
12 – 13	1176	1338	2515
13 – 14	1217	1207	2423
14 – 15	1416	1317	2733
15 – 16	1300	1423	2723
16 - 17	1423	1516	2939
17 – 18	1393	1384	2777
18 – 19	1377	1476	2852
19 – 20	1191	1321	2512
20 – 21	1143	1300	2442
21 – 22	1195	1218	2413
22 – 23	1174	1227	2401
23 – 0	1119	1267	2386
0 – 1	1102	1289	2390
1 – 2	1028	1323	2351
2 – 3	1019	1016	2035
3 – 4	1110	879	1989
4 – 5	1149	1075	2224
5 – 6	1178	1090	2268
6 – 7	1143	1309	2452
7 – 8	1306	1287	2592

Figure 1.0 indicates total traffic composition on NH-8 from Bharuch to Palej section. At Location near Nabipur village, vehicle's compositions by type and percentage of volume are 2-wheelers (3.13%), passenger car (17.75 %), Bus (7.66%), LCV (4%), 2-axle (21.48%), 3-axle trucks (15.18%) and Multi Axle (29.58%).
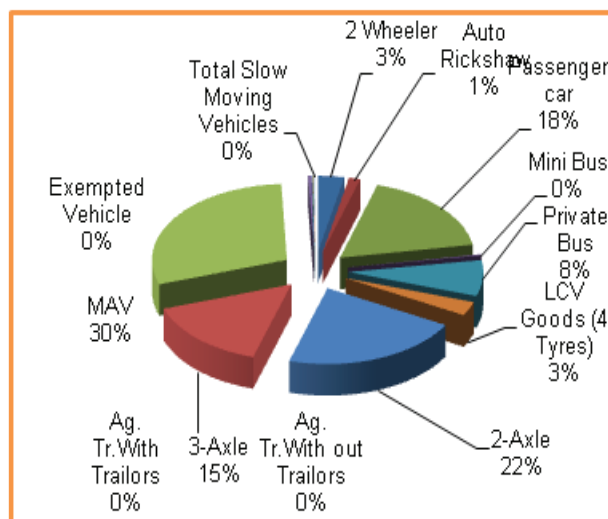

Fig. 1 :Trafic composition in PCU

Figure 2.0 indicates total day and night traffic composition percentage on old National Highway - 8 from Bharuch to Palej section.
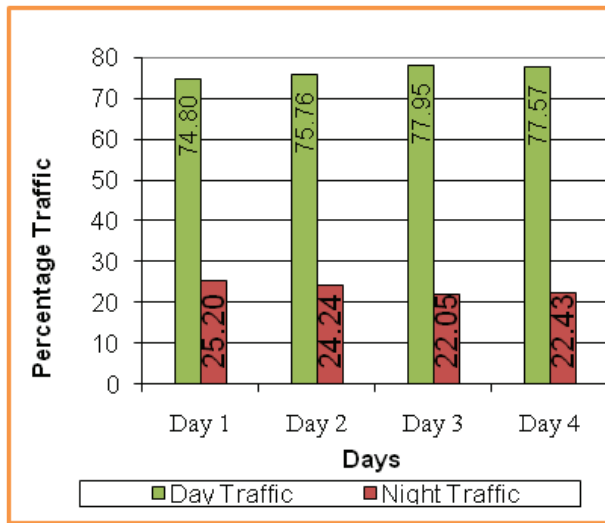
Fig. 2: Day and Night Traffic

RECOMMENDATIONS

Following recommendations are given from road safety inspection audit on project road.

Over Speeding

Traffic accidents were occurred as listed in Table 7 location at which Design speed limit of 50 km/hr accept Luwara junction where speed limit is 40 km/hr. This accident spots also recommended as traffic accident zone. Road users avoided these traffic regulation and drive with over speed limit which ultimately result into traffic accidents. Traffic accident zone sign is also provided by traffic division, Bharuch district. But such over speed is regulated by higher find charges to over speed road users with Traffic Interceptor Vehicle (TIV) etc.

Table 7: Overspeed Accidents Location

SR No.	Location of Accidents	No of Accident	Remarks
1	Near jandhar village	18	Overspeed, No Blinking signal
2	Near Atithi hotel	23	Overspeed, Poor speed limit sign
3	Kavitha Junction	9	Overspeed
4	Luwara jun. to Gurudwara	22	Overspeed
5	Near Ashuriya Village	15	Overspeed, No Blinking signal
6	Manch village	2	Overspeed,
7	Near Vagushna Junction	5	Over speed
8	Bostan hotel	5	Overspeed, Poor speed limit sign
9	Palej Overbridge	15	Over speed

In above Table 7, Accidents Location details due to over speed limit are given. Yellow blinking signal is provided at Near Jandhar and Asuriya village. Speed limit sign is in poor condition at Atithi and Bosten Hotel which needs to improve.

Abrupt change in carriageway width

There is sudden changed in carriageway width from 6 lane to 4 lane at km 176+400 bridge which also leads to accident. Location of narrow bridge is near to Manch village as shown in Table 8 which is also one of factor for accident. Such type of abrupt change in carriageway width on higher speed carriageway resulted into road accidents. So, Bridge width is increased and developed to 6 lanes to avoid accidents.

Table 8: Narrow Bridge Accident Location

Sr. No.	Location of Accident	No of accide-nt	Remarks
1	Manch village	2	Near by narrow bridge,

Roadside Parking

Majority road side parking is found on project road which results into poor rod sight distance at intersections. Accident locations due to road side parking are shown in Table 9. Road side parking on project road is found due to 47 no of rest area on the project road.

Table 9: Road side Parking Accidents Location

Sr. No	Locations of Accident	No of accident
1	Luwara junction to Gurudwara	22
2	Manch village	2
3	Bostan hotel	5
4	Near Varediya Junction	23
5	Hotel Decent	2

Overtaking lane is blocked by Slow Moving Vehicle

It is observed that majority trucks drivers are moved in overtaking lanes with low speed compared to cars as shown in photograph above which force to car users to move in wrong direction for overtaking which ultimate results into accident. So, Lane discipline driving is necessary to reduce such kind of accidents which is implemented by providing higher find charges by traffic police. Land discipline signs are also provided on project road.

CONCLUSIONS

The following conclusion made from the road safety inspection from Bharuch to Palej on NH-8.

1. Accident Severity Index (ASI) is decreased from 44.08 in 2014 to 32.78 in 2015 and higher than 2011 in which total no of accident occurred 109 compared to 61 in 2015. which are due to increase in traffic volume on project road.

2. Weighted severity index (WASI) is decreased from 4.034 in 2014 to 2.885 in 2015 which similar to 2.991 as in 2016. WASI indicates that traffic overall accidents severity is decreased in 2015 due to traffic regulation even though traffic volume is increase.

3. According to traffic composition and traffic accidents composition, the traffic volume of trucks is 65% and involvement in accidents is 33 % as traffic volume of car is around 18% and involvement in accidents is 29%. that indicates the car user's involvement compared to traffic composition is high which is due to higher speed and poor driving sense.

4. Looking to the traffic and accident composition, car and truck users having major involvement in road accident which indicates that poor sense of driving by them.

5. Majority accidents occurred between 6.00AM to 12.00PM and 3.00PM to 9.00 PM and which require strong traffic regulation during this time zone.

REFERENCES

1. Antov D Road Safety Inspection and RSA as the main tool for Infrastructure safety improvement in rapidly motorizing countries, Journal of International Scientific Publications, Vol.6 (1), 1996. Available on: http://www.science-journals.eu

2. Chauhan D. V, et al. Road Safety Audit: A Case Study of Stretch from Garudeshwar Chokdi to Kalaghoda Circle at Rajpipala, International Journal of Science and Modern Engineering, Vol.3, Issue 6, 2015.

3. Chaurasia V. K, et al. Accident Study on Identified Roads of Kurukshetra, Transportation Engineering, National Institute of Technology Kurukshetra, Haryana, India, 2015. E-mail address: vishal14290@gmail.com

4. Deshpande P Road safety and accident prevention in India: a review,Int. J Adv. Engg. Tech., vol.5, issue.2, 64-68, 2014.

5. Dr. Jain A. M, et al. Road safety audit is corridor of Narol to Narola National Highway-Ahmedabad city of Gujarat state, International Journal ofEngineering and Technical Research, Vol.2, Issue 3, 2014.

6. Dr. Jain S. S, et al.Road safety audit for four lane national highways, 2011.

7. Dr. Ravinder K, et al. Road Safety Audit of National Highways in India at Construction Stage, 13th WCTR, 2013.

8. European Transport Safety Council Road safety audit and safety impact assessment, 1997.

9. Gangopadhyay S and U K guru vittal Central Road Research Institute, Vol.108 (5), 2015.

10. Grewal G, Rahul bansal . Study on Accident Severity Index, Time of Accident and Vehicle involved in

Accident in Hisar City, International Journal of Enhanced Research in Science Technology & Engineering, ISSN: 2319-7463 Vol. 4 Issue 5, pp 128-135, may-2015, Impact Factor: 1.252

Available online at: www.erpublications.com

11. Indian Department of Transportation Highway safety improvement program local project selection guidance, 2014.

12. Kanellaidis G Aspects of road safety audits, Journal of transportation engineering, vol.125 (6), pp 481-486, 1999. Available on: http://www.in.gov/indot/div/engineering/shsp.html

13. Kanellaidis G Human factors in highway geometric design, Journal of construction engineering and management, vol.122 (1), pp 59-66, 1999.

14. Kim Y. A, et al. Major Accident Factors for Effective Safety Management of Highway Construction Projects, Journal of construction engineering and management, vol.139 (6), pp 628-640, 2013.

15. Mankar C. R, et al. Road Safety Audit: An Accident Studies of Selected Stretch Road, International Journal of Innovative Research and Development, Vol.3, Issue 5, 2014.

16. Patel D. G, et al. Road Safety Audit of Selected Stretch from Umreth Junction to Vasad Junction, International Journal of Science and Modern Engineering, Vol.1, Issue 6, 2013.

17. Shruthi P Accidents related to traffic, 2013.

18. Singh R. K, et al. "Accident Analysis and prediction of Model on National Highways" International Journal of advanced technology in civil Engineering, Volume 1, Issue 2, 2001.

19. Singh S. K, et al. Road safety analysis: A case study of Patna city, urban transportation journals, vol.2 (2), pp 60-75, 2004.

20. Spring G. S Road Safety: Discussion of State of Practice, Journal of construction engineering and management, vol. 131 (5), pp 329-332, 2005.

21. Wilson E. M, et al. "Road Safety Audits, a Synthesis of Highway Practice", 2014.

Design and Planning of a Bicycle Track for Urban Recreation and Commuting in Nashik City

Darshankumar Patel
Research Scholar
Department of Civil Engineering
Oriental University
Indore, Madhya Pradesh
✉ darshptl12354@gmail.com

Bikram Prasad
Associate Professor
Department of Civil Engineering
Oriental University
Indore, Madhya Pradesh

ABSTRACT

As urban areas continue to expand and prioritize sustainable transportation, the demand for well-designed bicycle paths has become increasingly critical. This summary introduces a comprehensive planning strategy for creating a bicycle path that serves both recreational and commuting purposes in urban settings. The proposed path is intended to encourage the adoption of eco-friendly transportation, promote healthy living, and enhance the overall quality of life in the community. The planning process involves a detailed examination of the local urban infrastructure, considering the current transportation network, population density, and existing recreational facilities. Special attention is given to seamlessly integrating the path into the urban landscape, ensuring connectivity to important destinations, and addressing potential safety issues. The design accommodates various user groups, catering to different skill levels and preferences, thereby promoting inclusivity and accessibility. Furthermore, the summary emphasizes the incorporation of sustainable practices and green technologies in the construction and maintenance of the bicycle. Strategies include the use of recycled materials, energy-efficient lighting, and the promotion of native plant landscaping to reduce environmental impact and contribute to the project's overall sustainability. By fostering collaboration among urban planners, landscape architects, transportation engineers, and community stakeholders, the proposed bicycle path aims to encourage social engagement, promote active lifestyles, and decrease carbon emissions. The summary concludes by discussing the expected positive effects of the bicycle on the urban environment, such as improved air quality, reduced traffic congestion and enhanced well-being for residents.

KEYWORDS : Educational, Workplace, Accessibility, Bicycle.

INTRODUCTION

Accessibility refers to assessing how various activities are spread out around a specific point, taking into account the ability and willingness of individuals or organizations to overcome obstacles in their surroundings [1]. This idea is widely used in areas like transportation planning, urban planning, and geography, and plays a significant role in creating policies [7]. It can be defined as the closeness of people, places, and services to the transportation system [5]. Accessibility indicates the capability of individuals to access services, goods, and activities, which is the primary aim of most transportation initiatives [11]. A community's increased accessibility to different activity areas corresponds to a higher potential for its development [1]. Notably, accessibility is a crucial characteristic for metropolitan regions and is often reflected in transportation and land-use planning goals [4]. Measures of accessibility are frequently used to evaluate policy plans for land-use and infrastructure, aiding policymakers and researchers in finding solutions [7].In terms of public transport accessibility levels, the PTAL (Public Transport Accessibility Levels) in Ahmedabad city was determined using various methods, eventually settling on the quintile method for mapping [16]. An analysis in Ahmedabad focused on the multi-modal accessibility to jobs for the urban poor, emphasizing the importance of improving public transport, non-motorized transport

feeder functions, and integrated urban land use and transport development strategies, while considering where the urban poor live and work [13]. Similarly, a study in Milan, Italy, examined potential changes to the surface public transportation system, highlighting the need for improvements in the system's efficiency and identifying areas for potential enhancements not only for residents but also for businesses within the city limits [14]. Furthermore, a study in Krefeld, Germany, aimed to enhance accessibility indicators for use in public transport plans, suggesting the use of a travel time budget indicator for analysing local accessibility by public transport, demonstrated through a GIS application in the case study city [8].Workplace accessibility, also known as job accessibility, is influenced by various factors such as modes of transportation, traffic congestion, road networks, and the level of competition for jobs among workers [6]. The spatial aspect of job access has significant implications, especially in inner-city areas, impacting residents and the overall dynamics of the city, including social disorder and criminal behaviour [3]. Socioeconomic factors, including vehicle ownership, may contribute to the lack of employment opportunities [2].Studies like the Amsterdam Job Accessibility Measure have shown that job accessibility can be measured and mapped in a GIS environment, emphasizing the significance of data related to transportation networks and activity locations. This information can be valuable in developing various policies [12]. In the context of London, the PTAL is calculated numerically and used in development plans to determine policies, including decisions on housing density, parking area locations, and allocations [15]. Efficient public transport significantly contributes to the level of accessibility, especially for work-related trips, which are considered essential and unavoidable. A primary survey conducted in Nashik city identified five major modes of transportation, including bicycles, motorcycles, cars, auto-rickshaws, and public buses. The Relative Accessibility Index (RAI) of public transport was calculated using these modes and mapped in a GIS environment using ArcMap. The study aims to provide a framework for local authorities to improve the city's transportation infrastructure, with RAI mapping offering insights to decision-makers and policymakers for shaping the city's development pattern with regard

to public transport. The study proposes a method called the Public Transport Accessibility Model (PTAM) for assessing public transport accessibility at a macroscopic level.

Below is a simple table that can guide the planning process for a bicycle track in a city

Table 1: Guidelines for planning process for a bicycle track in a city

Criteria	Description
1. City Demographics	Understanding the city's population density, age distribution, and cycling habits.
2. Existing Infrastructure	Assessing the current road network, public transportation, and bike-sharing systems.
3. Safety Measures	Ensuring adequate safety features such as proper lighting, clear signage, and designated crossing points.
4. Environmental Impact	Evaluating the impact of the track on the environment and nearby ecosystems.
5. Accessibility	Ensuring the track is easily accessible for people with disabilities and all members of the community.
6. Integration with Urban Design	Integrating the track seamlessly with the existing urban landscape and architectural features.
7. Land Use Planning	Identifying appropriate land areas for the track without encroaching on private properties or natural reserves.
8. Maintenance Plan	Developing a sustainable maintenance plan to ensure the track remains safe and functional in the long term.
9. Community Engagement	Involving the community in the planning process to understand their needs and address any concerns.

10. Cost-Benefit Analysis	Conducting a comprehensive cost-benefit analysis to evaluate the economic feasibility of the project.

This table can serve as a starting point for a comprehensive bicycle track planning process in a city.

Planning a bicycle track in India involves considering several key factors to ensure its success and integration into the existing infrastructure. Below is a comprehensive guideline that can help in planning a bicycle track in India:

- Conduct a feasibility study: Before initiating the planning process, conduct a comprehensive feasibility study to assess the practicality and potential of the bicycle track in the selected location. Consider factors such as population density, traffic patterns, and the existing infrastructure.

- Identify suitable locations: Identify areas with high bicycle usage or the potential for increased bicycle usage. Look for locations with low vehicular traffic, wide roads, or areas with scenic beauty to encourage more people to use the bicycle track.

- Collaborate with local authorities: Engage with local municipal corporations, urban planners, and relevant government bodies to gain support for the project. Obtain necessary permits and clearances before commencing any construction.

- Involve the community: Involve local communities and cycling enthusiasts in the planning process. Conduct public consultations and gather feedback to understand the requirements and expectations of potential users. Incorporate their suggestions into the planning process where feasible.

- Ensure safety measures: Prioritize the safety of cyclists by implementing safety measures such as clearly marked lanes, traffic signals, speed limit signs, and designated crossing points. Integrate safety barriers to separate the bicycle track from vehicular traffic.

- Consider environmental impact: Ensure the bicycle track is designed with environmental sustainability in mind. Incorporate green spaces, plant trees, and use eco-friendly construction materials wherever possible. Aim to minimize the ecological footprint of the project.

- Provide necessary amenities: Install bicycle parking stations, repair stations, and rest areas along the track. Include amenities such as water fountains, seating areas, and public restrooms to enhance the overall experience for cyclists.

- Integrate with public transport: Integrate the bicycle track with existing public transport systems, such as bus stops and metro stations, to facilitate seamless intermodal transportation. This integration will encourage more people to combine cycling with public transit.

- Ensure accessibility: Design the bicycle track to be accessible to people of all abilities. Incorporate features such as ramps, elevators, and other accessibility aids to accommodate individuals with disabilities.

- Regular maintenance and monitoring: Establish a regular maintenance schedule to ensure the bicycle track remains in optimal condition. Monitor the usage patterns, collect user feedback, and make necessary adjustments to improve the overall experience.

- Promote awareness and education: Launch awareness campaigns and educational programs to promote the benefits of cycling and the use of the bicycle track. Organize workshops and events to encourage more people to adopt cycling as a sustainable mode of transportation.

By adhering to these guidelines, you can effectively plan and develop a well-designed and functional bicycle track that contributes to a sustainable and eco-friendly transportation system in India.

STUDY AREA: NASHIK CITY

Nashik is a city located in the northwest region of the state of Maharashtra in India. It is situated on the banks of the Godavari River, one of the longest rivers in India. Nashik is known for its rich historical, cultural, and mythological significance. Nashik has a significant place in Indian history and mythology. It is believed to be the place where Lord Rama, the central figure of the Hindu epic Ramayana, spent a significant

part of his exile. The city is famous for its numerous temples and religious sites. The Kumbh Mela, one of the largest religious gatherings in the world, takes place in Nashik once every 12 years, drawing millions of pilgrims from around the country. The city has a well-developed educational infrastructure with several schools, colleges, and universities. It also has a good healthcare system, with many hospitals and medical facilities catering to the needs of the local population. The city has a well-developed educational infrastructure with several schools, colleges, and universities. It also has a good healthcare system, with many hospitals and medical facilities catering to the needs of the local population. [17].

Fig. 1: Nashik City's Position [17]

## AIM, OBJECTIVE AND METHODOLOGY

Aim

To propose bicycle track for identified area of Nashik city for better accessibility to educational services.

Objectives

• To understand demographic features of Nashik city

• To study transportation system of Nashik city

• To study existing condition of Educational Trips for Nashik city

• To evaluate existing accessibility index of Educational trips for identifying area of bicycle track

Methodology
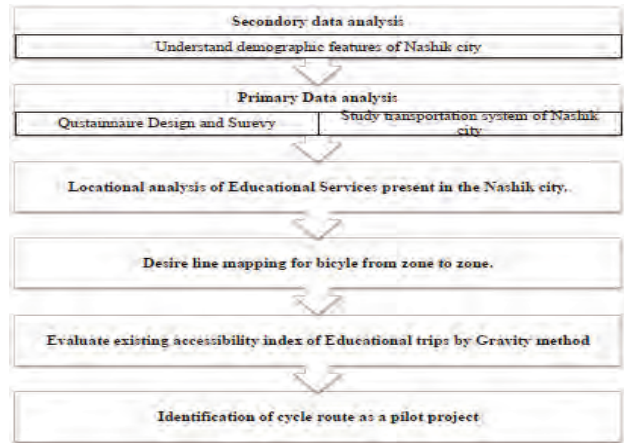
Zoning of Study Area

A preliminary investigation was carried out in Nashik city to examine the travel behavior within the core area of the city using a questionnaire. The findings of this study revealed that the commuting patterns included trips originating within the city limits and those from the surrounding peripheral areas. However, the survey did not include the Military area. In order to comprehensively assess accessibility, it was deemed necessary to incorporate this area into the zoning. Therefore, city has been divided in to six zones excluding military area. Figure no 2 providing the location of all six zones. This zoning of the city was very helpful while doing the detailed analysis of transportation systems of the city with the help of primary data collected with questionnaire design for survey purposes.
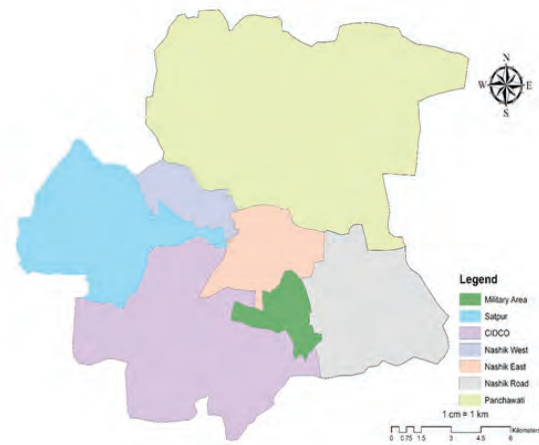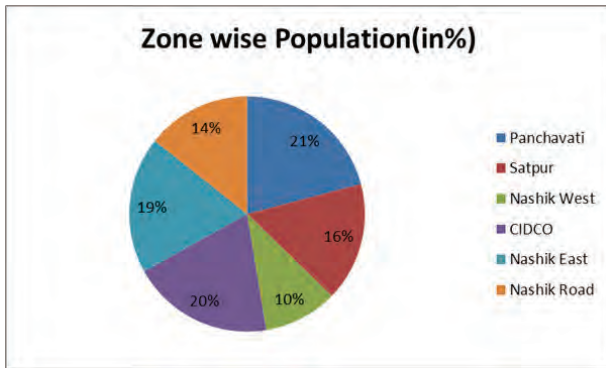

Fig. 2: Zones of Nashik City

Fig. 3: Zone wise Population of Nashik City

Analysis of Population Density of City

Fig. 4: Population density Map

The core area and CIDCO region of the city exhibit the highest population density. Ward number 10, located in the core area and in close proximity to the city centre, boasts the maximum population density of 1121 people per hectare (PPHa). On the other hand, ward number 70 showcases the lowest population density at 11 PPHa. The city's overall average population density is approximately 212 PPHa. Additionally, the population density demonstrates an exponential decrease as one moves away from the city centre, as depicted in the accompanying graph.
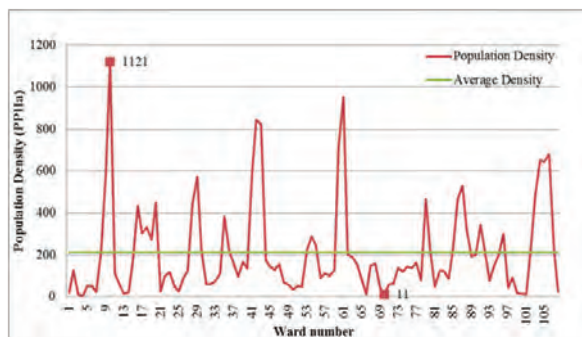
Fig. 5: Population density vs. Ward Number
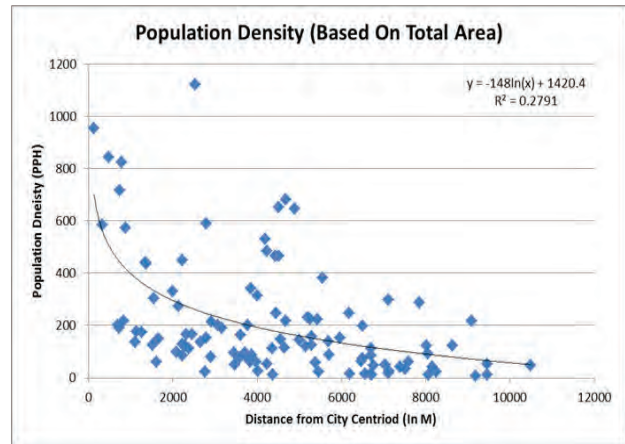
Fig. 6: Population Density Vs. Distance from Centroid of city

Public Transportation Present in City

Currently, the Maharashtra State Road Transport Corporation manages the city bus service in Nashik through its two depots, namely Nashik I depot and Nashik II depot situated close to old Adgaon. Nashik City has received 100 buses under the Jawaharlal Nehru National Urban Renewal Mission (JNNURM). On a daily basis, the bus system caters to approximately 145,000 passengers, including 45,000 students. Additionally, around 2,75,034 commuters use 392 schedules and 3280 trips to and from various parts of the State. The M.S.R.T.C. plays a pivotal role in the urban renewal and development of Nashik City. The projected expenditure for achieving its objectives is estimated to be Rs. 128.00 Cr.
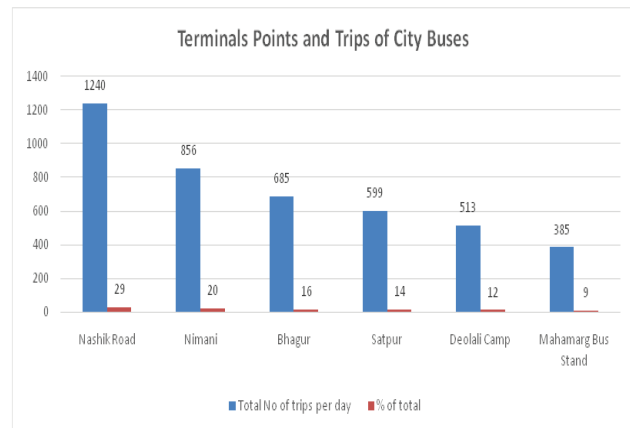
Fig. 7: Terminals Points and Trips of City Buses (Year 2011) [19]
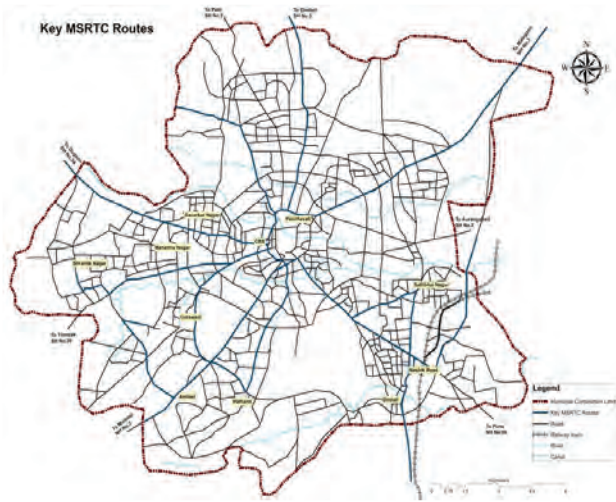
Fig. 8: Key MSRTC routes in Nashik City

Table 2: Number of bus routes and Passengers

Sr. No	Year	Total buses	No of total routes	No of Passengers	Growth in Passenger (%)
1	1995-96	130	285	117892	-
2	2000-01	145	305	123847	5.05
3	2005-06	185	346	140393	13.36
4	2010-11	190	376	155378	10.67

Vehicle Ownership Pattern
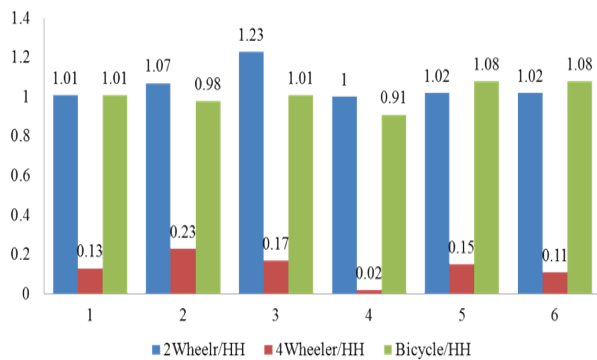
Fig. 9: Vehicle ownership pattern
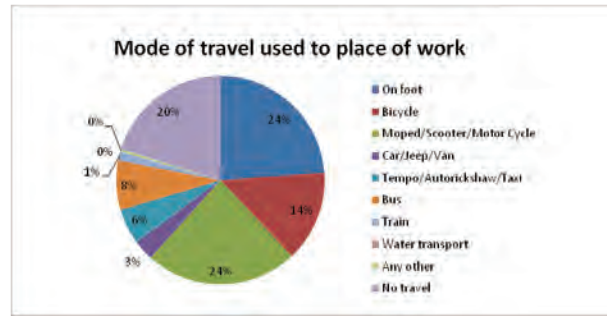
Fig. 10: Mode of travel used to place of work

Issues Related to Public Transport in Nasik City

• Insufficient availability of parking and growing issues with traffic, traffic safety, and congestion stem from the rising numbers of Auto Rickshaws and private vehicles.

• The scarcity of buses contributes to the problem, with private vehicles dominating the roads. Data indicates that buses serve as the sole public transportation option, accounting for a mere 4% of all trips, revealing their inadequacy in meeting the escalating transportation demands.

• Inadequate and poorly positioned bus depots lead to significant unproductive travel.

• Furthermore, the absence of link roads and bypass routes exacerbates the traffic gridlock.

• There is a pressing need to enhance the use of public transport, while the development of intersections, junctions, and pedestrian and cycle corridors has been largely overlooked.

EVALUATION OF ACCESSIBILITY INDEX

Gravity Accessibility Method

In this method attractiveness of each zone is consider along with the number of educational facilities, workplaces present in zone. Generalized cost function is considered for both educational and work trips separately. First accessibility index is calculated by type of mode for wok trips and educational trips zonewise. Then the average value is considering for finding total accessibility index for Wok trips and Educational Trips. The equation which is used for the calculating the accessibility index is as below:

$$A_i = \frac{\sum \{O_i * f(c_{ij})\}}{D_i * f(c_{ij})} * 100$$

Where,

O_i = Trips attracted by zone i from all other zones

$f(c_{ij})$ = Generalized cost Function

D_i = Number of activities presents in zone i

Fig. 11: Accessibility index for Work trips by type of mode

AI for Work trips by bicycle is maximum for Nashik east zone.
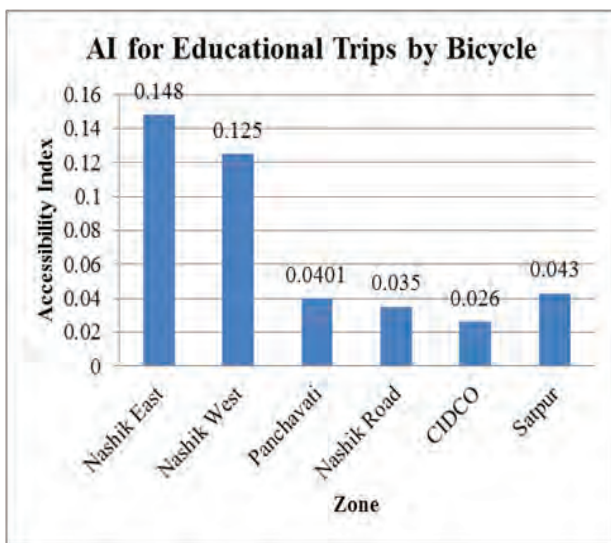
Fig. 12: Accessibility index for Educational trips by type of mode

AI for Educational Trips by bicycle is maximum for Nashik east zone. AI for Educational Trips by four wheelers is maximum for Satpur and Panchavati zone.

IDENTIFICATION OF CYCLE ROUTE AS A PILOT PROJECT

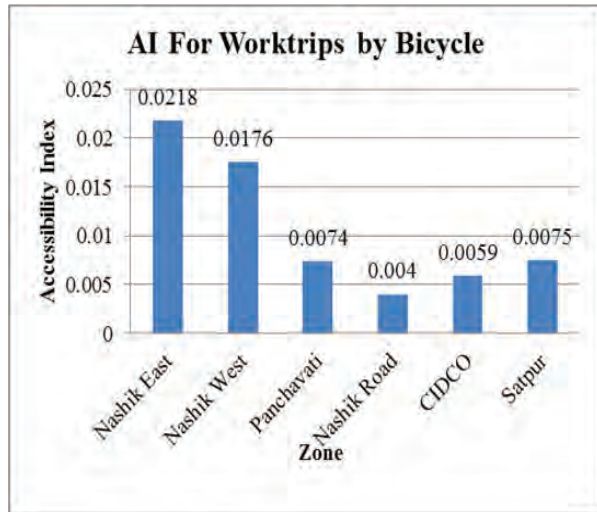Observing various parts of the city, such as Panchwati, Sharanpur, around Trimbak Road, Canada Corner, Pandit Colony, Lawate Nagar, Savarkar Nagar, and other areas, it is evident that there is a lack of dedicated and uninterrupted sidewalks. Even prominent routes like the Mumbai-Agra road, Trimbak Road, Sharanpur Road, and Gangapur Road, which are either wide or have been recently expanded, lack secure and continuous walkways, cycling lanes, and crossing points. While a physically separated sidewalk might not have been deemed necessary in the past due to low motorization and reduced speeds, the city is now witnessing a significant surge in private vehicles.

The expansion of roads and carriage width will present a hazard to non-motorized transportation (NMT) modes unless safe facilities for pedestrians and cyclists are incorporated. Given the significance of Non-Motorized Transportation and the increasing use of bicycles for commuting and educational purposes, a pilot project introducing Cycle routes has been suggested in Nashik city.

The steps undertaken to determine these cycle routes are outlined as follows.:The initial phase involves pinpointing areas where a substantial number of individuals rely on bicycles for commuting and educational purposes. This determination is based on the desire line map, which highlights that zones 1, 2, 5, and 6 exhibit the highest frequency of cycle trips. Furthermore, the accessibility index map for bicycles aids in identifying zones with limited bicycle accessibility. Following this, the subsequent stage entails the identification of current cycle tracks and preserved paths for Non-Motorized Vehicles (NMV) within these specific zones. In the third phase, the existing and planned bus terminals within these four zones are identified in order to seamlessly integrate them with the cycle routes. Taking all of these factors into consideration, a new cycle route is proposed for these designated zones
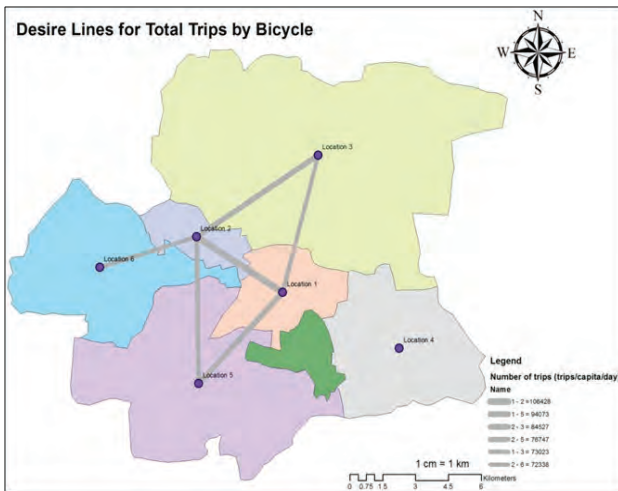
Fig. 13: Desire line map for total trips by Bicycle
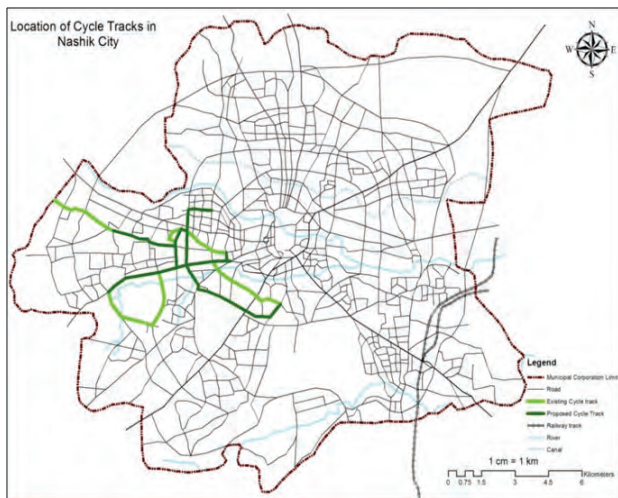
Fig. 14: Location of cycle track in Nashik city
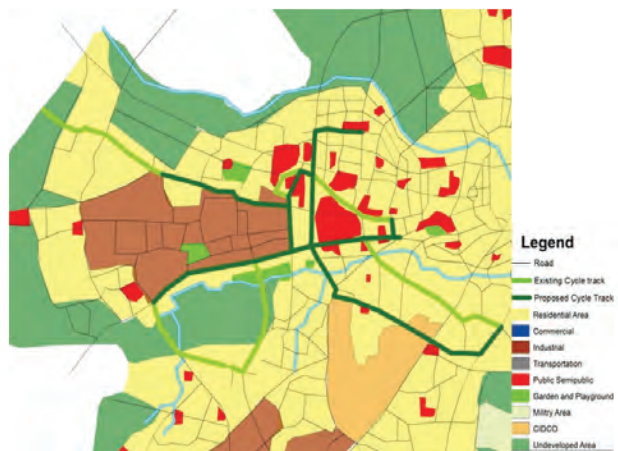
Fig. 15: Proposed Cycle Route Map

After introducing cycling paths in specific areas, the plan is to extend them to other regions using the same approach. This expansion aims to enhance bike accessibility for both work and educational commuting. Additionally, a bike-sharing program will be launched through collaboration with a private firm, allowing people to rent bicycles. This initiative forms part of the comprehensive traffic management strategy integrated into the smart city's overarching plan.

FINDINGS

Similar to work trips, the Satpur zone has the lowest accessibility index for educational visits, whereas Nashik East has the highest index. It demonstrates that the zones Satpur and Nashik Road have the highest commute times and expenses to go to work. Additionally, it demonstrates that, in comparison to other zones, Nashik East and Nashik West are the closest to educational institutions. These problems can be resolved by building connections between the zones, enhancing public transportation, and taking other appropriate measures, such as allocating facilities in that zone, among other things. The total AI, which uses the probability method, indicates that the zones of Panchavati, Nashik Road, and Northeast have lower levels of accessibility by public transportation for educational locations.This demonstrates the need for more infrastructure for public transportation in these zones. Nashik East has the highest accessibility index for work trips, while Satpur zone has the lowest. It demonstrates that the zones Satpur and Nashik Road have the highest commute times and expenses to go to work. It also demonstrates that, as comparison to other zones, Nashik East and Nashik West have the closest proximity to the workplace. This problem can be resolved by building connections between the zones, enhancing public transportation, and taking other appropriate measures, such as allocating facilities in that zone, among other things. The total AI, which uses the probability method, indicates that the zones of Panchavati, Nashik Road, and Northeast have lower levels of accessibility by public transportation to workplace locations. This shows that this zones need increase in public transport infrastructure. Accessibility ratio for Educational trip is maximum for Panchavati, Nashik road and Nashik East zone. It shows that

maximum number of peoples are using private mode of transportation for trip rather than public transport. It also shows that this zones have lack of public transport infrastructure Accessibility ratio for work trip is maximum for Panchavati, Nashik road and Nashik East zone. It shows that maximum number of peoples are using private mode of transportation for trip rather than public transport. It also shows that these zones have lack of public transport infrastructure.

REFERENCES

1. Hansen, W. G. (1959). How Accessibility Shapes Land Use. Journal of the American Institute of Planners, 25(2), 73-76. doi: 10.1080/01944365908978307

2. Taylor, B. D., & Ong, P. M. (1995). Spatial mismatch or automobile mismatch?An examination of race, residence and commuting in US metropolitan areas. Urban studies, 32(9), 1453-1473.

3. Freeman, R. B. (1996). Why do so many young American men commit crimes and what might we do about it? : National Bureau of Economic Research.

4. Handy, S. L., & Niemeier, D. A. (1997). Measuring accessibility: an exploration of issues and alternatives. Environment and planning A, 29(7), 1175-1194.

5. Sathisan, S., & Srinivasan, N. (1998). Evaluation of accessibility of urban transportation networks. Transportation Research Record: Journal of the Transportation Research Board (1617), 78-83.

6. Wang, F. (2003). Job proximity and accessibility for workers of various wage groups. Urban Geography, 24(3), 253-271.

7. Geurs, K. T., & Van Wee, B. (2004). Accessibility evaluation of land-use and transport strategies: review and research directions. Journal of Transport Geography, 12(2), 127-140.

8. Zwacarze and Bjorn, "Measuring Local Accessibility By Public Transport, Research and Teaching Assistant, University of Dortmund, Faculty of Spatial Planning Chair of System Theory and Systems Engineering, Germany.August-2006.

9. Zimon Cooper, Peter Wright and Rhodri Ball. "Measuring the Accessibility of Opportunities and Services in Dense Urban Environments: Experiences from London", Transport for London (2009).

10. Measuring Public Transport Accessibility Level, Transport for London, April 2010.

11. Litman, T. (2011). Evaluating accessibility for transportation planning. Victoria, BC: Victoria Transport Policy Institute.

12. J. Cheng and L. Bertolini."Measuring urban job accessibility with distance, competition and diversity." Journal of transport Geography, 2013: vol.30, pp.100-109.

13. ZUIDGEEST. M, Van den BOSCH, F. BRUSSEL, M. SALZBERG, A. MUNSHI, T. GUPTA and N. Van. "GIS for Multi-Modal Accessibility to Jobs for the Urban Poor in Ahmedabad ",13th WCTR: July15-18, Rio-de Janeiro, Brazil,2013.

14. Martino, Alessandro De. ""Geographic Accessibility Analysis and Evaluation of Potential Changes to Public Transportation System in City of MILAN", Department of Physical Geography and Ecosystem Science, Centre for Graphical Information System, S-22362, Sweden,2014.

15. Transport for London, Mayor of London. "Accessing transport connectivity on London, "Guide, April 2015.

16. Jay Shah, Transport Planning Consultant and Bharghav Adhvaryu, CEPT University. "Public Transport Accessibility Levels for Ahmedabad", Journal of Public Transportation, Vol.19, no.3,2016.

17. Nashik Draft Revised Development Plan,2016-2036.

Study on Microplastic Pollution in Lake Sediments of Ashtamudi Lake – A Case Study

Shibu K
Assistant Professor
Department of Civil Engineering
College of Engineering Trivandrum
Thiruvananthapuram, Kerala
✉ shibukrishnanp@gmail.com

Aswathy A
Former Postgraduate Scholar
Department of Civil Engineering
College of Engineering Trivandrum
Thiruvananthapuram, Kerala

Drisiya J
Postgraduate Scholar
Department of Civil Engineering
College of Engineering Trivandrum
Thiruvananthapuram, Kerala

ABSTRACT

Pollution due to plastic has become a critical environmental concern for both our planet and mankind. This study presents the first investigation into the microplastic in the sediment of Ashtamudi Lake, a Ramsar Site of international importance in South India. For the analysis five sediment samples were collected from the Kollam, Kureepuzha and Kallada region in May -June 2022 and were processed for microplastic extraction and analysed for polymer composition using Fourier Transform Infrared Spectroscopy. The study highlights the abundance of microplastics across the sampled sediments with mean and standard deviation ranging from 12±1, 11±1, and 9±1 per 100gm in the Kollam, Kureepuzha and Kallada regions respectively. The polymer composition study reveals the secondary origin of the Film and Fragment type microplastic with polyethylene, polypropylene and polystyrene as the predominant polymer group. The primary source of the Microplastics in the Ashtamudi Lake includes the disposal of plastic bags, packing material open dumping of waste into the lake through drains and sewer pipes.

KEYWORDS : *Ashtamudi lake, Microplastics, Fourier transform infrared spectroscopy.*

INTRODUCTION

Microplastic pollution has emerged as a significant concern in both freshwater and marine ecosystems in recent years. There is growing interest in comprehending the repercussions of microplastics on aquatic organisms, driven by the fact that their full impact remains inadequately understood[1, 2]. Microplastics were initially detected in North America during the 1970s, appearing as tiny spheres within plankton communities along the New England coast[3]. Subsequently, it has been revealed that the majority of significant water bodies, including lakes, rivers, and oceans, harbour microplastics. These microplastics are defined as plastic particles with a diameter smaller than 5 mm[4].Over the last seven decades, there has been a significant push for increased global plastic production, leading to widespread environmental distribution. This trend has culminated to the extent that it's apt to describe our current state as inhabiting a "plastic world."[5]. Synthetic polymers are environmental pollutants in their own right and act as carriers for a variety of chemical contaminants[6], Nevertheless, they are also regarded as reliable indicators of the contemporary and current era, often the mid-twentieth century. [7].

Microplastic particles are now often found in marine and freshwater habitats in a variety of forms, polymers, sizes, and concentrations. [8], agroecosystems[9], atmosphere[10], food[11]drinking water[12], biota[13], and other remote locations[14].Microplastics enter bodies of water in two ways: primary and secondary[4]. Primary microplastics are created from raw plastic materials, such as virgin plastic granules scrubbers, and microbeads[1, 4] that enter the ocean via runoff from land [15]. Secondary microplastic introduction happens when large plastic items enter the coastline or ocean and experience mechanical photooxidation and/or

biological disintegration[1, 2, 15, 16]. This degradation breaks down the larger portions into increasingly minute plastic particles, which are eventually invisible to the naked eye.

The majority of microplastics, including microbeads and fibres, are of a size that enables them to bypass wastewater treatment facilities and eventually enter water systems[1].Right now, nothing is known regarding the way microplastics damage animals. Nonetheless, it has been demonstrated that a wide range of creatures, which includes invertebrates along with vertebrates, consume microplastics. Scientists are concerned that creatures swallowing plastic waste may be exposed to toxins sorbed into the plastic[17]. Chemical pollutants use plastic trash as both a source as well as a sink. Additives used in the production of plastic can seep into the marine environment[15]. Conversely, hydrophobic pollutants contained in water may capture plastic particles[3, 15, 17]. Thus, microplastics provide a way to carry concentrated pollutants into organisms[1].

We may declare that we live in a plastic world since plastic manufacturing has increased dramatically over the past 70 years all over the world. These polymers' attributes, including their affordable cost of manufacture, have made them indispensable in today's world. The majority of microplastics, including microbeads and fibres, are of a size that enables them to bypass wastewater treatment facilities and eventually enter water systems[18].

Plastics are highly tenacious, resulting in slower breakdown and rapid buildup[19]. In the current context, the global presence of a smaller percentage of plastics, which means microplastics (MPs) as well as nanoplastics (NPs), is garnering major attention from researchers worldwide due to their negative environmental repercussions[20].

According to the study reported by[21], The United States leads in plastic waste production, generating approximately 42 million metric tons annually. Following closely are the European Union, India, China, Brazil, Indonesia, the Russian Federation, Germany, and various other nations. MPs are formed through the steady accumulation of these as well as their subsequent fragmentation. Unfortunately, studies on this topic are still relatively restricted, and out of the 192 countries, only 22.9% have conducted research on MPs[22].

Depending upon the surrounding matrix, these MPs can have a wide range of effects. In aquatic environments, these can be swallowed by the dwelling species by mistaking MPs as food, or sometimes organisms are subjected to MPs owing to their inherent metabolism, such as filter-feeding organisms[23]. Microplastics (MPs) are recognized for their impact on the ecological dynamics of various terrestrial ecosystems, including the behaviour and functioning of species such as soil-dwelling invertebrates, pollinating insects, and fungi[24, 25].Because of their higher bioavailability, subsequent modifications can occur in soil's physical, chemical, and biological aspects, which may also alter terrestrial vegetation[26]. Furthermore, MPs can undergo trophic transfer or bioaccumulation[25, 27]. MPs' increased reach has led to harmful contamination of air, water, and soil, and they are known to be absorbed by humans through ingestion or inhalation processes[28–32]have discovered in their investigation that MPs have pierced the human placentaand possible routes of delivery are proposed via the respiratory and gastrointestinal systems. Furthermore, the adsorption of toxic compounds such as persistent organic pollutants (POPs), heavy-metal herbicides, antibiotics, pathogenic microbes, and destructive algal blooms on the surface of MPs results in synergistic consequences[33, 34]) have also identified ballast water as a major conduit for the channelization of such tainted MPs in global environments.

India is located in southern Asia and is bounded by the Arabian Sea to the southwest, the Bay of Bengal to the southeast, with the Indian Ocean to the south. It lies between latitude 8°4′ and 37°6′ N and longitude 68°7′ to 97°25′ E, with a coastline of 7517 km[35].

As things stand, few publications address the effects of MPs being in various areas of India's environment. The risks associated with MP pollution, including its movement and build-up in the atmosphere, water, and land are being studied worldwide, yet India only makes up a small portion of this global database.

STUDY AREA

Estuaries are environmentally sustainable and commercially significant coastal areas and among the most biologically prolific places on the planet. [36, 37] and sustain a great array of macrobenthic invertebrates. [38].The Ashtamudi estuary system is the 2nd largest on India's southwest border and a Ramsar site[39].

Ashtamudi Lake, commonly referred to as Ashtamudi Kayal (meaning "lake with eight braids"), is Kerala, India's second-largest brackish lake. Figure 1 depicts the coordinates (8°56′46.18″N, 76°33′16.33″E). It is a large, palm-shaped Ramsar wetland on India's southern coast[40].The Kallada River, which originates in the Kulathupuzha foothills of the Western Ghats, acts as the Ashtamudi estuary's sole source of fresh water. This river system is produced by the convergence of three minor rivers: Kulathupuzha, Chenthurnipuzha, and Kalthuruthipuzha. The Kallada River meets the Ashtamudi wetland ecosystem at Peringalam, Kollam. The Arabian Sea and the lake are inextricably linked, with daily tidal oscillations exchanging the lake's water. The wetland system's bedrock lithology is primarily made up of deposits of sediments from the Quaternary and Tertiary periods.The Tertiary sediments consist of laterite, sandstones, and mixed clays from the Warkalai formation, while the Quaternary deposits are marine, fluvial, and alluvial in origin[41]The basin's areas of drainage are 1700 km², with an average yearly rainfall of 2400 mm. The average yearly temperature is between 25.5 to 31.4ºC[41]Apart from December and January, the weather in the region is hot and humid. The Ashtamudi wetland environment offers a rich array of plant species, including mangroves including Avicennia officinalis, Bruguiera gymnorrhiza, and Sonneratia caseolaris, along with accompanying marshy vegetation. Numerous researchers have conducted detailed analyses of meteorological data, organic matter sources, bioaccumulation studies, and the natural history of islands in Ashtamudi's brackish waters[40–42].

The Ashtamudi Lake prominent tourist location in Kerala. It is home to more than 97 species of fish, 57 bird species, and 43 marshland mangrove species, with numerous species of significant conservation significance locally, nationally, and worldwide[43]. The Ministry of Environment, Forest, and Climate Change (MoEFCC) classified Ashtamudi Lake as wetlands of international importance according to the framework of the Ramsar Convention in 2002. Ashtamudi has been assigned as a Ramsar Convention site under Criterion 1 (indicative, rare, or unique instances of a natural or near-natural wetland form), Criterion 2, (which aids vulnerable, endangered, or threatened species, as well as supporting ecological groups at risk.) Criterion 3(which sustains populations of plant and/or animal species crucial for maintaining biodiversity within a

specific biogeographic area.,) and Criterion 8 (which is an essential source of food for fishes[44].

The primary purposes of a city lake can be categorised under a variety of headings, such as environmental services including cargo and ferry services, flood avoidance, pollution reduction, fishing and wildlife protection, support for species diversity, recreation, and aesthetics (tourism). Other advantages offered by this lake include fishing, inland navigation, and a fishing harbour at Neendakara.

Data from household surveys indicated that 10% of the households living around Ashtamudi Lake had direct dependence on Ashtamudi for livelihoods. Of these, a majority (93%) engage in fishing, including clam collection, while the rest derive sustenance from tourism and coir processing. The remaining households engage in small business, and livestock farming and those migrated to the Gulf region for livelihoods. Thousands of people live around the Ashtamudi Lake shoreline in the Kollam district. The present Kollam City's population 26,29,703 is expected to reach 4,00,000 by 2031. (Census of India, 2011). Due to the construction of new government buildings and industrial projects, Kollam City has grown quickly, which has increased Ashtamudi Lake's pollution burden. Kollam Municipal Corporation uses Ashtamudi Lake as a trash sink for both domestic and municipal solid waste, making it one of the majorsources of pollution. The disposal of waste from the ceramic, paper, palm oil, and coconut husk retting industries, as well as from hospitals, cashew factories, and the tourism industry, has an impact on the southern portion of Ashtamudi Lake. Kureepuzha and Mammoottikkadavu are the other waste-dumping locations for dumping untreated waste into lakes. Kollam Bus Stand is nearby. Large quantities of non-biodegradable plastic bags and containers are also present. The waste from the hospital and the slaughterhouse is not properly managed in the city. Small-scale industries' untreated effluents, inefficient fishing methods, food processing plants, boat construction yards, and oil spills all exacerbate the situation.

Water Quality in Ashtamudi Lake is generally alkaline, mixosaline to eusaline with pockets of depleted oxygen. Surface water temperature varies between 26˚C to 33˚C

throughout the year, with the maximum during the Summer and minimum during the monsoons. Salinity one of the key determinants of ecological productivity ranged between 13 to 33.5 ppt during 2012-2015[46] Samples taken from the mouth region had higher salinity owing to the influence of the Arabian Sea. The influx of Seawater and low discharge of freshwater during the pre-monsoon period shifts the lake towards saline conditions [46]The gradual predominance of coastal processes is evident in increased salinity in upstream stretches, with mixosaline conditions noted in river stretch adjoining Sasthamkotta Lakeup to Njankadavu bridge. The increasing population of Paphia malabarica(a clam that is generally found in mixosaline and estuarine conditions) in all parts of the lake is also an indicator of such a change[47]. Kollam canal, a major drain carrying sewage through Kollam city, located in the South of Ashtamudi lake has led to severe oxygen depletion as well.

Ashtamudi Lake is surrounded by clay mines as well as clay refining industries and the effluents from the same are discharged into the lake. Coconut coir retting along with related operations are widely scattered throughout coastal lengths and significantly contribute to the lake's organic pollution load. Neendakara port region has high instances of leaching of oil, grease and other lubricants from the boats using the port. Waste management operations in the 50-odd tourist houseboats that operate within the Ashtamudi Lake are not appropriate. The wash of adjoining slaughterhouses is also released into the Ashamudi Lake[48].

The concentration of nitrate and phosphate in Ashtamudi Lake ranged from 4.1 to 11.3 mg/L and 0.1 to 4.1 mg/L respectively with higher values during the monsoon period with a decline during the post-monsoon season. This may be due to the sediment in the runoff from the upstream as well as fertilisers from the agricultural field. Ashtamudi Lake has thus become a cesspool of waste and the pollution is likely to become a serious health hazard by moving through food chains. The pollution loading is way beyond its natural renewal capacity as well.
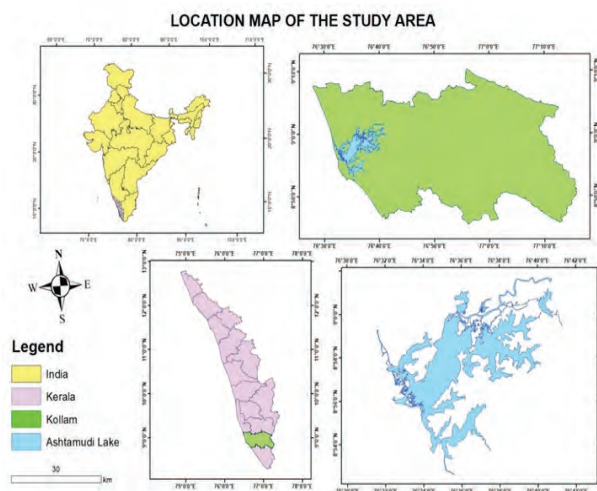
Fig. 1: Location map of Ashtamudi Lake
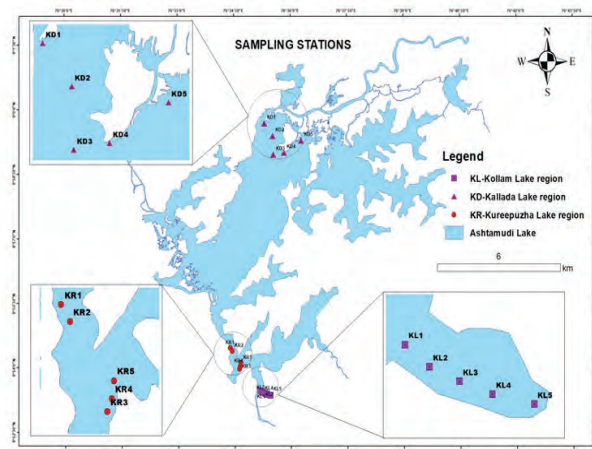
Fig. 2: Location map of Samplingstations.

METHODOLOGY

Samples were taken from the lake areas of Ashtamudi in the Kollam district, Kerala, specifically in the Kollam, Kureepuzha, and Kallada regions. The sampling stations' coordinates were recorded using a handheld GPS device (GARMIN eTrex® 30), as detailed in Table 1 and shown in Figure 2. Sediments were collected with a Van Veen grab sampler on May 14th and 28thof 2023 for Kollam and Kureepuzha, and on June 4th of 2023 for Kallada. All sampling stations were situated within 5 to 10 meters from the lake shore. The collected samples were air-dried, weighed, and sifted through a 4.75 mm sieve to eliminate large particles, with the sieve passings reserved for subsequent analysis.

Table 1: Designation and co-ordinates of the sampling stations selected

Designation of Sampling Stations		Latitude	Longitude
Kureepuzha Lake Region	KR1	76˚34'22.4"E	8˚ 54' 26.54''N
	KR2	76˚34'25.582"E	8˚ 54' 22.172''N
	KR3	76˚34'37.224"E	8˚ 53' 57.203''N
	KR4	76˚34'38.694"E	8˚ 54' 0.71''N
	KR5	76˚34'39.339"E	8˚ 54' 5.668''N
Kollam Lake Region	KL1	76˚35'10.97"E	8˚ 53' 26.979''N
	KL2	76˚35'13.869"E	8˚ 53' 24.555''N
	KL3	76˚35'17.603"E	8˚ 53' 22.954''N
	KL4	76˚35'21.685"E	8˚ 53' 21.559''N
	KL5	76˚35'26.876"E	8˚ 53' 20.434''N
Kallada Lake Region	KD1	76˚35'18.236"E	8˚ 59' 38.855'' N
	KD2	76˚35'32.02"E	8˚ 59' 21.576''N
	KD3	76˚35'32.341"E	8˚ 58' 58.953''N
	KD4	76˚35'49.677"E	8˚ 58' 58.462''N
	KD5	76˚36'16.82"E	8˚ 59' 15.138''N

The Sediment-Microplastic Isolation (SMI) unit was constructed with ball valves and 63 mm PVC piping, standing at a height of 440 mm. A 63 mm cap was placed on the base for easy cleaning and sediment removal. The unit was designed to allow smooth particle movement, preventing microplastics from getting trapped with their internally smooth surfaces. To remove microplastics from collected sediments, various high-density salt solutions were used, with the density flotation technique used to separate lighter plastic polymers from denser sediment particles. Sodium chloride (NaCl) solutions were made by dissolving salts in ultrapure water. with a density of 1.3 g/cm3. Before use, the solution was filtered through a 30-µm pore size Whatman nucleopore membrane to eliminate impurities, resulting in the preparation of the flotation media.

Before each experiment, all parts of the SMI unit were cleaned with ultrapure water. A sodium chloride solution (1.3 g/cm3) was poured into the SMI unit, ensuring that the ball valve was immersed completely. The ball valve was primed by repeatedly opening and closing it, filling the interior chamber, and limiting agitation during the processing of the sample. The solution was filled to roughly 90 mm above the open valve, allowing external contaminants to float to the surface. The device remained undisturbed for 5 minutes. The solution was then filtered via a 30-µm membrane into a clean flask for later use, and the unit was rotated to remove any contaminants from the interior walls. The valve was then pushed open. This technique, which lasted no more than 10 minutes, was performed again before each extraction.

For each extraction, a 40-g dry sediment sample and sodium chloride solution as floatation media were added to the SMI unit. The mixture was stirred for 5 minutes to allow trapped air bubbles to escape. The unit was left to settle until the supernatant was free of sediment. After closing the valve carefully, sodium chloride was collected for later use, and the supernatant was filtered through a 30-µm membrane to remove microplastic particles from the floatation media. To recover any remaining particles, the headspace was rinsed with ultrapure water. The apparatus was cleaned after each extraction. Hydrogen peroxide was added to break down organic matter. The investigation continued with four additional representative samples, and the microplastics collected in filter membranes were examined under a microscope.

The inspected microplastics were categorized on their shape and size. The shape, colour, size, and density affect the potential availability of microplastics to aquatic organisms. Based on shape, it was classed as fragments, film lines or fibres, pellets and foam. Based on size, it was classified as large microplastics (LMP) and small microplastics (SMP). Large microplastics (LMP) ranged in size from 1 to 5 mm, whereas small microplastics (SMP) were less than 1 mm.

Light microscopy is aneffective tool for detecting microplastics, but it does not impart the chemical information needed to identify the specific polymers involved. However, figuring out this identification is essential to understanding the significance and origin of the found microplastics. As a result, the most popular method used in microplastic research is FTIR microscopy. Microplastic particles interact with infrared (IR) radiation to produce recognizable IR absorption patterns. The type of polymer is then determined using these spectrum patterns. Each sampling station's microplastic samples were taken and put through Fourier Transform Infrared Spectroscopy to analyse their polymer composition.

RESULTS AND DISCUSSION

The microplastics were extracted from collected and processed samples of each site using an SMI unit on the principle of density separation. The microplastic abundance varied according to the locations. Table 2 shows the microplastic abundance of sediments from selected sampling stations of the lake region. The microplastic abundance in the lake area of Kollam is on an average of 12 ±1 items per 100g of air-dried sediments. The microplastic abundance in the lake area of Kureepuzha and Kallada is on an average of 11±1 and 9 ±1 particles per 100g of dry sediments respectively.

Table 2: Quantity of Microplastics extracted from sediment samples

Designation of Sampling Stations		Latitude	Longitude	MP abundance (Particles per 100 grams of sediment) Mean ± SD
Kureepuzha Lake Region	KR1	76°34'22.4"E	8° 54' 26.54''N	8
	KR2	76°34'25.582"E	8° 54' 22.172''N	11
	KR3	76°34'37.224"E	8° 53' 57.203''N	16
	KR4	76°34'38.694"E	8° 54' 0.71''N	12
	KR5	76°34'39.339"E	8° 54' 5.668''N	13
Kollam Lake Region	KL1	76°35'10.97"E	8° 53' 26.979''N	13
	KL2	76°35'13.869"E	8° 53' 24.555''N	9
	KL3	76°35'17.603"E	8° 53' 22.954''N	11
	KL4	76°35'21.685"E	8° 53' 21.559''N	8
	KL5	76°35'26.876"E	8° 53' 20.434''N	15
Kallada Lake Region	KD1	76°35'18.236"E	8° 59' 38.855'' N	8
	KD2	76°35'32.02"E	8° 59' 21.576''N	5
	KD3	76°35'32.341"E	8° 58' 58.953''N	9
	KD4	76°35'49.677"E	8° 58' 58.462''N	12
	KD5	76°36'16.82"E	8° 59' 15.138''N	11

The microplastics extracted from sediment samples were inspected under the Olympus CX21i microscope under 40X magnification and sorted manually based on shape and size.

The colour of microplastics could influence the digestion pattern of aquatic creatures due to the resemblance of prey items. The majority of extracted microplastics are transparent and white and were found in a discoloured state due to the presence of organic content. Based on shape, microplastics were classed as fragments, films, fibres, pellets and foam. From Table 3 and Table 4, it can be inferred that in the Lake Area of Kollam and Kureepuzha region, the number of film particles was comparatively higher than the fibre and pellet types and this increases the bioavailability of MP to organisms due to its reduced size. The probable source of film particles is observed to be disintegrated plastic carry bags. In the Kallada region, the percentage of fragment particles

predominated. The pellets extracted from sediments were seen as hard plastic materials of relatively higher thickness and were almost irregular in shape. Figure 3 shows the microplastic distribution based on the shape categorization.
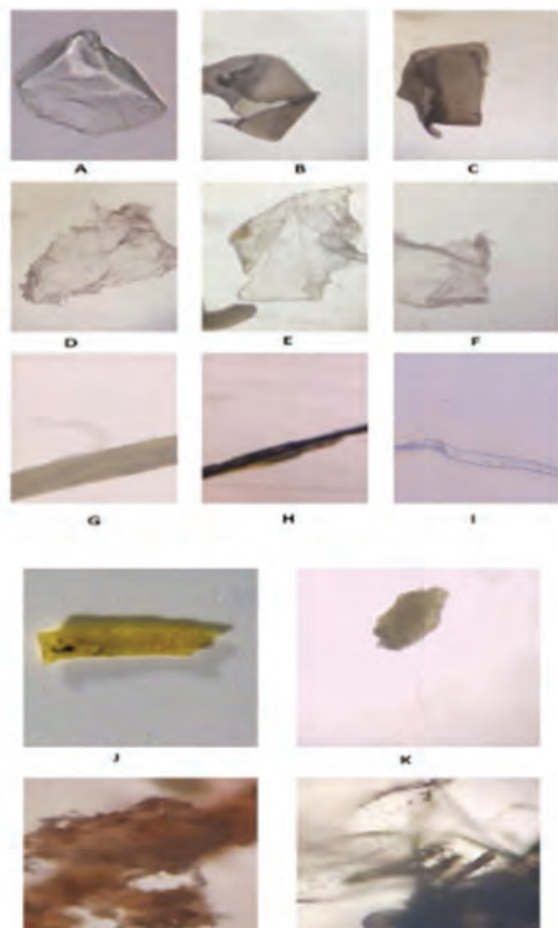

Figure 3 Microplastics that correspond to each category of shape type. Fragment (A-C), Film (D-F), Fiber/ Line (G –I), Pellet (J-K), Foam (L-M).

Table 3 Categorization of microplastic based on shape from the Kollam Lake area

Designation of Sampling Site		Frag-ment	Film	Fib-re	Pellet	Foam
Kollam Lake Region	KL1	3	5	0	0	0
	KL 2	5	4	1	1	0
	KL 3	6	6	1	2	1
	KL 4	2	6	2	2	0
	KL 5	4	5	2	2	0
	TOTAL	20	26	6	7	1

Table 4: Categorization of microplastic based on shape from the Kureepuzha Lake area

Designation of Sampling Site		Frag-ment	Film	Fib-re	Pellet	Foam
Kureepuzha Lake Region	KR 1	5	4	2	1	1
	KR 2	5	4	0	0	0
	KR 3	1	4	3	2	1
	KR 4	2	4	0	2	0
	KR 5	7	5	1	1	1
TOTAL		20	21	6	6	3

Table 5 Categorization of microplastic based on shape from the Kallada Lake area

Designation of Sampling Site		Frag-ment	Film	Fib-re	Pellet	Foam
Kallada Lake Region	KD 1	2	3	3	0	0
	KD 2	0	3	1	0	1
	KD 3	3	2	3	0	1
	KD 4	7	4	1	0	0
	KD 5	8	2	1	0	0
TOTAL		20	14	9	0	2

Based on the size of the microplastic obtained, there were small microplastics (SMP), less than 1mm in size and large microplastics (LMP) with a size range between 1mm and 5mm. From Table 6 showing the categorization based on size, it can be found that large microplastics are more abundant in all sampling sites.

Table 6 Categorization of microplastics based on size

Size	No. of Microplastics per 100 grams of sediment		
	Kollam	Kureepuzha	Kallada
SMP	17	21	12
LMP	43	35	33
TOTAL	60	56	45

The Fourier Transform Infrared Spectrometer was usedto determine the type of microplastic recovered from sediments using the SMI unit (Thermos Scientific Nicolet iS50 FTIR). FTIR spectrum of microplastic extracted from the Kollam Lake region is shown in Figure 4. The obtained FTIR spectrum was found to be similar to that of polyethylene. The polyethylene is used extensively for the production of food covers and wrappers, plastic carry bags, and plastic drinking bottles.

The microplastics extracted from sediments originated from the degradation of these plastic particles disposed into the lake region.
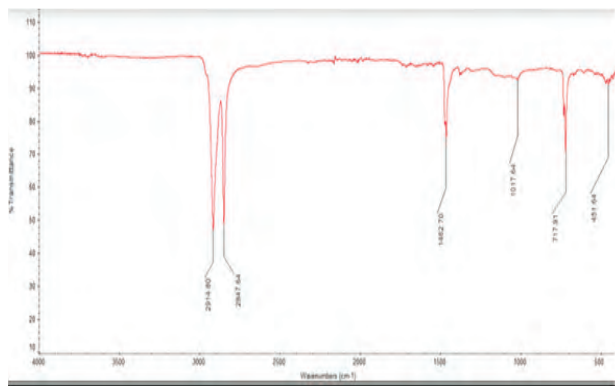

Fig. 4 FTIR spectrum of Microplastics extracted from the Kollam Lake Region

When the FTIR spectrum of microplastic extracted from the Kureepuzha lake region as shown in Figure5 was similar to that of polypropylene. This might be due to plastic bottles and caps, plastic ropes, packaging materials, toys, syringes from hospitals etc. The abandoned solid waste dump yard at Kureepuzha has been recognized as the primary supplier of plastic pollution in the lake. A portion of the dump yard is located on the shores of Ashtamudi Lake, and it is surrounded by residential structures, two temples, and other land. Microplastic generation is also influenced by the effluent discharge into the lake from the Parvathy mill, Milma diary Plant and various small-scale industries located near the lake region. There is also discharge from coconut husk retting grounds into the lake at the region.
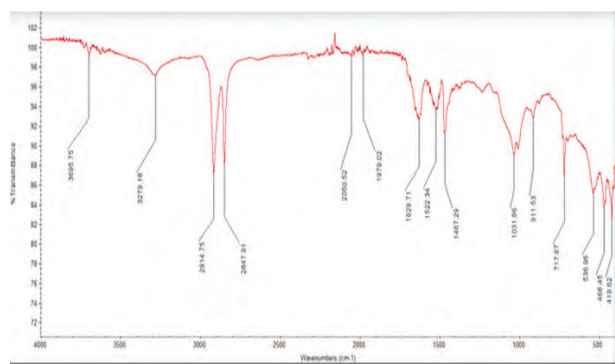

Fig. 5 FTIR spectrum of Microplastics extracted from the Kureepuzha lake region

When the FTIR spectrum of microplastic extracted from the Kallada lake region as shown in Fig. 6 was similar to that of polystyrene. Polystyrene is used in plastic disposable cutlery, foam packaging, luggage and houseware items. The selected region is known for the Tourism industry and fish Farming is also practised as a source of livelihood. There is an absence of large-scale industries here. The Kallada River joins the lake in the selected study area and thus there is an influence of sediment deposition by the river in the region.
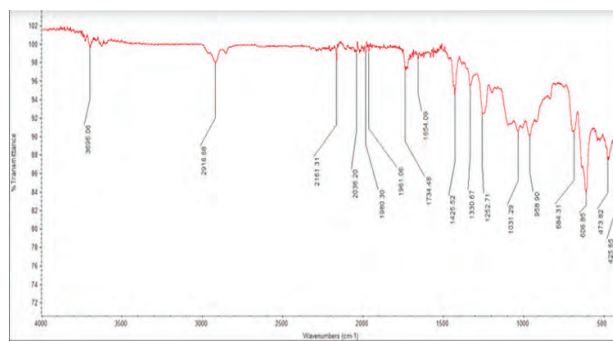
Figure 6 FTIR spectrum of microplastics extracted from the Kallada Lake region

CONCLUSION

Utilizing a practical, small-scale, and portable approach for microplastic extraction, the study sought to measure, classify, and figure out the sort of microplastic contamination prevalent in the lake's sediments of chosen sections of the Ashtamudi backwaters.The work is crucial for future investigations into the spread and effects of this growing contaminant on aquatic biota.The widespread dispersion of microplastics in the lake is indicated by their presence in all sediment samples. Microplastic abundance estimated as Mean ± SD values in sediments taken from the lake areasof Kollam, Kureepuzha and Kallada sample stations were 12±1, 11±1 and 9±1 microplastic particles per 100 grams of sediment collected respectively. The extracted microplastics were categorized by shape, which revealed their secondary origin. In the lake sediments taken from the Kollam Lake region, the film particles that typically result from the breakdown of carry bags were predominant. The Kureepuzha lake area was dominated by particles of the Film and Fragment types. The weathering of solid plastic litter is the principal cause of fragment formation. Sediments

in the Kallada Lake Region were primarily composed of fragment particles. Additionally, fibre particles were discovered in the three locations, which may have been created by the breakdown of fabrics, ropes, and fish nets. In all of the chosen sites, a greater percentage of the retrieved microplastics were large microplastics (size more than 1mm).The Polymer identification of existing microplastic pollution in the sampling sites revealed polyethylene, polypropylene and polystyrene as the predominant polymers contained in the lake sediments from Kollam, Kureepuzha and Kallada areas respectively. This is due to the presence of plastic bags, disposals of consumer products, bottles, packing materials etc. caused by the improper methods of plastic waste treatment and its disposal, open dumping of waste into the lake and sewer pipes and drains opening into the lake area acting as a carrier of plastic debris. The microplastics extracted from sediments originated from the degradation of these plastic particles disposed into the lake region. Because of the Ashtamudi wetland's unique and fragile ecosystem, it is essential to conserve it from the harmful impacts of microplastic pollution, safeguarding both its ecological balance and the well-being of the communities relying on its resources.

REFERENCES

1. Browne, M. A.; Galloway, T.; Thompson, R. (2007). Microplastic—an emerging contaminant of potential concern? Integrated Environmental Assessment and Management, Vol. 3, No. 4, 559–561. doi:10.1002/ieam.5630030412

2. Thompson, R. C.; Olsen, Y.; Mitchell, R. P.; Davis, A.; Rowland, S. J.; John, A. W. G.; McGonigle, D.; Russell, A. E. (2004). Lost at Sea: Where Is All the Plastic?, Science, Vol. 304, No. 5672, 838–838. doi:10.1126/science.1094559

3. Carpenter, E. J.; Anderson, S. J.; Harvey, G. R.; Miklas, H. P.; Peck, B. B. (1972). Polystyrene Spherules in Coastal Waters, Science, Vol. 178, No. 4062, 749–750. doi:10.1126/science.178.4062.749

4. Arthur C; Baker J; Bamford H. (2008, September 9). Proceedings of the International Research Workshop on the Occurrence, Effects, and Fate of Microplastic Marine Debris., NOAA Technical Memorandum NOS-OR&R-30

5. Roscam Abbing, M. (2019). Plastic Soup: An Atlas of Ocean Pollution, Island Press, Washington [District of Columbia]

6. Wagner, M.; Lambert, S. (Eds.). (2018). Freshwater Microplastics: Emerging Environmental Contaminants? (Vol. 58), Springer International Publishing, Cham. doi:10.1007/978-3-319-61615-5

7. Zalasiewicz, J.; Waters, C. N.; Ivar Do Sul, J. A.; Corcoran, P. L.; Barnosky, A. D.; Cearreta, A.; Edgeworth, M.; Gałuszka, A.; Jeandel, C.; Leinfelder, R.; McNeill, J. R.; Steffen, W.; Summerhayes, C.; Wagreich, M.; Williams, M.; Wolfe, A. P.; Yonan, Y. (2016). The geological cycle of plastics and their use as a stratigraphic indicator of the Anthropocene, Anthropocene, Vol. 13, 4–17. doi: 10.1016/j.ancene.2016.01.002

8. Campanale, C.; Stock, F.; Massarelli, C.; Kochleus, C.; Bagnuolo, G.; Reifferscheid, G.; Uricchio, V. F. (2020). Microplastics and their possible sources: The example of Ofanto river in southeast Italy, Environmental Pollution, Vol. 258, 113284. doi: 10.1016/j.envpol.2019.113284

9. Rillig, M. C.; Ingraffia, R.; De Souza Machado, A. A. (2017). Microplastic Incorporation into Soil in Agroecosystems, Frontiers in Plant Science, Vol. 8, 1805. doi:10.3389/fpls.2017.01805

10. Prata, J. C. (2018). Airborne microplastics: Consequences to human health?Environmental Pollution, Vol. 234, 115–126. doi: 10.1016/j.envpol.2017.11.043

11. Waring, R. H.; Harris, R. M.; Mitchell, S. C. (2018). Plastic contamination of the food chain: A threat to human health?Maturitas, Vol. 115, 64–68. doi: 10.1016/j.maturitas.2018.06.010

12. Pivokonsky, M.; Cermakova, L.; Novotna, K.; Peer, P.; Cajthaml, T.; Janda, V. (2018). Occurrence of microplastics in raw and treated drinking water, Science of The Total Environment, Vol. 643, 1644–1651. doi: 10.1016/j.scitotenv.2018.08.102

13. Rezania, S.; Park, J.; Md Din, M. F.; Mat Taib, S.; Talaiekhozani, A.; Kumar Yadav, K.; Kamyab, H. (2018). Microplastics pollution in different aquatic environments and biota: A review of recent studies, Marine Pollution Bulletin, Vol. 133, 191–208. doi: 10.1016/j.marpolbul.2018.05.022

14. Cook, T. (2019). How Are Microplastics Transported to Polar Regions?, Eos, Vol. 100. doi:10.1029/2019EO134237

15. Andrady, A. L. (2011). Microplastics in the marine

environment, Marine Pollution Bulletin, Vol. 62, No. 8, 1596–1605. doi: 10.1016/j.marpolbul.2011.05.030

16. Cooper, D. A.; Corcoran, P. L. (2010). Effects of mechanical and chemical processes on the degradation of plastic beach debris on the island of Kauai, Hawaii, Marine Pollution Bulletin, Vol. 60, No. 5, 650–654. doi: 10.1016/j.marpolbul.2009.12.026

17. Teuten, E. L.; Rowland, S. J.; Galloway, T. S.; Thompson, R. C. (2007). Potential for Plastics to Transport Hydrophobic Contaminants, Environmental Science & Technology, Vol. 41, No. 22, 7759–7764. doi:10.1021/es071737s

18. Koehler, A.; Anderson, A.; Andrady, A.; Arthur, C.; Baker, J.; Bouwman, H.; Gall, S.; Hidalgo-Ruz, V.; Köhler, A.; Law, K. L.; Leslie, H.; Kershaw, P.; Pahl, S.; Potemra, J.; Ryan, P.; Shim, W. J.; Thompson, R.; Hideshige Takada; Turra, A.; Vethaak, D.; Wyles, K. (2015). SOURCES, FATE AND EFFECTS OF MICROPLASTICS IN THE MARINE ENVIRONMENT: A GLOBAL ASSESSMENT. doi:10.13140/RG.2.1.3803.7925

19. Barnes, D. K. A.; Galgani, F.; Thompson, R. C.; Barlaz, M. (2009). Accumulation and fragmentation of plastic debris in global environments, Philosophical Transactions of the Royal Society B: Biological Sciences, Vol. 364, No. 1526, 1985–1998. doi:10.1098/rstb.2008.0205

20. Wright, S. L.; Thompson, R. C.; Galloway, T. S. (2013). The physical impacts of microplastics on marine organisms: A review, Environmental Pollution, Vol. 178, 483–492. doi: 10.1016/j.envpol.2013.02.031

21. Law, K. L.; Starr, N.; Siegler, T. R.; Jambeck, J. R.; Mallos, N. J.; Leonard, G. H. (2020). The United States contribution of plastic waste to land and ocean, Science Advances, Vol. 6, No. 44, eabd0288. doi:10.1126/sciadv. abd0288

22. Ajith, N.; Arumugam, S.; Parthasarathy, S.; Manupoori, S.; Janakiraman, S. (2020). Global distribution of microplastics and its impact on marine environment—a review, Environmental Science and Pollution Research, Vol. 27, No. 21, 25970–25986. doi:10.1007/s11356-020-09015-5

23. Dowarah, K.; Patchaiyappan, A.; Thirunavukkarasu, C.; Jayakumar, S.; Devipriya, S. P. (2020). Quantification of microplastics using Nile Red in two bivalve species Perna viridis and Meretrix meretrix from three estuaries in Pondicherry, India and microplastic uptake

by local communities through bivalve diet, Marine Pollution Bulletin, Vol. 153, 110982. doi: 10.1016/j.marpolbul.2020.110982

24. De Souza Machado, A. A.; Kloas, W.; Zarfl, C.; Hempel, S.; Rillig, M. C. (2018). Microplastics as an emerging threat to terrestrial ecosystems, Global Change Biology, Vol. 24, No. 4, 1405–1416. doi:10.1111/gcb.14020

25. Vikas Madhav, N.; Gopinath, K. P.; Krishnan, A.; Rajendran, N.; Krishnan, A. (2020). A critical review on various trophic transfer routes of microplastics in the context of the Indian coastal ecosystem, Watershed Ecology and the Environment, Vol. 2, 25–41. doi: 10.1016/j.wsee.2020.08.001

26. Bi, M.; He, Q.; Chen, Y. (2020). What Roles Are Terrestrial Plants Playing in Global Microplastic Cycling?Environmental Science & Technology, Vol. 54, No. 9, 5325–5327. doi: 10.1021/acs.est.0c01009

27. Goswami, P.; Vinithkumar, N. V.; Dharani, G. (2020). First evidence of microplastics bioaccumulation by marine organisms in the Port Blair Bay, Andaman Islands, Marine Pollution Bulletin, Vol. 155, 111163. doi: 10.1016/j.marpolbul.2020.111163

28. Daniel, D. B.; Ashraf, P. M.; Thomas, S. N. (2020). Abundance, characteristics and seasonal variation of microplastics in Indian white shrimps (Fenneropenaeus indicus) from coastal waters off Cochin, Kerala, India, Science of The Total Environment, Vol. 737, 139839. doi: 10.1016/j.scitotenv.2020.139839

29. Mason, S. A.; Welch, V. G.; Neratko, J. (2018). Synthetic Polymer Contamination in Bottled Water, Frontiers in Chemistry, Vol. 6, 407. doi:10.3389/fchem.2018.00407

30. Ragusa, A.; Svelato, A.; Santacroce, C.; Catalano, P.; Notarstefano, V.; Carnevali, O.; Papa, F.; Rongioletti, M. C. A.; Baiocco, F.; Draghi, S.; D'Amore, E.; Rinaldo, D.; Matta, M.; Giorgini, E. (2021). Plasticenta: First evidence of microplastics in human placenta, Environment International, Vol. 146, 106274. doi:10.1016/j.envint.2020.106274

31. Selvam, S.; Manisha, A.; Venkatramanan, S.; Chung, S. Y.; Paramasivam, C. R.; Singaraja, C. (2020). Microplastic presence in commercial marine sea salts: A baseline study along Tuticorin Coastal salt pan stations, Gulf of Mannar, South India, Marine Pollution Bulletin, Vol. 150, 110675. doi:10.1016/j.marpolbul.2019.110675

32. Zhang, J.; Wang, L.; Kannan, K. (2020). Microplastics

in house dust from 12 countries and associated human exposure, Environment International, Vol. 134, 105314. doi:10.1016/j.envint.2019.105314

33. Naik, R. K.; Naik, M. M.; D'Costa, P. M.; Shaikh, F. (2019). Microplastics in ballast water as an emerging source and vector for harmful chemicals, antibiotics, metals, bacterial pathogens and HAB species: A potential risk to the marine environment and human health, Marine Pollution Bulletin, Vol. 149, 110525. doi:10.1016/j.marpolbul.2019.110525

34. Sathish, M. N.; Jeyasanta, I.; Patterson, J. (2020). Microplastics in Salt of Tuticorin, Southeast Coast of India, Archives of Environmental Contamination and Toxicology, Vol. 79, No. 1, 111–121. doi:10.1007/s00244-020-00731-0

35. V. Sanil Kumar; K. C. Pathak; P. Pednekar; N. S. N. Raju; R. Gowthaman. (2006). Coastal processes along the Indian coastline, Current Science Association, Vol. 19, No. 4, 530–536

36. Costanza, R.; d'Arge, R.; De Groot, R.; Farber, S.; Grasso, M.; Hannon, B.; Limburg, K.; Naeem, S.; O'Neill, R. V.; Paruelo, J.; Raskin, R. G.; Sutton, P.; Van Den Belt, M. (1998). The value of the world's ecosystem services and natural capital, Ecological Economics, Vol. 25, No. 1, 3–15. doi:10.1016/S0921-8009(98)00020-2

37. Kennish, M. J. (2002). Environmental threats and environmental future of estuaries, Environmental Conservation, Vol. 29, No. 1, 78–107. doi:10.1017/S0376892902000061

38. Fujii, T. (2012). Climate Change, Sea-Level Rise and Implications for Coastal and Estuarine Shoreline Management with Particular Reference to the Ecology of Intertidal Benthic Macrofauna in NW Europe, Biology, Vol. 1, No. 3, 597–616. doi:10.3390/biology1030597

39. Babu, K. N.; Omana, P. K.; Mohan, M. (2010). Water and sediment quality of Ashtamudi estuary, a Ramsar site, southwest coast of India—a statistical appraisal, Environmental Monitoring and Assessment, Vol. 165, Nos. 1–4, 307–319. doi:10.1007/s10661-009-0947-0

40. Krishnakumar, A.; Saranya, P.; Prasad, P. G.; Rakhi, C. (2015). Holocene Records of Human Driven Geological Impacts in a Ramsar Wetland of India, Aquatic Procedia, Vol. 4, 373–380. doi:10.1016/j.aqpro.2015.02.050

41. Chinnadurai, S.; Mohamed, K. S.; Sharma, J.; Venkatesan, V.; Kripa, V. (2016). Assessment of bio-accumulation of bacteria in oysters from shellfish growing waters in Ashtamudi Lake (Kerala, India): A RAMSAR wetland, Regional Studies in Marine Science, Vol. 7, 118–122. doi:10.1016/j.rsma.2016.05.016

42. Ankit, Y.; Mishra, P. K.; Kumar, P.; Jha, D. K.; Kumar, V. V.; Ambili, V.; Anoop, A. (2017). Molecular distribution and carbon isotope of n-alkanes from Ashtamudi Estuary, South India: Assessment of organic matter sources and paleoclimatic implications, Marine Chemistry, Vol. 196, 62–70. doi:10.1016/j.marchem.2017.08.002

43. LePage, B. A. (Ed.). (2011). Wetlands: Integrating Multidisciplinary Concepts, Springer, Dordrecht ; New York

44. Ramsar Convention Bureau. (1997). The Ramsar Convention Manual: A Guide to the Convention on Wetlands of International Importance Especially as Waterfowl Habitat (2nd. ed.), Ramsar Convention Bureau, Gland

45. census of India. (2011). Census tables

46. Sujatha, C H; Benny Nify; Raveendran, Ranjitha; Fanimol C.L; Samantha N.K. (2009). Nutrient dynamics in the two lakes of Kerala, India, Indian Junal of Marine Sciences, Vol. 38, No. 4, 451–456

47. Ampili, M; Shiny Sreedhar. (2016). Hydrologic and sediment parameters affecting the distribution of the Venerid clam, Paphia malabarica in two estuaries, International Journal of Scientific and Research Publications, Vol. 6, No. 3

48. R. Sajeev; V. Subramanian. (2003). Land Use/Land Cover Changes in Ashtamudi Wetland Region of Kerala - A Study Using Remote Sensing and GIS, Geological Society of India, Vol. 61, No. 5, 573–580

A Performance Study of Prestressed Concrete Beams Reinforced with Bamboo Fibers (BFR) and Sisal Fiber (SFR)

K. Srinivasan, M. Sudharsasan
Assistant Professor
Department of Civil Engineering
Dr. Mahalingam College of Engg. and Technology
Pollachi, Tamil Nadu
✉ salemvasan@gmail.com

✉ sudharshanmail01@gmail.com @gmail.com

R. Anuja
Assistant Professor
Department of Civil Engineering
Dr. Mahalingam College of Engg. and Technology
Pollachi, Tamil Nadu

S. Srigeethaa
Assistant Professor
Department of Civil Engineering
P. A. College of Engineering and Technology
Pollachi, Tamil Nadu
Email: srigeethaa2009@gmail.com

ABSTRACT

The present study of "Prestressed Concrete Beams Reinforced with Bamboo and sisal Fibers" is one of the green reinforcement in concrete structures. Nowadays the rate of steel and production of steel bars are very expensive. Bamboo Fiber ropes (BFR) and sisal fiber rope (SFR), exemplified by their high strength in tension, light heaviness, and stumpy expenditure, be able to employ since a fractional substitution of normal steel bars to diminish the structure cost. The current investigation is a novel move towards making use of bamboo and sisal ropes (the method employing Non-shrink adhesive epoxy mortar coated) like a fractional substitution (25%, 50%, 75%, and 100%) of conventional rebar. 12 beams by a dimension of 150 mm x250 mm and 1200 mm span are organized to study one metre. Those steel bars in the beams were supplemented by bamboo or sisal strands during the casting process. Beams are subjected to a series of trials to determine the optimal amount of bamboo and sisal ropes to use in place of steel. Approximately 75% of the direct beam's load capacity was successfully given to bamboo and sisal ropes that were better in their deform capabilities feature (DCF), parameters Associated capability feature (LAF), and reliability factor (RF) (toughened through steel only). Using bamboo cables instead of metal ones will save money and promote economic growth.

INTRODUCTION

Every country, it may be developed or developing is facing problems of construction materials, especially steel resources. At the time of steel production will create more pollution to the environment. So every researcher is searching for eco-friendly materials and also for low-cost ones. One objective of this study would be to analyse how different commonly-used fiber materials (bamboo and sisal fiber) processed with Johnberg 1660 Epoxy resin for the fractional replacement of normal steel bar reinforcement.

When compared to other types of lingo-cellulose fibres, the composites made from bamboo fibre and processed bamboo wires has superior qualities due to the simultaneous enhancement of both mild robust and given to different. Conventional string, such as coir filament, bamboo strands, sisal strands, and jute strands, therefore functions in the same way. favored designed for the creature in the neighborhood reachable [1]. Sisal and bamboo plants are available in the hot weathered countryside. Even these types of natural materials are very superior amplification mechanisms

in polymeric complex intended for its light-weight and more strength. Present learning intended at examines the consequence of using bamboo fibers as a substitute for normal steel reinforcement in an undemanding concrete structural part. The performance The bending stress of a sisal fibre reinforced concrete beams were analysed. Many transformations of the strengthening would be identified to enhance the efficiency of reinforcement [2]. The length, cross-segment, shape, fibre composition, and connection characteristics of FRP are all important considerations for its application in armament reinforcement [3]. Nonetheless, it has been proven that bamboo rope can be used as reinforcing in cement discovered medium [6].

SIGNIFICANCE OF RESEARCH

This investigation is intended to explore the option of making use of bamboo and sisal wire cables towards the concrete building because of the strands' cheap cost, low weight, and durability. Rust prevention is the primary goal when using bamboo wire ropes in concrete. The main objective of the research is to gather information on the effectiveness of beams strengthened using bamboo cables as a substitute for conventional rebar.

EXPERIMENTAL WORK

A collection of productive examinations are approved elsewhere on top of concrete elements (beams and cylinders) which are put together with bamboo wire ropes since a fractional substitute of steel bars to learn the presentation of the substitution and evaluate the experiment outcome through conservative beams which in employment by usual reinforcing bars made

of steel, nothing more. For the purpose of learning the modulus of elasticity of centers of mass fibre ropes, nine beams with dimensions of 150x250x1200 mm with an apparent length of 1000 mm were fitted through categorization, while nine cylinders with measurements of 150x200 mm with two types of reinforcement (steel, bamboo wire rope) in categorization in the path to gain knowledge the adhesion even though pull-out test were constructed.

Materials

OPC cement was used, and properties of cement were passed as per the requirement of the Indian Standard. M sand was used for fine aggregate and 20 mm coarse aggregate was used for concreting. All material properties were matched with the conventional concrete. Another important material study was done for bamboo and sisal wire rope and found the following tensile properties.

The bamboo was seasoned and made like fiber with the help of fiber making machine. The bamboo fiber was twisted with the help of threads-making equipment. It was twisted in the form of four hooks with fixed rotation. The samples of bamboo fiber rope as shown in fig1.

Fig. 1 Bamboo rope with the diameter of 12mm

Fig. 2 Sisal rope with the diameter of 12mm

Table 1 Compressive strength of 12mm size bamboo rope

Sample	Load (N)	Elongation (mm)	standard Strength (Mpa)	critical Strength(Mpa)	Breaking strength (Mpa)
1	516.5	40.6	18.27	29.23	17.32
2	490.6	34.26	17.35	28.2	16.79
3	467.8	34.00	16.55	27.65	14.36
Mean	491.63	36.29	17.39	28.36	16.16

Pullout Test

Totally 9 cylinders (3 sample designed for every experiment) were arranged. Within every cylinder specimen, Bamboo and sisal ropes and Normal steel bar were kept in center of cylinder specimen. The embedded length of bamboo rope and steel bars are tabulated, 10cm length of each rope kept outside the cylinder to find the pull out test. The specimens were placed in universal testing machine and found the bonding.

Table 2 Pull out test, Sisal and Normal steel bar bonding strength with 8mm diameter

Specimen Number	Type of bar/rope	Length of Embedment (mm)	Strength of Bonding (Mpa)	Avg Bond Strength (Mpa)
1	Steel Bar 12 mm Dia	200	2029.360	1931.899
2	Steel Bar 12 mm Dia	150	1976.876	
3	Steel Bar 12 mm Dia	100	1789.461	
4	Bamboo ropes 12mm Dia	200	1102.526	1063.872
5	Bamboo ropes 12mm Dia	150	1098.658	
6	Bamboo ropes 12mm Dia	100	990.433	
7	Sisal ropes 12mm Dia	200	876.260	818.320
8	Sisal ropes 12mm Dia	150	810.360	
9	Sisal ropes 12mm Dia	100	768.340	

Fig. 3 bonding breakdown after Experiment

Casting of Specimen and Mix Proportion

A 1200mm×250mm×150mm steel mould was made-up and used for beam casting. The mix proportion ratio was designed to attain the characteristic compressive strength of concrete about 30MPa. The ingredients of mix ratio used were cement-420kg: 831.6 kg fine aggregate: 1009kg coarse aggregates mixed with 212kg of water. Nine moulds were cast for the reinforcement of 4 numbers of 12mm rebar rods in the stress regions of footing, and 2No's of 12mm dia steel bars at top starting with 0% rope replacement which represents control beam (beam without ropes). further 8 beams with 25%, 50%,75%, and 100% bamboo and sisal fiber rope beams were cast respectively to observe the result and it is inexpensive substance ropes and facilitate actual in both tension and compression as well the reduction of Normal steel reinforcement quantity and hence lead to cost effective construction.

Experiments on Beam

The concrete beams were tested by loading frame with the capacity of maximum 1000kN. Loads on beams arranged as two point load method and it was used for all beams. Dial gauges were fixed at the location of center of the beams to measure the center bottom deflection of beams. Before the loading of beams the dial gauge plungers touching the bottom surface of center of beams were verified. A characteristic two point load investigational position is shown in the Fig.4. The fracture form was further more witness on each load augmentation. Each and every beam was experimented up to breakdown. The curvature of the beam was measured with dial gauge arrangement to compute strain of beam; it is exposed in the Fig.6.
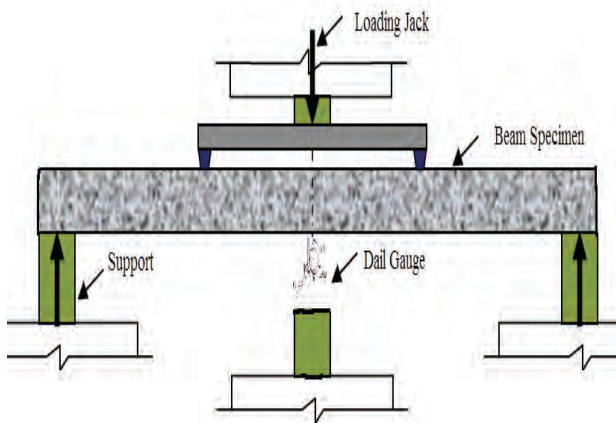
Fig 4. Two point load investigational position

Fig 5. Dial gauge arrangement to compute strain of beam

Effect of Bamboo and Sisal Ropes with Various Percentage

Corresponding to the load vs deflection relations of concrete beams include bamboo or sisal wires at the same time as a fractional proportion of conventional steel beam. Within these beams with bamboo ropes illustrate lesser deflections and higher critical loading than sisal rope reinforced beam. Though, reinforced beams with more than 50 % of bamboo or sisal rope replaced beams are giving you an idea about lower ultimate load and superior deflections in evaluation with the conventional beam. Since the breaking potency of sisal rope is lesser than bamboo ropes. Therefore, the final beam loads of sisal fiber wires were lesser than the reinforced beams of bamboo ropes next to the similar sisal fiber rope proportion.

Reinforced Beams with (75% Steel Bars + 25% BFR or SFR Ropes)

Figure. 6 show the Load vs Deflection relationship when the beams cast with75% steel bars and 25% of either BFR or SFR and compared with control beam. The collapse of the beams with bamboo or sisal wire ropes takes strength around 85 and 83% of the control beam, breakdown load correspondingly. At the time duration, the given load is in anticipation of breakdown. The final maximum carrying the load of the bamboo fiber ropes reinforced beams were on the subject of three percent superior than sisal fiber wires reinforced beams and show evidence of around 4 percentages less deflection than the sisal fiber ropes reinforced beam.

Table 3 Load Vs Deflection for Reinforced Beams with 75% Steel Bars + 25% BFR or SFR Ropes

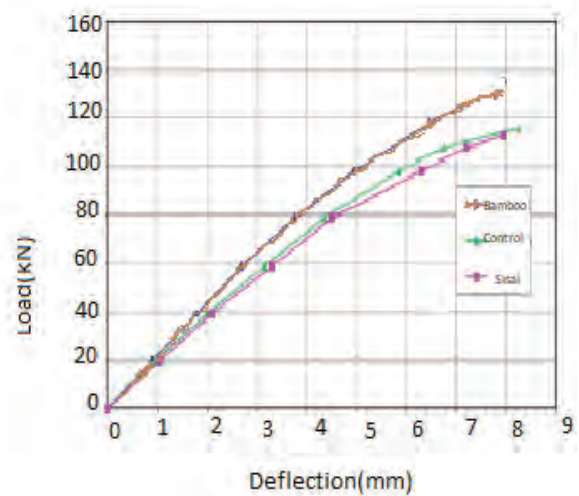| Load(kN)	Deflection(mm)		
	Control Beam	Bamboo Reinforced Beam	Sisal Reinforced beam
0	0	0	0
20	1	1	1
40	2	1.8	2.1
60	3.1	2.6	3.2
80	4.2	3.8	4.4
100	5.8	5	6.4
120	7	6.6	7.4

Fig 6. Reinforced Beams with 75% Steel Bars + 25% BFR or SFR Ropes

Reinforced Beams with 50% Steel Bars + 50% BFR or SFR Ropes

Load Vs deflection relationship of reinforced beams with (50% steel bars + 50% BFR & SFR Ropes) were compared with conventional beam (with 100% reinforced Normal steel bars), in Fig7. It was experimented with the breakdown loading beams with sisal and bamboo fiber ropes were 68% and 72% for conventional beam, correspondingly. Conversely, the deflection of beams with BFR and SFR were comparable to the conventional beam. Beams with sisal fiber rope proved more deflections than that of bamboo fiber rope reinforced beam. The deformation of SFR beams is around 6.8% while the deformation of BFR beams is around 4.5% for particular loadings.

Table 4 Load Vs Deflection for Reinforced Beams with 50% Steel Bars + 50% BFR or SFR Ropes

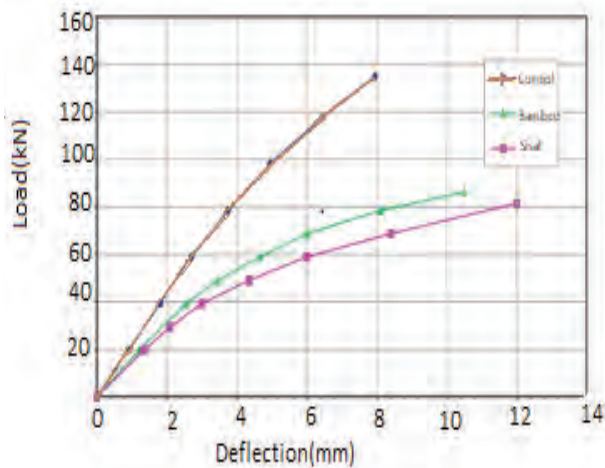| Load(kN)	Deflection(mm)		
	Control Beam	Bamboo Reinforced Beam	Sisal Reinforced beam
0	0	0	0
20	1	0.8	1
40	2	1.8	2.1
60	3.1	2.6	3.4
80	4.4	3.6	4.6
100	5.8	4.9	6.4
120	6.8	6.6	7.8

Fig 7. Reinforced Beams with 50% Steel Bars + 50% BFR or SFR Ropes

Reinforced Beams with 25% Steel Bars+ 75% BFR or SFR Ropes

The Load vs deflection relations of beams with 25% STEEL BARS+ 75% BFR or SFR Ropes were compared with a conventional beam as shown in Fig8. The breakdown ultimate stresses of the bamboo and sisal rope-reinforced beams approximately 67% and 62%, respectively, to a failure load in the standard frame. Both BFR and SFR fibre ropes showed deformations which were on par with those of a standard beam. At the point of failure, the bamboo and sisal rope bend more than 32 and 50 percent more than the control beam, respectively. More bending occurred in beams reinforced with sisal ropes than with bamboo fibre cables.

Table 7 Load Vs Deflection for Reinforced Beams with 25% Steel Bars + 75% BFR or SFR Ropes

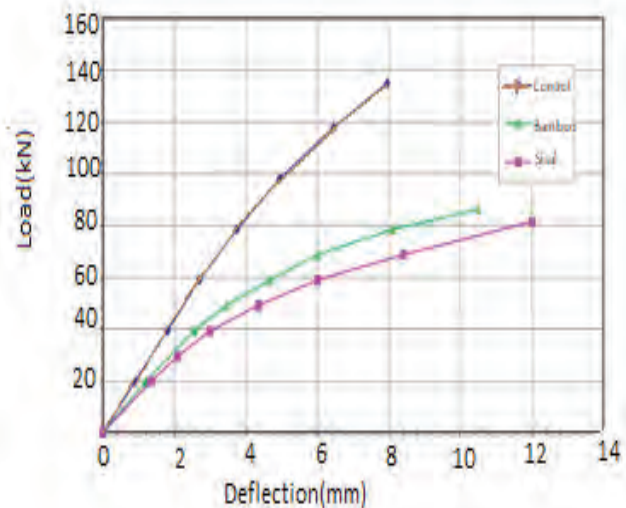| Load(kN)	Deflection(mm)		
	Control Beam	Bamboo Reinforced Beam	Sisal Reinforced beam
0	0	0	0
20	0.6	0.6	0.8
40	1.9	2.4	2.6
60	2.4	4.4	6.0
80	3.8	8.0	12
100	4.6	-	-
120	6.2	-	-

Fig 8. Reinforced Beams with 25% Steel Bars + 75% BFR or SFR Ropes

Beams Strengthened with Either BFR or SFR Fibre Ropes at A Ratio of 1:1

The load vs deflection relations of fiber-reinforced beams with100% BFR or SFR Ropes as exposed as in Fig.9. The load failure of the reinforced beam through completely bamboo and sisal fiber ropes reduced to about 48% and 43% of the conventional beam, correspondingly, while the beam deflections up to 78% ropes with fiber confirm more deflections when compared to the conventional beam on the identical load acting throughout steadily until the loading failure. At the time of breakdown, reinforced beams with bamboo fiber and sisal fiber ropes illustrate elevated deflections of around 109% and 128% of conventional steel reinforced beams.

Table 8 Load Vs Deflection for Reinforced Beams with 100% BFR or SFR Ropes

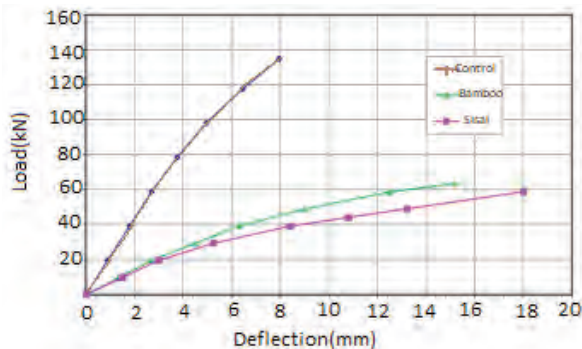| Load(kN)	Deflection(mm)		
	Control Beam	Bamboo Reinforced Beam	Sisal Reinforced beam
0	0	0	0
20	0.6	2.4	2.4
40	1.8	6.2	8.2
60	2.4	8.4	18
80	3.8	10	-
100	4.6	-	-
120	6.2	-	-

Fig 9. Reinforced Beams with 100% BFR or SFR Ropes

CONCLUSIONS

As per the experimental results of the various percentages of bamboo and sisal fiber rope replaced concrete beam Reponses are given below:

1) Substitute of 25% concrete beam normal steel reinforcement with bamboo fiber ropes, around maximum load failure and comparable deflection of the conventional beams were attained. Rising the substitution up to 50% of fiber rope concrete reduces the maximum failure load by about 70% and is greater than before the beam deflection by around 16% compared to the conventional steel-reinforced beam. The ultimate load breakup is reduced to about 64% of the typical beam, and the measured deviation further increases to around 43%, even after increasing the replacement to 75%.

2) From the experimental test on when fiber ropes reinforcement fraction particularly in sisal ropes fiber-reinforced beams, first load cracking become visible previous to the conventional beam.

3) Rising fiber rope reinforcement proportion decreases the investigational to hypothetical load cracking and Maximum beam load carrying.

4) The attempt is required to attain the study on reinforced concrete beams with BFR & SFR ropes in dissimilar periods extended.

5) The concrete and ropes were compatibility have to be considered cautiously to so numerous limitation particularly thermal expansion coefficient.

REFERENCES

1. Tara Sen, H. N. Jagannatha Reddy, "Application of Sisal, Bamboo, Coir and Jute Natural Composites in Structural Upgradation ", International Journal of Innovation, Management and Technology, Vol. 2, No. 3, June 2011.

2. MURTIADI Suryawan and AKMALUDDIN, "Sisal Fiber as Steel Bar Replacement of Lightweight Concrete under Flexural Loading", Applied Mechanics and Materials, ISSN: 1662-7482, Vol. 845, pp 202-207, (2016).

3. Önal M. Mustafa, "Reinforcement of Beam by Using Carbon Fiber Reinforced Polymer in Concrete

Buildings", Scientific Research and Essay, Vol. 4, No. 10 (2009), pp. 1136-1145.

4. Libo Yan, NawawiChouw and Krishnan Jayaraman, "Flax fiber and its composites –A review", Composites Journal: Part B, 56,(2014), pp (296:317).

5. Saswat Mohapatra, "evaluation of performance of flax fiber in the SMA Mix using slag as aggregate replacement", National Institute of Technology, Rourkela, (2013.)

6. Yogesh Ravindra Suryawanshi and Jitendra D Dalvi, "Study Of Sisal Fiber As Concrete Reinforcement Material In Cement Based Composites, 2(3), March - 2013, pp(1:4).

7. H. Mohammad hosseini, A.S.M. Abdul Aaal, "physical and mechanical properties of concrete containing fibers from industrial carpet waste", International Journal of Research in Engineering and Technology, 2(12), (2013), pp(464:468)

8. Mohini Saxena, AsokanPappu, RuhiHaque, and Anusha Sharma, "Sisal Fiber Based Polymer Composites and Their Applications", Handbook of materials chapter 22, Berlin, (2011), pp (589:659).

9. Kawkab Habeeb Al Rawi and MoslihAmerSalih Al Khafagy, "effect of adding sisal fiber and Iraqi bauxite on some Properties of concrete", Technical Institute of Babylon, (2009), pp (16).

10. Flavio de Andrade Silva, Nikhilesh Chawla and Romildo Dias de Toledo Filho, "tensile behavior of high performance natural (sisal) fibers", Composites Science and Technology, 68, (2008), pp (3438:3443).

13. Ashraf Mohamed Heniegal, Fawkia Fahim El-Habiby and Radwa Defalla Abdel Hafez, "Performance of Concrete Incorporating Industrial and Agricultural Wastes", IOSR Journal of Engineering, 4 (2014), pp (1:11).

16. H.A. McKenna, J.W. S. Hearle and N. O'Hear, "Handbook of fibre rope technology", The Textile Institute Wood head Publishing, Cambridge (2010(.

17. R. Senthil Kumar, "Textiles for Industrial Applications", CRC Press, Taylor & Francis Group, LLC (2014).

19. Ashraf M. Heniegal, "Strengthening and Repair of Selfelf Compacting Concrete Beams", Mansoura Engineering Journal, V. 37, No. 2, pp. (28-49), June 2012.

Performance Evaluation of Soaked CBR of Expansive Soil Treated with Combination of Wollastonite Powder, Fly Ash and Lime

A. I. Dhatrak
Associate Professor
Department of Civil Engineering
Government College of Engineering
Amravati, Maharashtra
✉ anantdhatrak@rediffmail.com

P. V. Kolhe
PhD Research Scholar
Department of Civil Engineering
Government College of Engineering
Amravati, Maharashtra
✉ piyushkolhe007@gmail.com

Aishwarya A. Maindkar
PG Scholar
Department of Civil Engineering
Government College of Engineering
Amravati, Maharashtra
✉ aishwaryamaindkar@gmail.com

ABSTRACT

A limestone that has undergone thermal modifications has a Wollastonite powder (WP) as a constituent. It may also occur when sediments changed by pollution from igneous rocks undergo metamorphisms that are affected by silicon. The prior research illustrates how the type of soil and subsequent elements, such as the quantity of Wollastonite powder, curing time, clay content, etc., affects the usage of Wollastonite powder in the field. As a result, the current work intends to investigate the impact on expansive soil (BCS) treated with varying concentrations of Wollastonite powder over curing periods of 7, 14, 21, 28 and 45 days on values of its Soaked California Bearing Ratio (CBR). Primarily the ingredients in minerals like Wollastonite powder are silicon, calcium, and oxygen. Wollastonite powder has the molecular formula $CaSiO_3$, and its approximate theoretical composition is around 49% CaO and roughly 51% SiO_2. Iron, Aluminium, potassium, magnesium, sodium, and other elements may be found in trace levels in natural Wollastonite mineral. From the compaction test, it was detected that maximum dry density was decreased whereas optimum moisture content of soils increased with increase in dosage of WP. The California Bearing Ratio values of soils treated with WP increased up on addition of 10% WP then, a slight decrease was observed. However, this value was higher than the untreated soil up on 10% addition of WP at 45 days of curing. Thus, outcome demonstrates a notable improvement in Soaked CBR values across all percentages of Wollastonite powder treatment. After 45 days of treatment, the greatest increase in strength was attained. The comparison research aids in determining the optimum value of Wollastonite powder, CBR value rise and maximum percentage for treating expansive soil.

KEYWORDS : Soaked CBR, Wollastonite mineral, Lime, Fly ash, Soil stabilization, Expansive soil, Curing period.

NOMENCLATURE

BCS =   Black Cotton Soil

CD =   Curing Period   (Days)

CH =   Highly Compressible Clay

FA =   Fly Ash

IS = Indian Standards

L = Lime

LL =   Liquid Limit   (%)

MDD = Maximum Dry Density (kN/m³)

OMC = Optimum Moisture Content (%)

PA =   Physical Appearance

PC =   Proctor Compaction

PI = Plasticity Index   (%)

PL =   Plastic Limit   (%)

SG =   Specific Gravity

SL =   Shrinkage Limit(%)

CBR = California Bearing Ratio (%)

WP =   Wollastonite Powder

INTRODUCTION

The BCS are very compressible and have a very low bearing capacity. The soils have exceptional shrinkage and swelling properties. BCS, like other soil types, has an extremely poor load-bearing capacity, which contributes to a variety of foundation failures, including punching failure and general shear failure. As a result, enhanced stabilisation should be achieved for each structure that has different properties. Certain stabilising procedures, such as lime stabilisation and cement stabilisation, however, have negative impacts on the BCS and other environmental components. A green technique, such as adding mineral powdered Wollastonite to soil in order to increase its strength capabilities, can be beneficial in the field of geotechnical engineering in this respect. Wollastonite is a mineral having a simple chemical composition that carries the name of Sir W. H. Wollaston (1766-1828), an English mineralogist and chemist. Wollastonite is created when impure dolostone or limestone is subjected to extreme pressure and heat. Wollastonite is a calcium silicate mineral (CaSiO3) found in a variety of locations under the earth's surface, although it can also include trace amounts of other minerals such as iron, magnesium, and manganese. The percentages of WP, L, and FA used in a field vary depending on the kind of soil utilised and its performance. The current study effort focuses on establishing the optimal ratios of individual WP, L, and FA, as well as their impact on expanding soil's CBR values, since higher Soaked CBR values reflect the intended effect of soil stabilisation.

Wollastonite is rarely pure and frequently contains impurities like as calcite, garnet, and dropsied, which are removed during the extraction process. By appropriately toning a suitable matching agent at the right concentration level, polymer compositions can be enhanced.

When used in resin, it improves processing and increases dispersion. Wollastonite has a wide range of applications, including practical ones in paints and ceramics. Wollastonite can generate a sequence of stable arrangements in the $CaSiO_3$-$FeSiO_3$ framework or an aqueous combination of stages in the $MnSiO_3$-$CaSiO_3$ framework to boost soil strength.

$$SiO_2 + CaCO_3 = CaSiO_3 + CO_2$$
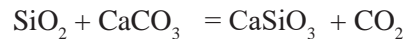
(Silica + limestone = Wollastonite + Carbon Dioxide)

LITERATURE REVIEW

In the recent past, several researchers stabilised BCS using varying concentrations of WP to evaluate the impact on soil strength. However, few of them are listed below.

In a study published by V. Mohanlakshmi et al. in 2016, investigated the effects of adding WP at various concentrations, including 5%, 10%, 15%, and 20%, on red soil. In Annur, Tamil Nadu, red soil was collected, identified, and then Wollastonite was applied. After this, the qualities and strength of the soil were discovered using a variety of experimental studies, such as LL, PC test, UCS, and CBR, among others. The results revealed that parameters including UCS CBR and dry density increased by up to 15% with the addition of WP, and that this parameter decreased with additional WP. Finally, they draw the conclusion that WP has a significant influence on the stabilisation of red soil and that 15% is the ideal amount of WP for red soil. From the experimental investigations, it was clear that with addition of 15% of Wollastonite powder which was further considered as optimum dosage, strength, liquid limit, CBR values were increased and however OMC values were decreased. The overall conclusions from the study were as follows:

i.   The addition of Wollastonite powder improves the wetting and bonding properties of red soil.

ii. The increased CBR values by the addition of Wollastonite enhanced the strength of red soil.

iii. The additions of Wollastonite to the red soil lead to reduction in OMC and increase of MDD values.

A review article titled civil engineering application and prior study on Wollastonite was published by R. Jagdeesh Kumar et al. in 2017. The article mostly focused on the information regarding Wollastonite, its uses in numerous industries, prior studies on soil stabilisation and concrete technology, as well as its potential future applications. The authors concluded that the application of Wollastonite might be carried out in sub branches of civil engineering like pavement engineering, geotechnical engineering, concrete technology based on suitable codes. The authors also suggested that the research may be prolonged in various other types of soils. In addition to individual utilization of Wollastonite, it might be added together with some pozzolanic materials like Fly ash, etc in a view of getting good results.

P. Sai Nikhil et al. in 2020 carried out research focused on employing WP as an addition to enhance the strength qualities of BCS. Two expansive soil samples were taken from two different places and named as sample S1 and S2 respectively. Following a review of these samples for various geotechnical properties, WP was added in concentrations of 5%, 7.5%, 10%, 12.5%, and 15% and the results revealed that as the amount of Wollastonite increased, the peak stress increased by 12.5%, followed by a slight loss in strength. From the experimental investigations, it was concluded that,

i. From the compaction tests, it was found that maximum dry density decreased whereas optimum moisture content of soils increased with increase in dosage of WP.

ii. The Unconfined compressive strength values of soils treated with WP increased up on addition of 12.5% Wollastonite powder then, a slight decrease was observed. However, this value was higher than the untreated soil up on 15% addition of Wollastonite powder. Peak stress was observed to 393.6% and 253.9% as compared to untreated soils on addition of 12.5%Wollastonite powder at 28 days of curing.

iii. Thus, the results showed that, Wollastonite powder was effective additive for soil, which could boost

stability and condense the cost of process in addition to improve strength and properties.

The motivation behind this investigation is its research gap as from the literature review it was observed that many studies have been carried out on Wollastonite powder in concrete material and few on Wollastonite powder in soil stabilization but there was no study available on the effect of Wollastonite powder on soil treated with the combination of pozzolanic material i.e. Fly Ash and Lime. Therefore the persistence of this investigation is to explore the usability of Wollastonite powder in improving problematic soils. Also it was observed that, very few studies are available on black cotton soil stabilized with Wollastonite Powder for improving the strength characteristics of soil. No work has been done to study the effect of Wollastonite powder in combination with fly ash and lime. No work has been done to study the effect of Wollastonite powder on swelling characteristics of soil. This reveals that there is great is need to carry out the experimental evaluation of Wollastonite stabilization of black cotton soil along with pozzolanic material like fly ash and lime for studying the effect of various dosage and curing period on different properties of soil.

MATERIALS AND METHODOLOGY

A large BCS sample was collected from the campus of Government College of Engineering, Amravati for this investigation. According to the applicable IS Codes, laboratory tests such the LL, PL, SL, SG, and PC tests were conducted on it, and the BCS was categorised as CH, or high compressible clay. Table 1, 2, 3 shows properties of WP, L and FA used in Experimental investigation. The varied percentages of WP, L, and FA were used to stabilize the BCS, with curing period of 7, 14, 21, 28, 45 days. Table 4 shows detailed study program and different percentages of stabilizers for experimental testing program. For the CBR experiments, soil samples were produced in a lab using various stabilized concentrations, appropriately stored in water for curing. Testing was done after curing, to determine the improvement in CBR of stabilized soil, further the findings of treated BCS samples were compared to untreated BCS. The outcome will be helpful in determining the ideal ratios of WP, L, and FA. Soaked CBR test specimens were soaked

in water, soaking denotes adverse moisture conditions from heavy rainfall or flooding. Specimen formation procedure includes compaction process and preparation usually involves soaking each specimen in water for 3 days before the penetration test.

Table 1. Properties of WP used in Experimental Investigation

Sr. No.	Properties	Results
1	PA	White
2	Hardness	4.5 – 5.5
3	pH	8.9 – 9.7
4	Melting Point (oC)	1540
5	CaO	43 – 47%
6	SiO2	45 – 75%
7	SG	2.8 – 3.09%

Table 2. Properties of L used in Experimental Investigation

Sr. No.	Properties	Results
1	PA	Dry White Powder
2	SG	1.2 – 1.5
3	SiO2	5.62%

4	Al2O3	0.46%
5	CaO	65.3%
6	MgO	0.10%
7	SO3	0.72%
8	Density	0.63 gm/cm3

Table 3. Properties of FA used in Experimental Investigation

Sr. No.	Chemical Constituents	Average (%)
1	SiO_2	40.18
2	Fe_2O_3	6.48
3	CaO	1.23
4	TiO_2	0.04
5	K_2O	0.18
6	MgO	0.14
7	P_4O_{10}	0.19
8	SO_3	0.04
9	Na2O	0.05
10	Al	1.42
11	Mn	0.02

Table 4. Detailed Study Program and Different Percentages of Stabilizers for Experimental Testing Program

Sr. No.	Materials	Tests	Remarks
1	BCS	A. Atterberg's Limit 1. LL Test 2. PL Test 3. SL Test B. Other tests 4. SG Test 5. PC Test 6. UCS 7. Soaked CBR	The classification of BCS was carried out as per IS classification system.
2	BCS + WP	1. PC Test : 5%, 10%, 15%, 20% of WP 2. UCS : 5%, 10%, 15%, 20% of WP (For CD 7, 14, 21,28, 45) 3. Soaked CBR : 5%, 10%, 15%, 20% of WP (For CD 7,14, 21,28, 45)	To find optimum dose of WP.
3	BCS + FA	1. PC Test : 3%, 6%, 9%, 12%, 15% of FA 2. UCS : 3%, 6%, 9%, 12%, 15% of FA (For curing period of 7 days)	To find optimum dose of FA .
4	BCS + L	1. PC Test : 2%, 4%, 6%, 8%, 10% of L 2. UCS : 2%, 4%, 6%, 8%, 10% of L (For curing period of 7 days)	To find optimum dose of L.

5	BCS + WP + FA	1. UCS : Optimum Dose of WP + OptimumDose of FA + BCS (For CD 7, 14, 21, 28, 45) 2. Soaked CBR : Optimum Dose of WP + Optimum Dose of FA + BCS (For CD 7, 14, 21, 28, 45)	The tests were carried out for the optimum dosage of FA along with WP.
6	BCS + WP + L	1. UCS : Optimum Dose of WP + OptimumDose of L + BCS (For CD 7, 14, 21, 28, 45) 2. Soaked CBR : Optimum Dose of WP + OptimumDose of L + BCS (For CD 7, 14, 21, 28, 45)	The tests were carried out for the optimum dosage of L along with WP.
7	BCS + WP + L + FA	1. UCS : Optimum Dose of WP + OptimumDose of FA + Optimum Dose of L + BCS (For CD 7, 14, 21, 28, 45) 2. Soaked CBR : Optimum Dose of WP + OptimumDose of FA + Optimum Dose of L + BCS (For CD 7, 14, 21, 28, 45)	The tests were carried out for the optimum dosageof FA,L along with WP.

RESULTS AND DISCUSSION

The outcomes of this research have provided in results and discussion section. Optimum results of WP, FA and L were found as 10%, 9% and 8% respectively. Fig. 1 illustrate the compaction curve for untreated soil and shows OMC = 24.3 % and MDD = 14.8 kN/m3 .Untreated BCS was found to have an soaked CBR of 1.64 %. Table 5, summarizes the findings of numerous tests conducted on untreated BCS, including different consistency limits, SG, PC and UCS testing.
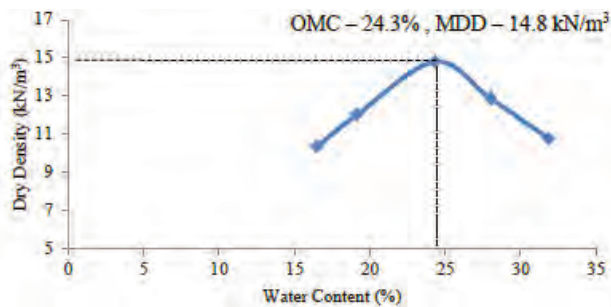

Fig. 1. Compaction Curve for Untreated BCS

Table 5. Test Results for Untreated BCS

Sr. No.	Properties of Untreated BCS	Value
1	LL (%)	60.80
2	PL (%)	26.30
3	SL (%)	18.12
4	PI (%)	34.50
5	IS Classification of Soil	CH
6	OMC (%)	24.3

7	MDD (kN/m³)	14.8
8	SG	2.67
9	UCS (kN/m²)	150.40
10	Soaked CBR (%)	
1.64		

To determine the compaction properties of each percentages of WP, a series of compaction experiments were carried out on treated BCS samples. MDD was shown to decrease whereas OMC increased. Maximum OMC and MDD values were determined to be 28% and 14.8 kN/m3. Table 6 demonstrates the variation in OMC and MDD values of stabilized BCS. Fig. 2 and 3 represents the variation in OMC and MDD values of BCS treated with WP respectively.

Table 6. Compaction Characteristics of BCS Stabilized with WP

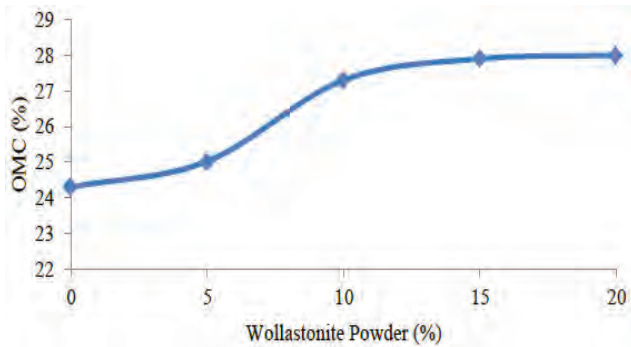| Sr. No.	WP (%)	OMC (%)	MDD (kN/m³)
1	0	24.3	14.8
2	5	25.02	13.88
3	10	27.3	13.5
4	15	27.9	13.2
5	20	28	13

Fig. 2. Variation in OMC of BCS Stabilized with Different Percentages of WP
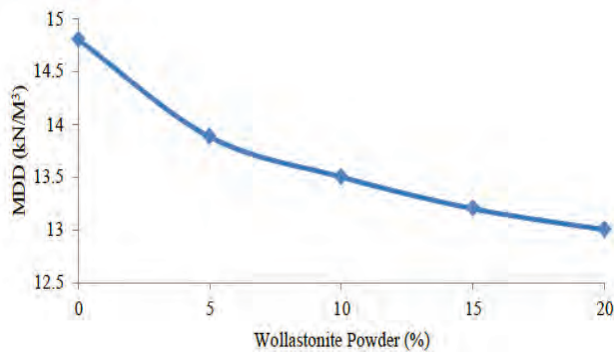

Fig. 3. Variation in MDD of BCS Stabilized with Different Percentages of WP

For each percentage of WP, the results of many Soaked CBR tests on a combination of BCS and WP were calculated. The test findings demonstrate that Soaked CBR values rise with an increase in curing time of every percentage. The CBR values of BCS treated with WP at different percentages and CD are shown inTable 7. For a WP proportion of 10% and a 45 days curing time, Soaked CBR increased by a maximum of about 213.41%. Fig. 4, Fig. 5, Fig. 6 and Fig. 7 represents the Load vs Penetration curves of soil treated with WP of different percentages. Fig. 8 represents variation in Soaked CBR readings of BCS treated with WP of different percentages and different CD.

Table 7. Soaked CBR Test Results for BCS Treated with WP

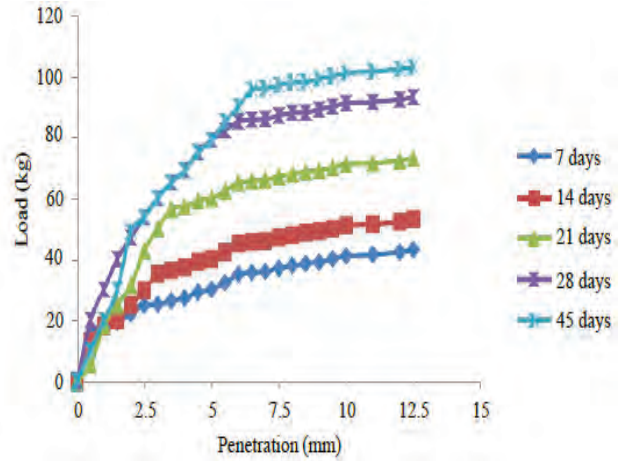| Sr. No.	Wollas-tonite powder (%)	Curing Period (Days)				
		7	14	21	**28**	45
		California Bearing Ratio (%) (Soaked)				
1	5	1.82	2.18	3.11	3.92	4.1
2	10	2.41	3.12	4.16	5.04	5.14
3	15	2.01	2.85	3.68	4.32	4.56
4	20	2.31	2.91	3.45	4.1	4.32

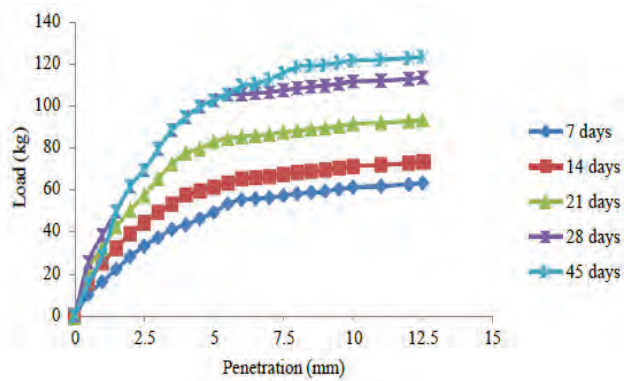Fig. 4. Results of Soaked CBR for BCS Treated with 5% WP

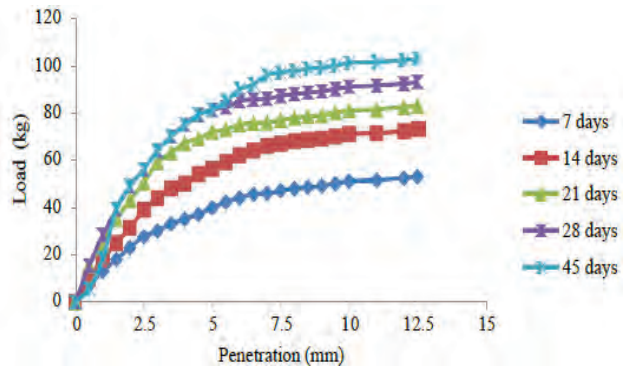

Fig. 5. Results of Soaked CBR for BCS Treated with 10% WP

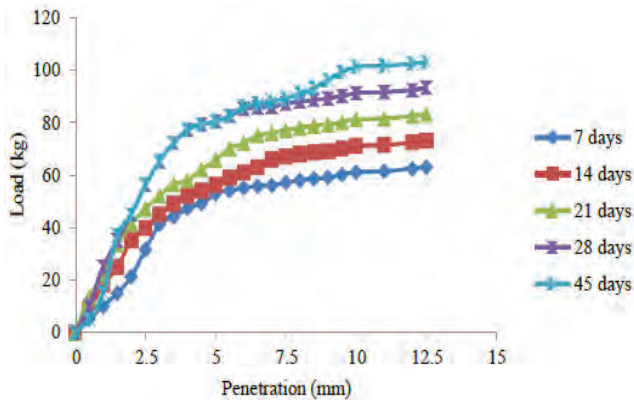Fig. 6. Results of Soaked CBR for BCS Treated with 15% WP

Fig. 7. Results of Soaked CBR for BCS Treated with 20% WP

1	Soil + Wollastonite powder (10%) + Fly ash (9%)	California Bearing Ratio (%) (Soaked)				
		2.45	2.71	3.62	4.45	5.56

Table 8 shows the Soaked CBR values of BCS treated with WP (10%) and FA (9%) at different CD. With varied CD, it was found that CBR values increased for each percentage of WP and FA. With an ideal proportion of 10% WP and an ideal percentage of 9% FA and a 45 days curing period, the highest percentage increase in soaked CBR was around 239.02%. Fig 9 illustrates the Load vs Penetration curves for Soaked CBR values of a mixture of BCS and WP (10%) coupled with FA (9%) with regard to different CD. Fig 10 shows the variation in Soaked CBR of soil treated with WP and FA for different CD.
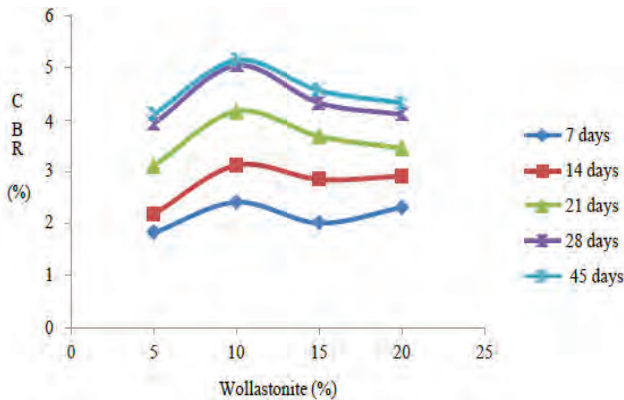

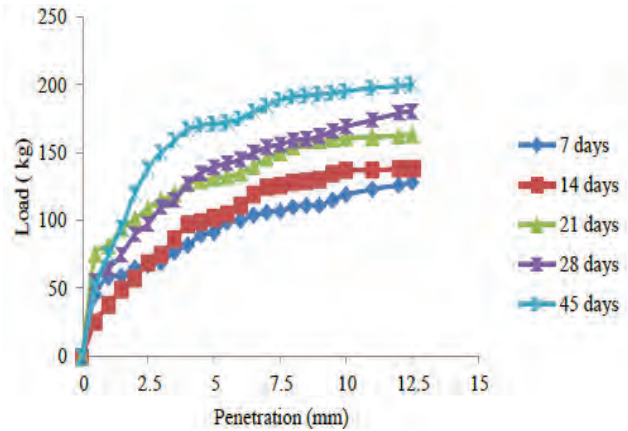
Fig. 9. Load vs. Penetration curves for Saoked CBR Tests Treated with Optimum Percentage of WP (10%) and FA (9%)

Fig. 8. Test results of Soaked CBR of BCS treated with Wollastonite powder

Table 8. Soaked CBR Test Results for BCS Treated with Wollastonite Powder and Fly ash

		Curing Period (Days)				
Sr. No.	Materials	7	14	21	28	45
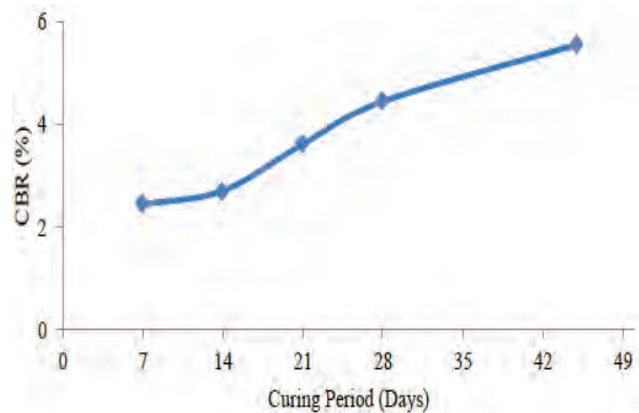
Fig. 10. Variation in CBR of BCS treated with WP (10%) and FA (9%) for different CD

The Soaked CBR values of the BCS treated with WP (10%) and L (8%) with varying CD are shown in Table 9. It was found that CBR values are improved as CD increases, with the maximum percentage increase in UCS being around 335.97% for the optimum percentage of WP, which is 10%, and the optimum percentage of L, which is 8% with curing period of 45 days. Fig. 11 shows the Load vs Penetration curves for CBR of BCS treated with WP, and L with regard to different CD. Fig. 12 indicates the variation in CBR of a BCS treated with WP, and L.

Table 9. Soaked CBR test results for BCS treated with WP (10%) and L (8%)

Sr. No.	Materials	Curing Period (Days)				
		7	14	21	28	45
1	Soil + Wollastonite powder (10%) + Lime (8%)	California Bearing Ratio (%) (Soaked)				
		4.91	5.03	6.5	7.11	7.15

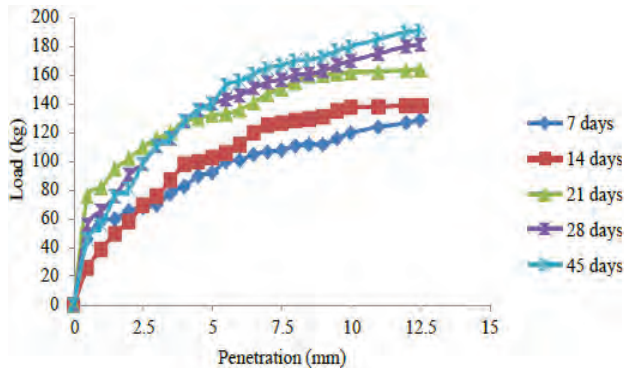**Fig. 11. Load vs penetration curves for Soaked CBR tests of BCS Treated with WP (10%) and L (8%) for different CD.**
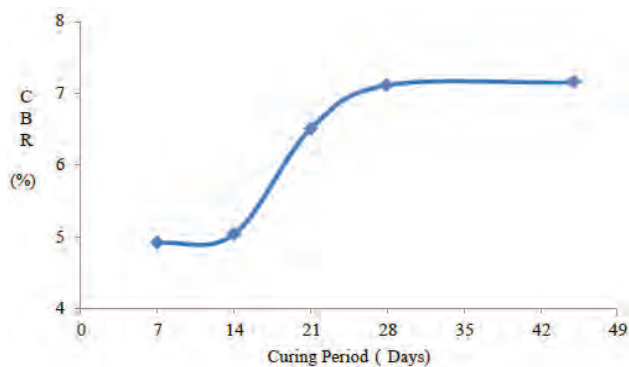

Fig. 12. Variation in CBR of BCS Treated with WP (10%) and L (8%)

Table 10 shows the CBR values of BCS treated with L (8%), FA (9%), and WP (10%) and the various CD. When WP, FA, and L were used in the recommended amounts with a 45-days curing time, the greatest percentage increase in UCS was around 528.04%. Fig. 13 describes the Load vs penetration curves for CBR of BCS treated with WP (10%), FA (9%), and L (8%) with different CD. Fig. 14 describes the variation in CBR of a BCS mixture including WP (10%), FA (9%), and L (8%).

Table 10. Soaked CBR Test Results for BCS Treated with WP (10%) , FA(9%) and L (8%)

Sr. No.	Materials	Curing Period (Days)				
		7	14	21	28	45
1	Soil + Wollastonite powder (10%) + Fly ash (9%) + Lime (8%)	California Bearing Ratio (%) (Soaked)				
		7.18	8.52	9.23	10.1	10.3

Fig. 13. Load vs Penetration curves for Soaked CBR of BCS Treated with WP (10%), FA (9%) and L
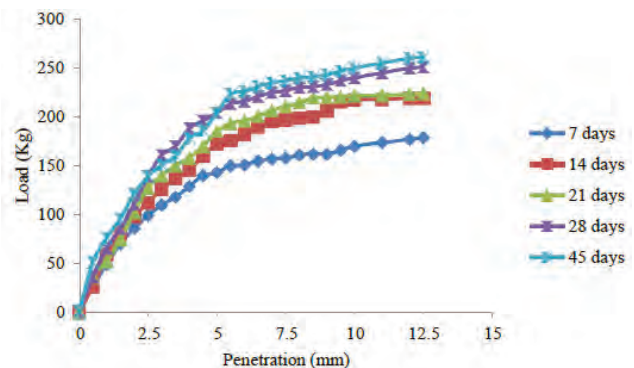
Fig. 14. Variation in UCS of BCS Treated with WP (10%), FA (9%) and L (8%)

CONCLUSIONS

- Wollastonite Powder was proven to be effective in all cases to improve both compaction and strength behavior when compared to untreated BC Soil, but the combination of Wollastonite Powder with pozzolanic material i.e. Lime and fly ash was more effective than use of Wollastonite Powder only.

- Wollastonite Powder with Lime is more effective than Wollastonite Powder with fly Ash.

- The soaked CBR values of expansive BC Soil increased with increase in dosages, curing days and constant soaking period of (3 days) for all combinations.

- The curing period supports in improving the CBR values of BC Soil.

- After treating the BC soil with Wollastonite powder, the OMC of treated soil increased from 24.3% to 28% and MDD decreased from 14.8% to 13%.

- CBR (Soaked) value increases up-to approximately 213.41% when treated with optimum dose of Wollastonite powder i.e., 10% as compared to untreated soil sample after 45 days of curing.

- CBR (Soaked) value increases upto approximately 239.02% when treated with optimum doses of Wollastonite powder and Fly ash i.e., 10% and 9% as compared to untreated soil sample after 45 days of curing.

- CBR (Soaked) value increases up-to 335.97% when treated with optimum doses of Wollastonite powder i.e., 10% and Lime i.e., 8% as compared to untreated soil sample after 45 days of curing.

- CBR (Soaked) value increases up-to approximately 528.04% when treated with optimum doses of Wollastonite powder, lime and Fly ash i.e., 10%, 8% and 9% as compared to untreated soil sample after 45 days of curing.

REFERENCES

1. Amu Olugbenga Oludolapo, Bamisaye Oluwole Fakunle and Komolafe Iyiola Akanmu, "The suitability andlime stabilization requirement of some lateritic soil sample as pavement", International journal of pure and applied sciences and technology, 2011.

2. Parbat Dhananjay, Mahajan S.M.,Bureau of Indian standards, "Methods of test for soils, determination of water content dry density relation using light compaction," IS 2720 (Part VII-1980), 1–16, 2011. Effects of Fly ash on Engineering Properties of BC Soil, International journal of research in engineering science and technologies(IJREST), 2015.

3. Bureau of Indian standards, "Indian Standard, Methods of test for soils, Part 5: Determination of liquid limit and plastic limit," Bur. Indian Stand. New Delhi, India,

vol. Reaffirmed, no. 2006, pp. 1–16 , 1985.

4. Amu Olugbenga Oludolapo, Bamisaye Oluwole Fakunle and Komolafe Iyiola Akanmu, (2011). "The suitability and lime stabilization requirement of some lateritic soil sample as pavement", International journal of pure and applied sciences and technology, Vol. 1, Issue 2, 2-4.

5. Parbat Dhanajay, Mahajan S.M.,Bureau of Indian standards,(2015). "Methods of test for soils, determination of water content dry density relation using light compaction," IS 2720 (Part VII-1980), , 2011. Effects of Fly ash on Engineering Properties of BC Soil, International journal of research in engineering science and technologies(IJREST), Vol 2, Issue 1, 1–16.

6. Bureau of Indian standards, (2006).'Indian Standard, Methods of test for soils, Part 5: Determination of liquid limit and plastic limit," Bur. Indian Stand. New Delhi, India, Vol. 2, pp. 1–16.

7. Cheng Y., s. Wang J., Li J., Huang X., Li C., Wu J.,(2018). "Engineering and mineralogical properties of stabilized expansive soil compositing lime and natural pozzolans", Construction Building Material,Vol-2,

2-7.

8. Hauashdh A.,Radin M, Mohamed S., Jailani J., and rahman Abd, (2020). "Stabilization of Peat Soil Using Fly Ash,Bottom Ash and Portland cement: Soil Improvement and Coal Ash Waste Reduction Approach," IOP Conf. Ser. Earth Environ. Sci., Vol. 4, 1-12.

9. IS 2720 (PART 10), "Indian Standard: Methods of test for soils, Part 10 Determination of unconfined compressive strength", Bur. Indian Stand. New Delhi, no. Reaffirmed 2006.

10. Indian standard, vol. Reaffirmed 2002.

11. IS: 2720 (PART 3) – 1964, Determination of Specific Gravity of soil.

12. IS: 2720 (Part 6) – 1972, Determination of Shrinkage Limit of soil.

13. IS : 2720 (Part XL)-1971 and IS :2720 (Part XLI) Determination of Free Swell Index.

14. IS: 2720 (part 16) – 1987, Determination of California Bearing Ratio.

15. IS : 2720 (Part 15) – 1986, Determination of Consolidation characteristics.

16. Mohanalakshmi V., Adhithiyan V. M., Kumar Jagadeesh, Agnes preethi,(2016). "Geotechnical Properties of Soil Stabilized with Wollastonite", International Journal of Engineering Research & Technology (IJERT) ISSN: 2278-0181, Vol. 5, Issue 3, 3-6.

17. Moradi R.,Marto A., Rashid A., Moradi M., Ganiyu A., Abdullah M., Horpibulsuk S.,(2019). "Enhancement of Soft Soil Behaviour by using Floating Bottom Ash Columns and Wollastonite", KSCE Civil Engineering conference of material ,Vol-3, 5-13.

18. Nikhil P, Ravichandran P., krishnan Divya,(2020). "Stabilization and characterization of soil using Wollastonite powder", Scientific committee of the 4th International Conference on Recent Advances in Material Chemistry, 6- 17.

19. Navagire Omkar, Sharma Shashikant, Rambabu D.,(2021). "Stabilization of black cotton soil with coal bottom ash and Wollastonite", International Conference on Smart and Sustainable Developments in Materials, Manufacturing and Energy Engineering, Vol-1, 3-9.

20. Prof. Kumar Jagadeesh, Prof. Rajan Soundara, Mohanalakshmi V., prof. Asikumar A.,(2017). "Civil Engineering Application And Earlier Research On Wollastonite – A Review", Journal of Emerging Technologies and Innovative Research (JETIR) (ISSN-2349-5162) Volume 4, Issue 02,1-9.

21. Sudhakaran S. P., Sharma A. K., Kolathayar S.,(2018). "Soil Stabilization Using Bottom Ash and Areca Fiber: Experimental Investigations and Reliability Analysis", Journal of Material Civil Engineering conference, Issue 1, 1-3.

22. Zha Fusheng, Songyu A., Liu E., Du Y., Cui K.,(2018). "Behavior of expansive soils stabilized with fly ash", Springer, Nat hazardsVol-3, 3-7.

Status of Construction & Demolition Waste in Pune City: A State of Framework

Sneha K Sawant, Ashwini R Patil
Assistant Professor
Department of Civil Engineering
D Y Patil College of Engineering Akurdi
Pune, Maharashtra
✉ sneha.ganpule007@gmail.com

Ashok B More
HOD & Professor
Department of Civil Engineering
D Y Patil College of Engineering Akurdi
Pune, Maharashtra

ABSTRACT

Construction industry in India mainly comprises of real estate and also urban development segment. Pune city is also known as IT hub city which has created numerous jobs opportunities and also has contributed growth of other sectors. Construction is one such sector dynamic construction and real estate industry has led to generation of construction and demolition waste in the city. Construction is not an eco-friendly activity by nature. The present paper mainly focuses on current practices of C&D waste in India with a case study of Pune city. The provisions to recover the waste material is discussed through the possibilities and proper methodology and how it can be used for new construction is also discussed. This study is limited to C&D waste parameter of residential and non-residential buildings in Pune city, other infrastructures are not considered. Various field surveys were carried out through different stakeholders to get statistics of C&D waste of Pune region. Detailed analysis of present status of C&D management with respect to legal policies, rules and regulations, current management practices is also presented in this paper. This review will be helpful as scope to researchers to explore the utilization of C&D waste by the process of reuse, recycle and recharge

KEYWORDS : Construction, C&D waste, Policies, Rules, Regulations.

INTRODUCTION

Pune is referred to as the IT hub, and this has helped the city's overall development. The construction industry is expanding concurrently and at the same rate. One of the primary elements worldwide that has contributed to the rise in environmental performance standards in the construction industry is sustainable development. The amount of waste generated by construction activities is one of the main cause of concern and subsequently waste disposal at sites of landfill.

The main objective of this article is an analysis of Pune's residential and non-residential structures. To ascertain the specific construction and demolition waste scenario in Pune City, the author carried out fieldwork and interviews. A comprehensive analysis of the various laws, legal system, and management strategies now in place in Pune City was carried out.

Construction and demolition waste in India

The building materials taken into account throughout the construction demolition process are broken down into two primary categories in the flow chart below.
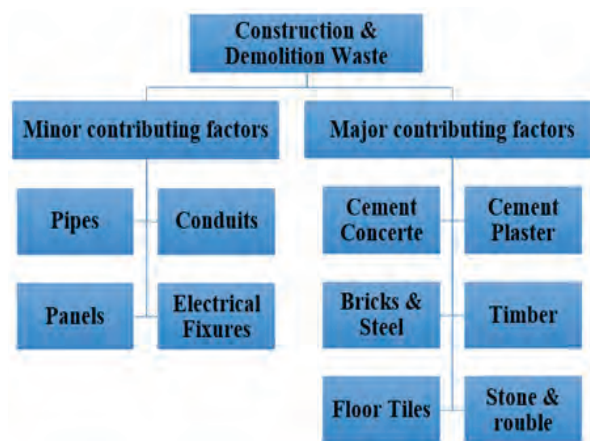

Fig. 1: Construction & Demolition Waste

The statics of constituents of core construction activities are as mentioned as per table

Table 1. Constituent in % per year

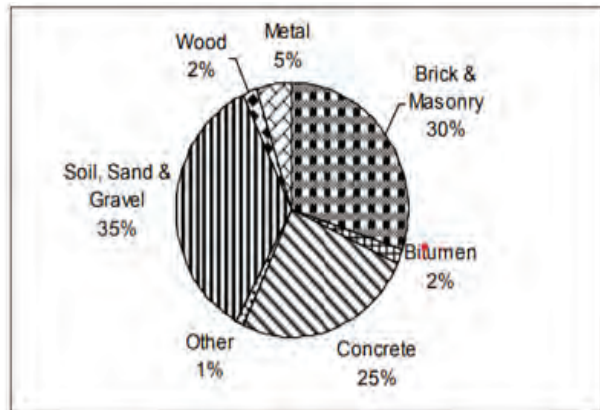| Constituent	Million tonnes/ yr.
Concrete	2.40 to 3.67
Soil, Sand and gravel	4.20 to 5.14
Bricks and masonry	3.60 to 4.40
Metals	0.60 to 0.73
Bitumen	0.25 to 0.30
Wood	0.25 to 0.30
Others	0.10 to 0.15

Fig. 2: Construction materials composition

Current condition and issues related to C&D waste in Pune

Due to the technological advancement and enhanced lifestyle, number of redevelopment projects are coming up in Pune. Out of total MSW, C& D waste in Pune constitutes 40%. According to environmental status report submitted to PMC it reflects that illegal dumping of construction rubble in the riverbeds is carried out in the city. Many times, the debris is thrown in river obstructing the natural flow of water.

According to TOI 2018 flash floods at Mula river in 2010 was due to dumping of debris on both the sides of river. Width of river has reduced at both the sides at

Pune city due to dumping of debris and it has also led to river obstruction. The flora and fauna of river is also reduced due to the same reason.

Fig. 3: Dumping of C&D waste illegally done at Pune City

Fig. 4: Dumping of C&D waste illegally done outside the construction premises of Pune City

Pune Municipal Corporation was facing a major issue of construction debris. It was first decided by Pune Municipal Corporation that C&D waste dumping should be done at Urali site but due to larger distance and increased cost of transportation builders were opposing same but due to protest of resident PMC took action against the builders and contractors.

With increasing construction and demolition waste in merged villages, Pune Municipal Corporation (PMC) has proposed to set up a debris waste processing plant in the western part of the city.

Fig. 5: Pune Municipal Corporation (PMC) has proposed to set up a debris waste processing plant in the western part of the city.

Fig. 6: C&D waste processing plant at Wagholi

Construction debris is often seen dumped around roadside, or the riverbed. The city currently generates over 400-450 tonnes of construction and demolition debris per month. However, PMC has only a 250 tonnes per day (TDP) processing plant in the Wagholi, which was constructed in 2020. PMC solid waste department will either set up the plant on Design-Build-Finance-Operate-Transfer (DBFOT) or Public Private Partnership (PPP) model. According to PMC officials, this new processing plant will cover Katraj, Wadgaon Budruk, Sinhagad Road, Karve Road, Kothrud, Baner, Balewadi, Pashan, Aundh and 13 out of the 23 merged villages in PMC limits.

Redevelopment and new construction projects were included in surveys conducted by authors ranging from medium to large scale projects. The area of redevelopment project varied from 6000 SFT to 30000 SFT. The age of the construction of buildings which are demolished in redevelopment projects ranges from 25-40years. RCC framed building to load bearing building percentage ratio was 70-40% and the waste generated includes concrete, bricks, cement plaster, gypsum boards and iron. 35% of the materials like blocks and bricks are segregated and sold at the 35-55 % of market rate after removal of mortar. Reusable materials are bought by slum dwellers. Straightening of Reinforcing steel is done on site to increase the resale value and sold as a scrap or sold. Refilling of other left over material are done on the same site or transported to the other construction site of same builder. Nowadays private contractors handle the collection, transportation and disposal of C & D waste. These contractors do disposal of C & D waste to the site of same builder or they identify site of for land filling. These private agencies will charge Rs. 1000-2000/one and half to two brass to both receiver and sender builder. The transportation charges will change according the location of site whether it is in the municipal limits or outside the municipal limits.

Need

Construction and Demolition waste should be done on priority basis as there is a global concern with regards to conservation of natural resources and energy. C&D waste management can be executed through various strategies like recycling and reuse and by forming a good and effective legislative and administrative framework for implementing of same.

Advantages

- Proper recycling and reuse helps in reduction of environmental impact.

- Construction activity required large amount of natural resources like gravel, sand, timber tree oil but with proper C&D waste management recovery and reuse of valuable materials can be done due to which there is reduction in demand of virgin resources and which ultimately helps in conservation of resources.

- Landfills are one of the important sources of greenhouse gas emission mainly methane.

By proper C&D Waste management through recycling and other methods of recovery instead of landfilling the emissions issues can be mitigated

Various compositions of C&D waste

Construction and Demolition is one of the solid wastes generated at large amount globally from various activities like construction, demolition, renovation it mainly includes

- Concrete: Concrete has largest contribution in C&D waste like concrete blocks, rubble and bricks.

- Wood: It includes various types of brick material.

- Gypsum: Waste from plasterboard and drywall/

- Plastics: It Includes plastics construction material, pipes and also includes packaging material.

- Asphalt: It is mainly from road construction material.

- Glass: It is mainly from windows, doors and other glass materials

Methods involved in recycling of waste material is as follows

- Separation of the Materials: Sorting C&D materials for recycling either manually or by automated process using sorting equipment and conveyor belts.

- Recycling of Wood: Wood waste processing in different forms such as wood chips which can be used for landscaping.

- Recycling of Glass: Glass waste is melted which can be used for production of new glass materials or using crushed glass as an aggregate.

- Recovery of Metal: Reusing metals like steel and aluminium by melting it down in manufacturing process or in construction activities.

Recovery and Recycling of C&D waste can be useful in various aspects like it helps in conservation of natural resources, lowering greenhouse emissions and reducing the landfill space. Only thing required for proper recovery is effective waste management practices and infrastructure proper sorting facility should be there.

Table No 2 Components of construction and demolition waste

Waste Components	Reuse and Recycle Methods
Concrete and Masonry	Concrete can be used as an aggregate in new concrete production mainly the crushed concrete hence the need for virgin aggregates is reduced
	Bricks and masonry can together be crushed and can also be used as an aggregate or it can be used in road base construction.
Metals	Aluminium and Steel and some other metals can also be recycled and used in production of new metal.
	Copper piping can be reused by melting it down.
Gypsum	Gypsum can be used from drywall and can be recycled and used in the production of new drywall
Plastics	Some Types of plastics can also be recycled like PVC pipes.
	Plastic sheeting can also be recycled into new plastic products.
Glass	Glass from windows, doors and other glass materials can be recycled and used as aggregate in concrete or in the production of new glass products .
Plaster	Plaster waste can also be recycled and used in production of new plaster products or as a soil amendment.
Tiles and Ceramics	Tiles and other ceramic materials can be crushed and also used as an aggregate.
Asphalt	Asphalt pavement can also be used as aggregate in new asphalt or for road base construction by crushing it.
Insulation	Fiberglass is one of the insulation material which can be recycled and used in the production of new insulation products.

II LEGISLATIVE FRAMEWORK OF PUNE CITY

- In Pune City, various departments of Pune Municipal Corporation, MLGL, Telephone Companies, Private Developers etc are undergoing Construction and Demolition work through which

large amount of Construction and Demolition Waste is generated. The solid waste management department has planned to set up a separate system for collecting and transporting the said construction debris.

- CPCB has brought various guidelines on Environmental Management of C&D wate in compliance with C&D Waste Management Rules 2016 and has tried to elaborate the negative impact if the waste management not done properly.

- Before the Construction and Demolition plant was set up, the Construction and Demolition collected from the city was be used for land filling at Uruli / Fursungi as per requirement. Also, part of the Construction and Demolition waste at Wagholi is be used for levelling.

- Rs. 19/per Mega. ton/per km rate is fixed for collecting the C&D waste from the city The distance will be measured by the GPS system. A separate toll-free cell Phone no.18002339595 has been made available by the department and municipal offices as well as citizens can also register information regarding the lifting of radars.

- Accordingly, there is a plan to collect the waste generated by various departments of Pune Municipal Corporation, MLGL, telephone companies, private developers through all the concerned developers and deposit it at a specific place directed to them and ensure that the said waste is not dumped on the side of the river bed, drain or road, highway in the city. In order to transport the entire C&D waste to the Wagholi plant project and process it.

Steps of C&D waste process at Pune City

1. For the disposal of construction and demolition waste generated under the regional offices, any kind of tender should not be called for and work should be done separately through the regional offices and further action should be taken in coordination with the solid waste department of the central office.

2. In order for the regional offices to dispose of the daily construction and demolition waste generated in their working area, the regional office should determine the place under the possession of the Pune municipality and create a feeder point at that place and see the management of the place, keeping records and taking further action regarding the disposal.

3. Small construction and demolition waste (less than 10 cubic meters) generated by various departments of Pune Municipality should be deposited at the collection centre (Feeder Point) of the concerned regional office.

4. From all departments / zonal offices, the contractor should pay the transportation cost of minor (less than 10 cubic meters) construction materials to the nearest collection point (Feeder Point) and Rs. Per 11 May. ton transport cost and Rs.195 per month. Locking of budget provision like tonne processing cost should be given to solid waste management department.

5. The provision for construction and demolition waste disposal of other departments, offices should be classified in the budget of solid waste management department.

6. Small amount of waste in the working room of the field office and due to increased construction / internal alteration of the building should be deposited at the feeder point of the field office and Rs. 19 per May. Tons of transportation costs should be recovered. Rs. 195 per May. Tons of processing costs should not be recovered.

7. Circular has been issued regarding production of the bulk qty of the construction and demolition waste. As per circular after transfer by the regional office to the recycling plant decided by Municipality, the authorized officer/ agency staff of the said place shall issue a challan with signature and stamp of the concerned. Date in the challan, wagon number, weight of empty wagon and full wagon, place S. No./developer should be mentioned

8. At present, regarding the construction and demolition waste accumulated in various parts of the city illegally, the contractor may. Action should be taken regarding the disposal by contacting SA Infra on toll free number and reporting the same to the solid waste department in written form (with photograph).

Ward offices - C&D collection centres in Pune City

- Nagar road and Kharadi – Kharadi

- Shivaji nagar-Ghole road - Vadarwadi, Gondhal chowk, Paul estate, Janwadi

- Kothrud-Bhavdhan – Sutarwadi

- Dhankawadi-Sahakarnagar – Ambegaon

- Sinhagad road –Mahadevnagar, ward 34 near canal, pharshi oil, Dattawadi, Janata vasahat

- Warje-Karvenagar - survey number 86

- Hadapsar - survey number 49 and 51, Kalepadal

- Wanwadi-Ramtekadi - HM royal parking, Amenity space Kondhwa

- Kondhwa-Yewalewadi - HM royal parking, Amenity space Kondhwa

- Kasba-Vishrambaughwada - Dambar kothi, near Chhatrapati Shivaji Maharaj statue

Table 3. C& D waste authorities in India

Place	Corporations	Municipal Corporation Class A	Municipal Corporation Class A	Municipal Corporation Class A	Nagar Panchyats	Cantonment Board
Mumbai	1	--	-	-	-	-
Navi Mumbai	1	--	-	1	-	-
Kalyan	3		-	-	3	-
Thane	3	2	2	1	3	-
Raigad	1	--	1	8	6	-
Kolhapur	3	--	5	18	18	--
Amravati	2	1	14	15	9	
Chandrapur	1	1	8	13	24	-
Nagpur	1	3	7	17	18	1
Pune	3	3	8	21	18	3
Nashik	5	2	15	25	17	2
Aurangabad	4	4	14	32	26	1
Total	28	16	74	151	142	7

Table 4. C& D waste Plants in Pune

Name of Corporation	Plant Capacity (TPD)	Present Status
Pune Municipal Corporation	250	In Operation
Pimpri Chinchwad Municipal Corporation	200	In Operation

Table 4. C&D Waste Urban Local Body

Name of Urban Local Body (ULB)	Class	Population	Total Qty of C & D waste Generated during whole year in MT	Total Qty of C & D waste processed/ recycled in MT	Total Qty of C & D waste Disposed by landfilling without processing (last option) or filling low lying area	Number of Storage Facilities for C&D Waste Storage	Transportation (Truck, Tractor, Dumper placer, other)	Transportation Municipal magistrates appointed for taking penal action for noncompliance with these rules.
Pune Municipal Corporation	MC-CLASS A	4294220	213410	124523	0	0	64	Yes

Pimpri-Chinchwad Municipal Corporation	MC-CLASS B	2965609	20683	20683	1440	0	12	Yes

Role of Stakeholders in Construction and Demolition Waste Management

The various stakeholders involved in C&D waste management are the builders, contractor's developers, the local authorities, architect's engineers, the research institutes

Responsibility of Engineer and architects are as follows:

● Proper Designing for Deconstruction and Dismantling.

● Parallel Disassembling should be done instead of sequential dissembling.

● Proper survey of site should be done before demolition.

● Use of minimum non toxic materials should be done.

● Proper development of waste management plan should be done.

Responsibility of Municipal authorities are as follows

● Proper identification of Landfill sites should be done.

● Existing landfill site should be properly managed.

● Proper infrastructure should be provided for collection, storage, segregation, transportation, processing and recycling as well as disposal of C&D waste.

● Awareness sessions should also be provided to other departments regarding C&D waste management.

Responsibility of Waste Source Generator

● Disposal of waste should be according to Municipal Solid Waste management rules.

● Disposal of waste should not be done outside area stipulated by municipal authorities.

CONCLUSION

The construction and demolition waste has become a major issue due to number of redevelopment projects taking place in Pune City. Though Construction and Demolition Wate Management Rules 2016 is introduced still there is need of proper implementation to be followed. This paper has come to a conclusion that if following waste management practices are followed we will be achieving a sustainable approach for waste management.

Following methods can be used for effective waste management practices.

1. Plans should be assessed by the engineer in terms of Design for Adaptability and Deconstruction.

2. Awareness campaign should be undertaken for all stakeholders for effective management of Construction and Demolition Waste.

3. Financial Incentives should be given to the builder's contractors and owners of the building if they are using recyclable material.

4. Those the guidelines are introduced still on ground the work is not executed as per the rules so checklist should be prepared and fines should be imposed to whomever not following the rules.

REFERENCES

1. Sourabh Jain, Shaleen Singhal, Nikunj Kumar Jain 2019. "Construction and Demolition Waste Generation in Cities of India: An Integrated Approach." International Journal of Sustainable Engineering: 1-7.

2. Daniel R. Rodinal-Oviedo 2021. "Construction and demolition waste management in developing countries: a diagnosis from 265 construction sites in the Lima Metropolitan Area." International Journal of Construction Management.

3. Sourabh Jain, Shaleen Singhal, Nikunj Kumar Jain 2019. "Construction and demolition waste (C&DW) in India: generation rate and implications of C&DW

recycling." International Journal of Construction Management: 1-7.

4. Mario Ramos, Graça Martinho 2022. "An assessment of the illegal dumping of construction and demolition waste." Cleaner Waste Systems,1-8

5. Guidelines on Environmental Management of Construction and Demolition (C&D) Waste

6. Annual Report of Construction and Demolition Waste Management Rules ,2016

7. Pune Municipal Corporation and Pimpri Chinchwad Municipal Corporation Official Website.

8. Field Survey from stakeholders and Interview with PCMC Officials.

Investigation on Performance and Emission Characteristics of Diesel Engine using Various Biodiesels

S. Raju
Research Scholar
Dept. of Mechanical Engineering
Chaitanya Deemed to be University
✉ Suramraju2@gmail.com

B. Mohan
Dept. of Mechanical Engineering
CDU

M. Srinivas Naik
Associate Professor
Dept. of Mechanical Engineering
JNU Delhi

ABSTRACT

The demand for energy has significantly increased as a result of rapid industrialization and population development. The depletion of petroleum resources is the result of careless use of fossil fuels. The ecosystem has been severely harmed by the pollutants that diesel engine emissions have generated. Our main goal is to resolve these problems. The usage of algae, animal fats, and vegetable oils are potential future biodiesel production methods. This article summarizes the studies on how biodiesel affects diesel engine performance and emissions. Being more viscous is the main issue with using other oils directly in engines; however, this can be overcome by employing Tran's esterification reaction to turn them into biodiesel instead. It was determined that the diesel and biodiesel's viscosity, flash point, and calorific value were equivalent to those of petroleum diesel. Variable loads and constant RPM diesel engine operation has been the subject of an experimental investigation. Graphs pertaining to engine performance parameters, such as brake power (BP), brake thermal efficiency, brake specific fuel consumption (BSFC), and engine effects on carbon monoxide (CO), carbon dioxide (CO2), hydrocarbon (HC), nitrogen oxides (Nox), sulphur oxides (Sox), etc., have been plotted.

KEYWORDS : *Biodiesels, Diesel engine, BTE, BSFC, Emission, Tran's esterification.*

INTRODUCTION

Almost every country depends on petroleum fuel to meet its energy needs. Increased energy consumption due to population growth has an influence on subterranean fossil fuel sources. To solve this problem, researchers are looking into alternative energy sources. Biodiesel is one of the potential replacements for diesel derived from petroleum since its properties are fairly comparable to those of diesel. Furthermore, the bulk of feedstocks used to produce biodiesel is renewable and comprise animal fats, edible and inedible oils, and both. A major focus in recent years has been on producing biodiesel from culinary oils, such as cottonseed, sunflower, coconut, chicken, and fish oils. Since using edible oils could have a negative effect on agriculture by lowering the availability of food crops, non-edible oils are used in the production of biodiesel. Portability, availability, enhanced lubricating qualities; lower sulfur content, higher cetane number, higher biodegradability, domestic origin, and a higher flash point are the main advantages of using biodiesel. Researchers have shown that emissions of nitrogen oxide (NOX) increase but emissions of hydrocarbons (HC), carbon monoxide (CO), and particulate matter (PM) decrease when biodiesel is used in place of conventional diesel fuel. Thus, the emissions generated by diesel engines powered by biodiesel are the main subject of this paper.

Objectives

1. Preparing biodiesel from waste cocking oil, chicken oil, fish oil.

2. Testing the chemical properties of prepared biodiesels.

3. Comparison between diesel and biodiesels.

4. How to Use of waste cooking oil, chicken oil and fish oil as an alternative fuel for diesel engine.

5. To study Performance and emissions of engine by using biodiesels.

Advantages of Biodiesel over Petroleum

Compared to diesel based on petroleum, biodiesel, which is made from renewable resources such as vegetable or animal fats, has the following benefits:

Unlike petroleum, which is a finite fossil fuel, biodiesel may be produced from renewable resources such used cooking oil, rapeseed oil, and soybean oil. When burning; biodiesel typically emits fewer greenhouse gases than petroleum fuel, particularly carbon dioxide (CO_2). As a result, a more closed carbon cycle can be created. Biodiesel's carbon comes from freshly harvested plants that took up CO_2 during their growth. Because biodiesel is non-toxic and biodegradable, it poses less of a risk to the environment in the event of spills or leaks than petroleum diesel. Many countries have the capacity to produce biodiesel on their own soil, reducing dependency on imported fossil fuels and enhancing energy security. Because it can be transported through the current diesel fuel infrastructure and utilized in diesel engines that are currently in use with little to no modification, biodiesel is a reasonably simple transition fuel. Because biodiesel has better lubricating properties than petroleum diesel, engine wear is decreased and engine life is increased. Biodiesel production can boost rural economic growth by creating jobs in agriculture and biodiesel production facilities. Burning biodiesel improves air quality and improves the health of urban populations by reducing pollution from sources like sulfur oxides and particle matter. For the purpose of producing biodiesel, a range of feedstock's are available, providing flexibility in the acquisition of raw materials and possibly lowering price volatility. When the entire lifecycle is considered, biodiesel produced from waste oils or agricultural leftovers nearly reaches carbon neutrality. Biodiesel has a significantly reduced carbon footprint.

LITERATURE REVIEW

Biodiesel is one of the most extensively researched biofuels for CI engines. It is a renewable fuel Made by Trans esterifying vegetable or animal fats. In terms of cetane number and lubricity, Biodiesel is comparable to regular diesel fuel. However, it has the benefit of emitting less carbon Monoxide (CO) and particulate matter (PM).

Researchers like Agarwal and Kar(2017) and Rakopoulos et al. (2015) have conducted experimental investigations that show the potential of Biodiesel blends to enhance engine performance and lower exhaust emissions, especially when combined in different ratios with conventional diesel fuel.

Yadav and Sharma (2016) and Schifter et al. (2018). These studies emphasize the Significance of fuel injection strategy optimization and engine calibration for enhanced Combustion stability. A further viable choice for CI engine applications is biogas, a renewable gaseous fuel made from the anaerobic digestion of organic waste. Methane (CH_4) and carbon dioxide (CO_2) make up most biogas, with trace amounts of other gases like ammonia (NH_3) and hydrogen sulfide (H_2S).

Authors like Yusaf et al. (2014) and Krishnan et al. (2019) have studied the combustion characteristics and emission performance of biogas-fueled CI Engines, demonstrating the fuel's potential as a low-emission and sustainable choice.

To maximize engine performance and emissions, researchers have also looked into mixed fuels and dual-fuel combustion techniques in addition to specific biofuels. Some of the advantages of diesel fuel can be preserved while reducing its environmental impact by blending biofuels with regular diesel fuel. By simultaneously injecting diesel and biofuels, dual-fuel combustion maximizes the benefits of both fuels, resulting in reduced emissions and increased efficiency. Studies on the impact of different blending ratios and dual-fuel combustion techniques on the performance and emissions of CI engines have been conducted by authors such as Avinash et al. (2017) and Ramadhas et al. (2020).

ENGINE SETUP AND ITS SPECIFICATION

Single-cylinder, four-stroke diesel engines make up the experimental arrangement. The pressure sensor is fixed to the cylinder head, which is exposed to the

combustion chamber, and it measures the in-cylinder combustion pressure in relation to the crank angle. To measure the crank angle, an encoder was installed on the crank shaft. For loading the engine, an eddy current dynamometer was employed. The pressure-crank angle data were collected and afterwards analyzed using the data gathering system. Throughout the testing, the engine speed (1500 rpm) and static injection time remained unchanged.

Fig. 1: Four Stroke Single Cylinder Diesel Engines

TheFigure1Explain the working of a four-stroke single-cylinder diesel engine. Four stroke single cylinderis the conversion of chemical energy from diesel fuel into mechanical energy by means of four separate piston strokes within the cylinder. A four-stroke single-cylinder diesel engine uses a controlled sequence of intake, compression, power, and exhaust strokes to convert diesel fuel into mechanical power. This method is dependable and effective. Every stroke is essential to the engine's continued running and ability to produce power.

Table 1. Specification of four stroke single cylinder Diesel Engine.

Engine	Kirloskar Diesel engine
Speed	1500rpm
Number of cylinders	1
Compression ratio	16.5:1
Maximum H.P	7H.P

Stroke	110mm
Bore	80mm
Type	Water cooled
Method of loading	Rope brake

A diesel engine with a single cylinder and four strokes may have different specifications depending on its intended use and design as show in the Table 1. Knowing these specs makes it easier to choose the right engine for a certain application, ensuring that it satisfies performance standards while taking into account variables like environmental effect, efficiency, and dependability.

Table 2. Properties of Neat Oils.

Property	Fish Oil	Chicken Oil	WCO	Diesel
DENSITY AT 15°C(Kg/ m3)	878	926	913	832
Kinematic viscosity at 40°c(mm^2/ sec)	49.9	38.10	5.03	3.5
Calorific value (kj/ kg)	32430	39398	35560	41950
Flash point C^o	240	267	208	75
Fire point C^o	266	296	220	82

The Table 2 is brief explains about the properties of oils. By exploiting these properties effectively, industries can optimize combustion processes, improve energy efficiency, reduce emissions, and enhance overall system performance. Advances in combustion technology and fuel formulation continue to offer opportunities for further efficiency gains and environmental benefits.

Table 3. Properties of Methyl esters

Property	Fish Oil Me	Chicken Oil Me	Wcome
Density at 15°C (Kg/ m^3)	880	874	885

Kinematic viscosity at 40°c(mm²/sec)	5.27	6.2	5.7
Calorific value(kj/kg)	3917	43780	38650
Flash point C°	174	164	160
Fire point C°	190	171	164

The Table 3 is brief explains about the properties of different methyl ester oils. Methyl esters, also referred to as biodiesel when made from vegetable or animal fats, have unique qualities that can be used to good use in a variety of contexts. Methyl esters can be used in a variety of applications, including as power production, transportation, and heating, to meet regulatory criteria and achieve environmental sustainability, energy security, and regulatory compliance. The performance and suitability of methyl esters as a renewable fuel alternative are intended to be further improved by ongoing research and technical developments.

RESULTS AND DISCUSSION

Brake power, thermal efficiency, and specific fuel consumption were compared after the performance characteristics investigation of the various fuels had been completed.

Comparison of the experimental performance characteristics of diesel and various oil methyl esters
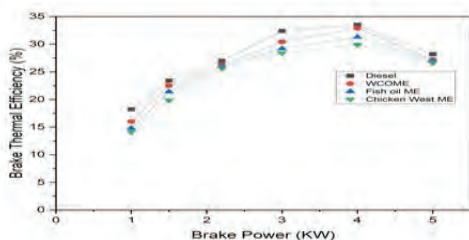

Figure 2. Comparison of brake thermal efficiency with respect to brake power for three methyl esters and diesel

Brake thermal efficiency indicates how well heat is transformed into work, depending on the fuel type and engine configuration. The brake power-to-fuel energy ratio is used to calculate braking force. With increasing load, BTE increases for all fuels. The Figure 2 displays

the variance. Four kW of brake power yields the maximum efficiency. The efficiency values for diesel methyl esters, fish, poultry, waste cooking, and 29.9%, 32.9%, and 33.5%, respectively, were reported. Methyl esters' braking thermal efficiency decreased by 1% to 4% when compared to diesel. Because of their high calorific value, these Ester oils are more efficient than diesel. Part of the decreased efficiency can be ascribed to the increased density and viscosity of esters.
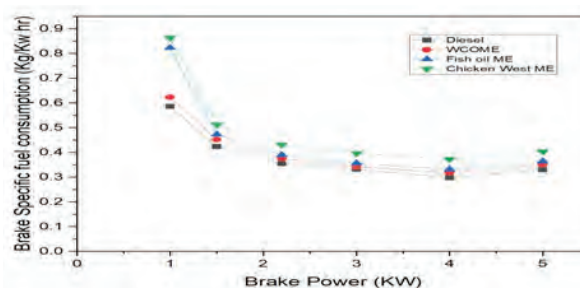

Figure 3. Comparison of specific fuel consumption with respect to brake power for three methyl esters and diesel

The calculation of brake-specific fuel consumption involves dividing the engine's power output at a given load by the fuel consumption rate. This important metric is critical since it reflects engine performance and is inversely related to BTE. The Figure 3 shows the particular fuel usage in response to braking power. As the load increases, the BSFC rises.5 kW of braking power was the least used. VOME had a higher BSFC than Diesel. Fish oil, chicken oil, waste frying, and diesel had BSFCs of 0.823 kg/kW-hr, 0.868 kg/kWhr, 0.623 kg/kWhr, and 0.586 kg/kWhr, in that order. The proportion of BSFC that increased for cooking waste, fish oil, and poultry oil The comparison of methyl esters and diesel showed that, respectively, 40.6%, 47.2%, and 6.3% more specific energy consumption was the reason behind the rise in the BSFC of Methyl esters. One reason for the increase in consumption is the increasing density and viscosity.

COMPARISON OF EXPERIMENTAL EMISSION CHARACTERISTICS OF METHYL ESTERS WITH DIESEL

Carbon Monoxide (CO) Emissions

Carbon monoxide emissions for all fuels are depicted in Figure 4 with more braking force, the emissions rise.

The CO emissions for diesel used cooking oil, fish oil, and chicken oil at 5 kW of braking power there were three methyl esters: 0.5, 0.4, and 0.44. When compared to diesel, the CO emissions for the aforementioned four methyl esters decreased by 20%, 16%, and 12%, respectively.

Incomplete combustion results in the generation of CO, which is dependent on the rate of combustion of the fuel-air combination and the amount of carbon in the fuel. Carbon is transformed into carbon monoxide when it cannot create carbon dioxide. The cetane number and oxygen concentration of ME are both high. Combustion is caused by the elevated oxygen level. Full combustion fuel is produced by the promoter. Therefore methyl esters reduce CO a by-product of incomplete combustion.
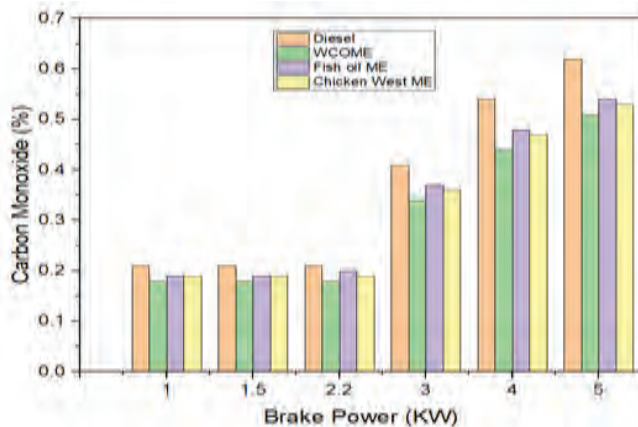
Figure 4. Comparison of carbon monoxidewith respect to brake power for three methyl esters and diesel

Hydrocarbon (HC) Emissions:

The emission of hydro carbons for each of the four fuels in relation to braking power is shown in Figure 5 as braking power increases, emissions rise. Diesel used cooking oil, fish oil, and methyl esters of chicken and fish oils all had HC emission levels that were, respectively, 88 PPM, 72 PPM, 75 PPM, and 76 PPM. Methyl esters of waste cooking oil, fish oil, and chicken oil had lower hydrocarbon emission rates than diesel at 18.18%, 14.8%, and 13.64 percent, respectively. Because of incomplete combustion, there are emissions. Only until the fuel correctly atomizes and combines with the air can efficient combustion take place, which in turn depends on the viscosity and surface tension of the fuel. Methyl esters burn more efficiently than diesel

due to their characteristics as a fuel. Because biodiesel has a greater cetane number than diesel, it displays shotter ignition delay time.
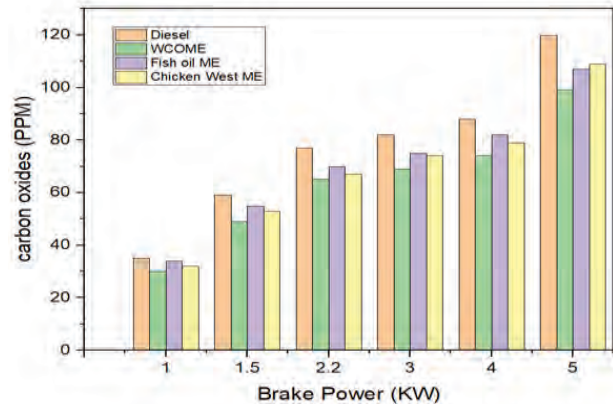

Figure 5. Comparison of carbon Oxides with respect to Brake power for three methyl esters and diesel

Nitric oxides

The Figure 6 shows the emission of nitric oxide for all the four fuels with respect to brake power. The emission increases with brake power. The emission of Nox for diesel, waste cooking oil, fish oil, and chicken oil methyl esters were 832PPM, 821PPM, 815PPM and 813PPM respectively. The decrease in NOx emission waste cooking oil, fish oil, and chicken oil methyl esters 1.3%, 1.7%, and 2.3%, than diesel respectively. NOx emission depends on oxygen content adiabatic flame temperature and spray properties. Spray characters is based upon droplet size, momentum, degree of mixing with air and penetration rate. The nitrogen content of the fuel also contributes to NOx production.
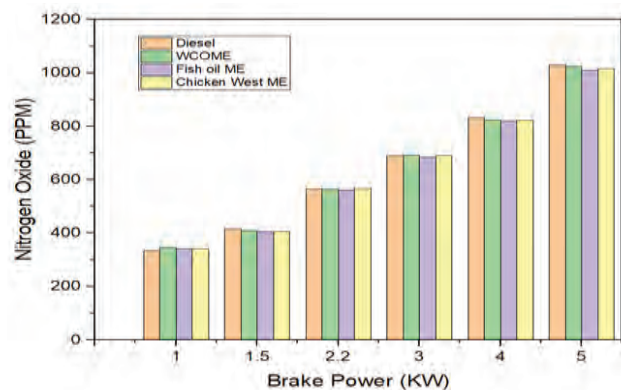

Figure 6. Comparison of Nitric Oxides with respect to brake power for three methyl esters and diesel

CONCLUSION

Compared to diesel, fish oil has a 1.6% lower brake thermal efficiency. The cooking oil waste is 0.6%, while the chicken waste is 3%. When compared to diesel, the consumption of brake-specific fuel increased by 48.1% for waste chicken oil, 40% for waste cooking oil, and 40% for fish oil. Waste cooking oil, fish oil, and chicken waste oil reduce their carbon monoxide emissions by 20%, 16%, and 14%, respectively, when compared to diesel. Waste cooking oil, fish oil, and chicken waste oil reduce hydrocarbon emissions by 18%, 16%, 15%, and 13%, respectively, when compared to diesel. Compared to diesel, waste cooking oil, fish oil, and chicken waste oil reduce nitrogen oxide emissions by 11.4%, 10%, and 8.5%, respectively.

The performance and emission characteristics of diesel engines employing several types of biodiesels were investigated, and the results provide some interesting directions for sustainable energy sources. Blends of biodiesel have shown promise in increasing engine efficiency and lowering hazardous emissions via extensive testing and research. The significance of alternative fuels in improving energy security and reducing environmental effect is highlighted by this research. Achieving global sustainability targets is greatly aided by adopting biodiesel technology, which also promotes the shift to greener transportation.

REFERENCES

1. J. Van Gerpen, Biodiesel processing and production, Fuel Processing Technology, 86 (2005), pp. 1097-1107 DOI: 10.1016/j.fuproc.2004.11.005

2. B.K. Barnwal, M.P. Sharma, Prospects of biodiesel production from vegetables oils in India, Renewable and Sustainable Energy Reviews, 9 (2005), pp. 363-378 DOI: 10.1016/j.rser.2004.05.007

3. S. K. Godiganur, The effect of Karanja oil methyl ester on Kirloskar HA394 diesel engine and exhaust emission, Thermal science, 14 (2010), pp. 957-964 DOI: 10.2298/TSCI1004957G

4. A. Demirbas, Biodiesel production from vegetable oil via catalytic and non-catalytic supercritical methanol transesterification methods, Prog Energy Combustion Sci., 31 (2005), pp. 466-487 DOI: 10.1016/j.pecs.2005.09.001

5. S.K. Karmee, A. Chala, Preparation of biodiesel from crude pongamiapinnata, BioresourceTechnol, 96 (2005), pp. 1425-1429 DOI: 10.1016/j.biortech.2004.12.011

6. M.P. Dorado, E. Ballesteros, J.M. Arnal, J. Gomez, F.J. Lopez, Exhaust emission from a diesel engine fuelled with transesterified waste olive oil, Fuel, 82 (2003), pp. 1311-1315 DOI: 10.1016/S0016-2361(03)00034-6

7. S. Puhan, N. Vedaraman, G. Sankarnarayanan, V. Bopanna, R. Bharat, Performance and emission study of mahua oil (MadhucaIndica oil) ethyl ester in a four stroke naturally aspirated direct injection diesel engine, Renew Energy (2004), pp. 1-10 DOI: 10.1186/1477-7525-2-1

8. R. Altin, S. Centikaya, H.S. Yucesu, The potential of using vegetable oil fuel as fuel for diesel engines, EnergyconverManag, 42 (2001), pp. 529-538 DOI: 10.1016/S0196-8904(00)00080-7

9. Y.D. Wang, T. Al-Shemmeri, P. Eames, J. Mcmullan, N. Hewitt, Y. Huang, An experimental investigation of the performance and gaseous exhaust emission of a diesel engine using blends of vegetable oil, Applied Thermal Energy, 26 (2006), pp. 1684-1691 DOI: 10.1016/j.applthermaleng.2005.11.013

10. F. Ma, M.A. Hanna, Biodiesel production: A Review, Bioresources Technology, 70 (1999), pp. 1-15, DOI: 10.1016/S0960-8524(99)00025-5

Comparative Analysis of Honeycomb Structure Panels with Different Cell Shapes and Material for Bus Flooring

Raja Sekhar
Professor & Head
Department of Mechanical Engineering
Methodist College of Engineering and Technology
Hyderabad, Telangana
✉ arsekhar06@gmail.com

Ch. Uday Kumar
Department of Mechanical Engineering
Methodist College of Engineering and Technology
Hyderabad, Telangana
✉ uday398kumar@gmail.com

Prasad Matam
Y. Madhu Maheswara Reddy
Associate Professors
Department of Mechanical Engineering
Methodist College of Engineering and Technology
Hyderabad, Telangana
✉ prasadmatam@methodist.edu.in
✉ mmr315@methodist.edu.in

ABSTRACT

This research paper presents a comprehensive comparative analysis of honeycomb structure panels designed for bus flooring, focusing on the influence of various cell shapes and materials. Honeycomb structures are renowned for their lightweight and high strength properties, making them ideal candidates for applications such as bus flooring. However, the performance of honeycomb panels can vary based on the specific design parameters.

The study investigates three main aspects: different cell shapes, various materials, and their combined effects on the mechanical and structural properties of honeycomb panels. The research aims to provide valuable insights into optimizing bus flooring to enhance safety, durability, and overall performance.

This project deals with the modelling and analyses of two sets of HSPs, made of different cell shapes(Square, Circular, Hexagonal & Triangular) with Al6061 as core material and as face sheet for one set and Stainless steel 316L as the face sheet material for other set of HSPs for comparing the Strength and Stiffness properties. Upon acquiring the results after doing a comparative analysis, it is found that, the Square cell type of HSP made of Stainless steel 316L-Al6061 combination giving better results is the better choice for Bus flooring.

KEYWORDS : *Honeycomb structure, Bus flooring, Cell shapes, Materials, Comparative analysis, Mechanical properties, Structural optimization.*

INTRODUCTION

The honeycomb structure, whether found in nature or engineered by humans, is a fascinating design characterized by hexagonal cells. This intricate geometry serves a dual purpose, minimizing both material usage and overall weight, consequently reducing costs. The cells, typically columnar and hexagonal, are strategically arranged to achieve this balance. In applications where mechanical structures demand a delicate equilibrium of stiffness, strength, and weight efficiency, the adoption of sandwich construction has emerged as a noteworthy trend.

These sandwich panels, known as honeycomb sandwich panels (HSPs), have found extensive utility across diverse industries, including aerospace (satellites, spacecraft, and aircraft), transportation (trains, boats, and trucks), and more. The distinctive feature of HSPs lies in their composition robust face plates bonded on the upper and lower sides encase a core material in between. The choice of core material is a critical consideration,

contingent upon the specific performance requirements of the application at hand.

Furthermore, the face sheet material of HSPs can be fashioned from either metal or non-metal materials, providing flexibility to tailor the construction to meet specific environmental and application needs. This adaptability is crucial in achieving optimal performance across a spectrum of conditions.

A notable advantage of honeycomb sandwich structures is their exceptional strength-to-weight and stiffness-to-weight ratios. This structural arrangement ensures that the resulting panels exhibit high levels of stiffness and strength while maintaining a minimized overall weight. This characteristic has rendered honeycomb sandwich panels indispensable in industries where achieving optimal structural performance with minimal material usage is a priority. In essence, the honeycomb structure and its application in sandwich panels exemplify an ingenious engineering solution that harmonizes efficiency, strength, and cost-effectiveness across a broad range of industries.
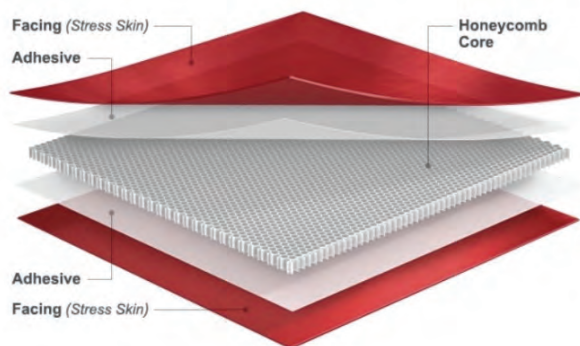

Fig-1: Sandwich Construction

LITERATURE REVIEW

The following are the list of research papers, that have been gone through to get a proper understanding of Honeycomb Structures and Bus flooring to determine the scope of work.

1. In the study by Gopi Chand [1], the bending behavior of copper core honeycomb panels with stainless steel facing was experimentally investigated under 3-point bending for various core heights and loads. The results indicated that a lower core height led to a higher gradient of the deflection curve, while higher core height resulted in lower stress.

2. Amy F.Domae [2] compared cell shapes in a honeycomb structure, emphasizing the strength of different shapes. The study found that circular columns exhibited greater strength, with the ranking of structures from strongest to weakest being cylinder, hexagon, square, and triangle. The results suggested that shapes with fewer flat faces, such as cylinders, tended to be stronger.

3. P.S.B. Chowdary [3] conducted a numerical investigation into the effect of cell shape on the behavior of honeycomb structure panels. The study concluded that stainless steel-copper panels with a square honeycomb core exhibited better resistance to deformation, leading to lower stress. Modal analysis revealed that aluminum-aluminum square honeycomb structure panels had higher natural frequencies.

4. G.Epasto [4] researched aluminum honeycomb structure panels for protective structures in earth-moving machines. The study focused on providing technical solutions for impact protection, concluding that lightweight aluminum honeycomb cores were suitable for designing absorber devices in vehicle protective structures to ensure occupant safety.

5. Sathish Kumar. P [5] studied the strength and behavior analysis of honeycomb structure composite plates made of various fibers and hybrids. The results indicated that composite plates filled with sawdust and coconut coir showed better flexural strength compared to empty composite plates.

6. Prof. A.B. Yadav [6] explored the design of honeycomb structure panels and their validation with bus flooring plates. The study found that the designed honeycomb structure panels exhibited a significantly higher stiffness-to-weight ratio and lower deflection under three-point bending compared to regular floor plates.

7. Hee-Young Ko, Kwang-Bok Shin, Kwang-Woo Jeon, and Seo-Hyun Cho [7] investigated the crashworthiness and rollover characteristics of low-floor buses made of composite structures. The

numerical simulation focused on a frontal accident at a speed of 60 km/h.

8. Chinnu Gigi, Dalmiya Rajan [8] conducted a study on honeycomb structures and hybrid structures. The analysis included buckling analysis, bending analysis, and dynamic analysis, revealing that hexagonal shapes exhibited better results, with hybrid structures providing thermal and mechanical advantages along with increased strength and energy absorption.

9. Jonathan Irwin, Keshav Srinivasan, Pesala Anudeep, Rahul Maddimani [9] modeled and analyzed honeycomb structure panels, comparing deformations, stresses, and displacements for varying thicknesses of hexagon cells and facing plates. The study also incorporated the proposed honeycomb structure panel into a car bumper, demonstrating its potential for improved safety during impacts.

10. Ms. Poonam Joshilkar, Prof. R. D. Deshpande, Prof. R. B. Kulkarni [10] analyzed the behavior of honeycomb structures with steel facing plates and a 5mm honeycomb core height under three-point bending. The study explored different honeycomb core materials and thicknesses of faceplates and core walls, finding that increasing the thickness of faceplates and core walls reduced deflection and increased load-carrying capacity. The failure load and stress variation at failure load were consistent when faceplate material was steel in all models.

SUMMARY OF LITERATURE REVIEW

In the review of prior research, various applications of Honeycomb Sandwich Panels (HSPs) have been extensively investigated by earlier scholars. Summarizing the key findings and highlights from the previous works:

➤ Core Geometry Comparison: Some previous studies focused on comparing two types of core geometries. However, these comparisons often did not encompass multiple material combinations, limiting the scope of the analysis.

➤ Material and Core Comparative Analyses: Previous research undertook comparative analyses by considering a single core geometry paired with different material combinations. Additionally, comparisons were made between hexagonal HSPs and conventional flooring plates used in buses.

➤ Loading Analysis with Non-metallic Material: An exploration into loading analyses of HSPs involved the use of non-metallic materials. This aspect broadened the scope by incorporating different material types beyond traditional metallic compositions.

➤ Variation in Core Height and Face Plate Thickness: Previous works included a comparative study involving variations in core height and face plate thickness. This approach provided insights into the influence of these structural parameters on the performance of HSPs.

RESEARCH GAPS

➤ Limited Core Materials and Combinations

➤ Absence of Environmental Impact Assessment

➤ Lack of Comparative Studies Across Different Loading Conditions

➤ Insufficient Exploration of Repair Techniques

➤ Limited Exploration of Hybrid Structures

➤ Absence of Real-world Application Studies

➤ Limited Consideration of Dynamic Characteristics

➤ Inadequate Exploration of Thermal Properties

PROBLEM STATEMENT

➤ The conventional use of plywood flooring in buses poses several challenges - Easy to mold or rot, weight concerns, Formaldehyde release and limited durability. Also, Poor resistance to sound and vibration.

➤ In light of these issues, the exploration of using alternative materials such as honeycomb panels for bus flooring becomes essential due to desirable properties.

➤ So, upon conducting a loading analysis, among HSPs of different core geometries and material combination ,the panel which can offer maximum resistance will be the appropriate choice for bus flooring.

OBJECTIVES

This research aims to compare the performance of honeycomb structure panels with different cell shapes and materials for bus flooring. The specific objectives include:

➢ Analyzing the mechanical properties of honeycomb panels with various cell shapes.

➢ Investigating the influence of different materials on the structural behavior of honeycomb panels.

➢ Optimizing the combination of cell shapes and materials for enhanced bus flooring performance.

PROCESS FLOW CHART
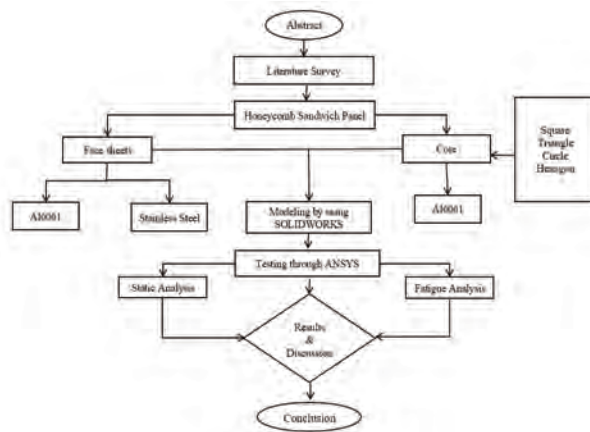
DESIGN OF HSP

Material selection

The utilization of stainless steel has witnessed a notable upswing across various components in the field of transportation over an extended period. While Al6061 remains the predominant material for bus flooring, the global acceptance of stainless steel in public transport systems is undeniable. The selection of Al6061 and stainless steel is driven by their combined advantages, including enhanced corrosion resistance and a consequential reduction in overall weight, attributed to the lower density of aluminum. This weight reduction translates into significant fuel savings, contributing to improved fuel economy in the realm of transportation.

Moreover, the adoption of stainless steel brings additional benefits, such as outstanding toughness, thereby bolstering the safety features of bus structures.

This heightened toughness contributes to the overall durability and resilience of the bus body, ensuring a superior level of safety for passengers and occupants.

The strategic use of stainless steel alongside Al6061 not only addresses corrosion concerns but also leverages the advantageous properties of both materials. The combination results in a synergistic effect, offering considerable weight reduction, corrosion resistance, and enhanced safety features in public transport systems. This dual-material approach represents a conscientious effort to optimize the performance and longevity of transport components while aligning with global trends in transportation material preferences.

DIMENSIONS OF HSP

In the initial phase of analysis, the design process involves the creation of two distinct sets of Honeycomb Sandwich Panels (HSPs). Set-1 is crafted using Al6061 for both the face plates and the core material. Correspondingly, Set-2 is formulated using Stainless Steel 316L for the face plates and Al6061 for the core material. Within each set, four HSPs are meticulously constructed, each characterized by a diverse core geometry – Circle, Triangle, Square, and Hexagonal. This results in a total of eight uniquely configured HSPs.

The dimensional parameters required for the fabrication of these HSPs are derived from tabulated data sheets obtained from "HONYLITE PRIVATE LIMITED," located in Greater Noida, Uttar Pradesh. These data sheets serve as the foundational reference for calculating the specific dimensions of the HSPs. The meticulous consideration of these dimensional details ensures precision and accuracy in the construction process.

By importing and relying on the tabulated data sheets, the design team ensures a standardized and industry-proven approach to dimensioning the HSPs. This method not only facilitates consistency in the manufacturing process but also aligns the design with established standards provided by a reputable source. The incorporation of these detailed dimensions is paramount for the subsequent stages of analysis, ensuring that the HSPs are constructed with precision and adherence to specified parameters

Table 1: Al 6061 - Al 6061 Combination

Honeycomb Core type		Al Ø9.0 - 54kg/m³ - 3003				
Total thickness (mm)		10	12	15	20	25
Skin thickness (mm)	Top	1.0	1.0	1.0	1.0	1.0
	Bottom	1.0	1.0	1.0	1.0	1.0
Core thickness (mm)		8	10	13	18	23
Weight kg/m²		6.7	6.8	6.9	7.2	7.5

Table-2: Stainless Steel - Al 6061 Combination

Honeycomb Core type		Al Ø 9.0 - 54kg/m³ - 3003				
Total thickness (mm)		10	12	15	20	25
Skin thickness (mm)	Top	0.8	0.8	0.8	0.8	0.8
	Bottom	0.8	0.8	0.8	0.8	0.8
Core thickness (mm)		8.4	10.4	13.4	18.4	23.4
Weight kg/m²		14.2	14.3	14.5	14.7	15.0

Building upon the information derived from the aforementioned tables, a standardized approach is adopted for dimensional calculations, taking the Circular cell as the reference with a diameter of 9mm and a total core height of 10mm. These values serve as the baseline for establishing comparable dimensions for the remaining cell shapes.

The cross-sectional area of the Circular cell becomes the pivotal parameter for these calculations. By equating this cross-sectional area to the relevant formulae for the other cell shapes, the corresponding side lengths for each shape can be determined. This systematic methodology ensures a consistent and cohesive approach to dimensional calculations, allowing for a standardized comparison across diverse cell geometries.

This approach not only streamlines the dimensional calculations for efficiency but also maintains a rigorous adherence to the principles of equivalence and comparability. By basing the calculations on a well-defined standard, the resulting dimensions for each cell shape can be accurately determined, contributing to the overall precision and reliability of the subsequent stages of analysis for the Honeycomb Sandwich Panels (HSPs).

Total thickness of Honeycomb sandwich panels = 10mm

Core height of Honeycomb sandwich panels

➢ For Al6061 face plates = 8mm

➢ For Stainless Steel 316L face plates = 8.4mm

In both the Sets Al6061 material is used for core part.

Face plate Thickness of Honeycomb sandwich panels (Top &bottom)

➢ For Al6061 face plates = 1mm

➢ For Stainless Steel 316L face plates = 0.8mm

Wall thickness of Honey comb core = 0.5mm

Cell size of Honeycomb sandwich panels

➢ Circular cell= 9mm diameter;

➢ Area = 63.617 sq. mm

➢ Volume = 508.98 cubic mm

➢ Square cell= 7.976mm
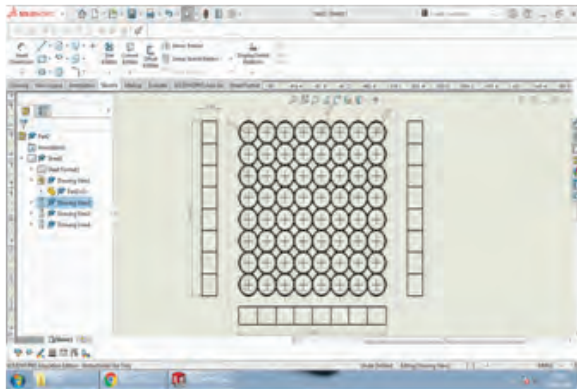
➢ Triangular cell= 12.121mm

➢ Hexagonal cell= 4.948mm

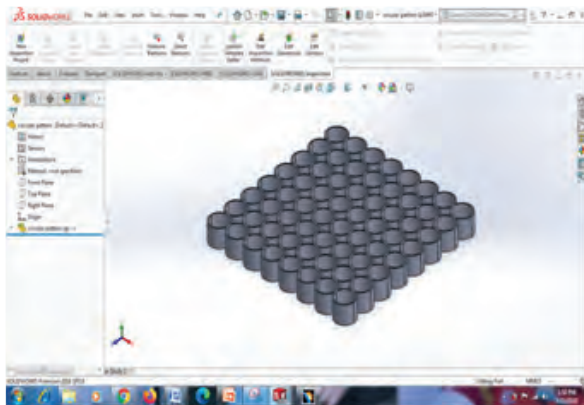**Fig 3: Circular cell HSP core 2D view**

Fig-4: Circular cell HSP core 3D view

As shown above, in the similar way Square, Triangular, Hexagonal shaped core parts will be prepared. The provided table outlines the mechanical properties utilized in the subsequent analysis phase. Subsequent pages showcase informative images derived from the Static and Fatigue Analysis conducted through the utilization of ANSYS.

Table-3: Input values of materials for ANSYS

Material	Young's Modulus	Poisson's ratio
Aluminium6061	68.9 Gpa	0.33
Stainless steel 316L	193 Gpa	0.25

METHODOLOGY

Following the completion of the modeling process for the eight Honeycomb Sandwich Panels (HSPs), comprehensive testing is undertaken to assess their performance under two distinct loading conditions

Static and Fatigue. The primary objective of the Static analysis is to ascertain critical parameters such as deformation, strain, and stress values. This examination provides crucial insights into how the HSPs respond to sustained loading scenarios, allowing for a thorough understanding of their structural behavior.

Concurrently, the Fatigue analysis is conducted to evaluate the endurance and longevity of the specimens. In this phase, loads are repetitively applied over a specified number of cycles. The Fatigue analysis specifically aims to determine the life expectancy of the HSPs, quantify potential damage accumulation, and establish a safety factor. By subjecting the panels to cyclic loading, the Fatigue analysis provides valuable information on the robustness and durability of the HSPs under real-world conditions.

These dual analyses serve as comprehensive assessments, shedding light on both the static and dynamic aspects of the HSPs' structural performance. The Static analysis unveils the panels' immediate response to static loading, while the Fatigue analysis extends the evaluation to predict their endurance and resilience over a prolonged operational lifespan. This meticulous approach ensures a thorough understanding of the HSPs' mechanical behavior in diverse scenarios, facilitating informed decision-making in the context of their application in transport flooring

Static Analysis

During the Static Loading phase, the Honeycomb Sandwich Panels (HSPs) undergo a standardized Three-point bending test wherein a consistent static load of 16KN is applied [4]. Throughout the loading process, meticulous observations are conducted to discern any alterations in the behavioral characteristics of the panels, particularly focusing on deformation, strain, and stress.

To ensure uniformity and comparability, the identical static load is applied to all eight HSPs. This systematic approach is employed to gain comprehensive insights into the behavioral responses of the panels and to identify the maximum values of deformation, strain, and stress under the specified load. Furthermore, the examination extends to visually identifying highly impacted zones within the panels. This visual observation is facilitated

through figures accompanying the analysis, aiding in the identification and interpretation of areas where the HSPs exhibit notable sensitivity or concentration of stress. By subjecting the HSPs to a consistent static load and closely monitoring their responses, this testing phase aims to provide crucial information about the structural integrity and performance characteristics of the panels. Such a meticulous approach ensures a detailed assessment of how the HSPs respond under applied static loads, contributing to a thorough understanding of their suitability for applications, particularly in scenarios such as bus flooring within various transportation contexts.

Fig. 6: Total Deformation
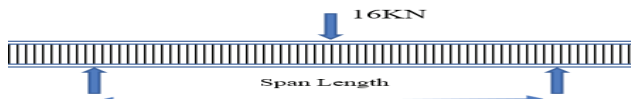
Fig. 5: Three-point Bending test

Case 1-Al 6061 and Al 6061

➢ Face plate material- Al 6061

➢ Core material- Al6061

To commence the analysis, a Honeycomb Sandwich Panel constructed from an Al6061-Al6061 material combination, featuring a circular core pattern, is exposed to a load of 16KN using the Three-point bending method. Throughout the loading procedure, meticulous records are maintained, documenting the extent of deformation, the occurrence of strain, and the induction of stress within the Honeycomb Sandwich Panel (HSP).

Detailed observations pertaining to the deformation, strain, and stress experienced by the HSP are visually depicted in the accompanying figures. These figures serve as illustrative aids, offering a comprehensive representation of the behavioral responses exhibited by the panel under the applied load. This systematic approach ensures a thorough understanding of how the Honeycomb Sandwich Panel, crafted from the specified material combination and core pattern, reacts to the Three-point bending method with a 16KN load. By documenting the deformation, strain, and stress parameters, the analysis aims to provide valuable insights into the structural performance and integrity of the HSP under these specific loading conditions.
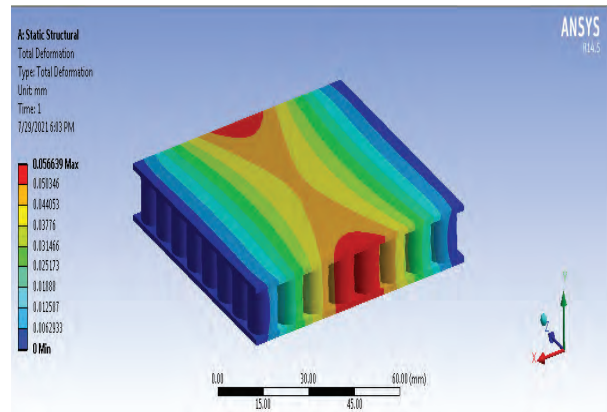

Fig. 7: Stress

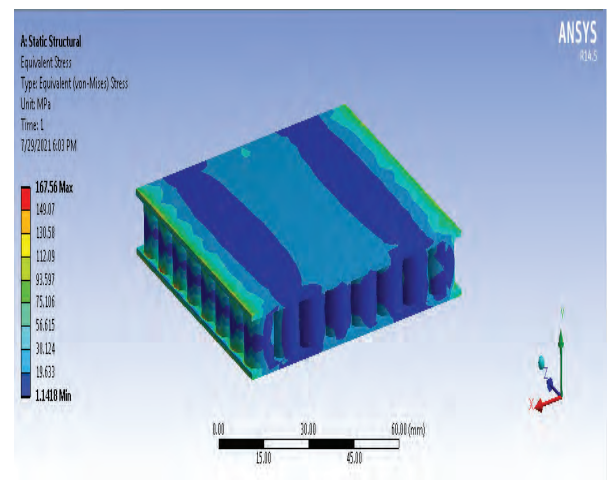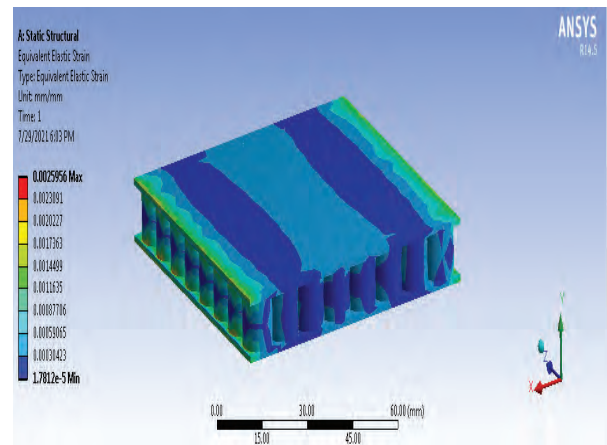**Fig. 8: Strain**

Case 2 –stainless steel316l and al6061

➢ Face plate material- Stainless Steel 316L
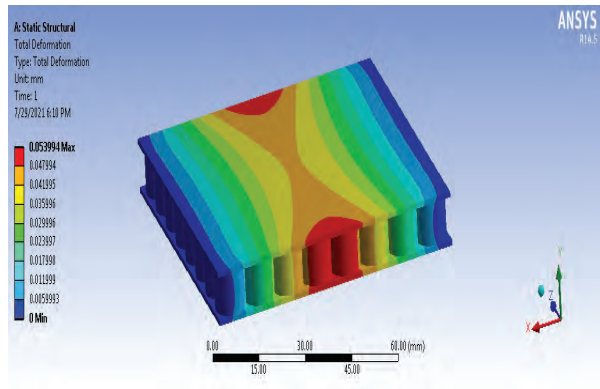
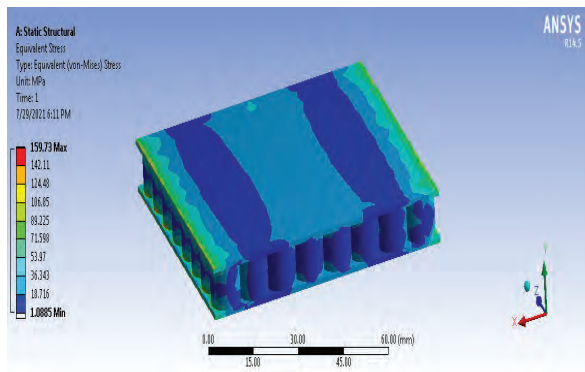➢ Core material- Al6061

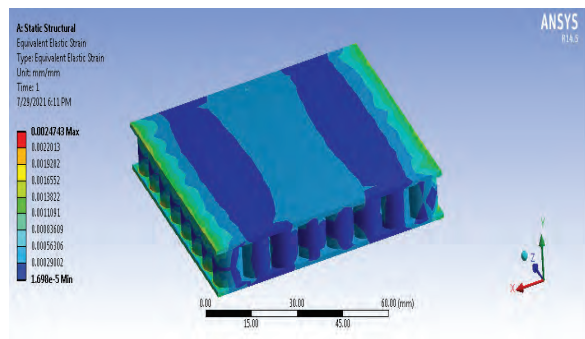**Fig. 9: Total Deformation**

Fig. 10: Stress

Fig. 11: Strain

Fatigue analysis

Within the realm of Fatigue analysis, objects undergo repetitive loading to ascertain the total number of load cycles leading to failure. This methodology is instrumental in understanding the behavior of materials, encompassing aspects such as Life, Damage, and Safety factor, particularly when subjected to fluctuating loads. The subsequent information provides insights into the response of the Honeycomb Sandwich Panels (HSPs) under Fatigue loading conditions.

Case 1-Al6061 and Al 6061

➢ Face plate material- Al6061

➢ Core material- Al6061

A Honeycomb Sandwich Panel, fabricated from an Al6061-Al6061 material combination and featuring a circular core pattern, undergoes repetitive loading of 16KN for 10,000 cycles. This cyclic loading is employed to assess and understand the responses of the Honeycomb Sandwich Panels (HSPs) in terms of Life, Damage, and Safety factor. The ensuing figures provide a visual representation of the observations made during this extended cyclic loading process.
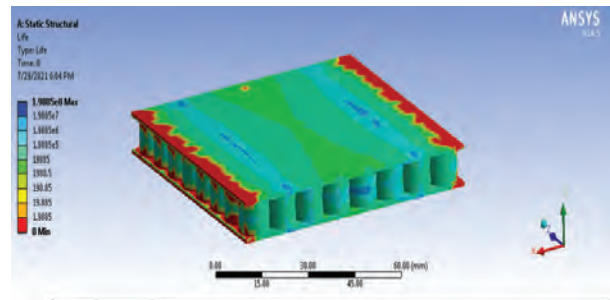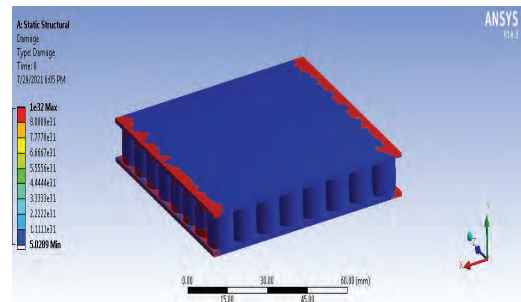

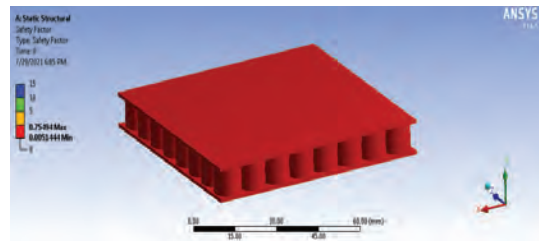
Fig. 12: Life

Fig. 13: Damage

Fig. 14: Safety Factor

Case 2 –stainless steel 316land Al 6061:

➢ Face plate material- Stainless Steel 316L
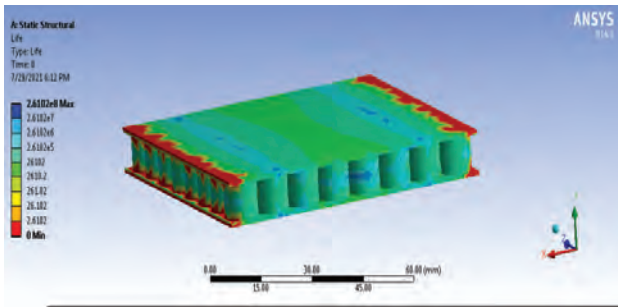
➢ Core material- Al6061
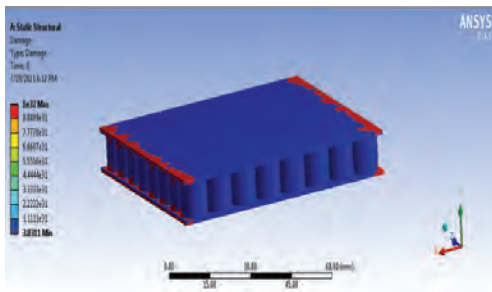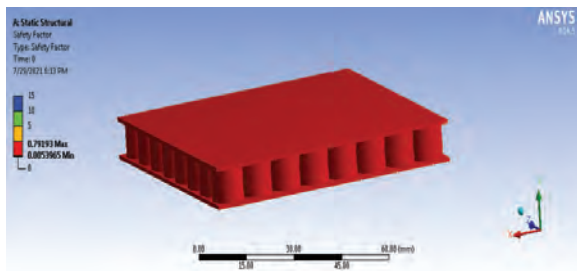
Fig. 15: Life

Fig. 16: Damage

Fig. 17: Safety Factor

In similar way, other HSPs made of Square, Triangleand Hexagonalcore patterns are tested for Static and Fatigue analyses in the same way for the two material combinations namely, Al6061-Al6061 and Stainless Steel 316L-Al6061.

RESULTS AND DISCUSSION

The design and comparative static and fatigue analyses encompass two sets of Honeycomb Sandwich Panels: one with an Al6061-Al6061 combination and the other with a Stainless Steel 316L-Al6061 combination. Both sets feature Square, Triangle, Circle, and Hexagon cell shapes. The objective is to discern the superior choice for bus flooring applications. Throughout testing, values for Deformation, Strain, Stress, and Safety factor are meticulously recorded and tabulated, as illustrated below.

Table 4: Static Analysis Results

Material	HSP core shape	Deformation (mm)	Stress N/mm²	Strain (mm/mm)
Al 6061-Al 6061	Circular	0.05669	167.56	0.0025956
	Triangle	0.05735	211.5	0.001244
	Hexagonal	0.040625	226.79	0.001235
	Square	0.016503	145.56	0.00079872
Stainless Steel 316L-Al6061	Circular	0.053944	159.73	0.0024743
	Triangle	0.054676	201.62	0.0011859
	Hexagonal	0.038727	216.2	0.0011773
	Square	0.015732	138.76	0.00076141

Table 5: Fatigue Analysis Results

Material	HSP core shape	Safety factor
Al 6061-Al 6061	Circular	0.75494
	Triangle	0.0040256
	Hexagonal	0.0038008
	Square	1.25
Stainless Steel 316L-Al6061	Circular	0.79193
	Triangle	0.00427553
	Hexagonal	0.0039871
	Square	1.6084

CONCLUSION

The design and comparative static and fatigue analyses were conducted on two sets of Honeycomb Structure Panels, employing Al6061-Al6061 and Stainless Steel 316L-Al6061 combinations, with Square, Triangle, Circle, and Hexagon cell geometries. The primary objective was to determine the optimal Honeycomb Structure Panel (HSP) for bus flooring applications.

The Three-point Bending test, executed on the Honeycomb Structure Panels under a 16kN load, facilitated the observation of deformations, strains, and stresses during Static Analysis. Simultaneously, the Life, Damage, and Safety factors of HSPs were assessed through Fatigue Analysis. The comparative analysis of results led to the following conclusions.

Minimal Deviation: Results indicated a negligible deviation between the two material combinations for all core geometries.

Superiority of Square Cell Type: In both material combinations, the Square cell type of HSPs consistently outperformed other cell shapes.

Optimal Resistance: Among all eight panels, it was observed that the Stainless Steel 316L-Al6061 material combination, featuring a Square cell geometry, demonstrated the highest resistance against loading in both Static and Fatigue analyses.

Conclusive Metrics for Square Cell Geometry with Stainless Steel 316L-Al6061:

Deformation: 0.015732mm

Strain: 0.00076141

Stress: 138.76N/mm2

Safety Factor: 1.6084

In light of these conclusions, it is evident that the Square cell geometry of HSP with a Stainless Steel 316L-Al6061 material combination is exceptionally well-suited for bus flooring applications. This configuration exhibited maximum resistance and optimal performance in both Static and Fatigue analyses. Additionally, the Al6061-Al6061 combination with the same Square cell geometry emerged as a commendable choice among the other tested panels.

FUTURE SCOPE

In the present study, Honeycomb Sandwich Panels (HSPs) were systematically compared across four distinct core geometries and two material combinations, maintaining a consistent total thickness. While this research provides valuable insights, there exist several avenues for future exploration in the domain of Honeycomb Structures. The following areas offer potential directions for further investigation and applications:

1. Exploring Improved Materials: Investigate novel materials such as high-strength composites or nanomaterials to create bus floors that are not only lighter but also stronger.

2. Intelligent Design Strategies: Collaborate with experts in materials, engineering, and design to identify the optimal combination of cell shapes and materials for bus flooring, ensuring strength, cost-effectiveness, and environmental friendliness.

3. Practical Safety Testing: Conduct real-world tests on honeycomb panels under various conditions, including heavy loads and sudden impacts, to ensure their effectiveness in keeping bus passengers safe.

4. Environmental Considerations: Evaluate the environmental impact of different panel designs throughout their lifecycle, considering material sourcing, manufacturing processes, and end-of-life disposal.

5. Incorporating Smart Features: Investigate the integration of panels with sensing capabilities or self-repair mechanisms to enhance adaptability and durability in bus flooring.

6. Real-world Validation: Take promising designs out of the laboratory and subject them to extensive testing in actual bus environments, ensuring their practical functionality and adherence to expectations.

REFERENCES

1. A. Gopichand, R. Mohan Rao, N.V. S Sankar, G. Rama Balaji, P. Sandeep Kumar; Design and Analysis of Copper Honeycomb Sandwich Structure, (IJEAT) ISSN: 2249 – 8958, Volume-2, Issue-4, April 2013.

2. Amy F. Domae, Cell Shape in a Honeycomb Structure vs. Structure Strength, CALIFORNIA STATE SCIENCE FAIR, J0311.

3 Ch. Naresh, A. Gopi Chand, K. Sunil Ratna Kumar, P.S.B.Chowdary, Numerical Investigation into Effect of Cell Shape on the Behavior of Honeycomb Sandwich Panel. Vol. 2, Issue 12, IJIRSET-2013.

4. A. Bonannoa, V. Crupib, G. Epastob, E. Guglielminob, G. Palombab, Aluminium honeycomb sandwich for protective structures of earth moving machines, AIAS 2017 International Conference on Stress Analysis, AIAS 2017, 6-9 September 2017, Pisa, Italy.

5. Sathish Kumar.P, Neethimanickam. I, R. Robinston Jeyasingh Swikker, Maheswari. K. S, Strength And Behavior Analysis Of Honey Comb Sandwich Composite Structure, International Journal Of Scientific & Technology Research Volume 9, Issue 01, January 2020.

6. Rohit Domb, Sushil Jadhav, Suraj Gajare, Nilesh Kadam, Prof. A.B.Yadav, Design of Honeycomb Sandwich Panel and Its Validation with Flooring Plate of Bus, (IRJET) Volume: 05 Issue: 07 | July 2018.

7.   Hee-Young Ko, Kwang-Bok Shin, Kwang-Woo Jeon and Seo-Hyun Cho A study on the crashworthiness and rollover characteristics of low-floor bus made of sandwich composites

8.   Shubham V. Rupani, Shivang S. Jani, G.D.Acharya, Design, Modelling and Manufacturing aspects of Honeycomb Sandwich Structures: A Review, April 2017 IJSDR | Volume 2, Issue 4.

9.   Martec Limited Prevost Car, Intercity Bus Weight Reduction Profram Phase, (2000).

10. C. C. Foo, G. B. Chai and L. K. Seah, A Model to Predict Low-Velocity Impact Response and Damage in Sandwich Composite, Composites Science and Technology, Vol. 68 (2008), 1348-1356.

11. J. S. Kim, S. J. Lee and K. B. Shin, Manufacturing and Structural Safety Evaluation of a Composite Train Carbody, Composite Structures, Vol. 20, No. 9 (2007), 465-476.

12. J. Y. Lee, K. B. Shin and S. J. Lee, A Study on Failure Evaluation if Korean Floor Bus Structure made of Hybrid Sandwich Composite, Korean Society of Automotive Engineers, Vol. 15, No. 6 (2007), 50-61.

Finite Element Simulation of Ballistic Impact on Combat Helmet

Deepak Verma
Research Scholar
Mechanical Engineering Department
IPS College of Technology and Management
Gwalior, Madhya Pradesh

Shatrughan Mishra
Associate Professor
Mechanical Engineering Department
IPS College of Technology and Management
Gwalior, Madhya Pradesh

Manoj Narwariya
Professor
Mechanical Engineering Department
IPS College of Technology and Management
Gwalior, Madhya Pradesh
✉ drmanoj.academic@gmail.com

Anurag Garg
Professor
Electronics and Communication Engineering Dept.
IPS College of Technology and Management
Gwalior, Madhya Pradesh

ABSTRACT

The use of combat helmets has greatly reduced penetrating injuries and saved lives of many soldiers. However, behind helmet blunt trauma (BHBT) has emerged as a serious injury type experienced by soldiers in battlefields. BHBT results from non-penetrating ballistic impacts and is often associated with helmet back face deformation (BFD). In this study the helmet and other components required for simulation is designed by solid works and the simulations of modern combat helmet on striking with 9 mm bullet is performed on commercial package ANSYS. The study cover the stress and maximum deformation of helmet due to impact of bullet at 610 m/s in different directions and at different angles. The same procedure is repeated to study the impact of bullet over all sides of helmet. We did the designing of all the components of helmet and bullet using SOLIDWORKS and all these simulations are done using finite element method in explicit dynamic analysis with the setting of AUTODYN in ANSYS.

KEYWORDS : *Stress, Deformation, AUTODYN, FEM, Solidworks, Dynamic analysis.*

INTRODUCTION

High energy wave produce due to impact of high speed billet causes not only damage/deformation of helmet but also causes serious brain injury normally termed as Behind Helmet Blunt Trauma (BHBT) [1-7]. This high energy wave can even result in traumatic cell death [2, 7]. Generally 50% of the total bullet impact injured persons will suffer with moderate to high brain injury [3-4]. Main mechanisms responsible for such brain trauma injury are not much clear till date [7]. Combat helmet of armor fiber reinforced composite are now a days more popular. The main merits of them are light weight, high strength to weight ratio, long life and comfort [7]. Physical validation through experimentation is the best method for verification of the durability of the helmet. It also justifies the quality and safety of the helmet and the bearer of it [8-12].

Beside other methods, human head surrogates is the best method of performing the real time test and evaluate the level of injury caused by the 9 mm pistol full metal body bullet [13-14]. FEM provide a comparative easy tool among other numerical analysis tool available, to evaluate and predict the injury and damage caused by the impact of bullet on the helmet and head of the bearer [15-16].

In this present work the impact of 9 mm bullet on helmet supported on human head surrogates filled with gelatin is simulated on commercial package Ansys. Simulation is validated with past literature present in open domain.

The bullet is assumed to hit the target with a muzzle velocity of 400 m/s. As bullet can strike the bearer at any place thus different position of striking the bullet is taken into consideration in the study.

MATERIALS AND METHODS

3D Model of the Helmet

In this work, student version of commercial package SOLIDWORKS is utilized to prepare the 3D model human head, 9 mm bullet and helmet and its components to perform the impact simulation. The helmet have two parts in it one is the outer part made of Kevlar fiber composite and the other in the inner padding layer. As already discussed the main aim of outer Kevlar composite layer is to decrease the velocity of impacting bullet by absorbing maximum energy. The padding layer is used in this study to decrease the effect of protrusion trauma caused due to deformation of outer layer and reduce the effect of head injury to solders. These both layers are prepared separately in SOLIDWORKS and for analysis they are assembled to get the final ACH helmet. Table 1 shows the thickness of the both layers used in the study for fabrication of helmet. Fig. 1 shows the complete assembly of complete helmet. From the Fig 3.1, we can see that the helmet is now comes in one solid shape with no loose parts i.e. all parts are intact in the helmet. Teharia et al. [12] show the properties of PLA as given in Table 1.

**Table 1. Thickness of different layers present in ACH.**

| Layers of ACH	Thickness
Kevlar layer	4mm
Padding layer	25mm

Fig. 1. Full assembly model of ACH prepared on Solidworks

3D Model of 9mm bullet

The 2D model along with the dimension and 3D model prepared with a similar dimension of 9 mm brass bullet is shown in Fig. 2(a and b) respectively. This bullet model is used by Tham et al (2008) and is taken similarly in the present case also [9].
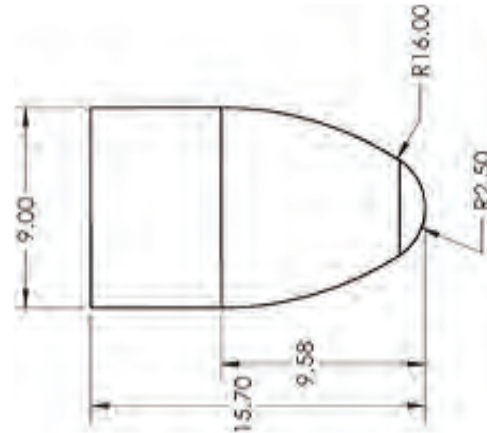
(a)
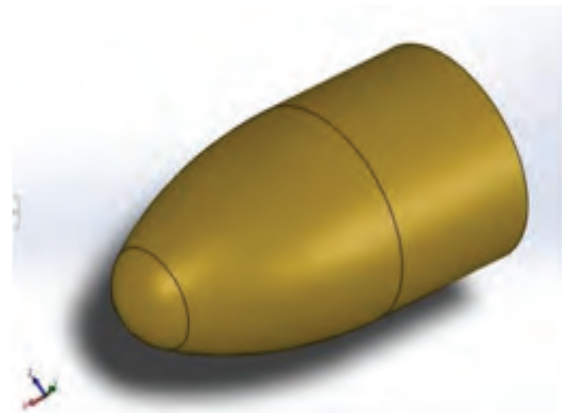
(b)

Fig. 2. (a) 2D geometry of 9 mm brass bullet (b) 3D model of 9 mm bullet

Final Assembly

Final Assembly of the dummy soldier head and the complete helmet for impact analysis is glued together about the central axis with no relative motion between the head and the helmet. The 9 mm bullet for striking the helmet is placed about 100 mm apart from the helmet in all cases of impact and a velocity of 610 m/sec is given to the bullet for impact on the helmet.
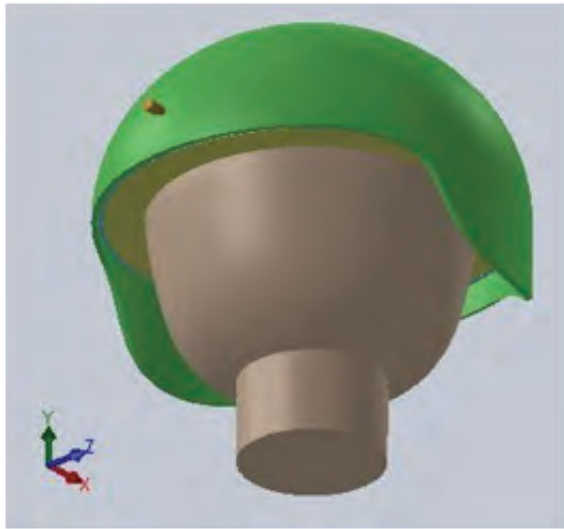
respectively. Table 3 shows the number of nodes in respective layers and components considered in the study.

(a)

(b)

Fig. 4. (a) Meshing of full assembly (b) Meshing of bullet

Fig. 3. 3D model of full assembly of ACH and bullet

Material properties

Material properties of Polyurethane foam and brass are available in the engineering data library of ANSYS. Material properties of Kevlar and skull are taken from Elsenburg et al (1996) [7] and Zhaoxia Li et al. (2010) [8] respectively. The detailed material properties of all the components are shown in Table 2.
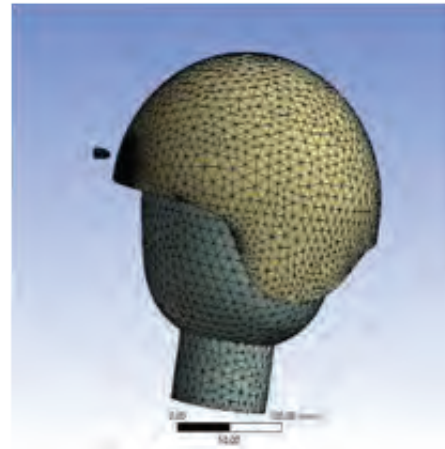
Table 2. Mechanical properties of all components

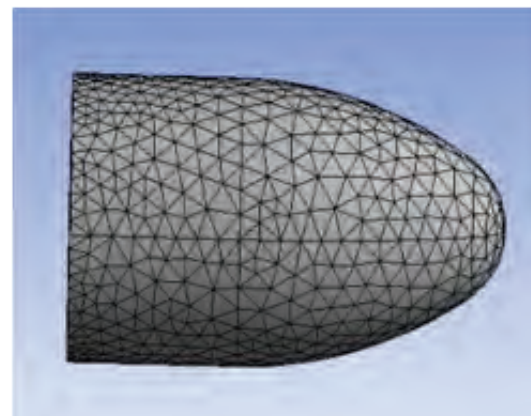| Assignment	Kevlar	Polyurethane foam, flexible	Brass	Skull
Density kg/ mm3	1.38e-006	3.19e-008	8.52e-006	2.08e-006
Young's Modulus MPa	76000	4.9e-002	115	6650
Poisson's Ratio	0.23	0.279	0.31	0.22
Bulk Modulus MPa	46914	3.6953e-002	100.88	3958.3
Shear Modulus MPa	30894	1.9156e-002	43.893	2725.4

Meshing

Fine meshing is generated at the area of impact with the help of the sphere of influence in the ANSYS module whereas the part far beyond the impact region has comparatively coarse mesh. Figs. 4(a and b) show the mesh generated on the helmet with bearer and bullet

Table 3. Number of nodes and elements present in all

Assignment	9 mm bullet	Kevlar layer	Head	Padding
Nodes	196	5441	1225	759
Elements	756	20832	5388	970

RESULTS AND DISCUSSION

The location of impact is so varied to visualize the overall effect of striking the bullet on the helmet and to study the injury effect onthe head of the soldier. The

analysis has been done to show the impact of bullets on helmets on the following locations.

• Impact of a bullet on the front of the helmet.

• Impact of a bullet on the rear of the helmet

• Impact of a bullet on the top of the helmet.
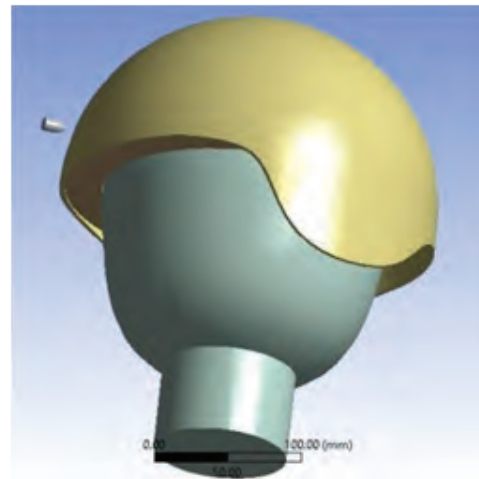
• Impact of a bullet on one side over the ear

Table 4 shows the summarized values of the maximum stress and deformation in the helmet during the analysis. From the table, it can observed that the average stress and deformation are very low and the person wearing the helmet will not feel very erratic during the impact and it will be very safe for the user and the chances of trauma is reduced.

Table 4. Result of Maximum deformation and equivalent stress for various impacts

Assignment	Helmet with Padding		Penetration
	Max Deformation (mm)	Equivalent Stress (M Pa)	
Front	23.370	2294.20	No
Rear	22.338	1977.70	No
Top	14.837	4484.30	No
One Side over the ear	23.812	2519.20	No

Figs. 5(a) to 5(d) show the boundary condition of the helmet and the bullet used in the study. From the Figures, it is clear that before the impact there was no sign of any stress or deformation. The skull is an intact clue with the helmet and there is no sign of delamination of its layer.

Fig. 6 to fig. 9 show the deformation pattern of the helmet when the bullet strikes on various locations of the helmet. From the figures, it can clearly be observed that the deformation in most of the parts is very low and the helmet material is capable of absorbing the impact of the bullet without bulging. Even the localized deformation is also very less and the padding is sufficient to cover the ill effect produced by the impact of the bullet. Thus we can say that the impact energy will be absorbed by the helmet layer and intermediate padding layer.

(a) Front side
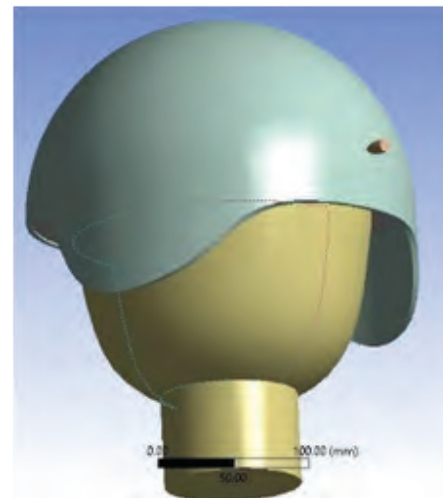
(b) Rear Side
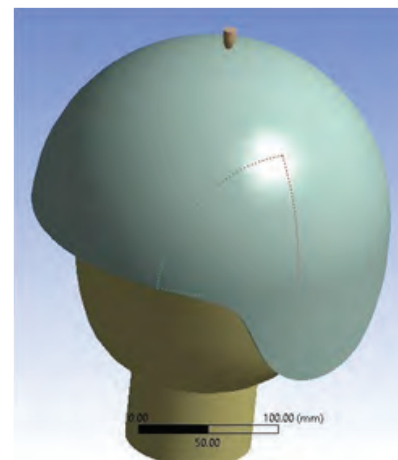
(c) Top side
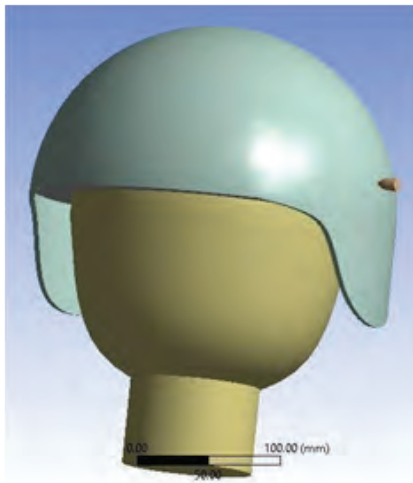
(d) one side over the ear

Fig. 5. Presents the visual of the impact of a bullet from various locations of the helmet

(a)

(b)

Fig. 6 (a) Presents the deformation pattern and (b) stress developed on the helmet when the bullet strikes from the front side of the helmet.
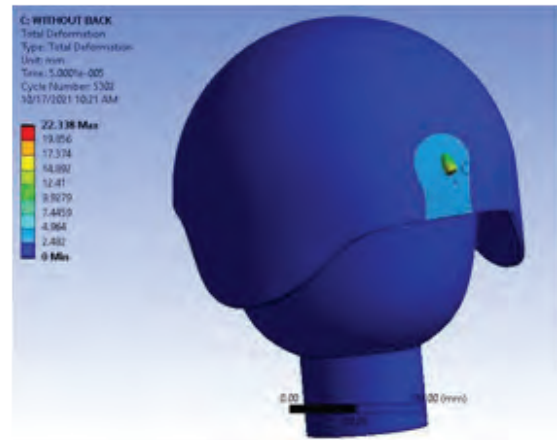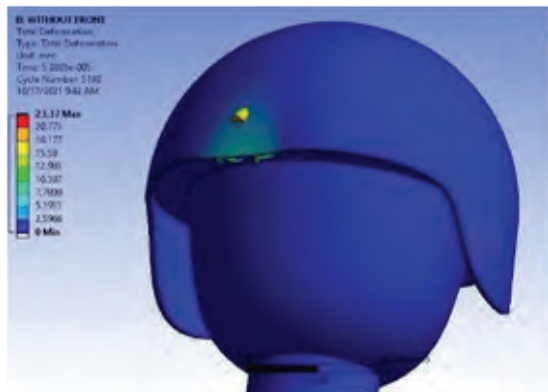
(a)

(b)

Fig. 7 (a) Presents the deformation pattern and (b) stress developed on the helmet when the bullet strikes from the rear side of the helmet

(a)

(b)

Fig. 8 (a) Presents the deformation pattern and (b) stress developed on the helmet when the bullet strikes from the top side of the helmet.

(a)

(b)

Fig. 9 (a) Presents the deformation pattern and (b) stress developed on the helmet when the bullet strikes from one side over the ear of the helmet.

CONCLUSIONS

In this present work, the impact of 9 mm bullet on helmet supported on human head surrogates filled with gelatin is simulated on commercial package ANSYS. Simulation is validated with past literature. The bullet is assumed to hit the target w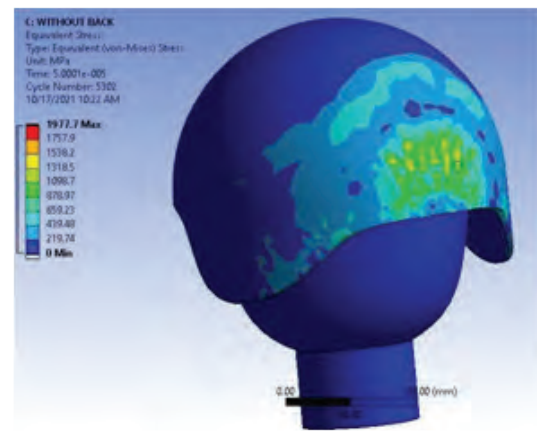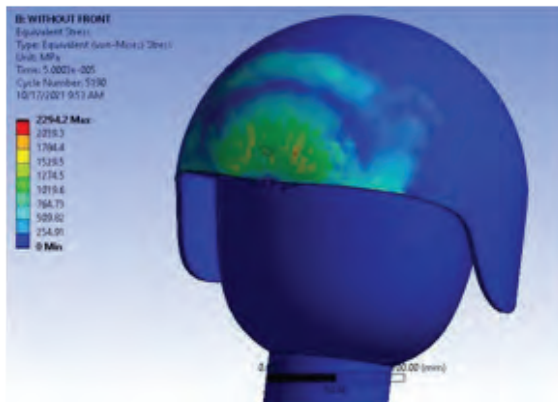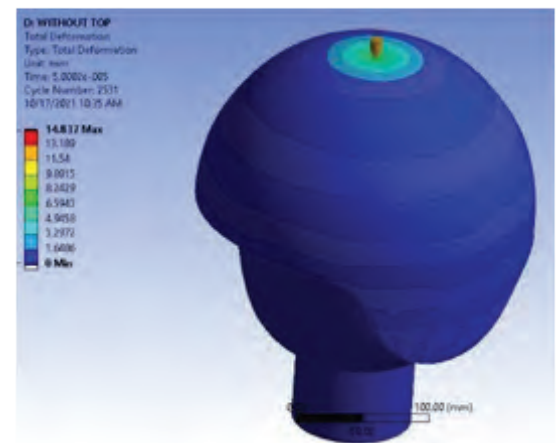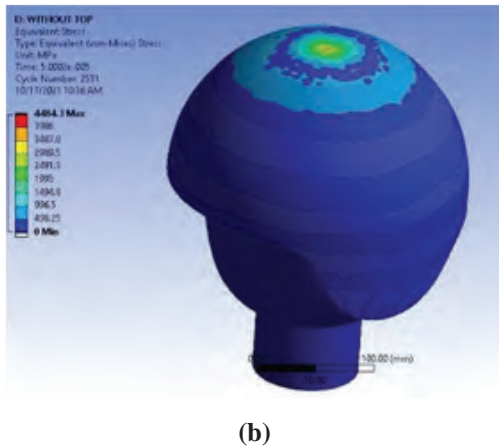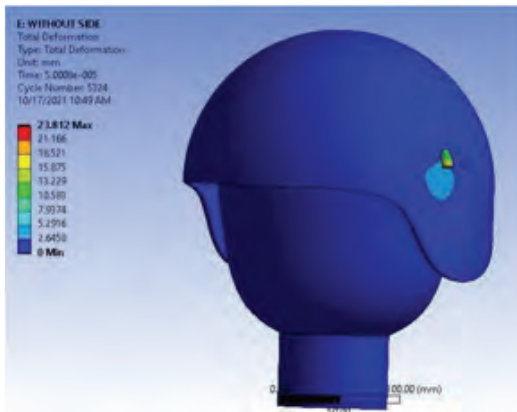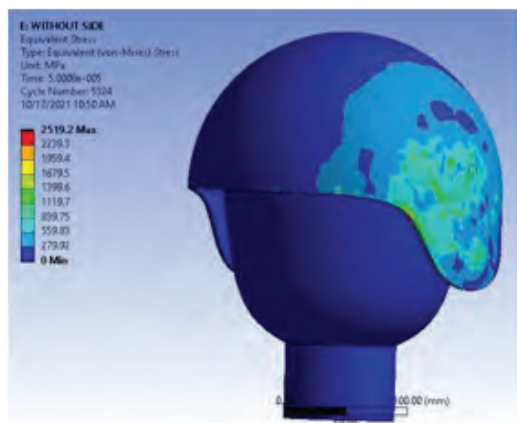ith a muzzle velocity of 400 m/s. From the study it can be concluded that the Bullet does not penetrate the kevlar layer, whereas the deformation in the helmet is measurable. The deformation of the helmet is reduced significantly without increasing the weight by using padding after the kevlar layer. Deformation of the helmet is maximum when a bullet strikes at side of the helmet, the value of deformation is 23.812 mm. The minimum deformation is 14.837 mm when the bullet strikes from the top of the head. Maximum stress is recorded as 4484.30 MPa in case of impact from the top center of the head, and minimum to the value of stress induced is 1977.70 MPa when the bullet strikes from the rear. Thus on the basis on the FEA analysis the helmet with padding is safe to be used against the 9 mm bullet.

REFERENCES

1. L. Cannon, "Behind armour blunt trauma-an emerging problem," Journal of the Royal Army Medical Corps, vol. 147, no. 1, pp. 87–96, 2001.

2. Kong LZ, Zhang RL, Hu SH, Lai JB. Military traumatic brain injury: a challenge straddling neurology and psychiatry. Mil Med Res 2022;9:2. https://doi.org/10.1186/s40779-021-00363-y.

3. Hemphill MA, Dauth S, Yu CJ, Dabiri BE, Parker KK. Traumatic brain injury and the neuronal microenvironment: A potential role for neuropathological mechanotransduction. Neuron 2015;85:1177–92. https://doi.org/10.1016/j. neuron.2015.02.041.

4. Traumatic Brain Injury Center of Excellence. 2022. DOD TBI Worldwide Numbers. Health.mil.DoD numbers for traumatic brain injury: worldwide totals 2000-2021 Q4, as of. February 11, 2022. https://health.mil/Military-Health-Topics/Centers-   of-Excellence/ Traumatic-Brain-Injury-Center-of-Excellence/DOD-TBI-Worldwide- Numbers (accessed July 13, 2022).

5. C. J. Freitas, J. T. Mathis, N. Scott, R. P. Bigger, and J. Mackiewicz, "Dynamic response due to behind helmet blunt trauma measured with a human head surrogate," International Journal of Medical Sciences, vol. 11, no. 5, pp. 409–425, 2014.

6. K. A. Rafaels, H. C. Cutcliffe, R. S. Salzar et al., "Injuries of the head from backface deformation of ballistic protective helmets under ballistic impact," Journal of Forensic Sciences, vol. 60, no. 1, pp. 219–225, 2015.

7. Li Y, Fan H, Gao XL. Ballistic helmets: recent advances in materials, protection mechanisms, performance, and head injury mitigation. Compos Part B Eng 2022; 238:109890. https://doi.org/10.1016/j.compositesb.2022.109890.

8. Rodríguez-Mill´an M, Ito T, Loya JA, Olmedo A, Migu´elez MH. Development of numerical model for ballistic resistance evaluation of combat helmet and experimental validation. Mater Des 2016;110:391–403. https://doi.org/10.1016/j. matdes.2016.08.015.

9. Rubio I, Rodríguez-mill´an M, Marco M, Olmedo A, Loya JA. Ballistic performance of aramid composite combat helmet for protection against small projectiles. Compos Struct 2019;226:111153. https://doi.org/10.1016/j. compstruct.2019.111153.

10. Tham CY, Tan VBC, Lee HP. Ballistic impact of a KEVLAR® helmet: experiment and simulations. Int J Impact Eng 2008;35:304–18. https://doi.org/10.1016/j. ijimpeng.2007.03.008.

11. Nguyen LH, Ryan S, Cimpoeru SJ, Mouritz AP, Oriici AC. The eficiency of ultra- high molecular weight polyethylene composite against fragment impact. ExpMech 2016;56:595–605. https://doi.org/10.1007/s11340-015-0051-z.

12. Lim JS, Kim JH. Ballistic behavior of Heracron®-based composites: effect of iber density and fabrication method. Compos Interfaces 2014;21:543–52. https://doi. org/10.1080/15685543.2014.889966.

13. Miranda-Vicario A, Bravo PM, Coghe F. Experimental study of the deformation of a ballistic helmet impacted with pistol ammunition. Compos Struct 2018;203: 233–41. https://doi.org/10.1016/j.compstruct.2018.07.012.

14. Freitas CJ, Mathis JT, Scott N, Bigger RP, MacKiewicz J. Dynamic response due to behind helmet blunt trauma measured with a human head surrogate. Int J Med Sci 2014;11:409–25. https://doi.org/10.7150/ijms.8079

15. Rodriguez-Millan M, Tan LB, Tse KM, Lee HP, Miguelez MH. Effect of full helmet systems on human head responses under blast loading. Mater Des 2017;117:58–71. https://doi.org/10.1016/j.matdes.2016.12.081

16. LUO Xiaohao , WEN Yaoke , YAN Wenmin, ZHANG Junbin4 , CAO Yanfeng, DONG Fangdong and HUANG Xueying. Protective performance of PASGT combat helmet under pistol bullet impact. J-Global. 2022; 39(7): 3629-3640.https://doi.org/10.13801/j.cnki.fhclxb.20210823.002

17. SHEN Zhouyu, WEN Yaoke, YAN Wenmin, DONG Fangdong, ZHANG Junbin and LI Ying. Behind☐ Helmet Blunt Trauma of a Pistol Bullet Striking Ballistic HelmetCovered Human Head and Neck Target. 2022; 9: 2101-2112.

Optimization of Technological Process Parameters for Wire Electric Discharge Machining on Nimonic 75 Alloy

Saidulu. G
Research Scholar
Mechanical Engineering Dept.
JNTU
Kukatpally, Hyderabad
✉ gilla.saidulu@gmail.com

P. Prasanna
Associate Professor
Mechanical Engineering Dept.
JNTU
Kukatpally, Hyderabad
✉ prajntu@jntuh.ac.in

ABSTRACT

The current experimental work primarily WEDM to machine the slots on Nimonic alloy 75. A WEDM was utilized for the experimental investigation, and the process parameters that were examined were Peak Current, Ton (on-time), Toff (off-time), and gap voltage (V). To maximize the machining properties, the Taguchi L-9 (OA) Orthogonal Array DOE were used. The primary response factors that were examined were material removal rate (MRR) and microhardness, utilizing 0.18mm and 0.25mm brass electrodes for diameter. Utilizing analysis of variance (ANOVA), the most significant parameter impacting the MRR and microhardness was determined.

KEYWORDS : *WEDM, Taguchi L-9 orthogonal array, DOE, MRR, Microhardness, ANOVA.*

INTRODUCTION

Nimonic 75 is an alloy containing approximately 20% chromium and 80% nickel. Its qualities include high tensile strength and hardness, resistance to creep and deformation under mechanical stress, and strong resistance to oxidation and corrosion. It was initially utilized for turbine blades in jet engine prototypes throughout the 1940s. These days, it is utilized in numerous applications, including heat treatment, turbine blades, aircraft, furnaces, hot-working automobiles, and more. The Nimonic alloy75 have good weldability. For fabrication, TIG, MIG, and submerged arc welding techniques can be applied. Nimonic alloy 75's drawbacks when using conventional machining include that chips weld to the cutting tool due to its low thermal diffusivity and that it becomes work-hardened during machining, resulting in burr development. An unusual machining procedure was used to get around these issues. A wire electrode can be used to cut a workpiece during the thermo-electrical machining, the procedure that is referred to as wire-cut electrical discharge machining.

Utilizing wire-cut EDM, significant performance results by changing the input parameters T on, T off, Peak current, Gap voltage, MRR, and microhardness have been measured.
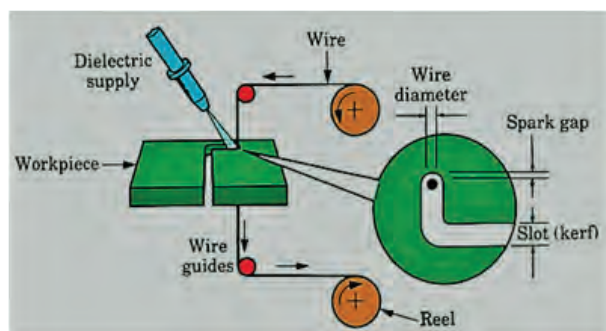

Fig. 1: Working principle of Wire cut EDM

LITERATURE REVIEW

Sabindra Kachhap et al. conducted research on the WEDM process parameters for the alloy Al 5454. Brass wire coated in zinc with a diameter of 0.25 mm was used in the machining process. Input parameters including pulse on time (Ton), current, power, wire feed

rate, wire tension, and flushing pressure are considered in order to enhance MRR and surface roughness. The study used the Taguchi L-16 OA design to maximize MRR and surface roughness. The key parameters were identified using the ANOVA approach. At a wire feed rate of 165 mm/min, wire tension of 15 N, power of 25 W, peak current of 15 A, pulse on time of 32 μs, and flush pressure of 7 bar, these are the ideal process results. MRR is primarily influenced by two factors: timing pulse and current. Surface roughness depends significantly on the current [1].

Pudi Charan et al. used the Inconel 800 super alloy to conduct wire-cut EDM research. Surface roughness and MRR are the main process outcomes. Current, wire feed rate, wire tension, Ton, and Toff are the selected input variables. The Taguchi L-27 design was utilized in the trial design in order to maximize both MRR and surface roughness. The experimental analysis indicates that wire feed and pulse off have a bigger effect on the process's outcomes [2].

The effects of wire EDM process variables on titanium alloy Grade 5-Ti-6Al-4V were investigated by Dheeraj Mathew Paulson et al. The pulse-on time, pulse-off duration, and peak current (A) are the input variables. The Taguchi L-18 OA design of the trials was utilized to optimize MRR and surface roughness. The ANOVA showed that peak current and SR had the greatest influence on MRR, with Toff and peak current also having an effect [3].

Rao Muralidhara et al. used WEDM machining to work on high-carbon steels. The selection of parameters included pulse time and pulse current. The procedure results included microhardness and the recast layer's thickness. Based on the experimental findings, it was discovered that the recast layer's thickness ranges from 16 to 25 μm. Surface roughness ranges from 2.4 to 4.2 μm, and both surface roughness and recast layer thickness increased with current [4].

Ti6Al4V was studied for wire EDM process parameters by K. Hareesh et al. To examine the surface finish, feed rate, wire speed, and voltage are taken into account as input factors. Higher feed rates and slower wire speeds result in a rise in the surface roughness value; higher voltages produce better surface finishes [5].

The impact of WEDM parameters on Inconel 718 was examined by Thejasree et al. T on, T off, and peak current are the metrics for analyzing the SR and MRR. The machining parameters that had the biggest impact were found using the ANOVA approach [6].

EXPERIMENTAL METHODS

The workpiece size of length 100 mm x width 200 mm x thick 2 mm was taken into consideration throughout the experiments, which were carried out on the wire-cut EDM model EZEECUT NXG. The suggested experimental setup is displayed below.
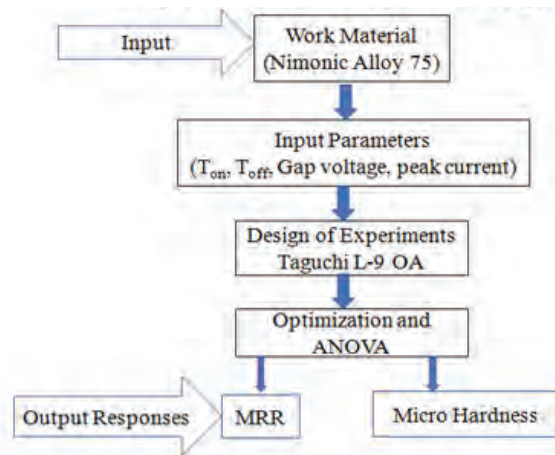
Fig. 2: Flow chart of experimental methodology

Table 1: Details of the wire-cut EDM

Details	In numbers
X, Y axis travel in numbers	320 X 400mm
Workpiece maximum dimensions:	360 X 600mm
Maximum cutting a taper Angle	3 degrees at 100mm job height
Brass and molybdenum wire diameters range	0.18 to 0.25 mm
Cutting speed Max.value)	80 square millimeters per minute
Z height maximum (mm)	400 mm
Workpiece weight limit	400 kg
Tool size for the machine	2000 X 1600 X 2100 mm

The details for Nimonic Alloy 75

Table 2: Nimonic Alloy 75's constituents

Name of element	Ni	Cr	C	Fe	Mn	Si	Cu	Ti
Chemical Composition, %	77.7	18.0–21.0	0.08–0.15	5.0 max.	1.0 max.	1.0 max.	0.5 max.	0.2–0.6

Specifications for Brass Wire

Table 3: The chemical composition of the electrode made of brass wire

Element	Ni	Cu	Fe	P	Sn	Zn	Pb	Cu	others total
Composition in %	0.05	71.0	0.02	0.3	0.1	28.5	0.05	71.0	0.1

Fig.4: Fixing of workpiece on machine table

Fig.5: Nimonic alloy 75 workpiece after machining.

Parameters of WEDM

The ranges of wire cut WEDM settings are displayed below.

Range of Wire EDM

Table 4: Parameter range for WEDM

S. No.	Parameter	Range
1	T on (µs)	0 to 200
2	Toff (µs)	0 to 100
3	Peak current (A)	1 to 5
4	Wire feed rate (m/min)	0 to 100
5	Sensitivity	1 to 200
6	Gap Voltage (V)	1 to 100

Orthogonal DOE

The experiment design made use of an L-9 orthogonal array, and three levels of input parameter selection were made: T on, T off, Peak current, and Gap voltage. For each experiment, the microhardness and metal removal rate are calculated. The levels and protocols listed below have been selected.

Table 5: Control Factors –Levels

Parameter	Peak current (amps)	T ON (µs)	T OFF (µs)	Gap voltage (v)
Symbol	A	B	C	D
Level :1	1	30	32	55
Level :2	2	34	36	65
Level :3	3	38	40	75

Table 6: The design of the Taguchi L9 OA

Expt. No	Peak current (amps)	T on (µs)	Toff (µs)	Gap voltage (v)
1.	1	30	32	55
2.	1	34	36	65
3.	1	38	40	75
4.	2	30	32	75
5.	2	34	36	55
6.	2	38	40	65
7.	3	30	32	65
8.	3	34	36	75
9.	3	38	40	55

The table displays the control parameters and their respective levels for wire-cut EDM. The Taguchi L-9 Orthogonal array is the target application for these control parameters.

Experimental Results

The formula below is used to determine MRR, while the stopwatch method is used to calculate cutting speed.

In a work process, the rate of impact is equal to the product of the cutting depth, cut breadth, and feed rate. Usually, the impact rate is mentioned in gram per minute.

MRR= Vc x dw x T

Where

   Vc =cutting speed (mm/min)

   dw =wire diameter

   T= Thickness of work piece (mm)

Microhardness

A Vickers hardness tester (Model no. BV250(S) was used to quantify microhardness. 15 N of force was applied, and the dwell time was 15 seconds.
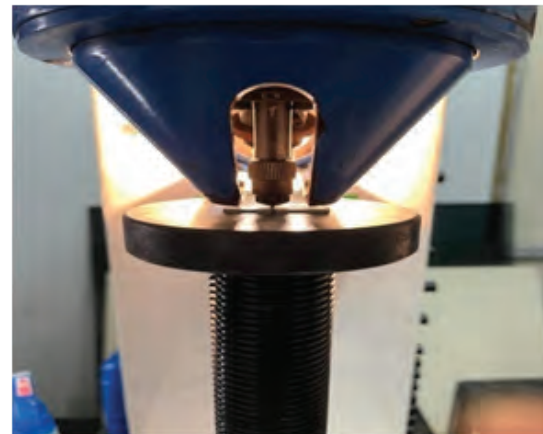
Fig. 6: Microhardness tester

The conformance test formula is as follows:

$$"Y_{Opt} = m + (MA_{opt} - m) + (MB_{opt} - m) + (MC_{opt} - m) + (MD_{opt} - m)"\,(1)\,[7].$$

m (mean) = Total value/No. of experiments

RESULT & DISCUSSION

Three levels of peak current (IP), T on, T off, and Gap voltage were selected, and the Taguchi OA was chosen to carry out the tests. The microhardness and MRR (g/min) of the process outputs are shown in the table.

Table 7: Experiment results of MRR and microhardness

Expt. No	0.25 mm diameter Brass wire		0.18 mm diameter Brass wire	
	Material removal rate (mm³/min)	Micro hardness	Material removal rate (mm³/min)	Micro hardness
1	1.295	213	1.209	200
2	1.325	209	1.206	193
3	1.325	214	1.206	186
4	1.320	219	1.202	195
5	1.325	212	1.202	195
6	1.325	213	1.213	193
7	1.300	224	1.216	202
8	1.350	215	1.216	204
9	1.300	219	1.213	201

The comparison of MRR with 0.25mm and 0.18mm diameter wires are shown in the graph.
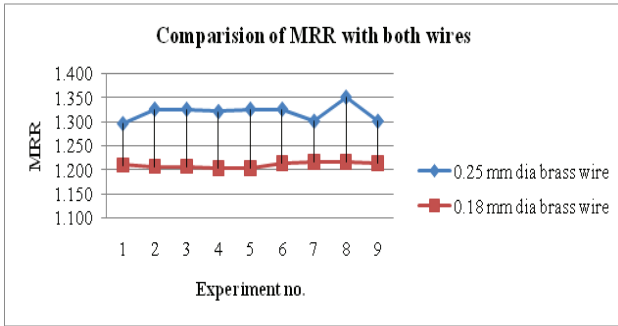
Fig.7: Comparison of MRR

The comparison of Micro hardness with 0.25mm and 0.18mm diameter wires are shown in the graph.
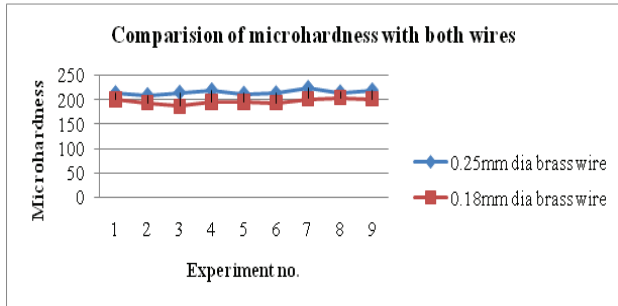
Fig.8: Comparison of Microhardness

Factors influencing MRR with 0.25mm brass wire

"The parameters- peak current 2 (amp), Ton 34 (s), T off 32 (s), and gap voltage 75 (v) were plotted and determined, the material removal rate combination is A2B2C1D3" [7]. It is not compatible with the Taguchi L9 OA, and the combination for MRR is A2B2C1D3. Thus, a confirmatory test was conducted.

Table 8: MRR- Response chart for S/ N Ratios

| Level	peak current	Ton	Toff	Gap voltage
1	1.393	1.343	1.302	0.01427
2	1.324	1.313	1.354	0.01357
3	1.43	1.467	1.443	1.342
Delta	0.0011	1.33	0.00093	0.0007
Rank	2	1	3	4

From equation (1), conformation value of MRR= 1.326 mm³/min
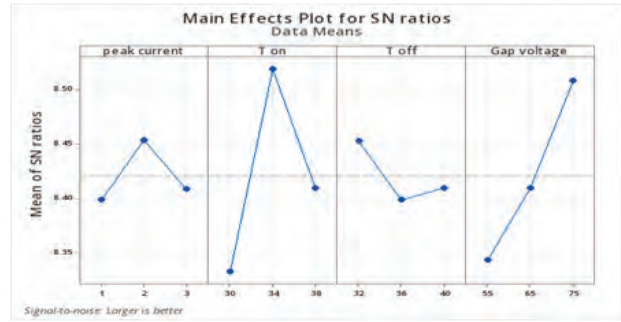
Fig. 9: S/N ratios of MRR on Nimonic Alloy 75 using 0.25mm dia Brass electrode.
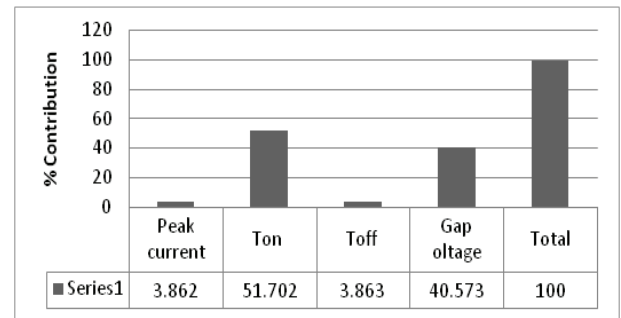
Fig. 10: % contribution MRR (ANOVA)

According to the ANOVA, Ton had the greatest influence on MRR. The parameters that have the least impact are peak current and T off.

Factors influencing MRR with 0.18mm brass wire

"The material removal rate combination is A3B3C1D2 when the input values parameters peak current 3 (amp), Ton 38 (μs), T off 32 (μs), and gap voltage 65 (v) are displayed and recognized" [7]. It is not compatible with the Taguchi L9 OA, and the combination for MRR is A3B3C1D2. Thus, a confirmatory test was conducted.

Table 9: MRR -Response chart for S/N Ratios

Level	peak current	Ton	Toff	Gap voltage
1	1.353	1.353	1.214	0.01327
2	1.214	1.203	1.364	0.01457
3	1.431	1.457	1.433	1.272
Delta	0.0011	1.323	0.00093	0.0007
Rank	2	1	3	4

From equation (1), conformation value of MRR= 1.276 mm³/min
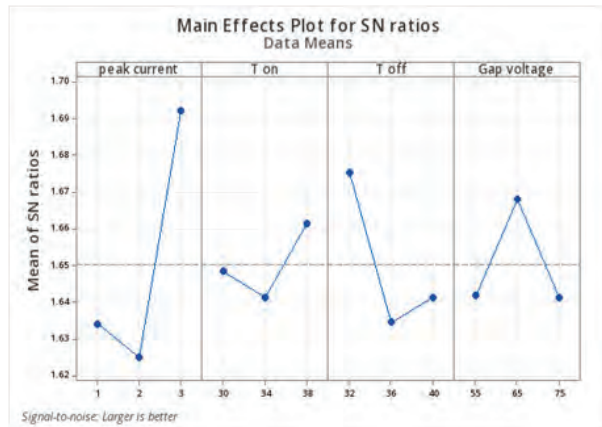
Fig. 11: S/N ratios of MRR on workpiece using 0.18mm dia Brass wire
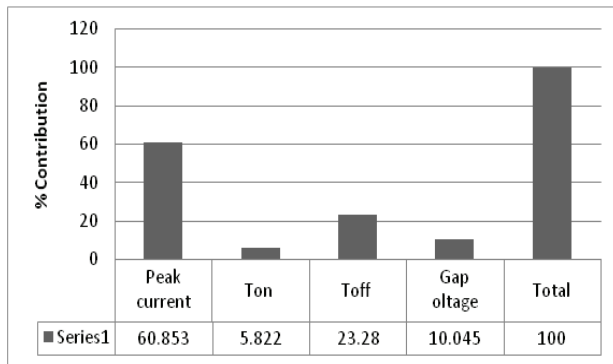
Fig. 12: % contribution MRR (ANOVA)

Peak current is the variable that influences MRR the greatest, according to the ANOVA. The parameter with the least influence is T on.

Factors influencing Microhardness with 0.25mm brass wire

Plotting and identification of the MRR combination A3B1C3D3 using these variables: Peak Current 3amp, T-on 30 µs, T-off 40 µs, and Gap Voltage 75v. The MRR combination, A3B1C3D3, is incompatible with the Taguchi L9 orthogonal array. Confirmation testing was therefore applied.

Table 10: Micro Hardness-Response chart for S/N Ratios

Level	peak current	T on	T off	Gap voltage
1	211.4	214.2	214.1	214.8
2	215.1	211.2	215	214.9
3	215.7	215.8	213.1	216.5

Delta	8.2	8	3	1.8
Rank	1	2	3	4

From equation (1), conformation value of Microhardness = 214.5
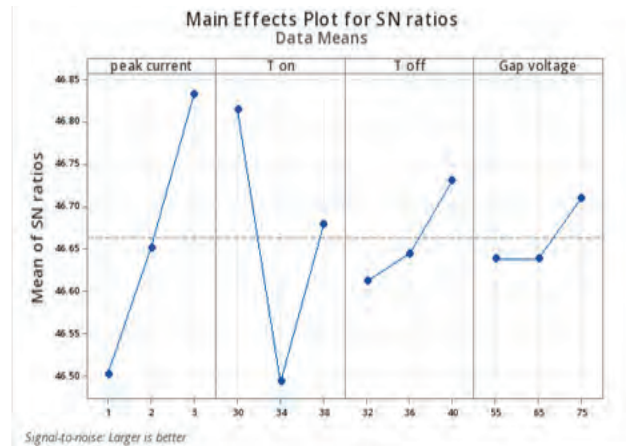
Fig. 13: S/N ratios of Microhardness on Nimonic Alloy 75 using 0.25mm dia Brass electrode.
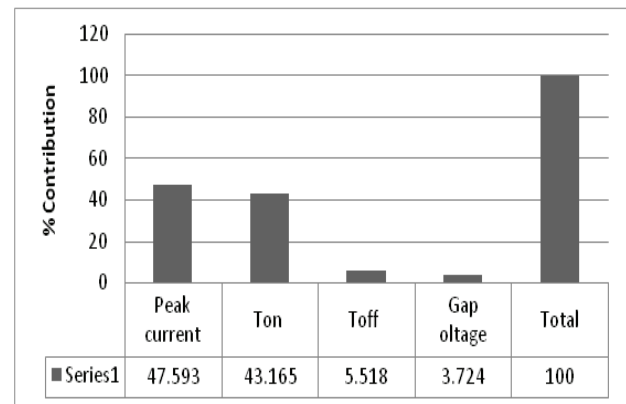
Fig.14: % contribution MRR (ANOVA)

Peak current is the parameter that influences microhardness the most, according to the ANOVA. The parameter that has the least influence is gap voltage.

Factors influencing Microhardness with 0.18mm brass wire

The input values peak current 3 amp, Ton 30 µs, T off 32 µs, and gap voltage 55v have been plotted and identified, resulting in the material Removal Rate combination A3B1C1D1. It is not compatible with the Taguchi L9 OA, and the combination for MRR is A3B1C1D1. Thus, a confirmatory test was conducted.

Table 11: Micro Hardness-Response chart for S/N Ratios

Level	Peak current	T on	T off	Gap voltage
1	193	195.1	194.8	197.7
2	194.9	197.6	196.3	196.8
3	197.6	193.9	194.5	195.2
Delta	9.8	5.3	5.2	3.4
Rank	1	2	3	4

From equation (1), conformation value of Microhardness = 194
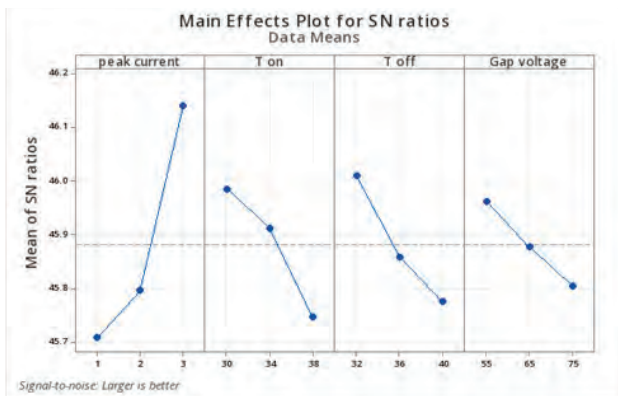
**Fig. 15: S/N ratios of Microhardness on Nimonic Alloy 75 using 0.18mm dia Brass electrode.**
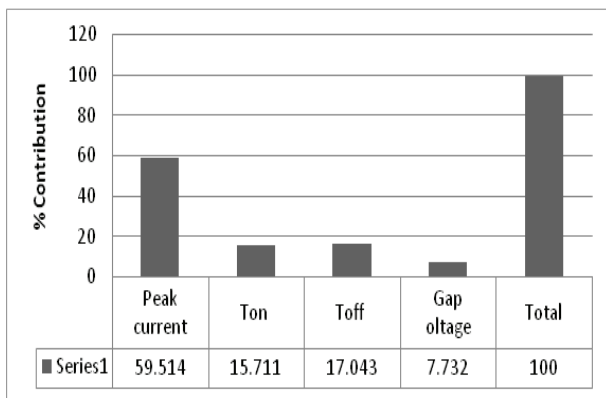
Fig. 16: % contribution MRR (ANOVA)

Peak current is the parameter that influences microhardness the most, according to the ANOVA. The parameter that has the least influence is gap voltage.
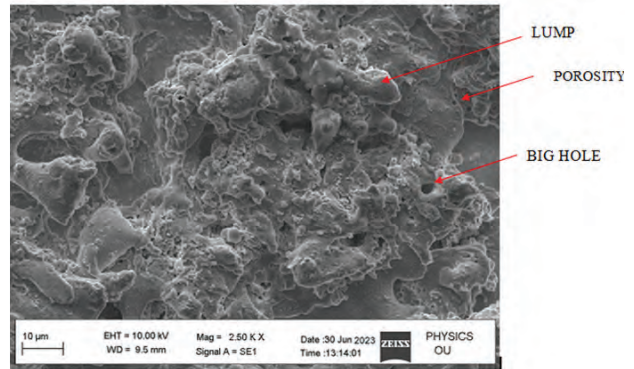
Fig. 17: SEM image of sample no.5
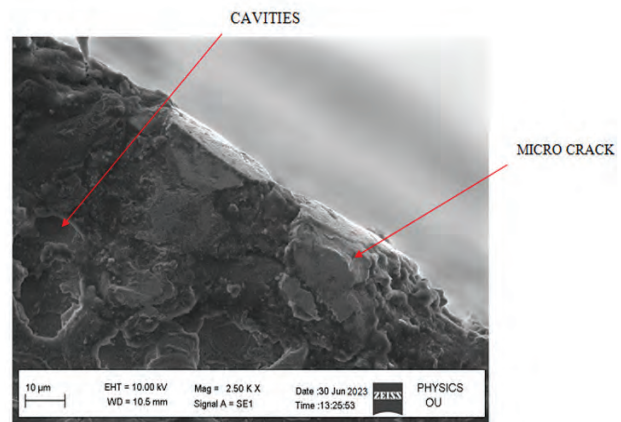
Fig. 18: SEM image of sample no. 7 edge

Using a scanning electronic microscope (model no. ZEISS -EVO 18), SEM images were obtained. As seen in figures 17 and 18, there are lumps, cavities, porosity, large holes, and micro cracks on the edge of the machined surface.

CONCLUSION

1. The MRR is mostly influenced by the Ton and Peak currents; increasing these values leads to a rise in the MRR as well.

2. Thicker wires release more heat energy than thinner wires, which increases the hardness value. On the other hand, thinner wires release less heat energy, which decreases the hardness value.

3. When using brass wire with a 0.25 mm diameter, the MRR is 1.326 mm3/min.

4. The removal rate of material by a brass wire with a 0.18 mm diameter is 1.276 mm^3/min.

5. The microhardness number obtained by machining with 0.25-mm brass wire is 214.5.

6. When 0.18mm brass wire is used for machining, 194 microhardness no. is obtained.

7. Micro cracks are observed on edge of the workpiece and Lumps, cavities, porosity and big holes are observed on machined face.

REFERENCES

1. Sabindra Kachhap, Pabitra Kumar Sahu, Punyapriya Mishra, Investigation and optimization of wire EDM process parameters for Al 5454 alloy machining, Materials Today: Proceedings, 2023, ISSN 2214-7853.

2. Pudi Charan & Chandrasekhara, Mekala. (2018). experimental investigation of wire edm parameters for surface roughness and MRR in machining of inconel 800 super alloy. Journal of Scientific Research and Development. 7. 677-684.

3. Dheeraj Mathew Paulson, Mohd Saif, Mohd Zishan, Optimization of wire-EDM process of titanium alloy-Grade 5 using Taguchi's method and grey relational analysis, Materials Today: Proceedings, Volume 72, Part 1, 2023, Pages 144-153, ISSN 2214-7853.

4. Muralidhara Rao, Vijeesh Vijayan, Athul Anil, Prithvi Kumar Rai, Nirmith R. Jain, Effect of wire electrode discharge machining process parameters on the surface roughness, hardness, and microstructure of the high carbon steels, Materials Today: Proceedings, Volume 46, Part 7, 2021, Pages 2625-2629, ISSN 2214-7853.

5. K. Hareesh, K.V. Nalina Pramod, N.K. Linu Husain, K.B. Binoy, R. Dipin Kumar, N.K. Sreejith, Influence of process parameters of wire EDM on surface finish of Ti6Al4V, Materials Today: Proceedings, Volume 47, Part 15, 2021, Pages 5017-5023, ISSN 2214-7853.

6. P. Thejasree, J.S. Binoj, N. Manikandan, P.C. Krishnamachary, Ramesh Raju, D. Palanisamy, Multi objective optimization of wire electrical discharge machining on Inconel 718 using Taguchi grey relational analysis, Materials Today: Proceedings, Volume 39, Part 1,6. 2021, Pages 230-235, ISSN 2214-7853.

7. U. Ashok Kumar, G. Saidulu, P. Laxminarayana, Experimental investigation of process parameters for machining of Nimonic alloy 75 using wire-cut EDM, Materials Today: Proceedings, Volume 27, Part 2, 2020, Pages 1362-1368, ISSN 2214-7853.

Development of 4D Printed Thermoplastic Urethane Insoles to Reduce/Redistribute Plantar Pressure In Diabetic Foot Ulcer Patients

Amol N. Patil

Department of Mechanical Engineering
Ajeenkya DY Patil School of Engg., Lohegaon, Pune
Research Scholar, JSPM's Jayawantrao Sawant
College of Engineering Hadapsar, Savitribai Phule
Pune University, Pune, Maharashtra
✉ patil.amol2015@rediffmail.com

S. H. Sarje

Department of Mechanical Engineering
JSPM Narhe Technical Campus
Savitribai Phule Pune University
Pune, Maharashtra
✉ suhassarje7235@gmail.com

ABSTRACT

The prevalence of the diabetes population is increasing day by day across the Globe, almost doubled in the last 23 years. This is also leading to the incidence of diabetic ulcers, sensation loss in the plantar region of the foot, and, in the most severe cases, the necessity for amputation. Non-healing diabetic foot ulcers (gangrene) are a major health concern nowadays, reducing the quality of life of individuals and families. From the research, one important factor that prevents foot ulcers from developing or recurring is the redistribution/reduction of peak plantar pressure. Customizing shoe insoles, offloading orthosis, and other strategies can help to mitigate these issues to some extent. However, customizing shoe insoles by the conventional method is laborious, requires special skills, and is costlier, time-consuming, and non-waterproof. Nowadays, a reverse engineering workflow, i.e., scanning, 3D modeling, and 3D printing, can fabricate customized insoles more accurately and quickly, as per the patient's requirements, creating novel prospects for regional healthcare product development. In this paper, low-cost and reduced plantar pressure 'novel 4D printed smart insoles' of shape memory thermoplastic urethane, in particular for low- and middle-income countries, using a reverse engineering workflow method, that has better performance than conventionally crafted insoles, have been developed.

KEYWORDS : 4D Printing, Plantar Pressure, Diabetic Foot Ulcer (DFU), Insoles, Shape Memory Thermoplastic Urethane (SMTPU).

INTRODUCTION

Diabetes is a group of metabolic disorders identified and characterized by hyperglycemia, insulin resistance, and a relative decrease in insulin secretion when treatment is not received [1]. It is a severe, chronic illness that affects people's lives and general well-being on a global scale, affecting communities, families, and individuals. It was estimated to have caused 4 million deaths worldwide in 2017, placing it among the top 10 causes of death for adults. Global health spending on diabetes was projected to reach USD 727 billion in 2017 [2]. Type 1 diabetes (T1D), type 2 diabetes mellitus (T2D), and gestational diabetes mellitus (GDM) are the three main forms of this disease. The International Diabetes Federation (IDF) has published data on diabetes prevalence at the regional, national, and international levels since 2000 for an age group of 20-79 yrs. The number of people with diabetes including T1D and T2D was found to be 285 million in 2010, leading to 366 million in 2011, 382 million in 2013, 415 million in 2015, 425 million in 2017, and recently 537 million in 2021. It is shocking to hear the prediction that it will increase up to 693 million by 2045, if not taking any effective preventive measures[3]. Aging, fast urbanization, and obesogenic environments are three prime causes of this rising trend in T2D, which makes up about 90% of cases. The proportion of diabetes is on the rise due in part to rising T1D incidence rates. It is still unknown the cause of this rise. Better survival of

diabetics (in certain populations) due to early diagnosis, better diabetes management, and a resulting decline in premature mortality is another factor contributing to the increased prevalence [3]. And finally, because they live longer, the growing number of younger adults with T2D in recent years also adds to the rise in T2D prevalence overall [4]. In recent decades the global burden of diabetes (GBD) has grown significantly by type of diabetes, region, and country and it is predicted to continue in coming decades too. Researchers provided the data required for health service planning and priority setting to fulfill the World Health Organization's global action plan for preventing and controlling such noncommunicable diseases (NCDs) by 2025 [5].

Most of the times, patients with diabetes have deep tissue ulceration, infection, and foot destruction, along with neurological abnormalities and peripheral vascular disease in the lower limbs are known to be diabetic foot ulcer (DFU) patients as per WHO and IWGDF guidelines [6]. Peripheral vascular disease and infection susceptibility prevents injury healing and increase gangrene risk. Currently, diabetic foot ulcers, with non-healing chronic wounds i.e. gangrene are a prime health issue, which reduces the life quality of individuals and families worldwide [7]. It is predicted that almost 40-60% of patients with diabetes will experience diabetic neuropathy at some point in their lives. Neuropathy may eventually cause additional complications that end in limb amputation or even loss of life [8]. Pressure ulcers or injuries are one of the major causes of developing diabetic foot ulcers, which arises from uneven, uncontrolled pressure distribution between the foot and supporting surfaces i.e. shoe insoles, creating localized regions of high pressure. Such peak/plantar pressures damage the soft tissues, compress the vascular networks, reduce the supply of nutrients and oxygen, and cause tissue ischemia i.e. breakdown of tissues. The resulting chronic ulcer causes discomfort, and severe pain, reduces the quality of life, causes amputation, and may even lead to death if infections are superimposed [9]. Limb amputation needed to be performed due to the combination of ischemia and infection[6]. It is estimated that a lower extremity is lost somewhere in the world every 30 seconds as an effect of diabetes. Therefore, it is of utmost importance to study this parameter because it has been proved that, redistribution and reduction of

plantar pressure between the neuropathic foot and insole prevents ulceration and its recurrence to the maximum extent which is an effective ulcer prevention strategy [7].

Nowadays 3D printing, an additive manufacturing technique has gained popularity across the globe. Fused filament fabrication (FDM), is one of the most commonly used additive manufacturing technologies that can be used for fabricating shoe insoles. It has been demonstrated by some authors that, customized insoles for DFU patients can be developed by 3D scanning, solid modeling, and 3D printing techniques[10]. This strategy may be quite useful for fabricating highly customized smart shoe insoles in less time than conventional techniques, which could reduce the peak/plantar pressure to a maximum extent by redistributing it properly. Plantar pressure may vary from person to person because the contact area will be different in each case. Thus, 3D printing fabricated shoe insoles/surfaces can fulfill such individual requirements for clinical treatments with different shapes, materials, internal patterns, etc.[11]. When new shoe insoles are suggested by the practitioner, the peak plantar pressure parameter permits him to verify the fabrication of the correct device and monitor the treatment. 3D-printed insoles have been reported and evaluated in earlier research. 15 participants in Korea were assessed while walking actively with 3D-printed insoles. It was investigated that wearing insoles changed the center of pressure (COP) path when walking quickly, enhancing the distribution of load evenly across the foot during the standing phase [12]. Some researchers focused on plantar pressure variations during a light walk. They designed customized insoles by scanning the feet of selected individuals for study. Three different conditions were used to test these insoles in contact with other surfaces: the original shoe insole, an ethyl vinyl acetate custom insole, and a 3D-printed biomechanical insole. The findings showed that customized insoles affect the distribution of plantar pressure, particularly in those with high-arched foot deformities or flat feet [10]. Using the finite element method, some authors have assessed the materials and design of customized insoles, defining the static and dynamic loads that may be applied to the insole, from a mechanical point of view [13]. The infill, or filling pattern, of 3D-printed

insoles made of semi-rigid materials, was analyzed in another report utilizing a variety of measurements and tests, like traction, bending, and hardness resistance [14]. Some investigators in China studied the impact of customized 3D printed insoles as compared with conventional prefabricated insoles in flat foot symptom patients. They found that plantar pressure on metatarsals is reduced to a maximum extent by redistributing it over the midfoot area [15]. Some other researchers developed and fabricated an elastomeric soft and flexible insole that can measure capacitive pressure. Four pressure-sensing zones were included in the design of this insole, and tests conducted under various conditions revealed reliable responses up to 300 kPa [16]. Another study employed a similar methodology, fabricated electronic insoles through 3D printing to measure plantar pressure. Using a microcontroller, the authors were able to send data wirelessly and in real-time to an Android app on a mobile device. This app displayed a plot of the force gradient across the insole [17].

Insoles manufactured by the conventional method are used for DFU patients by taking proper care using Boyner insole technology at the advanced wound care department of DMH hospital, Pune, India as per the patient's specific requirement, the results were encouraging. The GAIT analysis was performed by wearing these insoles. Analysis was repeated immediately after 2 months to observe the improvement. It has been observed that, there was a reduction of plantar pressure around wounds, improved foot ambulation performance score (FAP), and accelerated wound healing after 4 months [7].

However, it is laborious work, requires special skill, is costlier, time-consuming, and is permeable (non-waterproof)[18]. In addition to this, most of the time, while manufacturing the insole by conventional method, it is necessary to bring together both the patient and podologist for customization. Also, this method may contain hazardous material particles that can cause respiratory failure. Thus, a pre-fabricated insole by the conventional method is unsuitable because each DFU patient may have different limb sizes, anatomies, deformities, etc. Mass production may not be appropriate for each DFU individual to match his/

her specific need and may deteriorate the illness instead of orthotic comfort. It indicates that, for proper plantar pressure distribution, custom fitting is a vital parameter. To achieve this, recent technologies like 3D scanning, 3D geometry construction, and additive manufacturing are of utmost importance for producing patient-specific foot insoles [19].

Up till now lot of research has been carried out to reduce the plantar pressure in DFU patients by fabricating the shoe insoles conventionally and by using 3D printing techniques. But insole fabrication by 3D printing of shape memory polymers (SMPs)/ smart materials i.e. by '4D printing technique' has not been explored yet. In this method, static 3D printed structures/surfaces can be converted into dynamic ones i.e. shape changing, in the presence of external stimuli like heat, light, hot water, etc.[20]. SMPs are an exciting class of stimuli-responsive smart materials that can show reactive and reversible changes by switching between various states due to external stimuli [9]. Thus, it may be possible to reduce peak pressure i.e. to reduce the foot pain, by redistributing it properly, in the presence of environmental heat or that generated inside the shoe by rubbing the contacting surfaces as a stimulus. Many SMPs like polycaprolactone (PCL), polylactic acid (PLA), thermoplastic urethane (TPU), ethyl vinyl acetate (EVA), Neoprene and ABS can be used to develop DFU insoles[21,22]. But each SMP has its own merits and demerits. Amongst all, PU-based thermoplastic urethane i. e. 'Shape Memory Thermoplastic Urethane' (SMTPU) is the best-suited material for this biomedical application, verified so far, as having a low glass transition temperature range (35-45°C) which is around human body temperature range, more flexible, economical, biocompatible and easily available in filament form for 3D printing additively. [23]

Thus, the authors report on the development of customized shoe insoles of SMTPU for peak pressure redistribution, that exhibits controllable changes in dynamic pressure redistribution capability at a low glass transition temperature (~35 °C) i.e., around human body temperature, ideally suited to matching modulations in body contact pressure for dynamic pressure relief (e.g., pressure ulcer effects or for alleviation).

MATERIALS AND METHODS

Initially, the shape memory polymers/ smart materials selected for this course of the study are ethyl vinyl acetate (EVA), poron, and thermoplastic urethane (SMTPU), from the reported literature [21–24]. To check the suitability for the proposed biomedical application, these materials were characterized through a series of tests i.e. differential scanning calorimeter (DSC) test, scanning electron microscope (SEM) test to find glass transition temperatures (T_g), and porosity ratios(r) respectively [24-25]. Then, thermomechanical behavior was checked by loading and unloading the material samples uniaxially in the universal testing machine with a built-in temperature-controllable chamber for high-temperature experiments in the nitrogen atmosphere to find shape fixity ratios (R_f) and shape recovery ratios (R_r) as a behavior parameters. Shape fixing makes it possible to achieve a predefined shape before applying the foot, which may increase the coverage area and reduce the pressure. After evaluation, these parameters were tabulated (Table 1).

Table 1. Shape memory characteristics of polymers.

Parameter	EVA	Poron	SMTPU
T_g (°C)	45	44	35
r (%)	13	11	18
R_f (%)	89	83	95
R_r (%)	88	79	91

SMTPU finds many advantages over other SMPs and conventional materials. It is more flexible, easily available in 3D printing filament form, less costly, durable, and waterproof, and satisfies major requirements of the proposed application [26]. Besides this, one of the major advantageous parameters is its transition temperature, T_g (~35°C), which is around the human body temperature. Thus, there may be the chances of shifting the pressure points naturally which may release the contact stresses due to temperature fluctuations in the body and environment (~30−50 °C) [9] . Thus, using 3D-printed smart/active surfaces of SMTPU i.e. 4D Printing Technology may reduce excessive stress during plantar loading to reduce the pressure ulcer effects. Hence, for this study, SMTPU has been selected as an optimum material. Also, a reverse engineering workflow (Fig. 1) has been implemented for this work, wherein the general steps involved are digital scanning, point cloud data collection, geometry clean-up, 3D model generation, and 4D Printing.

A 'TPU- 3D printing filament' of 1.75mm diameter with 72 shore hardness(flexible) was purchased from Wol3D, Pune, India. This biocompatible polymer is generally used for fabricating 3D printed medical implants with interesting properties, tensile strength: 30Mpa, density: 108 g/cm3, and break elongation %: 900. In the entire fabrication workflow, a male adult patient with good health was recruited as a user to evaluate the performance of developed insole to validate the concept. The information about the patient's data was made strictly confidential, kept in a database, and password-protected so that only the researchers could access it. 'IST informatique' foot pressure scanner/ plate was used to measure the plantar pressure with 'Footwork' software for its analysis.

Diabetic foot insole development:

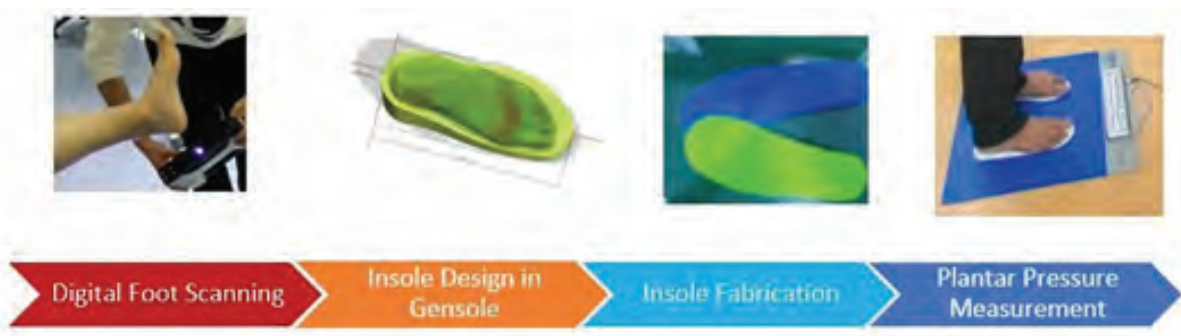Reverse engineering i.e. development workflow (Fig. 1) of smart insole is explained in detail:

Figure 1. Reverse engineering workflow for 4D printed insoles

Digital Foot Scanning

Scanning of the patient's foot was performed at AMS 3D India Pvt. Ltd., Pune, India with a ZG handheld portable scanner, model CereScan, with laser source of blue lines, high accuracy of 0.01mm and stand-off distance of 150mm-300mm, in a fine mode. The foot was placed in a resting posture and the scanner was turned around to finish the scanning process. The process took around 5 minutes per foot.

Insole Modeling

Point cloud data of scanned feet was sent to 3D modeling software for geometry clean-up. A full-proof 3D solid model of the foot is then imported into Gensole software [27] for insole modeling. Gensole is a freely available web-based application that enables the user to create insole models that are optimized for 3D printing with Filaflex (TPU/TPE) type materials by FDM technique. The upper surface of the insole was formed to resemble the foot model. To improve comfort fitting within the shoes, the right density of padding was selected, and the insole was given contour curves. The following parameters were chosen for the insole design:

- Weight of patient: 81Kg

- Total shoe insole length: 270 mm

- Measurements at insole ends: 10 and 25mm

- % infill at the largest contact area shown by green color: up to 60%

- Least thickness of insole: 5mm

All these parameters are used to print left and right insoles.

Insole Fabrication (3D printing of shoe insole)

Fused filament fabrication (FDM) method of 3D printing was used to print the insole. The generated AMF file (additive manufacturing file format) was then sent to a 3D printer through a pen drive, which includes G and M code data for machine axes movement and for building the insole model during the fabrication process. A 3D printer, model 'Creality Ender 3S1 Pro' was used for insole fabrication. The following printing parameters were set before actual printing: highest resolution was 0.2 mm per layer (layer height), extrusion temperature of nozzle at 225°C, temperature of bed at 60°C, room temperature at 22°C, printing/ building speed at 50 mm/s, filament diameter used of 1.75 mm and infill percent at 60 % with zigzag pattern and no supports. The printing bed size was 220x220x270 mm, can use up to 10 different printing filaments. Two insole pairs were fabricated with SMTPU material.

Plantar Pressure Measurement System

To measure peak plantar pressure, a force platform, FootWork electronic model, electronic baropodometry, and IST Informatique, France were used. This instrument was duly calibrated in an accredited lab and measurement was performed at the Advanced Wound Care Department (AWCD), of Deenanath Mangeshkar Hospital (DMH), Pune, India. The platform is composed of a 645x520x25mm rigid base and 2704 pressure sensors(7.62x7.62mm) that record individually up to $100 \, N/cm^2$ pressure. Sensor spread over an active area of 40x40 cm, enables baropodometry analysis of pressure loads in kgf/cm^2, in a standing posture. This pressure plate has a sampling frequency of 150 kHz with a 16-bit A/D converter. It was connected to a Pentium III personal computer.

Experimentation

After printing, trials related to plantar pressure measurement were performed at the GAIT lab of AWCD of DMH, Pune, India, on a developed insole. The authors followed the straightforward clinical protocol suggested by the podologist, which includes feet and postural examinations, GAIT analysis, and interviews for design purposes. Foot deformities and types of feet whether normal, planus, or high arch were checked and defined for feet examination. Postural examination evaluated the mobility and alignment of the hip, knee, and ankle joints. 2D GAIT analysis was then performed indoors on a concrete floor using the GAITRite tool to evaluate the FAP score. As per the podologist, the FAP score always lies between 95-100 for a normal person and it is between 80-100 for a normal Indian. If it is less than 80 then there is a risk of fall. To improve the FAP score, he suggests using fully customized shoe insoles to reduce plantar pressure and taking follow-up calls after two months to observe improvement in FAP [7]. The test was performed with three walk-trials of 180 seconds each with barefoot condition. To evaluate hip, knee, and ankle alignment, the patient was allowed to

walk forth and back in the presence of a physiotherapist. Videos of each walk trial were recorded for analysis. To detect rotational and axial abnormalities in the walking trail, reference points were marked in video frames. The patient was allowed to walk with his regular speed and habit to detect real problems. The FAP score observed was 98. The patient was then informed to stand on a foot pressure scanner plate to measure peak plantar pressure. Three trials of pressure measurement were taken viz. barefoot condition, with the developed 4D printed insole at ambient temperature (i.e. without thermomechanical programming) and with programmed insole (Fig. 2).

Figure 2. Plantar pressure measurement by foot scanner: (a) Barefoot, (b) SMPTU insole at ambient temperature, and, (c) Programmed SMTPU insole.

Peak pressure readings were recorded and compared with the conventionally crafted insole and tabulated (Table 2).

Table 2. Plantar pressure measurement of feet

Trial	Pressure on the bottom of feet (kPa)				Pressure on selected Areas (kPa)			
	Mean		Maximum		Mean		Maximum	
	LH	RH	LH	RH	LH	RH	LH	RH
Barefoot Condition	100.71	76.44	206.5	187.02	135.42	103.20	282.0	181.55
SMTPU Insole w/o programming	53.35	51.95	129.11	128.54	105.02	57.10	151.65	142.33
Programmed SMTPU Insole	52.60	42.71	135.6	109.0	68.26	46.95	113.01	79.05
Traditionally Crafted EVA Insole	78.21	81.42	155.3	160.22	102.39	61.7	147.3	121.73

In the third trial, to achieve the minor shape change, and thus reduce/redistribute the peak pressure by accommodating the foot profile, the developed insole was subjected to thermomechanical programming in the presence of thermal heat as an external stimulus. This transformation i.e. static 3D printed SMTPU insole (passive surface) into dynamic (active surface) can be achieved by heating it in the oven above T_g (at 50 to 60 °C). The patient then suggested to stand on the foot imprinter, model: POUSSOU of AMcube make to imprint the exact foot profile by inflating the silicon bladders (Fig.3(b)) for 5 minutes. After that, the heated insole, comparatively more flexible, was positioned in the molded cavity of the bladder and informed the patient to stand on it, in the previous posture for 5 minutes. It has been observed that heated insoles conformed to the exact shape of the foot profile due to his own weight and temperature (Fig. 3).

Gaining of a temporary shape (i.e. shape fixing) due to heat plus compressive load of the patient's self-body weight and then unloading (i.e. shape recovery), assumed to complete a thermo-mechanical cycle/programing, simulates real wearing condition with surrounding temperature as a stimulus. Thus, it can be assured that, when the developed insole is put into actual practice, the same thermomechanical shape-changing cycles of shape fixing and shape recovery will be repeated and

will surely help to redistribute high-pressure points and may provide relief to the DFU patients. Pressure measurement was then completed with programmed/molded/shape changed insole. Noticeable change in plantar pressure readings has been detected as compared to the first two trial conditions (viz. barefoot, at ambient temperature) and with the crafted insole.

Tabulated plantar pressure values help to understand that, the maximum pressure is comparatively lower in the case of programmed insole than that in barefoot condition and insole without programming. Thus, it can be stated that the programmed SMTPU insole can be used to distribute the plantar pressure effectively and hence can be used in the treatment of patients suffering from diabetic foot ulcers.
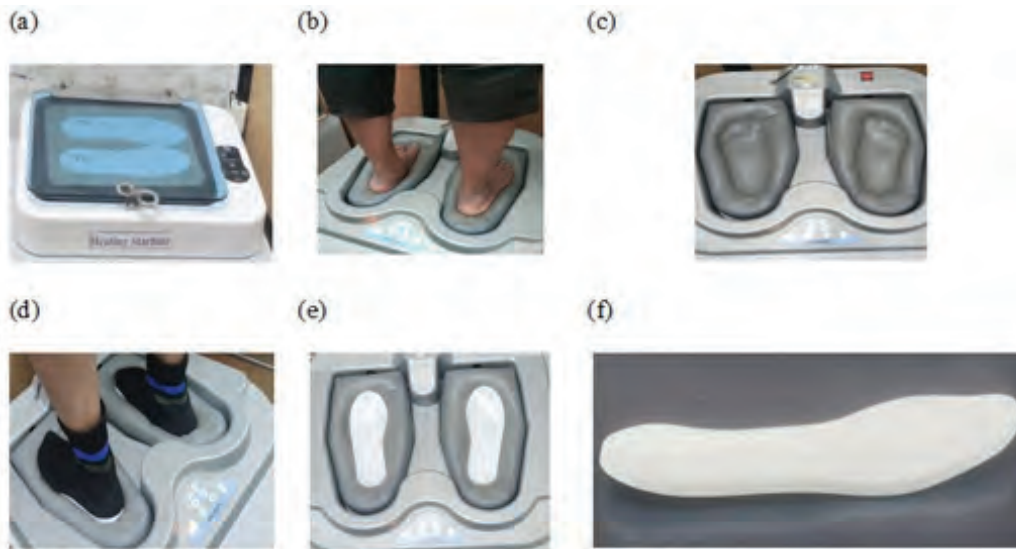

Figure 3. Thermomechanical programming of 4D printed SMTPU insole: (a) heating above T$_g$, (b) conforming foot profile using imprinter, (c) mold creation, (d) thermo-compressive loading, (e) insole programmed, conforming foot profile and. (f) shape fixing according to foot profile

RESULTS AND DISCUSSION

The reverse engineering workflow started with the scanning of the feet. A 3D solid model of the left and right foot was properly rebuilt with geometry cleanup tools. The insole 3D model generated by Gensole was fabricated by FDM technology. Insole pairs were manufactured with SMTPU as a soft, flexible shape memory polymer in a day. Out of all the steps, 3D printing took the longest time, almost 17 hours to print a single insole pair. No redesign or postprocessing was required for the insole. Also, need not be given dimensional allowances, etc., during mold creation as the material is flexible and can accommodate foot profile shape accurately after fabrication. Before measuring the plantar pressure using fabricated insoles, patient GAIT analysis was performed. Peak pressure results of the insole with, without programming, and barefoot condition were recorded and tabulated.

Average peak pressure was the only parameter that was selected for quantitative analysis and comparison, as it is most significant and responsible for pressure ulcer generation in DFU patients. It has been calculated by performing one-way ANOVA to compare the maximum values obtained from developed 3D printed insole and traditional crafted insole of EVA. The reference was the average of pressure measurement trials carried out with crafted insoles (148.52 kPa). The average pressure for the barefoot trial was 196.76 kPa, that for the unprogrammed insole was 138.5 kPa (p =0.04) and it was 130.94 kPa (p =0.001) for the programmed insole (Fig. 4). From the literature, peak pressure values recommended are of $\leq$ 200 kPa for diabetic footwear [28]. Variations in walk trials were observed at the standing posture in subjective gait analysis. Barefoot didn't allow the metatarsal to get proper contact with the concrete floor. During GAIT analysis, stability was

modified slightly and compensated by the patient. Step length was kept minimum. The flexion of the ankles, knees, and hips was obtained correctly. Faster walking speeds and longer length steps were detected in the GAIT cycle. According to the patient, he realized pain and discomfort in some steps, reported in an interview. There was not a significant variation in concentrations of the pressure on the metatarsal heels and heads during the trials.

Particularly, 3D printing has been advantageous in prevention and rehabilitation in enhancing accessibility to healthcare. Chronic diabetes mellitus is becoming more prevalent in low and middle-income countries like India. Approximately 77 million people in India have diabetes, making it one of the top nations in the world after China. By 2045, that figure is anticipated to increase to 35.7 million [29]. It has been predicted that about 25% of Indians with diabetes patients are expected to develop DFU [30]. Lack of public awareness, inadequate medical infrastructure, and financial constraints could cause this situation to worsen even more. DFU patients in such countries can take benefit of these 4D printed SMTPU customized insoles, for prevention, recurrence, or individual foot ulcer treatments. However, the majority of research employing this technology is still carried out in developed nations, and it is difficult and uneconomical to reproduce the manufacturing workflow. This study has demonstrated that, developed insoles can be produced and validated using a more interdisciplinary approach in low and middle-income countries. The protocol of digital manufacturing workflow has been defined well to promote reproducibility in such regions.

Figure 4. Quantitative analysis of insole by one-way ANOVA

Despite the mechanical properties of polymers, performance-wise, these 4D printed insoles can do better than conventional insoles, because pressure modification was not needed during insole design. Plantar pressure may be influenced by printing parameters due to various internal pattern configurations and density zones. For the design of insoles, simulations, and additional plantar surface measurement points may be useful.

Furthermore, some methodological limitations are reported in this investigation. Foot scanning requires a commercial 3D scanner which is yet costlier for low and middle-income countries and its availability is limited. Also, the development of a 3D solid model from point cloud data by scanning the body parts, called photogrammetry is a promising technique, that requires highly skilled operators. Photogrammetry can also be possible by Android smartphone apps but accuracy is too limited as compared to commercial 3D scanners. Only a single SMTPU flexible filament was used at the digital manufacturing stage with the same printing parameters in this study. It should be explored to investigate the effect on peak plantar pressure by changing the elements like, mixed-material 3DP filaments, infill percentage, patterns and printing parameters, etc. It would be interesting if the specially designed 3D printing filaments with antibacterial properties could prevent ulceration [31].

CONCLUSION

Clinical complications like foot ulceration or amputation result from diabetic neuropathy. As a part of diabetic foot management, orthopedic insoles are necessary for the prevention of ulcer formation, its recurrence, or wound healing by reducing/redistributing the plantar pressure. Usually, conventionally crafted/handmade insoles are used, but there are some drawbacks to traditional methods during their customization. As an emerging technology, it has been proved from numerous studies conducted in developed nations, that 3D printing has shown the potential benefits for insoles fabrication for foot ulcer treatment.

Authors tried the insole development by 3D printing of shape memory thermoplastic urethane i.e. 4D printing, and also demonstrated that reverse engineering process flow can be employed for insole fabrication
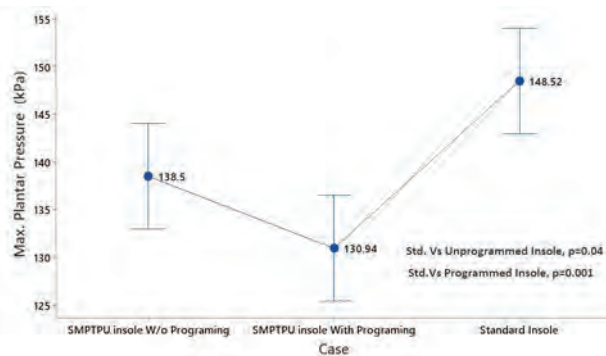
in middle-income countries like India, etc. To collect user information, a relatively easy clinical protocol has been proposed. Barefoot condition, insole at ambient temperature, and the above glass transition temperature cases were considered while measuring plantar pressure between foot and insole. Quantitative analysis of insoles was carried out by one-way ANOVA in Minitab. It has been finally concluded that the average peak pressure in the programmed insole is less i.e. well redistributed than in other cases. The patient reported that the programmed i.e. 4D printed SMTPU insole was more comfortable, experienced him. Hence, the developed insole can be used for DFU patients to reduce foot pain by redistributing or lowering the peak plantar pressure properly.

Future studies should explore emerging technologies like machine learning, and artificial intelligence to evaluate the insole plantar pressure for neuropathic diagnosis in diabetic patients. Similar techniques may be employed to decide which regions of insoles to be modified while fabricating the insole to reduce the pressure during the patient's walks.

REFERENCES

1. Classification of diabetes mellitus [Internet]. 2019. Available from: http://apps.who.int/bookorders.

2. Chan JCN, Lim LL, Wareham NJ, et al. The Lancet Commission on diabetes: using data to transform diabetes care and patient lives. Vol. 396, The Lancet. Lancet Publishing Group; 2020. p. 2019–82.

3. IDF Diabetes Atlas 10th edition [Internet]. Available from: www.diabetesatlas.org

4. Chatterjee S, Khunti K, Davies MJ. Type 2 diabetes. Vol. 389, The Lancet. Lancet Publishing Group; 2017. p. 2239–51.

5. Lin X, Xu Y, Pan X, et al. Global, regional, and national burden and trend of diabetes in 195 countries and territories: an analysis from 1990 to 2025. Sci Rep. 2020 Dec 1;10(1).

6. Nicholas Katsilambros, Konstantinos Makrilakis, Nicholas Tentolouris, et al. Diabetic Foot. In: Liapis Christos D., Balzer K, BVF and F e FJ, editor. Vascular Surgery [Internet]. Springer Berlin Heidelberg; 2007. p. 501–21. Available from: https://doi.org/10.1007/978-3-540-30956-7_45

7. Sinha A, Kulkarni D, Mehendale P. Plantar pressure analysis and customized insoles in diabetic foot ulcer management: Case series. Journal of Diabetology. 2020;11(3):204.

8. Zuñiga J, Moscoso M, Padilla-Huamantinco PG et al. Development of 3D-Printed Orthopedic Insoles for Patients with Diabetes and Evaluation with Electronic Pressure Sensors. Designs (Basel). 2022 Oct 1;6(5).

9. Kumar B, Noor N, Thakur S et al. Shape Memory Polyurethane-Based Smart Polymer Substrates for Physiologically Responsive, Dynamic Pressure (Re) Distribution. ACS Omega. 2019;4(13):15348–58.

10. Jandova S, Mendricky R. Benefits of 3D Printed and Customized Anatomical Footwear Insoles for Plantar Pressure Distribution. 3D Print Addit Manuf. 2022 Dec 1;9(6):547–56.

11. Ma Z, Lin J, Xu X et al. Design and 3D printing of adjustable modulus porous structures for customized diabetic foot insoles. International Journal of Lightweight Materials and Manufacture. 2019 Mar 1;2(1):57–63.

12. Ji-Yong Joo, Young-Kwan Kim. Effects of Customized 3D-printed Insoles on the Kinematics of Flat-footed Walking and Running. Korean Journal of Sport Biomechanics 2018; 28(4): 237-244

13. Cotoros D, Druga C, Stanciu A et al. Experimental Analysis of Corrective Insoles Materials. Macromol Symp. 2021 Apr 1;396(1).

14. Mogan Y, Tun U, Onn Malaysia H et al. Thermoplastic elastomer infill pattern impact on mechanical properties 3D printed customized orthotic insole Mohd Halim

Irwan Ibrahim [Internet]. 2016. Available from: https://www.researchgate.net/publication/304887411

15. Xu R, Wang Z, Ren Z et al. Comparative study of the effects of customized 3D printed insole and prefabricated insole on plantar pressure and comfort in patients with symptomatic flatfoot. Medical Science Monitor. 2019; 25:3510–9.

16. Ntagios M, Dahiya R. 3D Printed Soft and Flexible Insole with Intrinsic Pressure Sensing Capability. IEEE Sens J. 2023 Oct 15;23(20):23995–4003.

17. Majewski C, Perkins A, Faltz D, et al. Design of a 3D printed insole with embedded plantar pressure sensor arrays. In: UbiComp/ISWC 2017 - Adjunct Proceedings of the 2017 ACM International Joint Conference on Pervasive and Ubiquitous Computing and Proceedings of the 2017 ACM International Symposium on Wearable Computers. Association for Computing Machinery, Inc; 2017. p. 261–4.

18. Peker A, Aydin L, Kucuk S et al. Additive manufacturing and biomechanical validation of a patient-specific diabetic insole. Polym Adv Technol. 2020 May 1;31(5):988–96.

19. Mavroidis C, Ranky RG, Sivak ML, et al. Patient-specific ankle-foot orthoses using rapid prototyping. J Neuroeng Rehabil. 2011;8(1).

20. Patil AN, Sarje SH. Additive manufacturing with shape-changing/memory materials: A review on 4D printing technology. Mater Today Proc [Internet]. 2021 Jan 29 [cited 2021 Feb 7]; Available from: https://linkinghub.elsevier.com/retrieve/pii/S2214785320395833

21. Healy A, Dunning DN, Chockalingam N. Materials used for footwear orthoses: A review. Vol. 2, Footwear Science. Taylor and Francis Ltd.; 2010. p. 93–110.

22. Yick KL, Tse CY. Textiles and other materials for orthopedic footwear insoles. In: Handbook of Footwear Design and Manufacture. Elsevier Inc.; 2013. p. 341–71.

23. Patil, AN, Sarje SH. Shape memory and shape recovery characterization of thermoplastic urethane. Advances in Materials and Processing Technologies, 1–16. doi:10.1080/2374068X.2024.2379104

24. Wang Taoxi. Thesis: Elastic shape memory polymeric materials for comfort-fitting footwear. Doctoral Thesis. School of Mechanical and Aerospace Engineering, Nanyang Technological University, Singapore. 2019; Available from: https://hdl.handle.net/10356/104823.

25. Wu XL, Huang WM, Tan HX. Characterization of shape recovery via creeping and shape memory effect in ether-vinyl acetate copolymer (EVA). Journal of Polymer Research. 2013 Aug 1;20(8).

26. Ramezani M, Monroe MBB. Biostable Segmented Thermoplastic Polyurethane Shape Memory Polymers for Smart Biomedical Applications. ACS Appl Polym Mater. 2022 Mar 11;4(3):1956–65.

27. Gensole [Internet]. [cited 2022 Mar 4]. Available from: https://gensole.com/

28. M. Yavuz et al., "Temperature- and Pressure-Regulating Insoles for Prevention of Diabetic Foot Ulcers," Journal of Foot and Ankle Surgery, vol. 59, no. 4, pp. 685–688, Jul. 2020, doi: 10.1053/j.jfas.2019.05.009.

29. Kale DS, Karande GS, Datkhile KD. Diabetic Foot Ulcer in India: Aetiological Trends and Bacterial Diversity. Indian J Endocrinol Metab. 2023 Mar 1;27(2):107–14.

30. Shankhdhar K, Lk S, Shankhdhar U, et al. Diabetic foot problems in India: an overview and potential simple approaches in a developing country. Author information. Vol. 8, Curr Diab Rep. 2008.

31. Thavornyutikarn B, Lertwimol T, Kosorn W, et al. 3D-printing antibacterial composite filaments containing synergistic antibacterial activity of green tea and tannic acid. Polym Adv Technol. 2021 Aug 1;32.

Pupil Detection by Mask-R-CNN Model for the Classification of Relative Afferent Pupillary Defect and Cataract

M. Srinivas
Department of Biomedical Engineering
University College of Engineering(A)
Osmania University, Hyderabad
✉ msrinivas.ou@gmail.com

Anusha Verma Chandraju
Department of Computer Science and Engineering
University of Illinois
Urbana-Champaign, Champaign, USA
✉ canushaverma@gmail.com

D. Suman
Department of Biomedical Engineering
University College of Engineering(A)
Osmania University, Hyderabad
✉ dabbusuman@osmania.ac.in

Anthony Vipin Das
L V Prasad Eye Institute of Medical Sciences (LVPEI)
Hyderabad

ABSTRACT

Diagnosing cataract and Relative Afferent Pupillary Defect (RAPD) uses different tests widely used in clinical practice. However, these are subjective tests and quantification, and automatic detection of these diseases is needed due to the advent of machine Learning- based classification techniques. This study aims to automatically detect cataract and RAPD from pupil images by a machine learning algorithm. A total of 458 subjects were enrolled in the study and categorized into three groups: Cataract, n=178, RAPD, n=120, and Normal, n=160. A pupilometer With a Machine learning algorithm automates the process end to end, from capturing the eye images to pupil detection and subsequent classification into cataract, RAPD and Normal. The framework uses a custom-trained pupil detection Mask-R-CNN model with a mean average precision of 90.66, while the Random Forest classifier used for the eye disorder classification outperforms the other base models in classification performance with 94.7 percent accuracy.

KEYWORDS : *Cataract, RAPD, Pupil detection, Random Forest Classifier.*

INTRODUCTION

The World Health Organization reveals that 2.2 billion people worldwide have vision impairments that affect the patient's daily activities and cause discomfort, pain, and irritation[1]. This statistic highlights the essential need for early detection of ophthalmic disorders. Getting an early diagnosis is vital for rapid treatment to stop the progression of eye illness and minimise vision loss. Cataracts and RAPD are typical eye disorders that affect a patient's overall health and visual acuity. Cataracts mainly cloud the eye's natural lens, producing hazy or blurry vision [2]. In cataracts, The normally clear and transparent lens becomes progressively opaque, impeding light passage and causing visual impairment. On the other hand, Relative Afferent Pupillary Defect (RAPD) refers to an irregular pupillary response that highlights a distinction in how the pupils of the eyes react [3]. It often signifies underlying issues with the optic nerve or retina. Both these conditions are more associated with the elderly population. The early detection of these diseases is crucial since it could lead to worsening vision and more severe symptoms if left untreated.

RAPD is diagnosed from the pupil's images by comparing the pupillary response between the subject's two eyes [4]. A pupil, a black circular aperture in the middle of the iris, controls the quantity of light that enters the eye. Medical practitioners may get important information about various eye problems and neurological disorders by analyzing the features of the pupil, such as its size and how it responds to light stimuli. A Pupilometer is a specialized instrument used in the field of Ophthalmology to measure and examine the size of the pupil in addition to its reaction [5]. A Pupilometer

takes objective measurements and provides quantitative data, enabling reliable evaluations and comparisons. A disorder known as "RAPD" is characterized by an aberrant pupillary response in one eye compared to the other. It is often an indicator of malfunction in the optic nerve and other underlying neurological problems[6-9]. In addition, pupilometers are useful when determining cataracts' effect on pupil functioning [10]. According to Volpe et al. [11], despite diminished sensitivity, the pupillometer device can differentiate between healthy persons and patients with a Relative Afferent Pupillary Defect (RAPD) larger than 0.9 log units of neutral density filter. This is the case even if the RAPD threshold is higher for the patients than for healthy individuals. The research demonstrates that there is a statistically significant difference between normal people and those who have RAPD. A statistically significant association exists between patients with real "Afferent Pupillary Defects "(APD) and participants with RAPD triggered using neutral density filters. Cohen et al. [12] constructed a unique computerized pupillometer and studied pupillary responses in RAPD patients by delivering varied illumination intensities (LUX) to both eyes. This was done to test the pupillometer's accuracy. They discovered that detecting RAPD by the device agrees with the swinging flash test method. The research concluded that the device had excellent sensitivity and specificity in identifying the existence and degree of RAPD. As a result, it is the only device that is accessible and can be used for such detection.

Using a binocular television pupillometer, the researcher Cox et al. [13] recorded the pupillary responses of normal people after triggering RAPD using neutral density filters and analyzed the data. After studying and contrasting many RAPD indicators, such as minimum size, final size, and redilatation amplitude, the researchers concluded that contraction amplitude was the most accurate measurement. Radzius et al. [14] used an infrared pupilometer to assess the pupil's diameter and change in response to a light stimulus. The values that were measured were quite similar to those that were obtained using photographic measurements. Patients with optic atrophy due to unilateral open-angle glaucoma were the subjects of research that Kalaboukhova et al. [15] carried out. This group wanted to create a novel method for analyzing RAPD and finding the optimal stimulus settings for RAPD identification in these individuals. Additionally, to improve this method, They evaluated many different sets of stimulus-pause

combinations using a pupillometer that had been custom-built for them. According to the results of their study, the optimal conditions for diagnosing glaucoma were a light intensity of 1000 Lux combined with a stimulation length of 0.5 seconds and a pause time of 1 second.

Cataracts are cloudings that form on the eye's natural lens, which reduces one's ability to see [16]. A pupilometer may assist in determining the extent of the cataract by carefully measuring the size and responsiveness of the pupil [17]. This information can then guide judgments about needing surgical surgery [18].

The first step in diagnosing cataracts from images of the pupil is often capturing the image [19]. The use of specialist equipment such as a slit lamp or specific eye imaging cameras is required to produce images of the pupils that have a high resolution. These devices take precise eye images, enabling the lens and the pupil to be examined in more detail. Pre-processing procedures are done after the images have been captured to improve the image quality and eliminate any noise or artefacts that may have been present. Resizing the picture, removing noise, and altering the contrast are common pre-processing operations. Following these procedures guarantees that the subsequent analysis will be carried out on images of high quality. The pupil images are analyzed to extract relevant characteristics that may indicate the existence of cataracts[20]. Variations in the pixel intensities may result from cataracts since they can cause light to scatter or refract irregularly inside the eye. This can generate blurriness. The quantity of light scattering and its extent will be measured to assist in diagnosing cataracts. In addition, the shape of the pupil may be examined to look for any anomalies or deformations. Cataracts have been known to provide the appearance of a deformed or unequal pupil. A further indication that cataracts may be found by analyzing the shape of the pupil in the images. The pupil images can be analyzed using machine learning or deep learning techniques, and the results can be categorized as healthy or symptomatic of cataracts. These methods include training a model using a labelled dataset of pupil images, where the labels indicate whether or not cataracts are present in the subject's eye. Due to its capacity to learn and extract information from images, "Convolutional Neural Networks" (CNNs) are often utilized in this application. The model must be verified and assessed using a different dataset after training.

In computer vision and image processing, pupil detection is a well-researched subject. Akinlar, Cuneyt et al. [21] focused on accurately segmenting the pupil by proposing a Convolutional Neural Network (CNN) based approach. This involves training a CNN to classify input as pupil using multiple convolutional and pooling layers. The second stage consists of fitting an ellipse to the segmented pupil region, using an ellipse fit error regularization term to optimize and enforce geometric constraints. Khan et al. [22] present a method for pupil localization by detecting faces, using colour based segmentation and morphological operations, and localizing the pupil using a Convolutional Neural Network (CNN). The eye centre is estimated by calculating the centroid of the segmented pupil region, and a refinement step using Gaussian Mixture Models (GMMs) improves accuracy. The method outperforms other methods' accuracy and robustness, making it suitable for eye tracking, human-computer interaction, and bio-metrics applications. Lee, Jeon, and Song [23] developed a deep learning-based approach for pupil detection to improve eye-tracking systems' speed and accuracy. The method involves a convolutional neural network (CNN) to classify a pixel classification as a pupil and a post-processing algorithm to refine predictions. The authors introduce a circular voting scheme considering nearby confidence scores to determine accurate centre location. Wolfgang Fuhl et al. [24] developed a CNN-based approach called PupilNet to improve pupil detection using convolutional neural networks. The network uses convolutional and pooling layers and fully connected layers for classification. It uses a binary cross-entropy loss function for training and incorporates image pre-processing techniques like adaptive thresholding, edge detection, and morphological operations.

Pavani Tripathi et al [25] proposed a novel method for detecting cataracts using NIR eye images. The approach combines deep learning techniques with feature extraction and classification algorithms involving pre-processing, feature extraction, and classification. The authors use a pre-trained convolutional neural network (CNN) and an SVM classifier to classify the images into normal or cataractous categories. Tasmina Tasin and Mohammad Ashfak Habib et al [26] explored the usage of a random forest classifier for cataract detection.

The method involves image pre-processing, feature extraction, and classification, with the extracted features used as input to a random forest classifier. Renato R. Maaliw et al [27] developed a method for detecting and grading cataracts using ensemble neural networks and transfer learning techniques. The procedure involves image pre-processing, feature extraction, ensemble modelling, and grading. The authors use pre-trained CNNs for feature extraction and fine-tuning the CNNs for specific cataract grading categories. The ensemble of neural networks combines predictions to make final detection and grading decisions.

Though the diagnostic methods for RAPD and Cataracts exist, quantifying these diseases with accuracy and automatic detection is still not explored. Limited literature is available on the automatic detection of RAPD and cataracts by machine learning model with pupilometer images. This research proposes a framework for capturing pupil images with a pupilometer under a visual stimulus and automatically detecting the pupil's response. Diagnosis of Cataract and RAPD uses different tests widely used in clinical practice. However, a common method of using pupilometer images with a machine learning application is being proposed in this study. This study aims to automatically detect Cataract and RAPD from pupil images by a machine learning algorithm. A total of 458 subjects were enrolled in the study and categorized into three groups: Cataract, n=178, RAPD, n=120, and Normal, n=160. A pupilometer With a Machine learning algorithm automates the process end to end, from capturing the eye images to pupil detection and subsequent classification into cataract, RAPD and Normal. For pupil detection, we initially planned to use an instance segmentation model, which would give both the detection of the pupil and the edges of the detected pupil. Instead of only a bounding box, the Mask R-CNN model was implemented after reviewing the existing architecture literature. It is an advanced instance segmentation model that combines object detection and pixel-level segmentation. The detectron2 framework by Facebook was used to build and train this model using our custom dataset.

METHODOLOGY

The study involves the detection of RAPD and cataracts from the pupil images acquired using a pupilometer

under different conditions of an external stimulus. It involves five steps, shown in Fig.1. which are

1. Data Collection
2. Data annotation
3. Pupil detection
4. Classification data creation
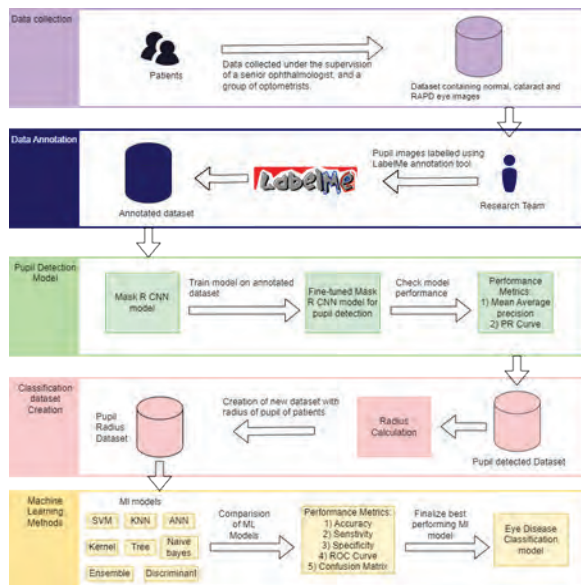5. Machine learning methods for classification.

Fig. 1. Methodology

Data Collection

This study aims to automatically detect cataract and RAPD from pupil images by a machine learning algorithm. Subjects enrolled in the study are from two hospitals, L V Prasad Eye Institute (LVPEI), Hyderabad, and Urban Primary Health Clinic (UPHC), Lalapet, under Telangana Kanti Velugu. The institutional ethical committee has approved the protocol of the study. Before inducting them into the study, written consent from all the participants was taken. Initial data collection started with the LVPEI under the supervision of a senior ophthalmologist and a group of optometrists. Later, the study also included data collected under the "Telangana Kanti Velugu program," a mass screening of eye diseases, a Government initiative. With permission from the District Med- ical and Health Officer (DMHO), Hyderabad, the data collection was performed for 30 days from 20/02/2023 to 11/04/2023. During this period, 1256 subjects visited the camp, and a team

of ophthalmologists and optometrists conducted the initial clinical investigation to identify the ophthalmic disorders. Out of 1256 subjects, 458 topics were enrolled in the study and categorized into three groups: Cataract, n=178, RAPD, n=120, and Normal, n=160. They were 18 years or older with a mean age of 46±7 and had the best visual acuity of 6/36 or better in the normal group, 54±8 having blurred vision in the Cataract group and RAPD. Exclusion criteria included are those with retinal abnormalities, ocular disorders, cloudy corneas, prior surgeries, and the use of miotic drugs. A pupilometer is used for obtaining the pupil images of the subjects under two different conditions, "under visual stimulus" and "without visual stimulus". This is similar to a swinging flash test to obtain the pupil's response to a visual stimulus. In our previous study, a pupillometer was designed and developed, and its accuracy in detecting RAPD is also validated against the clinical settings[12]. The experimental setup for the data collection consists of a pupillometer, intuvision fundus cam, visual acuity test, and auto refractometer, as shown in Fig.2. The initial clinical evaluation consists of a visual acuity test, swinging flash test, and Auto refractometer. From the results of these tests, participants are divided into three groups: Cataract, RAPD, and Normal. Among 1256 participants, 178 suffer from cataracts, 120 are diagnosed with RAPD, and 958 are normal. To build the ML model and uniformity in the data related to each group, only 160 normal subjects were considered to avoid errors in classification. The pupil images are acquired from each group of subjects under and without stimulus.

Fig. 2. Experimental setup for Data Collection during Telangana Kantivelugu program
1-Ophthalmologist, 2-Intuvision Fundus camera, 3-Optometrist, 4-Participant, 5-Pupilometer, 6-Attendant

The pupilometer obtains high-resolution images of the pupil. Typically, these images were acquired in a sterile setting with the proper lighting. Pre-processing techniques were applied to the obtained pupil images to improve image quality and eliminate artefacts or noise. Image enhancement techniques such as brightness, contrast, and sharpness were employed to ensure the quality of the image. Image processing methods separate the pupil area from the rest of the image and segment it accordingly. This stage contributes to the study by helping to concentrate, especially on the pupil's reaction. Analyzing the segmented areas in the images allows for the measurement of the diameter of each pupil. The variations in pupil size in response to varying illumination levels are used to determine each eye's pupillary response. Analysis of pupil size when light is shown to each eye and asymmetrical changes in pupil size by comparing the pupillary responses of both eyes is performed. The existence of RAPD was determined when there is a discernible variation in the degree to which each eye contracts or dilates. The asymmetrical reaction to RAPD was assessed or scored according to the response's degree of severity or amplitude. Ophthalmologists and optometrists have analyzed and interpreted pupil images during the swinging flash test performed on them. Their clinical competence was used for assessing and diagnosing RAPD and the severity of the disease from the pupil's diameter in response to the light stimulus.

This study uses these pupil images, and subsequently, a machine-learning algorithm was built to detect RAPD and cataracts. Sample images of the normal subjects without stimulus and under visual stimulation are shown in Fig.3.(a) and Fig.3.(b) of the RAPD patients without stimulus and under visual stimulus are shown in Fig.4.(a) and Fig.4.(b). The sample images of Cataract pa- tients without stimulus and under visual stimulation are shown in Fig.5.(a) and Fig.5.(b).

Fig. 3. (a)Normal subject's Right Eye without stimulus (b) Normal subject's Right Eye with stimulus
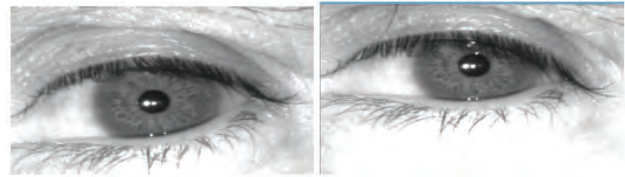
Fig. 4. (a)RAPD subject's right eye without stimulus (b) RAPD subject's right eye with stimulus
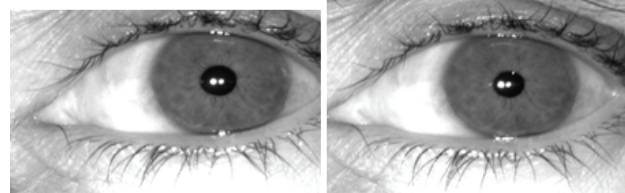
Fig. 5. (a) Cataract Patient's Right Eye without stimulus (b) Cataract Patient's Right Eye with stimulus

Data annotation

The pupil image datasets collected from the three groups are used as the input for the deep learning-based pupil detection model for finding the radius of the pupil under investigation. These data sets are initially annotated by using LabelMe software. LabelMe is an open-source Python tool for annotating the region of interest in an image. All the images of the three datasets and for each subject, four images right eye with stimulus, without stimulus, left eye with stimulus, left eye without stimulus of the Cataract, n=178*4, RAPD, n=120*4, and Normal, n=160*4 are considered for the model. A total of 1832 pupil images are annotated, and 75 per cent of these images, 1374, are used for the training. The remaining 458 prints are used for testing the pupil detection model.

Pupil Detection

The study's main objective is to detect the pupil from the eye images acquired using a pupilometer with and without stimulus. A dataset of Pupil images is prepared from three groups of participants consisting of four images of each subject listed as the left eye with stimulus, left eye without stimulus, right eye with stimulus, and right eye without stimulus. A single dataset is prepared with all theimages of three groups under different conditions to make it more dynamic in the detection of pupil diameter. It is ensured that the model must accurately predict pupil diameter irrespective of

whether a participant is normal or diseased. Var- ious machine learning models ate tested for performance by comparing metrics such as accuracy, sensitivity and specificity. For the task of pupil detection, we initially planned to use an instance segmentation model, which would give both the detection of the pupil and also the edges of the detected pupil instead of only a bounding box. The Mask R CNN model was implemented after reviewing the existing architecture literature. It is an advanced instance segmentation model that combines object detection and pixel-level segmentation. The detectron2 framework by Facebook was used to build and train this model using our custom dataset mentioned in the above section.

The Mask R-CNN model is shown in Fig.6. consists of a multi-stage architecture with a backbone network, a region proposal network (RPN), and a mask head.
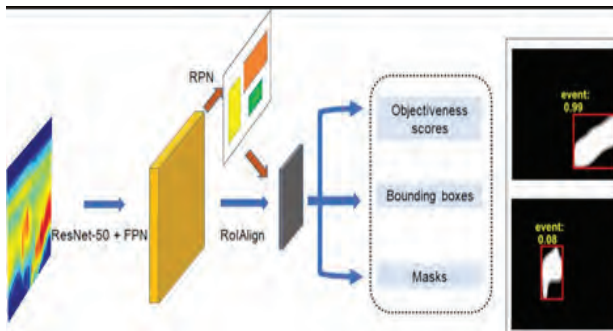

Fig. 6. Mask R CNN Architecture

The backbone network for Mask R-CNN is a feature extractor, conventionally a convolutional neural network (CNN) such as ResNet or VGG. The model used in this project is the ResNet 50 backbone.

Convolutional layers often process the input image and extract high-level information. These layers carry out convolutional operations, which are described mathematically as:

output[i, j, k] = (inputpatch *filter) + bias[k]

Output[i, j, k] represents the feature map's output value at position (i, j, k). filter means the convolutional filter

input patch is a local patch of the input image bias[k] is an optional bias term for each filter.

The RPN is the part of the architecture that creates the region proposals us- ing the feature maps it receives

from the backbone network. The bounding box offsets (x, y, w, h) and the objectness score (P(object)) are the two parameters that the RPN predicts for each anchor box.

Objectness score = P(object) = Probability of object presence Bounding box offsets= x, y, w, h = Adjustments to anchor box

The mask head is then given a list of chosen RPN regions. The mask head then carries out pixel-wise segmentation and refines the bounding box predic- tions. By combining these mathematical formulas with the power of convolu- tional neural networks, Mask R-CNN achieves impressive results in object de- tection and pixel-level segmentation tasks.

Here, for training, the training dataset consists of annotated 1832 pupil im- ages and 75 per cent of these images 1374, are used for the training, and the remaining 458 images are used for testing purposes of the pupil detection model.

Radius Calculation

Radius calculation from the detected pupil is achieved through the predicted mask from the trained model. Using In-Built OpenCV definitions, the countor of the pupil is found using the find Countour method and then finding the minimum enclosing circle. After seeing the smallest circle that encloses the generated mask, the circle's radius is detected, shown in Fig.7 and Fig.8 . This determines the radius of the pupil in the pixel metric. The pupil diameters in pixel metric of a few subjects of the three classes are given in Table 1.
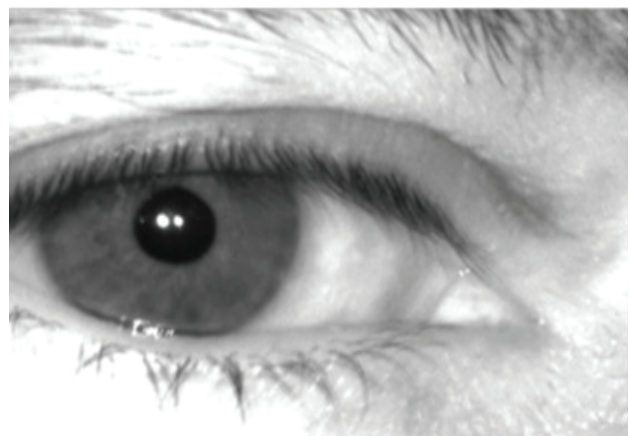

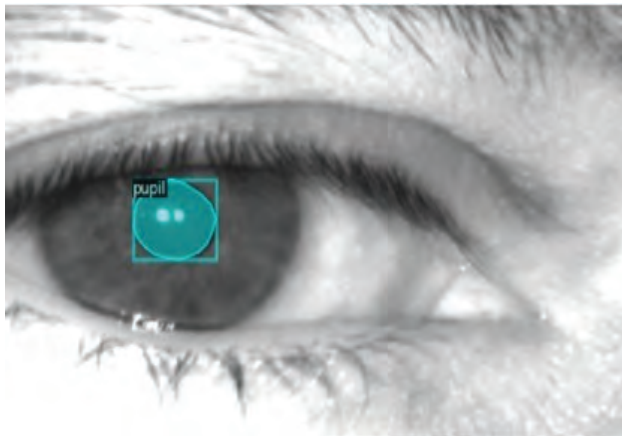**Fig. 7. Sample Eye image from dataset**

Fig. 8. Detected pupil

Table 1: Pupil diameters in Pixels of three groups under different conditions

S no	DLWS	DLS	DRWS	DRS	Class
1	67.64893	43.28165	56.48461	48.6622	normal
2	54.74039	42.31187	58.03183	46.93131	normal
3	53.76777	38.47087	52.28059	45.62082	normal
4	54.39921	31.97665	46.06042	32.26851	normal
5	30.11209	27.28563	30.51704	26.82421	normal
6	49.04235	38.14784	60.70614	45.1277	Cataract
7	55.54428	45.01398	55.10962	40.20582	Cataract
8	52.06976	37.07435	40.89325	33.45529	Cataract
9	56.39602	37.67018	44.64033	32.9622	Cataract
10	52.66175	37.26268	41.10059	34.03317	Cataract
11	65.15629	66.50619	68.18368	69.02608	RAPD
12	37.07663	36.64663	34.71321	37.57951	RAPD
13	40.94965	41.7802	41.8161	42.18447	RAPD
14	48.93117	48.33096	61.20467	62.40731	RAPD
15	64.77856	64.33775	68.47234	67.2552	RAPD

DLWS-Diameter of the left eye's pupil without stimulus
DLS-Diameter of the left eye's pupil with stimulus

DRWS-Diameter of the Right eye's pupil without stimulus DRS-Diameter of the Right eye's pupil with stimulus

Eye disease Classification

After calculating the radius of the pupil for the left and right eye with and without stimulus, training and testing data are created for the classifier model. The class distribution of subjects considered in the study is shown in Table 2.

Table 2: Classification Class Distribution

Subjects	Training	Testing	Total
Cataract	134	44	178
RAPD	90	30	120
Normal	121	40	161
Total	344	114	458

A multi-label classification model is created with multiple feature inputs as per Table.1.being the four radius and the predicted class being the eye condition prediction. Machine learning models are implemented on the train and test data in python for the classification of diseases. The classification models use 344 training data points and 115 testing data points. Eight machine learning models, SVM, KNN, Decision Tree, LDA (Linear Discriminant Analysis), Naive Bayes, Gradient Boosting Classifier, Random Forest Classifier and ANN, were used to detect the best-performing classification model.

Results and Discussions

The pupil detection model results are analyzed by using the mean average precision metric (mAP), which helps to determine the performance of an instance segmentation model and the accuracy of edge prediction.

The study has achieved the mAP metric for the bounding box prediction is 87.79, as shown in Table.3. Since the prediction of pupil is significant, a circular object, the bounding box prediction accuracy is lesser.

Table 3: Mask R-CNN performance for bounding box predictions

Performance metric and bounding box values	
AP	87.79766045177202
AP50	98.78758709204256
AP75	98.78758709204256
APs	70.0
APm	87.2493134206769
APl	92.17660871397331
AP-pupil	87.79766045177202

where

AP - Average PrecisionAP50 - Average Precision at 50 percent IoU threshold

AP75 - Average Precision at 75 percent IoU threshold
APs - Average Precision for small objects

APm - Average Precision for medium objects APl - Average Precision for large objects

In Table 4, the mAP metric for the segmented prediction achieved 90.66. This shows that the model performs well predicting the pupil's edges in the given image. Further, it was also explored that when the Intersection over Union (IOU) thresholds are 50 per cent and 75 per cent, the model performs better, with mAP reaching up to 98.8 for both metrics. IOU measures how well the prediction overlaps with the ground-truth segmentation. A 50 per cent threshold indicates that there must be at least a 50 per cent overlap for a case to be classified as a true positive.

Table 4: Mask R-CNN performance for Segmented values predictions

Performance metric	Segmented values
AP	90.66143674481549
AP50	98.78758709204256
AP75	98.78758709204256
APs	80.0
APm	89.74446141627017
APl	98.38067891296171
AP-pupil	90.66143674481549

where

AP - Average Precision

AP50 - Average Precision at 50 percent IoU threshold
AP75 - Average Precision at 75 percent IoU threshold
APs - Average Precision for small objects

APm - Average Precision for medium objects APl - Average Precision for large objects

In Fig 9, the precision-recall curve of the pupil detection model shows the trade-off between precision and recall for a binary classification model. This study has achieved a satisfactory balance between the two metrics for different thresholds for pupil detection. Hence, the study contributed to finding the pupil diameter by the Mask R-CNN model, which is significant in detecting pupil diameter.
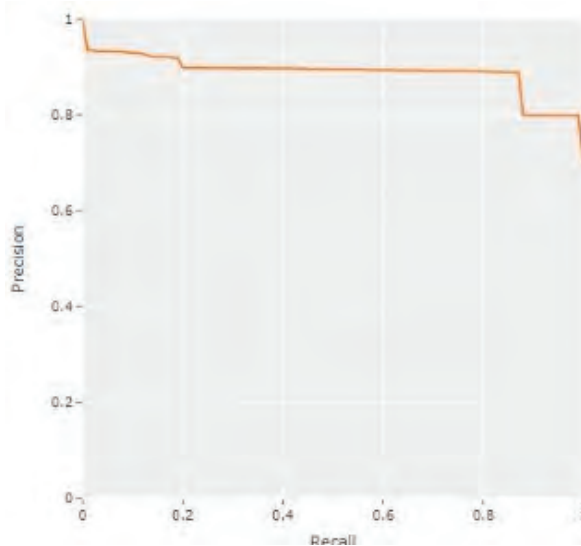
Fig. 9. PR Curve for pupil detection

The results of the machine learning model performance on the training data is an important performance metric to understand since it allows checking for possible overfitting or underfitting of the model.

In table 5, the accuracies of 8 machine learning models are recorded. Upon comparison, it becomes evident that the Random Forest Classifier outperforms the other models with the highest accuracy.

Table 5: Comparision of machine learning classifiers

Classifier Model	Accuracy(percent)
SVM	70.43
KNN	89.56
DT	93.91
LDA	68.69
NB	55.65
GB	93.04
ANN	65.21
RF	94.78

where

SVM - Support Vector Machine KNN- K Nearest Neighbour DT - Decision tree

LDA - Linear Discriminant Analysis

NB - Naive Bayes

GB - Gradient Boosting

ANN - Artificial Neural Network RF- Random Forest

The analysis begins with the training dataset outcomes using the random forest classifier. Subsequently, in Fig 10, the confusion matrix is leveraged to compute pivotal metrics, particularly specificity and sensitivity.
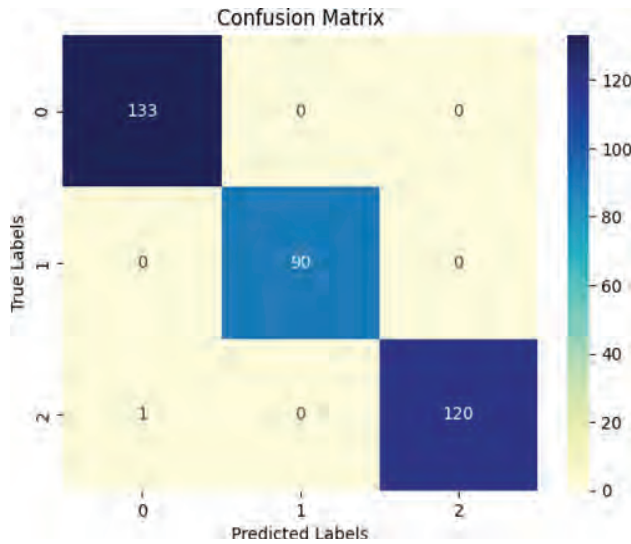
Fig. 10. Confusion matrix for training dataset

True Negative (TN) signifies the accurate identification of negative cases. False Positive (FP) denotes negative cases incorrectly labeled as positive. False Negative (FN) indicates positive cases mistakenly classified as negative. True Positive (TP) represents correctly identified positive instances. In Table 6, these metrics are listed for each of the classification class.

Table 6: Performance metrics for Classification Classes of Training Dataset

Class	TP	FP	FN	TN
Cataract	133	1	0	210
RAPD	90	0	0	254
Normal	120	0	1	223

Specificity and sensitivity are key factors in evaluating classification models. Specificity highlights the model's accuracy in identifying instances of the negative class. It represents the proportion of actual negatives that the model correctly classifies. In contrast, sensitivity assesses the model's effectiveness in detecting instances of the positive class. It signifies the ratio of actual positives that the model accurately identifies.

In Table 7, the RAPD class has the highest accuracy of prediction while the other classes are similar in accuracy. The specificity and sensitivity values are satisfactory, although the normal class could use some improvement with the detection of positive cases.

Table 7: Additional performance metrics of classification class on training dataset

Class	Accuracy	Specificity	Sensitivity	F1-Score
Cataract	0.997	0.995	1	1
RAPD	1	1	1	1
Normal	0.997	1	0.992	1

We take a look at the results given for the testing dataset on the trained random forest classifier.
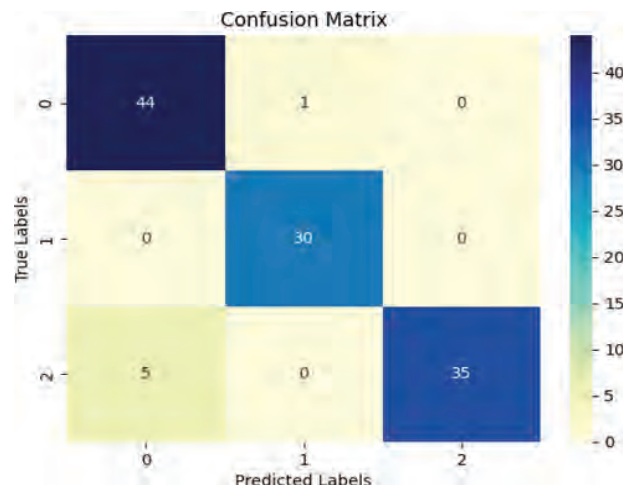
Fig. 11. Confusion matrix for testing dataset

Table 8: Performance metrics of classification class on testing dataset

Class	TP	FP	FN	TN
Cataract	44	5	1	65
RAPD	30	1	0	84
Normal	35	0	5	74

In Table 9, the RAPD class is again performing with the highest accuracy of prediction with Normal and cataract being followed respectively in terms of accuracy. The sensitivity of the normal class could be better improved since it is 0.875 but the specificity of the normal class is perfect; ie; the model detects the negative cases very well. The cataract class although not achieving perfect sensitivity nor specificity; performs very well.

Table 9: Additional Performance metrics of classification class on testing dataset

Class	Accuracy	Specificity	Sensitivity	F1 score
Cataract	0.9478	0.928	0.977	0.94
RAPD	0.9913	0.988	1	0.98
Normal	0.9561	1	0.875	0.93

The AUC-ROC curve of the Random Forest Classifier shows us the tradeoff between the True Positive Rate (The senstivity of the model) vs the false positive rate(1 - Specificity of the model). In fig 12, we see that all three classes perform satisfactorily with RAPD and Normal getting a AUC score of 1 over the thresholds and Cataract getting a AUC score of 0.98.

This study has contributed to the machine learning-based application for automatically detecting RAPD and cataracts from pupil images under visual stimulus.
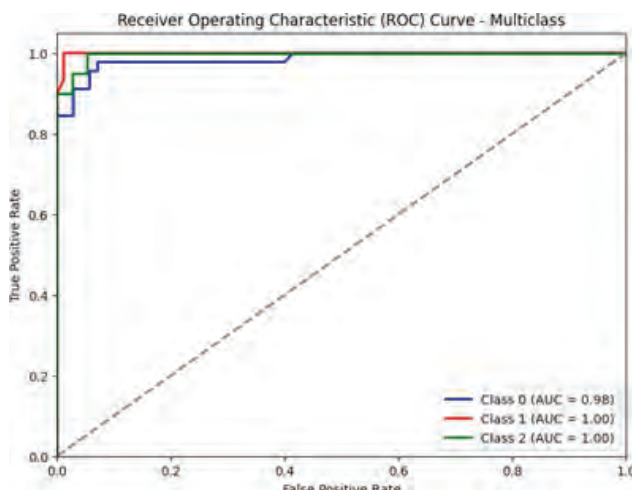
Fig. 12. AUC-ROC Curve for testing dataset

Table 10 depicts the comparative analysis of the recent studies related to our study. Very meagre literature is available on machine learning with the combination of Cataract and RAPD with the pupil images. Several studies are available on machine learning models that use either RAPD data sets or Cataracts but don't have the combination of these two classes. This is the main contribution of our study, and it uses pupil images to classify the two disease classes: cataract and RAPD. A study uses the high-resolution fundus images and IDRiD database with a 16-layer DNN classifier to classify cataract disease. This study has an ac- curacy of 99.13 with an F1 score of 99.07 [30]. Researchers used 1130 cataract and non-cataract fundus images and developed a CataractNet classifier to predict cataract disease. This study has reported an accuracy of 99.13 with an F1 score of 99 [31]. A study reported an accuracy of 99.0 with the F1 score of 99.0 in detecting Cataract from a dataset of eye images with the ImageNet classifier [32]. Even though the studies mentioned above reported a better accuracy than our model, the basic difference is our model is being built on a multiclass model with the three classes Normal, Cataract, and RAPD. Hence, the classification performance of our model is less than the other studies where they use only two classes, normal and either RAPD or Cataract. All the other studies reported the use of fundus images as the input for the detection of cataract and pupil images for the detection of RAPD. But none of them classify both diseases; this is the main contribution of our study. Another difference is that the model used in the study uses the pupil images as the input for both the disease classes, namely RAPD and Cataract, this makes the system more reliable, accurate, and dynamic. The performance of our model is reasonable in terms of accuracy, sensitivity, and specificity and meets the standards of classification systems in general, which will be significant in the detection of RAPD and Cataract.

Table 10: Discussion for cataract detection

Ref	Description	Dataset	Classifier	Accuracy	F1 score
[29]	Used a RAPD detecting approach using modifications done to the AlexNet object detection model	64 test cases	RAPDNet	90.6	-
[30]	Used a novel deep learning network to detect cataract in fundus images with comparision drawn to leading VGG16, VGG19 and Res Net-50 models; performing better than these base models in terms of accuracy and runtime	high reso- lution fundus +the fundus image regis- tration dataset++ colour fundus+ DRIVE IDRiD	16 layer DNN	99.13	99.07

[31]	Uses a novel 16 layer network architecture to detect cataract for computation optimization	cataract and non-cataract fundus	CataractNet	99.13	99
[32]	Uses Modified DenseNet model for cataract identification with a 10 percent increase in performance to base model	Data set of 5000 eye images	ImageNet	99	99
Our model	Used a fine tuned maskrcnn model for pupil detection and random forest for eye disease detection	Custom pupil dataset	Mask R- CNN+ Random Forest classifier	94.8	94

CONCLUSIONS

Then, we developed a fine-tuned image detection model to identify the pupil in the eye's image and determine its radius in pixels. After going through the leading instance segmentation models, it is decided on using the Mask R CNN model implemented by the detectron2 framework by Facebook [3]. The pupil diameters detected are further used for classifying into cataract, RAPD and normal by various classifiers. It is found that the Random Forest Classifier is best among all the classifiers to detect Cataract and RAPD.

Our proposed framework has recommended an end-to-end methodology for detecting cataracts and RAPD in patients. Through this project, we have collected a custom dataset containing eye images from two different eye diseases with the eyes of normal patients. With our custom-trained Mask R-CNN model for pupil detection on our dataset, we can get a mAP of 90.66, which is satisfactory, and the accuracy of the eye disease classification model for eye conditions, which is 95.4 per cent. After extensive evaluation of various machine learning techniques, the Random Forest Classifier gives the best classification accuracy performance.

The future work for the project lies on creating an application that allows for the automatic usage of the method end-to-end on a deployed application that is accessible to hospitals.

ACKNOWLEDGEMENTS

REFERENCES

1. WHO. World report on vision. 2019. 180 p.

2. Allen, David, and Abhay Vasavada. "Cataract and surgery for cataract." BMJ (Clin- ical research ed.) vol. 333,7559 (2006): 128-32. doi:10.1136/bmj.333.7559.128

3. Broadway, David C. "How to test for a relative afferent pupillary defect (RAPD)." Community eye health vol. 25,79-80 (2012): 58-9.

4. Donaldson, Laura, Ryan Rebello, and Amadeo R. Rodriguez. "Relative Afferent Pupillary Defect with Normal Vision: Unique Localisation to the Contralateral Brachium of the Superior Colliculus." Neuro-Ophthalmology 44, no. 2 (2020): 128-130.

5. Bindiganavale, Megha P., and Heather E. Moss. "Development and implementation of a handheld pupillometer for detection of optic neuropathies." Current eye research 46, no. 9 (2021): 1432-1435.

6. Piaggio, Davide, Georgy Namm, Paolo Melillo, Francesca Simonelli, Ernesto Iadanza, and Leandro Pecchia. "Pupillometry via smartphone for low-resource set- tings." biocybernetics and biomedical engineering 41, no. 3 (2021): 891-902.

7. Lussier, Bethany L., DaiWai M. Olson, and Venkatesh Aiyagari. "Automated pupillometry in neurocritical care: research and practice." Current neurology and neuro- science reports 19 (2019): 1-11.

8. Sarker, Prithul, Nasif Zaman, and Alireza Tavakkoli. "VR-SFT: Reproducing Swinging Flashlight Test in Virtual Reality to Detect Relative Afferent Pupillary Defect." In Advances in Visual Computing: 17th International Symposium, ISVC 2022, San Diego, CA, USA, October 3–5, 2022, Proceedings, Part II, pp. 193-204. Cham: Springer Nature Switzerland, 2022.

9.   Vairamani, Ajantha Devi. "Detection and diagnosis of diseases by feature extraction and analysis on fundus images using deep learning techniques." In Computational Methods and Deep Learning for Ophthalmology, pp. 211-227. Academic Press, 2023.

10. Nakamura, Makoto, Mari Sakamoto, Kaori Ueda, Mina Okuda, Fumio Takano, and Yuko Yamada-Nakanishi. "Detection of Relative Afferent Pupillary Defect and Its Correlation with Structural and Functional Asymmetry in Patients with Glaucoma Using Hitomiru, a Novel Hand-Held Pupillometer." Journal of Clinical Medicine 12, no. 12 (2023): 3936.

11. Volpe, Nicholas J., et al. "Portable pupillography of the swinging flashlight test to detect afferent pupillary defects." Ophthalmology 107.10 (2000): 1913-1921 1005-14-740117

12. Cohen, Liza M., et al. "A novel computerized portable pupillometer detects and quantifies relative afferent pupillary defects." Current eye research 40.11 (2015): 1120-1127

13. Cox, Terry A. "Pupillographic characteristics of simulated relative afferent pupil- lary defects." Investigative ophthalmology visual science 30.6 (1989): 1127-1131

14. Radzius, Aleksandras, et al. "A portable pupilometer system for measuring pupil- lary size and light reflex." Behavior Research Methods, Instruments, Computers 21.6 (1989): 611-618

15. Kalaboukhova, Lada, Vanja Fridhammar, and Bertil Lindblom. "An objective method for measuring relative afferent pupillary defect in glaucomatous optic neu- ropathy—stimulus optimization." Neuro-ophthalmology 30.1 (2006): 7-15

16. Kebapcı, Ayda, and Serpil Topcu. "Interrater reliability in pupillary assessment among intensive care nurses." Intensive and Critical Care Nursing 58 (2020): 102801.

17. Hayashi, Ken, Motoaki Yoshida, Sosuke Ishiyama, and Akira Hirata. "Pupillary light response after cataract surgery in healthy patients." Japanese Journal of Oph- thalmology 65, no. 5 (2021): 616-623.

18. Giede-Jeppe, Antje, Maximilian I. Spru¨gel, Hagen B. Huttner, Matthias Borutta, Joji B. Kuramatsu, Philip Hoelter, Tobias Engelhorn, Stefan Schwab, and Julia Koehn. "Automated pupillometry identifies absence of intracranial pressure eleva- tion in intracerebral hemorrhage patients." Neurocritical Care 35 (2021): 210-220.

19. Kumar, Yogesh, and Surbhi Gupta. "Deep transfer learning approaches to predict glaucoma, cataract, choroidal neovascularization, diabetic macular edema, drusen and healthy eyes: an experimental review." Archives of Computational Methods in Engineering 30, no. 1 (2023): 521-541.

20. Heruye, Segewkal H., Leonce N. Maffofou Nkenyi, Neetu U. Singh, Dariush Yalzadeh, Kalu K. Ngele, Ya-Fatou Njie-Mbye, Sunny E. Ohia, and Catherine A. Opere. "Current trends in the pharmacotherapy of cataracts." Pharmaceuticals 13, no. 1 (2020): 15.

21. Akinlar, Cuneyt, Hatice Kubra Kucukkartal, and Cihan Topal. "Accurate cnn- based pupil segmentation with an ellipse fit error regularization term." Expert Sys- tems with Applications 188 (2022): 116004.

22. Khan, Wasiq, et al. "Pupil localisation and eye centre estimation using machine learning and computer vision." Sensors 20.13 (2020): 3785.

23. Lee, Kang Il, Jung Ho Jeon, and Byung Cheol Song. "Deep learning-based pupil center detection for fast and accurate eye tracking system." Computer Vision–ECCV 2020: 16th European Conference, Glasgow, UK, August 23–28, 2020, Proceedings, Part XIX 16. Springer International Publishing, 2020.

24. Fuhl, Wolfgang, et al. "Pupilnet: Convolutional neural networks for robust pupil detection." arXiv preprint arXiv:1601.04902 (2016).

25. Tripathi, Pavani, et al. "MTCD: Cataract detection via near infrared eye images." Computer Vision and Image Understanding 214 (2022): 103303.

26. Tasin, Tasmina, and Mohammad Ashfak Habib. "Computer-Aided Cataract Detec- tion Using Random Forest Classifier." Proceedings of the International Conference on Big Data, IoT, and Machine Learning: BIM 2021. Springer Singapore, 2022.

27. Maaliw, Renato R., et al. "Cataract detection and grading using ensemble neural networks and transfer learning." 2022 IEEE 13th Annual Information Technology, Electronics and Mobile Communication Conference (IEMCON). IEEE, 2022.

28.   Sarki, Rubina, et al. "Automated detection of mild and multi-class diabetic eye diseases using deep learning." Health Information Science and Systems 8.1 (2020): 32.

29.   D. Temel, M. J. Mathew, G. AlRegib and Y. M. Khalifa, "Relative Afferent Pupillary Defect Screening Through Transfer Learning," in IEEE Journal of Biomedical and Health Informatics, vol. 24, no. 3, pp. 788-795, March 2020, doi: 10.1109/JBHI.2019.2933773

30.   Panda, Saroj Kailash, and Nikhil Panjwani. "Cataract Detection Using Deep Learning." (2023).

31.   Junayed, Masum Shah, et al. "CataractNet: An automated cataract detection sys- tem using deep learning for fundus images." IEEE Access 9 (2021): 128799-128808.

32.   C̦etiner H, C̦etiner İ, 2022. Classification of Cataract Disease with a DenseNet201 Based Deep Learning Model. Journal of the Institute of Science and Technology, 12(3): 1264 - 1276.

Smart Investing in the Digital Era: The Dynamics of Financial Literacy, Experience, Behavioral Finance, and Fintech Applications

Pinisetty Ram Kishore
Research Scholar
VIT-AP School of Business
VIT-AP University
Amaravati, Andhra Pradesh
✉ kishore.21phd7040@vitap.ac.in

Raghavendra
Professor & Associate Dean
VIT-AP School of Business
VIT-AP University
Amaravati, Andhra Pradesh
✉ raghavendra@vitap.ac.in

ABSTRACT

Many investors believe fintech can transform the financial sector by introducing greater transparency and safety, easing the exchange of products and services, expanding service providers, and providing superior risk mitigation. Fintech's rapid expansion is driven by investors' willingness to use their money to lower risk. However, only 36% of individual investors in India use fintech investing platforms, highlighting the importance of other factors in investment decisions. Variables such as investor knowledge, financial behaviour, financial literacy, and financial experience significantly influence investment choices, regardless of fintech use. This study employs quantitative methods to investigate these research concerns, prioritizing unbiased measurements and data analysis. With 200 participants, the data was processed using SPSS. The objective is to provide significant insights for stakeholders, including the Indian government, fintech groups (particularly in digital payments), and fintech platform users.

KEYWORDS : Fintech, Financial literacy, Financial experience, Investment, Behavioral finance.

INTRODUCTION

The advancement of technological advances in communication and information has significantly transformed how contemporary financial operations are executed. Financial transactions were previously usually conducted via a wired network or in person. Nonetheless, the internet and the dissemination of mobile devices made it feasible to carry out financial transactions online. Fintech applications are supported by several kinds of devices and programmes that facilitate online transactions(Leon A. Abdillah, 2019). A technological breakthrough in the financial industry known as fintech (financial technology) can be utilised to assist financial services to enhance monetary operations (Mention, 2019).

Fintech, as opposed to the conventional way, delivers speed and ease in the financial transaction process(Caisar Darma et al., 2020). Long-held beliefs on the connection between financial services, technology, and business models are being challenged by the fintech industry's fast changes (Muthukannan et al., 2021). Fintech payment solutions are designed to overcome the drawbacks of the traditional payment system. For example, people in distant places with restricted access to bank offices can perform transactions with the help of mobile money services.Online payment systems streamline payments and enable large-scale transactions beyond typical business hours. Fintech may enhance the entire payment system in many different ways altogether(Harsoyo & Zulaikha, 2021).

India's MSME sector has a $380 billion credit gap, according to the World Bank. Investment bank Avendus Capital predicted a $530 billion MSME credit deficit. Only 14% of India's 64 million MSMEs have loans, data shows. A 3.8x debt-to-equity ratio put debt-based financing demand at $1,544 billion, while MSMEs demanded $1,955 billion(MSME Desk, 2023).India

now has the third-largest startup ecosystem in the world; 59,593 startups from 57 distinct industries—1,860 of which are in the FinTech sector—have been recognised by DPIIT. Over 17 Fintech startups in India as of December 2021 have achieved "Unicorn Status," with a valuation exceeding $1 billion USD(PIB, 2021).

Because fintech promotes product diversity, offers greater risk management, and is a larger service provider, various investors believe that fintech can wholly transform the financial industry and make it safer and more transparent. Investor interest in utilising fintech investments to lower risk has increased as a result(Bollaert et al., 2021). Four categories of fintech are established by the Financial Stability Board (FSB) according to the type of innovation: Payment, Peer to Peer (p2p) the lending process, Market Aggregator, Capital Management and Crowdfunding(Leon A. Abdillah, 2019).

Fintech consists of technologies that transform the financial sector. First, these fintech Payment, Settlement, and Clearing solutions aim to streamline digital payment processes. Second, Market Aggregator platforms provide financial information to help clients compare financial goods and make smart choices. Thirdly, wealthtech, a digital financial counselor, helps people assess their finances and make smart decisions. Crowdfunding and peer-to-peer (P2P) lending use technology to let borrowers and lenders access online borrowing and lending(Safitri, 2020).

The SBI poll found 4.47 million new retail investor accounts, showing a growth in retail engagement in Indian stock markets. In FY 2021, 12.25 million CDSL accounts and 1.97 million NSDL accounts were opened, bringing the total number of individual investors to 1.42 million. According to NSE data, retail investors made up 39% of stocks exchange turnover in March 2021 and 45% today (Livemint, 2021).Recent years have seen more investment in the Indian stock market. Stock market investors are still a small part of the nation's household population, but they are growing.

"There are 80 million direct stock market investors now. We have 80 million PANs and hope to achieve 90 million soon. Once duplicates are removed, the NSE has 80 million distinct accounts out of 160–170 million. Most new investors joined in the past two to three years,

thus numbers are rising. Mobile phones and apps are helping people save money in the stock market. The 80 million direct stock market investors in India comprise 50 million families, or 17% of all Indian households. Ashishkumar Chauhan, MD & CEO of the National Stock Exchange, noted that they generally enter through IPO markets.(Ashish Rukhaiyar, 2023).

Forecasts indicate that the fintech market might be worth $2.1 trillion by 2030. The financial technology sector holds the position of the second most funded venture industry in India as of 2022.Fintech startups in India amassed a total of $5.65 billion in funding in 2022. The total count of distinct institutional investors in the Indian fintech sector had a significant rise from 535 to 1019, or an almost twofold increase, during the period spanning from 2021 to 2022(Raghav Dhanuka, 2023).

But it's crucial for all investors to understand that, even in the absence of financial technology, some factors can influence investing choices. Among these, having solid financial literacy and awareness is essential for selecting investments that are smart and well-informed(Nag & Shah, 2022). Internal factors like financial skill and conduct can also affect investment decisions. Since experience-based understanding and awareness influence investing decisions, investors must have them. Lack of industry understanding and competence may hurt an investor's reputation(Karmacharya, 2023). We can conclude that financial experience, literacy, investor awareness, and behavioral finance influence investing decisions.

We did this study to help people make smart financial decisions, preferably using fintech as an investing platform. Investors are increasingly interested in fintech. Its secondary goal is to study how investors' financial market knowledge, behaviors, literacies, and experience affect their investing decisions.

LITERATURE REVIEW

Financial Literacy

Everybody's life is greatly impacted by financial literacy since it allows each person to get a deeper grasp of how to handle their finances responsibly. Financial literacy may help in making critical decisions and assessments about the prudent use and management of money (Baker

et al., 2019). The ability to manage money in a variety of ways, including savings, investments, insurance and loans, is denoted to as financial literacy (Sujono et al., 2023). A person's conception of the financial world, including how to record,manage, and invest money, will grow as they gain greater financial literacy. However, a person may find it difficult to manage their resources appropriately, which might put them at danger, if they lack adequate knowledge pertaining to financial literacy. They will also have trouble seeing the possible hazards when they make an investment (Novianggie & Asandimitra, 2019). In addition, consumers of digital financial services and technologies possess a deeper comprehension of financial instruments, techniques, and linkages. Therefore, when it comes to making financial decisions, those who routinely use digital financial services technology and/or are financially literate are fiscally responsible (Rasumovskaya et al., 2020). Based on the preceding discourse, the postulated hypothesis is as follows:

H1: Investment Decision is positively influenced by Financial Literacy

Financial Experience

Financial experience is the sum of an individual's personal financial events, including loans, investments, savings, and transactions(Arifin & Widjaya, 2022a). Someone with greater financial expertise will know what they can and cannot do while making financial decisions. Furthermore, it can make sound financial management decisions about loans, savings, and investments (Husnain et al., 2019). An individual's understanding of the financial world, including how to handle money, keep track of finances, and invest, increases with their level of financial literacy. On the other hand, a person may find it difficult to manage their finances appropriately, which might put them at danger, if they lack adequate information about financial literacy. They will also have some trouble recognising potential threats when they are making investments. There may be a relationship between financial literacy and financial experience, with those with more experience managing their finances more skilfully than others (Ameliawati & Setiyani, 2018). This explanation demonstrates the importance of both knowledge and experience in the financial world for each person. Financial literacy

enables investors to manage their money wisely, while experience teaches people what to do and what not to do when handling their finances (Baihaqqy et al., 2020).Based on the preceding discourse, the postulated hypothesis is as follows:

H2:Investment Decision is positively influenced by Financial Experience.

Behavioral Finance

During the 1980s, the term "behavioural finance" gained popularity and prominence due to the inclusion of cognitive, psychological, and behavioural aspects in the realm of financial and economic managerial process. It also seeks to investigate human characteristics in order to provide an explanation for people's rationale while making investment decisions(Costa et al., 2019). The area of behavioural finance, which is a modern application of psychology to finance, demonstrates how behavioural finance influences market behaviour. Behavioural finance looks on the sociological and psychological factors that affect how individuals and institutions make investment decisions (Atif Sattar et al., 2020). Many instances of activities that confront reason have been discovered in the field of behavioural finance research; these actions fall into two categories: cognitive bias and constrained rationality. Due to a lack of easily accessible and thorough information, bounded rationality suggests that decision-making is dependent on partial knowledge and can lead to heuristic decision-making, delay, and the uneven weighting of evident features(Jain et al., 2019).When choosing investments, each investor will have a different set of risks and potential rewards. An investor's appraisal and comprehension of risk can influence their investing decisions, helping to minimise possible losses as well as rewards. This is because investors may be influenced by financial psychology to make erroneous investing decisions or to stray from reason altogether (Madaan & Singh, 2019).Based on the preceding discourse, the postulated hypothesis is as follows:

H3:Investment Decision is positively influenced by Behavioral finance.

Investor Awareness

To earn lucrative investment returns, investors must be able to recognise specific risks that exist within the

financial markets and take steps to safeguard themselves. This is where investor awareness comes into play. Knowledge and information are essential for obtaining effective investment returns as they prevent investors from suffering significant losses if they lack sufficient information on stock market performance (Ndung'u & Kung'u, 2022). Investor awareness gives investors access to knowledge about investments and helps them comprehend risks associated with the securities they acquire. Moreover, investor knowledge helps investors build their own defence mechanisms against fraud and loss. Investor knowledge of current financial assets is influenced by the information portfolio providers share about the securities they issue (Karmacharya, 2023). As a result, investors' decisions to invest profited from their knowledge of economic circumstances and policies, which inevitably raised stock performance. Based on the preceding discourse, the postulated hypothesis is as follows:

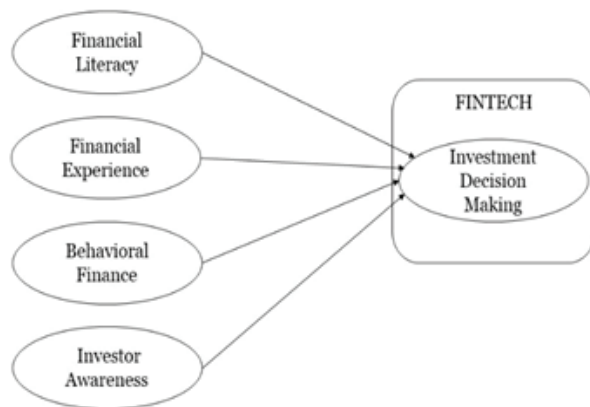H4:Investment Decision is positively influenced by Investor Awareness.

Fig:1 Research Framework

METHODOLOGY

The current research adoptsthe quantitative techniques that emphasizes the use of objective evaluation and statistical analysis of data collected using questionnaires to methodically analyze responses from the research participants. Indian respondents make up the sample population for the current research. A structured Google Forms questionnaire will be used to gather information on the respondents' thoughts.200 samples were acquired through distributing questionnaires.

A fintech application was used as a platform for the investment made by the 200 responders who met the criterion. To confirm the reliability and validity of the questionnaire, we initially conducted a normalcy test on 20 respondents. An additional 180 respondents were employed to meet the research's requirements after the validity of the questions had been established. Male or female samples meeting the age range of 18 to 65 are acceptable. Targeted occupations are Students, Employees, Professionals, Business people, and Housewives.

The Likert scale was used for this survey to rate each item, with 1 denoting strong disagreement and 5 signifying strong agreement. To highlight and present significant features, trends, and patterns in the data, descriptive analysis techniques will be applied to the obtained data in the Statistical Product and Service Solution (SPSS). During participant selection, the Simple Random Sampling (SRS) approach was employed to guarantee the populace's representativeness. Reducing bias, ease of use, simple analysis, generalisation, and observational independence are the goals of adopting SRS.

RESULTS AND INTERPRETATIONS

Demographic Analysis

In all, 200 respondents participated in the data gathering process that the author carried out; 189 of them had previously made fintech investments, and 11 had never made one. Majority of the respondents who have used the fintech to invest are women, accounting for 119 (62.8%) of the sample, while males make up the remaining 70 respondents (37.2%). In terms of ages 18–24 accounted for 51.3 percent of replies, with 25–34 accounting for 43.9 percent and 35–44 accounting for 4.8%. Private employees make up the majority of the workforce (100 persons, or 52.91%), followed by students (62 people, or 32.80%), professionals (19 people, or 10.5%), and housewives (8 people, or 4.24%).

Reliability and Validity Analysis

Financial Experience, Financial Literacy,Investor Awareness and Behavioural Finance were the four independent variables employed in this study. Only Fintech-related questions make up the 23 total questions in this study, with three to eight questions for each independent variable. The SPSS programme

is used to calculate each question's r-value, which is then compared to the R-table to assess each question's validity. Using a df = 187 value and a two-way significance level of 5%, the R-table yields a value of 0.1435 on the significance level. It is possible to deem aquestion valid if the R-value above the R-Table, as this study indicated.

Table 1. Validity Test Results

Df = No. ofresponses -2	Sig. Level	R-Table	R-Value
187	0.05	0.143	0.5342

Items on the questionnaire will be evaluated for validity using Cronbachs' alpha; items with an alpha greater than 0.70 will be considered reliable. Results showing a Cronbachs' alpha greater than 0.70 imply that the instruments are reliable.

Reliability Test Results

A Cronbach's α of 0.831 indicates strong internal consistency among 23 items. Typically, Cronbach's α values above 0.7 are acceptable, 0.8 is outstanding, and 0.9 is exceptional. With an α of 0.831, the scale or test is considered reliable, showing well-correlated items that presumably assess the same construct.

Classic Assumption Test

The classic assumption test, which includes checks for heteroscedasticity, normalcy, and multicollinearity, is used in this study. As a normalcy test, we have used the (Kolmogorov-Smirnov) K-S test, which generates asynchronously significant data when tested with two tails. The results in this investigation exhibit a normal distribution since the asymptotic significance level (Asymp. Sig., 2-tailed) is 0.65, which is greater than the threshold of 0.50 required to declare a normal distribution test.

It is reasonable to assume that no signs of multicollinearity exist when both the tolerance value and the VIF are greater than 0.100 but less than 10.00. All independent variables in the tests conducted for this study had tolerance values greater than 1.000 and VIFs less than 10.00, indicating the absence of multicollinearity indications.

Table 2. Multicollinearity Results

Model	Collinearity Statistics	
	Tolerance	**VIF**
Financial Experience	0.546	1.866
Financial Literacy	0.484	2.082
Investment Awareness	0.762	1.398
Behavioral Finance	0.584	1.741

Heteroscedasticity will be assessed using the Glejser test. Heteroscedasticity is not evident in the data if the significance value is more than 0.05. There are no indications of heteroscedasticity in this study becausethe significant values of all the exogenous variables are greater than 0.05.

Table 3. Heteroscedasticity Test Result

Model	T	Sig.
Financial Experience	0.546	1.866
Financial Literacy	0.484	2.082
Investment Awareness	0.762	1.398
Behavioral Finance	0.584	1.741

Descriptive Simulant Test

The regression model's significance value is examined in order to run the F test. In the absence of a significance level lower than 0.05, the exogenous variable has concurrently substantial impact on the endogenous variable. The regression's significance value (Sig.) in this study is less than 0.05 (i.e., 0.000), suggesting that the independent variables influence the dependent variable significantly at the same time in the test carried out in this investigation with the F-score of 43.884.

Hypothesis Test

The impact of each exogenous variableon endogenous variable is determined using the T-test. All of the hypotheses are supported generally, with the exception of investment awareness, for which there is a significance value greater than 0.05. A positive and significant influence is shown by the remaining independent factors. It is possible to conclude that H1, H2, and H3in which Behavioural Finance demonstrates a highly significant influence on Investment Decisionsare statistically supported.

Table 4. Hypothesis Testing

Hypothesis	T	Sig.	Decision
H1	4.708	0.000	Supported
H2	5.442	0.000	Supported
H3	5.058	0.000	Supported
H4	-1.944	0.054	Rejected

Multiple linear regression is a statistical method used to analyze the relationship between an endogenous variable and multiple exogenous variables; the equation for this type of analysis is:

$$Y= 0.703+0.217\ FL+ 0.149\ BF + 0.272\ FE - 0.061\ IA+ e \ \ldots\ldots\ (1)$$

According to the equation given earlier, the value of the investment decision is 0.703 when the constant value is Zero. For every one percentrise in the constructs of Financial Experience, Financial Literacy, and Behavioral Finance leads torise in the Investment Decision value by 0.272, 0.217, and 0.147 There is a 0.061 drop in Investment Decision value for every 1% rise in Investment Awareness.

R-Square Analysis

The purpose of R-Square analysis is to assess how well the model can explain how much the exogenous variable affects the endogenous variable. The result of the coefficient of determination test produces an adjusted R-squared score of 0.489. This study reveals that the four exogenous variables, namely financial experience, financial literacy, financial behavior, and investment awareness, collectively have a significant impact on the investment choice variable, accounting for a total of 48.9%. Other variables that were not considered in this analysis affect the remaining 51.1%.

DISCUSSION

Our findings shed important light on the connections between these factors and how they affect the way decisions are made about investments. People with greater levels of financial literacy were able to analyse and assess financial products and services more effectively, which led to better financial decision-making. Financial literacy is crucial for promoting investment decision-making since informed individuals are more probable to vigorously use fintech goods and services. This finding is consistent with a prior study by (Hamza & Arif, 2019), which found that financial literacy significantly and favourably influences investing choices.

Financial experience is the term used to describe the hands-on engagement and exposure people receive when managing their investments, personal finances, and monetary transactions over time. People who possess a substantial amount of financial expertise have a greater comprehension of risk assessment, market dynamics, and investing concepts. They are better able to assess investment prospects and make wise selections as a result of this experience. Similar to previous research by (Arifin & Widjaya, 2022b),which has highlight the significant correlation between financial experience and investment selections, underscoring the favorable and large influence of financial expertise on investment choices.

Moreover, behavioural finance exerts a substantial influence on investing choices. Overconfidence, confirmation bias, experience bias, loss aversion, disposition bias, and familiarity bias are examples of behavioural biases that are employed in this study that can cause people to make irrational decisions that affect investing outcomes. People may take intelligent and profitable investment decisions by matching their decisions with their financial objectives and using behavioural finance concepts to their decision-making process. This is in line with previous research by(Jain et al., 2019), which confirmed behavioural finance has a favourable and substantial influence on investing decisions.

Nevertheless, in fintech applications, it was discovered that investor awareness had no discernible impact on investment decision-making, which was unanticipated. This result runs counter to other studies(Harsoyo & Zulaikha, 2021; Ramanujam, 2018), that have shown the important influence of investor awareness on the choice to make an investment. To well appreciate the significance of investor knowledge in the milieu of fintech applications, more study is required to investigate the causes of this mismatch.

CONCLUSION

The study's prime goal is to identify the variables that may affect investing choices. The deciding constructs in this study include financial experience, financial literacy and financial behaviour. Data was gathered

from 200 respondents in India. Of the 200 respondents, 189 had previously made an investment via fintech, while the remaining 11 had never done so. According to the study's findings, three of the four independent variables it examined had a statistically significant beneficial impact on investment choices. Increasing one's degree of financial literacy, expertise with money, and understanding behavioural finance all help to encourage and simplify investing decisions.

This suggests that people are more probable to captivate in investing activities if they have greater financial knowledge, real-world experience, and an awareness of behavioural biases. The wellbeing of society as a whole, including individuals with little financial means, can also be enhanced by this accessibility to financial goods and services. The study findings offer valuable insights for several stakeholders, such as the Indian government, the fintech association, especially in the digital payment industry, and fintech platform users. The study's conclusions can help others understand the relationship between investor awareness, financial behaviour, financial experience, and financial literacy and how these elements might affect investing decisions. Fintech associations may also use these data to improve their services and platforms, which will eventually help their users and advance the fintech sector.

REFERENCES

1. Ameliawati, M., & Setiyani, R. (2018). The Influence of Financial Attitude , Financial Socialization , and Financial Experience to Financial Management Behavior with Financial Literacy as the Mediation Variable. International Conference on Economics, Business and Economic Education, 2018, 811–832. https://doi.org/10.18502/kss.v3i10.3174

2. Arifin, A. Z., & Widjaya, I. (2022a). The Effect of Financial Knowledge, Financial Experience, and Locus of Control Towards Investment Decision of Non-Depository Investors. 3rd Tarumanagara International Conference on the Applications of Social Sciences and Humanities (TICASH 2021). https://doi.org/10.2991/assehr.k.220404.120

3. Arifin, A. Z., & Widjaya, I. (2022b). The Effect of Financial Knowledge, Financial Experience, and Locus of Control Towards Investment Decision of Non-Depository Investors. https://doi.org/10.2991/assehr.k.220404.120

4. Ashish Rukhaiyar. (2023). 17% of all Indian households invest in the Indian stock markets, says NSE CEO. Business Today. https://www.businesstoday.in/markets/stocks/story/17-of-all-indian-households-invest-in-the-indian-stock-markets-says-nse-ceo-403824-2023-10-30

5. Atif Sattar, M., Toseef, M., & Fahad Sattar, M. (2020). Behavioral Finance Biases in Investment Decision Making. International Journal of Accounting, Finance and Risk Management, 5(2), 69. https://doi.org/10.11648/j.ijafrm.20200502.11

6. Baihaqqy, I., Rizaldy, M., & Sari, M. (2020). The effect of financial literacy on the investment decision. Budapest International Research and Critics Institute-Journal (BIRCI-Journal), 3(4), 3073–3083.

7. Baker, H. K., Kumar, S., Goyal, N., & Gaur, V. (2019). How financial literacy and demographic variables relate to behavioral biases. Managerial Finance, 45(1), 124–146. https://doi.org/10.1108/MF-01-2018-0003

8. Bollaert, H., Lopez-de-Silanes, F., & Schwienbacher, A. (2021). Fintech and access to finance. Journal of Corporate Finance, 68, 101941. https://doi.org/10.1016/j.jcorpfin.2021.101941

9. Caisar Darma, D., Lestari, D., & Muliadi, M. (2020). FinTech and Micro, Small and Medium Enterprises Development. Entrepreneurship Review, 1(1), 1–9. https://doi.org/10.38157/entrepreneurship-review.v1i1.76

10. Costa, D. F., Carvalho, F. de M., & Moreira, B. C. de M. (2019). BEHAVIORAL ECONOMICS AND BEHAVIORAL FINANCE: A BIBLIOMETRIC ANALYSIS OF THE SCIENTIFIC FIELDS. Journal of Economic Surveys, 33(1), 3–24. https://doi.org/10.1111/joes.12262

11. Hamza, N., & Arif, I. (2019). Impact of Financial Literacy on Investment Decisions: The Mediating Effect of Big-Five Personality Traits Model. Market Forces Research Journal, 14(1), 43–60. https://kiet.edu.pk/marketforces/index.php/marketforces/article/view/386

12. Harsoyo, E. C., & Zulaikha. (2021). the Impact of Investor Awareness Levels of the Red Flagging on Investment Decisions With Investor Risk Tolerance As Intervening Variable. International Journal of Business and Law, 24(6), 1–10.

13. Husnain, B., Shah, S., & Fatima, T. (2019). Effect of Neuroticism, Conscientiousness on Investment Decisions, Mediation Analysis of Financial Self-Efficacy. City University Research Journal, 09(1), 15–

26. https://www.proquest.com/docview/2190973695?fromopenview=true&pq-origsite=gscholar#:~:text=The results of the study supported a positive,self-efficacy between neuroticism%2C conscientiousness and long-term investment decision.

14. Jain, J., Walia, N., & Gupta, S. (2019). Evaluation of behavioral biases affecting investment decision making of individual equity investors by fuzzy analytic hierarchy process. Review of Behavioral Finance, 12(3), 297–314. https://doi.org/10.1108/RBF-03-2019-0044

15. Karmacharya, B. (2023). Determinants of Investor Awareness in Nepalese Capital Market. Journal of Business and Management, 7(01), 1–15. https://doi.org/10.3126/jbm.v7i01.54540

16. Leon A. Abdillah. (2019). An Overview of Indonesian Fintech Application. The 1st International Conference on Communication, Information Technology and Youth Study (I-CITYS2019), Figure 1, 8–16.

17. Livemint. (2021). Why more and more individual investors in India are investing in stock market. MInt. https://www.livemint.com/market/stock-market-news/why-more-and-more-individual-investors-in-india-are-investing-in-stock-market-11624337297582.html

18. Madaan, G., & Singh, S. (2019). An Analysis of Behavioral Biases in Investment Decision-Making. International Journal of Financial Research, 10(4), 55. https://doi.org/10.5430/ijfr.v10n4p55

19. Mention, A.-L. (2019). The Future of Fintech. Research-Technology Management, 62(4), 59–63. https://doi.org/10.1080/08956308.2019.1613123

20. MSME Desk. (2023). MSME Minister Narayan Rane says no study undertaken to evaluate MSME credit gap post Covid. Financial Express. https://www.financialexpress.com/business/sme-msme-minister-narayan-rane-says-no-study-undertaken-to-evaluate-msme-credit-gap-post-covid-3194963/

21. Muthukannan, P., Tan, B., Chian Tan, F. Ter, & Leong, C. (2021). Novel mechanisms of scalability of financial services in an emerging market context: Insights from Indonesian Fintech Ecosystem. International Journal of Information Management, 61, 102403. https://doi.org/10.1016/j.ijinfomgt.2021.102403

22. Nag, A. K., & Shah, J. (2022). An Empirical Study on the Impact of Gen Z Investors' Financial Literacy to Invest in the Indian Stock Market. Indian Journal of Finance, 16(10), 43. https://doi.org/10.17010/ijf/2022/v16i10/172387

23. Ndung'u, D. T., & Kung'u, J. N. (2022). Influence of investor awareness on performance of real estate investment trusts in Kenya. Pressacademia. https://doi.org/10.17261/Pressacademia.2022.1632

24. Novianggie, V., & Asandimitra, N. (2019). The Influence of Behavioral Bias, Cognitive Bias, and Emotional Bias on Investment Decision for College Students with Financial Literacy as the Moderating Variable. International Journal of Academic Research in Accounting, Finance and Management Sciences, 9(2), 92–107. https://doi.org/10.6007/IJARAFMS/v9-i2/6044

25. PIB. (2021). Fintech Sector. Ministry of Commerce & Industry. https://pib.gov.in/PressReleasePage.aspx?PRID=1781857#:~:text=Furthermore%2C India now hosts the 3rd largest ecosystem,with a valuation of over USD 1 billion.

26. Raghav Dhanuka. (2023). BFSI – Fintech & Financial Services. Invest India. https://www.investindia.gov.in/sector/bfsi-fintech-financial-services

27. Ramanujam, V. (2018). Does Investment Awareness Have Effect On Decision Making Among The Information Technology Professionals? Does Investment Awareness Have Effect On Decision Making Among The Information Technology Professionals? Does Investment Awareness Have Effect On Deci. International Journal of Business and Management Invention (IJBMI) ISSN, 7(8), 2319–2801. www.ijbmi.org

28. Rasumovskaya, E. A., Rasumovskyi, D. Y., & Ovsyannikova, E. Y. (2020). Impact Of The Digital Financial Technology To The Financial Literacy Of Population. European Proceedings of Social and Behavioural Sciences, 380–388. https://doi.org/10.15405/epsbs.2020.03.55

29. Safitri, T. A. (2020). The Development of Fintech in Indonesia. Proceedings of the 1st Borobudur International Symposium on Humanities, Economics and Social Sciences (BIS-HESS 2019). https://doi.org/10.2991/assehr.k.200529.139

30. Shingrup, M. M. (2020). Financial Literacy : A Momentum Towards Financial Stability in Society. 42–44.

31. Sujono, Mirosea, N., & Hajar, I. (2023). Effect of Financial Literacy and Behaviour on Investment Decisions (Study on Southeast Sulawesi investors). KnE Social Sciences. https://doi.org/10.18502/kss.v8i2.12766

GENERAL GUIDELINES FOR PREPARING AND SUBMITTING PAPERS

First Author*, Second Author†

*Institution and Country of first author's affiliation

†Institution and Country of second author's affiliation

Abstract

It should consist of a concise summary of the material discussed in the article below. It is preferable not to use footnotes in the abstract or the title. The acknowledgement for funding organizations etc. is placed in a separate section at the end of the text.

Keywords

Maximum 3 keywords may be placed after the abstract.

Introduction

Provide a historical perspective regarding the subject of your paper.

Background

Provide broad definitions and discussions of the topic and incorporate views of others (literature review) into the discussion to support, refute or demonstrate your position on the topic.

Main Thrust of the Paper

Present your perspective on the issues, controversies, problems, etc., as they relate to theme and arguments supporting your position. Compare and contrast with what has been, or is currently being done as it relates to your specific topic and the main theme of the volume.

Future Trends

Discuss future and emerging trends. Provide insight about the future of the topic from the perspective of published research on the topic. If appropriate, suggest future research opportunities within the domain of the topic.

Conclusion

Provide discussion of the overall coverage of the topic in your manuscript and conclusion should include key findings of the paper & concluding remarks.

References

References should follow the conclusions. The references should be listed in numerical order with the corresponding number cited inside the printed manuscript within square brackets at appropriate places [1, 2].

For example:

1. Hake, Richard R. 1998. Interactive-engagement versus traditional methods. A six-thousand student survey of mechanics test data for introductory physics courses. American Journal of Physics 66(1): 64-74

2. Steif, Paul S., and Anna dollar, 2003. A new approach to teaching and learning statics. In Proceedings of the ASEE Annual Conference and Exposition. Nashville, TN

GENERAL GUIDELINES FOR PREPARING AND SUBMITTING PAPERS

Acknowledgement

The acknowledgement for funding organizations etc. should be placed in a separate section at the end of the text.

Biodata

Please include brief bio data of the author (s) within 300 words and also attached a scanned copy of the latest passport size colour photograph of author (s)

Style

Manuscript should be printed on A4 size good white paper. Papers must be typed in English using MS Word. Kindly follow the instructions given below for all the pages

Margins:	:	Top	1.2"
		Bottom	1.2"
		Left	1.2"
		Right	1.2"
Orientation:	:	Portrait	
Font	:	Arial / 12 pt	
Heading	:	14 point	
Sub Heading	:	13 pt	
Spacing	:	Single line spacing	
Para Indent	:	6 point	

Length of Paper

The length of manuscript should not exceed 15 pages, including, figures/ photographs and references. The minimum number of pages should be 7 pages

Figures

All figures should be captioned and printed / pasted in appropriate place of the paper. Caption for the figures should be printed below the figures and numbered consecutively throughout the text. Tables should be placed closest to the text of citation and the title of the table to be printed on top of the table.

All figures, tables, drawings, screen shots are to be sent in a separate file preferably in an editable form.

Submission of the full paper

The final paper(s) may kindly be submitted to at the following address by post or to email : **editor@isteonline.org**

> **The Editor**
> (Indian Journal of Technical Education)
> Indian Society for Technical Education
> IIT Campus, Shaheed Jeet Singh Marg,
> Near Katwaria Saria, New Delhi - 110 016
> Phone : +91-11-26963542,26963431

Subscription details:

For subscribing the IJTE kindly visit our website www.isteonline.in and download the necessary forms.

ABOUT THE JOURNAL

Periodicity : Quarterly   **Subject :** Multidisciplinary

Indexed in the UGC-Care Journal list

The Indian Journal of Technical Education is published by the Indian Society for Technical Education on quarterly basis with the aim to provide an appropriate platform presenting well considered, meaningful, constructively thought provoking, non-political and non-controversial but critically analyzing and synthesizing present and future aspects of Technical Education System with particular reference to our country. The contributors are expected to highlight various issues of Technical Education (a broad outline of the journal objective is to promote the theory and practice of Engineering, Science, Technology, Management, Architecture, Pharmacy, Applied Arts and Crafts, Hotel Management and Computer Applications) along with meaningful suggestions for solution, refinement and innovations.

The following guidelines must be carefully followed.

1. IJTE is a peer reviewed Journal.

2. Manuscripts submitted to the journal will be initially screened by the editors. Those considered inappropriate will be returned to the sender.

3. The Authors are fully responsible for the contributions.

4. The Authors should be the Life Member of ISTE, if not, while submitting the paper they can apply for the membership by clicking https://membership.isteonline.in

5. The Copyright clearance will be the sole responsibility of authors for their papers. Enough precaution should be taken to make the manuscript error free.

6. Upon acceptance of a paper, the author(s) will be requested to provide an electronic copy of the paper, compatible with Microsoft Word.

7. The selection of papers for publication will be based on their relevance, clarity, topicality and originality.

8. The manuscript should be submitted and author's details should be mentioned in the beginning. The author should not be identified anywhere else in the article. The authors details should include full name, affiliation, e-mail address etc.

9. Manuscripts should not exceed 7,500 words (about 15 A-4 size pages, typed one and half space only)

10. Submit an abstract of about 200 words. The articles should be in clear, coherent and concise English language. Author/s should upload manuscript in MS-Word,

11. Tables should be numbered and referred to in the text as Table 1, Table 2, etc. Tables should not duplicate results in graphs. The minimum amount of descriptive text should be used on graphs and drawings (label curves, points, etc. with single letter symbols). The tables and figures should be clearly visible, readable and monochromatic in nature. Avoid inserting pictures of tables and figures in the manuscript.

12. In view of the large responses from Technical Education fraternity and limited space available in the Journal, the publication may take usually 3 months to 6 months from the date of receipt of the manuscript subject to approval by the reviewers.

13. All contributors are requested to please co-operate by observing the above mentioned Guidelines strictly while sending the paper for publication in the Indian Journal of Technical Education.

Note : Articles will be selected by the Editorial Board and are subject to editorial modification, if necessary